

Long-term impacts of preeclampsia on the cardiovascular system using murine models

Yolanda Correia

Doctor of Philosophy

ASTON UNIVERSITY

June 2023

© Yolanda Correia, 2023

Yolanda Correia, 2023 asserts her moral right to be identified as the author of this thesis.

This copy of the thesis has been supplied on condition that anyone who consults it is understood to recognise that its copyright belongs to its author and that no quotation from the thesis and no information derived from it may be published without appropriate permission or acknowledgement.

Aston University

Long-term impacts of preeclampsia on the cardiovascular system using murine models

Yolanda Correia

Doctor of Philosophy

June 2023

Thesis Abstract

Preeclampsia (PE) is a multisystemic pregnancy disorder accounting for 76,000 maternal and 500,000 perinatal deaths annually, often leaving survivors with severe long-term complications.

Angiogenic imbalance and compromised protective pathways are implicated in PE pathogenesis. Soluble fms-like tyrosine kinase 1 (sFlt-1), a soluble form of the vascular endothelial growth factor receptor 1 (VEGFR-1) extracellular ligand-binding domain, a crucial anti-angiogenic factor released by the placenta, plays vital role in PE pathogenesis. Hydrogen Sulphide (H₂S), an endogenous gaseous transmitter, is a potent vessel dilator, responsible for cellular physiology. Cystathionine- γ -lyase (CSE) is the main enzyme in cardiovascular system to produce H₂S. Its Dysregulation is associated with PE.

sFlt-1 overexpression and CSE malfunction have been used to induce PE-like symptoms in mice. However, the long-term impact on cardiovascular outcomes post-PE in these models remains unclear. We hypothesized that sFlt-1 induces PE-like symptoms and cardiovascular maladaptations during pregnancy and leads to long-term cardiovascular dysfunction. Using echocardiography, we found that pregnancy induced cardiovascular adaptations took place in mice treated with adenovirus empty vector (AdCMV). While as in sFlt-1 overexpressing pregnant mice, these adaptations were compromised alongside with PE-like symptoms, increased arterial pressure and reduced foetal weight. Furthermore, the cardiac dysfunction persisted beyond the immediate postpartum. We also investigated the role of CSE in the maternal cardiovascular adaptation. Echocardiography revealed that compared to CSE wild-type (CSE WT), pregnancy induced cardiac adaptation was compromised and associated with increased mitochondrial DNA content. Finally, significant differences in the gene profiles in sFlt-1 overexpressing mice during pregnancy and postpartum were identified using RNA-sequencing, suggesting exposure of sFlt-1 has long-term consequences in cardiovascular system.

In conclusion, our research enhances the understanding of the immediate and enduring effects of sFlt-1 and the underlying mechanisms of PE attributable to H₂S dysregulation.

Key words: soluble Flt-1, hydrogen sulphide, cystathionine- γ -lyase, preeclampsia

Acknowledgments

This thesis is dedicated to my mother, who has consistently offered unwavering support throughout not only my doctoral journey but also my entire academic career. Despite not having the same opportunities during her youth, she has made every conceivable effort to guarantee my success.

They say that it is people who make a moment, a place or a stage of your life beautiful, and I couldn't agree more.

First and foremost, I extend my deepest appreciation to the European Union Horizon 2020 Innovative Training Network (ITN) under the Marie Skłodowska-Curie Action, which provided the financial support needed to conduct the research presented in this thesis. Additionally, I am grateful to my supervisor, Dr. Keqing Wang, for giving me the opportunity to pursue a doctoral degree and for working and dealing with me on a day-to-day basis to achieve the final result. Her patience and advice have significantly helped my growth not just as a researcher but as a person. I would also like to express my gratitude to Dr. Colin Murdoch and the iPlacenta consortium, along with its exceptional Early-Stage Researchers.

I would also like to express my deepest gratitude to Dr. Sophie Broadway-Stringer, who imparted training on the majority of the research showcased in this thesis. Her patience, benevolence, and guidance have been pivotal in attaining the comprehensive understanding exhibited in this work.

I would also like to thank the whole team at Aston Medical school as well as Caroline Brocklebank, who consistently offered assistance in addressing any difficulties I encountered.

Next, I would like to express my gratitude to the remarkable women with whom I have had the pleasure of learning from and working alongside with, both within and beyond the confines of Aston university. I am grateful to Dr. Sophie Broadway-Stringer, Dr. Milda Grubliauskiene, Dr. Lorena Diaz Sanchez, Dr. Hala Abdelmohaimen Shokr, Dr. Homira Rezai, the soon-to-be Dr. Re Ea Tay, for sitting down with me and assisting in piecing things together when everything around me seemed to be falling apart, for their kindness, positivity, and cheerfulness, especially in the moments when research did not progress as anticipated.

Finally, I would like to thank my mom, my family, especially my aunts and cousins for supporting and believing in me from afar. Special thanks to my partner, Reece B., for his love, encouragement, and unwavering belief in me.

Table of Contents

| | |
|-----------------------------------------------------------------------------|-----------|
| List of abbreviations | 16 |
| Chapter 1 | 25 |
| 1. Introduction | 26 |
| 1.1 Pregnancy | 26 |
| 1.2 Hormone changes in pregnancy | 27 |
| 1.3 Cardiac Adaptations to Pregnancy and Postpartum | 28 |
| 1.3.1 Volume of Blood in Circulation | 29 |
| 1.3.2 Cardiac Systolic Functions | 30 |
| 1.3.3 Cardiac Diastolic Functions | 32 |
| 1.3.4 Remodelling of the Cardiovascular System | 37 |
| 1.4 Uterine flow | 40 |
| 1.5 Dysfunctional Adaptations to Pregnancy | 40 |
| 1.6 Preeclampsia | 41 |
| 1.6.1 Current Hypotheses behind PE | 44 |
| 1.6.2 Potential underlying mechanisms | 60 |
| 1.6.3 Vascular predisposition and abnormal Cardiovascular adaptations in PE | 64 |
| 1.7 Long-Term Cardiovascular Risk | 68 |
| 1.7.1 Cardiovascular Disease risk | 69 |
| 1.7.2 Genetics of preeclampsia | 70 |
| 2. Aims and Hypotheses | 76 |
| 2.1 Aims | 76 |
| 2.2 Hypotheses | 77 |
| 3. Materials and Methods: | 79 |
| 3.1 Animals: | 79 |
| 3.1.1 Time Mating | 80 |
| 3.1.2 Transgenic Model | 80 |

| | | |
|------------|-------------------------------------------------------------------------------------------------------------|------------|
| 3.1.3 | Genotyping | 80 |
| 3.1.4 | Adenovirus Treatment In Vivo | 81 |
| 3.2 | Mean Arterial Pressure Measurement | 81 |
| 3.2.1 | Probe Calibration | 81 |
| 3.2.2 | Data Collection | 82 |
| 3.3 | Ultrasound Imaging | 83 |
| 3.3.1 | Parasternal Long Axis and Left Mid-papillary Short Axis of the Heart | 83 |
| 3.3.2 | M-Mode | 84 |
| 3.3.3 | B-Mode | 87 |
| 3.3.4 | Mitral Inflow | 89 |
| 3.3.5 | Uterine Artery | 91 |
| 3.4 | Tissue Collection | 93 |
| 3.4.1 | Plasma isolation | 93 |
| 3.4.2 | Tissue Collection post-euthanasia | 93 |
| 3.4.3 | Interval in-vivo Blood Collection | 93 |
| 3.5 | ELISA | 95 |
| 3.6 | Gene Expression | 95 |
| 3.6.1 | RNA Isolation | 95 |
| 3.6.2 | cDNA Synthesis | 96 |
| 3.6.3 | Quantitative polymerase chain reaction (qPCR) | 97 |
| 3.6.4 | mRNA Sequencing | 97 |
| 3.7 | Statistical analysis | 98 |
| 4. | Cardiac changes during pregnancy in PE model – sFlt-1 overexpression model | 100 |
| 4.1 | Background | 100 |
| 4.2 | 4.2 Normotensive Pregnancy Adaptations | 102 |
| 4.3 | Overexpression of sFlt-1 in pregnancy increases maternal blood pressure and decreases foetal weight. | 105 |
| 4.3.1 | sFlt-1 overexpression was successful. | 106 |

| | | |
|------------------|--------------------------------------------------------------------------------------------------------------------------|------------|
| 4.4 | Effects of sFlt-1 overexpression on cardiac function during pregnancy | 107 |
| 4.4.1 | Effects of sFlt-1 on Cardiac Systolic Functions in Pregnancy | 108 |
| 4.4.2 | Overexpression of sFlt-1 altered diastolic functions in pregnancy. | 110 |
| 4.4.3 | Overexpression of sFlt-1 impacted the cardiac structural changes. | 112 |
| 4.4.4 | Overexpression of sFlt-1 did not alter the uterine artery blood flow | 115 |
| 4.5 | Discussion | 117 |
| 4.6 | Limitations | 123 |
| 5. | Long-term effects of sFlt-1 induced preeclampsia on cardiovascular health | 125 |
| 5.1 | Long-term effects of sFlt-1 | 126 |
| 5.1.1 | sFlt-1 level in plasma | 126 |
| 5.1.2 | Long-term effects of sFlt-1 on Cardiac Systolic Functions | 128 |
| 5.1.3 | Long-term effects of sFlt-1 on Diastolic Functions | 130 |
| 5.1.4 | Long-term effects of sFlt-1 on Cardiac Structural Changes | 134 |
| 5.1.5 | Long-term effects of sFlt-1 on uterine artery blood flow | 137 |
| 5.2 | Discussion | 138 |
| 5.2.1 | sFlt-1 levels in plasma reached baseline by 8 weeks | 138 |
| 5.2.2 | Long-term effects of sFlt-1 overexpression led to systolic and diastolic dysfunctions | 139 |
| 5.2.3 | Long-term effects of sFlt-1 overexpression resulted in abnormal structural changes | 141 |
| 5.2.4 | Long-term effects of sFlt-1 overexpression induced sustained increased uterine artery pressure up to 8 weeks post-partum | 142 |
| 5.2.5 | Short-term exposure of sFlt-1 causes long-term impact on cardiovascular functions | 144 |
| 5.3 | Limitations | 146 |
| Chapter 6 | | 147 |
| 6. | The role of CSE on cardiovascular adaptation during pregnancy | 148 |
| 6.1 | CSE KO in pregnancy | 149 |
| 6.1.1 | Effects of CSE KO on cardiac systolic functions during pregnancy | 150 |
| 6.1.2 | Effects of CSE KO on cardiac diastolic functions during pregnancy | 151 |
| 6.1.3 | Effects of CSE KO on cardiac structural changes | 152 |
| 6.1.4 | Effects of CSE KO on uterine artery blood flow | 154 |

| | | |
|------------|---------------------------------------------------------------------------------------------|------------|
| 6.1.5 | Cardiac mitochondrial content is influenced by endogenous H ₂ S _____ | 155 |
| 6.2 | Discussion _____ | 157 |
| 6.2.1 | CSE KO effect on adaptations to pregnancy _____ | 157 |
| 6.2.2 | CSE KO on mitochondrial function _____ | 158 |
| 6.3 | Conclusion _____ | 160 |
| 6.4 | Limitations _____ | 161 |
| 7. | Gene Expression in PE models _____ | 163 |
| 7.1 | Gene expression CSE KO mice _____ | 164 |
| 7.1.1 | Gene expression in cardiac tissue of non-pregnant CSE KO vs CSE WT mice _____ | 164 |
| 7.1.2 | Gene expression in the cardiac tissues of pregnant vs non-pregnant CSE WT mice _____ | 171 |
| 7.1.3 | Gene expression in the cardiac tissues of pregnant CSE KO vs CSE KO non-pregnant mice. ____ | 178 |
| 7.2 | Gene expression in pregnant mice overexpressing sFlt-1 _____ | 192 |
| 7.2.1 | Gene expression in cardiac tissue of AdsFlt-1 vs AdCMV mice in pregnancy _____ | 193 |
| 7.2.2 | Gene expression in cardiac tissue of AdCMV postpartum vs AdCMV in pregnancy _____ | 200 |
| 7.2.3 | Gene expression in cardiac tissue of AdsFlt-1 postpartum vs AdsFlt-1 mice in pregnancy ____ | 206 |
| 7.2.4 | Gene expression in cardiac tissue of postpartum AdsFlt-1 vs AdCMV in mice _____ | 213 |
| 7.2.5 | Gene expression in cardiac tissue of AdsFlt-1 postpartum vs pregnant AdCMV mice _____ | 221 |
| 7.3 | Discussion _____ | 228 |
| 7.3.1 | Gene expression in CSE KO in cardiac tissue _____ | 229 |
| 7.3.2 | Gene expression in AdsFlt-1 _____ | 235 |
| 7.3.3 | Gene expression in AdsFlt-1 postpartum _____ | 237 |
| 7.4 | Conclusion _____ | 247 |
| 7.4.1 | CSE KO and pregnancy _____ | 247 |
| 7.5 | Limitations _____ | 248 |
| 8. | General Discussion and Conclusions _____ | 251 |
| 8.1 | Summary of findings _____ | 251 |
| 8.1.1 | sFlt-1 effects on Cardiovascular functions _____ | 251 |
| 8.1.2 | The role of CSE on cardiovascular adaptations to pregnancy _____ | 256 |
| 8.2 | Conclusions and Future Work _____ | 257 |

| | | |
|------|------------------------------------------|-----|
| 8.3 | Limitations | 258 |
| 9. | References | 260 |
| 10. | Appendices | 390 |
| 10.1 | Appendix A – Consumables and Instruments | 390 |
| 10.2 | Appendix B – Supplementary Material | 392 |
| 10.3 | Appendix C – Supplementary Methods | 393 |
| | C.1 Novogene mRNA Sequencing protocol | 393 |
| 10.4 | Appendix E – Publications | 399 |

List of Figures

| | |
|-------------------------------------------------------------------------------------------------------------------------------------------------------------------------|-----|
| Figure 1.1 Illustration of hormonal and Cardiovascular Adaptations to pregnancy. _____ | 28 |
| Figure 1.2 The measurement of cardiac time intervals is shown schematically. _____ | 37 |
| Figure 1.3 Hypotheses behind PE. _____ | 44 |
| Figure 1.4 Oxidative Stress illustration. _____ | 50 |
| Figure 1.5 The relationship between preeclampsia and angiogenesis involves the traditional theory of angiogenic imbalance. _____ | 54 |
| Figure 1.6 H ₂ S effects on mitochondria. _____ | 60 |
| Figure 3.1 Summary of materials and methods. _____ | 79 |
| Figure 3.2 Echocardiography analysis. Echocardiography analysis. _____ | 85 |
| Figure 3.3 Simpson's measurements in M-mode SAX. _____ | 88 |
| Figure 3.4 Mitral Flow Measurements. _____ | 90 |
| Figure 3.5 Typical illustrations of uterine artery measurements. _____ | 92 |
| Figure 4.1 Systolic functions of left ventricle in pre-gravid and pregnant mice at E17.5. _____ | 103 |
| Figure 4.2 Uterine artery flow in pre-gravid and pregnant mice at E.17.5. _____ | 104 |
| Figure 4.3 Mean arterial blood pressure (MAP) in the mother and foetal weight was recorded. _____ | 105 |
| Figure 4.4 ELISA assay for plasma sFlt-1 level measurement. _____ | 106 |
| Figure 4.5 Systolic functions of left ventricle in CMV and sFlt-1 mice during pregnancy. _____ | 109 |
| Figure 4.6 Diastolic functions of left ventricle in CMV and sFlt-1 mice during pregnancy. _____ | 111 |
| Figure 4.7 Representative images of the mitral inflow colour Doppler trace in pregnancy. _____ | 112 |
| Figure 4.8 Structural functions of left ventricle in CMV and sFlt-1 mice during pregnancy. _____ | 114 |
| Figure 4.9 Uterine artery flow in CMV and sFlt-1 mice during pregnancy. _____ | 116 |
| Figure 5.1 Plasma samples were collected at different timepoints during pregnancy (in the graph this is noted as week 0) and post-partum. _____ | 127 |
| Figure 5.2 Systolic functions of left ventricle in CMV and sFlt-1 mice during pregnancy and post-partum. _____ | 129 |
| Figure 5.3 Uterine artery flow in CMV and sFlt-1 mice during pregnancy and post-partum. _____ | 137 |
| Figure 6.1 Systolic functions of left ventricle adaptations in Wild type (WT) and knockout (KO) mice. _____ | 150 |
| Figure 6.2 Diastolic functions of left ventricle adaptations in Wild type (WT) and knockout (KO). _____ | 151 |
| Figure 6.3 Structural functions of left ventricle adaptations in Wild type (WT) and knockout (KO). _____ | 153 |
| Figure 6.4 Uterine artery flow adaptations in Wild type (WT) and knockout (KO). Uterine artery flow was measured in WT and KO mice before pregnancy and on E17.5. _____ | 155 |
| Figure 6.5 Bar plot showing the effect of CSE Knockdown on mitochondrial DNA (mtDNA) of pregnant versus non-pregnant mice. _____ | 156 |

| | |
|---------------------------------------------------------------------------------------------------------------------------------------------------------------------------------------------------------|-----|
| <i>Figure 7.1 The DEG in cardiac tissue of non-pregnant of CSE KO (n=2) vs CSE WT mice (n=2), was visually represented by a volcano plot and a heatmap.</i> | 165 |
| <i>Figure 7.2 GO enrichment Analysis of DEG on CSE KO vs CSE WT non-pregnant cardiac tissue.</i> | 168 |
| <i>Figure 7.3 KEGG pathway enrichment analysis of DEGs from RNA-seq data.</i> | 170 |
| <i>Figure 7.4 The differential expression of genes (DEG) in cardiac tissue of CSE WT pregnant (n=2) vs CSE WT non pregnant mice (n=2), was visually represented by a volcano plot and a heatmap.</i> | 172 |
| <i>Figure 7.5 GO enrichment Analysis of DEG on CSE WT pregnant vs CSE WT non-pregnant cardiac tissue.</i> | 176 |
| <i>Figure 7.6 KEGG pathway enrichment analysis of DEGs from RNA-seq data.</i> | 177 |
| <i>Figure 7.7 The differential expression of genes (DEG) in cardiac tissue of pregnant of CSE KO (n=2) vs CSE KO non-pregnant mice (n=2), was visually represented by a volcano plot and a heatmap.</i> | 179 |
| <i>Figure 7.8 GO enrichment Analysis of DEG on CSE KO pregnant vs CSE KO non-pregnant cardiac tissue.</i> | 183 |
| <i>Figure 7.9 KEGG pathway enrichment analysis of DEGs from RNA-seq data.</i> | 184 |
| <i>Figure 7.10 The differential expression of genes (DEG) in cardiac tissue of pregnant of CSE KO (n=2) vs CSE WT pregnant (n=2) mice, was visually represented by a volcano plot and a heatmap.</i> | 186 |
| <i>Figure 7.11 GO enrichment Analysis of DEG on pregnant CSE KO vs CSE WT in cardiac tissue.</i> | 189 |
| <i>Figure 7.12 KEGG pathway enrichment analysis of DEGs from RNA-seq data.</i> | 191 |
| <i>Figure 7.13 The differential expression of genes (DEG) in cardiac tissue of pregnant of AdsFlt-1 vs AdCMV pregnant mice, was visually represented by a volcano plot and a heatmap.</i> | 194 |
| <i>Figure 7.14 GO enrichment Analysis of DEG on the cardiac tissue of AdsFlt-1 vs AdCMV in pregnant mice.</i> | 197 |
| <i>Figure 7.15 KEGG pathway enrichment analysis of DEGs from RNA-seq data of the cardiac tissue in pregnancy of AdsFlt-1 vs AdCMV mice.</i> | 199 |
| <i>Figure 7.16 The differential expression of genes (DEG) in cardiac tissue of pregnant of AdCMV postpartum vs AdCMV in pregnant mice, was visually represented by a volcano plot.</i> | 201 |
| <i>Figure 7.17 GO enrichment Analysis of DEG in cardiac tissue of pregnant of AdCMV postpartum vs AdCMV in pregnant mice.</i> | 204 |
| <i>Figure 7.18 KEGG pathway enrichment analysis of DEGs from RNA-seq data of the cardiac tissue in AdCMV postpartum vs AdCMV in pregnant mice.</i> | 205 |
| <i>Figure 7.19 The differential expression of genes (DEG) in cardiac tissue of postpartum AdsFlt-1 vs AdsFlt-1 in pregnant mice, was visually represented by a volcano plot and a heatmap.</i> | 207 |
| <i>Figure 7.20 GO enrichment Analysis of DEG in cardiac tissue of postpartum AdsFlt-1 vs AdsFlt-1 in pregnant mice.</i> | 210 |
| <i>Figure 7.21 KEGG pathway enrichment analysis of DEGs from RNA-seq data of the cardiac tissue in AdsFlt-1 postpartum vs AdsFlt-1 in pregnant mice.</i> | 212 |

| | |
|------------------------------------------------------------------------------------------------------------------------------------------------------------------------------------------|-----|
| <i>Figure 7.22 The differential expression of genes (DEG) in cardiac tissue of postpartum AdsFlt-1 vs AdCMV mice, was visually represented by a volcano plot and a heatmap.</i> | 214 |
| <i>Figure 7.23 GO enrichment Analysis of DEG in cardiac tissue of postpartum AdsFlt-1 vs AdCMV mice.</i> | 217 |
| <i>Figure 7.24 KEGG pathway enrichment analysis of DEGs from RNA-seq data in cardiac tissue of postpartum AdsFlt-1 vs AdCMV mice.</i> | 220 |
| <i>Figure 7.25 The differential expression of genes (DEG) in cardiac tissue of postpartum AdsFlt-1 vs pregnant AdCMV mice, was visually represented by a volcano plot and a heatmap.</i> | 222 |
| <i>Figure 7.26 GO enrichment Analysis of DEG in cardiac tissue of postpartum AdsFlt-1 vs pregnant AdCMV mice.</i> | 225 |
| <i>Figure 7.27 KEGG pathway enrichment analysis of DEGs from RNA-seq data in cardiac tissue of postpartum AdsFlt-1 vs pregnant AdCMV mice.</i> | 227 |
| <i>Figure S10.1 Workflow of directional library construction.</i> | 394 |
| <i>Figure S10.2 Genotyping of cystathionine gamma lyase (CSE) knockout and</i> | 397 |
| <i>Figure S10.3 Echocardiographic MV E/A classification according to (Danzmann et al. 2008)</i> | 398 |

List of Tables

| | |
|-----------------------------------------------------------------------------------------------------------------------------------------------------------------------------------------------------------------------------------------|-----|
| Table 1.1 Cardiovascular Adaptations to Normal Pregnancy and Postpartum. | 35 |
| Table 1.2 Abnormal Cardiovascular Adaptations in Preeclampsia. | 66 |
| Table 3.1 B-Mode Measurements using Parasternal Long Axis View (PSLAX). | 84 |
| Table 5.1 Cardiac diastolic functions during pregnancy and post-partum analysed using echocardiography and M-mode of parasternal long axis view in CMV and sFlt-1. | 132 |
| Table 5.2 Cardiac structural functions during pregnancy and post-partum analysed using echocardiography and M-mode of parasternal long axis view in CMV and sFlt-1. | 136 |
| Table 7.1 Table of top 5 upregulated genes with a cut-off at p adjusted of 0.05, ordered in descending order from the most upregulated gene to the least upregulated gene in non-pregnant KO mice versus non-pregnant WT mice. | 166 |
| Table 7.2 Table of top 5 downregulated genes with a cut-off at p adjusted of 0.05, ordered in ascending order from the most downregulated gene to the least downregulated gene in non-pregnant KO mice versus non-pregnant WT mice. | 167 |
| Table 7.7.3 Table of top 5 upregulated genes with a cut-off at p adjusted of 0.05, ordered in ascending order from the most downregulated gene to the least downregulated gene in pregnant CSE WT mice versus non-pregnant CSE WT mice. | 173 |
| Table 7.7.4 Table of top 5 downregulated genes with a cut-off at p adjusted of 0.05, ordered in ascending order from the most upregulated gene to the least upregulated gene in pregnant CSE WT mice versus non-pregnant CSE WT mice. | 174 |
| Table 7.5 Table of top 5 upregulated genes with a cut-off at p adjusted of 0.05, ordered in ascending order from the most upregulated gene to the least upregulated gene in pregnant CSE KO mice versus non-pregnant CSE KO mice. | 180 |
| Table 7.6 Table of top 5 downregulated genes with a cut-off at p adjusted of 0.05, ordered in ascending order from the most downregulated gene to the least downregulated gene in pregnant CSE KO mice versus non-pregnant CSE KO mice. | 181 |
| Table 7.7 Table of top 5 upregulated genes with a cut-off at p adjusted of 0.05, ordered in ascending order from the most upregulated gene to the least upregulated gene in pregnant CSE KO mice vs CSE WT mice. | 187 |
| Table 7.8 Table of top 5 downregulated genes with a cut-off at p adjusted of 0.05, ordered in ascending order from the most downregulated gene to the least downregulated gene in pregnant CSE KO mice vs CSE WT mice. | 188 |

| | |
|--------------------------------------------------------------------------------------------------------------------------------------------------------------------------------------------------------------------------------------------------------------------|-----|
| Table 7.9 Table of top 5 upregulated genes with a cut-off at p adjusted of 0.05, ordered in ascending order from the most upregulated gene to the least upregulated gene in pregnant AdsFlt-1 vs AdCMV mice. _____ | 195 |
| Table 7.10 Table of top 5 downregulated genes with a cut-off at p adjusted of 0.05, ordered in ascending order from the most downregulated gene to the least downregulated gene in pregnant AdsFlt-1 vs AdCMV mice. _____ | 195 |
| Table 7.11 Table of top 5 upregulated genes with a cut-off at p adjusted of 0.05, ordered in ascending order from the most upregulated gene to the least upregulated gene in postpartum AdCMV vs pregnant AdCMV mice. _____ | 202 |
| Table 7.12 Table of top 5 downregulated genes with a cut-off at p adjusted of 0.05, ordered in ascending order from the most downregulated gene to the least downregulated gene in postpartum AdCMV vs pregnant AdCMV mice. _____ | 203 |
| Table 7.13 Table of top 5 upregulated genes with a cut-off at p adjusted of 0.05, ordered in ascending order from the most upregulated gene to the least upregulated gene in postpartum AdsFlt-1 vs pregnant AdsFlt-1 mice. _____ | 208 |
| Table 7.14 Table of top 5 downregulated genes with a cut-off at p adjusted of 0.05, ordered in ascending order from the most downregulated gene to the least downregulated gene in postpartum AdsFlt-1 vs pregnant AdsFlt-1 mice. _____ | 208 |
| Table 7.15 Table of upregulated DEG with a cut-off at p adjusted of 0.05, ordered in ascending order from the most upregulated gene to the least upregulated gene in postpartum AdsFlt-1 vs AdCMV mice. Only one DEG was significantly upregulated. _____ | 215 |
| Table 7.16 Table of downregulated regulated DEG with a cut-off at p adjusted of 0.05, ordered in ascending order from the most downregulated gene to the least downregulated gene in postpartum AdsFlt-1 vs AdCMV mice. _____ | 215 |
| Table 7.17 Table of upregulated DEG with a cut-off at p adjusted of 0.05, ordered in ascending order from the most upregulated gene to the least upregulated gene in postpartum AdsFlt-1 vs pregnant AdCMV mice. Only one DEG was significantly upregulated. _____ | 223 |
| Table 7.18 Table of downregulated regulated DEG with a cut-off at p adjusted of 0.05, ordered in ascending order from the most downregulated gene to the least downregulated gene in postpartum AdsFlt-1 vs pregnant AdCMV mice. _____ | 223 |
| Table S10.1: Laboratory Instruments and Software _____ | 391 |
| Table S10.2 Laboratory Consumables and Kits _____ | 392 |

| | |
|-----------------------------------------------------------------------------------------------------------|-----|
| Table S10.3: Primer sequences for assessing the effectiveness of transgenic generation (Yang et _____) | 392 |
| Table S10.4 Mitochondrial DNA Primers _____ | 393 |

List of abbreviations

| ABBREVIATION | MEANING |
|---------------------|------------------------------------------------------------------------|
| ° | Degree |
| °C | Degree Celsius |
| µg | Microgram |
| µl | Microliter |
| µm | Micrometre |
| 3-MST | 3-Mercaptopyruvate Sulfurtransferase |
| AdCMV | Empty vector of Adenovirus /Cytomegalovirus injection |
| AdsFit-1 | Adenovirus injection overexpressing Soluble Fms-Like Tyrosine Kinase 1 |
| ANG | Angiotensin |
| Angptl4 | Angiopoietin-Like Protein 4 |
| Angptl7 | Angiopoietin-Related Protein 7 |
| Apold1 | Apolipoprotein L Domain Containing 1 |
| ATP | Adenosine Triphosphate |
| β-HCG | beta-human chorionic gonadotropin |
| B2M1 | Beta-2-Microglobulin |
| BBB | Blood–Brain Barrier |

| | |
|------------------------|-----------------------------------------------------|
| BC002163 | cDNA sequence BC002163 |
| BP | Biological Processes |
| BSA | Bovine Serum Albumin |
| BSX | Brain Specific Homeobox |
| Ca²⁺ | Calcium |
| cAMP | Cyclic Adenosine Monophosphate |
| CAT | Cysteine Aminotransferase |
| CBS | Cystathionine-B-Synthase |
| CC | Cellular component |
| cDNA | Complimentary Deoxyribonucleic Acid |
| cDNA | Complementary Deoxyribose Nucleic Acid |
| Cftr | Cystic Fibrosis Transmembrane Conductance Regulator |
| cm | Centimetre |
| CMV | Cytomegalovirus |
| CNS | Central Nervous System |
| CO | Cardiac Output |
| CORM-2 | Co-Releasing Molecule-2 |
| COX | Cyclooxygenase |
| Cox6a2 | Cytochrome C Oxidase Subunit 6a2 |

| | |
|-----------------------------------|--------------------------------------------------------|
| Csdc2 | cold shock domain containing C2, RNA binding |
| CSE | Cystathionine Gamma-Lyase |
| CSE^{-/-} / CSE KO | CSE Knockout |
| Ct | Cycle Threshold |
| CVD | Cardiovascular Disease |
| Cxcl13 | C-X-C Motif Chemokine 13 |
| Cyp26b1 | Cytochrome P450, Family 26, Subfamily B, Polypeptide 1 |
| d | Diastole |
| DAO | D-Amino Acid Oxidase |
| DEG | Differentially Expressed Genes |
| DNA | Deoxyribonucleic Acid |
| dNTPs | Deoxyribonucleotide Triphosphates |
| Drps | Dynamin-related proteins |
| E | Embryonic Day |
| ECM | Extracellular Matrix |
| Ednrb | Endothelin Receptor Type B |
| EDTA | Ethylenediaminetetraacetic Acid |
| EF | Ejection Fraction |
| Eif3j1 | eukaryotic translation initiation factor 3, subunit J1 |

| | |
|-----------------------|---------------------------------------------------|
| EKV | Electrocardiogram-Gated Kilohertz Visualisation |
| ELISA | Enzyme Linked Immunosorbent Assay |
| eNOS | Endothelial Nitric Oxide Synthase |
| Entpd4b | ectonucleoside triphosphate diphosphohydrolase 4B |
| ETC | Electron Transport chain |
| EVT | Extravillous Trophoblasts |
| fEPSPs | field excitatory post- synaptic potentials |
| FGR | Foetal Growth Restriction |
| FoxO | Forkhead box O |
| FS | Fraction Shortening |
| Gm14085 | predicted gene 14085 |
| GO | Gene Ontology |
| H₂S | Hydrogen Sulphide |
| HK2 | Hexokinase 2 |
| HO | Haem Oxygenase |
| HR | Heart Rate |
| HUVEC | Human Umbilical Vein Endothelial Cells |
| IC | Inconsistent – No Consensus Found |
| ICM | Internal Cellular Mass |

| | |
|---------------|-----------------------------------------|
| IL | Interleukin |
| IL1B | Interleukin 1 Beta |
| ITG | Integrin |
| ITGa2b | Integrin Alpha 2b |
| IVCT | Isovolumetric Contraction Time |
| IVRT | Isovolumetric Relaxation Time |
| IVS | Interventricular Septum |
| KATP | Potassium ATP |
| KEGG | Kyoto Encyclopedia of Genes and Genomes |
| Ldhc | Lactate Dehydrogenase C |
| lncRNA | Long non-coding RNA |
| LTP | Long-term potentiation |
| LV | Left Ventricle |
| LVID | Left Ventricle Internal Diameter |
| LVPW | Left Ventricle Posterior Wall |
| LVWT | Left Ventricular Wall Thickness |
| MAP | Mean Arterial Pressure |
| MAPK | Mitogen Activated Protein Kinase |
| MF | Molecular Functions |

| | |
|----------------|-----------------------------------------------------------|
| MPI | Myocardial Performance Index |
| mRNA | Messenger Ribonucleic Acid |
| mtDNA | Mitochondrial DNA |
| MV Area | Mitral Area |
| MV E/A | mitral valve early-to-late filling velocity ratio |
| Mybpc3 | Myosin Binding Protein C, Cardiac |
| Myh7b | Myosin, Heavy Polypeptide 7, Cardiac Muscle, Beta |
| MyI2 | Myosin Light Polypeptide 2 |
| NADH | Nicotinamide Adenine Dinucleotide |
| ND1 | Nadh Dehydrogenase Subunit I |
| Ndufa1 | Nadh:Ubiquinone Oxidoreductase Subunit A1 |
| Ndufb3 | Nadh Dehydrogenase Ubiquinone 1 Beta Subcomplex Subunit 3 |
| Ndufs5 | Nadh:Ubiquinone Oxidoreductase Core Subunit S5 |
| NFκB | Nuclear Factor Kappa B |
| NLRP3 | NLR family pyrin domain containing 3 |
| NO | Nitric Oxide |
| NOS | Nitric Oxide Synthase |
| Nr4a1 | Nuclear Receptor Subfamily 4, Group A, Member 1 |
| Nr4a3 | Nuclear Receptor Subfamily 4, Group A, Member 3 |
| Nrgn | Neurogranin |

| | |
|-----------------|------------------------------------------------------------------------|
| Nxpe4 | neurexophilin and PC-esterase domain family, member |
| PBS | Phosphate Buffered Saline |
| PBS-T | Pbs-0.025% Tween |
| Pcna-ps2 | proliferating cell nuclear antigen pseudogene 2 |
| Pdzd3 | PDZ domain containing 3 |
| PE | Preeclampsia |
| Penk | Preproenkephalin |
| PFU | Plaque Forming Unit |
| PGC-1 | Peroxisome proliferator-activated receptor 1 |
| PI | Pulsatility Index |
| Pilrb2 | Paired Immunoglobulin-Like Type 2 Receptor Beta 2 |
| PIGF | Placental Growth Factor |
| PP | Post-partum |
| PPCM | Peripartum cardiomyopathy |
| ppm | Part per million |
| PPRC | Peroxisome proliferator-activated receptor-coactivator-related protein |
| Prkcg | Protein Kinase C, Gamma |
| qPCR | Quantitative Real-Time Polymerase Chain Reaction |
| RAAS | Renin-Angiotensin Aldosterone System |

| | |
|----------------|------------------------------------|
| RI | Resistance Index |
| RNA-seq | RNA Sequencing |
| ROS | Reactive Oxygen Species |
| Rpl29 | ribosomal protein L29 |
| Rpl34 | ribosomal protein L34 |
| s | Systole |
| S.E.M. | Standard Error of The Mean |
| SBP | Systolic Blood Pressure |
| sEng | Soluble Endoglin |
| sFlt-1 | Soluble Fms-Like Tyrosine Kinase 1 |
| SIRT-3 | Sirtuin 3 |
| Sln | Sarcolipin |
| Snca | Synuclein, Alpha |
| SQR | Sulfide Quinone Oxidoreductase |
| SV | Stroke Volume |
| SVR | Systemic Vascular Resistance |
| TCA | Citric Acid Cycle |
| TE | Trophectoderm |
| TGFβ | Transforming Growth Factor beta |

| | |
|----------------|-----------------------------------------------|
| Thbs1 | Thrombospondin 1 |
| tRNA | Transfer RNA |
| TTN | Titin |
| uNK | Uterine Natural Killer Cells |
| VEGF | Vascular Endothelial Growth Factor |
| VEGFA | Vascular Endothelial Growth Factor A |
| VEGFR-1 | Vascular Endothelial Growth Factor Receptor 1 |
| VGCC | Voltage Gated Calcium Channel |
| W | Weeks Post-partum |
| WHO | World Health Organisation |
| Wif1 | Wnt Inhibitory Factor 1 |

Chapter 1

Introduction

1. Introduction

1.1 Pregnancy

Pregnancy is a complex biological process that describes the period that ranges from fertilization all the way to birth (Taranikanti 2018). The full human gestation period (pregnancy) is 40 weeks (9 months), however the median time from ovulation to birth is 268 days (38 weeks and 2 days) (Jukic et al. 2013).

The human pregnancy is subcategorised into 3 trimesters (3 months or 12 weeks) and with each trimester as the foetus grows, the body of the mother changes. The first trimester is comprised by the beginning of the menstrual cycle, the fertilization (union of an ovum with a sperm, resulting into a fertilized egg), the cleavage (divisions of the fertilized egg, as it passes the fallopian tube), the blastulation (formation of cells following several cleavages), the gastrulation (differentiation and separation off embryonic cells following implantation) ("Muhr et al. 2022_Embryology, Gastrulation - StatPearls - NCBI Bookshelf" n.d.), the neurulation (formation of the spinal cord) and the organogenesis (organ formation). The second trimester is mostly comprised of further organogenesis and particularly the formation of the heart. The third trimester includes further growth and differentiation of the organs, and the foetus starts to gain movement and even grasping reflexes. The end of gestation is marked by the birth or parturition of the baby.

Throughout all three trimesters, the mother undergoes various changes to accommodate for the increased physiological demands to support the growing foetus. These changes are adaptations to pregnancy, an example of that are the ramifications on the cardiovascular, the gastrointestinal, the renal and pulmonary systems, as all these adaptations are needed to support the mass effect of the growing foetus (Kepley *et al.* 2022).

Due to the complexity in moral and ethical matters, exploring and studying human pregnancy is a rare occasion. However, mouse and rat models have widely been used to study diseases

and complications associated with pregnancy. The main reasons murine models have been used, include their haemochorial placentation (Andersen et al. 2018; Carter 2020; Waker et al. 2021a), their short gestation time (21 days), their similar cardiovascular adaptations during pregnancy (A. Y. H. Wong et al. 2002; Kulandavelu et al. 2006; Q. Yu et al. 2008; Burke et al. 2011), and their similarities in gene expression (70 percent of the same protein-coding gene sequences) (LaFee 2014).

Thus, to study pregnancy and PE in murine models, one must first understand what the adaptations to pregnancy are in a healthy human and in a healthy mouse.

1.2 Hormone changes in pregnancy

As the maternal body changes to accommodate for the growing foetus, different changes occur within the body. Endocrinological modifications during human pregnancy induce significant metabolic changes that affect the physiological state of the mother-foetus interface (Magon & Kumar 2012; Kodogo *et al.* 2019). The first change is a hormone change is seen with beta-human chorionic gonadotropin (β -HCG) (Magon & Kumar 2012). The hypothalamus, pituitary gland, and placenta contribute to the endocrine adaptations of pregnancy by producing a variety of hormones, including oestrogen, beta-human chorionic gonadotropin (β -HCG), and progesterone (J. Z. J. Chen *et al.* 2012). These hormones play a crucial role in conserving the cardiovascular adaptations observed during pregnancy, and their levels fluctuate dynamically throughout gestation and postpartum. In particular, β -HCG produced by the placenta prevents the corpus luteum from regressing after 10 days of ovulation, ensuring the continued release of progesterone by ovarian granulosa cells. Additionally, β -HCG is one of the earliest released substances by the conceptus, making it a valuable diagnostic indicator of pregnancy. The placental production of β -HCG reaches its maximum at around 100,000 IU/L in the maternal circulation, followed by a lower plateau that persists for the remainder of the pregnancy. Similarly, oestrogen and progesterone levels gradually rise throughout pregnancy and peak in the fourth trimester before declining shortly after delivery. The corpus luteum initially produces both oestrogen and progesterone during the first 10 weeks of pregnancy, but eventually, the placenta takes over. In the third trimester, progesterone levels range from 100 to 200 ng/ml, and the placenta secretes about 250 mg per day.

1.3 Cardiac Adaptations to Pregnancy and Postpartum

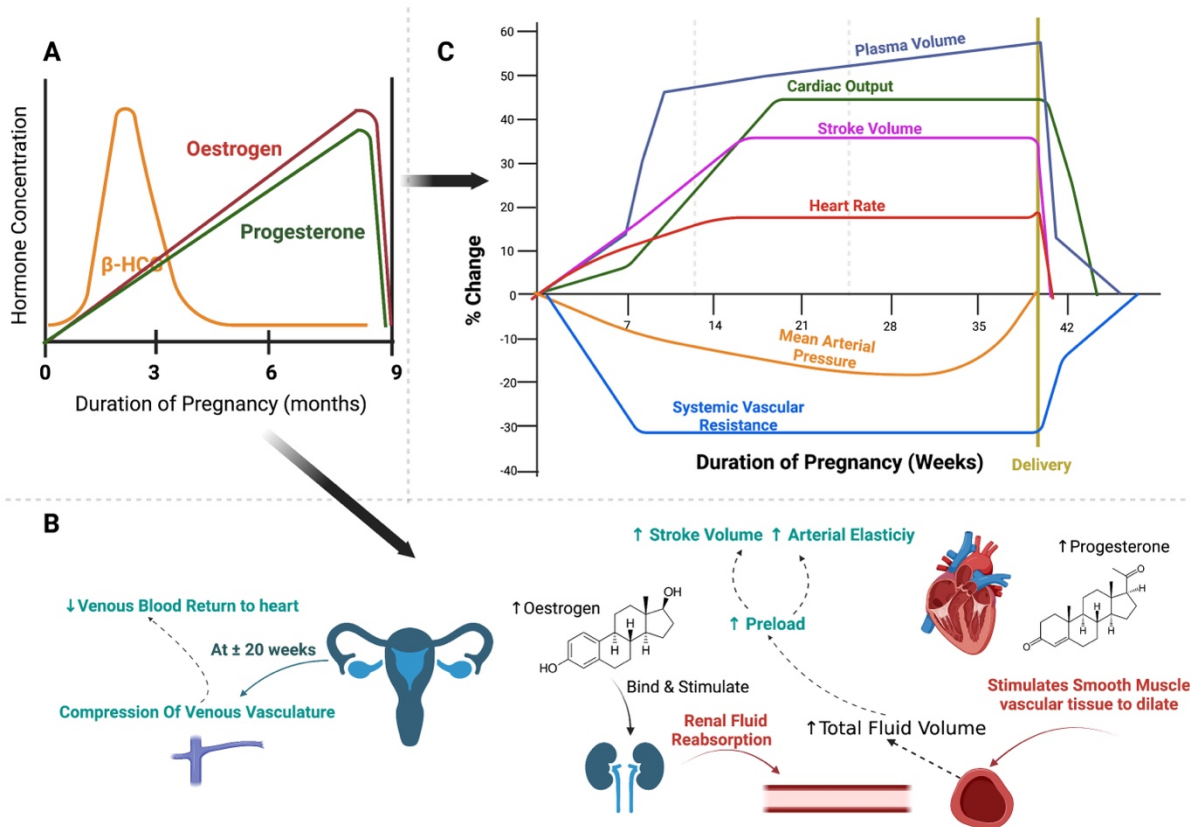


Figure 1.1 Illustration of hormonal and Cardiovascular Adaptations to pregnancy.

Figure was created in Bio-Render.com.

Pregnancy involves a series of cardiovascular changes (table 1.1), which, according to several authors, start around the fifth week of gestation and continue up to one year after delivery (S. C. Robson et al. 1987, 1989; Hunter & Robson 1992; Duvekot & Peeters 1994; Clapp & Capeless 1997; Desai et al. 2004; Hall et al. 2011; Karen Melchiorre et al. 2012). Despite numerous papers mentioning the beginning of these cardiovascular changes, the scientific community has not reached a consensus on their onset, duration, and magnitude. The three main reasons behind the lack of a consensus in the scientific community are; that certain variables relating to maternal characteristics have not been corrected, different estimation techniques have been used, and finally that baseline values from either the first trimester or

postpartum have been used instead (S. C. Robson et al. 1987, 1989; Hunter & Robson 1992; Carla Van Oppen et al. 1996; Clapp & Capeless 1997; Ford et al. 1997).

1.3.1 Volume of Blood in Circulation

During gestation, blood volume rises progressively until week 34 by 40-50% (1200-1778ml), redistributing 25% of total cardiac output to the uterus, 20% to the kidneys, 10% to the breasts and 2% to the skin. Oestrogens and progesterone are responsible for this increase (Lund *et al.* 1967; Stachenfeld & Taylor 1991; Thornburg *et al.* 2000; Turan *et al.* 2008). The majority of this 50% increase happens by week 34 of pregnancy and is proportionate to the baby's birth weight (Kasula et al. 2017). This results in increased hemodynamic stress that causes physiologic changes in the circulatory system. One of these changes is the uterine contractions forcing blood out of the intervillous region and into the central circulation, thereby augmenting the blood volume even more during labour (Kasula et al. 2017). After delivery, the uterus involutes and placental circulation stops, resulting in an autotransfusion of about 500 mL of blood (F J Dagher *et al.* 1965; Rovinsky & Jaffin 1965; Campbell & MacGillivray 1972; Salas *et al.* 2006). Eight weeks after parturition, blood volume gradually returns to normal.

Similarly, to humans, the blood volume in C57BL/6 mice increases during pregnancy (Kulandavelu *et al.* 2006). Contrarily to humans, in mice, the blood volume rises later in gestation (John H Fowler & Donald J Nash 1968; Norton *et al.* 2009). The blood volume reverts back to pre-pregnancy levels 2 weeks postpartum (Gokina et al., 2021; L D Longo, 1983; Monika Sanghavi & John D. Rutherford, 2014).

1.3.2 Cardiac Systolic Functions

1.3.2.1 Cardiac output, vascular resistance, heart rate, and stroke volume

The heart, just like the rest of the organs in the body needs to adapt to accommodate for the growing foetus and the increased strain on the mother. The first cardiac adaptation, in the same manner as during physical activity; is an increase in heart rate (HR) (of up to 15-30% which is more than 20 beats/minute compared to non-pregnant women) (Mashini *et al.* 1987; William C Mabie *et al.* 1994; Clapp & Capeless 1997) and cardiac output (CO) (Geva *et al.* 1997; Gilson *et al.* 1997; Hall *et al.* 2011; Kepley *et al.* 2022). Around 12 weeks after delivery, the HR values return to normal, although there is dissension as to the exact time of recovery (Clapp & Capeless 1997; Karen Melchiorre *et al.* 2012).

Additionally, an increase in CO can also happen as a result of an increased stroke volume (SV) (15-18%), which is associated with higher levels of circulating progesterone (Soma-Pillay *et al.* 2016). The CO reaches its maximum increase (30-50%) around 24 weeks gestation (Mashini *et al.* 1987; Datta *et al.* 2010). However, there is discrepancy in its behaviour in the third trimester, with decreases, no variation and increases. Additionally, as the pregnancy progresses, a decrease in SV can then be observed towards the end of the third trimester (Zoey N. Pascual & Michelle D. Langaker 2022). To account for that decrease in SV, the maternal HR continues to raise thus allowing the CO to remain elevated up until term (Jukic *et al.* 2013). Cardiovascular output can increase by as much as 150% above non-pregnant readings and 80% above pre-labour values in the immediate postpartum period (S. C. Robson *et al.* 1987; Datta *et al.* 2010b). Cardiac output significantly decreases 24 – 72 hours postpartum but only reverts back to its pre-pregnancy levels 6 – 8 weeks after parturition.

To facilitate maternal circulation, a decrease in systemic vascular resistance (SVR), which is reduced by up to 30% at around week 28 of gestation, after which it gradually increases until the end of pregnancy can be observed (Geva *et al.* 1997; Gilson *et al.* 1997; Bamfo *et al.* 2007; Zentner *et al.* 2012). This decrease in SVR is caused by the elevation of nitric oxide (NO) by oestrogen as well as by the action of progesterone (Figure 1.1), relaxin, prostaglandins and prolactin and by the new utero-placental circulation (Mone *et al.* 1996;

López-Jaramillo *et al.* 2004). In addition, this decrease implies a reduction in left ventricular afterload which favours the increase of blood volume and CO. Afterload reaches its minimum value during mid-pregnancy and tends to increase in the third trimester, coinciding with the increase in SVR from 28 weeks onwards (Figure 1.1) (Savu *et al.* 2012). Postpartum, systemic vascular resistance reverts back to values approaching those of pre-pregnancy, however no specific time period for the reversal has been reported (Sanghavi & Rutherford 2014).

Studies conducted on pregnant rodents have shown alterations in vascular function, including increased vasodilation, and decreased SVR and blood pressure (Gilbert *et al.* 2007; Cindrova-Davies *et al.* 2013; Mulder *et al.* 2022). The CO and the HR in mice increases due to an increase in SV (Eghbali *et al.* 2005). In mice, the HR is decreased in the early stages of pregnancy when compared to the late stages and starts to decrease back to pre-pregnant three days after delivery, ultimately getting back to pre-gravid levels by day seventeen (A. Y. H. Wong *et al.* 2002).

1.3.2.2 Ejection Fraction and Fraction Shortening

The overall performance of the heart as a pump is often evaluated and described by left ventricular ejection fraction (EF) and the left ventricular fractional shortening (FS) (Desai *et al.* 2004; Savu *et al.* 2012). The EF is the percentage of blood that is pumped out with each contraction (D. Williams *et al.* 2021; Sebastião *et al.* 2022). The FS represents the percentage difference in the left ventricular diameter during systole (Otto 2021). Recent studies have utilized EF to determine cardiac function (Du *et al.* 2002; Jovin *et al.* 2013; Ciftci *et al.* 2014; D. Williams *et al.* 2021). A decreased EF has been linked to heart failure, which can be caused by various factors and can manifest as coronary artery disease, cardiomyopathy, and valvular heart disease (Goffart *et al.* 2004; Jovin *et al.* 2013; Di Salvo *et al.* 2015; D. A. Brown *et al.* 2017; D. Williams *et al.* 2021; M. Liu *et al.* 2022).

Nevertheless, studies suggest that EF and FS measurements during pregnancy are not consistent, reflecting improvement, stability or deterioration, with the greatest deterioration occurring in the third trimester (R. Katz *et al.* 1978; Mone *et al.* 1996; Geva *et al.* 1997; Gilson

et al. 1997; Mesa et al. 1999; Kametas et al. 2001; Simmons et al. 2002; Desai et al. 2004; Eghbali et al. 2005; Zenther et al. 2009; Estensen et al. 2013).

Both mice and human studies of pregnancy have reported unchanged (no significant changes) ejection fractions as well as fraction shortening values for pre-pregnancy, during pregnancy (occasionally increased) and postpartum (A. Y. H. Wong et al. 2002; Sanghavi & Rutherford 2014; Che et al. 2019).

1.3.3 Cardiac Diastolic Functions

Left ventricular diastolic function can be assessed through mitral flow include E (early ventricular filling) and A (late ventricular filling) wave velocity, E/A ratio and E wave deceleration time, the myocardial performance index (MPI), isovolumetric contraction time (IVCT) and relaxation time (IVRT)(Savu *et al.* 2012).

1.3.3.1 Mitral Inflow

The main measurements of mitral flow include E (early ventricular filling) and A (late ventricular filling) wave velocity, E/A ratio and E wave deceleration time (H. Valensise *et al.* 2000; Nagueh *et al.* 2016). E and A wave velocities of the mitral valve are increased during gestation. While research in the past ten years does not come to a consensus as to a specific percentage, most research papers report an increased E/A ratio in the first trimester due to an initially greater rise in passive left ventricular filling (E-wave peak velocity) compared to active left ventricular filling during diastole (A-wave peak velocity)(Mesa et al. 1999; Fok et al. 2006; Adeyeye et al. 2016; Kasula et al. 2017). Due to a stabilising E - wave peak velocity and a rise in A-wave peak velocity, the E/A ratio gradually drops as gestation progresses to term (Mesa et al. 1999; H. Valensise et al. 2000; Christiana M Schannwell et al. 2002; Estensen et al. 2013). The maximum E/A ratio is seen in the second trimester of pregnancy and a lower E/A ratio is observed by the end of the third trimester and postpartum. Some studies have even

reported the lowest E/A ratio (lower than during early pregnancy or even postpartum) to be at the third trimester (Fok et al. 2006; Adeyeye et al. 2016; Kasula et al. 2017). These E-wave and A-wave velocity adaptations have been shown to return to normal within 8 weeks postpartum (Christiana M Schannwell et al. 2002).

Similar changes in E-wave and A-wave velocity adaptations have been observed in C57BL/6 mice (Eghbali *et al.* 2005).

Cardiovascular Adaptations to Normal Pregnancy And Postpartum In Humans

| | Change | Proportion | 1 st T | 2 nd T | 3 rd T | PP |
|------------------------------------------|--------|------------|-------------------|-------------------|-------------------|----|
| SVR | ↓ | 30% | ↓ | ↓ | ↑ | ↑ |
| Blood Volume | ↑ | 40 – 45% | ↑ | ↑ | — | ↓ |
| Remodelling of the Cardiovascular System | | | | | | |
| Arterial Elasticity | ↑ | 30% | ↑ | — | — | ↓ |
| Heart Size | ↑ | 30% | ↑ | ↑ | ↑ | ↓ |
| Left Atrium | ↑ | 16 – 40% | ↑ | ↑ | ↑ | ↓ |
| Systolic Functions | | | | | | |
| CO | ↑ | 30 – 50% | ↑ | ↑ | ↑ | ↓ |
| HR | ↑ | 10 – 30% | ↑ | ↑ | ↑ | ↓ |
| SV | ↑ | 25 – 30% | ↑ | ↑ | ↑ | ↓ |
| Diastolic Functions | | | | | | |
| MV E/A | ↑ | 15 – 33% | ↑ | ↑ | ↓ | ↓ |
| ESV | ↑ | 20% | ↑ | | | |
| EDV | ↑ | 23% | ↑ | ↑ | — | ↓ |
| Cardiac Structural Functions | | | | | | |
| LV Mass | ↑ | | ↑ | ↑ | — | ↓ |
| LVID;S-D | ↑ | 20% | ↑ | ↑ | ↑ | — |

Table 1.1 Cardiovascular Adaptations to Normal Pregnancy and Postpartum.

1st T; First Trimester, 2nd T; Second Trimester, 3rd T; Third Trimester, PP; Postpartum, SVR; Systemic Vascular Resistance, CO; Cardiac Output, HR; Heart Rate, MV E/A; Mitral Inflow E (Early Ventricular Filling) And A (Late Ventricular Filling) ratio, ESV; End Systolic Volume, EDV; End Diastolic Volume, LV MASS; Left Ventricular Mass, LVID;S-D; Left Ventricle Internal Diameter During Systole. This table was adapted using various papers (Castleman et al., 2016, 2023; Jingyuan Li et al., 2012).

1.3.3.2 Isovolumetric contraction

Isovolumetric contraction time (IVCT) is the time when the short time when the ventricles contract without any change in their volume, essentially it is the time between the closure of the mitral and tricuspid valves and before the opening of the aortic pulmonary valves (Figure 1.2) (Lauboeck 1980; Feher 2012). This measurement is often also used as a marker to assess the diastolic function performance (Khandoker *et al.* 2016). During pregnancy, this time can be impacted by changes in hormones, such as progesterone and oxytocin (Yin *et al.* 2018; Peavey *et al.* 2021). A longer IVCT can cause less blood to be sent to the mother and baby, while a shorter time can lead to higher pressure in the vascular system (Alhakak *et al.* 2020). Similarly, to EF, IVCT, and its increase specifically has also been reported as a predictor of incident heart failure (Alhakak *et al.* 2020).

However, research has reported conflicting changes in IVCT during pregnancy, while Kim *et al.* reported an increase in IVCT during pregnancy, Khandoker *et al.* reported a decrease in IVCT during pregnancy (Khandoker *et al.* 2016; S. M. Kim & Ye 2021). One study even reported a IVCT higher in postpartum than during pregnancy (Bamfo *et al.* 2007). Due to the conflicting evidence with regards to the changes in IVCT pre-pregnancy, during pregnancy or postpartum reported by different papers, no concrete conclusion with regards to IVCT can be made (A. Y. H. Wong *et al.* 2002; Estensen *et al.* 2013; Khandoker *et al.* 2016). Similarly, to studies conducted with regards to IVCT pre-pregnancy, during pregnancy and postpartum, studies relating left ventricle (LV) contractility itself have also reached different conclusions. Some studies have seen an increase in left-ventricle contractility (Duvekot & Peeters 1994; Mesa *et al.* 1999; Karen Melchiorre, Sharma, *et al.* 2012; Karen Melchiorre *et al.* 2016a;

DeVore & Polanco 2023), whereas other studies observed a decrease in contractility (Rubler *et al.* 1973; Mone *et al.* 1996; A. K. Pandey *et al.* 2010).

In C57BL/6 mice, IVCT increases significantly at the beginning of the pregnancy due to hormonal changes that shift the balance between afterload and preload. At the pregnancy mid-point up until delivery, the IVCT remains relatively stable. This is due to an increased release of progesterone which helps to relax the smooth muscle found in arterioles and can result in less pressure on the vascular system (Wen-Sen Lee *et al.* 1997). The IVCT in mice descends back to its normal levels approximately two weeks postpartum (A. Y. H. Wong *et al.* 2002).

1.3.3.3 Isovolumetric relaxation time

Isovolumetric relaxation time (IVRT) is the period of time between the end of the aortic ejection and the start of the ventricular filling (Figure 1.2) (de Madron 2015). In humans, a reduced volume of circulating blood and an increased oxygen-carrying capacity of the vessels occurs through vascular relaxation adaptations in pregnancy including a decrease in blood pressure and an increase in the diameter of the blood vessels (Wen-Sen Lee *et al.* 1997; Goldsmith & Weiss 2009; Yin *et al.* 2018; Peavey *et al.* 2021).

During the first trimester of pregnancy both humans and C57BL/6 mice experience a significantly decreased IVRT due to hormonal changes (Figure 1.2) that cause both an increase in afterload, mean arterial pressure, vasoconstriction. To balance these changes, progesterone is released thereby inducing vasodilation and afterload reduction. This in turn results in the return of IVRT to baseline levels. Similar changes have been reported in mice.

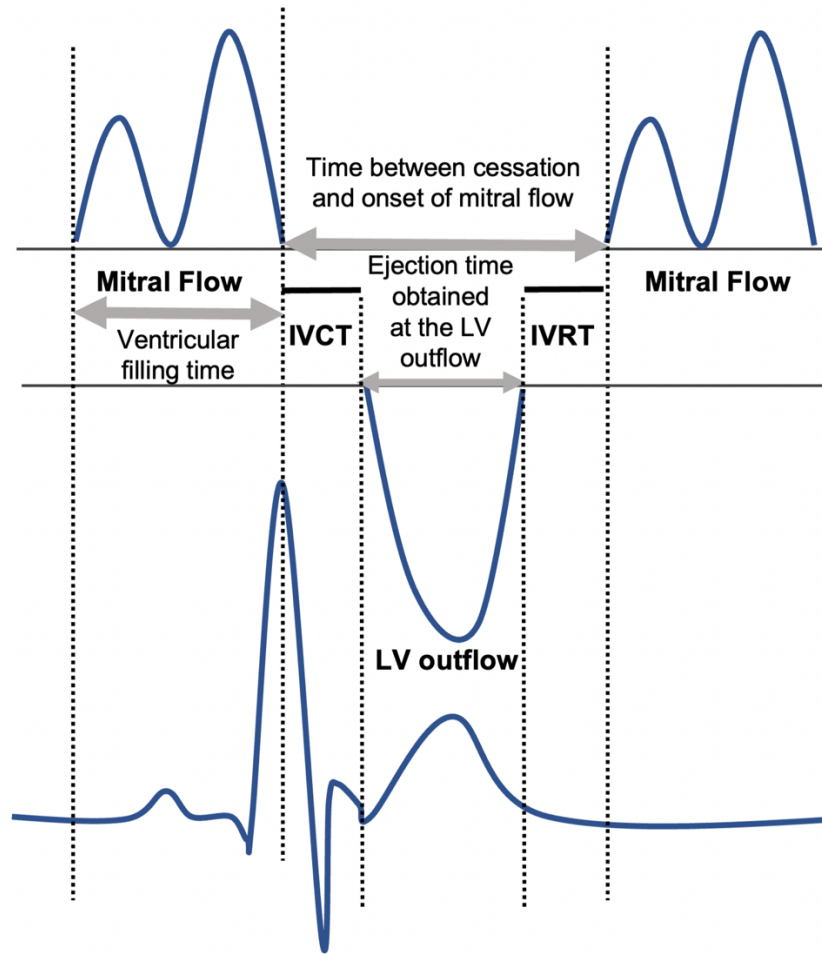


Figure 1.2 The measurement of cardiac time intervals is shown schematically.

IVCT for intraventricular contraction time, IVRT stands for isovolumetric relaxation time, and LV stands for left ventricle. This figure was inspired by (Kato et al. 2005; S. M. Kim & Ye 2021).

1.3.4 Remodelling of the Cardiovascular System

Structural adaptations in the heart are essential for a successful pregnancy. In humans, and in mice, intraventricular septum thickness, left ventricular mass and LV internal diameter are significantly increased by the end of gestation. As the heart itself goes through remodelling to accommodate for the growing foetus, an increased left ventricular wall thickness (LVWT) and an increased end-diastolic chamber size can be observed in healthy pregnant women (Monika Sanghavi & John D. Rutherford 2014; Zoey N. Pascual & Michelle D. Langaker 2022). An increased myocardial contractility is also observed and accounts for the increased LVWT

(Kasula et al. 2017; Kepley et al. 2022). Lastly, blood pressure decreases in the 1st and 2nd trimester but increases to non-pregnant levels in the 3rd trimester (Savu et al. 2012; Monika Sanghavi & John D. Rutherford 2014; Taranikanti 2018).

1.3.4.1 Arterial Compliance

During a healthy pregnancy, blood pressure modestly decreases and gradually returns to pre-pregnancy levels as the pregnancy progresses (Hunter & Robson 1992; Sanghavi & Rutherford 2014). Simultaneously, systemic vascular resistance rapidly drops throughout the first trimester and remains low until delivery (Clapp & Capeless 1997; Geva *et al.* 1997; Gilson *et al.* 1997; Hall *et al.* 2011). This is due to vasodilation, which leads to decreased total vascular resistance, as well as an increase in global arterial compliance (also referred to as arterial elasticity), resulting in decreased vascular stiffness (V. R. Turi et al. 2022).

The increase in global arterial compliance during pregnancy is highly adaptive, as it allows for increased intravascular volume without raising mean arterial pressure (MAP). It also aids in preserving the effectiveness of mechanical energy transfer from the left ventricle to the arteries and maintains coronary perfusion pressure by lessening aortic diastolic pressure decay. Overall, these changes in arterial compliance and systemic vascular resistance contribute to the efficient adaptation of the maternal cardiovascular system to meet the metabolic needs of both the mother and the developing foetus.

Studies have revealed that pregnancy and the postpartum period significantly alter vascular compliance in C57BL/6 mice. Global arterial compliance rises during pregnancy, enabling an increase in CO and uterine blood flow to promote foetal growth and development. It is thought that hormonal changes, notably the rise in oestrogen levels, are to blame for this increase in arterial compliance. However, after giving birth, arterial compliance falls, as a result of the drop in oestrogen levels (Evans et al. 2011a; Akçay & Özdemir 2021). The increased risk of cardiovascular disease (CVD) seen in postpartum women may be caused by this reduction in arterial compliance. These results imply that arterial compliance is essential for the adaptation of the maternal cardiovascular system throughout pregnancy and for its recovery following delivery.

1.3.4.2 Structural and Vascular adaptation to pregnancy

Just like the heart adapts to pregnancy, so does the rest of the body, especially the blood vessels, as these connect the heart to the rest of the organs (Sandoo *et al.* 2010). Angiogenesis: meaning the growth of new vessels from other already formed vessels, and Vasculogenesis; meaning growth of blood vessels from differentiating endothelial cells (or angioblasts during embryogenesis) (Zygmunt *et al.* 2003; Gupta & Zhang 2005; D.-B. Chen & Zheng 2013), are very important parts of the adaptations that occur during normal pregnancy (Boeldt & Bird 2017). An increase in blood flow helps to sustain the growth and development of the growing foetus by providing essential nutrients and oxygenations (Remien & Majmundar 2022). Other structural changes occur throughout the body including vasodilation, decreased viscosity, and enhanced vessel repair mechanisms, to accommodate this extra blood flow (Boeldt & Bird 2017; Osol *et al.* 2019). In addition to CO increases, there are also several other vascular adaptations that take place during pregnancy.

These other vascular adaptations include increased capillary permeability and reduced venous resistance (M. A. Brown *et al.* 1989). The increased permeability is necessary for nutrient exchange between mother and baby as well as for waste removal (M. A. Brown *et al.* 1989; Vanwijk *et al.* 2000). The reduced venous resistance allows the additional blood to be efficiently transported back to the heart where it can then be circulated throughout the body (Hall *et al.* 2011). The vascular adaptations in pregnancy also include increased circulating plasma volume which helps reduce hematocrit levels, thereby improving oxygen delivery to both mother and baby (F Hytten 1985; Vricella 2017). Additionally, there is an increase in endothelial NO synthase (eNOS) activity which leads to vasodilation and improved tissue perfusion (V. H. J. Roberts *et al.* 2018). This helps further improve oxygenation as well as nutrient exchange between mother and foetus. Lastly, there are increased levels of fibrinolysis, which help with vessel repair mechanisms so that any damaged vessels can heal faster (Hale *et al.* 2012). Overall, the numerous vascular adaptations that take place during pregnancy help to ensure that both the mother and the foetus receive an adequate supply of oxygen and nutrients. These adaptations are essential for a healthy pregnancy and can help to prevent complications such as PE.

The vascular system of pregnant C57BL/6 mice and humans differ in a number of ways. In humans, there is an increase in total blood volume during pregnancy, whereas this is not seen in C57BL/6 mice (Kulandavelu *et al.* 2006). The human placenta also secretes vasoactive molecules, such as prostacyclin and NO, which are not seen in the mouse placenta (Sandoo *et al.* 2010). These molecules are not secreted by the placenta of pregnant C57BL/6 mice. Despite these differences, the changes in vascular structure and function during pregnancy seen in both humans and C57BL/6 mice are similar.

Pregnancy is associated with profound changes in a woman's vascular system to insure the health of the mother and the foetus. In C57BL/6 mice, these changes involve both structural and functional adaptations of the vessels, including increased vessel wall thickness, vessel wall permeability and reduced vasoconstriction. These adaptations are believed to be necessary for improved uterine perfusion and nutrient delivery to the foetus, as well as maternal health.

1.4 Uterine flow

In addition to left ventricular mass adaptations during gestation, uterine artery undergoes structural changes to accommodate for the increased blood flow needs to the placenta. Additionally, uterine artery flow is an indication of uteroplacental perfusion and has been studied in humans and C57BL/6 mice (Oloyede & Iketubosin 2013; Browne *et al.* 2015). An increase in uterine artery pulsatility (UA PI) and uterine artery resistance indices (UA RI), alongside early diastolic notching have been correlated to a dysfunctional placentation (Naeh *et al.* 2022).

1.5 Dysfunctional Adaptations to Pregnancy

The physiological adaptations that the cardiovascular system undergoes during pregnancy are of utmost importance for ensuring a successful pregnancy. However, any malfunction or aberration in these adaptations can result in undesirable outcomes for the mother and the developing foetus. Emerging research indicates that even subtle maladaptations at the time

of implantation can trigger poor trophoblast invasion and abnormal hemodynamic adaptation, ultimately culminating in endothelial dysfunction (Y. Zhou *et al.* 1992; Duvekot *et al.* 1995; Spaanderman *et al.* 2001). The cascade of events triggered by endothelial dysfunction, abnormal hemodynamic adaptations, or other maladaptations to pregnancy are known to contribute to the development of various pregnancy-related disorders such as PE (Schrier & Dürr 1987; Duvekot *et al.* 1993, 1995; Spaanderman *et al.* 2001).

1.6 Preeclampsia

PE is a multisystemic disorder, defined as a de novo onset of hypertension ($\geq 160/110$ mmHg) plus the involvement of at least one organ system (Trogstad *et al.* 2011; Lambert *et al.* 2014; Tranquilli *et al.* 2014; Fatmeh & Farahnaz 2018; Mark A. Brown *et al.* 2018). The proteinuria (spot urine protein/creatinine > 30 mg/mmol or > 300 mg/day), after 20 weeks of gestation, is no longer (as of 2014) a required criteria for the diagnosis of PE (Tranquilli *et al.* 2014; Mol *et al.* 2016). PE affects between 5 and 8 out of every 100 pregnant women worldwide and accounts for 76 000 maternal deaths and 500 000 infant deaths yearly (“IPLACENTA” n.d.; Walker 2000; Ramma & Ahmed 2014) .

Over the past 15 years a growing interest has developed as scientists linked a defective placenta to various pregnancy diseases such as PE (Mutter & Karumanchi 2008a; Trogstad *et al.* 2011; Turanov *et al.* 2018; Turco *et al.* 2018; Vento-tormo *et al.* 2018). Evidence from clinical findings showed that hydatiform moles or molar pregnancies (absent foetus) with placentas can still develop preeclamptic phenotypes (Acosta-Sison 1956; Kristoffersen & Jørgensen 1970; Billieux *et al.* 2004; Mutter & Karumanchi 2008a; Trogstad *et al.* 2011; Ottanelli *et al.* 2012; Vitoratos *et al.* 2012; Atuk *et al.* 2018), thereby indicating that the placenta plays a key role in PE and other pregnancy diseases. The process of placentation is a critical step in ensuring a successful pregnancy outcome (Fox & Elston 1978; P. R. Burton *et al.* 2007; Romero *et al.* 2011; Katie Delach 2016; Graham J. Burton & Jauniaux 2018). However, when disturbed, it can have devastating consequences for foetal health. Recent studies suggest that disturbances in angiogenesis underlie the phenomenon of poor placentation (Noback 1946; Kirsten R. Palmer *et al.* 2015; K. R. Palmer *et al.* 2017; L. Zhou *et al.* 2019). Specifically, there is evidence to suggest that an imbalance in the levels of pro- and anti-angiogenic factors such as placental growth factor (PlGF), vascular endothelial growth factor (VEGF), and fms-like

tyrosine kinase-1 (sFlt-1) play a pivotal role in this process (Mehendale et al. 2007; Iman Gurnadi et al. 2015; Kirsten R. Palmer et al. 2015; Szalai et al. 2015a; Kirsten R Palmer et al. 2016; K. R. Palmer et al. 2017; Lorenz-Meyer et al. 2022). Additionally, the inappropriate activation of the renin-angiotensin-aldosterone system (RAAS) has also been implicated in the aetiology of poor placentation (Inoue *et al.* 1995; Silva *et al.* 2015; Denney *et al.* 2016; Leal *et al.* 2022).

Though the main actor in PE seems to be the placenta, over the years, scientific research showed that preeclamptic women have an increased chance of developing cardiovascular, neurological and kidney diseases later in life, even after the placenta has been delivered (Walker 2000; Irgens et al. 2001; Sibai et al. 2003; D. W. Brown et al. 2006; Mutter & Karumanchi 2008a; Ayansina et al. 2016). A 2007 journal article by the BMJ (British Medical Journal) looked at cohort studies from 1960 to 2006 and found that PE was strongly correlated with the development of hypertension, ischaemic heart disease, stroke and venous thromboembolism, later in life (Bellamy *et al.* 2007). Additionally, a longitudinal study from 2001 revealed that preeclamptic women who delivered pre-term were 8 times more likely to die from cardiovascular causes than non-preeclamptic women (Irgens *et al.* 2001). Accordingly, recent discoveries suggest that other factors besides solely the placenta may be at the centre of this condition (Sánchez-Aranguren et al. 2014; Possomato-Vieira & Khalil 2016a; Apicella et al. 2019). Several predisposing factors such as multifoetal pregnancies, chronic high blood pressure, personal or family history of PE, pre-existing diabetes, thrombophilia, and obesity, have been linked to the appearance of the disease (English *et al.* 2015).

Finally, the exact pathogenesis behind PE is still unclear but it is believed to be multifactorial (B. Huppertz 2008; S. Ahmad et al. 2015). Several theories have come forth as a potential cause for PE, such as: angiogenic imbalance (physiological balance between the stimulatory and inhibitory signals for blood vessel growth), systemic inflammation and oxidative stress (I. Brosens 1964; Hoeben et al. 2004; S. Maynard et al. 2008; J. M. Roberts & Escudero 2012; Rana et al. 2012; Burke & Ananth Karumanchi 2013; Raghupathy 2013; Candela et al. 2017;

Atakul 2019; Barneo-Caragol et al. 2019; Doganlar et al. 2019; Haram et al. 2019; J. Hu et al. 2019; Stojanovska et al. 2019).

Early-onset and late-onset PE are distinguished as separate conditions. A study exploring cardiac function at 24 weeks gestation found that women who later developed PE displayed different hemodynamic states based on whether they developed early or late PE (Wójtowicz *et al.* 2019). Early PE was associated with a higher incidence of bilateral notching of the uterine artery, lower total vascular resistance, and higher cardiac output, implying defective placental development. In contrast, late PE is more common in women with a high body mass index and low total vascular resistance, suggesting constitutional factors like obesity as possible origins.

Vascular changes associated with PE can be detected long before symptoms manifest. Endothelium-derived vasoconstrictors, which regulate blood flow, are disrupted in PE, leading to increased blood pressure and peripheral arterial waveform resistance. Notably, other peripheral arteries also exhibit impaired function in early pregnancy, indicating a generalized abnormal vascular physiology in PE.

These findings point to a shared predisposition to PE and cardiovascular disease, underscoring the importance of investigating cardiovascular function to better understand PE pathophysiology. The current management strategies for PE include compounds commonly used in cardiology, like statins and nitric oxide donors, which have shown promise in PE prevention and treatment. This indicates that the heart could be greatly affected by both forms of PE, emphasizing the need for early detection and management to mitigate cardiovascular risks.

However, despite the extensive research into the potential causes and mechanisms of PE presented in these studies, there isn't a cure for PE. To date preeclamptic patients are usually treated for their symptoms (hypertension, proteinuria...etc.) and most of the time these women are rushed to deliver prematurely, as this is the only method of resolving PE (Lambert *et al.* 2014; Perry *et al.* 2018). Therefore, there is urgent need for a better understanding and better managements for PE.

1.6.1 Current Hypotheses behind PE

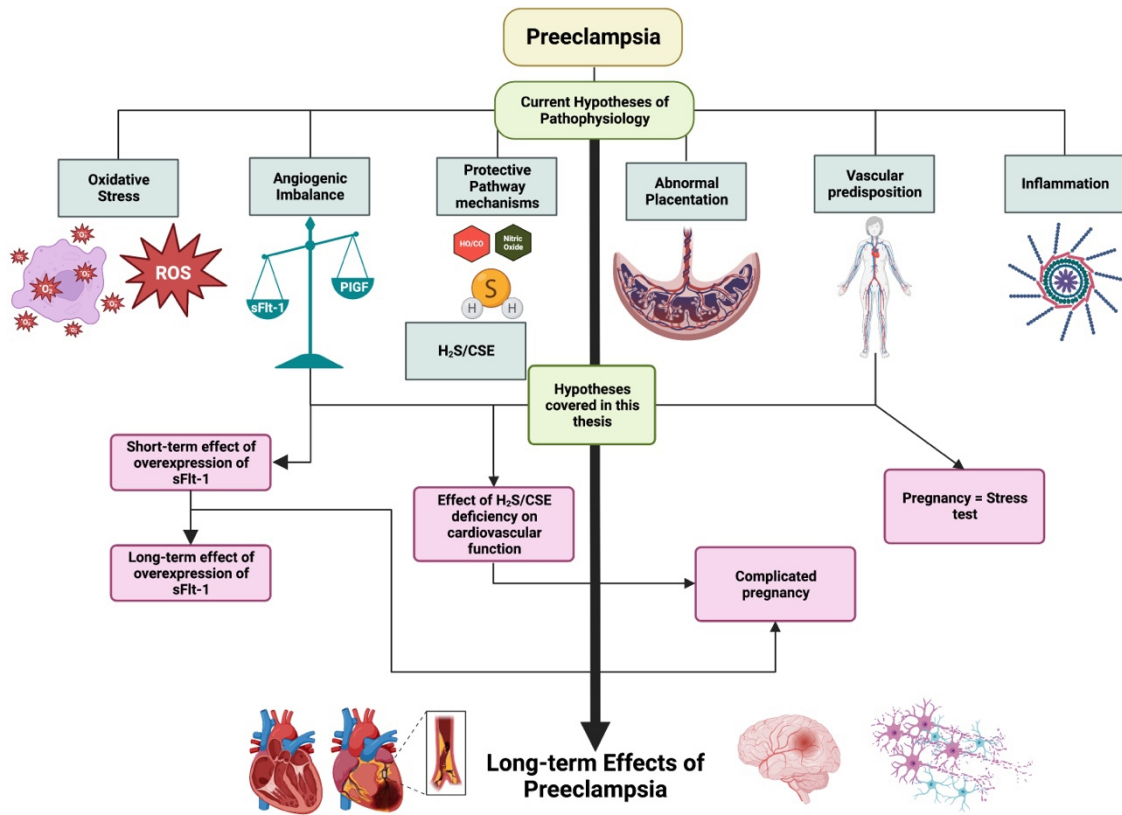


Figure 1.3 Hypotheses behind PE.

PE is a complex, multifactorial disease that is thought to occur in two stages. The first stage is characterized by abnormal placentation, leading to decreased placental perfusion during the early stages of the first trimester. In the second stage, a maternal syndrome arises in the later second and third trimesters, which is marked by an excess of antiangiogenic factors. Several hypotheses have been proposed to explain the pathophysiology of this condition, including abnormal placentation, oxidative stress, dysregulation of protective pathway mechanisms, and inflammation. Despite extensive research into the aetiologies and mechanisms underlying PE, its exact pathogenesis remains elusive. However, given the significant number of studies pointing to the involvement of angiogenic imbalance and protective pathway mechanisms, this thesis aims to investigate these specific aspects of PE. Figure was created in Bio-Render.com.

Despite the lack of clear knowledge behind the pathophysiology of PE, it is accepted that the placental disease is said to occur in two stages: stage 1 is synonym of abnormal placentation (decreased placental perfusion) early in the first trimester and stage 2 is a “maternal syndrome in the later second and third trimesters characterized by an excess of antiangiogenic factors”

(J. M. Roberts et al. 1989; Lain & Roberts 2002; J. M. Roberts & Gammill 2005; Jim Roberts 2007; D. J. Roberts & Post 2008; J. M. Roberts & Escudero 2012; Rana et al. 2019). Two reviews looking at the main theories (as seen in Figure 1.3) of the pathophysiology of PE (abnormal spiral artery remodelling, elevation in systemic inflammation, maternal endothelial dysfunction, and gaseous signalling molecules) suggested that all the suggested causes behind PE should be evaluated according to the Bradford Hill criteria for disease causation (Van Reekum et al. 2001; Ramma & Ahmed 2014; A. Ahmed & Ramma 2015a). Briefly, the Bradford Hill criteria involves criteria such as the temporality, the dose response, the strength, the consistency, the specificity, the coherence and the plausibility of the disease causation (Van Reekum *et al.* 2001).

1.6.1.1 Normal versus abnormal placentation

The normal human placenta develops by forming the outer layer of the pre-implantation embryo: a trophoblast (J. D. Boyd & W. J. Hamilton. Heffer, 1970; Turco & Moffett, 2019). The trophoblast (TE) forms approximately 5 days post fertilization of the blastocyst and is segregated into two lineages: the internal cellular mass (ICM) (the ICM form the embryoblast, the umbilical cord, the amnion, and the embryo) and the TE (Moser *et al.* 2019). The polar end of the TE binds to the epithelium of the uterus which is termed endometrium. To date, the first stages of implantation haven't been visualized in humans (J. D. Boyd & W. J. Hamilton. Heffer 1970). However, given the physiological observations from samples of superior primates it is believed that 6 to 7 days after fertilization, the TE develops into a primary syncytium. This development is referred to as the prelacunar phase of the placental development (J. D. Boyd & W. J. Hamilton. Heffer 1970; Turco & Moffett 2019). After invasion of the endometrium by the primary syncytium, the endometrium develops into a specialized tissue known as the decidua (Schlafke & Enders 1975; Turco & Moffett 2019). At 14 days post fertilization, the blastocyst is now fully ingrained in the decidua and coated by the surface of the epithelium (A. T. Hertig *et al.* 1956; Turco & Moffett 2019). Lacunae start forming together with the syncytial mass. These then enlarge and merge together to splice the biological system into trabeculae. This stage is known as the lacunar stage. The syncytium now disintegrates to form decidual glands and thereby allows secretions to enter the syncytial mass. The villous stage of development then occurs by proliferation of the trophoblasts which in turn form projections through the primary syncytium to form primary villi. The villi proliferate further and form into

villous trees and the lacunae develop into intervillous space (Turco & Moffett 2019). Cytotrophoblasts invade the primary syncytium and fuse laterally by enveloping the conceptus in a continuous cytotrophoblast shell between the villi and the decidua (Turco & Moffett 2019). Finally, the blastocyst is now coated by three layers: the chorionic plate, the villi which are separated by the intervillous space and the cytotrophoblast shell with the decidua (Turco & Moffett 2019). This results in a spherically shaped placenta (Moser *et al.* 2019).

At approximately 10 to 18 days post fertilization, the mesenchymal cells go through the villous core to form secondary villi. The secondary villi is also the term used to describe the cytotrophoblast layer between the mesenchymal cells and the maternal tissues (Moser *et al.* 2019). At the 18th day post fertilization, when the vasculogenesis starts (foetal capillaries emerge at the core), thereby initiating the development of the secondary villi into tertiary villi (Moser *et al.* 2019; Turco & Moffett 2019). A system of villous trees is formed by the continuous branching of the villous tree. Individual cytotrophoblast leave the shell when they come into contact with the decidua to invade the decidua in the form of extravillous trophoblasts (EVT) (Turco & Moffett 2019). Thus, whole development process of the placenta is established by the first trimester by secondary villi turning into tertiary villi and by the branching of vasculogenesis (Turco & Moffett 2019). The distinct branching of vasculogenesis is imperative for the proper development of the placenta and is highly dependent on the intraplacental low oxygen supply during the first trimester (Moser *et al.* 2019).

The supply of intraplacental low oxygen is essential for trophoblast plugs within the uterine spiral arteries to be formed. These temporary trophoblast plugs, which occur as a consequence of the EVT invasion into the spiral arteries, allow for the vessels to morph and their smooth muscle cells in the wall to deplete, thereby losing their elastic lamina. The loss of elasticity of the vessels, leads to the dilation of the arteries (and this extends to the inner third of the myometrium) and increase of luminal width and hence insures the uteroplacental blood flow during pregnancy (J. M. Roberts & Escudero 2012; Moser *et al.* 2019). The spiral arteries become low resistance vascular channels and therefore the blood flow is increased for maximum blood flow to the placenta and the foetus and becomes independent of control by

the maternal vasculature (independent of humoral or neural signals) (Pijnenborg *et al.* 2006; Cartwright *et al.* 2010; Pennington *et al.* 2012).

In a healthy placenta, the maternal spiral arteries change to allow for the increased blood flow in the placenta. However, in preeclamptic pregnancies, these changes are only observed in some cases, whereas in most of the preeclamptic pregnancies the remodelling of the vessels does not occur. In the preeclamptic pregnancies where the remodelling of the spiral arteries does occur, it does not extend to the myometrium (W. B. Robertson *et al.* 1967; I. A. Brosens 1972; W. Robertson *et al.* 1973; T. Y. Khong *et al.* 1986; Lyall 2002). Despite, a lot of evidence pointing to the main issue being the inability of these spiral arteries to dilate during PE, new evidence points to the main issue being the depth of the vascular modification rather than the dilating of the spiral arteries (G. J. Burton *et al.* 2009). The inability of the spiral arteries to invade the myometrium combined with the persistence of the smooth muscle (the spiral arteries remain contractile in PE) (that is lost in a healthy pregnancy) results in a reduced utero-placental circulation and in increased oxidative stress, as well as a release of placental factor into the maternal circulation (Trogstad *et al.* 2011; Coroyannakis & Khalil 2019). Moreover, given that the spiral arteries remain contractile during PE, this may generate a potential perfusion/reperfusion scenario which can subsequently generate oxidative stress (J. M. Roberts & Escudero 2012).

Additionally, some studies have shown that uterine natural killer cells (uNK), (which populate the uterine spiral arteries) are involved in the spiral artery remodelling (A. Robson *et al.* 2012). An increase of uNKs have been observed in some preeclamptic pregnancy studies, whereas a decrease in uNKs have been observed normotensive pregnancies (Stallmach *et al.* 1999; Bachmayer *et al.* 2006; P. J. Williams *et al.* 2009). However, given the evidence shown from an in vivo study conducted on immune deficient Rag2 *-/-*/yc-/- double knockout mice (who appear to lack spiral artery remodelling), that demonstrated that although these mice lacked spiral artery remodelling, no preeclamptic phenotype was found, in this mouse model (Burke *et al.* 2010). The lack of a preeclamptic phenotype in these mice disproves the theory that spiral artery remodelling are the main cause for placental dysregulation (Burke *et al.* 2010).

Not to mention, it has also been shown that defects in spiral artery remodelling occur in other diseases such as foetal growth restriction and foetal death and are not specific to PE.

Further, a single-cell RNA sequencing study that analysed first-trimester placental and decidual cells from healthy subjects found that three distinct fibroblast populations within the placenta and decidua were found unexpectedly within each tissue type (Hemant Suryawanshi *et al.* 2018). The most abundant cluster of fibroblasts was a primary source of DLK1 which is a gene involved in encoding an endocrine signalling molecule (present in high concentrations in maternal circulation). The second cluster of fibroblasts that was specifically expressed was the EGFL6 gene which is responsible for promoting endothelial cell migration and angiogenesis. Lastly, the third cluster of fibroblasts found expressed proinflammatory genes such as IL6, PTGDS, CFD, CXCL2, REN and AGTR1, which are implicated in the regulation of blood pressure, sodium and fluid homeostasis (S. Wu *et al.* 2018). This finding suggests a dysregulation of these genetic changes/fibroblast clusters may be a main factor leading to pregnancy complications such as PE (Hemant Suryawanshi *et al.* 2018).

Moreover, gross pathological changes have also been observed in placentas from PE (J. M. Roberts & Escudero 2012). Dypvik *et al.* looked at placental weight for centile for gestational age and found that infants with placentas less than the 30th centile were smaller in preeclamptic pregnancies, while those with placental weight greater than the 90th centile were larger (Dypvik *et al.* 2017). Furthermore, studies have also observed that the shape of the placentas from PE are different from those with a normotensive pregnancy (Kajantie *et al.* 2010). Placentas from PE had a significantly lower surface area and a surface that was more oval than placentas from normotensive pregnancies. Overall, the thickness of the placenta was increased in placentas from PE and their shape was more oblong compared to circular in normotensive placentas (Kajantie *et al.* 2010). Lesions such as villous-free placental lakes, fibrin deposition and inflammation, that reflect maternal malperfusion caused by failure of spiral arteries remodelling were also observed in placentas from PE (Pathak *et al.* 2011; Falco *et al.* 2017; Sebire 2017). Although these lesions were not specific to PE, they were found to be four to seven times more common in preeclamptic placentas than normotensive placentas.

Additionally, microscopical studies also showed that placental lesions such as swelling of the mitochondria, necrosis of the syncytiotrophoblasts with loss and distortion of the microvilli, dilation of the endoplasmic reticulum cisternae were also linked to PE (Jones & Fox 1980; Holland *et al.* 2017; J. G. Burton *et al.* 2019).

Some studies supported that these morphological changes were linked to higher levels of placental stress at the molecular level. An increase of oxidative stress and of unfolded protein response (UPR) (protein that is associated with the suppression of non-essential protein synthesis) were found in early onset PE compared to late onset PE (Yung *et al.* 2014; J. G. Burton *et al.* 2019). This increase of oxidative stress and of UPR explains why growth restriction is often associated with early onset PE (Graham J. Burton & Jauniaux 2018; J. G. Burton *et al.* 2019). Despite, the wide range of research on the placenta and the different hypotheses on abnormal placentation and how it relates to PE, a significant amount of uncertainty remains. Extensive research still needs to be conducted to elucidate this uncertainty.

1.6.1.2 Oxidative Stress

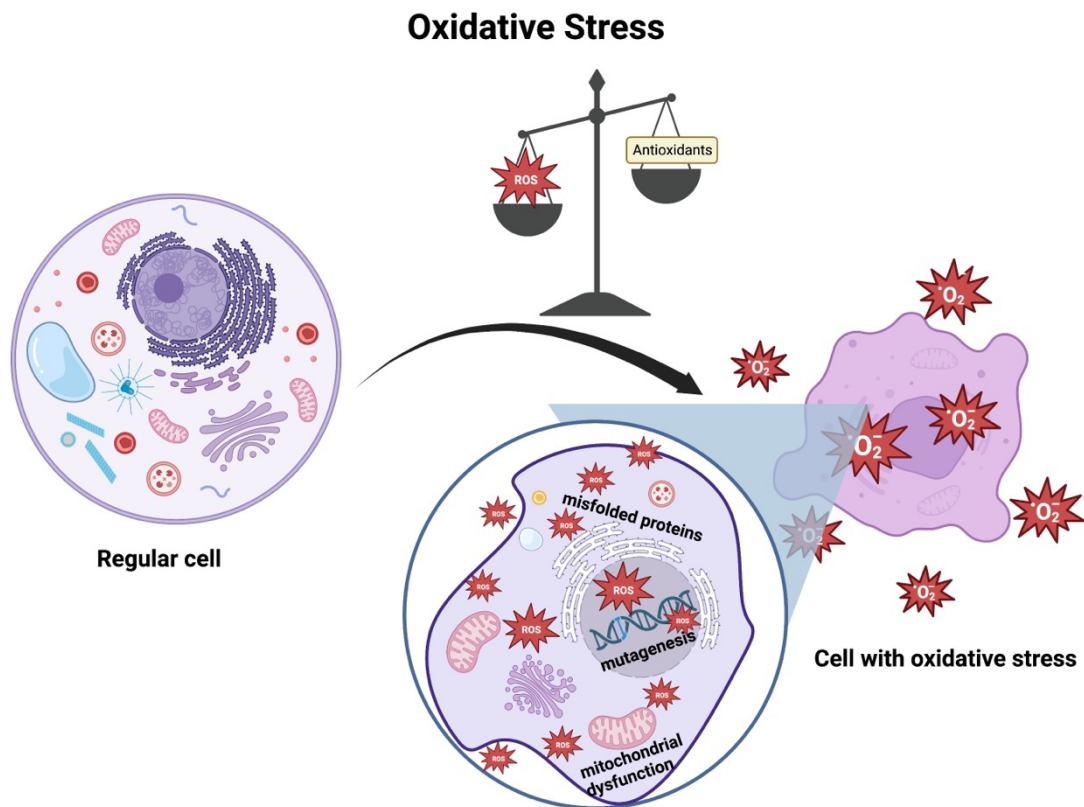


Figure 1.4 Oxidative Stress illustration.

Figure was created in Bio-Render.com.

Oxidative stress is considered to occur as a consequence of an overproduction of reactive oxygen and nitrogen species (ROS), or as a result of an insufficient supply of antioxidants needed to dispose of the free radicals (Wisdom *et al.* 1991; Graham J Burton & Jauniaux 2004; Myatt & Cui 2004a; Graham J. Burton & Jauniaux 2011). Oxidative stress is produced when an excess of free radicals exceeds the buffering capacity of the cellular defence mechanisms (Haram *et al.* 2019). This excess of free radicals combined with a diminution of antioxidants are said to be at the centre of the pathogenesis behind PE (Graham J. Burton & Jauniaux 2011; Poston *et al.* 2011; Goksu Erol *et al.* 2012). Toescu *et al.* investigated oxidative stress in a longitudinal study of seventeen normotensive pregnancies and looked at the oxidative stress present at the end of each trimester and after the 8 weeks postpartum (Toescu

et al. 2002). This investigation showed that late pregnancy was associated with the formation of oxidative stress. This, and more studies have shown that oxidative stress is expected in healthy placental development. Nonetheless, increased oxidative stress and reduced placental protective factors have been observed in preeclamptic phenotypes, in both the maternal circulation and the placenta (Wickens *et al.* 1981; Rodgers *et al.* 1988; A. Ahmed *et al.* 2000; K. Wang *et al.* 2013). A paper in 2016 speculated that epitheliochorial placentation in which the foetus remains separated from the maternal blood throughout gestation evolves as a protective mechanism against oxidative stress from pregnancy (Elliot 2016). The paper suggested that the lack of evolution of the epitheliochorial placentation thereby causes PE to arise (Elliot 2016).

On the other hand, Cester *et al.* looked at the basal content of lipid peroxides in the syncytiotrophoblasts plasma membranes from pregnant women with hypertension and showed an increase in oxidative stress (Cester *et al.* 1994). Following this study, Wang *et al.* hypothesized that PE mitochondria, which are sources of oxygen and are enriched by polyunsaturated fatty acids, could be an important source of oxidative stress and lipid peroxidation (Y. Wang & Walsh 1998). After analysing placentae that were obtained immediately after delivery from normal and preeclamptic pregnancies, the findings of this study concluded that placental mitochondria contribute to the abnormal increase in lipid peroxidation that occurs in PE by both an increase in their amount and an increase in their susceptibility to oxidation and mitochondrial generation of superoxide which in turn could lead to an important source of oxidative stress being produced in PE.

Further, a review suggested the conjunction of oxidative stress and tissue damage cause a breach to the placental barrier and thus creates a leak of foetal and placental-derived factors into the maternal circulation (Hansson *et al.* 2015). This leakage of foetal material into the maternal blood stream leads to maternal endothelial damage, elevated oxidative stress, and systemic inflammation (Smarason *et al.* 1993; Knight *et al.* 1998; Hahn & Holzgreve 2002; Tjoa *et al.* 2006). Moreover, this review also suggested that the shedding of nanoparticles such as free Haemoglobin (which causes kidney damage) and miRNA might further

exacerbate the inflammation, vascular damage from the placenta as well as the systemic oxidative stress (Redman & Sargent 2008; Tannetta *et al.* 2013; Cronqvist *et al.* 2014; Rudov *et al.* 2014). Interestingly, although smoking causes oxidative stress, smoking has also been shown to have a protective effect against PE (Conde-Agudelo *et al.* 2011). Karumanchi *et al.* 2010 explained this paradox by the fact that smoking has been linked to a decreased soluble fms-like tyrosine kinase 1 (sFlt-1) by carbon monoxide (Karumanchi & Levine 2010).

Mitochondria (especially mitochondrial DNA (mtDNA)) which are responsible for the production of ATP and the consumption of oxygen, are particularly sensitive to ROS in proximity to oxygen generation site of the electron transport chain (Myatt & Cui 2004a; Agarwal *et al.* 2015). This causes extensive damage to mtDNA and causes mutations to occur, which leads to impaired energy production and risk of further electron leakage which in turn causes an increase in oxidative stress (Agarwal *et al.* 2015). Mitochondrial DNA levels in the maternal circulation play an important role both in PE and as an indicator of placental abruption. An increase in maternal mtDNA levels has been linked to an increase in oxidative stress (Qiu *et al.* 2012; M. A. Williams *et al.* 2013; Holland *et al.* 2017). This increase is thought to be due to the hypoxic conditions associated with placental insufficiency and thus a diminution of placental blood flow (Costa *et al.* 1988; Jansson & Powell 2006; H. M. Lee *et al.* 2007; Holland *et al.* 2017). Hypoxic stress has been shown to increase the biogenesis of mitochondria, this generating more circulating mtDNA. However, unchanged, as well as both increased and decreased levels of mtDNA have been found in the same pathogenesis of pregnancy through different studies (Y. Wang & Walsh 1998; He *et al.* 2004; Lattuada *et al.* 2008; Qiu *et al.* 2013; Mandò *et al.* 2014; R. Hastie & Lappas 2014; Poidatz *et al.* 2015; Vishnyakova *et al.* 2016).

The potential causative correlation of oxidative stress and PE has long been debated (Agarwal *et al.* 2015). Some studies suggested that PE arose as a consequence of an excessive amount of oxidative stress, whereas other studies supported that increased oxidative stress occurs as a consequence of PE. However, evidence gathered by more recent studies, showing that oxidative stress also occurs in other pathologies such as diabetes, cancer, and

neurodegenerative diseases, suggests that oxidative stress occurs as a side-effect of PE rather than the alternative.

1.6.1.3 Angiogenesis

Angiogenesis is the process by which blood vessels form and is essential for the delivery of nutrients to the body. Though angiogenesis has been described in the placenta, as early as 18 days after conception (Noback 1946; Ottanelli et al. 2012; J. Hu et al. 2019), the bulk of the attention has been focused on cancer studies. The key molecules involved in angiogenesis are pro-angiogenic factors such as the vascular endothelial growth factors (VEGF), and anti-angiogenic factors such as the soluble fms-like tyrosine kinase 1 (sFlt-1) (Cross *et al.* 2012). VEGF can bind 3 receptors, but its activity is mediated by two main tyrosine kinase receptors, VEGFR-1 and VEGFR-2 which is also known as foetal liver kinase 1 Flk-1 (Kendall & Thomas 1993a). Soluble Flt-1, which is generated by alternative splicing of the VEGFR-1 (also known as Flt-1 gene), is a soluble form of VEGFR-1 extracellular ligand-binding domain, and it can bind to all isoforms of VEGF, as well as to the placental growth factor (PlGF) (Kendall & Thomas 1993a; A. Ahmed et al. 2000; S. Ahmad & Ahmed 2004; Eddy et al. 2018).

PlGF plays many roles in pregnancy amongst such as angiogenesis by promoting the growth of new blood vessels, placental development, blood pressure regulation, and foetal growth.

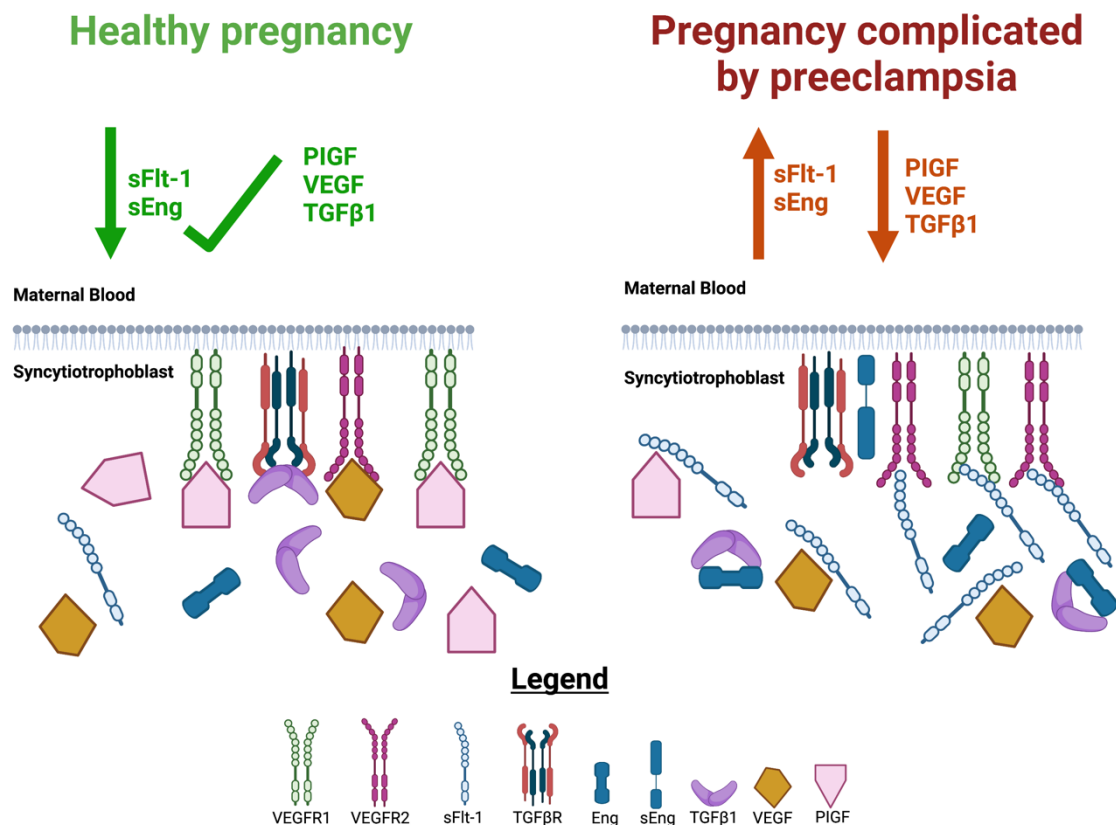


Figure 1.5 The relationship between preeclampsia and angiogenesis involves the traditional theory of angiogenic imbalance.

This theory suggests that preeclampsia is characterized by increased levels of circulating soluble tyrosine kinase-1 (sFlt-1) and soluble endoglin (sEng), which are similar to fms. As a result, the levels of free vascular endothelial growth factor (VEGF)/placental growth factor (PIGF) and TGF decrease, leading to endothelial dysfunction. The figure was created using BioRender.com. This figure was inspired by (Torres-Vergara et al. 2022).

One of the hypotheses behind PE (Figure 1.3) is that anti-angiogenic factors (Figure 1.5), specifically sFlt-1 are increased and in turn counteract the pro-angiogenic effects of VEGF (A. Ahmed 1997; Hiratsuka et al. 2001; Koga et al. 2003; S. E. Maynard, Min, Merchan, Lim, Li, Mondal, Libermann, Morgon, et al. 2003; Chaiworapongsa et al. 2004; S. Ahmad & Ahmed 2004; Romero et al. 2011). If sFlt-1 is free in serum, it can bind to VEGF and thus hinder it from binding to its cognate receptors and thus inhibit pro- angiogenic effects from occurring (Mutter & Karumanchi 2008a). The asymmetry of pro-angiogenetic and anti-angiogenic factors has been linked to endothelial dysfunction and decreased angiogenesis, hence exhibiting a

preeclamptic phenotype (hypertension, proteinuria)(S. E. Maynard, Min, Merchan, Lim, Li, Mondal, Libermann, Morgon, et al. 2003; Mutter & Karumanchi 2008a).

Maynard et al showed that after the administration of sFlt-1, pregnant rats started to develop PE-like phenotypes such as hypertension, proteinuria and glomerular endotheliosis (S. E. Maynard, Min, Merchan, Lim, Li, Mondal, Libermann, Morgon, et al. 2003). Similarly, a study on mice demonstrated that one single injection of the combination of; anti-mouse VEGF neutralizing antibodies and sFlt-1, into healthy non-pregnant mice, induced proteinuria, as well as massive glomerular endothelial cell detachment/damage and suppression of nephrin (a glomerular epithelial slit diaphragm apparatus-associated protein) (Sugimoto et al. 2003a). Both of these studies underline that sFlt-1 plays a crucial role in PE.

Another study, conducted in 2012 showed that non-pregnant women displayed symptoms of acute PE when suffering from bevacizumab (a humanized recombinant monoclonal IgG antibody that binds VEGF) toxicity, which mimics acute PE. The discontinuation of bevacizumab resulted in a reversible effect of the PE-like manifestations, which advocated for the fact that sFlt-1 is the main culprit behind PE (Cross *et al.* 2012).

Furthermore, as previously discussed, under-perfusion of the placenta causes ischemia and hypoxia. A study using in situ hybridization, found that hypoxic placentas secrete increased VEGF levels (Forsythe *et al.* 1996). However, the level of sFlt-1 secreted increases to a greater extent than the amount of VEGF secreted, thereby generating an imbalance of anti-angiogenic factors. Studies have also shown that circulating levels of sFlt-1 correlate with the severity of PE (Koga et al. 2003; S. E. Maynard et al. 2003; Sugimoto et al. 2003a; A. Hertig et al. 2004; Chaiworapongsa et al. 2005; Levine et al. 2005; Powers et al. 2005). On the other hand, sFlt-1 levels return to normal after delivery and all the preeclamptic syndromes are alleviated, which indicates the importance of this protein in pathogenesis (Eddy *et al.* 2018).

Over the years, different therapies have been proposed to deal with angiogenic imbalance. Apheresis is a therapy that removes substances from the blood and was shown to be safe for pregnant patients (Teruel *et al.* 1995). Thadhani *et al.* and Fan *et al.* both looked at the use of apheresis (therapy used to remove substances from the blood) for the removal of sFlt-1 from the plasma of preeclamptic patients (Fan *et al.* 2014; Angela Makris *et al.* 2016; Thadhani *et al.* 2016). While both of these studies were successful in diminishing the amount of plasma sFlt-1 and reducing the total protein/creatinine ratio, these studies were both pilot studies that only involved a small cohort, nor did these studies correct for other factors that might have been removed as a consequence of the (non-specific ion-exchange chromatography used and dextran sulphate apheresis) non-specific apheresis (Thadhani *et al.* 2011, 2016; Eddy *et al.* 2018).

Using the supplementation of VEGF or PlGF as the buffering mechanisms for excess sFlt-1 has been tested in different animal PE models (Eder & McDonald 1987; Rees *et al.* 1990; Miquerol *et al.* 2000; Alexander *et al.* 2002; Sholook *et al.* 2007; Zhihe Li *et al.* 2007; D. Chen *et al.* 2008; Bergmann *et al.* 2010; Gilbert *et al.* 2010; Woods *et al.* 2011; Logue *et al.* 2017). For example, adenoviral delivery of VEGF121 in pregnant BPH/5 mice inhibits the spontaneous development of PE-like symptoms (Woods *et al.* 2011). Adenoviral delivery of VEGF165 in sFlt-1 overexpressing pregnant mice leads to reduced blood pressure and kidney injury (Bergmann *et al.* 2010). Additionally, different forms of PlGF have also been tested in different animal models (Maglione *et al.* 1991; J. E. Park *et al.* 1994; Persico *et al.* 1999; Iyer *et al.* 2001; Gigante *et al.* 2006). It has been demonstrated that the administration of placental growth factor-2 (PlGF-2) and VEGF in pregnant mice overexpressing sFlt-1, decreased the mean blood pressure of these mice. Spradley *et al.*, looked at the 5-day infusion of recombinant human form of PlGF at gestational day 14 on pregnant rats that had undergone RUPP procedure and demonstrated an abolishment of the effects seen after the RUPP procedure, such as an increase in glomerular filtration rate, a decrease in the mean arterial blood pressure and a decrease of plasma sFlt-1 (Spradley *et al.* 2016).

However, several adverse effects were correlated with the supplementation of VEGF for the treatment of angiogenic balance (D. Chen *et al.* 2008; Fan *et al.* 2014). These adverse effects included; a diminution in pup and placenta weight, low platelet count, oedema formation, abnormalities in the heart, an augmented number of reabsorptions (in pregnant mice), and a diminished amount of viable pups, (Meyer & Chilkoti 1999; Miquerol *et al.* 2000; George *et al.* 2014, 2015; Nouri *et al.* 2015; Despanie *et al.* 2016; Logue *et al.* 2017). These adverse effects suggested that VEGF may express a dose dependent toxicity (Eddy *et al.* 2018). On the other hand, no adverse effects were observed when using PlGF for treatment, given that PlGF has the ability to bind only to sFlt-1. However, it was observed that PlGF-based therapies had a very short lifetime which complicated the drug-delivery system in pregnancy (Suzuki *et al.* 2009; Eddy *et al.* 2018).

Overall, more extensive research is still needed to assess the use of these angiogenic factors as potential treatments to reverse, counteract or even hinder PE.

1.6.1.4 Protective Pathway Mechanisms

A 2015 review metaphorically compared PE to a car with accelerators and breaks (A. Ahmed & Ramma 2015). In this metaphor, the “car” is the pregnancy, the “accelerators” are the inflammation, oxidative stress and angiogenic imbalance and the “breaks” are the endogenous protective pathway mechanisms (A. Ahmed & Ramma 2015). If the braking system (here the protective pathway mechanisms) of the car (pregnancy) doesn’t work, the accelerator (inflammation, oxidative stress and angiogenic imbalance) goes out of control until it crashes and materialises itself in the form of PE. The metaphorical “braking system” (or protective pathway mechanism) is composed of three main mechanisms: the haem oxygenase pathway (HO/CO system), the hydrogen sulphide (H₂S) pathway and the NO pathway (A. Ahmed & Ramma 2015).

1.6.1.5 Hydrogen Sulphide Pathway

Hydrogen sulphide (H₂S) is gasotransmitter (gas signalling molecule) that plays a role in various functions such as vasodilation, angiogenesis stimulation, inflammation, and cytoprotection against cellular damage (Abe & Kimura 1996a; W. Zhao et al. 2001; P. Kamoun 2004; Zanardo et al. 2006a; Blackstone & Roth 2007; Elrod et al. 2007; Papapetropoulos et al. 2009). H₂S also influences the opening of ATP-sensitive potassium channels in smooth muscle cell and increases the VEGF expression (K. M. Holwerda *et al.* 2012). Endogenous H₂S is produced by three enzymes cystathionine-synthase (CBS) and Cystathionine γ -lyase (CSE) and 3-mercaptopyruvate sulfurtransferase (3-MST), all of which are present in the human uterus and the placenta (Abe & Kimura 1996; H. Kimura 2014). CSE is the main H₂S-producing enzyme expressed in cardiovascular system (Yan *et al.* 2004). It has been demonstrated that continuous administration of DL-propargylglycine (PAG), a CSE inhibitor, resulted in elevated blood pressure and vascular remodelling, as well as a decreased level of both CSE and H₂S (Yan *et al.* 2004). Genetically depletion of CSE in mice lead to the development of hypertension, hyperhomocysteinemia (abnormally high levels of homocysteine which can contribute to arterial damage and blood clots) and endothelial dysfunction (G. Yang et al. 2008; Akahoshi et al. 2019).

Recently, it has been shown that the knockdown of CSE by small interfering RNA, in human umbilical vein endothelial cells (HUVEC), augmented the level of sFlt-1 and soluble endoglin (Kim M. Holwerda *et al.* 2014). It was also shown that adenoviral overexpression of CSE in HUVEC cells inhibited the release of sFlt-1 and soluble endoglin (D. B. Yang *et al.* 2013). Wang et al. showed that by treating pregnant mice with DL-propargylglycine (a CSE inhibitor), subsequent PE-like symptoms (such as induced hypertension, liver damage, promoted abnormal vascularization in the placenta and decreased foetal growth) developed (K. Wang *et al.* 2013). Contrarily, when a slow releasing H₂S compound was administered, inhibition of anti-angiogenic factors (sFlt-1 and soluble endoglin) and restored foetal growth in mice that were previously compromised by DL-propargylglycine were observed. Thus, endogenous H₂S

is required for healthy placental development and a dysfunction or diminution of the levels of CSE/H₂S, contributes to the pathogenesis of PE.

Yang et al. (2008) studied the blood vessels, the blood pressure and the vessel relaxation of CSE knockout mice (which displayed hypertension and diminished endothelium-dependent vasorelaxation) versus the ones from wild type mice (Shin-Young Kim et al. 2004; G. Yang et al. 2008). They established that CSE knockout mice had an increased blood pressure and decrease in systolic pressure, when compared to wild type mice. Thus, this study concluded that H₂S is a physiologic vasodilator and a regulator of blood pressure.

Several studies have shown that H₂S/CSE plays an imperative role in the pathogenesis of PE, the regulation of blood pressure and the angiogenic activity. Nevertheless, research is still needed for the evaluation of H₂S as a potential therapy for PE.

1.6.2 Potential underlying mechanisms

7.1.1.1.1 H₂S and its control on the mitochondria

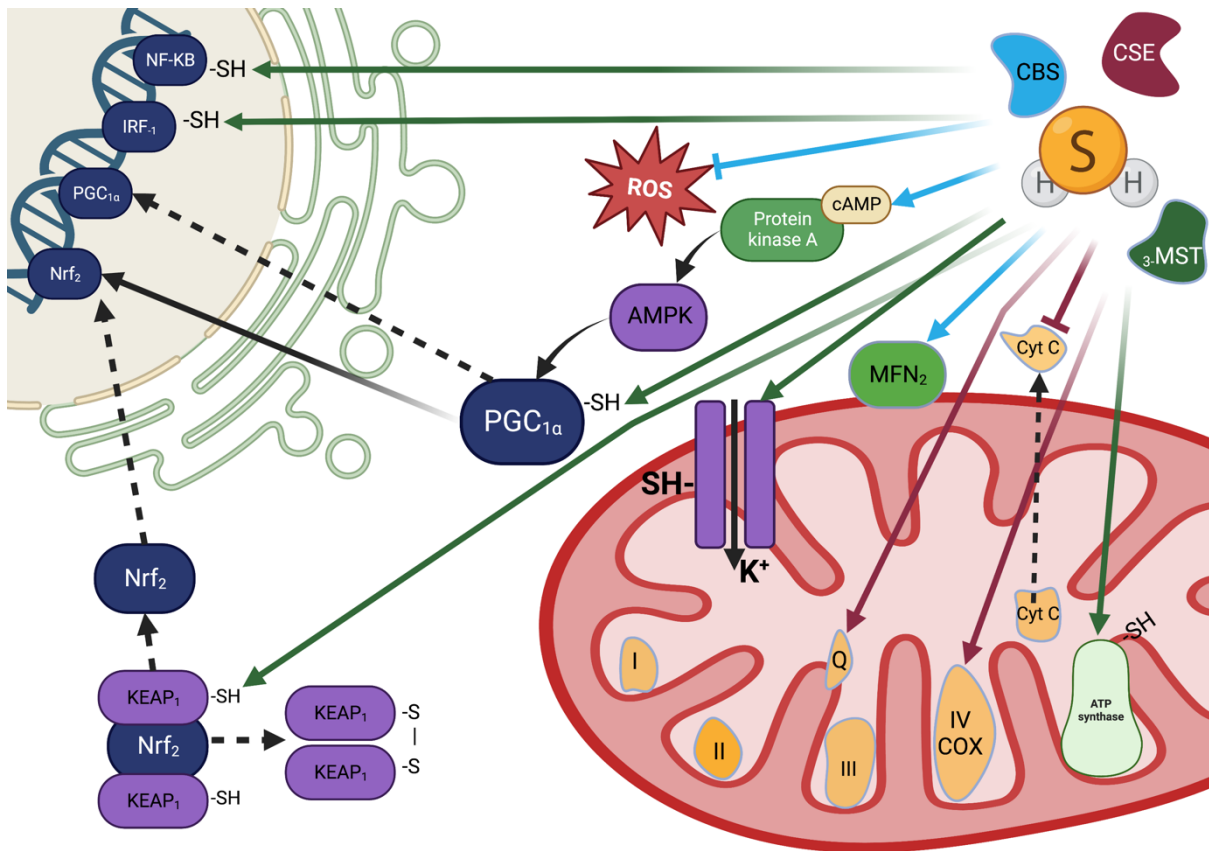


Figure 1.6 H₂S effects on mitochondria.

Persulfidation signaling is denoted by green arrows, antioxidant effects are denoted by blue arrows, and metalloprotein interactions by H₂S are denoted by red arrows. H₂S can persulfidate many transcription factors, including Nf-KB, IRF-1, and PGC-1a, to encourage the transcription of a number of mitochondrial biogenesis and anti-apoptotic genes. H₂S can also boost PGC-1a expression by coactivating Nrf2, which encourages pathways for cellular survival, and cAMP/PKA/AMPK activation, which boosts its transcriptional stimulation of mitochondrial biogenesis. H₂S can also activate Nrf2 by causing it to dissociate from its complex with Keap1 as a result of persulfation. Additionally, it has been demonstrated that H₂S activation of mitoKATP channels via persulfidation directly inhibits apoptosis. Finally, upon its activation, cytochrome c (Cyt c) released into the cytosol from the mitochondria can be bound to by H₂S and sequestered, preventing apoptosis. Additionally, H₂S can promote mitochondrial bioenergetics. ATP synthesis in the mitochondria is stimulated by persulfidation of ATP synthase and direct H₂S electron transfer to the ETC via SQR/ubiquinone and COX interactions. Finally, it has been demonstrated that H₂S production keeps mitochondrial fusion intact and prevents mitochondrial fission. The redox-sensitive maintenance of the outer mitochondrial membrane fusion protein MFN2 is one way it accomplishes this. Image adapted from (Murphy et al. 2019). Figure was created on Bio-render.com.

The mitochondria are crucial organelles that play a central role in many biological functions such as respiration, apoptosis, biogenesis, and shape. As part of its signalling pathway, H₂S directly targets the mitochondria (Figure 1.6). H₂S has been shown to impact the activity of the Electron Transport Chain (ETC) in a concentration-dependent manner. At low concentrations, H₂S acts as a substrate through Sulfide Quinone Oxidoreductase (SQR) metabolism, which provides an electron to the ETC, encourages ATP production, and oxidative phosphorylation (Nicholls et al. 1982; Völkel et al. 1996; Theissen et al. 2008).

However, high concentrations of H₂S can inhibit the ETC, disrupt redox balance, alter metabolism, and eventually cause mitochondrial depolarization and death (Eghbal *et al.* 2004; Libiad *et al.* 2019). Nevertheless, cells can adapt by up-regulating uncoupling protein 2 to protect themselves from oxidative stress and reduce COX subunits, saving valuable energy while ATP synthesis is disturbed.

H₂S can induce apoptosis through the mitochondrial permeability transition pore formation and opening, cytochrome c release, activation of proapoptotic proteins, and down-regulation of anti-apoptotic proteins (Baskar *et al.* 2007; Adhikari & Bhatia 2008). Moreover, H₂S at lethal concentrations can cause mitochondrial swelling, decreased membrane potential, and increased permeability transition pore induction, leading to cell death (DeMoura et al. 2019).

Interestingly, H₂S has an anti-apoptotic effect under specific conditions and at harmless concentrations. For instance, H₂S can stop apoptosis even after an apoptotic event has been initiated by persulfidating procaspase 9, which inhibits the caspase cascade and mitochondrion-dependent apoptosis (Libiad *et al.* 2019). Moreover, H₂S can inhibit apoptosis by directly persulfidating NF- κ B, which improves its ability to bind to the promoters of multiple anti-apoptotic genes (N. Sen *et al.* 2012). H₂S has also been shown to regulate mitochondrial biogenesis, or the production of new mitochondria. The process is masterfully regulated by Peroxisome proliferator-activated receptor 1 (PGC-1), which coactivates Nrf2 to activate TFAM and cause the transcription of nuclear-encoded mitochondrial proteins. Endogenous CSE-dependent H₂S generation increases PGC-1 via activation of the cAMP/PKA pathway in primary hepatocytes, and persulfidation brought on by H₂S increases PGC-1 activity (Untereiner, Wang, et al. 2016). H₂S can also preserve mitochondrial biogenesis in osteoblasts subjected to increased homocysteine levels, which restores osteoblast function, ATP generation, and redox equilibrium (Zhai *et al.* 2019).

Finally, H₂S controls mitochondrial morphogenesis by controlling the expression of GTPases that control the processes of mitochondrial fusion and fission. H₂S has been demonstrated to decrease mitochondrial fragmentation by decreasing the levels of phosphorylated Drp1/Drp1, preventing ROS accumulation and apoptosis (N. Liu *et al.* 2017). It has also been shown to block mitochondrial fission in mouse neuroblastoma cells *in vitro* through an ERK1/2-dependent loss of Drp1 at the mRNA and protein level (Qiao *et al.* 2017a).

7.1.1.1.2 H₂S and cardiac disease

The functions of H₂S in cardiac tissue are diverse and significant due to its role as a signalling gas and a potential cardioprotective agent. H₂S has been demonstrated to be endogenously produced in vascular smooth muscle cells, eliciting vasorelaxation in rat aorta tissues (Abe & Kimura 1996; W. Zhao & Wang 2002). Its involvement in metabolizing homocysteine through the transsulfuration pathway, links defective CBS/CSE function to hyperhomocysteinemia, a serious CVD risk characterized by excessive levels of homocysteine in the blood (X. Chen *et al.* 2004; Kruger 2017).

Dysfunctional endothelial cells, which line the interior of blood and lymphatic vessels, have been associated with various cardiovascular disorders such as atherosclerosis and hypertension (Gimbrone & García-Cardena 2016; Konukoglu & Uzun 2017). H₂S has demonstrated potential as a treatment for these disorders by reducing ROS production, mitochondrial membrane hyperpolarization, and boosting ETC complex III activity and mitochondrial metabolism in endothelial cells under glucose stress (Gerő *et al.* 2016). Furthermore, H₂S may prevent apoptosis in endothelial cells by reducing oxidative stress and preserving mitochondrial health (Zong *et al.* 2015).

H₂S has also shown promise as a treatment for atherosclerosis due to its effects on lipid hydroperoxide synthesis in LDL, defending against oxidized LDL cytotoxicity, preventing cytotoxic lipid accumulation, and foam cell development (Jeney *et al.* 2009; Muellner *et al.* 2009; Z. Z. Zhao *et al.* 2011). Additionally, H₂S is thought to mitigate atherosclerosis through

redox restoration and by affecting vascular smooth muscle cells and monocytes (E. Yu *et al.* 2013). Persulfidation of proteins such as superoxide dismutase and medium-chain specific acyl-CoA dehydrogenase has been observed, which are crucial for maintaining redox balance and metabolizing lipids in the mitochondria (Cheung & Lau 2018).

H₂S has also been found to inhibit the generation of foam cells originating from macrophages, a key step in atherogenesis, through the activation of the KATP/ERK1/2 pathway (Z. Z. Zhao *et al.* 2011). Moreover, H₂S has been shown to lessen myocardial ischemia injury by preserving mitochondrial function and potentially through mitochondrion-mediated macrophage M2 polarization (Xie *et al.* 2014; Miao *et al.* 2016).

In ischemia/reperfusion injury, H₂S has been demonstrated to protect mitochondria during I/R to enhance respiration and promote biogenesis (Elrod *et al.* 2007). The mitochondrion-targeted H₂S donor AP39 has been shown to protect against myocardial ischemia/reperfusion injury by blocking mitochondrial permeability transition pore in a cyclophilin d-dependent manner when administered during reperfusion (Karwi *et al.* 2017). Additionally, AP39 has exhibited repeatable protection against I/R in kidney and brain damage (H. Pan *et al.* 2014; Ikeda *et al.* 2015; A. Ahmad *et al.* 2016).

1.6.2.1 H₂S in pregnancy and PE

The placenta can synthesize H₂S from CSE and CBS, particularly under hypoxia (P. Patel *et al.* 2009). Women with PE have higher plasma levels of homocysteine, cystathionine, and cysteine, which may be related to weakened endothelium-dependent vascular relaxation observed in CBS-deficient pregnant mice (G. Yang *et al.* 2008; U. Sen *et al.* 2010). Decidualization is also compromised in mice lacking the CBS gene. Moreover, PE women may have reduced CSE mRNA and H₂S levels in their blood, which is associated with an angiogenic imbalance linked to PE symptoms (L. L. Pan *et al.* 2011; Tao *et al.* 2013). Oxidized low-density lipoprotein levels may be a potential mechanism for the downregulation of CSE in

PE, as oxidized low-density lipoprotein was found to decrease CSE expression in human aortic endothelial cells (Zhen Li et al. 2018; Fanfan Li et al. 2019; Xiaomei Li et al. 2022).

Animal studies suggested that CSE, H₂S, and PE formation are interrelated (G. Yang et al. 2008; K. Wang et al. 2013; S. Ahmad et al. 2015). Studies on transgenic CSE knockout mice showed age-dependent hypertension, endothelial dysfunction, and hyperhomocysteinemia, traits linked to PE (G. Yang et al. 2008; K. Wang et al. 2013). Pregnant mice treated with the CSE inhibitor DL-Propargylglycine exhibited hypertension, an elevation in anti-angiogenic factors, aberrant placental vascularization with foetal growth restriction (FGR), and other symptoms associated with PE. Interestingly, the slow-releasing H₂S donor GYY4137 rescued alteration of placental vasculature and FGR in DL-Propargylglycine-treated animals and controlled the development of the additional protective enzyme haem oxygenase 1 (M. J. Wang *et al.* 2010). CSE is highly expressed in various tissues, including the heart, vascular endothelium, liver, kidney, uterus, placenta, and pancreatic islets. Regulation of CSE activity, such as its mitochondrial translocation via Tom20, may compete for substrates, thereby affecting CSE's activity (Bos *et al.* 2015). In conclusion, CSE/H₂S plays a crucial role in the vasculature, and impaired production and activity of CSE promote the development of CVD.

1.6.3 Vascular predisposition and abnormal Cardiovascular adaptations in PE

The elucidation of the physiological adaptations that occur during pregnancy and postpartum is crucial to grasp the pathophysiological discrepancies associated with PE. Echocardiography studies have identified different changes in maternal cardiac function even in uncomplicated normotensive pregnancies. Specifically, an excessive and significant increase in left ventricular mass combined with diastolic dysfunction has been observed, which reverts back to its pre-pregnancy state postpartum (Savu et al. 2012; Karen Melchiorre et al. 2016).

Moreover, maternal echocardiography studies demonstrated severe cardiac dysfunction prior to and at the onset of clinical symptoms of PE (Thilaganathan & Kalafat 2019a). Furthermore, a considerable reduction in cardiac output in early onset as well as an abnormal ventricular geometry paired with diastolic function has been observed in the majority of women affected by PE (Herbert Valensise et al. 2008; K. Melchiorre et al. 2013).

Among the most significant prognostic biomarkers for PE in the first trimester are maternal mean arterial blood pressure and uterine artery resistance (Rolnik *et al.* 2017). A combination of 36 cohort studies' evaluation of 815 preeclamptic women, by Castleman *et al.* (2016), revealed increased vascular resistance and left ventricular mass as the most common symptoms of preeclampsia (Castleman *et al.* 2016). Left ventricular wall thickness of 1.0 cm, excessive reduction in early diastole/atrial contraction, and lateral e' of 14 cm/s, which are indicative of diastolic dysfunction, were distinctive features of abnormal pregnancy (Castleman *et al.* 2016).

Increases in blood pressure and peripheral arterial waveform resistance have also been noted preceding the onset of PE (Thilaganathan & Kalafat 2019a). Recent findings indicate that maternal peripheral arteries, including the ophthalmic artery and brachial artery, exhibit impaired function during early pregnancy indicating abnormal generalized vascular physiology in PE rather than a localized vascular defect in the uteroplacental circulation as previously hypothesized (Weissgerber *et al.* 2016; Porto *et al.* 2017; V. A. Lopes van Balen *et al.* 2017; Kalafat *et al.* 2018). Foo *et al.* (2018) demonstrated that women who later developed PE had lower cardiac output and higher peripheral resistance even prior to conception compared to healthy pregnancies (Foo *et al.* 2018). Comparable results have been observed in women with chronic hypertension who eventually develop PE, as well as normal women at mid-gestation, accompanied by ventricular remodelling and hypertrophy (K. Melchiorre *et al.* 2013; Ambia *et al.* 2018). These findings provide evidence that PE shares a vascular predisposition with cardiovascular morbidity in non-pregnant individuals and suggest that further research into cardiovascular function may reveal insights into the pathophysiology and clinical effects of PE (Myredal *et al.* 2010; Matsuzawa *et al.* 2015; Sedaghat *et al.* 2018).

The modifications that arise in normotensive pregnancy have been outlined in a study and summarized in Table 1.4.1. However, besides discerning the hemodynamic changes that manifest during normotensive pregnancy, evaluating the timing of these variations is necessary. Notably, a systematic review published in 2018 suggested that the first hemodynamic changes include augmented heart rate, stroke volume, and cardiac output coupled with a decline in systemic vascular resistance, leading to high-volume, low-resistance circulation, peaking in the early third trimester (Perry *et al.* 2018). Following these changes, there is a reduction in the cardiac output and stroke volume (Perry *et al.* 2018).

| | PARAMETERS | NORMAL PREGNANCY | PREECLAMPSIA |
|---------------------|----------------------|------------------|--------------|
| | Changes in pregnancy | | |
| HEMODYNAMIC CHANGES | SVR | ↓ | ↑ |
| | Blood Volume | ↑ | ↓ |
| SYSTOLIC FUNCTION | SV | ↑ | ↓ |
| | HR | ↑ | ↑ |
| DIASTOLIC FUNCTION | MV E/A | ↑ | ↓ |
| CARDIAC STRUCTURE | Arterial Stiffness | - | ↑ |
| | LV Mass | ↑ | ↑↑ |

Table 1.2 Abnormal Cardiovascular Adaptations in Preeclampsia.

This table was adapted using various papers (Thornburg *et al.* 2000; Castleman *et al.* 2016, 2023; Perry *et al.* 2018; Forrest *et al.* 2022).

As gestation progresses, systemic vascular resistance progressively increases towards the 40th week of gestation, correlating with changes in blood pressure. Early in gestation, blood pressure decreases, and it subsequently increases during the third trimester (Thornburg *et al.* 2000; Poston *et al.* 2011; Mahendru *et al.* 2014; Meah *et al.* 2016; Perry *et al.* 2018; Vinayagam *et al.* 2018). Subsequently, in late pregnancy, a plateau is observed as the hemodynamic changes begin to wane (Dunsworth *et al.* 2012; Perry *et al.* 2018). Intriguingly, echocardiography studies conducted on normotensive pregnancies revealed an upsurge in the left ventricular mass and remodelling, which is typically indicative of diastolic dysfunction (Savu *et al.* 2012; Karen Melchiorre *et al.* 2016). However, this excessive increase in the left

ventricle in normotensive pregnancies commonly reverts to baseline after delivery, highlighting the remarkable adaptability of the heart to meet the demands of both the mother and foetus during pregnancy (Savu et al. 2012; Karen Melchiorre et al. 2016). Conversely, the reversal of cardiac remodelling after delivery is only observed more extensively in 40% of preeclamptic pregnancies (Karen Melchiorre et al. 2011). Melchiorre et al. demonstrated a link between PE and structural alterations in the heart, such as biventricular systolic dysfunction (observed in 26% of pre-term PE cases compared to 4% term PE pregnancies) and severe left ventricular hypertrophy (detected in 19% of pre-term PE cases compared to 2% term PE pregnancies) (Karen Melchiorre et al. 2011, 2012).

Recent cohort studies have demonstrated that women who develop PE display defective myocardial relaxations, as well as diastolic and systolic ventricular dysfunctions before the onset of the condition (Muthyala *et al.* 2016; Thayaparan *et al.* 2019). These studies have highlighted a crucial connection between cardiac function and the development of PE, which could potentially enable new methods of diagnosing and preventing this hypertensive disorder. In addition, Khalil et al. found that an increase in arterial stiffness was observed in pregnant women who later developed PE, as early as the first trimester of pregnancy (Khalil *et al.* 2012; K Melchiorre *et al.* 2013). This suggests that pregnancy acts as a "stress test" by revealing poor cardiovascular reserves and dysfunctions, which were previously invisible can lead to further complications later in life (Craici *et al.* 2008). Reduced stroke volume, diastolic dysfunction, and left ventricular remodelling are most prominent in severe and early-onset preeclampsia and are associated with adverse maternal and foetal outcomes, regardless of the traditional classification of preeclampsia based on clinical severity or gestational onset (Christiana M Schannwell et al. 2002; Jovin et al. 2013; Marcolan Quitete et al. 2015).

A growing body of evidence has revealed that women who develop PE are at a higher risk of developing additional cardiovascular complications later in life (Walker 2000; Irgens et al. 2001; Sibai et al. 2003; D. W. Brown et al. 2006; Bellamy et al. 2007; Mutter & Karumanchi 2008a; Ayansina et al. 2016). While past and current research has largely focused on examining hemodynamic changes associated with pregnancy and PE after the onset of diagnosis, very little attention has been given to the pre-pregnancy/pre-PE onset and post-delivery/post-PE phases. Further investigation is necessary to fully elucidate the hemodynamic changes underlying both normotensive pregnancy and PE. A better comprehension of the mechanistic basis for the development of this condition would facilitate

the development of more effective prophylactic measures to mitigate its long-term impact on maternal health.

1.7 Long-Term Cardiovascular Risk

A growing body of research indicates that women with a history of PE may face long-term health implications, particularly an increased susceptibility to CVD in later life (Bellamy et al. 2007; Evans et al. 2011; Karen Melchiorre et al. 2011; R. Ahmed et al. 2014; Amaral et al. 2015; English et al. 2015; Bokslag et al. 2017;; Tomimatsu et al. 2017; Escouto et al. 2018; Dayan & Nerenberg 2019; Garrido-Gimenez et al. 2020; Ngene & Moodley 2020; Washington C. Hill et al. 2020; Booz et al. 2021; Sarhaddi et al. 2022) These studies have found that women with a history of PE are more likely to develop hypertension, strokes, and ischemic heart disease compared to those without such a history (Garovic *et al.* 2010; Garovic & August 2013; R. Ahmed *et al.* 2014; Washington C. Hill *et al.* 2020).

Additionally, an increased risk of metabolic syndrome (Rafeeina *et al.* 2014; Cho *et al.* 2019; Hooijschuur *et al.* 2019), diabetes (Libby *et al.* 2007; Allison 2013; Weissgerber & Mudd 2015), and renal disease (Veronica Agatha Lopes van Balen *et al.* 2017; Kristensen *et al.* 2019; Kattah 2020) has been associated with a history of PE. Recent research has also demonstrated a link between PE and cerebrovascular disease, including stroke and transient ischemic attack (Bushnell & Chireau 2011; E. C. Miller 2019; De Havenon et al. 2021; J. A. Kitt et al. 2021; J. Kitt et al. 2021; Beckett et al. 2023).

In particular, women who experienced severe PE during their pregnancy appear to be at a higher risk of developing cerebrovascular disease later in life (Bushnell & Chireau 2011; E. C. Miller 2019; Turbeville & Sasser 2020; De Havenon et al. 2021; J. Kitt et al. 2021; Beckett et al. 2023). Different studies have reported a five-fold to eight-fold increased chance of future CVD in women with a history of severe PE (Gammill *et al.* 2018; Hallum *et al.* 2023; Sophia Antipolis 2023).

Women with a history of PE may face significant long-term health risks, particularly an increased susceptibility to cardiovascular and cerebrovascular diseases.

1.7.1 Cardiovascular Disease risk

Pregnancy complications, particularly preeclampsia, have been identified as risk factors for CVD in women (Irgens et al. 2001; Sattar & Greer 2002; G. N. Smith 2014; P. Wu et al. 2017; Behrens et al. 2019; Leon et al. 2019; Khosla et al. 2021). Women with a history of preeclampsia are more likely to experience CVD events in the future which cannot be explained by controlling for confounding factors (Sattar & Greer 2002; Leon *et al.* 2019; ACOG 2020). Numerous studies demonstrate a substantial risk of further cardiovascular events following a preeclamptic incident, including higher rates of hospitalization and death from ischemic heart disease and myocardial infarction, as well as higher coronary artery calcium scores and an increased risk of major cardiovascular events such as myocardial infarction, cardiac shock, malignant dysrhythmia, cerebrovascular accidents, or any other condition requiring percutaneous cardiac intervention, coronary artery bypass surgery, an implantable cardiac defibrillator, or thrombolysis (J. M. Roberts & Gammill 2005; Mosca *et al.* 2011; R. Ahmed *et al.* 2014; Seely *et al.* 2021).

Patients with PE also have a higher chance of developing hypertension, further increasing their risk of CVD later in life. In addition, PE-affected women had a higher rate of protein-altering mutations in the genes linked to idiopathic or peri-partum cardiomyopathy than reference populations, and the titin (TTN) gene, which produces the sarcomeric protein titin, was the site of the majority of variations (Ehler 2018; Gammill *et al.* 2018). PE and cardiomyopathy share genetic risk factors that may eventually shed light on pathogenesis, define clinical phenotypes among these clinically diverse illnesses, and forecast long-term risk (J. M. Roberts & Gammill 2005; Ehler 2018; Gammill *et al.* 2018; Jia *et al.* 2018; Behrens *et al.* 2019; Moolla *et al.* 2022; Mubarik *et al.* 2023). These pregnancy-specific exposures may lead to peripartum cardiomyopathy in women with TTN variants developing the disease earlier than idiopathic cardiomyopathy.

More importantly, the Cardiovascular Health After Maternal Placental Syndromes (CHAMPS) population-based cohort study analysed 1.03 million women who were enrolled in the Ontario Health Insurance Plan between 1990 and 2004 (Ray *et al.* 2005). These women were healthy before their first documented delivery, and their data was linked to hospital admissions data from the Canadian Institute for Health Information Discharge Abstract Database and death data from the Canadian Registered Persons Database in order to analyse outcomes (C. E.

Brown *et al.* 2023). Despite this extensive study of 2005, finding biomarkers with high predictive value for postpartum CVD in women with a history of PE still remains to be established.

In contrast, the development of PE has been associated with elevated levels of angiogenic factors like soluble endoglin and elevated ratios of sFlt-1: PlGF, which have been found to be clinically useful predictive and diagnostic biomarkers (Turbeville & Sasser 2020). However, no specific markers for future CVD risk have been found to date (C. E. Brown *et al.* 2023).

While traditional CVD risk factors, such as chronic hypertension and obesity, can explain much of the increased CVD risk associated with a history of preeclampsia, a significant portion, 20% to 40%, cannot be explained by these factors (Haug *et al.* 2019; Stuart *et al.* 2020). Preeclampsia serves as an early warning system for future CVD risk, predicting a doubling of CVD risk even before the manifestation of traditional CVD risk factors (Timpka *et al.* 2017, 2018).

1.7.2 Genetics of preeclampsia

Since the 19th century, PE has been observed to cluster within families, suggesting a genetic component to the condition (Chesley *et al.* 1968; Graves *et al.* 1993). However, identifying the genetic contribution to PE is difficult because the phenotype manifests only in parous women.

Initial twin studies that aimed to determine the relative contributions of hereditary and environmental factors to PE, revealed frequent discordance between monozygotic twin sisters, suggesting minimal heritability from maternal genes (Thornton & Macdonald 1999). However, more recent studies using extensive Swedish registries have estimated the heritability of PE to be around 55%, including contributions from both maternal and foetal genes. Subsequent research has demonstrated equal prevalence of concordance and discordance in monozygotic twins (O'Shaughnessy *et al.* 2000).

The candidate gene method, frequently used in PE research, focuses on maternal genotype, selecting a single gene based on existing knowledge of PE pathophysiology (Colhoun *et al.* 2003; Mütze *et al.* 2008; Yong *et al.* 2018; Mohamad *et al.* 2020).

Many biological (>70) candidate genes represent various pathophysiological processes, but results have been inconsistent, with no widely recognized susceptibility gene identified (P. J. Williams & Broughton Pipkin 2011). Small sample sizes and population variation contribute to these inconsistencies (P. J. Williams & Broughton Pipkin 2011).

The most popular candidate genes can be classified into groups based on their functional characteristics and conceivable functions in pathophysiology, such as Thrombophilia, Haemodynamics and endothelial activity, oxidative stress and lipid metabolism (Graves *et al.* 1993; Mütze *et al.* 2008; P. J. Williams & Broughton Pipkin 2011; Gammill *et al.* 2018; Yong *et al.* 2018; Balan *et al.* 2020; Mohamad *et al.* 2020a).

Thrombophilia: Adequate placental circulation is crucial for a successful pregnancy. Thrombophilias are believed to increase the risk of placental insufficiency due to their effects on trophoblast growth and differentiation, as well as placental micro- or macro-vascular thrombosis (Isermann *et al.* 2003). Abnormalities in the clotting cascade are well-established in women with PE (Brenner 2002; Kohli *et al.* 2016). PE can cause endothelial damage, which is associated with a procoagulant phenotypic shift and reduced endothelially mediated vasorelaxation. This trait may be present prior to PE in pregnancy or could develop as a result of damage caused by placental injury. A small proportion of women also experience frank thrombocytopenia, often accompanied by haemolysis, elevated liver enzymes, and low platelet counts (HELLP syndrome).

PE has been linked to the three most extensively studied thrombophilic factors—factor V Leiden (F5), methylenetetrahydrofolate (MTHFR), and prothrombin (F2)—but numerous studies have also reported conflicting findings (Mütze *et al.* 2008). A recent meta-analysis found no associations between the 1691G>A mutation in F5 and PE or MTHFR or F2; however, it did reveal a two-fold increase in risk (Lin & August 2005). To date, more studies

have disproved a relationship between these three genes and PE than those supporting it. Attempts to replicate associations with the inhibitor of fibrinolysis plasminogen activator factor-1 gene have also been unsuccessful (Fabbro *et al.* 2003; A. Gerhardt *et al.* 2005; Dalmáz *et al.* 2006).

Haemodynamics and endothelial activity: The renin-angiotensin system (RAAS) plays a vital role in regulating cardiovascular and renal changes during pregnancy. The RAAS has been implicated in the pathophysiology of PE in several studies (Shah *et al.* 2006). Consequently, RAAS genes have been considered likely candidates for PE. Extensive research has been conducted on angiotensin-converting enzyme, angiotensin II type 1 and type 2 receptors, and angiotensinogen in the context of PE (Inoue *et al.* 1995). Recent meta-analyses have found that the T allele of AGT M235T is associated with an increased risk of PE, and similar increases in disease risk have been identified for angiotensinogen and the angiotensin-converting enzyme I/D polymorphism (Medica *et al.* 2007). A rare functional mutation in angiotensinogen that causes leucine to be replaced by phenylalanine at the site of renin cleavage has been linked to severe PE (Inoue *et al.* 1995).

Reduced activity of the vascular remodelling and vasodilation enzyme endothelial NO synthase 3 (eNOS3) has been observed in PE (Brennecke *et al.* 1997). However, association studies in other ethnic populations have yielded both positive and negative results. The E298D polymorphism, previously associated with PE in Colombian women, was not found to be linked with increased risk in a meta-analysis (Medica *et al.* 2007). Vascular endothelial growth factor (VEGF) is essential for endothelial cell proliferation, migration, survival, and regulation of vascular permeability. Few studies have investigated single nucleotide polymorphisms in the genes of the VEGF system. The polymorphisms in VEGF have been associated with severe PE in two small studies, but they are not currently considered significant risk factors (Papazoglu *et al.* 2004; Bányász *et al.* 2006).

Oxidative stress & lipid metabolism: Oxidative stress is crucial in the aetiology of PE, with rapid changes in local oxygen tension and potential hypoxia-reperfusion required for maternal placental perfusion near the end of the first trimester. This process involves increased antioxidant expression and activity, including glutathione peroxidase, catalase, and superoxide dismutases (Jauniaux *et al.* 2000). Diminished antioxidant response may trigger poor placentation events. Recent research has assessed evidence for reduced antioxidant activity in PE (Perkins 2006). Lipid peroxidation, a candidate causal agent for endothelial damage in PE, could exacerbate endothelial dysfunction if genes involved in reactive oxygen species formation or inactivation are deficient (Wickens *et al.* 1981).

Despite the strong correlation between oxidative stress and PE, only a few genes have been studied. Functional polymorphisms in the genes for glutathione S-transferase (GST) and microsomal epoxide hydrolase (EPHX) have shown associations, but conflicting findings also exist (Laasanen *et al.* 2002; Ohta *et al.* 2003; G. S. Gerhardt *et al.* 2004; Canto *et al.* 2008). Abnormal lipid profiles in PE are linked to lipid peroxidation induced by oxidative stress. Lipoprotein lipase (LPL) and apolipoprotein E (ApoE), the main lipid metabolism regulators, have been proposed as potential candidate genes (Y. J. Kim *et al.* 2001; Descamps *et al.* 2005). A recent study found that PE is associated with altered glycosylation of circulating ApoE isoforms (Atkinson *et al.* 2009). The most promising genetic variant is the missense mutation Asn291Ser in LPL, which has been associated with increased dyslipidemia and reduced LPL activity, although replication has been inconsistent (Hubel *et al.* 1999; Y. J. Kim *et al.* 2001; C. Zhang *et al.* 2006). It has also been demonstrated that foetal genotype affects maternal lipoprotein metabolism (Descamps *et al.* 2005).

1.7.2.1 Genome-wide association studies (GWAS)

GWAS use single nucleotide polymorphisms (SNPs) to search for associations across the entire genome. With over 10 million common single nucleotide polymorphisms, identifying those that influence disease susceptibility is challenging (P. R. Burton *et al.* 2007). Linkage disequilibrium allows genotyping of fewer representative tag-single nucleotide polymorphisms, capturing most human genome variation (Lander & Kruglyak 1995; Arngrímsson *et al.* 1999; Moses *et al.* 2000; Zintzaras *et al.* 2006). Focusing on regions linked to diseases helps identify causal variants, often requiring significant re-sequencing. For GWAS to be reliable and useful,

several conditions must be met, including sufficient study power, strict statistical significance thresholds, and appropriate population-based control samples (Mohamad *et al.* 2020). Over 2000 common variations linked to common diseases have been discovered through GWAS, with hundreds successfully replicated. However, small effect sizes in well-replicated GWAS loci emphasize the need for large sample sizes and functional research to clarify molecular mechanisms underlying disease pathology. GWAS for susceptibility DNA changes related to PE are ongoing in various centres, with results eagerly awaited (P. R. Burton *et al.* 2007). These studies have potential implications for understanding complex disorders like bipolar disorder, coronary artery disease, and type 2 diabetes (Mohamad *et al.* 2020)

Chapter 2

Aims and Hypotheses

2. Aims and Hypotheses

2.1 Aims

The human body undergoes drastic changes in its cardiovascular, hormonal, and metabolic system. Maladaptations to pregnancy can be the pointer of underlying, previously undetectable heart disease, making pregnancy a nature's stress test (Sanghavi & Rutherford 2014). Indeed, cardiovascular disease remains the most prevalent non-obstetric cause of death in pregnancy and the postpartum period.

Women who suffered from PE are at increased risk of developing cardiovascular disease and stroke in the future, even years after having had PE (Walker 2000; Sibai et al. 2003; D. W. Brown et al. 2006; Bellamy et al. 2007; Mutter & Karumanchi 2008; Karen Melchiorre et al. 2011; R. Ahmed et al. 2014; Amaral et al. 2015; Ayansina et al. 2016; Tomimatsu et al. 2017; Cho et al. 2019). A study by Hallum et al. (2023) even reported that women who suffered from severe PE were 5 times more likely to have a stroke than those without a preeclamptic pregnancy (Hallum *et al.* 2023).

A thorough comprehension of cardiac structure and function during pregnancy is paramount to enable timely recognition of deviations from normalcy and facilitate appropriate interventions to prevent pregnancy complications such as PE. Echocardiography represents a non-invasive, safe, and accurate method to evaluate cardiac structure and function during pregnancy.

Thus, the primary aim of this study was to determine the cardiovascular adaptation in normal pregnancy and murine models of PE; and to investigate the long-term impact of PE on cardiovascular functions.

Objectives:

- I. To determine the physiologic adaptations in normal pregnancy and two murine models of PE, CSE KO model and sFlt-1 overexpression model, using echocardiography as the principal assessment tool.
- II. To investigate the effects of sFlt-1 overexpression during pregnancy on cardiovascular functions postpartum.
- III. To evaluate:
 - the gene profile associated with CSE KO during pregnancy,
 - the gene profile associated with sFlt-1 overexpression during pregnancy,
 - the genes associated with long-term effects of sFlt-1 overexpression.

2.2 2.2 Hypotheses

- I. Loss of CSE leads to cardiovascular maladaptations during pregnancy without any significant pre-pregnancy differences. A difference in genetic markers can be observed in CSE KO mice when compared to CSE WT mice.
- II. Overexpression of sFlt-1 causes cardiovascular maladaptations during pregnancy.
- III. Overexpression of sFlt-1 leads to long-term cardiovascular changes that can be observed post-partum.

Chapter 3

Materials And Methods

3. Materials and Methods:

To investigate the long-term impact of PE on cardiovascular functions, this study murine models of PE were used. The methods were summarised in Figure 3.1.

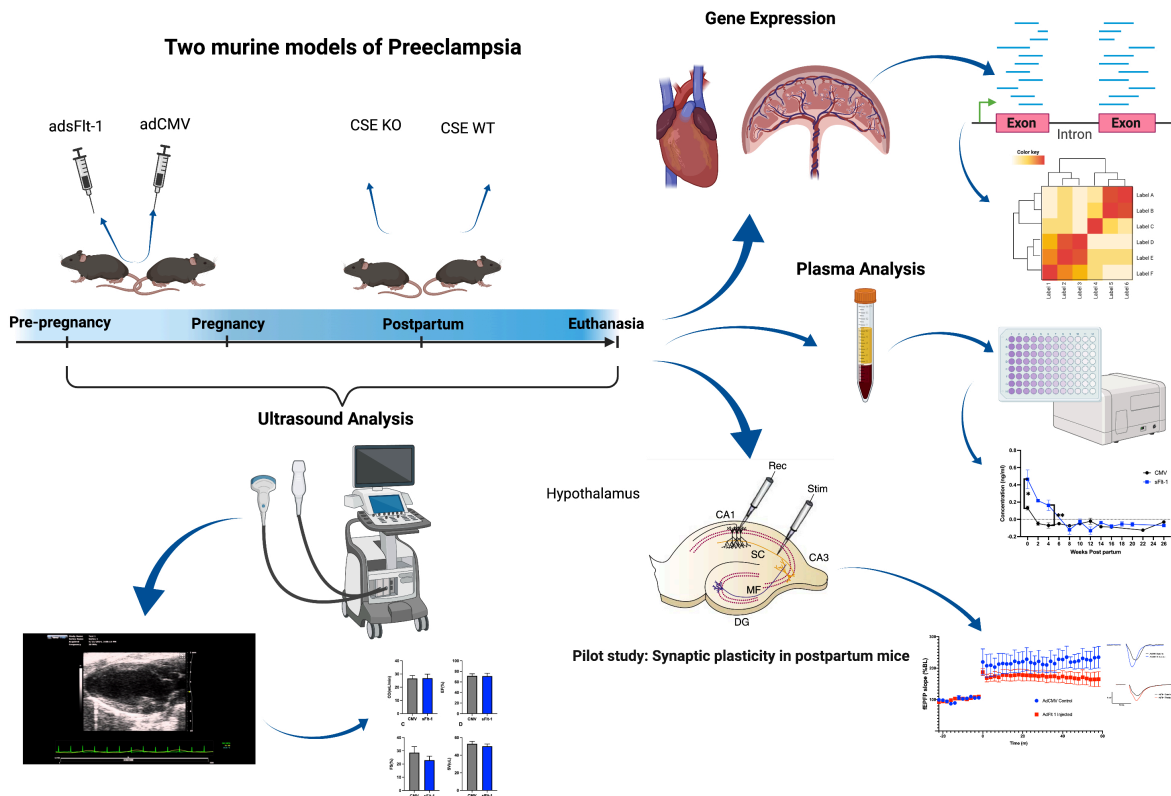


Figure 3.1 Summary of materials and methods.

Figure was created with Bio-render.com.

3.1 Animals:

All experimental mouse work was conducted by following a departmental laboratory induction and completing Home Office licence modules A-C in safe animal handling, anaesthesia and specialised procedures like echocardiography, in accordance with the UK Home Office Animals (Scientific Procedures) Act 1986. All the animal work in this project was conducted in the biomedical research facility at Aston University. The mice were housed at the biomedical research facility at Aston University in well-ventilated cages, with sex-matched littermates (2–

5 mice/cage). This housing of the animals was kept at controlled standard conditions: 12 hours light/dark cycle, 22°C and 55% humidity. All the mice in the experiment were maintained on a normal chow diet unless otherwise mentioned. Food and water were given ad libitum.

3.1.1 Time Mating

Eight- to twelve-week-old female mice were paired with stud males for a period of 12 hours. Following time-mating, the female mice were then separated from the male and housed back into their respective cages. The onset of pregnancy was indicated by E0.5, after which the mice were weighed incrementally. Deviations from the typical growth pattern, such as excessive weight gain, provided evidence of pregnancy in the mice.

3.1.2 Transgenic Model

G. Yang (2008) generously donated the CSE wild-type and knockout mice (CSE WT/CSE KO). The generation of CSE KO mice has already been described (G. Yang et al. 2008b).

3.1.3 Genotyping

Ear clips were taken by our in-house technician from our CSE KO and our CSE wild type (WT) mice. Genotyping was done by lysing the ear clips with 200µl of DirectPCR® lysis reagent containing proteinase K solution (1:100). These samples were then incubated overnight at 37°C to allow for digestion of the tissue. Following the overnight treatment, a further incubation for 45 minutes at 85°C assured for proteinase K deactivation. The digested samples were centrifuged at 12,000 RPM for one minute to pellet remaining debris.

Genotyping was determined using a three-primer assay that was applied across two reactions as previously described (G. Yang et al. 2008b). Target alleles were identified using N1 primer sequence, wild type alleles were identified using the F1 primer. Downstream insertion of the targeted allele (Table S.3.7) was identified using the R1 primer. Reaction 1 contained F1 and R1 primers to successfully identify wildtype mice, while reaction 2 contained N1 and R1 primers to identify the knock-out genotype.

The master mix was prepared by combining primers in equal parts with GoTaq® and nuclease-free water. In PCR reaction tubes, DNA was added (2µl) to 18µl of the master mix. Denaturation at 94°C for 30 seconds, annealing step at 60°C for 35 seconds, and elongation at 72°C for 60 seconds were the thermal cycling conditions. Before cooling to 4°C, this three-temperature cycle strategy was done 30 times. By gel electrophoresis with a 1% agarose gel at 110 volts for an hour in TBE buffer, the resulting PCR products were separated. When examined using the G:BOX Syngene system, the PCR result had 400 bp. The proof of the genotyping is in figure S10.2 (see appendix).

3.1.4 Adenovirus Treatment In Vivo

AdsFlt-1 or an empty vector of cytomegalovirus (AdCMV) was diluted in saline solution to a volume of 100µl at a concentration of 0.5×10^9 PFU/ml.

With the goal of limiting stress on the animal and lowering the chance of miscarriage/total resorption, pregnant mice were led into a mouse restrainer on E10.5. In order to see the blood vessels, a humid warmed tissue was wrapped around the length of the tail. A 0.3ml insulin syringe was used to deliver the virus to the mouse. Prior to injection, the syringe barrel was gently tapped to eliminate all air bubbles. The virus was slowly injected into the bloodstream after the needle was placed into a clearly visible tail vein. For 30 seconds, the puncture location was under pressure to minimise bleeding. To avoid any adverse side effects, mice were monitored for 24 hours following any treatment.

3.2 Mean Arterial Pressure Measurement

3.2.1 Probe Calibration

The bridge amplifier was connected to the Millar Mikro-Tip® pressure catheter. To stabilise the pressure trace in the LabChart® software, the probe was placed in a beaker with distilled water for 30min. Following stabilisation, the probe was gently inserted and fastened onto a T-piece with a plastic dome. The pressure was raised cumulatively between 0 and 180mmHg linked to the same T-piece with plastic dome. In the LabChart® program, the recorded area

was highlighted, and multipoint calibration was chosen. Next, the values were adjusted in accordance with the calibration values.

3.2.2 Data Collection

Mice were given 2% isoflurane (IsoFlo[®]) anaesthesia before being put into the supine position on a heated surface with their extremities restrained with tape. To check the temperature of the body's core, a rectal probe was inserted. To verify sufficient unconsciousness, a pedal reflex test was performed. This was done repeatedly throughout the protocol. There was a minor cut done over the trachea. The carotid artery's surrounding fat and connective tissues were then gently removed to reveal the length of the left vessel.

To protect the vagus nerve, which runs parallel to the carotid artery, it was carefully isolated from the vessel wall. To stop blood flow, a little piece of suture was put in a tight knot at the anterior end of the vessel, avoiding the nerve. At the opposite end of the vessel, a loose knot was tied using a different suture. The posterior of the vessel received one more loop of suture. The extra suture was pulled by the weight of a pair of clamp scissors, which caused the vessel to bend slightly and momentarily cut off the blood flow to a tiny portion of the isolated vessel.

An incision large enough for the Miller-tip pressure catheter probe was made in the vessel using a needle that had been modified to produce a tiny hook. The loose knot was tightened to secure the probe once it was inserted into the vessel. After removing the clamp scissors, a microscope was used to verify that blood flow had come back to the vessel. LabChart[®] was used to measure the mean arterial pressure (MAP), systolic blood pressure (SBP), diastolic blood pressure (DBP), heart rate, and core body temperature in real time. The readings were averaged during a steady 10-minute period during which the subjects' bodies were 37°C and their heart rates were greater than 500BPM. Saline solution was used to maintain moisture in exposed regions.

3.3 Ultrasound Imaging

Ultrasound imaging was performed on CSE KO and CSE WT, pre-gravid (one week before time-mating) and on E17.5. AdsFlt-1 mice and AdCMV mice were monitored via ultrasound imaging on E17.5 and postpartum (table 3.7).

Vevo® 3100 system (VisualSonics, Amsterdam, Netherlands) was used to measure cardiovascular structure and function. The mice were anaesthetised in an induction chamber filled with 3% isoflurane and supplied with 1.5 L/min medical oxygen flow. Once the animals were seemingly unconscious, anaesthesia was confirmed by foot pinch, the animal was transferred to heated platform and its mouth and nose were placed in an anaesthetic mask. The paws were taped to the conductance gel-coated electrode pads on the heating platform. To keep eyes moist while under anaesthesia, eye cream was administered. The heart rate was kept at 450 ± 50 BPM. To control the temperature of the body's core, a lubricated rectal probe was inserted. Depilatory cream (Nair) was used to remove hair from the chest and abdomen. Pre-warmed ultrasonic gel was applied after hair was removed and the scanning region was cleansed with water to prevent the introduction of bubbles. Ultrasound imaging was performed at different time points (table 3.7).

3.3.1 Parasternal Long Axis and Left Mid-papillary Short Axis of the Heart

The stage was slightly inclined to the left once the mouse was securely placed on the hot platform, exposing the left side of the chest to the probe. The mouse sternum served as the guide as the probe was lowered into the ultrasound gel until the heart was visible on the display. The probe was progressively rotated anticlockwise after finding the aorta until the entire heart's apex was seen. Both standard B mode pictures and electrocardiogram-gated kilohertz visualisation (EKV) images were captured. Figure 3.2A depicts the diastolic profile from the parasternal long axis view, while Figure 3.2B depicts the systolic profile. LV trace analysis was performed by tracing the heart wall while utilising Vevo® labs software.

The short axis of the heart was then scanned after acquiring the parasternal long axis. The mouse remained in place while the probe was turned 90° (Figure 3.2C). For upcoming analysis, the same measurements were taken once more.

| LABEL | DESCRIPTION | UNITS | FORMULA |
|--------------|----------------------|--------------|-----------------------------------------------------------|
| EDV | End Diastolic Volume | μl | $\left(\frac{7.0}{2.4 + LVID; d}\right) \times LVID; d^3$ |
| ESV | End Systolic Volume | μl | $\left(\frac{7.0}{2.4 + LVID; s}\right) \times LVID; s^3$ |

Table 3.1 B-Mode Measurements using Parasternal Long Axis View (PSLAX).

This table was adapted from the Vevo® Lab user manual.

3.3.2 M-Mode

M-mode analysis was chosen on the Vevo® 3100 system once the probe was correctly positioned over the short axis of the cardiac region (Figure 3.2 C). This provided a cross-sectional image for calculating the end diastolic (EDV) and end systolic volume (ESV) (Table 3.2). The intraventricular septum (IVS) left ventricle internal diameter (LVID), and left ventricle posterior wall (LVPW) are the distance measures produced by this model (Figure 3.2D). The cubic formula used to compute the LV mass using M-mode analysis is shown in Table 3.3.

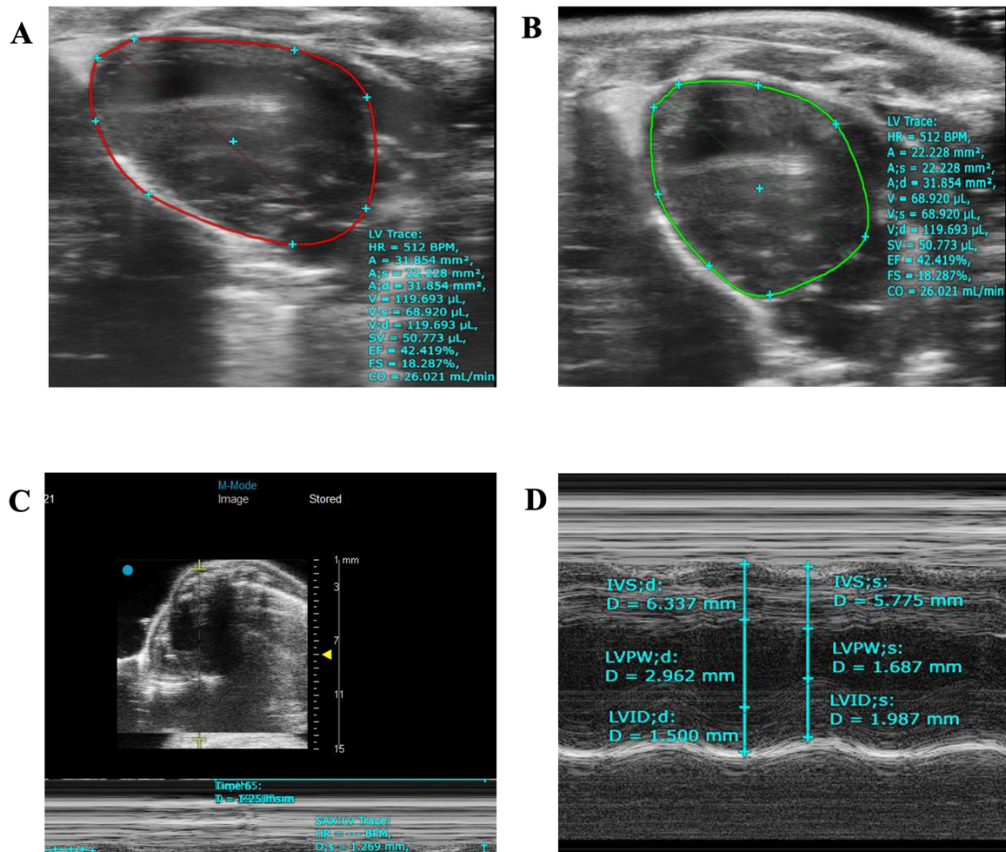


Figure 3.2 Echocardiography analysis. Echocardiography analysis.

(A) Diastolic long axis image of the heart. Red line represents the internal wall. (B) Systolic long axis image of the heart (green line represents the internal wall). (C) To capture the short axis view of the heart, the probe was turned 90 degrees clockwise around its axis. (D) A cross sectional image of the heart's outer walls was taken in M-mode. Different distance measurements were assessed. IVS; Interventricular septum, LVID; Left ventricle internal diameter, LVPW; Left ventricle posterior wall, d; diastole, s; systole.

| Label | Description | Units | Generic Type | Mode | Chain |
|-------|------------------------------------|-------|--------------|--------|--------|
| IVS;d | Interventricular Septum (diastole) | mm | Depth | M-Mode | LVID;d |
| IVS;s | Interventricular Septum (systole) | mm | Depth | M-Mode | LVID;s |

| | | | | | |
|--------|-----------------------------------------------|----|-------|--------|---------|
| LVID;d | Left ventricular internal diameter (diastole) | mm | Depth | M-Mode | LVPW;d |
| LVID;s | Left ventricular internal diameter (systole) | mm | Depth | M-Mode | LVPW;s |
| LVPW;d | Left ventricular posterior wall (diastole) | mm | Depth | M-Mode | |
| LVPW;s | Left ventricular posterior wall (systole) | mm | Depth | M-Mode | |
| LW;d | Left ventricular lateral wall (diastole) | mm | Depth | M-Mode | LV Mass |
| LW;s | Left ventricular lateral wall (systole) | mm | Depth | M-Mode | LV Mass |

Table 3.2 Short Axis View (SAX) Measurements.

This table was adapted from the Vevo® Lab user manual.

| Label | Description | Units | Formula |
|--------------------|------------------------------|-------|-----------------------------------------------------------|
| LV Mass | LV Mass Uncorrected (M-mode) | mg | $1.053 \times [(LVID; d + LW; d + IVS; d)^3 - LVID; d^3]$ |
| LV Mass Correction | LV Mass Corrected (M-Mode) | mg | $AM - LV Mass \times 0.8$ |

Table 3.3: Anatomical M-Mode Left Ventricle Calculations.

This table was adapted from the Vevo® Lab user manual.

3.3.3 B-Mode

Following on from the M-mode image acquisitions, the B-Mode was selected on the Vevo® 3100 system.

3.3.3.1 Simpson's

Simpson's calculations and measurements were used to calculate different parameters (Table 3.4), as this allows for greater precision in situations where the heart geometry is abnormal or altering over time, this enables greater precision. These measurements were taken on B-Mode images of the heart, using one long axis view (Figure 3.3D) and three short axis views evenly spaced around a mid-level view (Figure 3.3A) at the papillary muscles, one toward the apex or distal portion of the heart (Figure 3.3B), and one toward the base or proximal portion of the heart (Figure 3.3C). All of these measurements were taken both during systole and diastole allowing for parameters such as the cardiac output (CO) (Table 3.4), the stroke volume (SV), the ejection fraction (EF) and the fraction shortening (FS).

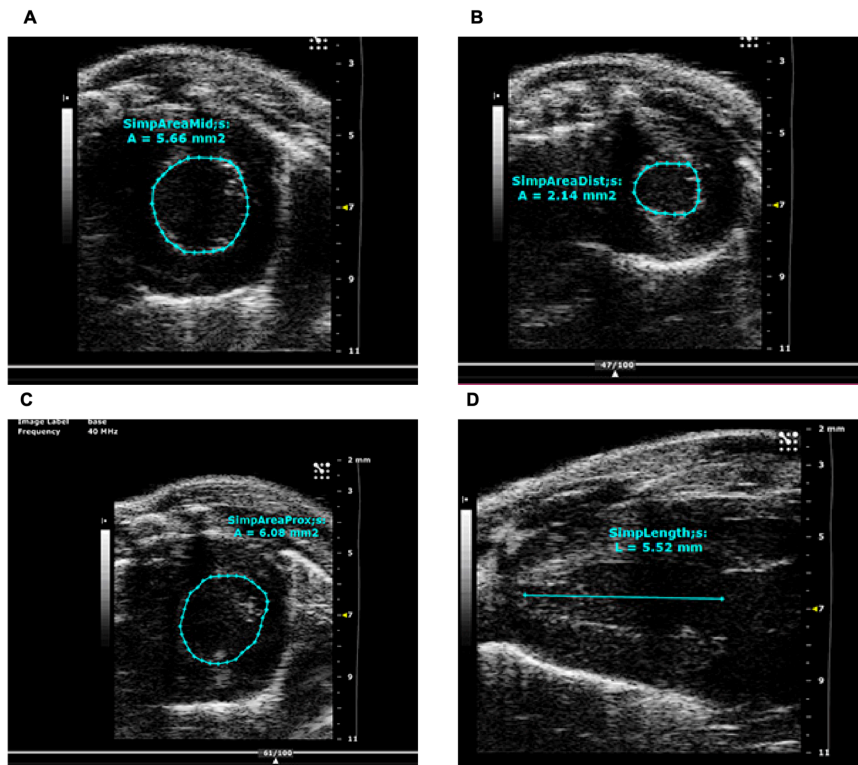


Figure 3.3 Simpson's measurements in M-mode SAX.

(A) short axis views around a mid-level view was taken during systole and diastole (diastole not pictured). (B) short axis views around distal portion of the heart were taken during systole and diastole (diastole not pictured). (C) short axis views around apex or distal portion of the heart were taken during systole and diastole (diastole not pictured). (D) Long axis view was taken during systole and diastole (diastole not pictured).

| Label | Description | Units | Formula |
|----------|--------------------------------|---------------|-----------------------------------------------------------------------------------------------------------------------------------------------------------------------------|
| Volume;d | Volume calculation in diastole | μL | $ \begin{aligned} & (Simp\ Area\ Dist; d \\ & + Simp\ Area\ Mid; d \\ & + Simp\ Area\ Prox; d) \times \frac{h}{3} \end{aligned} $ <p>h=Simpson Length in diastole</p> |

| | | | |
|----------|-------------------------------|---------------|------------------------------------------------------------------------------------------------------|
| Volume;s | Volume Calculation in systole | μL | $(\text{Simp Area Dist}; s + \text{Simp Area Mid}; s + \text{Simp Area Prox}; s) \times \frac{h}{3}$ |
| SV | Stroke Volume | μL | $\text{Volume}; d - \text{Volume}; s$ |
| EF | Ejection Fraction | % | $100 \times \left(\frac{SV}{\text{Volume}; d} \right)$ |
| FS | Fraction Shortening | % | $100 \times \left(\frac{\text{Length}; d - \text{Length}; s}{\text{Length}; d} \right)$ |
| CO | Cardiac output | mL/min | $\frac{SV \times \text{Heart Rate}}{1000}$ |

Table 3.4: Simpson’s Calculations and formulas in M-mode.

This table was adapted from the Vevo[®] Lab user manual.

3.3.4 Mitral Inflow

Mitral inflow was assessed to gauge cardiac diastolic function. The platform was then positioned in the Trendelenburg position (feet 15–30 degrees higher than the head) after the imaging of the left papillary short axis view of the heart. The probe was kept in the same orientation, but the overall placement was changed to align with the apex of the heart and follow the plane of the chest rather than the sternum.

Blood flow across the mitral valve was measured using colour Doppler. EKV mode was used to photograph the valve's movement. The measurement gate was positioned over the region where the open tip of the valve would have touched. Based on the flow angle and the location of the heart, the angle was fixed at vertical $\pm 10^\circ$ (Figure 3.4A). The isovolumetric contraction time (IVCT), isovolumetric relaxation time (IVRT), and aortic ejection time (AET) were obtained

from this Doppler waveform using Vevo® laboratories software, and the myocardial performance index (MPI) was calculated using Equation 3. The velocities were also measured (Figure 3.4A) if distinct E (early filling velocity) and A (late filling velocity) peaks were discernible.

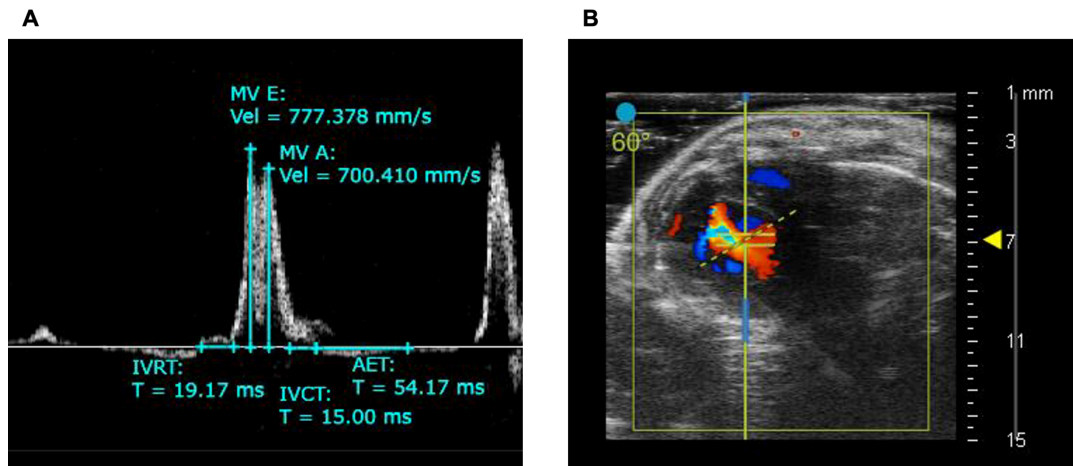


Figure 3.4 Mitral Flow Measurements.

(A) Illustration of the mitral flow Isovolumetric contraction time, isovolumetric relaxation time, and aortic ejection time are all terms used in the Doppler waveform. (B) A depiction of the mitral valve. Waveform for Doppler. Doppler colour image of blood flow across the mitral valve with a yellow gate across it.

| Label | Description | Units | Formula |
|------------|-------------------------------------------------------|-------|---------------------------|
| MV E/A | Mitral Valve E to A ratio (Power Doppler Mode) | | $\frac{MV E}{MV A}$ |
| LV MPI NFT | Left Ventricle Myocardial Performance | | $\frac{NFT - AET}{AET}$ |
| LV MPI IV | Left Ventricle Performance Index (PW Doppler Mode) | | $\frac{IVRT + IVCT}{AET}$ |

| | | | |
|--------|----------------------------------------|----|-----------------------------------|
| MV PHT | MV Area (simplified) (PW Doppler Mode) | ms | 0.29 × <i>MV Decel in time</i> |
|--------|----------------------------------------|----|-----------------------------------|

Table 3.5: Mitral Flow Calculations and Formular.

This table was adapted from the Vevo[®] Lab user manual.

3.3.5 Uterine Artery

The uterine artery was originally located using the bladder as a landmark (Figure 3.5C). In both pregnant, non-pregnant and postpartum mice, uterine artery blood flow was visualised using the colour Doppler mode. The relevant flow was gated in the direction of the flow and at an angle greater than 40° after the flow had been located. Power Doppler mode was then applied. Using Vevo[®] Labs software, the resistance index and pulsatility index (Table 3.6) were determined (Figure 3.5A-B).

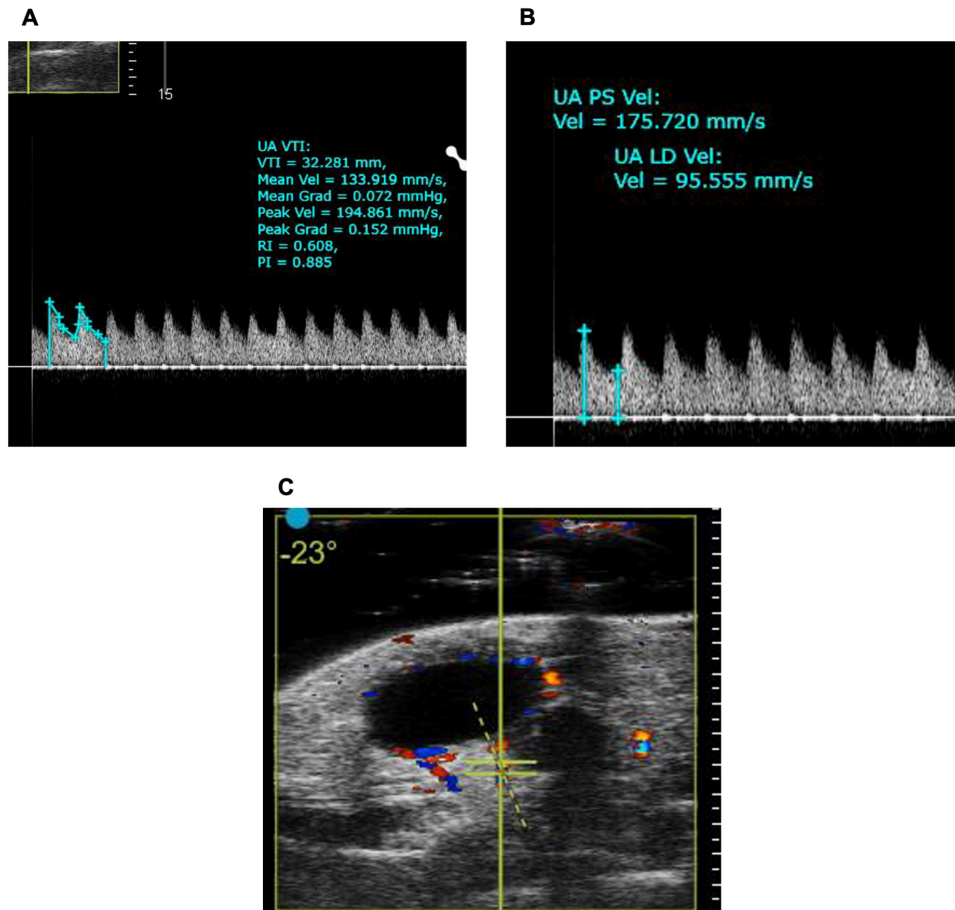


Figure 3.5 Typical illustrations of uterine artery measurements.

(A) Illustration of a single cardiac cycle used to determine the mean velocity. **(B)** A typical uterine artery flow Doppler waveform. **(C)** The uterine artery is located using the bladder as a preliminary.

| Label | Description | Formula |
|-------|----------------------------------|------------------------------------------------|
| UT RI | Uterine Artery Resistive Index | $\frac{UT\ PSV - UT\ EDV}{UT\ PSV}$ |
| UT PI | Uterine Artery Pulsatility Index | $\frac{UT\ PSV - UT\ EDV}{UT\ VTI\ Mean\ Vel}$ |

Table 3.6: Umbilical Arteries Calculations and Formulas.

This table was adapted from the Vevo[®] Lab user manual.

3.4 Tissue Collection

3.4.1 Plasma isolation

Following mean arterial pressure measurement, a cardiac puncture was performed to collect blood. Below the ribcage, at a small inclination to the left of the sternum, a needle and syringe were slowly inserted. Then, to prevent clotting, blood was drawn and put into a blood collection tube coated with EDTA (Ethylenediaminetetraacetic Acid). To separate cells from plasma, whole blood was centrifuged at 10,000 RPM for 10 minutes. The resultant supernatant was taken out and kept at -80°C for future analysis.

3.4.2 Tissue Collection post-euthanasia

Animals were euthanised through cervical dislocation. A cut was made in the abdomen to reveal the mesentery. The organs were painstakingly dissected, cut into sections, and either stored in 4% paraformaldehyde for further histological staining or into dry ice for later molecular testing. The kidneys, liver, placenta (if appropriate), heart and brain were also collected.

3.4.3 Interval in-vivo Blood Collection

Blood was collected via tail vein at different time points (table 3.7). The animal was anaesthetised in an induction chamber filled with 3% isoflurane and supplied with 1.5 L/min medical oxygen flow. Once the animal was seemingly unconscious, anaesthesia was confirmed by foot pinch, the animal was transferred to a flat surface and its mouth and nose were placed in an anaesthetic mask. Similarly, to the procedure for injection, a humid warmed tissue was wrapped around the length of the tail. Once the tail vein was located a small incision (± 3 mm) was made and 2-3 droplets of blood were collected into a blood collection tube coated with EDTA (Ethylenediaminetetraacetic acid) to prevent clotting. To separate cells from plasma, whole blood was centrifuged at 10,000 RPM for 10 minutes. The resultant supernatant was taken out and kept at -80°C until further analysis.

| Time Point | Tissue type collected | Analysis conducted | | | |
|---------------------------------|-----------------------|--------------------|------------|-----------------|-----------|
| | | ELISA | Ultrasound | Gene expression | CSE model |
| Pre-pregnancy (8-week-old mice) | Plasma | ELISA | Ultrasound | Gene expression | CSE model |
| E17.5 | Plasma | ELISA | Ultrasound | Gene expression | CSE model |
| 7 days Postpartum | Plasma | ELISA | Ultrasound | / | / |
| 2 weeks postpartum | Plasma | ELISA | Ultrasound | / | / |
| 4 weeks postpartum | Plasma | ELISA | Ultrasound | / | / |
| 8 weeks postpartum | Plasma | ELISA | Ultrasound | / | / |
| 10 weeks postpartum | Plasma | ELISA | Ultrasound | / | / |
| 12 weeks postpartum | Plasma | ELISA | Ultrasound | / | / |
| 14 weeks postpartum | Plasma | ELISA | Ultrasound | / | / |
| 16 weeks postpartum | Plasma | ELISA | Ultrasound | / | / |
| 18 weeks postpartum | Plasma | ELISA | Ultrasound | / | / |
| 20 weeks postpartum | Plasma | ELISA | Ultrasound | / | / |
| 30 weeks postpartum | / | / | Ultrasound | / | / |
| 32 weeks postpartum | / | / | Ultrasound | / | / |
| 36 weeks postpartum | / | / | Ultrasound | Gene expression | / |
| 40 weeks postpartum | / | / | Ultrasound | / | / |

Table 3.7: Tissue collection and analysis for a given time point.

3.5 ELISA

Using the sandwich Enzyme-Linked Immunosorbent Assay (ELISA), the presence of sFlt-1 in plasma was determined for different time points. The mouse sFlt-1 DuoSet (DY471) (R&D Systems, Minnesota, US) was used to analyse sFlt-1 in the plasma in accordance with the manufacturer's recommendations.

In accordance with the manufacturer's guidelines, the recombinant sFlt-1 standard was reconstituted in distilled water to a stock concentration. Then, a seven-point standard curve was created using a two-fold serial dilution in the kit's provided reagent diluent. A microplate spectrophotometer was used to transfer the plate and read the optical density at 450 nm. The reading was corrected for wavelength, bringing it to 540 nm. By computing an unknown sample concentration and producing a four-parameter logistic (4-PL) curve-fit, the standard curve was produced.

3.6 Gene Expression

3.6.1 RNA Isolation

In 700 μ l of QIAzol reagent, following the manufacturer's instructions, total RNA from previously obtained tissues was isolated using a Qiagen miRNeasy isolation kit. Snap-frozen tissues previously collected, were cut using a scalpel, weighed (about 30 mg) and mechanically homogenised using ceramic beads. After homogenization, Qiagen QIAshredder columns were used to perform a full-speed centrifugation of the lysate to eliminate any potentially harmful material. The resulting flow-through was taken out and combined in clean Eppendorf tubes with 140 μ l of chloroform. Each sample was vortexed for 15 seconds at its highest setting. After two minutes at ambient temperature, samples were centrifuged at 12,000 RPM for 15 minutes.

Total RNA was isolated using the miRNeasy isolation kit (Qiagen) in accordance with the manufacturer's instructions. A clean Eppendorf tube was used to collect the ensuing supernatant's clear phase, which was then combined with 1.5 litres of 100% ethanol. 700 μ l of

the solution was put to the available columns after the solution was gently mixed using repeated pipetting. These columns were centrifuged for 15 seconds at 10,000 RPM, and the resulting runoff was thrown away. After adding 700 μ l of RWT severe washing buffer to the column, the centrifugation procedure was repeated, and the runoff was discarded. To eliminate any remaining salts in the spin columns, 500 μ l of RPE buffer, a mild washing buffer, was added to the spin columns and centrifuged for an additional 15 seconds at 10,000 RPM. Runoff was removed. A second time (500 μ l) of RPE buffer was added, and the spin columns were centrifuged for two minutes at 10,000 RPM. The spin columns were withdrawn from their collection tubes once this portion of the protocol was finished, and fresh collection tubes were used to collect any liquid that was left over after the membrane-drying stage (centrifuge at full speed for one minute).

To enable RNA collection after membrane drying, spin columns were added to clean Eppendorf tubes. To elute the RNA, 25 μ l of RNase-free water was added. The centrifuge was run at 10,000 RPM for one minute. To obtain a higher RNA concentration, eluted RNA was once again passed through the column (final centrifugation repeated).

The resultant concentration (ng/ml) prepared for cDNA reverse transcription was measured using a NanoDrop™ 1000/1000c (Thermo Fisher Scientific, Loughborough, UK). The 260/230 ratio served as a measure of the RNA purity after extraction. The predicted range for the value was 2.0–2.2. When the sample values were below this ratio, the sample was rejected because of contamination.

3.6.2 cDNA Synthesis

The concentrations obtained from the NanoDrop™ were used to calculate the volume of RNA needed to result in a concentration of 1 μ g. The kit components were kept on ice and were centrifuged prior to use. The cDNA synthesis was completed according to the manufacturer's (Evoscript Roche) instructions. A consistent 4 μ l volume of reaction buffer, which contained the appropriate primers, dNTPs, oligo(dT)18, and Mg(OAc)₂, was added to each PCR reaction

tube. For each sample, a total volume of 18 μ l was created by adding the specified amount of extracted RNA and RNase-free water. After centrifuging the final mixes to make sure all the ingredients were combined, they were placed on ice for five minutes to allow the primers to anneal to the template. Each PCR tube received 2 μ l of the enzyme mixture before being quickly centrifuged once more. The cDNA was produced using the manufacturer's recommended standard reverse transcription technique. The samples were heated to 65°C for 30 minutes and then cooled to 4°C as part of this.

3.6.3 Quantitative polymerase chain reaction (qPCR)

The lyophilised reverse and forward primers (Table S1.3 & S1.4) were reconstituted to a final concentration of 100 μ M. Master mixes for each gene of interest, including housekeeping genes such as Actin were made using a ratio of 1:1. The master mixes each contained 3.8 μ l of RNase-free water, 0.2 μ l of primer working stock, and 5 μ l of LightCycler® 480 SYBR Green I master, containing DNA polymerase and double strand specific dye (Roche). The master mix was then loaded into a 386 well plate, prior to loading the cDNA or the respective reaction standard. Each sample was loaded in duplicate for each gene of interest. Prior to centrifugation at 2400 RPM for one minute at 4°C, the plate was covered with a sterile adhesive foil. The qPCR plates were then loaded onto the thermocycler Roche LightCycler® 480 and the qPCR reaction was carried out using the following parameters: pre-incubation at 95°C for one cycle, amplification at 95°C for 45 cycles. A table S1.4 with the primers used can be found in the appendix B.

3.6.4 mRNA Sequencing

The "next generation sequencing" or "deep sequencing" approach, in which millions of cDNA fragments are processed in parallel, is the foundation for transcriptome profiling method known as RNA-seq. The previously extracted heart and placenta tissue samples were processed by Novogene (Novogene Ltd, Cambridge, UK) for RNA sequencing. The exact protocol for the Novogene (UK) Ltd (Cambridge) sequencing can be found in Appendix C.

3.6.4.1 Data Analysis

The pre-analysed (by Novogene) mRNA sequencing results were obtained in the form of Excel sheets. An initial screening of all the group comparisons and (significantly) differently expressed genes was completed. Further analysis of mRNA sequencing results was conducted using the cloud-based after-sales analysis tool NovoMagic[®] (independently created) by Novogene. Re-analysis and customization of the Novogene analysis results was done using the NovoMagic[®]. Additional analysis included looking at gene groups, examining gene expression, and finding genes that are differentially expressed.

3.7 Statistical analysis

Cell experiments were repeated at least three times and results are presented as mean \pm S.E.M. All *in vivo* experiments contain data from at least five animals unless stated and data are presented as mean \pm S.E.M. Statistical significance was calculated using Mann Whitney test for non-parametric data or Two-way ANOVA using GraphPad Prism 9 software (GraphPad, California, USA). $P < 0.05$ was considered statistically significant.

Chapter 4

Cardiac changes during pregnancy
in preeclampsia model – sFlt-1
overexpression model

4. Cardiac changes during pregnancy in PE model – sFlt-1 overexpression model

4.1 Background

During a healthy pregnancy, the cardiovascular system undergoes significant adaptations to accommodate the increased metabolic needs of both the mother and the foetus, as well as provide adequate uteroplacental circulation for foetal growth and development. These adaptations begin around the fourth to fifth week of gestation and persist for up to one year after delivery as per several reports (Capeless & Clapp 1991; Clapp & Capeless 1997; Desai et al. 2004; Hall et al. 2011; Karen Melchiorre, Sharma, et al. 2012). These changes include rises in arterial elasticity (Papaioannou *et al.* 2014), and CO, decreases in blood pressure and total systemic vascular resistance (Hall *et al.* 2011; Sanghavi & Rutherford 2014). The mean blood pressure steadily decreases during pregnancy, with the highest drop occurring between 16 and 20 weeks, followed by an increase towards pre-pregnancy levels in the middle of the third trimester (Hall *et al.* 2011; Sanghavi & Rutherford 2014).

Despite the immense research with regards to the onset of these cardiovascular alterations in various papers, the scientific community lacks consensus on their initiation, duration, and magnitude, owing to uncorrected maternal characteristic variables, differences in estimation techniques, and the use of baseline values from either the first trimester or postpartum (S. C. Robson et al. 1987, 1989; Hunter & Robson 1992b; Clapp & Capeless 1997).

However, maladaptations during pregnancy can reveal underlying, previously undetectable heart disease, making pregnancy a nature's stress test (Sanghavi & Rutherford 2014). Thus, it is important to understand and pinpoint the normal adaptations to pregnancy in order to manage women with cardiovascular disease during pregnancy (Hunter & Robson 1992b). PE and intrauterine growth restriction are examples of disorders related to maladaptations during pregnancy that can cause maternal and foetal morbidity if they are not treated.

PE is a multisystem illness that affects 3-5% of all pregnancies and is one of the leading causes of maternal morbidity (9-26% maternal deaths) and mortality in women (Garrido-Gimenez *et al.* 2020; Shahd A. Karrar & Peter L. Hong. 2023). Although decades of research have improved knowledge of clinical risk factors and genetic predispositions, the exact pathophysiology of PE is still unknown. Over the years, different hypotheses as to the cause for PE have been suggested, including: angiogenic imbalance (physiological balance between the stimulatory and inhibitory signals for blood vessel growth) (I. Brosens 1964; Hoeben *et al.* 2004; S. Maynard *et al.* 2008; Rana *et al.* 2012; Burke & Ananth Karumanchi 2013; Atakul 2019) , systemic inflammation (Raghupathy 2013; Candela *et al.* 2017; J. Hu *et al.* 2019; Stojanovska *et al.* 2019) and oxidative stress (J. M. Roberts & Escudero 2012; Barneo-Caragol *et al.* 2019; Doganlar *et al.* 2019; Haram *et al.* 2019). Nonetheless, over the years, especially within the 21st century, research has started to point fingers at angiogenic imbalance, as the main culprit for it being a significant factor in the development of PE (Ramma & Ahmed 2011a; A. Ahmed & Ramma 2015).

Soluble Fms-like tyrosine kinase receptor-1 (sFlt-1), a soluble form of vascular endothelial growth factor receptor 1 (VEGFR-1), is an anti-angiogenic protein released by the placenta during pregnancy. This anti-angiogenic factor binds to VEGF or placental growth factor (PlGF) and impedes VEGF-signalling by acting as a decoy receptor, preventing VEGF-mediated pro-angiogenic effects. Although maternal circulating sFlt-1 levels rise during normal pregnancy, they are significantly higher in PE than normal pregnancy before the onset of the disease. Studies have shown that the presence of sFlt-1 is associated with the development of PE as a splice variant of membrane-bound VEGFR-1 that inhibits the activity of pro-angiogenic VEGF and PlGF, resulting in endothelial dysfunction (J. M. Roberts *et al.* 1989; James Roberts 1998; Kroll & Waltenberger 2000; Boeldt & Bird 2017). Additionally, an increase sFlt-1 was shown to be present even before the onset of the clinical signs of PE (Levine *et al.* 2005). However, a severe PE phenotype could not be induced solely by the presence of sFlt-1; it required the administration of anti-angiogenic soluble endoglin to pregnant rats (S. E. Maynard, Min, Merchan, Lim, Li, Mondal, Libermann, Morgan, *et al.* 2003; Ramma & Ahmed 2011a). This caused endothelial dysfunction that led to the development of a severe PE-like phenotype, including HELLP syndrome, according to Venkatesha (2006) (Venkatesha *et al.* 2006; Walshe, Dole, *et al.* 2009; Walshe, Saint-Geniez, *et al.* 2009). Another study by Vogtmann *et al.* (2021) using double-transgenic hsFLT1/rtTA dams showed that pregnant

mice overexpressing sFit-1 developed hypertension, aortic wall thickening, and elastin breakdown, glomerular endotheliosis, podocyte damage, proteinuria and growth restriction (Vogtmann *et al.* 2019, 2021).

We hypothesised that the administration of adenovirus overexpressing sFit-1 during pregnancy would cause PE-like symptoms to appear alongside cardiac maladaptations to pregnancy. To test this hypothesis, C57BL/6j pregnant mice were given adenoviral vectors that encoded either with sFit-1 (AdsFit-1) or a blank vector of Cytomegalovirus (AdCMV) on embryonic day 10.5. Their pregnancy outcomes were assessed, including vascular function, on embryonic day 17.5. To monitor cardiac adaptations, ultrasound scans were performed pre-pregnancy and during pregnancy. Circulating sFit-1 was measured in plasma during pregnancy and postpartum.

4.2 4.2 Normotensive Pregnancy Adaptations

To confirm the adaptations in a normotensive pregnancy, 8- to 12-week-old, pre-gravid and pregnant mice at E17.5, were scanned.

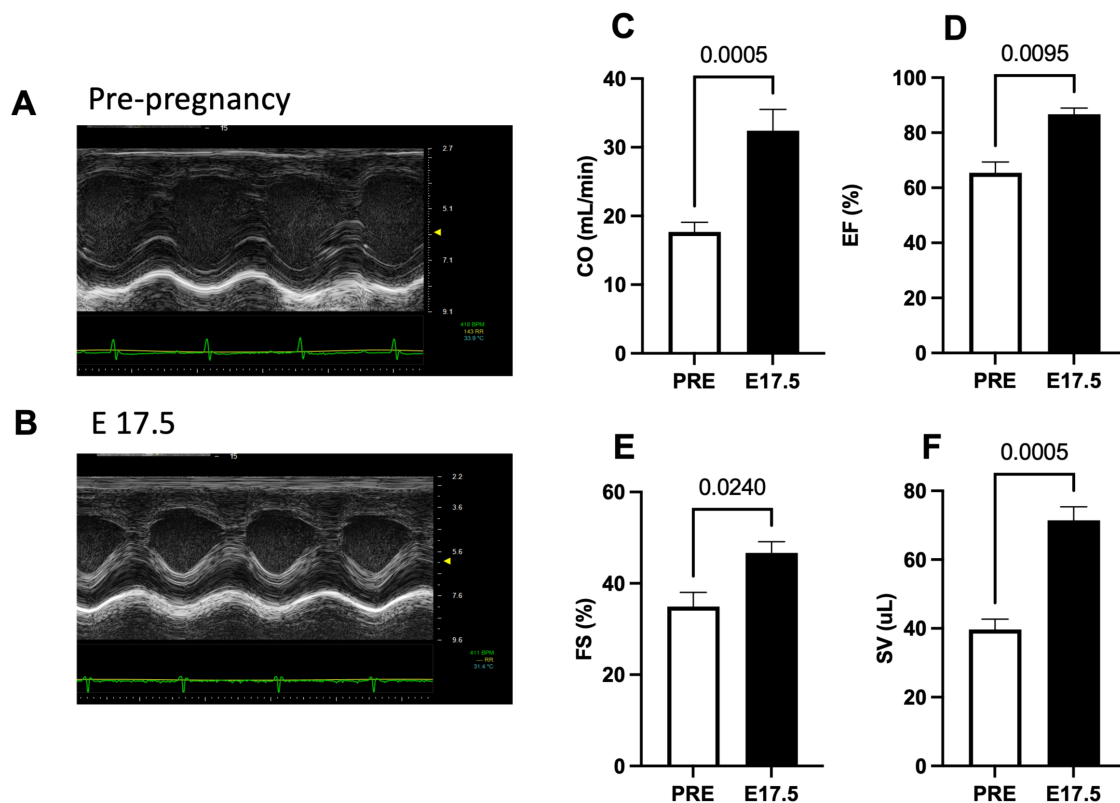


Figure 4.1 Systolic functions of left ventricle in pre-gravid and pregnant mice at E17.5.

Representative M-mode images of the heart in parasternal long axis view of pre-gravid (**A**) and pregnant mice at E17.5 (**B**). Ultrasound analysis was carried out on pre-gravid mice and on pregnant mice at E17.5 (n=6/group). Different measurements were taken: cardiac output (**C**) was significantly increased in the pregnant mice when comparing to the pre-gravid mice, the ejection fraction (**D**) was significantly increased in the pregnant mice when comparing to the pre-gravid mice, the fraction shortening (**E**) as significantly increased in the pregnant mice when comparing to the pre-gravid mice, and stroke volume (n=6) (**F**) was significantly decreased during pregnancy when comparing to the pre-gravid mice. Statistical comparison was performed using Mann Whitney test.

As expected, an increase in CO, FS, and SV was seen during pregnancy, simulating what has been reported in the literature of normotensive pregnancies.

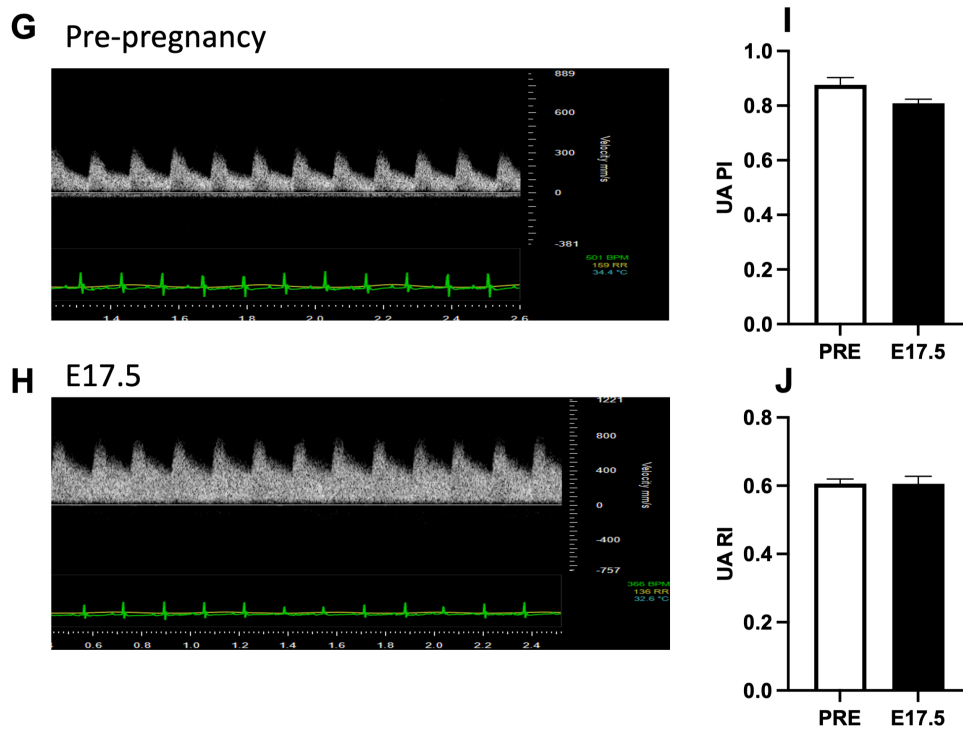


Figure 4.2 Uterine artery flow in pre-gravid and pregnant mice at E.17.5.

Representative Doppler waveforms from pre-gravid mice (**G**) and on E17.5 of pregnancy (**H**). Uterine artery flow was measured on E17.5 on both sFlt-1 and CMV injected group (n=8/group). Resistive index (RI) (**J**) and pulsatility index (PI) (**I**) remained unchanged in both groups. *Statistical comparison was performed using Mann Whitney test. Neither of these measurements were significantly different.

No significant difference was seen in the uterine artery flow. However, from the representative Doppler waveforms images from pre-gravid mice (Figure 4.2G) and pregnant mice (Figure 4.2H) a difference can be observed.

Overall, the adaptations seen in mice from pre-gravid to pregnant mice correspond to what has been described in the literature.

4.3 Overexpression of sFlt-1 in pregnancy increases maternal blood pressure and decreases foetal weight.

The main symptom of PE is hypertension plus the involvement of at least one organ system (Trogstad et al. 2011; Lambert et al. 2014; Tranquilli et al. 2014; Fatmeh & Farahnaz 2018; Mark A. Brown et al. 2018). To substantiate earlier findings and confirm the validity of this sFlt-1 model of PE, mean arterial pressure was measured on embryonic day 17.5 via carotid artery ligation using a Millar tip catheter.

Overexpression of sFlt-1 resulted in a significantly higher mean arterial blood pressure (MAP) in pregnant mice when compared to the control (AdCMV) pregnant mice (Figure 4.3A) indicating that sFlt-1 overexpression induced PE-like symptoms, which is in consistent with previous published research (S. E. Maynard et al. 2003; Amraoui et al. 2014; Szalai et al. 2014, 2015; Vogtmann et al. 2019, 2021; Walentowicz-Sadlecka, Domaracki, Sadlecki, Siodmiak, Grabiec, Walentowicz, Moliz, & Odrowaz-Sypniewska 2019).

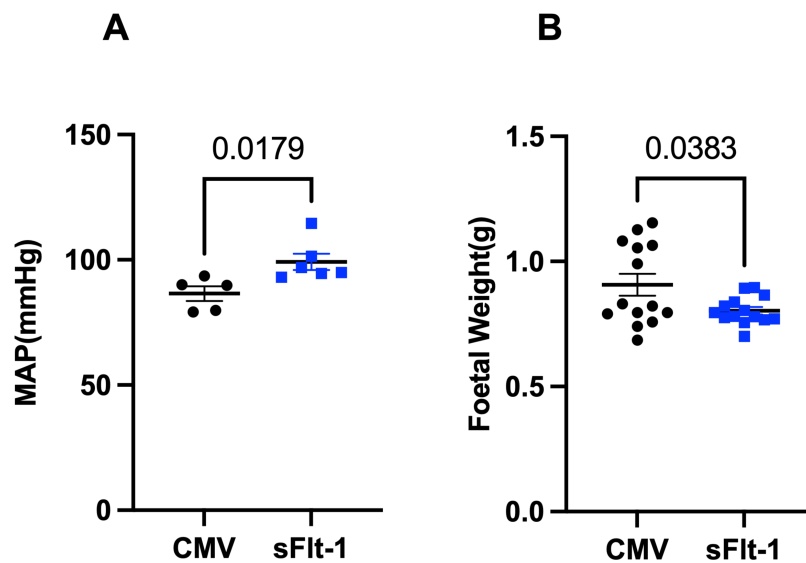


Figure 4.3 Mean arterial blood pressure (MAP) in the mother and foetal weight was recorded.

(A) A significant increase in blood pressure was observed in sFlt-1 mice compared to CMV. This was done using carotid artery ligation and Millar Tip catheter on E17.5 of pregnancy in both CMV (n=5) and sFlt-1 mice (n=6). **(B)** Foetal weight was recorded for both groups at E17.5. A significant decrease in foetal weight was observed in the sFlt-1 mice (n=14) compared to the CMV mice (n=14). Data are expressed as mean \pm S.E.M. Statistical comparison was performed using Mann Whitney test.

Foetal growth restriction can often be associated with PE or pregnancy maladaptations (Duvekot et al. 1995; S. E. Maynard et al. 2003; Jansson & Powell 2006; P. J. Williams et al. 2009; Browne et al. 2015; Graham J. Burton & Jauniaux 2018; Tay et al. 2018; Youssef & Crispi 2020; Sławek-Szmyt et al. 2022). As expected, a significant decrease in foetal weight at E17.5 was seen in AdsFlt-1 pregnant mice, when compared to the AdCMV pregnant mice (Figure 4.3B).

These results of the mean arterial pressure together with those of foetal weight, demonstrate that this adenoviral sFlt-1 overexpression model is a suitable model to study changes associated to PE.

4.3.1 sFlt-1 overexpression was successful.

Circulating sFlt-1 level in the plasma samples taken from AdsFlt-1 and AdCMV injected mice at E17.5 were measured to confirm the success of sFlt-1 overexpression via adenoviral injection in mice prior at E10.5. As anticipated, a significant increase in sFlt-1 level was detected in AdsFlt-1 mice compared to AdCMV mice. This result indicates successful overexpression of sFlt-1 in AdsFlt-1 mice.

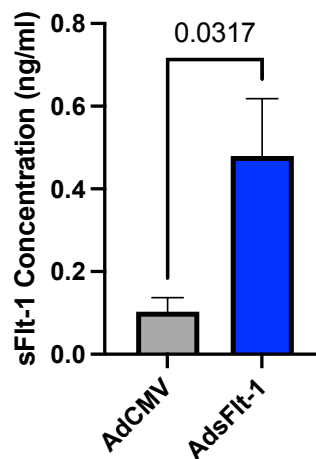


Figure 4.4 ELISA assay for plasma sFlt-1 level measurement.

Plasma samples (n=6/group) were collected at E17.5 during pregnancy. The sFlt-1 level in AdsFlt-1 mice was significantly higher when compared to the AdCMV pregnant mice. Mann-Whitney test was used for statistical analysis. Data are expressed as mean \pm S.E.M.

The findings indicated that the sFlt-1 level remained significantly higher during this time, which confirmed the continued overexpression of sFlt-1 in AdsFlt-1 mice. Mice with low sFlt-1 were considered to have had unsuccessful injection and were excluded from the following studies.

4.4 Effects of sFlt-1 overexpression on cardiac function during pregnancy

Research has shown that maladaptations to pregnancy be it on a hormonal level, on a cardiovascular level or even on a metabolic level, can have severe nefarious consequences for both the mother and the foetus (Duvekot et al. 1993; Duvekot & Peeters 1994; Vanwijk et al. 2000; S. E. Maynard et al. 2003; F Burbank 2009; Gyselaers et al. 2011; Amaral et al. 2015; Bokslag et al. 2017; Kazma et al. 2020). Specifically, cardiovascular maladaptations during pregnancy have been associated to cardiovascular and cerebrovascular diseases later in life (James Metcalfe 1963; A. Y. H. Wong et al. 2002; Evans et al. 2011; Karen Melchiorre et al. 2011; Mahendru et al. 2014; Amaral et al. 2015; Escouto et al. 2018; Lima et al. 2019; Washington C. Hill et al. 2020; DeMartelly et al. 2021; Hutchens et al. 2022; Beckett et al. 2023; Giorgione et al. 2023). Abnormal cardiac haemodynamic changes (Lambert et al. 2014, Perry et al. 2018, Crews et al. 2020, Mahendru et al. 2014, Savu et al. 2012, Castleman et al. 2016, Dennis et al. 2014, Amraoui et al. 2014, Mesa et al. 1999, Borghi et al. 2000) have been reported in PE, including a decrease in ejection fraction, decrease in mitral flow, a severe decrease in diastolic volume.

To investigate and compare the adaptive changes in cardiovascular functions and uterine artery blood flow during a normotensive pregnancy and PE, pregnant mice treated with AdsFlt-1 to induce PE-like symptoms. Mice treated with AdCMV were used as normal control. Cardiovascular functions were monitored via ultrasonography and colour Doppler before time-mating and near term on day E17.5.

In normotensive pregnancies, several critical alterations in cardiovascular function arise, which significantly affects the outcome of a successful pregnancy. The heart must adjust to guarantee adequate blood supply for all organs and prevent hypoxia during volume overload (Hall *et al.* 2011). Consequently, pregnancy leads to gradual increases in CO, SV, and heart rate, along with a decrease in blood pressure, an increase in arterial compliance, and an

increase in extracellular fluid volume, culminating in significant cardiovascular adaptations throughout pregnancy (Hall et al. 2011; Jing Li et al. 2012; Castleman et al. 2016, 2023).

4.4.1 Effects of sFlt-1 on Cardiac Systolic Functions in Pregnancy

To examine the cardiac function during pregnancy, four systolic parameters: CO, SV, EF, and FS (Figure 4.4) were measured. Compared to non-pregnant mice, CO were significantly increased in AdCMV and AdsFlt-1 (Figure 4.4A) treated pregnant mice, indicating that cardiac adaptation took place during normal pregnancy and PE. However, SV were significantly increased only in AdCMV treated pregnant mice (Figure 4.4B) suggesting that sFlt-1 overexpression led to impaired pregnancy induced cardiac adaptation. This finding was consistent with previous studies on non-injected mice. The study demonstrated that sFlt-1 is the factor that is influencing maladaptations to the heart in pregnancy.

In addition, SV (Figure 4.4B) was significantly reduced in AdsFlt-1 treated pregnant mice compared to AdCMV controls, suggesting that PE is linked to cardiac dysfunction and may interfere with the heart's adaptive changes during pregnancy.

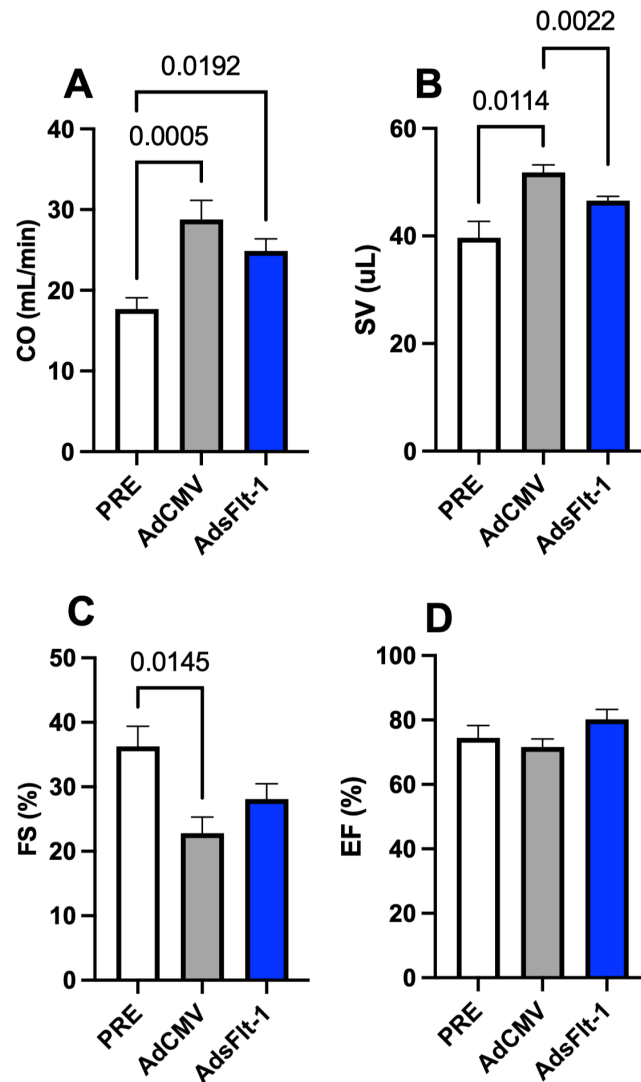


Figure 4.5 Systolic functions of left ventricle in CMV and sFlt-1 mice during pregnancy.

Ultrasound analysis was carried out on pre-gravid mice and on E17.5 of pregnancy for both sFlt-1 and CMV injected group (n=6/group). Different measurements were taken cardiac output (**A**) did not significantly change when comparing the sFlt-1 vector treated mice with the CMV vector treated mice. There was a significant increase in AdCMV and AdsFlt-1 mice when compared to pre-gravid mice. The stroke volume (**B**) was significantly decreased during pregnancy in the sFlt-1 vector treated mice when compared with the CMV vector treated mice. Additionally, there was a significant increase in the stroke volume in the AdCMV mice when compared to pre-gravid mice. The fractional shortening (**C**) did not significantly change when comparing the sFlt-1 vector treated mice with the CMV vector treated mice. There was a significant decrease in the fractional shortening in the AdCMV mice when compared to the pre-gravid mice. The ejection fractioning (n=6) (**D**) did not significantly change when comparing the sFlt-1 vector treated mice with the CMV vector treated or pre-gravid mice. Statistical comparison was performed using Mann Whitney test.

4.4.2 Overexpression of sFlt-1 altered diastolic functions in pregnancy.

Eight diastolic parameters: MV E/A, MV Area, MV PHT, LV MPI, IVCT, IVRT, ESV, and EDV, were measured to determine diastolic function during pregnancy. These functions are used to assess mitral flow velocities, ventricular filling, and myocardial performance.

Pregnant AdsFlt-1 mice showed a significant increase in MV E/A ratio, LV MPI, and MV PHT, while MV E/A Area decreased compared to pregnant AdCMV mice (Figure 4.6). It has been reported that women with PE showed increased IVRT and E/A ratio, as well as increased LV MPI (Shivananjiah et al. 2016; Thayaparan et al. 2019; Waker et al. 2021). An increase in LV MPI is linked to a deterioration of cardiac function. (Libanoff & Rodbard 1968; Tei et al. 1996; M. Kato et al. 2005; Rhee et al. 2011; Luewan et al. 2014; Ramadan et al. 2016; Omeroglu et al. 2023). Elevated levels of antiangiogenic factors, such as sFlt-1, are associated with a decline in cardiac function evidenced by an increase in LV MPI (Ramadan *et al.* 2016). Severe decreases in MV E/A area have been linked to various cardiac dysfunctions including mitral stenosis, hypertrophic cardiomyopathy, and peripartum cardiomyopathy (Kawahara et al. 1991; Tsiaras & Poppas 2009; de Haas et al. 2021; Kuć et al. 2022). Our results are consistent with previous studies indicating that sFlt-1 overexpression led to cardiac dysfunction.

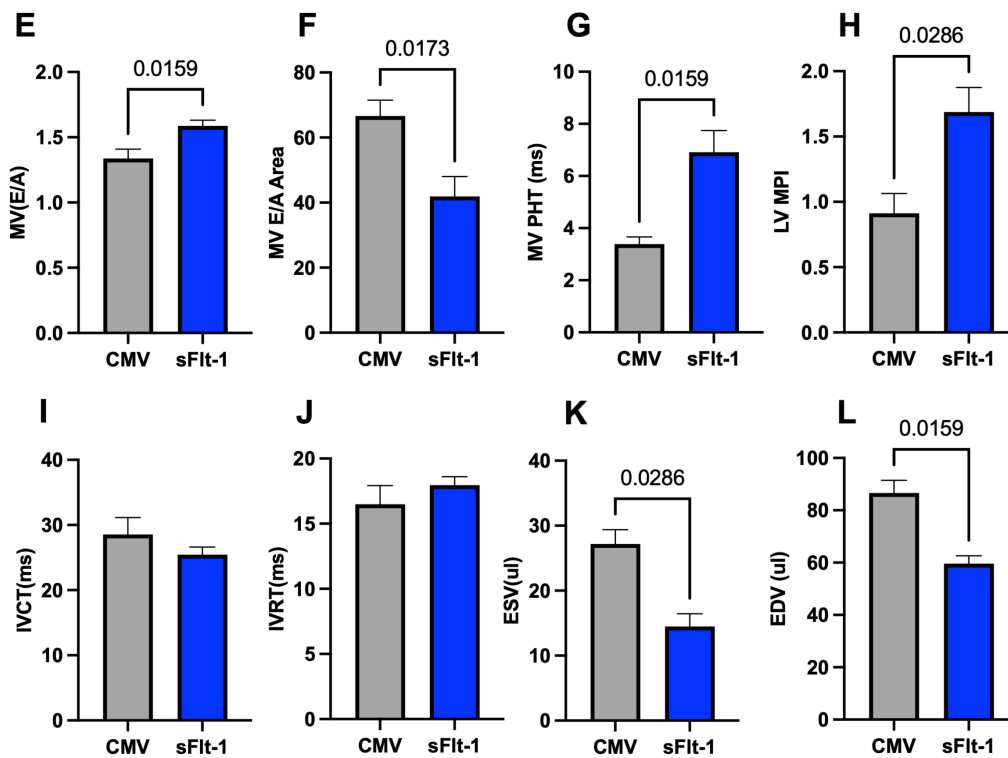


Figure 4.6 Diastolic functions of left ventricle in CMV and sFlt-1 mice during pregnancy.

Echocardiography was used to measure diastolic heart function on E17.5 on both sFlt-1 and CMV injected group (n=8/group). Mitral flow E/A ratio was significantly increased during pregnancy in the sFlt-1 vector treated mice when compared with the CMV vector treated mice, Mitral flow area (F) was significantly decreased during pregnancy in the sFlt-1 vector treated mice when compared with the CMV vector treated mice, Mitral valve by pressure half time (G) was significantly increased during pregnancy in the sFlt-1 vector treated mice when compared with the CMV vector treated mice, left ventricular Myocardial Performance Index (H) was significantly increased during pregnancy in the sFlt-1 vector treated mice when compared with the CMV vector treated mice, Isovolumetric relaxation time (I) did not significantly change when comparing the sFlt-1 vector treated mice with the CMV vector treated mice, Isovolumetric contraction time (J) did not significantly change when comparing the sFlt-1 vector treated mice with the CMV vector treated mice, end systolic volume (K) was significantly decreased during pregnancy in the sFlt-1 vector treated mice when compared with the CMV vector treated mice, and end diastolic volume (L) was significantly decreased during pregnancy in the sFlt-1 vector treated mice when compared with the CMV vector treated mice. Data is expressed as a mean \pm S.E.M and statistical comparison was performed using Mann Whitney test.

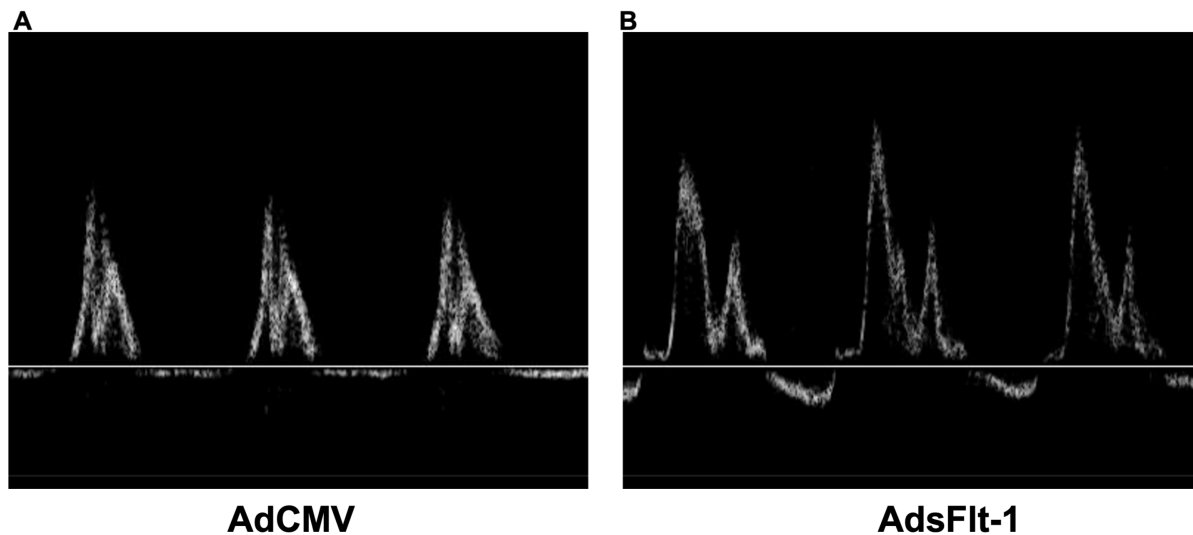


Figure 4.7 Representative images of the mitral inflow colour Doppler trace in pregnancy.

Echocardiography was used to measure heart function in pregnant AdCMV mice (**A**) and AdsFlt-1 mice (**B**).

Interestingly, ESV (Figure 4.5K) and EDV (Figure 4.5L) were significantly decreased in AdsFlt-1 treated pregnant mice compared to the controls, which is contrary to what is typically observed in PE. Previous literature suggests an increase in both measurements in women with PE (Simmons *et al.* 2002; Redman 2011; Shivananjiah *et al.* 2016; Lavie *et al.* 2018; Mostafavi *et al.* 2019). However, Zaman *et al.* (2018) compared a cohort of 34 normotensive women and 30 preeclamptic women and found no significant differences in ESV or EDV (Zaman *et al.* 2018). In addition, the mitral flow velocities pattern in AdsFlt-1 treated mice (Figure 4.7) corresponds to a Fixed restricted grade IV (Figure S.1.2) diastolic dysfunction (Christiana M Schannwell *et al.* 2002; Jovin *et al.* 2013; Muthyala *et al.* 2016). Taken together, these findings suggest that sFlt-1 overexpression may lead to restricted diastolic dysfunction.

4.4.3 Overexpression of sFlt-1 impacted the cardiac structural changes.

During a normotensive pregnancy, the maternal heart undergoes structural changes, including an increase in preload, a decrease in afterload, and an increase in LV wall thickness, LV mass, and chamber diameters (Simmons *et al.* 2002; Karen Melchiorre *et al.* 2012, 2014; Savu *et al.*

2012; Sanghavi & Rutherford 2014; Cong et al. 2015; Kasula Sunanda et al. 2017). Additionally, the sphericity index decreases, indicating a more spherical shape of the left chamber. The intraventricular septum and left ventricular posterior wall gradually increase with advancing gestational age (Christiana M Schannwell et al. 2002; Eghbali et al. 2005; Jingyuan Li et al. 2012a). Pregnancy triggers reversible hypertrophy, which is a natural adaptation to volume strain on the circulatory system (Hunter & Robson 1992b; Yuan et al. 2006).

The current study aimed to evaluate cardiac structural changes in a PE model by comparing seven structural measurements between AdsFit-1 and AdCMV pregnant mice at E17.5. The seven measurements were LV Mass, IVS during systole and diastole, LVID during systole and diastole, and LVPW during systole and diastole.

Significant increases in LV Mass, IVS during systole and diastole, LVID during diastole, and LVPW during systole were observed in pregnant AdsFit-1 mice compared to those treated with the AdCMV. These results are consistent with previous studies on PE.

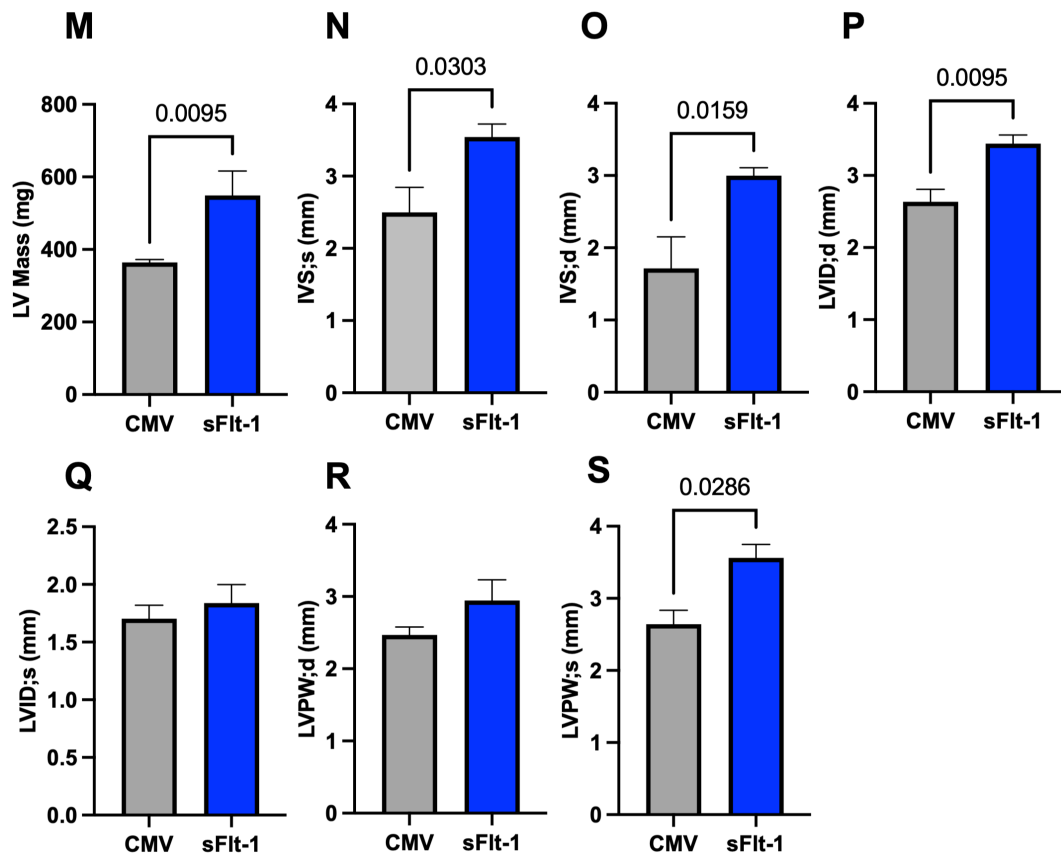


Figure 4.8 Structural functions of left ventricle in CMV and sFlt-1 mice during pregnancy.

Ultrasound analysis was carried out on mice on E17.5 of pregnancy on E17.5 on both sFlt-1 and CMV injected group (n=8/group). Different measurements were taken: LV Mass; left ventricle mass (**M**) was significantly increased during pregnancy in the sFlt-1 vector treated mice when compared with the CMV vector treated mice, IVS; intraventricular septum during systole (**N**) was significantly increased during pregnancy in the sFlt-1 vector treated mice when compared with the CMV vector treated mice, intraventricular septum during diastole (**O**) was significantly increased during pregnancy in the sFlt-1 vector treated mice when compared with the CMV vector treated mice, LVID; left ventricle internal diameter during systole (**P**) did not significantly change between the two groups, left ventricle internal diameter during diastole (**Q**) was significantly increased during pregnancy in the sFlt-1 vector treated mice when compared with the CMV vector treated mice, LVPW; left ventricular posterior wall during systole (**R**) did not significantly change when comparing the sFlt-1 vector treated mice with the CMV vector treated mice, left ventricular posterior wall during diastole (**S**) was significantly increased during pregnancy in the sFlt-1 vector treated mice when compared with the CMV vector treated mice. Data is expressed as a mean \pm S.E.M and statistical comparison was performed using Mann Whitney test.

PE is characterized by LV concentric remodelling, concentric hypertrophy, and asymmetrical LV remodelling/hypertrophy (Karen Melchiorre et al. 2011, 2012, 2014). These structural changes are linked to increased afterload, unfavourable LV remodelling, and LV concentric hypertrophy. LV diastolic dysfunction and segmental myocardial relaxation are present in

women predisposed to PE (Easterling et al. 1990; Bosio et al. 1999; H. Valensise et al. 2000; H Valensise et al. 2001; Aardenburg et al. 2005; Herbert Valensise et al. 2008; Gyselaers et al. 2011b; Scholten et al. 2011; Sep et al. 2011; Novelli et al. 2012; Karen Melchiorre et al. 2014). Studies show that PE leads to LV dysfunction (Borghi *et al.* 2000, 2011; Hamad *et al.* 2009; Tyldum *et al.* 2011; Shahul *et al.* 2012) increased aortic stiffness (Hibbard *et al.* 2005; Kaihura *et al.* 2009; Avni *et al.* 2010), decreased venous capacity (Gyselaers et al. 2011), and poor myocardial contractility (Lang et al. 1991; Simmons et al. 2002; Karen Melchiorre et al. 2011). PE can also cause biventricular chamber systolic dysfunction and significant hypertrophy accompanied by high-amplitude segmental post-systolic shortening at the level of the basal septum (Lang *et al.* 1991; Avni *et al.* 2010). Some studies have found an increased left atrial dimension in preterm PE, indicating elevated left-sided chamber filling pressures (Rubler *et al.* 1973; Zenther *et al.* 2009; Bokslag *et al.* 2016). Adverse left atrial remodelling is only observed in individuals with LV global diastolic failure, suggesting that the pregnant heart in PE is operating at its limit of capacity (Redman 2011; E. Chung & Leinwand 2014).

4.4.4 Overexpression of sFlt-1 did not alter the uterine artery blood flow

One of the most important factors in maintaining an appropriate intrauterine environment for foetal growth and development is maternal uterine artery blood flow. This is because maternal blood not only carries nutrients and removes waste products, but it also regulates the amount of oxygen that can reach the developing fetoplacental unit by perfusing the spiral arterioles that perfuse the intervillous area. To meet the needs of the fetoplacental unit, uterine vascular adaptations result in a five- to ten-fold dilatation, accompanied by considerable morphologic changes in the spiral arterioles (G. J. Burton et al. 2009; Ridder et al. 2019). When uterine vascular development is impaired, PE and foetal growth restriction may occur due to primary placental defects (S. L. Khong et al. 2015; Parks 2017). Understanding normal placentation and how it is impacted by PE and foetal growth restriction requires understanding the relationship between uterine artery blood flow and placental development. In PE the uterine artery pulsatility index (UA PI) and the uterine artery resistive index (UA RI) tend to be significantly higher, when compared to normotensive pregnancies. Several studies have

proposed that utilising the UA PI and UA RI for diagnostic purposes in PE may be beneficial (Crossen et al. 2008; S. L. Khong et al. 2015; Das et al. 2022).

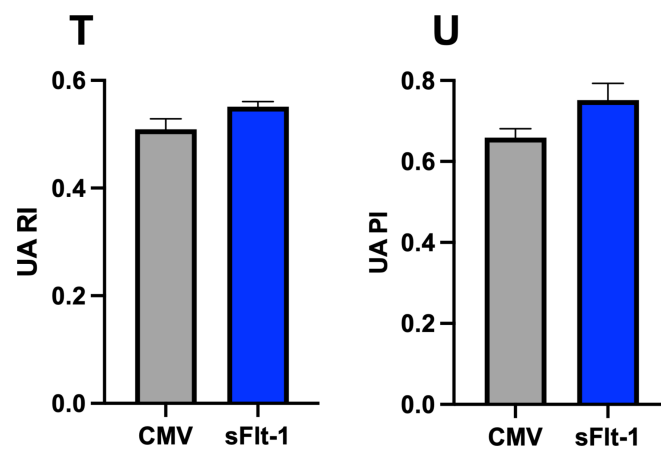


Figure 4.9 Uterine artery flow in CMV and sFlt-1 mice during pregnancy.

Uterine artery flow was measured on E17.5 on both sFlt-1 and CMV injected group (n=8/group). Resistive index (RI) (T) and pulsatility index (PI) (U) remained unchanged in both groups. *Statistical comparison was performed using Mann Whitney test. Neither of these measurements were significantly different.

To assess the uterine artery adaptation in PE model, two uterine artery blood flow measurements (Figure 4.8); the UA RI and the UA PI were recorded at E17.5 in AdsFlt-1 treated mice and on AdCMV treated controls. Surprisingly, no differences in uterine artery RI and PI were observed in the AdsFlt-1 treated mice when compared to AdCMV controls. Although, most literature has observed a significant increase in UA PI and UA RI when comparing preeclamptic patients with normotensive pregnant women, some studies have also demonstrated no significant difference when comparing both groups (Ridder et al. 2019b; a; Parnavitana et al. 2021; Tian & Yang 2022).

4.5 Discussion

Increased levels of sFlt-1 are associated with the development of PE as a splice variant of membrane-bound VEGFR-1 that inhibits the activity of pro-angiogenic VEGF and PlGF, resulting in endothelial dysfunction (S. E. Maynard et al. 2003; Ramma & Ahmed 2011a). This study showed that overexpression of sFlt-1 via adenoviral injection during pregnancy in mice resulted in the PE-like symptoms.

Animal models of PE have proven useful in investigating the biological disturbances underlying human PE and the development of PE-like symptoms, thereby providing insights into the molecular mechanisms of the condition (G. Yang et al. 2008; Bytautiene et al. 2010; Szalai et al. 2015; Vogtmann et al. 2019, 2021). However, some of these methods lack physiological relevance to the human condition and may thus hinder the development of new treatments. Moreover, these models exhibit a wide range of physiological endpoints that make it challenging to compare their effects across different models. While the models developed by Maynard *et al.* (2003) were the first to use AdsFlt-1 to induce PE-like symptoms in rat. However, studies using sFlt-1 overexpression PE model often did not include echocardiographic measurements, making human comparisons impossible (S. E. Maynard, Min, Merchan, Lim, Li, Mondal, Libermann, Morgan, et al. 2003; Vogtmann et al. 2019). As ultrasound scans of both the mother and the foetus are routinely conducted with any pregnancy, a better understanding of echocardiographic markers that indicate maladaptation are needed to insure early detection of PE (Preeclampsia Foundation 2022). Early detection of PE is critical, and deciphering these markers can aid in its timely diagnosis and effective management.

The present study is the first to demonstrate the combined symptoms associated with PE; hypertension, growth restriction alongside cardiac maladaptation, while also using diagnostic tools such as echocardiography akin to the ones used in humans.

4.5.1.1 Overexpression of sFlt-1 in pregnancy caused symptoms of PE in mice.

PE is characterized by hypertension and the involvement of at least one organ system, with pregnant women prone to PE exhibiting elevated levels of sFlt-1. Although the exact aetiology of the condition remains unclear, it has been hypothesized that sFlt-1 may play a key role (Lu et al. 2007; Makris et al. 2007; Szalai et al. 2014; Jiang et al. 2015; K. R. Palmer et al. 2017). In this study, we were able to induce PE-like symptoms, such as increased MAP and foetal growth restriction in pregnant mice using adenoviral encoded sFlt-1 overexpression. Overall, these results demonstrated the suitability of the adenoviral sFlt-1 overexpression model for studying changes associated with PE.

4.5.1.2 Overexpression of sFlt-1 hinder cardiac adaptations to pregnancy in diastolic and systolic functions.

The cardiovascular system undergoes significant adaptations to accommodate the increased metabolic needs of both the mother and the foetus. Increases in CO, decreases in blood pressure and total systemic vascular resistance (Hall et al. 2011; Sanghavi & Rutherford 2014) are part of these adaptations. It has been reported that women exhibit increased mitral valve E and A wave velocities, with a shorter IVCT phase and longer ejection phase representing the two ventricular contraction phases during pregnancy (Feher 2012).

Women with PE are often associated with cardiac dysfunction. Systolic dysfunction such as a decrease in CO and SV is expected in PE (Tay et al. 2018; Thilaganathan & Kalafat 2019; Mulder et al. 2022). In addition, PE is also associated with diastolic dysfunction such as an increase in IVRT and a greater increase in the MV E/A ratio (Shivananjiah et al. 2016; Thayaparan et al. 2019; Waker et al. 2021) compared to normal pregnancies (Rhee *et al.* 2011; Ramadan *et al.* 2016). Furthermore, a significantly increased LV MPI has been observed in preeclamptic women (Rhee *et al.* 2011; Ramadan *et al.* 2016), The deterioration of cardiac function, evidenced by an increase in LV MPI, correlated with high levels of antiangiogenic factors such as sFlt-1 (Libanoff & Rodbard 1968; M. Kato et al. 2005; Luewan et al. 2014; Ramadan et al. 2016; Omeroglu et al. 2023).

The pathophysiology of PE and the cardiovascular maladaptations that arise from it remain uncertain. The purpose of this investigation was to explore the differences in adaptations seen in normal pregnancies versus a murine model of PE, using ultrasound scans.

In the present study, we found that pregnancy induced cardiac adaptation did take place in AdsFlt-1 induced PE in mice, albeit to a lesser degree as evidenced by an increase in CO but no change in SV during pregnancy suggesting that PE may obstruct the heart's pregnancy-related adaptive changes. Furthermore, we observed the presence of systolic and diastolic dysfunctions following sFlt-1 overexpression in pregnant mice. These findings support the notion that sFlt-1 is responsible for the cardiac maladaptations observed during pregnancy. Whether cardiac dysfunction associated with PE is due to the direct effect of sFlt-1 on cardiac function or secondary to sFlt-1 induced endothelial dysfunction warrant further investigation.

4.5.1.3 Overexpression of sFlt-1 caused maladaptions to pregnancy in the cardiac structure.

In a normotensive pregnancy and in response to the foetal demands the maternal heart goes through structural alterations such as an enhanced preload, decreased afterload, and heart rate augmentation, along with increased stroke work indicating that myocardial fibres are working harder (Simmons et al. 2002; Cong et al. 2015; Kasula et al. 2017). Additionally, LV wall thickness, LV mass, and longitudinal and transverse chamber diameters increase, while the sphericity index decreases by the third trimester, indicating a more spherical shape of the left chamber that is reversed postpartum (Savu *et al.* 2012; Sanghavi & Rutherford 2014). The time it takes for the LV mass to be normalized postpartum has mixed conclusions, with some studies reporting normalization as early as 12 weeks to 6 months after delivery (Hunter & Robson 1992b; Simmons et al. 2002; Yuan et al. 2006; Savu et al. 2012; Ferreira et al. 2021), while others suggest modified mass persistence for up to a year (Clapp & Capeless 1997).

During early pregnancy, there is an increase in venous return to the left atrium (LA) (preload), which is reflected by an increase in LA size and LVID from the first to second trimesters,

leading to elevated LV filling rates (Melchiorre et al., 2016). As the pregnancy progresses, the myocardium grows physiologically larger to handle the chronic volume strain on the circulatory system (Kasula et al. 2017). In this context, IVS and LVPW gradually increase with advancing gestational age, while other studies report their gradual increase throughout the trimesters. Pregnancy induces reversible hypertrophy, also known as physiological hypertrophy, with no long-term effects on heart function (Christiana M Schannwell et al. 2002; Eghbali et al. 2005; Jingyuan Li et al. 2012a; b).

Following birth, the woman's heart goes through reverse remodelling, returning to its pre-gravid structure and function (Ferreira *et al.* 2021). Heart remodelling brought on by hemodynamic overload during pregnancy is characterized by LV eccentric hypertrophy and left atrium enlargement (Mone et al. 1996; Christiana M Schannwell et al. 2002; Eghbali et al. 2005; Schwartz & Schneider 2006; Jingyuan Li et al. 2012b; a; Borges et al. 2018). Cardiac hypertrophy is a critical coping mechanism that helps the heart keep up its pumping ability when the heart is under hemodynamic stress from pressure or volume overload (Savu et al. 2012; Kasula et al. 2017). In addition, hypertrophy is frequently considered the heart's main mechanism for reducing strain on the ventricle walls (Kasula et al. 2017). Heart hypertrophy can either be physiological, which is advantageous and adaptive, or pathological, which is a maladaptation and has adverse consequences (Jingyuan Li et al. 2012).

A significant increase in LV Mass, IVS during systole and diastole, LVID during diastole, and LVPW during systole was seen in pregnant mice treated with the sFlt-1 vector when compared to the pregnant mice treated with the CMV vector was observed. These results mimic the results previously described in PE.

In PE, LV concentric remodelling, concentric hypertrophy, and asymmetrical LV remodelling/hypertrophy which mostly affects the basal anteroseptum has been described (Karen Melchiorre et al. 2011, 2012, 2014). These structural changes are linked to increased afterload and unfavourable LV remodelling, as evidenced by significantly higher mean arterial

pressure, total vascular resistance index, relative wall thickness, and LV concentric hypertrophy (Karen Melchiorre et al. 2014). Additionally, modest LV diastolic dysfunction (30%) and segmentally reduced myocardial relaxation (70%), two risk factors for preterm PE, are present in women who are predisposed to the condition (Easterling et al. 1990; Aardenburg et al. 2005; Herbert Valensise et al. 2008; Scholten et al. 2011; Novelli et al. 2012; Karen Melchiorre et al. 2014). Numerous studies have demonstrated that PE causes LV dysfunction (Borghi *et al.* 2000, 2011; Hamad *et al.* 2009; Tyldum *et al.* 2011; Shahul *et al.* 2012), increased aortic stiffness (Hibbard *et al.* 2005; Kaihura *et al.* 2009; Avni *et al.* 2010), decreased venous capacity (Gyselaers et al. 2011), and poor myocardial contractility (Lang et al. 1991; Simmons et al. 2002; Karen Melchiorre et al. 2011). In particular, more severe or premature episodes of PE dramatically reduce cardiac contractility, as shown by lower segmental myocardial systolic and diastolic deformation indices, indicating poor myocardial contractility and relaxation (Lang *et al.* 1991; Avni *et al.* 2010). Moreover, biventricular chamber systolic dysfunction and significant hypertrophy are accompanied by high-amplitude segmental post-systolic shortening at the level of the basal septum in one-fifth of premature preeclamptic women (Rubler *et al.* 1973; Zenther *et al.* 2009; Bokslag *et al.* 2016).

In addition, some studies have found increased left atrial dimensions in preterm PE, which is a result of elevated left-sided chamber filling pressures (Karen Melchiorre et al. 2012). However, adverse left atrial remodelling was only discovered in individuals with LV global diastolic failure, suggesting that the pregnant heart in PE operates at its limit of capacity (Redman 2011; E. Chung & Leinwand 2014).

The overexpression of sFlt-1 resulted in left ventricular dysfunction, as indicated by structural maladaptations such as an increase in left ventricular mass, intraventricular septum, and left ventricular internal dimension. These structural maladaptations are comparable to those observed in women with PE (Simmons *et al.* 2002; Danzmann *et al.* 2008; Cong *et al.* 2015).

4.5.1.4 Overexpression of sFlt-1 does not impact adaptations in uterine artery.

Maternal uterine artery blood flow is crucial in maintaining an appropriate intrauterine environment for foetal growth and development, as it carries nutrients, removes waste products, and regulates oxygen levels that reach the developing fetoplacental unit (Oloyede & Iketubosin 2013; Browne *et al.* 2015; Ridder *et al.* 2019a; b). Uterine vascular adaptations during pregnancy result in a considerable morphologic change in the spiral arterioles - dilating by five- to ten-fold to meet the needs of the fetoplacental unit (A. Robson *et al.* 2012; Cui *et al.* 2013; Guedes-Martins *et al.* 2014; Small *et al.* 2016). Primary placentation defects occur when uterine vascular development is impaired, leading to PE and foetal growth restriction (Mu Junwu & Lee 2006; Gilbert *et al.* 2007; Sholook *et al.* 2007; Cnossen *et al.* 2008). Understanding the relationship between uterine artery blood flow and placental development is critical in comprehending normal placentation and its interaction with PE and foetal growth restriction. In normal pregnancy, the UA PI and UA RI tend to be lower than those seen in preeclampsia. The higher values of UA PI and UA RI in preeclampsia suggest impaired blood flow through the uterine arteries, which may lead to placental insufficiency and adverse foetal outcomes (Valiño *et al.* n.d.; Mu Junwu & Lee 2006; Guedes-Martins *et al.* 2014). Therefore, monitoring these indices can aid in the early detection and management of preeclampsia (Cnossen *et al.* 2008; Pedroso *et al.* 2018). The findings in this study of the uterine artery contradicted previous research as there was no significant differences in either UA PI or UA RI between the two groups.

In summary, the present study aimed to investigate the effects of sFlt-1 overexpression on cardiac adaptations and uterine vascular function in mice during pregnancy. The study used AdCMV mice as controls and found that AdsFlt-1 mice had significantly decreased foetal weight, increased circulating sFlt-1 plasma levels, and cardiac maladaptations in the structure, the diastolic and the systolic functions, consistent with previous studies on PE. Interestingly, there were no significant differences in uterine artery pressure measurements between the two groups. Although this contrasts with most literature that has observed a significant increase in UA P and UA RI in PE patients compared to normotensive pregnant women, some studies have demonstrated no significant difference between the two groups. The study met the diagnostic criteria for positive PE diagnosis, which included increased mean arterial pressure, decreased foetal weight, and an increase in plasma sFlt-1 levels. Additionally, the study demonstrated maladaptations to pregnancy in the cardiovascular system, suggesting

that this animal model is highly suitable for studying PE. The research proposes future studies should investigate the relationship between sFlt-1 overexpression and uterine vascular function, as the study found no significant differences in uterine artery pressure measurements between the two groups. Lastly, this study pinpointed the need for a more defined non-invasive standardised protocol for the diagnosis of PE.

4.6 Limitations

The sFlt level in plasma was only measured once at E17.5. However, other studies have highlighted the importance of conducting repeated measurements of sFlt-1 levels throughout pregnancy and even before conception to provide a comprehensive understanding of sFlt-1's role. Hagmann et al. further emphasize the added value of repetitive sFlt-1 measurements in their review (Hagmann *et al.* 2012). Additionally, given the growing interest in the sFlt-1/PIGF ratio (Perales et al. 2017; Quezada et al. 2020; Ohkuchi et al. 2021; Andrikos et al. 2022; Dathan-Stumpf et al. 2022; Verlohren et al. 2022; W. Chen et al. 2022), further investigations should include measurements of this specific ratio, rather than solely sFlt-1 levels. Future large-scale studies are needed to evaluate the additive value of repeated sFlt-1/PIGF ratio measurements relative to current assessments, as well as to establish cut-off values of the ratios' slopes with regards to pregnancy outcome. Furthermore, while the study conducted one ultrasound scan during pregnancy at E17.5, ideally, the entire pregnancy should have undergone regular ultrasound scans.

Chapter 5

Long-term effects of sFlt-1 induced preeclampsia on cardiovascular health

5. Long-term effects of sFlt-1 induced preeclampsia on cardiovascular health

An expanding body of research indicates that women with a history of PE may face long-term health consequences, particularly a heightened risk of cardiovascular disease in later life. Studies have found that these women are more likely to experience hypertension, strokes, and ischemic heart disease compared to those without a history of PE. Additionally, a history of PE has been associated with an increased risk of metabolic syndrome, diabetes, and renal disease (C. M. Schannwell *et al.* 2003; Gutgesell *et al.* 2009; Weissgerber & Mudd 2015; Maneerattanasuporn 2017; Aryal *et al.* 2019; Kristensen *et al.* 2019; Kattah 2020; Yijun Yang *et al.* 2021; Ying Yang & Wu 2022). Recent findings also suggest a link between PE and cerebrovascular disease, such as stroke and transient ischemic attack (Oehm *et al.* 2006; Warrington *et al.* 2015; Miller 2019; Coelho-Santos & Shih 2020; Miller *et al.* 2021; Shaaban *et al.* 2021; Beckett *et al.* 2023). Women who experienced severe PE during pregnancy appear to be at a higher risk of developing cerebrovascular disease later in life (Mayhan *et al.* 1988; S. W. Lee *et al.* 2003; Oehm *et al.* 2006; Bunik *et al.* 2008; Schoknecht *et al.* 2015; X. Liu *et al.* 2016; Borsche *et al.* 2021; J. Kitt *et al.* 2021; Chechko *et al.* 2022). Furthermore, studies have shown that women with a history of severe PE have a five- to eight-fold increased risk of developing cardiovascular disease in the future.

Investigating the long-term post-partum effects of increased sFlt-1 levels is crucial for understanding the potential consequences on maternal health. Recent studies have highlighted the persistence of elevated sFlt-1 levels in the post-partum period, raising concerns about the possible impact on cardiovascular and renal function (Quitterer & Abdalla 2021; Sarhaddi *et al.* 2022b). Furthermore, research has demonstrated that sFlt-1 can induce endothelial dysfunction and impair angiogenesis, which are critical processes in the maintenance of vascular health (Kendall & Thomas 1993b; L. Li *et al.* 2016). These findings underscore the importance of investigating the long-term effects of increased sFlt-1 levels to better elucidate the mechanisms underlying post-partum health complications and to develop targeted interventions aimed at mitigating the risks associated with persistent sFlt-1 elevation.

Ultimately, a comprehensive understanding of the role of sFlt-1 in post-partum health could pave the way for improved clinical management and prevention strategies for women at risk of PE-related complications.

Therefore, the aim of this study was to investigate the cardiovascular changes in AdsFlt-1 and AdCMV mice post-partum.

5.1 Long-term effects of sFlt-1

5.1.1 sFlt-1 level in plasma

Monitoring sFlt-1 levels can help predict the onset and severity of preeclampsia, enabling early intervention and better clinical management (Zeisler et al., 2016; Rolfo et al., 2020). Elevated sFlt-1 levels are associated with an increased risk of developing preeclampsia, and measuring these levels could serve as a valuable diagnostic tool, as it can provide insights into the long-term health implications for women who have experienced preeclampsia (Kattah 2020; Quitterer & Abdalla 2021).

In the context of this study, sFlt-1 levels were measured in the plasma of AdsFlt-1 mice and AdCMV mice at different timepoints. This was done to evaluate the effects of sFlt-1 on the cardiovascular and neurological changes.

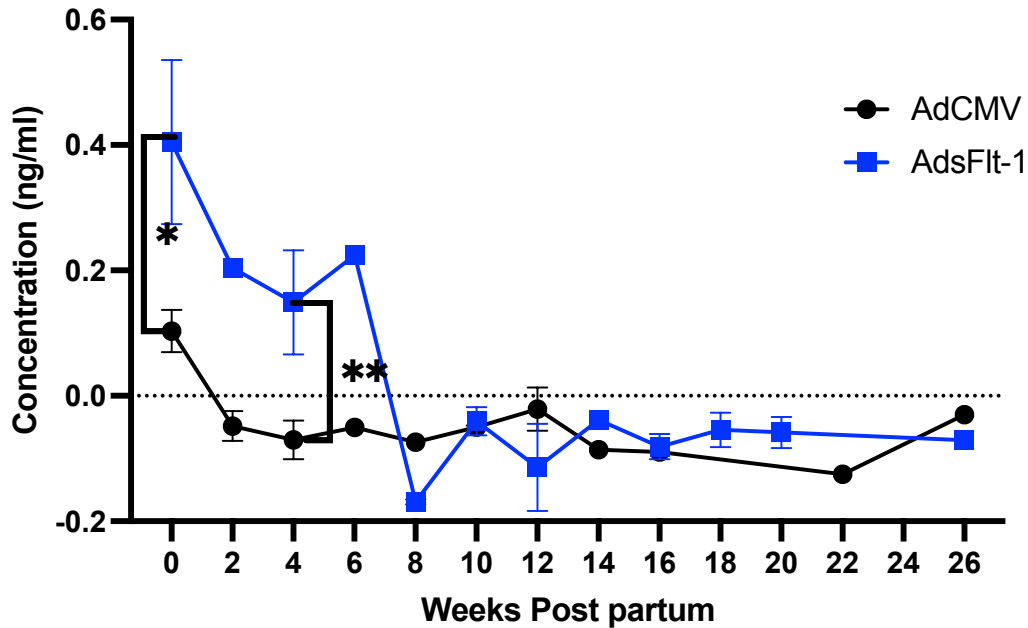


Figure 5.1 Plasma samples were collected at different timepoints during pregnancy (in the graph this is noted as week 0) and postpartum.

The sFlt-1 level in sFlt-1-overexpressing mice dropped back to normal 8 weeks post-partum. *P=0.031746, **P=0.028571 Mann-Whitney test was used for statistical analysis. Data are expressed as mean \pm S.E.M. ;(n= 2-6).

The sFlt-1 levels returned to baseline in the AdCMV group after the second week postpartum, while the AdsFlt-1 group showed a decrease only after the eighth week postpartum. This is consistent with previous studies showing that systolic and diastolic parameters generally revert to normal within eight weeks post-delivery (Christiana M Schannwell et al. 2002). Therefore, measurements of cardiovascular function were taken during pregnancy at E17.5, as well as at eight and thirty-three weeks postpartum.

5.1.2 Long-term effects of sFlt-1 on Cardiac Systolic Functions

To assess cardiac function during pregnancy, four systolic parameters, namely CO, EF, FS, SV (Figure 5.2), were quantified. No differences were observed between AdCMV and AdsFlt-1 mice in terms of CO or FS. However, a significant decrease was observed in the EF at 8 weeks, suggesting sFlt-1 could lead to cardiomyopathy (Umazume *et al.* 2018). Developing cardiomyopathy after preeclampsia has been reported by multiple studies and is usually characterized by a lower EF (typically below 45%) due to the weakened cardiac muscle (Borghetti *et al.* 2018; Maheu-Cadotte *et al.* 2019; Malhamé *et al.* 2019; Sethi & Kumar 2020).

Additionally, a significantly lower SV was detected in AdsFlt-1 mice at E17.5 and at 8 weeks postpartum when compared to AdCMV mice. According to the literature, the SV usually returns to non-gravid levels within 48-96 hours postpartum (Datta *et al.* 2010b; Foster *et al.* 2019; Aranda & McFarland 2023; Mubarik *et al.* 2023).

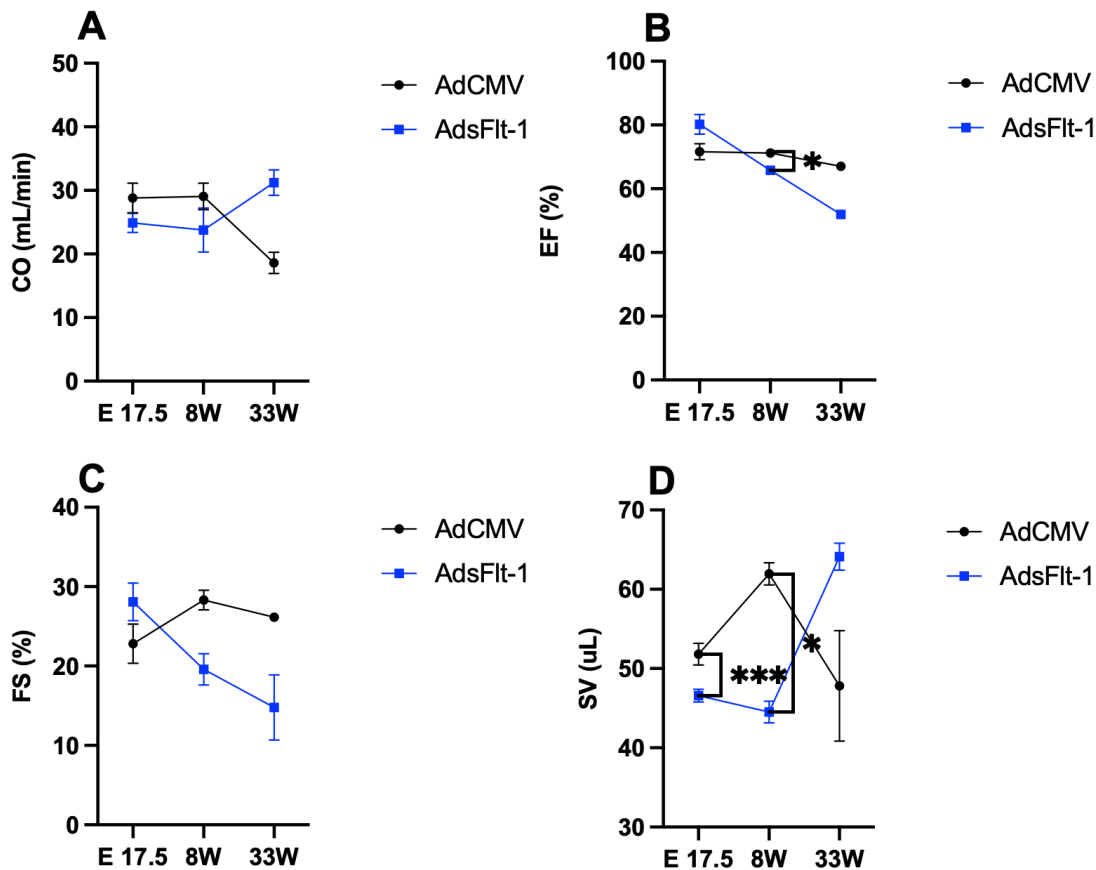


Figure 5.2 Systolic functions of left ventricle in CMV and sFlt-1 mice during pregnancy and post-partum.

Ultrasound analysis was carried out on mice at E17.5 (n=6) of pregnancy, 8 weeks post-partum (n=4) and 33 weeks post-partum (n=3-4). Different measurements were recorded: cardiac output (CO) **(A)** did not significantly change when comparing the sFlt-1 vector treated mice with the CMV vector treated mice. The ejection fraction (EF) **(B)** was significantly decreased in AdsFlt-1 mice when compared to AdCMV mice, at both 8weeks post-partum ($p=0.01587$) and 33 weeks post-partum ($p=0.0201$). The fraction shortening (FS) **(C)** did not significantly change when comparing the sFlt-1 vector treated mice with the CMV vector treated mice. There was a significant decrease in stroke Volume **(D)** in AdsFlt-1 mice when compared to AdCMV mice, at both E17.5 ($p=0.002165$) and 8 weeks post-partum ($p=0.0286$). Statistical comparison was performed using Mann Whitney test.

Although there was no discernible variation in EF at E17.5 between AdCMV and AdsFlt-1 treated mice, a continuous decline in EF was observed in sFlt-1 treated mice despite the normalization of sFlt-1 levels. These results suggest that the overexpression of sFlt-1 during pregnancy is associated with a progressive deterioration of cardiac function.

The decrease in EF and the decrease in SV suggest that sFlt-1 overexpression led to impaired reverse adaptations (from pregnancy to postpartum) (Ferreira *et al.* 2021). Thus, cardiac dysfunction is sustained, even after pregnancy (Karen Melchiorre *et al.* 2011; Guedes-Martins *et al.* 2015; Hutchens *et al.* 2022).

5.1.3 Long-term effects of sFlt-1 on Diastolic Functions

The diastolic measurements recorded, were comprised of MV E/A, MV E/A Area, LV MPI, IVCT, IVRT, ESV and EDV (Table 5.2). A significant decrease in MV E/A Area and a significant increase in MV E/A was observed during pregnancy and postpartum at 33 weeks postpartum, respectively. Several studies have reported that women with PE have an increased MV E/A ratio (James Metcalfe 1963; Karen Melchiorre *et al.* 2011; Shivananjiah *et al.* 2016; Thayaparan *et al.* 2019; Waker *et al.* 2021; Mubarik *et al.* 2023), while having a decreased MV E/A Area, which has also been linked to cardiac dysfunctions, including mitral stenosis, hypertrophic cardiomyopathy, and peripartum cardiomyopathy (Kawahara *et al.* 1991; J Jose 1993; Kuć *et al.* 2022).

| Left ventricle diastolic functions | | | | |
|------------------------------------|-----------|-----------------|-----------------|--------|
| Measurement | Timepoint | CMV | sFlt-1 | P |
| MV E/A | E17.5 | 1.338 ± 0.142 | 1.587 ± 0.097 | 0.0159 |
| | 8W | 1.217 ± 0.023 | 1.600 ± 0.132 | NS |
| | 33W | 1.136 ± 0.035 | 1.351 ± 0.035 | 0.0257 |
| MV Area(mm ²) | E17.5 | 66.636 ± 10.903 | 41.891 ± 15.045 | 0.0173 |

| | | | | |
|------------------|-------|-----------------|----------------|--------|
| | 8W | 75.115 ± 8.107 | 39.730 ± 6.645 | NS |
| | 33W | 61.770 ± 3.818 | 70.718 ± 5.550 | NS |
| MV PHT | E17.5 | 3.383 ± 0.616 | 6.912 ± 1.671 | 0.0159 |
| | 8W | 2.469 ± 0.180 | 3.699 ± 0.926 | NS |
| | 33W | 2.497 ± 0.228 | 3.094 ± 0.282 | NS |
| LV MPI IV | E17.5 | 0.913 ± 0.304 | 1.687 ± 0.378 | 0.0286 |
| | 8W | 0.970 ± 0.172 | 1.320 ± 0.110 | 0.0292 |
| | 33W | 0.969 ± 0.008 | 1.340 ± 0.082 | NS |
| IVCT (ms) | E17.5 | 28.553 ± 6.989 | 25.440 ± 2.649 | NS |
| | 8W | 33.333 ± 8.911 | 24.585 ± 2.647 | NS |
| | 33W | 29.580 ± 4.507 | 25.833 ± 2.227 | NS |
| IVRT (ms) | E17.5 | 16.499 ± 3.787 | 17.960 ± 1.602 | NS |
| | 8W | 22.037 ± 0.850 | 25.927 ± 2.780 | NS |
| | 33W | 22.775 ± 0.785 | 19.677 ± 0.815 | NS |
| ESV(μl) | E17.5 | 27.198 ± 4.382 | 14.483 ± 3.951 | 0.0356 |
| | 8W | 26.395 ± 4.605 | 37.665 ± 3.137 | NS |
| | 33W | 18.651 ± 4.097 | 32.322 ± 4.898 | 0.0106 |
| EDV(μl) | E17.5 | 86.588 ± 10.867 | 59.664 ± 5.874 | 0.0159 |

| | | | | |
|--|-----|-----------------|------------------|----|
| | 8W | 82.909 ± 17.335 | 115.153 ± 14.008 | NS |
| | 33W | 52.087 ± 7.921 | 99.359 ± 6.777 | NS |

Table 5.1 Cardiac diastolic functions during pregnancy and post-partum analysed using echocardiography and M-mode of parasternal long axis view in CMV and sFlt-1.

Ultrasound analysis was carried out on mice at E17.5 (n=6) of pregnancy, 8 weeks post-partum (n=4) and 33 weeks post-partum (n=3-4). MV E/A; mitral flow E/A ratio was significantly increased in AdsFlt-1 compared to AdCMV both during pregnancy at E 17.5 (p=0.0159) and 33 weeks postpartum (p=0.257), MV Area; mitral flow area was significantly decreased in AdsFlt-1 when compared to AdCMV during pregnancy (p=0.0173). MV PHT; mitral valve area by pressure half time was significantly increased during pregnancy (p=0.0159) in AdsFlt-1 when compared to AdCMV. LV MPI IV; Myocardial Performance Index was increased in AdsFlt-1 when compared to AdCMV both in pregnancy as well as at 8 weeks (p=0.0292) postpartum. IVCT; isovolumic contraction time was not significantly different in AdsFlt-1 when compared to AdCMV. IVRT; isovolumic relaxation time, was not significantly different in AdsFlt-1 when compared to AdCMV. ESV; end systolic volume was significantly decreased in pregnancy and significantly increased at 33 weeks postpartum. EDV; end diastolic time was significantly decreased in pregnancy in AdsFlt-1 compared to AdCMV. Statistical comparison was performed using Mann Whitney test.

An elevation in LV MPI was observed in AdsFlt-1 compared to AdCMV during pregnancy and at 8 weeks postpartum. This increase in LV MPI in PE relative to normotensive women, both during pregnancy and postpartum, aligns with previous findings (A. K. Pandey et al. 2010; Foster et al. 2019; Giorgione et al. 2023; Mubarik et al. 2023).

Moreover, a notable reduction in EDV and ESV was detected in pregnant AdsFlt-1 mice compared to AdCMV mice. A decrease in EDV during pregnancy can lead to a reduced cardiac output, as it means that less blood is being pumped out with each heartbeat and could indicate issues with the cardiovascular system, such as poor ventricular filling or diastolic dysfunction (Thornburg *et al.* 2000). In fact, a decrease in EDV may result in insufficient blood flow to the placenta and the developing foetus, potentially leading to complications like intrauterine growth restriction, low birth weight, or even preeclampsia (Thornburg *et al.* 2000; Jovin *et al.* 2013).

Additionally, a significant rise in ESV of AdsFlt-1 relative to AdCMV was observed at 33 weeks postpartum. Although earlier research indicates increased ESV and EDV in women with PE (Simmons *et al.* 2002; Redman 2011; Shivananjiah *et al.* 2016; Lavie *et al.* 2018; Mostafavi *et al.* 2019), Zaman *et al.* (2018) reported no significant differences between normotensive and preeclamptic women (Zaman *et al.* 2018). An increase in ESV during the postpartum period, it could suggest that the heart is not pumping blood as efficiently as it should, leaving more residual blood in the ventricles after each contraction (Soma Pillay *et al.* 2018; Giorgione *et al.* 2023a). The observed changes in EDV and end-systolic volume ESV are noteworthy for their correlation with the typical pathophysiology of cardiac hypertrophy (Dorn 2007; Jingyuan Li *et al.* 2012b; Jovin *et al.* 2013; Dual & Schmid Daners 2022).

Initially, heightened contractility from the thicker myocardium contributes to a decrease in EDV; however, as the hypertrophic response reaches its maximum potential, the myocardium undergoes remodelling and results in a decline in contractile function, ultimately leading to heart failure and an increase in EDV.

Diastolic dysfunction may be present in postpartum AdsFlt-1 mice compared to control mice AdCMV. This is supported by findings such as a significant decrease in MV E/A Area and increase in MV E/A ratio, increased LV MPI, and alterations in ESV and EDV. Although some studies report inconsistencies regarding ESV and EDV differences between normotensive and preeclamptic women, the overall evidence suggests potential cardiac dysfunctions in sFlt-1 overexpressing mice (Duvekot & Peeters 1994; Most *et al.* 2001; M. Kato *et al.* 2005; A. K. Pandey *et al.* 2010; Rhee *et al.* 2011; Harmelink *et al.* 2013; Karen Melchiorre *et al.* 2014; Sanghavi & Rutherford 2014; Di Salvo *et al.* 2015; Ramadan *et al.* 2016).

5.1.4 Long-term effects of sFlt-1 on Cardiac Structural Changes

PE is linked to persistent arterial stiffness, temporary cardiac changes, and dysfunction, including diastolic dysfunction and impaired endothelial function, hypertrophy, and cardiomyopathy (Mustonen & Alitalo 1995; Iemitsu et al. 2008; Erusalimsky 2009; Kaihura et al. 2009; Peter et al. 2009; Tyldum et al. 2012; Christensen et al. 2016; Possomato-Vieira & Khalil 2016; Boeldt & Bird 2017; Jia et al. 2019; Akçay & Özdemir 2021; Forrest et al. 2022; V. R. Turi et al. 2022). Postpartum assessment of cardiac structures can identify these changes, evaluate their reversibility, and timely intervention for improved long-term outcomes and reduced future cardiovascular risks. To determine sFlt-1's long-term impact on postpartum structural remodelling, or reverse remodelling, measurements (Table 5.2) such as LV Mass, IVS during systole and diastole, LVID during systole and diastole, and LVPW during systole and diastole, were recorded.

| Left ventricle structural changes | | | | |
|------------------------------------------|------------------|------------------|-------------------|----------|
| Measurement | Timepoint | CMV | sFit-1 | P |
| IVS;s(mm) | E17.5 | 2.497 ± 0.781 | 3.542 ± 0.442 | 0.0303 |
| | 8W | 3.647 ± 0.828 | 3.427 ± 0.028 | NS |
| | 33W | 3.827 ± 0.244 | 3.607 ± 0.326 | NS |
| IVS;d(mm) | E17.5 | 1.715 ± 0.876 | 2.998 ± 0.245 | 0.01587 |
| | 8W | 3.051 ± 0.584 | 2.659 ± 0.143 | NS |
| | 33W | 3.489 ± 0.307 | 3.494 ± 0.069 | NS |
| LV Mass(mg) | E17.5 | 364.199 ± 16.305 | 549.124 ± 163.993 | 0.0095 |
| | 8W | 367.655 ± 17.955 | 561.357 ± 29.679 | 0.0285 |
| | 33W | 283.266 ± 15.639 | 863.357 ± 29.679 | 0.0291 |
| LVID;d(mm) | E17.5 | 2.634 ± 0.348 | 3.442 ± 0.291 | 0.0095 |
| | 8W | 2.955 ± 0.347 | 3.540 ± 0.486 | NS |
| | 33W | 3.296 ± 0.314 | 3.569 ± 0.206 | NS |
| LVID;s(mm) | E17.5 | 1.703 ± 0.308 | 1.838 ± 0.396 | NS |
| | 8W | 1.669 ± 0.116 | 2.69 ± 0.422 | NS |

| | | | | |
|-------------------|-------|---------------|---------------|--------|
| | 33W | 1.408 ± 0.062 | 1.665 ± 0.166 | NS |
| LVPW;d(mm) | E17.5 | 2.469 ± 0.247 | 2.944 ± 0.578 | NS |
| | 8W | 2.577 ± 0.256 | 3.188 ± 0.317 | NS |
| | 33W | 2.633 ± 0.515 | 2.927 ± 0.513 | NS |
| LVPW;s(mm) | E17.5 | 2.641 ± 0.389 | 3.563 ± 0.368 | 0.0286 |
| | 8W | 2.871 ± 0.826 | 3.691 ± 0.571 | NS |
| | 33W | 2.618 ± 0.349 | 3.470 ± 0.475 | 0.0186 |

Table 5.2 Cardiac structural functions during pregnancy and post-partum analysed using echocardiography and M-mode of parasternal long axis view in CMV and sFlt-1.

Analysis was carried out on mice at E17.5 (n=6) of pregnancy, 8 weeks post-partum (n=4). IVS;s ; intraventricular septum during systole was significantly increased during pregnancy (p=0.0303) in the sFlt-1 vector treated mice when compared with the CMV vector treated mice. IVS;d; intraventricular septum during diastole was significantly increased (p=0.01587) during pregnancy in the sFlt-1 vector treated mice when compared with the CMV vector treated mice, LV Mass; left ventricle mass was significantly increased during pregnancy (p=0.0095), at 8 weeks postpartum (p=0.0285), and at 33 weeks postpartum (p=0.0291) in the sFlt-1 vector treated mice when compared with the CMV vector treated mice. LVID; left ventricle internal diameter during systole (P) did not significantly change between the two groups. LVID;d left ventricle internal diameter during diastole was significantly increased during pregnancy in the sFlt-1 (p=0.0095) vector treated mice when compared with the CMV vector treated mice/ LVPW;d ; left ventricular posterior wall thickness during diastole was not significantly different. LVPW; s left ventricle internal diameter during was significantly increased during pregnancy in the sFlt-1 vector treated mice when compared with the CMV vector treated mice. Data is expressed as a mean ± S.E.M and statistical comparison was performed using Mann Whitney test.

A notable elevation was observed in IVS; s, IVS; d, LV Mass, LVID; d, and LVPW; s during pregnancy. Concurrently, a marked increase was detected postpartum in LV Mass at 8 weeks and 33 weeks, as well as in LVPW; s at 33 weeks. These findings suggest that sFlt-1 overexpression during pregnancy leads to hypertrophic phenotype in the heart (Eghbali et al. 2005; Jingyuan Li et al. 2012b; Kumar et al. 2019; Vogtmann et al. 2021). These measurements align with findings reported in the literature. DeMartelly et al. (2021) discovered that cardiac dysfunctions persisted into the postpartum period, as demonstrated by an increased IVS in 10 years postpartum in women who had been affected by PE (DeMartelly et al. 2021). Similarly, Vasconcelos et al. (2023) corroborated the results of this study, revealing

a rise in IVS and LVPW even two months following delivery in women (Vasconcelos *et al.* 2023).

5.1.5 Long-term effects of sFlt-1 on uterine artery blood flow

Postpartum research indicates that although PI values decrease in preeclamptic women, they remain significantly higher than those in normotensive women (Guedes-Martins *et al.* 2015; Sharma *et al.* 2018). While some studies document a sustained increase in UA PI and UA RI after PE (Brainard *et al.* 2007; Browne *et al.* 2015; Guedes-Martins *et al.* 2015; S. M. Lee *et al.* 2016), there is a knowledge gap regarding the postpartum resolution of high UA PI or UA RI. This is despite delivery being viewed as the primary diagnostic for placental insufficiency disorders like PE. Consequently, UA PI and UA RI measurements were taken to investigate the changes seen postpartum in uterine artery.

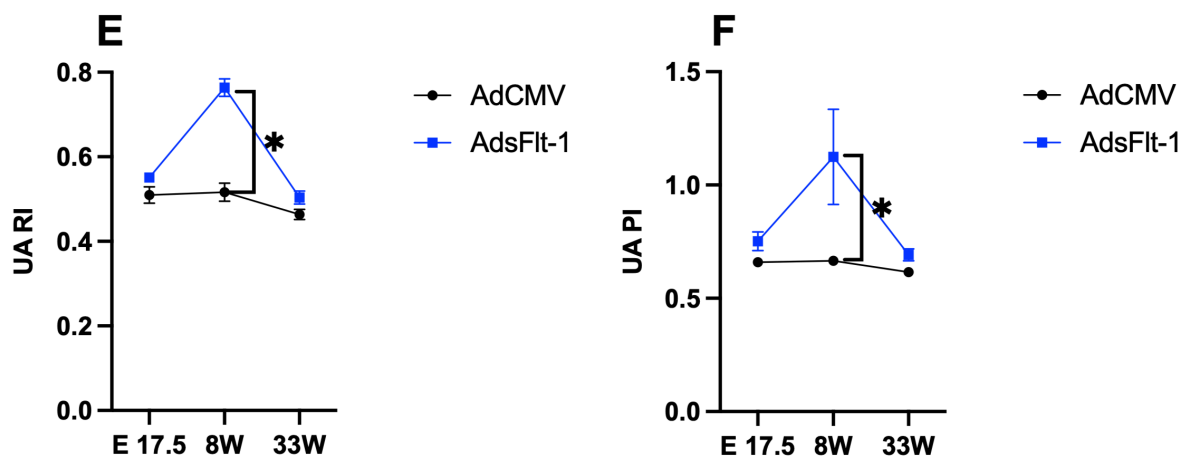


Figure 5.3 Uterine artery flow in CMV and sFlt-1 mice during pregnancy and post-partum.

Analysis was carried out on mice at E17.5 (n=6) of pregnancy, 8 weeks post-partum (n=4). Resistive index (RI) (E) was significantly increased ($p=0.028571$) at 8 weeks post-partum in the sFlt-1 vector treated mice when compared with the CMV vector treated mice. Pulsatility index (PI) (F) was significantly increased ($p=0.0300$) at 8 weeks post-partum in the sFlt-1 vector treated mice when compared with the CMV vector treated mice. *Statistical comparison was performed using Mann Whitney test.

Intriguingly, this study demonstrated a significant elevation in UA PI and UA RI in AdsFlt-1 mice for these measurements compared to AdCMV mice, peaking at 8 weeks postpartum and subsequently decreasing to levels below those noted during pregnancy. The UA PI and UA RI peak aligns with the time when sFlt-1 plasma levels in AdsFlt-1 mice normalize. While studies report postpartum increases in PE women, relative to normotensive women (Guedes-Martins *et al.* 2015; Vogtmann *et al.* 2021), no consensus exists regarding when the UA PI and UA RI decline following PE (S. M. Lee *et al.* 2016). This can be attributed to most studies concentrating on the immediate hours or days postpartum (Capeless & Clapp 1991; Guedes-Martins *et al.* 2015; Khan *et al.* 2016; S. M. Lee *et al.* 2016; Pedroso *et al.* 2018; Sharma *et al.* 2018; Giorgione *et al.* 2023; Vasconcelos *et al.* 2023).

5.2 Discussion

The predisposition to develop PE is heightened by the presence of antiangiogenic factors, such as sFlt-1 overexpression. In the previous study outlined in this thesis (Chapter 4), we successfully induced PE-like symptoms in pregnant mice by administering adenoviral encoded sFlt-1 in mice during mid-pregnancy at E10.5. This intervention resulted in notable reductions in foetal weight, increased circulating sFlt-1 plasma levels, and cardiac maladaptations in structure, diastolic, and systolic functions in AdsFlt-1 mice, aligning with prior research on PE. Recent evidence has shown that PE and the consequent elevation of sFlt-1 levels are associated with an increased risk of developing cardiovascular and cerebrovascular diseases later in life (Karen Melchiorre *et al.* 2011; Neuman *et al.* 2021; Naeh *et al.* 2022; Mubarik *et al.* 2023). The objective of this chapter was to evaluate the potential consequences and postpartum sFlt-1 levels, along with the impact on cardiac functions.

5.2.1 sFlt-1 levels in plasma reached baseline by 8 weeks

According to several earlier studies, a quick postpartum curettage in preeclamptic patients may improve maternal prognosis, with a reduction in maternal serum sFlt-1 levels observed

following curettage (Magann *et al.* 1994; Matsuo *et al.* 2007). However, more recent prospective randomized trials found that postpartum uterine curettage did not improve clinical or laboratory outcomes for mothers (Ossada *et al.* 2016; Hamza *et al.* 2019). Consequently, the precise influence of sFlt-1 postpartum, and whether its effects persist from pregnancy or stem from a preceding impact that triggers the elevation of antiangiogenic factors, warrants further elucidation.

The objective of this study was to examine the prolonged effects of increased levels of sFlt-1 during pregnancy on the maternal cardiovascular system. The investigation aimed to determine whether the relatively brief exposure to sFlt-1 has sustained implications on cardiovascular function. This conclusion supports our findings that sFlt-1 is in fact a risk factor but does not predict maternal outcomes. Indeed, the results presented in this study demonstrated that, sFlt-1 levels in AdsFlt-1 mice returned to baseline at 8 weeks postpartum, while in AdCMV mice, these levels reverted to baseline within less than a week.

5.2.2 Long-term effects of sFlt-1 overexpression led to systolic and diastolic dysfunctions

The development of PE significantly affects the cardiovascular system, resulting in cardiac dysfunction, severe hypertension, and peripartum cardiomyopathy in the short term (Bauer & Cleary 2009; Behrens *et al.* 2019). Research examining the heart's anatomy and function in PE has demonstrated that diastolic dysfunction and left ventricular remodelling occur during pregnancy onset (Bauer & Cleary 2009; Behrens *et al.* 2019). Notably, while these changes may be clinically apparent during pregnancy, they can sometimes be irreversible and persist into the postpartum period (Castleman *et al.* 2016).

Peripartum cardiomyopathy (PPCM), also referred to as postpartum cardiomyopathy, is a rare form of cardiomyopathy characterized by systolic dysfunction and frequently dilated heart

chambers (Honigberg & Givertz 2019). This condition typically manifests during the final month of pregnancy or within the weeks following delivery, although it can occur up to five months postpartum or later (Honigberg & Givertz 2019). In PPCM, the enlargement of heart chambers and weakening of the heart muscle result in a diminished volume of blood pumped with each heartbeat, quantified as the EF or fractional shortening FS. A weakened heart can cause fatigue and low blood pressure due to reduced blood flow to the body, as well as swelling in the legs and abdomen due to fluid build-up in organs such as the lungs and liver (Honigberg & Givertz 2019; Honigberg 2021).

The association between PE and PPCM suggests a possible shared pathogenesis (Honigberg & Givertz 2019; Honigberg 2021). A 2013 meta-analysis of 22 studies revealed that PE is more than four times more common in women with PPCM (Bello *et al.* 2013). Concurrently, 22.8% of the initial 411 women in the EURObservational Research Programme's PPCM registry developed PE (Sliwa *et al.* 2017). Further research is needed to elucidate the underlying mechanisms connecting PE and PPCM.

In the present study, diastolic and systolic measurements were utilized to assess cardiac function during pregnancy and postpartum. The observed reduction in EDV during pregnancy suggested the presence of poor ventricular filling or diastolic dysfunction. Additionally, the increase in ESV during the postpartum period indicated a potential decrease in the heart's pumping efficiency. Despite no significant difference in pregnancy in EF between AdCMV and AdsFlt-1 treated mice, the continuous decline in EF in sFlt-1 treated mice, even after the normalization of sFlt-1 levels, highlights a possible long-term impact on cardiac function. Furthermore, the observed postpartum dysfunctions could potentially suggest the occurrence of PPCM in this PE model, as the diagnostic criteria for PPCM are present (decreased EF or FS, occurring following pregnancy, potential increased LV Mass) (Hilfiker-Kleiner & Sliwa 2014; Foster *et al.* 2019; Honigberg & Givertz 2019; Aranda & McFarland 2023).

It is essential to acknowledge the challenges in classifying cardiomyopathies that incorporate both anatomical terms (e.g., hypertrophic and dilated) and functional ones (e.g., restricted), as previous attempts have not been successful in achieving this (Yancy *et al.* 2013; Bozkurt *et al.* 2016). Additionally, diagnosing cardiomyopathy requires standard diagnostic techniques

recommended for patients with heart failure or cardiomyopathy and necessitates a thorough understanding of the complex, diverse, and patient-specific pathophysiology involved (Yancy *et al.* 2013; Bozkurt *et al.* 2016). Consequently, further research is needed to conclusively diagnose the observed dysfunctions.

Crucially, the observed alterations in both diastolic and systolic functions suggest that even with a brief period of exposure to sFlt-1 overexpression, long-term consequences are evident. This finding may indicate that exposure to sFlt-1 during pregnancy not only contributes to the development of preeclampsia symptoms but also potentially causes irreversible damage to the cardiovascular system.

5.2.3 Long-term effects of sFlt-1 overexpression resulted in abnormal structural changes

The postpartum period is characterized by significant structural and hemodynamic alterations. Cardiac remodelling due to hemodynamic overload during pregnancy involves left ventricular eccentric hypertrophy, commonly referred to as physiological hypertrophy. After childbirth, the woman's heart undergoes reverse remodelling, reverting to its pre-gravid structure and function (Ferreira *et al.* 2021). Within four weeks following delivery, the physiological hypertrophy of the ventricular system, associated with normotensive pregnancy, returns to its pre-pregnancy state (Chauhan & Tadi 2022).

However, in instances of pathological hypertrophy, such as those seen in preeclampsia (PE), postpartum changes have been reported from 1 to 10 years after delivery (Karen Melchiorre *et al.* 2011; DeMartelly *et al.* 2021). The primary structural complications linked to PE include a notably higher prevalence of asymptomatic global left ventricular dysfunction, geometric abnormalities, and myocardial damage (Karen Melchiorre, Sutherland, Baltabaeva, *et al.* 2011b; Karen Melchiorre, Sutherland, Liberati, *et al.* 2011). Furthermore, women with a history

of preeclampsia have been observed to exhibit increased IVS, LVPW, and LV mass compared to those with a normotensive pregnancy history, with these elevated parameters persisting up to 10 years post-delivery (DeMartelly *et al.* 2021). These findings are consistent with the results observed in the present study.

In the past decade, evidence has emerged suggesting that lactation contributes to a decrease in physiological hypertrophy observed in normal pregnancies (Murata *et al.* 2013; C. Dai *et al.* 2020). Notably, lactation has been shown to reduce the risk of metabolic disorders and hypertension in mothers later in life (Murata *et al.* 2013; Poole *et al.* 2014; Countouris *et al.* 2016; Burgess *et al.* 2019). However, a study by Countouris *et al.* (2016) demonstrated that while lactation decreased systolic and diastolic blood pressure among women who developed gestational hypertension, it did not have the same effect on women who developed preeclampsia (Countouris *et al.* 2016).

In the current study, lactation length was not specifically monitored, with pups being weaned at four weeks postpartum. Consequently, determining the impact of lactation on blood pressure reduction and left ventricular remodelling remains challenging. Future research should investigate the combined effects of lactation, as well as examine the specific influence of AdsfIt-1 in the absence/ presence of lactation.

5.2.4 Long-term effects of sFlt-1 overexpression induced sustained increased uterine artery pressure up to 8 weeks post-partum

During a healthy pregnancy, uterine artery Doppler sonography demonstrates a series of structural changes in the uterine spiral arteries, characterized by low impedance and high-flow patterns (A. Robson *et al.* 2012; Burke & Ananth Karumanchi 2013; Cui *et al.* 2013). However, in pregnancies complicated by placental insufficiency, which manifests as PE and/or foetal intrauterine growth restriction, the anticipated decrease in uterine artery impedance is

reduced, typically resulting in elevated UA PI and UA RI values (D. J. Roberts & Post 2008; Collinot *et al.* 2018).

Regarding the normalization of uterine artery indices post-pregnancy, there is a lack of consensus among studies, even in normotensive pregnancies. Some research suggests that significant changes in these indices do not occur until day 28, with a complete return to baseline at 14 weeks (Mulic-Lutvica *et al.* 2007), while other studies report normalization as early as 6 weeks postpartum (Tekay & Jouppila 1993) or 8 weeks (Guedes-Martins *et al.* 2014, 2015).

While delivery is acknowledged as the primary effective treatment for conditions associated with placental insufficiency, there is limited information available on the postpartum resolution of elevated uterine artery UA PI and UA RI. The current study found that uterine artery indices reached peak elevation at 8 weeks postpartum, with normalization observed around 33 weeks postpartum. However, these results did not align with the sparse existing research examining PE and postpartum uterine artery indices specifically.

For example, a study conducted in a semi-rural region of South Africa involved postpartum follow-up of 122 women, including 36 previously affected by preeclampsia. This study found that uterine artery indices remained significantly higher in formerly pre-eclamptic women compared to non-pregnant controls up to three months after delivery (Namugowa *et al.* 2019). Additionally, the study reported that both central and brachial blood pressure indices were higher in previously pre-eclamptic women relative to nonpregnant controls up to one year postpartum. In contrast, a case-control study by Naeh *et al.* (2022) suggested a potential physiological recovery of uterine artery flow at 6 weeks postpartum in pregnancies impacted by PE (Naeh *et al.* 2022).

However, in the current study, a decrease in diastolic function and an elevation in uterine artery indices were observed at 8 weeks postpartum, rather than during pregnancy. This discrepancy may suggest the existence of arterial stiffness in AdsFlt-1 mice after delivery, which could potentially contribute to the prolonged time for normalization of uterine artery indices (Zieman *et al.* 2005; Everett *et al.* 2012; Namugowa *et al.* 2019). Previous research has established that PE is a risk factor for arterial stiffness and cardiomyopathy, which has also been found to affect uterine arteries (S. Kim *et al.* 2020). Consequently, it is plausible that sFlt-1 overexpression during pregnancy results in increased vascular stiffness even in the postpartum period (Kirkinen P *et al.* 1988; Tekay & Jouppila 1993; Kaihura *et al.* 2009; Everett *et al.* 2012; Namugowa *et al.* 2019). Arterial stiffening has been correlated with PE and is more pronounced in PE pregnancies compared to those experiencing gestational hypertension (Hausvater *et al.* 2012).

5.2.5 Short-term exposure of sFlt-1 causes long-term impact on cardiovascular functions

Various studies have proposed differing hypotheses regarding the pathophysiology of PE and, more importantly, the causes of long-term complications following PE (A. Ahmed & Ramma 2015; Thilaganathan & Kalafat 2019; Xiaomei Li *et al.* 2022).

Over the past two decades, the majority of research papers have implicated abnormal placentation and angiogenic factors as primary contributors to PE (J. D. Boyd & W. J. Hamilton. Heffer 1970; W. Robertson *et al.* 1973; Fox & Elston 1978; B. Huppertz 2008; Myatt & Powell 2010; Shu *et al.* 2014; Mandavilli 2018; Gebara *et al.* 2021). However, a more recent review by Thilaganathan & Kalafat (2019), suggested that pathophysiology, in fact, initiates prior to the onset of PE (Thilaganathan & Kalafat 2019). Notably, several cohort studies have reported abnormal cardiovascular functions before the clinical onset of PE (Herbert Valensise *et al.* 2008; Karen Melchiorre *et al.* 2012, 2014; K. Melchiorre *et al.* 2013; Thilaganathan & Kalafat 2019). Furthermore, pregnancy has been referred to as the "ultimate cardiac stress test," as it uncovers previously undetectable cardiovascular disease (Craici *et al.* 2008; E.

Chung & Leinwand 2014). Lactation has also been associated with increased cardiovascular load and instances of cardiac hypertrophy, which revert to normal after lactation in normotensive women (Katharina M. Hiller et al. 2014; Poole et al. 2014; Countouris et al. 2016; Hyatt et al. 2017; Burgess et al. 2019).

In the context of the present study, no evidence was found to support the theory of cardiovascular maladaptations prior to the onset of PE, as this PE model does not permit such conclusions. However, the mice in this study did lactate up to 3 weeks postpartum, raising the question of whether lactation in AdsFlt-1 mice further exacerbated the observed postpartum cardiovascular dysfunctions.

Additionally, diastolic, systolic, and structural dysfunctions in this study were found to correspond with symptoms of cardiomyopathy. Interestingly, increased arterial stiffness has also been demonstrated in cases of cardiomyopathy and even in patients considered recovered from cardiomyopathy (Johansson *et al.* 2021).

In conclusion, while previous studies have reported an association between elevated levels of sFlt-1 and PE as well as heart failure, the current study supports the hypothesis that even brief exposure to increased sFlt-1 levels may induce maladaptations during pregnancy, potentially leading to long-term irreversible damage to the cardiovascular system (Ky et al. 2011a; Gruson et al. 2016a; Tayal et al. 2017; Healthwise Staff 2019; D. Williams et al. 2021; Honigberg 2021).

5.3 Limitations

This study demonstrated that sFlt-1 contributes to postpartum cardiac dysfunctions; however, several limitations must be considered. First, the sample size was inconsistent throughout the study, with six mice per group during pregnancy, four at eight weeks postpartum, and 2-4 at 33 weeks postpartum. Increasing and maintaining a consistent sample size would strengthen the conclusions drawn. Second, although the study identified evident cardiac dysfunction postpartum, additional immunohistochemistry and arterial elasticity analyses should be performed to determine the most prevalent dysfunction in this model or if multiple dysfunctions coexist. Third, calculating the sFlt-1/placental growth factor (PIGF) ratio could enhance the understanding of the observed phenomena in conjunction with ultrasound analysis.

It is also crucial to recognize that recent studies have associated lactation with cardiac hypertrophy and altered cardiac reverse remodelling. Therefore, further investigation is needed to determine whether these long-term effects are indeed caused by sFlt-1, lactation, or if lactation exacerbates sFlt-1 effects on the cardiovascular system. Lastly, it is essential to acknowledge that ultrasound image quality may vary depending on the animal, which could complicate image analysis and interpretation of the results.

Chapter 6

The Role of CSE On Cardiovascular Adaptation During Pregnancy

6. The role of CSE on cardiovascular adaptation during pregnancy

H₂S is a multifunctional molecule with significant roles in various physiological processes, such as vascular tone regulation, mitochondrial function, and cellular homeostasis (R. Wang 2002; G. Yang et al. 2008; Bos et al. 2015). Genetic deficiencies in CSE, one of the enzymes responsible for H₂S production, lead to hypertension and endothelium-dependent vasorelaxation loss (G. Yang et al. 2008), while CBS heterozygotes exhibit elevated blood pressure (U. Sen *et al.* 2010). Mitochondria play a crucial role in cellular homeostasis (Andres et al. 2015; E. Murphy et al. 2016), and H₂S affects numerous processes related to them (Shimizu *et al.* 2018).

Preeclampsia, a pregnancy complication, is linked to H₂S deficiencies due to decreased CSE activity, resulting in an imbalance in angiogenic growth hormones and aberrant placentation (Cindrova-Davies *et al.* 2013; K. Wang *et al.* 2013). H₂S plays a role in various physiological processes during pregnancy, including reproduction, anti-inflammatory action, oxygen sensing, and vasodilation in the placenta (Carson & Konje 2014; X. Hu et al. 2021).

Mitochondria play a significant role in cellular homeostasis due to their functions in fuel utilization, calcium storage, intracellular signalling, and cell death (Andres et al. 2015; E. Murphy et al. 2016). Consequently, mitochondrial dysfunction contributes to the emergence of various diseases, including heart failure, cancer, diabetes, and neurodegenerative illness (E. Murphy et al. 2016). H₂S regulates numerous biological processes, including angiogenesis, proliferation, redox balance, inflammation, and cell death, and is produced by enzymes CBS, CSE, and 3MST. 3-MST mediates the intramitochondrial generation of H₂S and other sulfur species, which supports cellular bioenergetics and preserves mitochondrial electron transport (Shimizu *et al.* 2018). H₂S deficiency may be linked to preeclampsia and CSE-deficient mice display mild hypertension and weakened endothelium-dependent relaxant reactions (Nicholson & Calvert 2010; Kondo *et al.* 2013).

Investigating CSE knockout (KO) in pregnancy and the heart specifically is crucial to understanding the functional changes of uteroplacental vasculature under physiological and pathological states of pregnancy. Additionally, focusing on the mitochondria in the heart is

essential to explore the potential therapeutic applications of H₂S in cardiovascular disorders such as atherosclerosis, myocardial ischemia injury, and hypertension.

Despite numerous investigations into various models of H₂S deficiency, studies specifically examining the relationship between preeclampsia and H₂S deficiency are limited. Therefore, to explore the effects of H₂S deficiency on pregnancy and pre-pregnancy conditions, the cardiovascular system of previously validated CSE KO mice was assessed.

6.1 CSE KO in pregnancy

Preeclampsia, a pregnancy complication, is associated with an imbalance in angiogenic growth hormones and aberrant placentation. H₂S is a proangiogenic vasodilator mainly produced by CSE. A decrease in CSE activity can lead to altered angiogenic equilibrium, aberrant placentation, and maternal hypertension (K. Wang *et al.* 2013). In pregnancies with severe early-onset growth restriction and preeclampsia, there is decreased immunoreactivity of CSE in the placenta, leading to increased vascular resistance (Cindrova-Davies *et al.* 2013).

H₂S plays a role in various physiological processes, including reproduction. It has been found to act as an anti-inflammatory, oxygen sensor, and vasodilator in the placenta, or both to maintain uterine quiescence during pregnancy (Carson & Konje 2014). In gestational diabetes mellitus, a deficiency of H₂S synthetase in the placenta leads to increased activation of the NLRP3 inflammasome, which is involved in the release of inflammatory cytokines and initiation of maternal insulin resistance (Wu *et al.*, 2021).

Studies have demonstrated that maladaptations during pregnancy, whether hormonal, cardiovascular, or metabolic, can result in significant adverse outcomes for both the mother and the foetus (Duvekot *et al.* 1993; Duvekot & Peeters 1994; S. E. Maynard *et al.* 2003; F Burbank 2009; Fred. Burbank 2009; Gyselaers *et al.* 2011; Amaral *et al.* 2015; Bokslag *et al.* 2017; Kazma *et al.* 2020). Notably, cardiovascular maladaptations during pregnancy have been associated with an increased risk of cardiovascular and cerebrovascular diseases later in life (James Metcalfe 1963; A. Y. H. Wong *et al.* 2002; Karen Melchiorre, Sutherland, Liberati, *et al.* 2011; Amaral *et al.* 2015; Lima *et al.* 2019; Washington C. Hill *et al.* 2020; DeMartelly *et al.* 2021; Hutchens *et al.* 2022; Beckett *et al.* 2023; Giorgione *et al.* 2023a). Abnormal cardiac hemodynamic changes have been reported in PE, including a decrease in ejection fraction,

decrease in mitral flow, and a severe decrease in diastolic volume (Mesa *et al.* 1999; Borghi *et al.* 2000; Savu *et al.* 2012; Amraoui *et al.* 2014; Dennis & Castro 2014; Lambert *et al.* 2014; Castleman *et al.* 2016; Perry *et al.* 2018). Therefore, the aim of this study was to compare the adaptations observed in normotensive pregnancies with those seen in CSE KO models. Cardiovascular functions were monitored via ultrasonography and colour Doppler before time-mating and near term on day E17.5.

6.1.1 Effects of CSE KO on cardiac systolic functions during pregnancy

To investigate the role of CSE in cardiac adaptation during pregnancy, cardiac function in CSE WT and KO mice before pregnancy and during pregnancy at E17.5 were monitored. Four systolic parameters were assessed: CO, SV, EF, and FS (Figure 6.6.1). No significant difference was seen in CO.

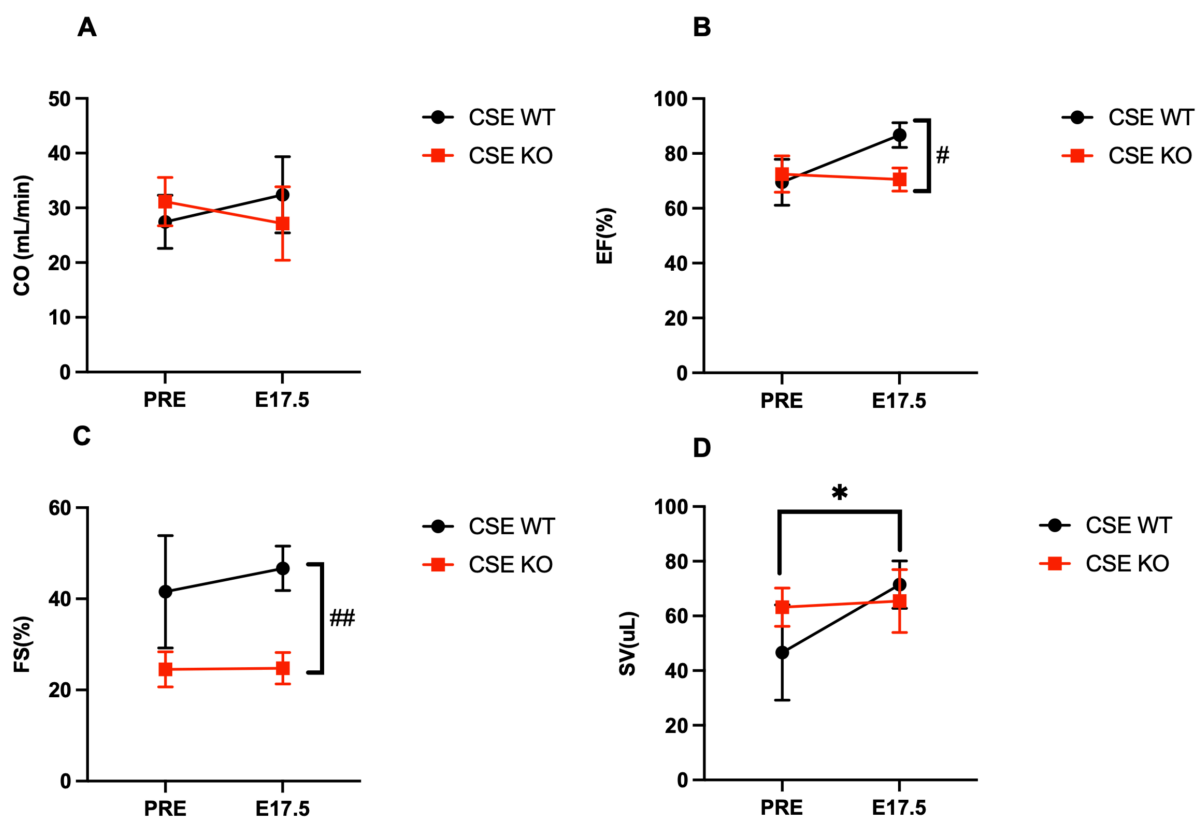


Figure 6.1 Systolic functions of left ventricle adaptations in Wild type (WT) and knockout (KO) mice.

Echocardiography analysis was carried out on mice before pregnancy (12 weeks old) and on E17.5 of pregnancy from both WT and KO mice. The cardiac output (**A**), the ejection fraction (**B**), the fraction shortening (**C**), and stroke volume (**D**) were measured in pre-pregnancy and during pregnancy at E17.5 (n=5/group). Cardiac output (A), Ejection fraction (B), fraction shortening (C) were similar pre-pregnancy and E17.5 in CSE WT mice. Stroke volume (D) was significantly increased in E17.5 when compared with pre-pregnancy in CSE WT. The ejection fraction (B) and the fraction shortening (C) were significantly increased in CSE WT mice when compared to CSE KO mice. Statistical comparison was performed using Mann Whitney test. #= $P < 0.005$ WT vs KO E17.5; ## $P < 0.001$ WT vs KO E17.5; * $P < 0.05$ WT Pre vs WT E17.5

Nonetheless, a notable elevation in EF and FS was observed in pregnant CSE WT mice compared to CSE KO mice (Figure 6.6.1B and Figure 6.6.1C). Additionally, while a significant increase in SV was detected in CSE WT mice when comparing pre-pregnant to pregnant states, no such difference was evident in the CSE KO mice. This indicates that cardiac adaptation took place in CSE WT mice. However, lack of CSE disrupted the adaptive changes of the heart during pregnancy.

6.1.2 Effects of CSE KO on cardiac diastolic functions during pregnancy

To evaluate diastolic function before and during pregnancy, eight diastolic parameters were assessed: MV E/A ratio, MV area, IVCT, and IVRT. No significant difference was seen in MV E/A nor in the MV Area.

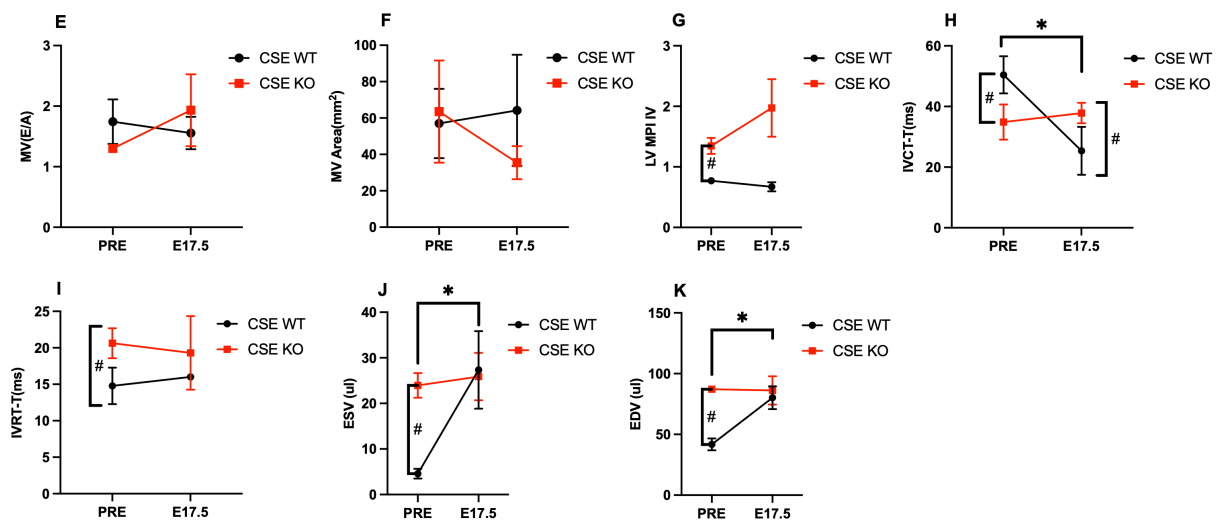


Figure 6.2 Diastolic functions of left ventricle adaptations in Wild type (WT) and knockout (KO).

Echocardiography was used to measure diastolic heart function in WT and KO mice before pregnancy and on E17.5. Mitral flow E/A ratio (MV E/A) (**E**) and Mitral flow area (MV Area) (**F**) were unchanged pre-pregnancy and during pregnancy in both WT and KO mice. Myocardial Performance Index (LV MPI) (**G**) was significantly increased in CSE KO mice in pre-pregnancy when compared to CSE WT mice. No significant change was observed during pregnancy in the LV MPI. Isovolumetric contraction time (IVCT) (**H**) was significantly decreased in CSE WT mice when comparing pregnant CSE WT mice to non-pregnant mice. Additionally, when compared to CSE KO mice, CSE WT mice had an increased IVCT in pre-pregnancy but a decreased IVCT during pregnancy, when compared to CSE KO mice. Isovolumetric relaxation time (IVRT) (**I**) was significantly increased in non-pregnant CSE KO mice, when compared to CSE WT mice. No significant difference was observed in the IVRT during pregnancy. End systolic volume (ESV) (**J**) was significantly decreased in CSE WT mice when compared to CSE KO mice in pre-pregnancy. Additionally, a significant increase in ESV was observed in CSE WT during pregnancy, when compared to pre-pregnancy. End systolic volume (ESV) (**K**) was significantly decreased in CSE WT mice compared to KO mice in pre-pregnancy. However, a significant increase was observed in WT mice during pregnancy, when compared to pre-pregnancy. Statistical comparison was performed using Mann Whitney test. #=P<0.005 WT vs KO *P<0.05 WT Pre vs WT E17.5

In the pre-pregnancy state, an elevated LV MPI was observed in CSE KO mice compared to CSE WT mice. Additionally, IVCT was significantly reduced in pregnant CSE WT mice relative to non-pregnant mice. When comparing CSE KO mice, the IVCT was increased in CSE WT mice during pre-pregnancy but decreased during pregnancy.

IVRT was found to be significantly elevated in non-pregnant CSE KO mice when compared to CSE WT mice. However, no notable difference was detected in IVRT during pregnancy. In terms of ESV, a significant reduction was observed in pre-pregnant CSE WT mice when compared to CSE KO mice. Furthermore, a substantial increase in ESV was noted in CSE WT mice during pregnancy relative to pre-pregnancy levels.

These findings suggest that CSE KO mice may exhibit altered cardiac function compared to CSE WT mice, particularly in the pre-pregnancy state. The differences in LV MPI, IVCT, IVRT, and ESV between CSE KO and WT mice imply potential dysfunction in CSE KO mice, which could affect their ability to adapt to the physiological changes associated with pregnancy.

6.1.3 Effects of CSE KO on cardiac structural changes

The objective of the present study was to assess cardiac structural alterations by comparing seven structural parameters between CSE KO and CSE WT pregnant mice before pregnancy and at E17.5 during pregnancy. The seven measurements (Figure 6.3) included LV mass,

interventricular septum (IVS) thickness during systole and diastole, left ventricular internal diameter (LVID) during systole and diastole, and left ventricular posterior wall (LVPW) thickness during systole and diastole. These findings provide insights into the potential differences in cardiac structure between CSE KO and WT mice, both before and during pregnancy. By examining these structural parameters, a better understanding on how CSE deficiency may influence cardiac adaptations in pregnant mice, particularly within the context of PE could be elucidated.

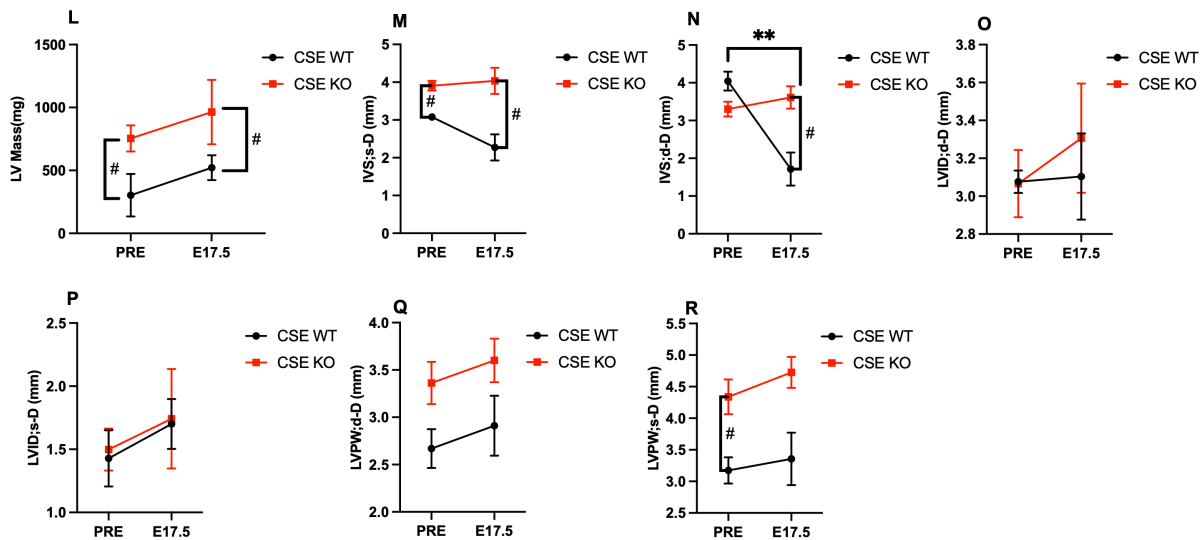


Figure 6.3 Structural functions of left ventricle adaptations in Wild type (WT) and knockout (KO).

Echocardiography was used to measure structural functions in WT and KO mice before pregnancy and on E17.5. While the left ventricle mass (LV Mass) (L) remained unchanged during pregnancy in both groups. A significant increase was observed in KO when comparing WT mice in both pre-pregnancy as well as E17.5. Interventricular septum (IVS;s) (M) thickness during systole remained unchanged during pregnancy in both groups. An increased IVS;s was observed both in pre-pregnancy and during pregnancy in CSE KO mice when compared to CSE WT mice. Interventricular septum (IVS;d) (N) thickness during diastole was significantly decreased in CSE WT mice during pregnancy when compared to pre-pregnancy. An increased IVS;d was observed in CSE KO during pregnancy when compared to CSE WT mice. Left ventricular internal diameter (LVID;d) (O) during diastole remained unchanged. No significant difference was observed between either group either. Left ventricular internal diameter (LVID;s) during systole (P) remained unchanged. No significant difference was observed between either group either. Left ventricular posterior wall (LVPW;d) (Q) thickness during diastole remained unchanged. No significant difference was observed between either group either. Left ventricular posterior wall (LVPW;s) (R) thickness during systole was significantly increased in KO when comparing WT mice in pre-pregnancy. No significant difference was observed during pregnancy. Statistical comparison was performed using Mann Whitney test. #= $P < 0.005$ WT vs KO

The LV Mass remained consistent during pregnancy for both CSE KO and CSE WT groups. However, a significant increase was observed in the KO group compared to the WT group in both pre-pregnancy and at E17.5. IVS;s remained unchanged during pregnancy in both groups, but an increased IVS;s was observed in CSE KO mice compared to CSE WT mice, both in pre-pregnancy and during pregnancy.

IVS;d exhibited a significant decrease in CSE WT mice during pregnancy compared to pre-pregnancy, whereas an increased IVS;d was observed in CSE KO mice during pregnancy relative to CSE WT mice. LVID;d remained constant, with no significant difference observed between the two groups. Similarly, LVID;s and LVPW;d thickness during diastole remained unchanged, with no noticeable difference between the groups.

However, LVPW;s demonstrated a significant increase in the KO group compared to the WT group in pre-pregnancy, while no substantial difference was found during pregnancy.

These findings suggest that there are differences in cardiac structure between CSE KO and WT mice, particularly in certain parameters such as LV Mass, IVS thickness, and LVPW;s thickness. These alterations in CSE KO mice may potentially impact their ability to adapt to the physiological changes associated with pregnancy, warranting further investigation into the implications of CSE deficiency on cardiac function.

6.1.4 Effects of CSE KO on uterine artery blood flow

In order to evaluate uterine artery adaptation, two blood flow parameters – the UA RI and the UA PI – were measured in CSE KO mice and CSE WT mice both before pregnancy and at E17.5.

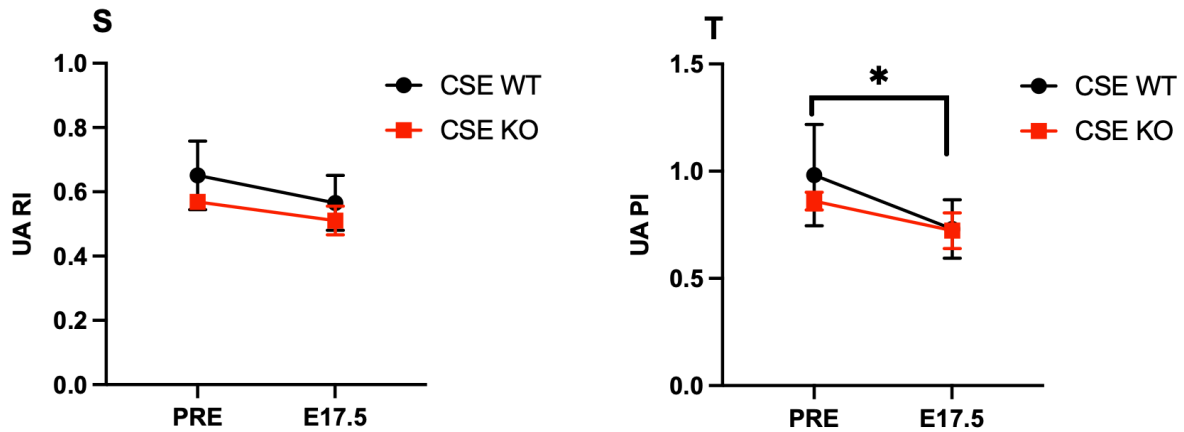


Figure 6.4 Uterine artery flow adaptations in Wild type (WT) and knockout (KO). Uterine artery flow was measured in WT and KO mice before pregnancy and on E17.5.

Resistive index (RI) (J) remained unchanged in both groups, but pulsatility index (PI) (K) was significantly decreased during pregnancy in WT mice. * $P < 0.05$ WT Pre vs WT E17.5 Statistical comparison was performed using Mann Whitney test.

The assessment (Figure 6.4) of uterine artery flow in both WT and KO mice revealed that the UA RI remained unchanged in both groups throughout the course of pregnancy. However, a significant reduction in the UA PI was observed in WT mice during pregnancy, indicating that uterine artery adaptation to pregnancy indeed occurred. Moreover, these findings suggest that in CSE KO mice, the vascular adaptation to pregnancy within the uterine artery was impaired, contrary to what was observed in the WT mice, further implying that a deficiency in H_2S hinders proper adaptation to pregnancy.

6.1.5 Cardiac mitochondrial content is influenced by endogenous H_2S

Although mitochondrial DNA (mtDNA), does not directly reflect mitochondrial functionality, it is associated with the activity of mitochondrial enzymes and the production of adenosine triphosphate (S. Li & Yang 2015; Castellani *et al.* 2020). This study aimed to investigate the potential association between cardiac mitochondrial content and H_2S deficiency. Cardiac samples were collected from CSE KO and CSE WT mice prior to conception and at E17.5 of pregnancy.

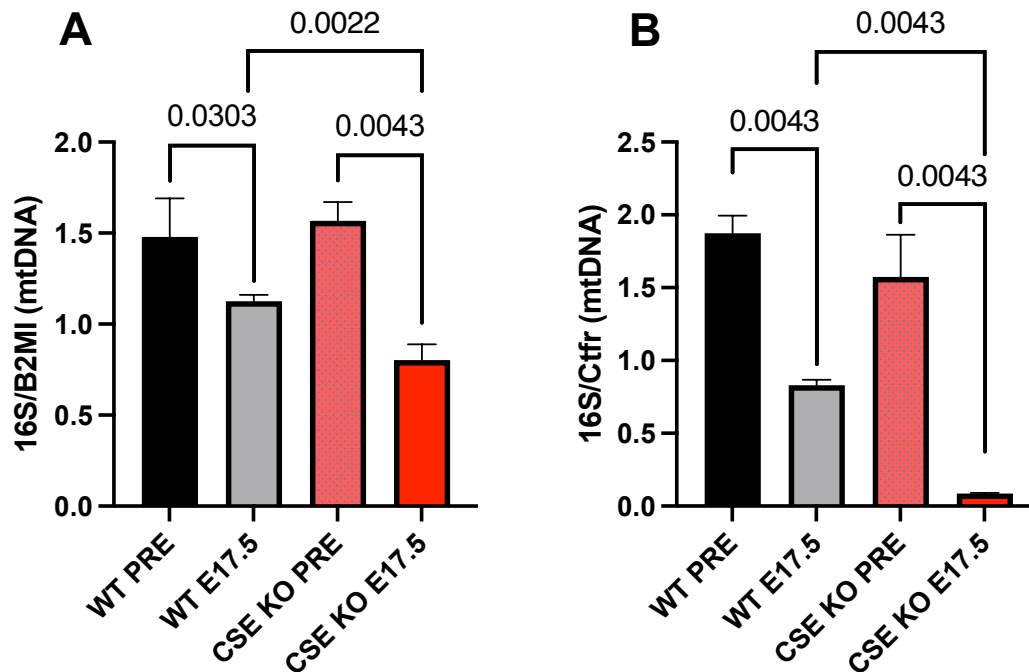


Figure 6.5 Bar plot showing the effect of CSE Knockdown on mitochondrial DNA (mtDNA) of pregnant versus non-pregnant mice.

Relative quantification was performed on the cardiac tissue of n=6 CSE WT and CSE KO mice both pre- pregnancy and during pregnancy, in duplicates using qPCR by amplification of 16S gene, normalised against B2MI (A) and Ctfr (B), nuclear genes. A significant decrease in mtDNA/nDNA ratio (A & B) were detected in the hearts of pregnant CSE WT and CSE KO mice compared to pre-pregnant CSE WT and CSE KO mice. A decrease in mtDNA was also seen in pregnant WT mice, when compared to non-pregnant WT mice. Statistical comparison was performed using Mann Whitney test.

Interestingly, significant decrease in mtDNA/nDNA ratio were detected in pregnant CSE WT and CSE KO mice compared to their non-pregnant controls (Figure 6.5) indicating a decrease in cardiac mitochondrial content relative to nuclear content during pregnancy. However, compared to pregnant CSE WT mice, the relative mitochondrial content was significantly decreased in CSE KO mice, suggesting loss of CSE led to impaired mitochondrial biogenesis.

Taken together, these findings indicate that cardiac mitochondrial content may be affected by endogenous H₂S concentrations. This postulates that CSE KO mice, which exhibit H₂S deficiency, may experience altered cardiac mitochondrial content compared to CSE WT mice. Understanding the implications of these differences could provide valuable insights into the role of H₂S in cardiac function and inform the development of therapeutic strategies to manage

heart-related complications associated with H₂S deficiency (Goffart *et al.* 2004; Rosca & Hoppel 2013; Fillmore *et al.* 2014).

6.2 Discussion

This study aimed to investigate the role of H₂S deficiency in cardiac function and uteroplacental vasculature during pregnancy, particularly in relation to PE. H₂S deficiency has been linked to preeclampsia due to decreased CSE activity. Examining CSE KO mice can provide insights into the functional changes of uteroplacental vasculature and potential therapeutic applications of H₂S in cardiovascular disorders. The study is crucial as maladaptations during pregnancy can lead to significant adverse outcomes for both the mother and the foetus and increase the risk of cardiovascular and cerebrovascular diseases later in life.

6.2.1 CSE KO effect on adaptations to pregnancy

H₂S is a key regulator of cardiovascular homeostasis and has been linked to cardiovascular disease with embryonic origins (Hsu & Tain 2021). H₂S-based therapies have uncovered its potential in reversing programming processes and preventing adult-onset cardiovascular disease in animal models (Wen *et al.* 2018; Zhen Li *et al.* 2018). H₂S has been identified as a significant factor in the development of hypertension, both in humans and animals (G. Yang *et al.* 2008; K. Wang *et al.* 2013). Recent data suggest that H₂S plays a vital role in inflammatory reactions within uterine tissues, which are associated with uterine activation for labour (X. J. You *et al.* 2011; X. You *et al.* 2017). The human myometrium produces H₂S via enzymes CSE and CBS during pregnancy (X. J. You *et al.* 2011). Investigations into the role of H₂S in maintaining uterine quiescence throughout pregnancy have revealed that it inhibits myometrial inflammation, thereby reducing the expression of contraction-associated proteins (Zanardo *et al.* 2006b; X. J. You *et al.* 2011), highlighting the importance of endogenous H₂S in preserving uterine quiescence during pregnancy (X. You *et al.* 2017).

The present study's findings show notable differences in various aspects of cardiac function and structure between CSE KO and CSE WT mice, particularly in the pre-pregnancy state.

These alterations include disparities in EF, FS, SV, LV mass, IVS, and LVPW. Moreover, the assessment of uterine artery flow revealed differences in blood flow adaptations between the two groups, specifically concerning the UA PI. These deviations in cardiac function and structure, as well as uterine artery blood flow adaptations, suggest that CSE KO mice may have a reduced ability to adapt to the physiological changes associated with pregnancy compared to CSE WT mice. This could potentially be due to the lack of endogenous H₂S and its inability to preserve uterine quiescence (X. You *et al.* 2017), as well as the importance of KATP channel activation in this process.

These findings imply that CSE deficiency may have significant implications for cardiac function during pregnancy, potentially leading to dysfunction and maladaptation. Crucially, this present investigation indicates that the observed maladaptations may be attributed to pre-existing cardiac dysfunction prior to pregnancy, as evidenced by the pre-pregnancy differences identified in this study.

6.2.2 CSE KO on mitochondrial function

Mitochondrial H₂S signalling influences respiration, apoptosis, biogenesis, and morphology in a concentration-dependent manner, affecting the electron transport chain (ETC) activity (P. Nicholls & Kim 1982; Peter Nicholls *et al.* 2013). H₂S also regulates mitochondrial biogenesis through PGC-1 activation and persulfidation-mediated activation of PGC-1, PPRC, and AMPK pathways (Untereiner, Fu, *et al.* 2016; Untereiner, Wang, *et al.* 2016; Shimizu *et al.* 2018; Zhai *et al.* 2019). H₂S modulates mitochondrial morphogenesis by controlling Drps in a SIRT3-dependent manner (Santel & Fuller 2001; Smirnova *et al.* 2001; Ishihara *et al.* 2004, 2006; N. Liu *et al.* 2017; Qiao *et al.* 2017b; Chakraborty *et al.* 2018; G. Meng *et al.* 2018; J. Zhang *et al.* 2018; M. Xu *et al.* 2019).

Research has demonstrated that protein sulfhydration is an important mechanism through which H₂S balances cellular signalling (Paul & Snyder 2012a). For example, H₂S sulfhydration of NFκB's p65 subunit is essential for the protein's antiapoptotic effects (N. Sen *et al.* 2012). H₂S also induces hyperpolarization and vasorelaxation in endothelial cells and smooth muscle cells by sulfhydrating ATP-sensitive potassium channels (Mustafa *et al.* 2011). Furthermore, H₂S controls cellular bioenergetics by impacting mitochondrial function, such as by donating

electrons to the mitochondrial ETC, stimulating mitochondrial bioenergetics (Fu *et al.* 2012; Módis *et al.* 2013). This activity complements and balances the bioenergetic role of Krebs cycle-derived electron donors and maintains mitochondrial electron transport (Módis *et al.* 2013). In contrast, H₂S acts as a potent and reversible inhibitor of mitochondrial function by regulating cytochrome c oxidase (complex IV of the mitochondrial ETC) (Hill *et al.* 1984).

Recent studies suggest that H₂S protects against cardiac damage through an eNOS-dependent mechanism (Minamishima *et al.* 2009; King *et al.* 2014) and enhances NO bioavailability and signalling (Kondo *et al.* 2013; Polhemus *et al.* 2013).

Moreover, during the early asymptomatic phase of PE (usually observed at 8 to 10 weeks of gestation), an ischemic placental environment, resulting from inadequate placental perfusion, inducing elevated oxidative stress has been demonstrated (Bilodeau 2014; Marschalek *et al.* 2018). This can be explained by the fact that preeclamptic placentas exhibit a slower antioxidant clearance rate due to increased oxidative stress present in both the placenta and maternal circulation during PE (Yuping Wang & Walsh 1996; Hubel 1999; Myatt & Cui 2004b). Studies have demonstrated that oxidative stress, diminished trophoblastic differentiation, and hindered invasion of trophoblastic tissue are all related to mitochondrial dysfunction, which may serve as a critical factor in PE (Qiu *et al.* 2012). Cells exposed to oxidative stress augment their production of mtDNA copies to repair damage and neutralize reactive oxygen species (Y. Wang & Walsh 1998; Graham J. Burton & Jauniaux 2011; Wen *et al.* 2013; Navarro-YepesJuliana *et al.* 2014; Papa Gobbi *et al.* 2018). Additionally, the lack of histone protection renders mtDNA highly susceptible to oxidative stress-related cellular damage (H. C. Lee & Wei 2000; J. Lu *et al.* 2009; Qiu *et al.* 2012; Marschalek *et al.* 2018). Alterations in peripheral blood mtDNA copy numbers have been proposed as potential biomarkers for mitochondrial failure in diseases induced by oxidative stress (Stark & Roden 2007; Ježek *et al.* 2010; Qiu *et al.* 2012).

The combination of these findings in current literature suggests mitochondrial dysfunction as a pathogenic mediator and mtDNA as a potential biomarker of oxidative stress, a pathophysiological component of PE (Elrod *et al.* 2007; Nicholson & Calvert 2010; Qiu *et al.* 2012; Murata *et al.* 2013; King *et al.* 2014; Shimizu *et al.* 2018; Sundquist *et al.* 2022). The objective of this study was to examine maternal cardiac-mtDNA levels in CSE KO mice, pre-pregnancy and during pregnancy.

MtDNA) levels in pregnant CSE KO and CSE WT mice were quantified. A significant elevation in mtDNA levels was observed in pregnant CSE KO mice compared to pregnant CSE WT mice. Moreover, an increase was noted when comparing non-pregnant WT mice to pregnant WT mice.

Intriguingly, our findings that mitochondrial DNA contents were relatively decreased during pregnancy were not in consistent with previous research positing that mtDNA levels increase during normotensive pregnancy (Srivastava et al. 2022). However, it has been demonstrated that reduced circulating mtDNA is associated with PE compared to normal pregnancy (Cushen et al. 2022). In the currently study, we found that the relative mtDNA content was significantly reduced in pregnant CSE KO mice compared to CSE WT mice. Our results supported the current understanding that endogenous H₂S plays an important role in maintaining the mitochondrial homeostasis (S. Paul et al. 2021). Loss of CSE/H₂S may lead to aberrant mitochondrial activity in cardiac tissue and subsequently result in cardiovascular dysfunction.

6.3 Conclusion

Overall, this study demonstrated significant differences in cardiac function, structure, uterine artery flow, and mitochondrial function between CSE KO and CSE WT mice, during pregnancy. These alterations in cardiac function, structure, and uterine artery flow adaptations indicated that CSE KO mice may have a reduced ability to adapt to physiological changes during pregnancy compared to CSE WT mice, potentially due to H₂S deficiency.

Mitochondrial H₂S signalling affects several processes (e.g., morphology in a concentration-dependent manner, influencing ETC activity) and modulates cellular bioenergetics (P. Nicholls & Kim 1982; Módis *et al.* 2013; Peter Nicholls *et al.* 2013). Furthermore, H₂S protects against cardiac damage through an eNOS-dependent mechanism and enhances NO bioavailability and signalling (Minamishima *et al.* 2009; King *et al.* 2014).

The observed maladaptations in cardiac function and structure may be attributed to pre-existing dysfunction prior to pregnancy, as evidenced by the pre-pregnancy differences identified in this study. These findings could imply that CSE deficiency or H₂S deficiency may lead to reduced ability to adapt to physiological changes during pregnancy, potentially causing dysfunction and maladaptation. Altered mitochondrial function may play a role in these

differences, and further research is necessary to understand the underlying mechanisms and potential clinical implications.

6.4 Limitations

This study revealed the impact of H₂S deficiency on pregnancy, as evidenced by structural and diastolic differences, as well as decreased mtDNA levels in cardiac tissue. This model therefore recapitulated the parameters observed in PE. Nonetheless, the study also presented several limitations such as, the lack of immunohistochemistry to examine specific structural changes associated with this PE model. Additionally, while a decrease in mtDNA levels was observed, mitochondrial function was not investigated. Therefore, it is recommended that future studies assess mitochondrial function using high-resolution respirometry or fluorescence-based assays to measure parameters such as mitochondrial calcium, superoxide, mitochondrial permeability transition, and membrane potential.

Furthermore, due to limited research on the long-term effects of H₂S deficiency, particularly in the CSE KO model, it is essential to extend investigations to these long-term consequences. This approach would provide further elucidation regarding whether pregnancy exacerbates the decline in mitochondria or if mitochondrial levels recover post-pregnancy, suggesting a potential rescue mechanism.

Chapter 7

RNA sequencing in heart tissue of PE models

7. Gene Expression in PE models

Over the past decade, scientific research in pregnancy disorders has focused on examining placental metabolism, phenotyping, and transcriptome analysis, which have been made possible by advancements in next-generation sequencing (Medina-Bastidas *et al.* 2020). These studies have successfully established a correlation between pregnancy complications and diminished placental function (Staff *et al.* 2013; J. M. Roberts 2014; Cox *et al.* 2015; McAninch *et al.* 2017; Graham J. Burton & Jauniaux 2018; Knöfler *et al.* 2019). Specifically, transcriptome research utilizing mRNA-seq or microarray techniques have been used to elucidate the molecular pathways underlying pathophysiology and to identify placenta-derived biomarkers that could enhance the prediction and diagnosis of PE (Staff *et al.* 2013; Cox *et al.* 2015). Messenger RNA, or mRNA, is a type of single-stranded RNA molecule that plays a crucial role in protein synthesis (S. K. Sen 2023). mRNA acts as this intermediary, transferring genetic information from DNA to the protein synthesis machinery. Thus, mRNA plays an essential role in the fundamental process of generating a living organism and is crucial in connecting the DNA code of life to the cellular machinery that produces proteins (S. K. Sen 2023). Disturbances in mRNA metabolism can lead to alterations in protein synthesis and secretion, which can contribute to the development of PE (Sammar *et al.* 2011; Gourvas *et al.* 2014; Prins *et al.* 2016). RNA sequencing studies have identified many genes that are dysregulated in PE, including some established biomarkers such as sFlt-1, and other promising candidates (Rezk *et al.* 2022).

In this study, the objective was to investigate the overall genetic profile, with a particular focus on cardiac and cerebrovascular genes and pathways. The main aim of this study was to compare the genetic profiles of distinct models of PE, namely the CSE KO model and the AdsFlt-1 model. We hypothesized that these models would exhibit similar genetic profiles, but that the AdsFlt-1 model postpartum would show a different genetic expression pattern. To test this hypothesis, mRNA expression profiles were assessed in tissues obtained from the placenta and heart of CSE KO mice, as well as from tissues derived from the heart of AdsFlt-1 mice, alongside their respective controls. These tissues were collected at E17.5 of pregnancy and at 34-37 weeks postpartum.

7.1 Gene expression CSE KO mice

To assess the mRNA expression profiles in heart tissues, Differential expression analysis was undertaken with the Novogene – Novomagic software.

7.1.1 Gene expression in cardiac tissue of non-pregnant CSE KO vs CSE WT mice

To determine the differentially expressed genes in the LV tissues in non-pregnant and pregnant CSE KO and CSE WT mice, the profile of gene expression was analysed. There were 23,646 differentially expressed genes (DEG) identified from non-pregnant CSE KO and CSE WT mice. Of these, 23,646 DEG, only 927 genes were significantly expressed. Among these DEG, 426 were up-regulated and 501 down-regulated ($\log FC > 1$, P value 0.05) were observed, which were depicted on a volcano map. Up-regulated genes were illustrated by red dots, down-regulated genes by blue dots, and non-significant DEG were represented by green dots. The expression profile of statistically significant DEG was presented in a heatmap (Figure 7.1B), where up-regulated genes were shown in red and down-regulated genes in blue. Both the heatmap and the volcano plot for the DEG were showcased in Figure 7.1 and analysed with Novomagic software.

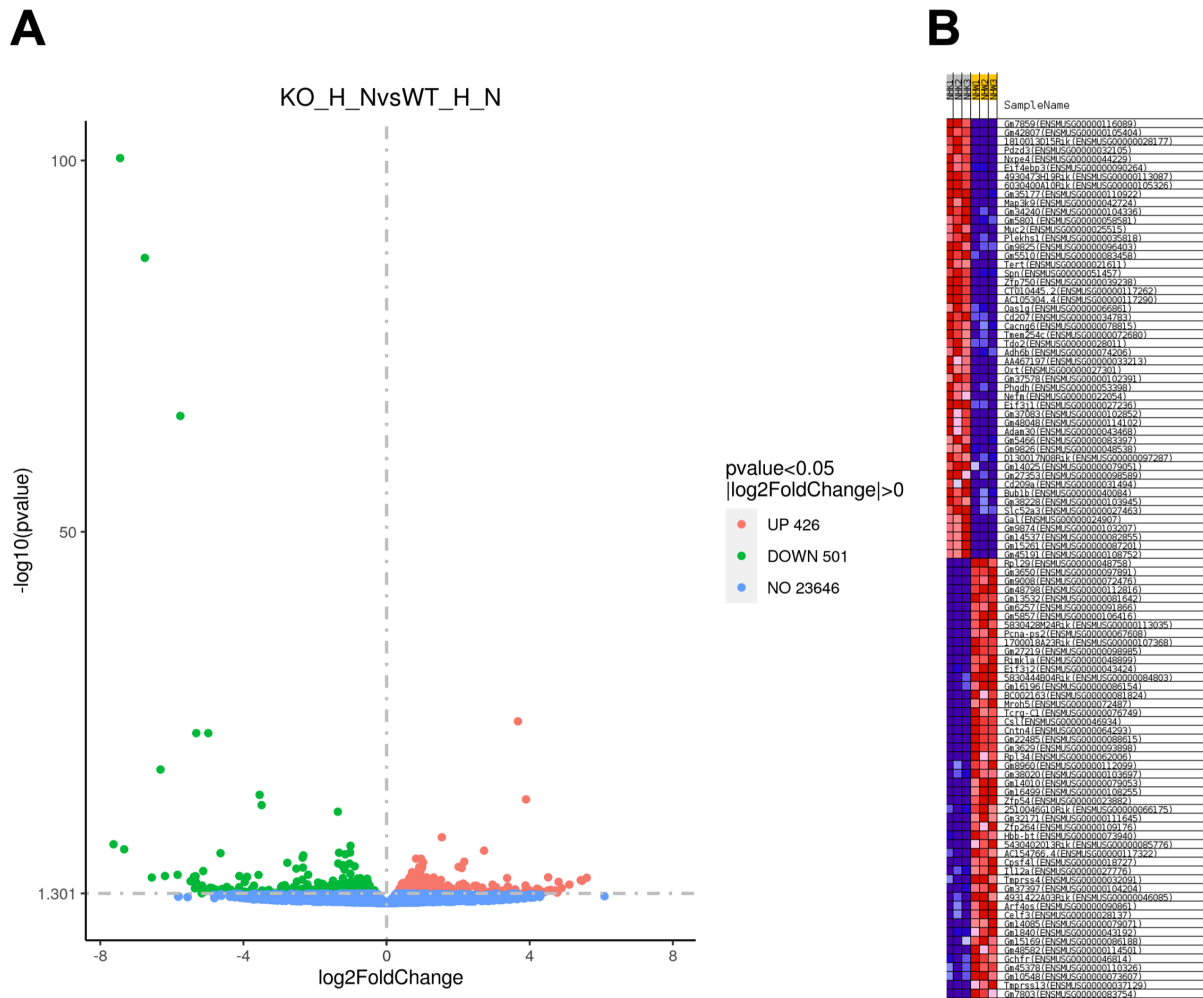


Figure 7.1 The DEG in cardiac tissue of non-pregnant of CSE KO (n=2) vs CSE WT mice (n=2), was visually represented by a volcano plot and a heatmap.

The volcano plot (A) illustrated up-regulated genes with red dots and down-regulated genes with green dots. The heatmap (B) depicted up-regulated genes as red and down-regulated genes as blue.

A table with the top 5 most upregulated (table 7.1) genes and most downregulated DEG (table 7.2) looking at non-pregnant CSE KO vs CSE WT, was integrated.

| Gene ID | Gene Name | Full Name | Adjusted P-value |
|---------|-----------|-----------|------------------|
|---------|-----------|-----------|------------------|

| | | | |
|--------------------|---------|-----------------------------------------------------------------------------------------------|----------|
| ENSMUSG00000044229 | Nxpe4 | neurexophilin and PC-esterase domain family, member 4 [Source:MGI Symbol;Acc:MGI:1924792] | 1.66E-05 |
| ENSMUSG00000032105 | Pdzd3 | PDZ domain containing 3 [Source: MGI Symbol; Acc: MGI:2429554] | 8.51E-97 |
| ENSMUSG00000027236 | Eif3j1 | eukaryotic translation initiation factor 3, subunit J1 [Source: MGI Symbol; Acc: MGI:1925905] | 6.86E-05 |
| ENSMUSG00000022066 | Entpd4b | ectonucleoside triphosphate diphosphohydrolase 4B [Source: MGI Symbol; Acc: MGI:5435040] | 1.17E-83 |
| ENSMUSG00000042109 | Csdc2 | cold shock domain containing C2, RNA binding [Source: MGI Symbol; Acc: MGI:2146027] | 2.67E-15 |

Table 7.1 Table of top 5 upregulated genes with a cut-off at p adjusted of 0.05, ordered in descending order from the most upregulated gene to the least upregulated gene in non-pregnant KO mice versus non-pregnant WT mice.

| Gene ID | Gene Name | Full Name | Adjusted P-value |
|--------------------|-----------|---------------------------------------------------------------|------------------|
| ENSMUSG00000048758 | Rpl29 | ribosomal protein L29 [Source: MGI Symbol; Acc: MGI:99687] | 1.09E-14 |
| ENSMUSG00000081824 | BC002163 | cDNA sequence BC002163 [Source: MGI Symbol; Acc: MGI:3612445] | 3.39E-25 |

| | | | |
|--------------------|----------|--------------------------------------------------------------------------------------|----------|
| ENSMUSG00000062006 | Rpl34 | ribosomal protein L34 [Source: MGI Symbol; Acc: MGI:1915686] | 8.68E-08 |
| ENSMUSG00000079071 | Gm14085 | predicted gene 14085 [Source: MGI Symbol; Acc: MGI:3702173] | 2.70E-06 |
| ENSMUSG00000067608 | Pcna-ps2 | proliferating cell nuclear antigen pseudogene 2 [Source: MGI Symbol; Acc: MGI:97505] | 1.86E-05 |

Table 7.2 Table of top 5 downregulated genes with a cut-off at p adjusted of 0.05, ordered in ascending order from the most downregulated gene to the least downregulated gene in non-pregnant KO mice versus non-pregnant WT mice.

To examine the functional roles of the DEG, Gene Ontology (GO) analysis was performed (Figure 7.2). The GO analysis can be categorized into three categories: biological processes (BP), cellular components (CC), and molecular functions (MF). In this study, upregulated DEG (Figure 7.2 A1) were significantly correlated with 98 BP, 8 CC and 0 MF, and the downregulated DEG (Figure 7.2 A2) were significantly correlated with 1 CC only.

The top 5 most upregulated BP included regulation of ERK1 and ERK2 cascade, mononuclear cell migration, eosinophil chemotaxis, negative regulation of neuron apoptotic process and negative regulation of immune system process.

The top 5 CC terms in upregulated DEG included membrane raft, membrane microdomain, plasma membrane raft, and ECM. The downregulated DEG were significantly (Figure 7.2 B2) correlated with only one CC term, spliceosomal complex.

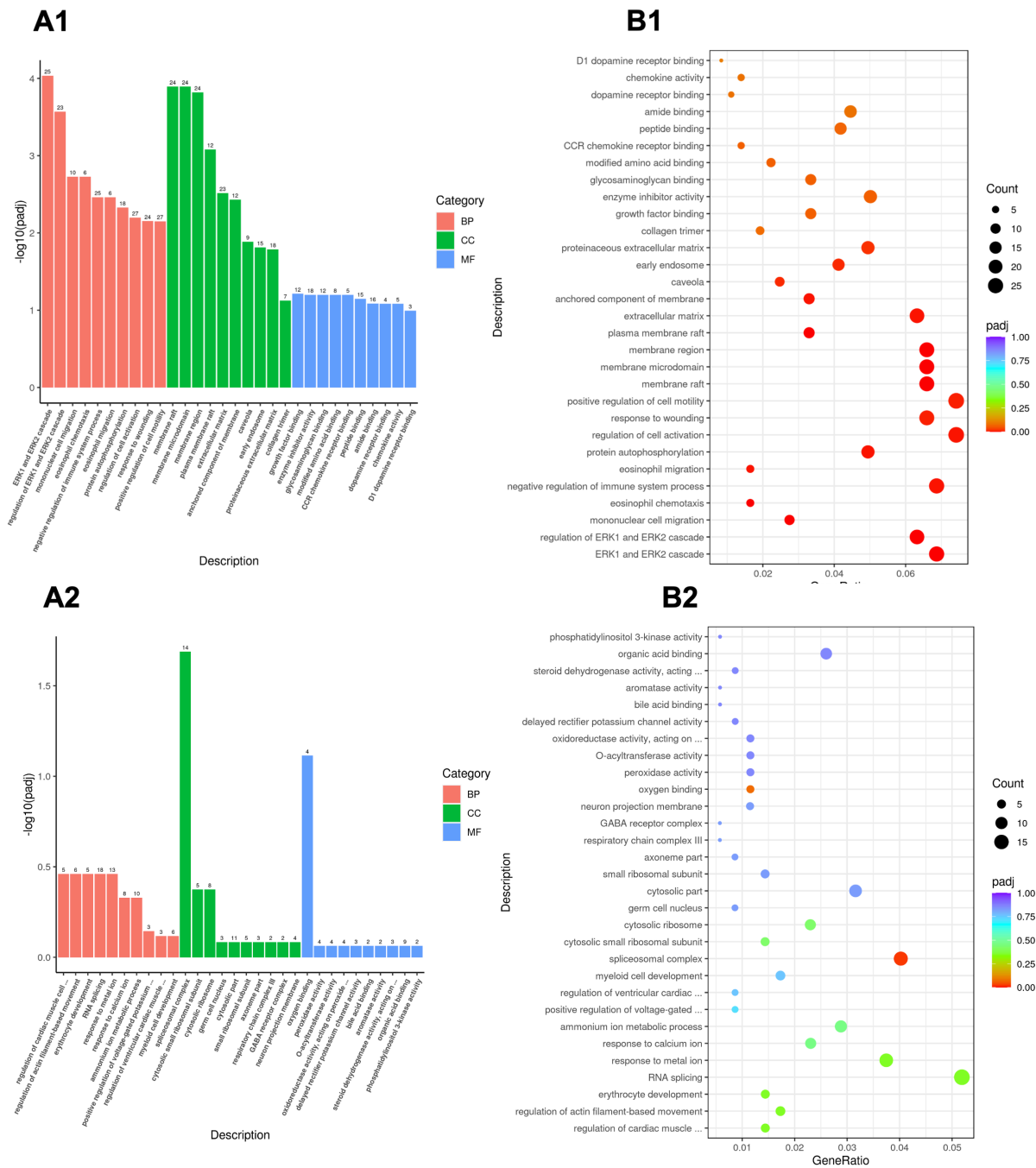


Figure 7.2 GO enrichment Analysis of DEG on CSE KO vs CSE WT non-pregnant cardiac tissue.

GO of upregulated genes (**A1**) and downregulated genes (**A2**) annotates genes to BP, MF, and CC in a directed acyclic graph structure. Round size represents the gene count of each pathway and the colour of red to purple represents the significance level cut-off at p adjusted of 0.05. This was done with both upregulated DEG (**B1**) and downregulated DEG (**B2**).

As Kyoto Encyclopaedia of Genes and Genomes (KEGG) is a more standardised method to annotate genes to pathway levels, KEGG analysis was performed using the Novomagic software (Figure 7.3). KEGG analysis revealed that the upregulated DEG (Figure 7.3A1) were identified to be significantly enriched in 4 pathways. These 4 pathways were *Staphylococcus aureus* infection, Central carbon metabolism in cancer, HIF-1 signalling pathway, Chagas disease (American trypanosomiasis). These pathways are related to immune responses, metabolic processes, and bacterial infections. In contrast, the downregulated DEG (Figure 7.3A2) were not significantly identified with any pathway (B3).

KEGG Pathway of Upregulated Genes

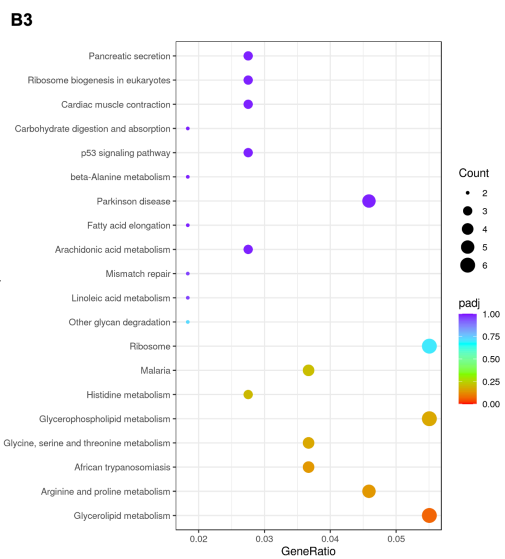
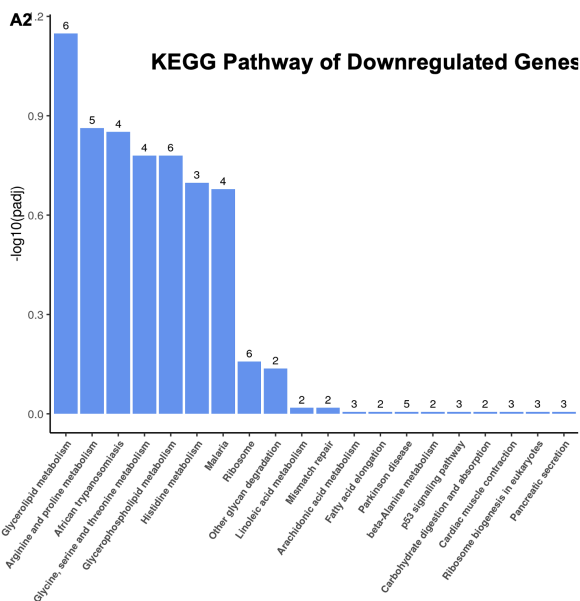
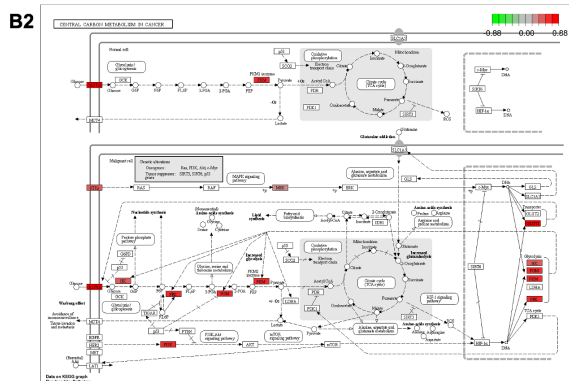
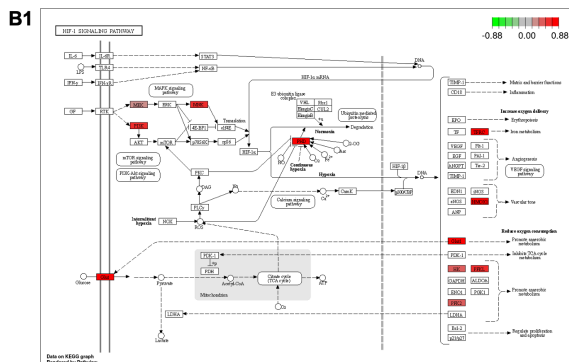
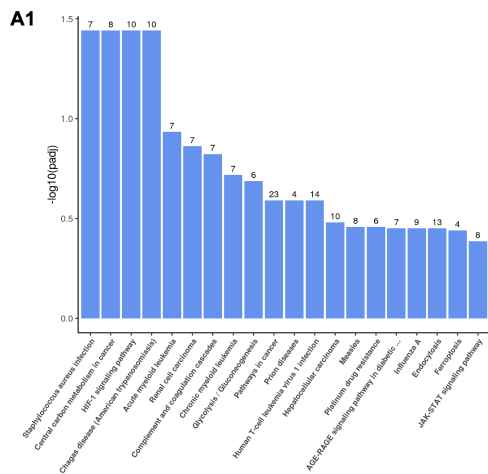


Figure 7.3 KEGG pathway enrichment analysis of DEGs from RNA-seq data.

The bar chart showed the top 20 significantly enriched KEGG pathways of DEG with the p adjusted value cut-off as 0.05. Four upregulated pathways (A1) were significantly correlated to DEG. The top two were Staphylococcus aureus infection (B1) and HIF-1 signalling pathway (B2). Central carbon metabolism in cancer, Staphylococcus aureus infection. The downregulated genes (A2) were not significantly enriched in any pathway (B3).

7.1.2 Gene expression in the cardiac tissues of pregnant vs non-pregnant CSE WT mice

In order to determine the differentially expressed genes (DEG) in the LV tissues in normal cardiac adaptations to pregnancy, a comparison was made between the mRNA profiles of CSE WT pregnant mice and CSE WT non-pregnant mice. The present investigation employed data derived from 23,771 DEG identified from CSE WT pregnant and CSE WT mice that were not pregnant. Of these, 23,771 DEG, only 766 genes were significantly expressed. Among the DEG, 361 up-regulated genes and 405 down-regulated genes ($\log FC > 1$, P value 0.05) were observed, which were depicted on a volcano map (Figure 7.4A). Up-regulated genes were illustrated by red dots, down-regulated genes by blue dots, and non-significant DEG were represented by green dots. The expression profile of statistically significant DEG was presented in a heatmap (Figure 7.4B), where up-regulated genes were shown in red and down-regulated genes in blue. Both the heatmap and the volcano plot for the DEG were showcased in Figure 7.4 and analysed with Novomagic software

| | | | |
|--------------------|--------|------------------------------------------------------------------------------|----------|
| | | [Source: MGI Symbol; Acc: MGI:88588] | |
| ENSMUSG00000112449 | Srp54b | signal recognition particle 54B [Source: MGI Symbol; Acc: MGI:3714357] | 4.75E-06 |
| ENSMUSG00000045573 | Penk | preproenkephalin [Source: MGI Symbol; Acc: MGI:104629] | 6.99E-07 |
| ENSMUSG00000064366 | mt-Tl2 | mitochondrially encoded tRNA leucine 2 [Source: MGI Symbol; Acc: MGI:102481] | 6.80E-07 |
| ENSMUSG00000024164 | C3 | complement component 3 [Source: MGI Symbol; Acc: MGI:88227] | 1.32E-05 |

Table 7.7.3 Table of top 5 upregulated genes with a cut-off at p adjusted of 0.05, ordered in ascending order from the most downregulated gene to the least downregulated gene in pregnant CSE WT mice versus non-pregnant CSE WT mice.

| Gene ID | Gene Name | Full Name | |
|--------------------|-----------|--------------------------------------------------------------------------------|----------|
| ENSMUSG00000027398 | Il1b | interleukin 1 beta [Source: MGI Symbol; Acc: MGI:96543] | 5.66E-05 |
| ENSMUSG00000046223 | Plaur | plasminogen activator, urokinase receptor [Source: MGI Symbol; Acc: MGI:97612] | 2.92E-05 |
| ENSMUSG00000114212 | Gm47985 | predicted gene, 47985 [Source: MGI Symbol; Acc: MGI:6097275] | 2.98E-06 |

| | | | |
|--------------------|---------|--------------------------------------------------------------------------------------------------|----------|
| ENSMUSG00000038894 | Irs2 | insulin receptor substrate 2 [Source: MGI Symbol; Acc: MGI:109334] | 1.69E-05 |
| ENSMUSG00000063415 | Cyp26b1 | cytochrome P450, family 26, subfamily b, polypeptide 1 [Source: MGI Symbol; Acc: MGI:2176159] | 2.95E-08 |

Table 7.7.4 Table of top 5 downregulated genes with a cut-off at p adjusted of 0.05, ordered in ascending order from the most upregulated gene to the least upregulated gene in pregnant CSE WT mice versus non-pregnant CSE WT mice.

To examine the functional roles of the DEG in pregnant CSE WT vs CSE non-pregnant mice, GO analysis was performed. Upregulated DEG (Figure 7.2 A1) were significantly enriched in 36 BP terms, 27 CC terms and 30 MF terms, and the downregulated DEG (Figure 7.2 A2) were significantly correlated with 112 BP terms, 11 CC terms, and 10 MF terms.

The top 5 BP terms positively regulated were cofactor metabolic process, monocarboxylic acid metabolic process, cofactor biosynthetic process, tetrapyrrole metabolic process, 2-oxoglutarate metabolic process, The top BP terms negatively regulated were ossification, cellular response to external stimulus, positive regulation of voltage-gated potassium channel activity, leukocyte differentiation, and response to extracellular stimulus.

The top 5 CC terms correlated with an upregulation were mitochondrial matrix, mitochondrial protein complex, mitochondrial inner membrane, organelle inner membrane, and organellar ribosome. On the other hand, the top 5 negatively regulated CC terms were actin filament bundle, actomyosin, stress fibre, contractile actin filament bundle, and cluster of actin-based cell projections.

The top 5 upregulated MF terms were cofactor binding, coenzyme binding, glutathione binding, oligopeptide binding, and oxidoreductase activity, and vitamin binding. The top 5 negatively regulated MF terms were MAP kinase tyrosine/serine/threonine, phosphatase activity, semaphorin receptor activity, MAP kinase phosphatase activity, actin binding, and transcriptional repressor activity, RNA polymerase II transcription regulatory region sequence-specific DNA binding.

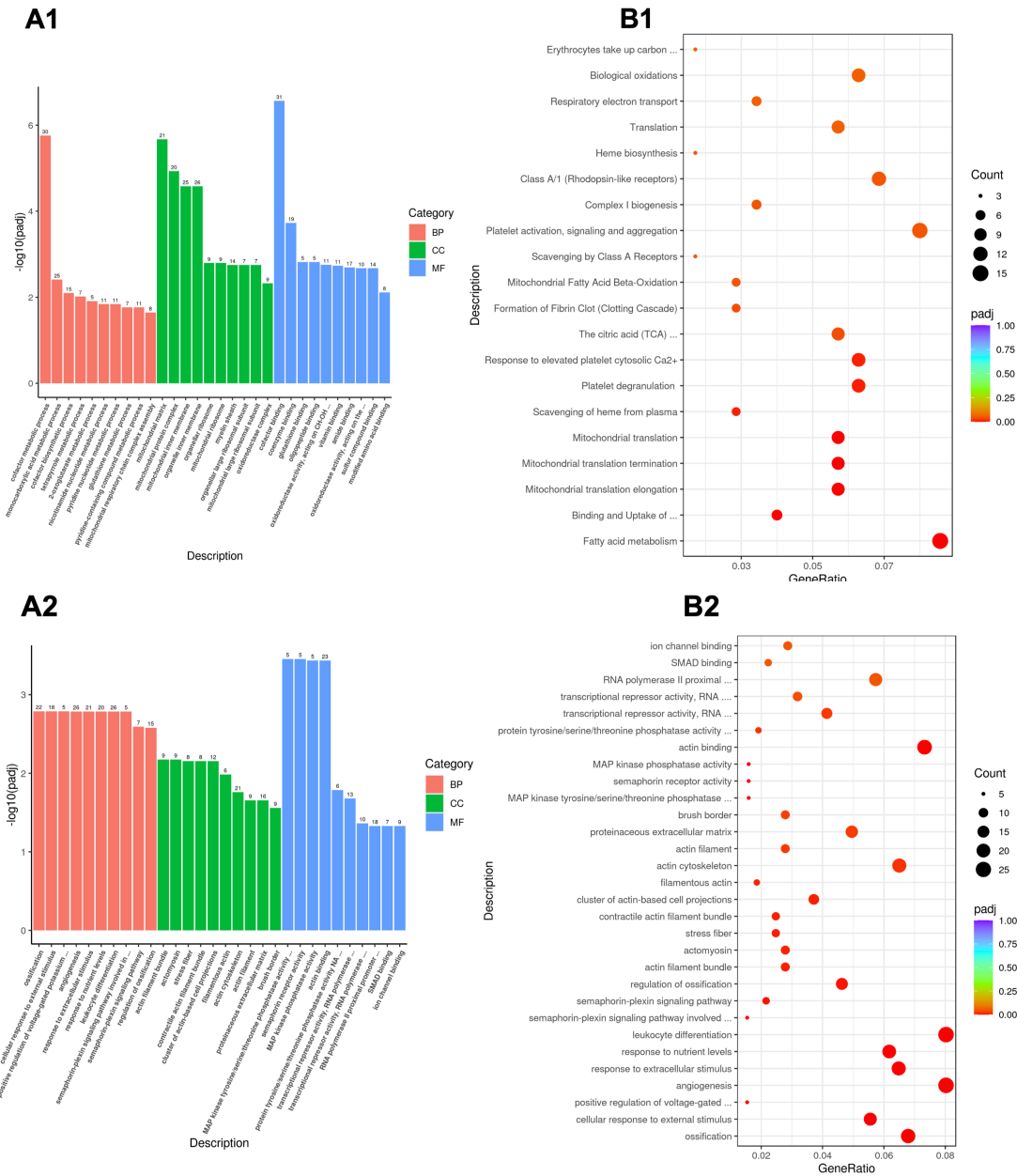


Figure 7.5 GO enrichment Analysis of DEG on CSE WT pregnant vs CSE WT non-pregnant cardiac tissue.

GO of upregulated genes (**A1**) and downregulated genes (**A2**) annotates genes to BP, MF, and CC in a directed acyclic graph structure. Round size represents the gene count of each pathway and the colour of red to purple represents the significance level cut-off at p adjusted of 0.05. This was done with both upregulated DEG (**B1**) and downregulated DEG (**B2**).

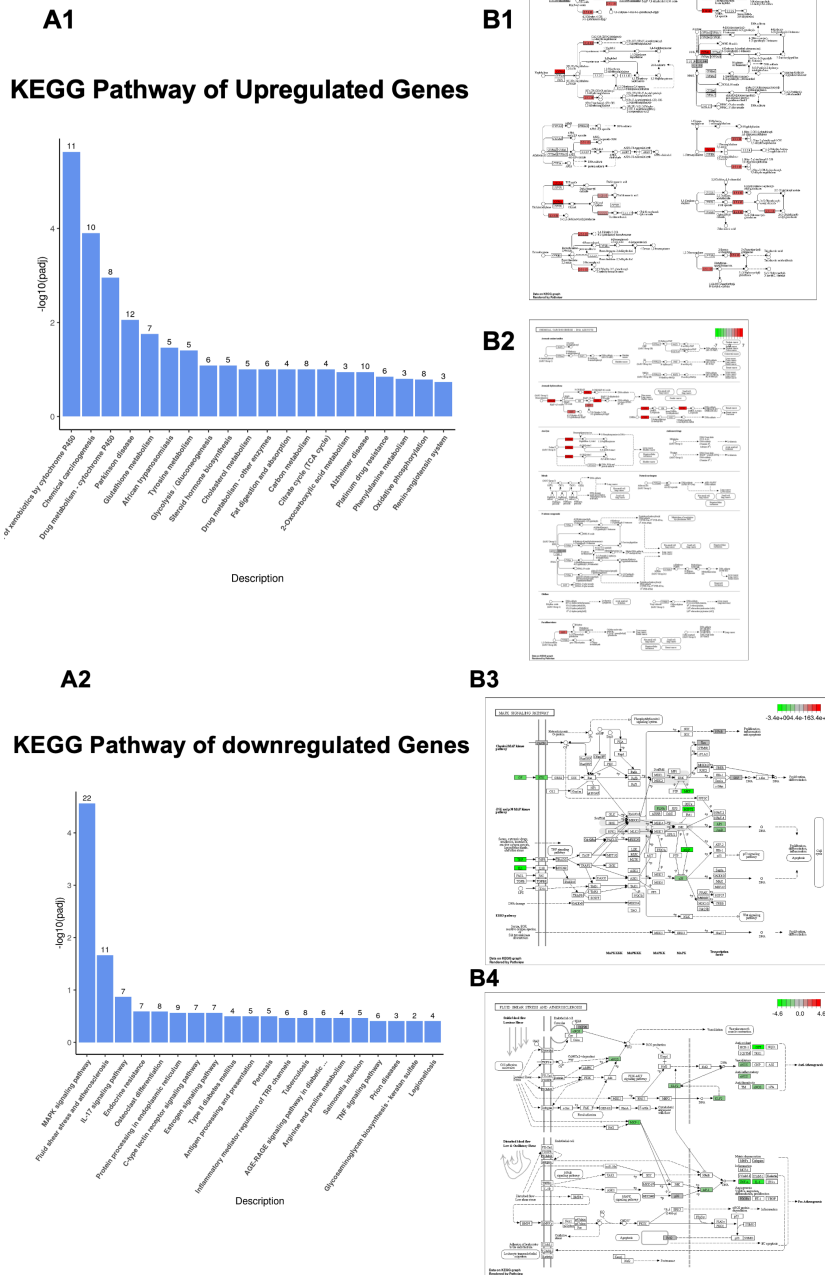


Figure 7.6 KEGG pathway enrichment analysis of DEGs from RNA-seq data.

The bar chart showed the top 20 significantly enriched KEGG pathways of DEG with the p adjusted value cut-off as 0.05. Seven significantly upregulated pathways (**A1**) were correlated with DEG, the top two were Metabolism of xenobiotics by cytochrome P450 (**B1**) and Chemical carcinogenesis (**B2**). Two significantly downregulated pathways (**A2**) were correlated with DEG in MAPK signalling pathway (**B3**) and Fluid shear stress and atherosclerosis (**B4**).

When looking at KEGG analysis, 7 pathways were significantly upregulated (Figure 7.6 A1), and two pathways were significantly downregulated (Figure 7.6 A2). The top 5 upregulated pathways were Metabolism of xenobiotics by cytochrome P450 (Figure 7.6 B1), Chemical carcinogenesis (Figure 7.6 B2), Drug metabolism - cytochrome P450, Parkinson disease, and Glutathione metabolism. The two downregulated pathways were MAPK signalling pathway (Figure 7.6 B3) and Fluid shear stress and atherosclerosis (Figure 7.6 B4).

7.1.3 Gene expression in the cardiac tissues of pregnant CSE KO vs CSE KO non-pregnant mice.

A comparison was made between DEG in the LV tissues of CSE KO pregnant mice and CSE KO non-pregnant mice. The present investigation employed data derived from 22,082 DEG identified from CSE KO pregnant and CSE KO mice that were not pregnant. Of these, 22,082 DEG, only 1620 genes were significantly expressed. Among the DEG, 608 up-regulated genes and 1012 down-regulated genes ($\log FC > 1$, P value 0.05) were observed, which were depicted on a volcano map (Figure 7.7A). Up-regulated genes were illustrated by red dots, down-regulated genes by blue dots, and non-significant DEG were represented by green dots. The expression profile of statistically significant DEG was presented in a heatmap (Figure 7.7B), where up-regulated genes were shown in red and down-regulated genes in blue. Both the heatmap and the volcano plot for the DEG were showcased in Figure 7.4 and analysed with Novomagic software.

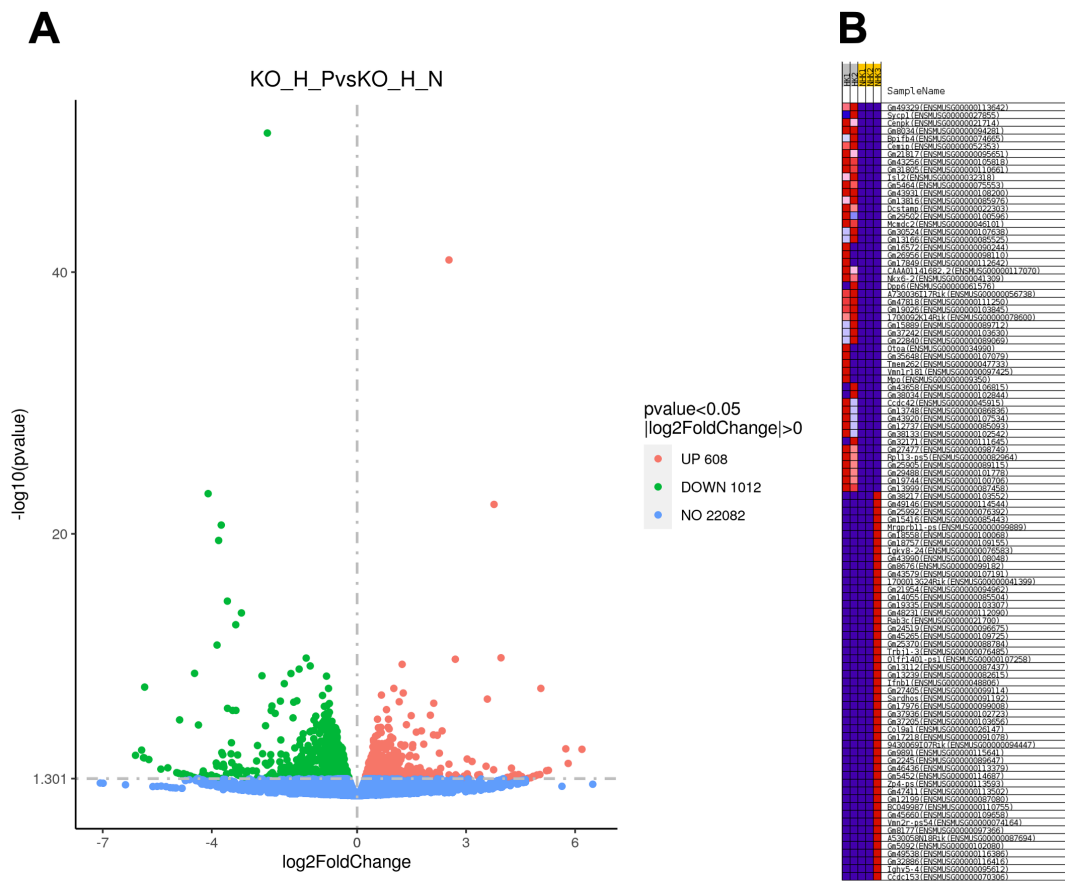


Figure 7.7 The differential expression of genes (DEG) in cardiac tissue of pregnant of CSE KO (n=2) vs CSE KO non-pregnant mice (n=2), was visually represented by a volcano plot and a heatmap.

The volcano plot (A) illustrated up-regulated genes with red dots and down-regulated genes with green dots. The heatmap (B) depicted up-regulated genes as red and down-regulated genes as blue.

A table with the top 5 most upregulated (table 7.5) DEG and most downregulated DEG (table 7.6) looking at pregnant CSE KO vs non-pregnant CSE KO mice, was composed.

| Gene ID | Gene Name | Full Name | Adjusted p-value |
|--------------------|-----------|--------------------------------------------------------------------------------------|------------------|
| ENSMUSG00000097891 | Gm3650 | predicted gene 3650 [Source: MGI Symbol; Acc: MGI:3781826] | 6.42E-09 |
| ENSMUSG00000067608 | Pcna-ps2 | proliferating cell nuclear antigen pseudogene 2 [Source: MGI Symbol; Acc: MGI:97505] | 2.94E-11 |
| ENSMUSG00000059040 | Eno1b | enolase 1B, retrotransposed [Source: MGI Symbol; Acc: MGI:3648653] | 5.62E-23 |
| ENSMUSG00000079071 | Gm14085 | predicted gene 14085 [Source: MGI Symbol; Acc: MGI:3702173] | 4.19E-08 |
| ENSMUSG00000025889 | Snca | synuclein, alpha [Source: MGI Symbol; Acc: MGI:1277151] | 3.79E-11 |

Table 7.5 Table of top 5 upregulated genes with a cut-off at p adjusted of 0.05, ordered in ascending order from the most upregulated gene to the least upregulated gene in pregnant CSE KO mice versus non-pregnant CSE KO mice.

| Gene ID | Gene Name | Full Name | Adjusted P-value |
|--------------------|-----------|---------------------------------------------------------------|------------------|
| ENSMUSG00000003545 | Fosb | FBJ osteosarcoma oncogene B [Source:MGI Symbol;Acc:MGI:95575] | 5.09E-09 |
| ENSMUSG00000101122 | Gm17971 | predicted gene, 17971 [Source:MGI Symbol;Acc:MGI:5010156] | 1.63E-06 |
| ENSMUSG00000033730 | Egr3 | early growth response 3 [Source:MGI Symbol;Acc:MGI:1306780] | 4.55E-10 |

| | | | |
|--------------------|-------|-------------------------------------------------------------------------------------|----------|
| ENSMUSG00000023034 | Nr4a1 | nuclear receptor subfamily 4, group A, member 1 [Source:MGI Symbol;Acc:MGI:1352454] | 3.99E-06 |
| ENSMUSG00000038418 | Egr1 | early growth response 1 [Source:MGI Symbol;Acc:MGI:95295] | 8.45E-24 |

Table 7.6 Table of top 5 downregulated genes with a cut-off at p adjusted of 0.05, ordered in ascending order from the most downregulated gene to the least downregulated gene in pregnant CSE KO mice versus non-pregnant CSE KO mice.

To examine the functional roles of the DEG, GO (Figure 7.8) analysis was carried out. The upregulated DEG (Figure 7.8 A1) exhibited significant enrichment in 15 BP terms, 5 CC terms, and 5 MF terms. Conversely, the downregulated DEGs (Figure 7.8 A2) exhibited significant enrichment in demonstrated a significant association with 421 BP terms, 76 CC terms, and 35 MF terms.

The 5 most prominently upregulated biological BP terms included fatty acid metabolism, monocarboxylic acid metabolism, cofactor metabolism, long-chain fatty acid metabolism, and regulation of cellular carbohydrate catabolism. Meanwhile, the top 5 downregulated BP terms encompassed muscle organ development, angiogenesis, striated muscle tissue development, cardiac muscle tissue development, and cardiac ventricle morphogenesis.

The 5 most significantly upregulated CC terms encompassed peroxisomes, microbodies, mitochondrial matrix, microbody components, and peroxisomal elements. In contrast, the top 5 downregulated CC terms included cytosolic ribosomes, cytosolic large ribosomal subunits, ribosomal subunits, ribosomes, and cytosolic portions.

The 5 most notably upregulated MF terms consisted of cofactor binding, peroxidase activity, antioxidant activity, coenzyme binding, and oxidoreductase activity, utilizing peroxide as the acceptor. Conversely, the top 5 downregulated MF terms encompassed structural constituents

of ribosomes, structural molecule activity, cell adhesion molecule binding, actin binding, and cadherin binding.

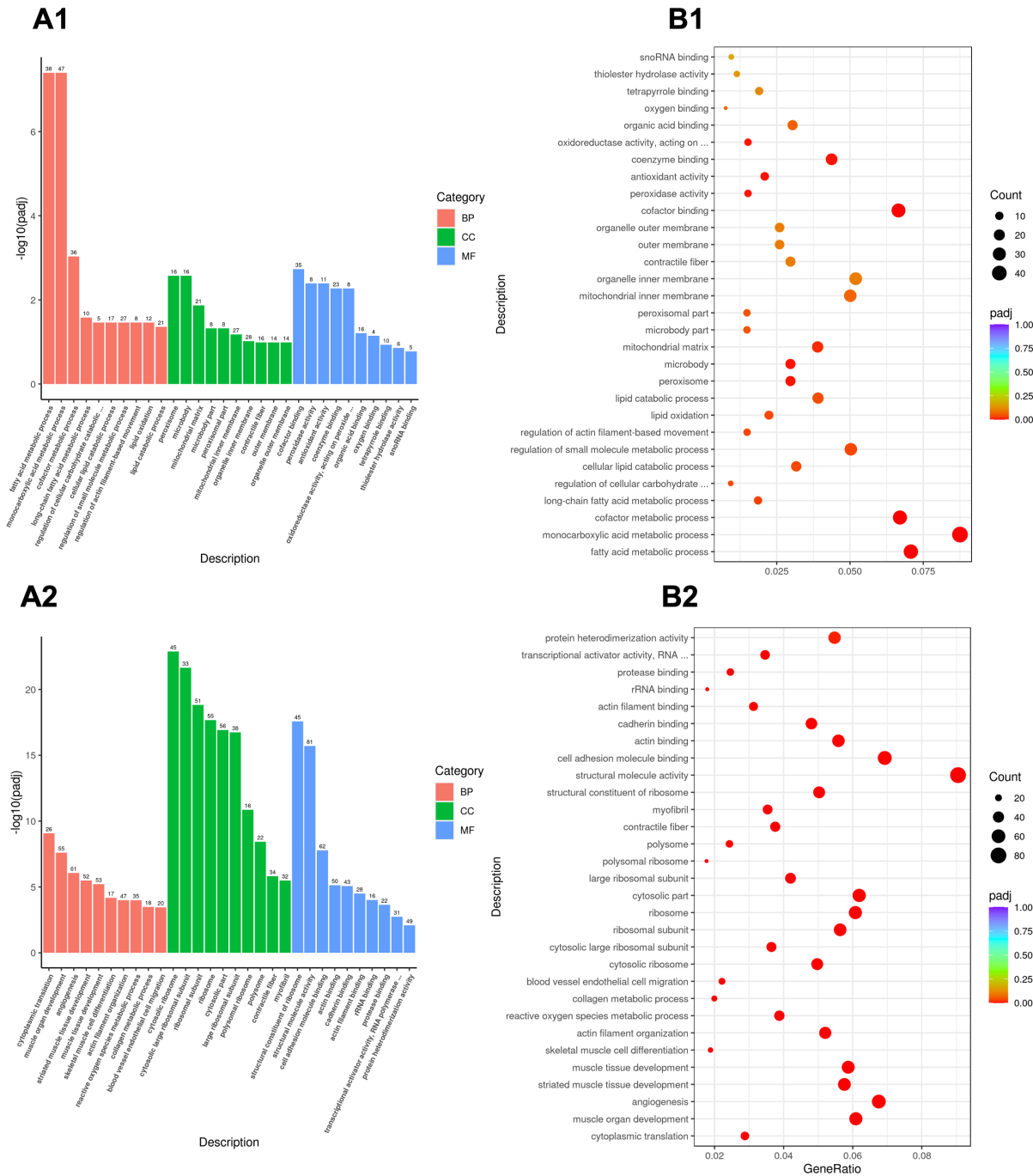


Figure 7.8 GO enrichment Analysis of DEG on CSE KO pregnant vs CSE KO non-pregnant cardiac tissue.

GO of upregulated genes (**A1**) and downregulated genes (**A2**) annotates genes to BP, MF, and CC in a directed acyclic graph structure. Round size represents the gene count of each pathway and the colour of red to purple represents the significance level cut-off at p adjusted of 0.05. This was done with both upregulated DEG (**B1**) and downregulated DEG (**B2**).

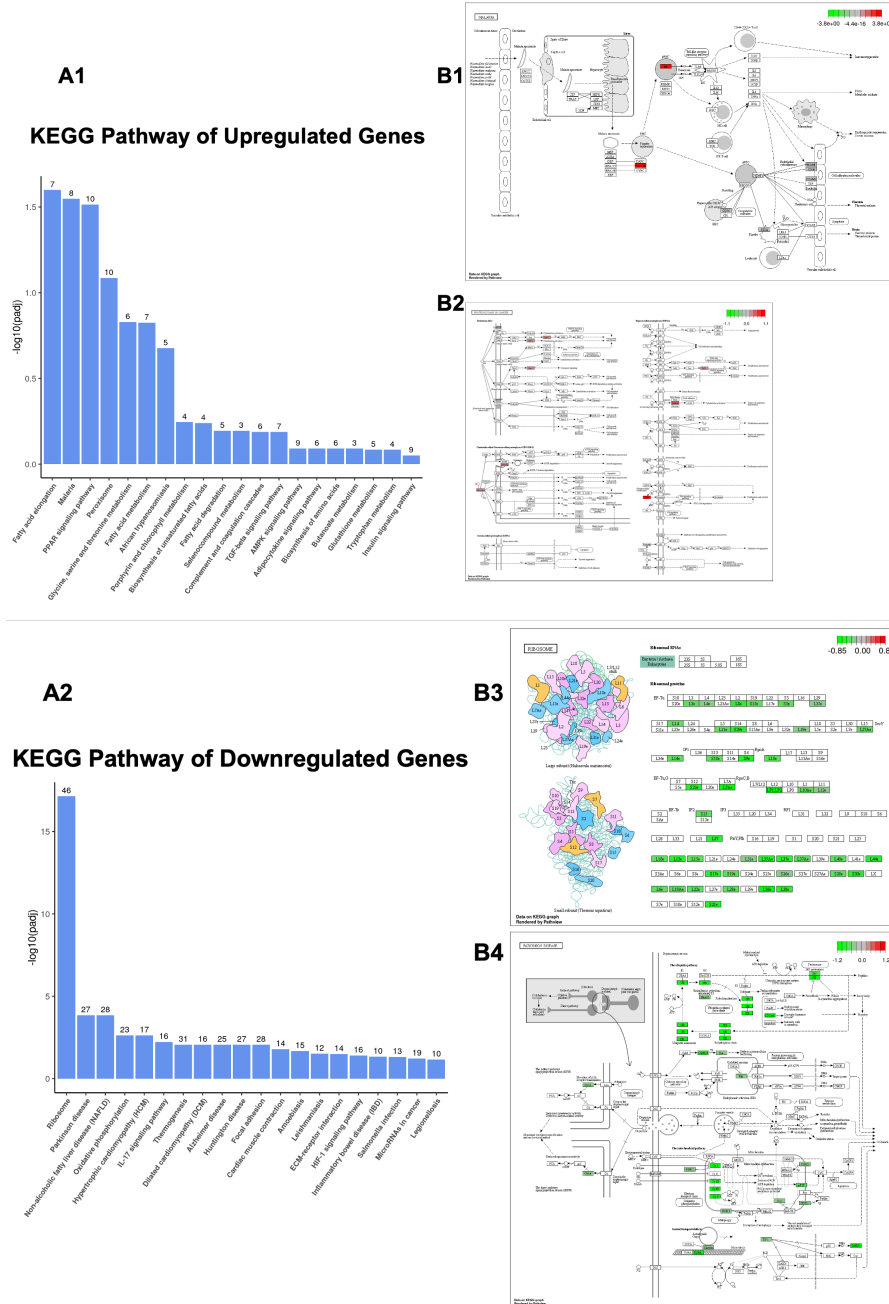


Figure 7.9 KEGG pathway enrichment analysis of DEGs from RNA-seq data.

The bar chart showed the top 20 significantly enriched KEGG pathways of DEG with the p adjusted value cut-off as 0.05. Two significantly upregulated pathways (A1) were correlated with DEG; Malaria (B1) and proteoglycans in cancer (B2). Ten significantly downregulated pathways (A2) were correlated with DEG, the top 2 were ribosome (B3) and Parkinson disease (B4).

The KEGG analysis (Figure 7.9) revealed 2 significantly upregulated pathways (Figure 7.9A1) and 10 significantly downregulated pathways. The 2 upregulated pathways were Malaria and proteoglycans in cancer. The top 5 downregulated pathways were ribosome, Non-alcoholic fatty liver disease (NAFLD), Parkinson disease (Figure 7.9 B3), Oxidative phosphorylation (Figure 7.9 B4), and Hypertrophic cardiomyopathy (HCM)

Gene expression in cardiac tissue of pregnant CSE KO vs CSE WT pregnant mice

A comparison was made between the DEG in the LV tissues of CSE KO pregnant mice and CSE WT pregnant mice. The present investigation employed data derived from 22,620 DEG identified from pregnant CSE KO and CSE WT mice. Of these, 22,620 DEG, only 929 genes were significantly expressed. Among the DEG, 411 up-regulated genes and 518 down-regulated genes ($\log FC > 1$, P value 0.05) were observed, which were depicted on a volcano map (Figure 7.10A). Up-regulated genes were illustrated by red dots, down-regulated genes by blue dots, and non-significant DEG were represented by green dots. The expression profile of statistically significant DEG was presented in a heatmap (Figure 7.10B), where up-regulated genes were shown in red and down-regulated genes in blue. Both the heatmap and the volcano plot for the DEG were showcased in Figure 7.4 and analysed with Novomagic software.

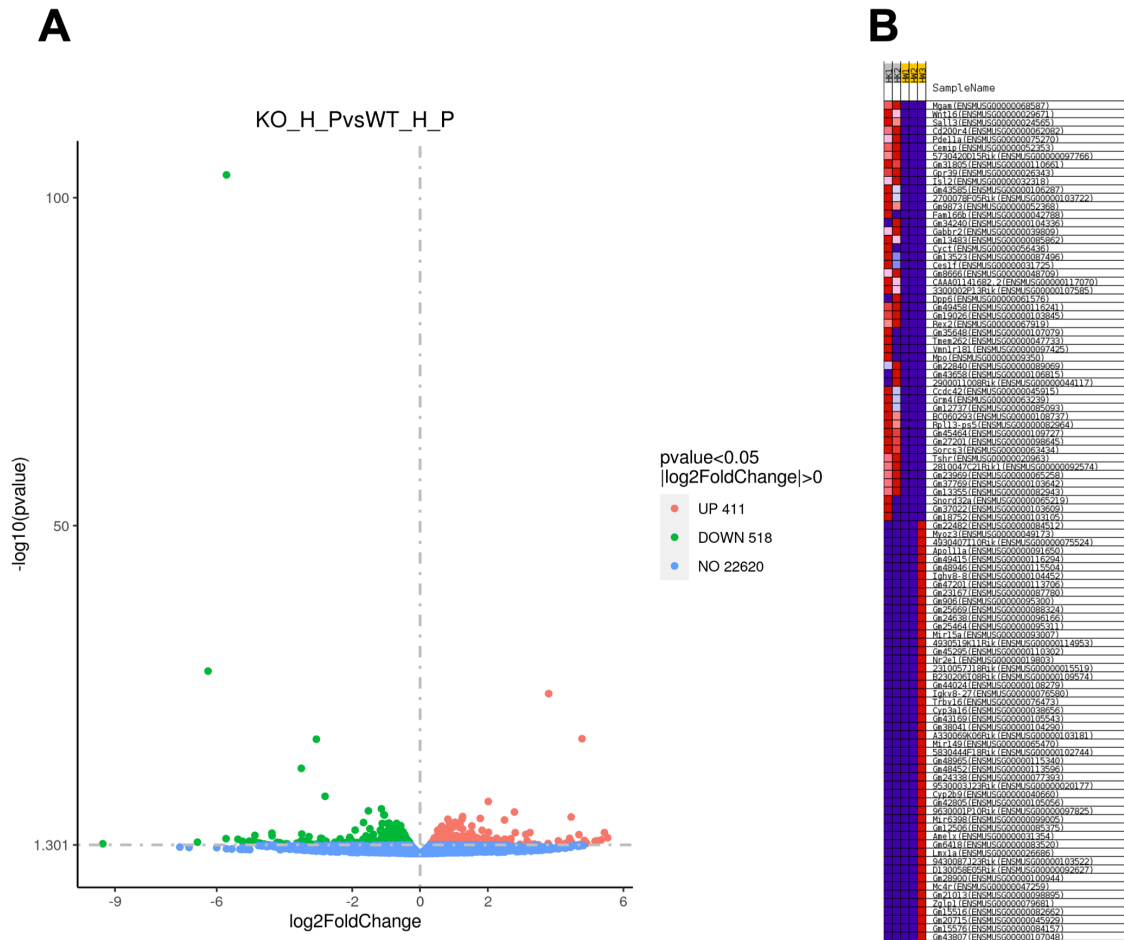


Figure 7.10 The differential expression of genes (DEG) in cardiac tissue of pregnant of CSE KO (n=2) vs CSE WT pregnant (n=2) mice, was visually represented by a volcano plot and a heatmap.

The volcano plot (A) illustrated up-regulated genes with red dots and down-regulated genes with green dots. The heatmap (B) depicted up-regulated genes as red and down-regulated genes as blue.

A table with the top 5 most upregulated (table 7.7) DEG and most downregulated DEG (table 7.8) looking at pregnant CSE KO vs CSE WT mice, was recorded.

| Gene ID | Gene Name | Full Name | Adjusted P-value |
|---------|-----------|-----------|------------------|
|---------|-----------|-----------|------------------|

| | | | |
|--------------------|---------|----------------------------------------------------------------------------------------------|------------|
| ENSMUSG00000044229 | Nxpe4 | neurexophilin and PC-esterase domain family, member 4 [Source: MGI Symbol; Acc: MGI:1924792] | 8.83E-15 |
| ENSMUSG00000059040 | Eno1b | enolase 1B, retrotransposed [Source:MGI Symbol;Acc:MGI:3648653] | 1.64E-21 |
| ENSMUSG00000030278 | Cidec | cell death-inducing DFFA-like effector c [Source:MGI Symbol;Acc:MGI:95585] | 0.00050705 |
| ENSMUSG00000096842 | Gm10736 | predicted gene 10736 [Source:MGI Symbol;Acc:MGI:3704412] | 0.00514527 |
| ENSMUSG00000020738 | Sumo2 | small ubiquitin-like modifier 2 [Source:MGI Symbol;Acc:MGI:2158813] | 1.76E-05 |

Table 7.7 Table of top 5 upregulated genes with a cut-off at p adjusted of 0.05, ordered in ascending order from the most upregulated gene to the least upregulated gene in pregnant CSE KO mice vs CSE WT mice.

| Gene ID | Gene Name | Full Name | Adjusted P-value |
|--------------------|-----------|---------------------------------------------------------------|------------------|
| ENSMUSG00000081824 | BC002163 | cDNA sequence BC002163 [Source: MGI Symbol; Acc: MGI:3612445] | 9.07E-25 |
| ENSMUSG00000062006 | Rpl34 | ribosomal protein L34 [Source: MGI Symbol; Acc: MGI:1915686] | 3.82E-100 |
| ENSMUSG00000043192 | Gm1840 | predicted gene 1840 [Source: MGI Symbol; Acc: MGI:3037698] | 2.05E-10 |

| | | | |
|--------------------|--------|-------------------------------------------------------------------------|----------|
| ENSMUSG00000032549 | Rab6b | RAB6B, member RAS oncogene family [Source: MGI Symbol; Acc: MGI:107283] | 8.83E-15 |
| ENSMUSG00000074280 | Gm6166 | predicted gene 6166 [Source: MGI Symbol; Acc: MGI:3645893] | 3.21E-06 |

Table 7.8 Table of top 5 downregulated genes with a cut-off at p adjusted of 0.05, ordered in ascending order from the most downregulated gene to the least downregulated gene in pregnant CSE KO mice vs CSE WT mice.

To explore the functional roles of DEG, a GO analysis was performed (Figure 7.11). The upregulated DEGs (Figure 7.11 A1) demonstrated significant enrichment in 204 BP terms, 20 CC terms, and 11 MF terms. Meanwhile, the downregulated DEGs displayed significant enrichment in 76 BP terms, 43 CC terms, and 29 MF terms.

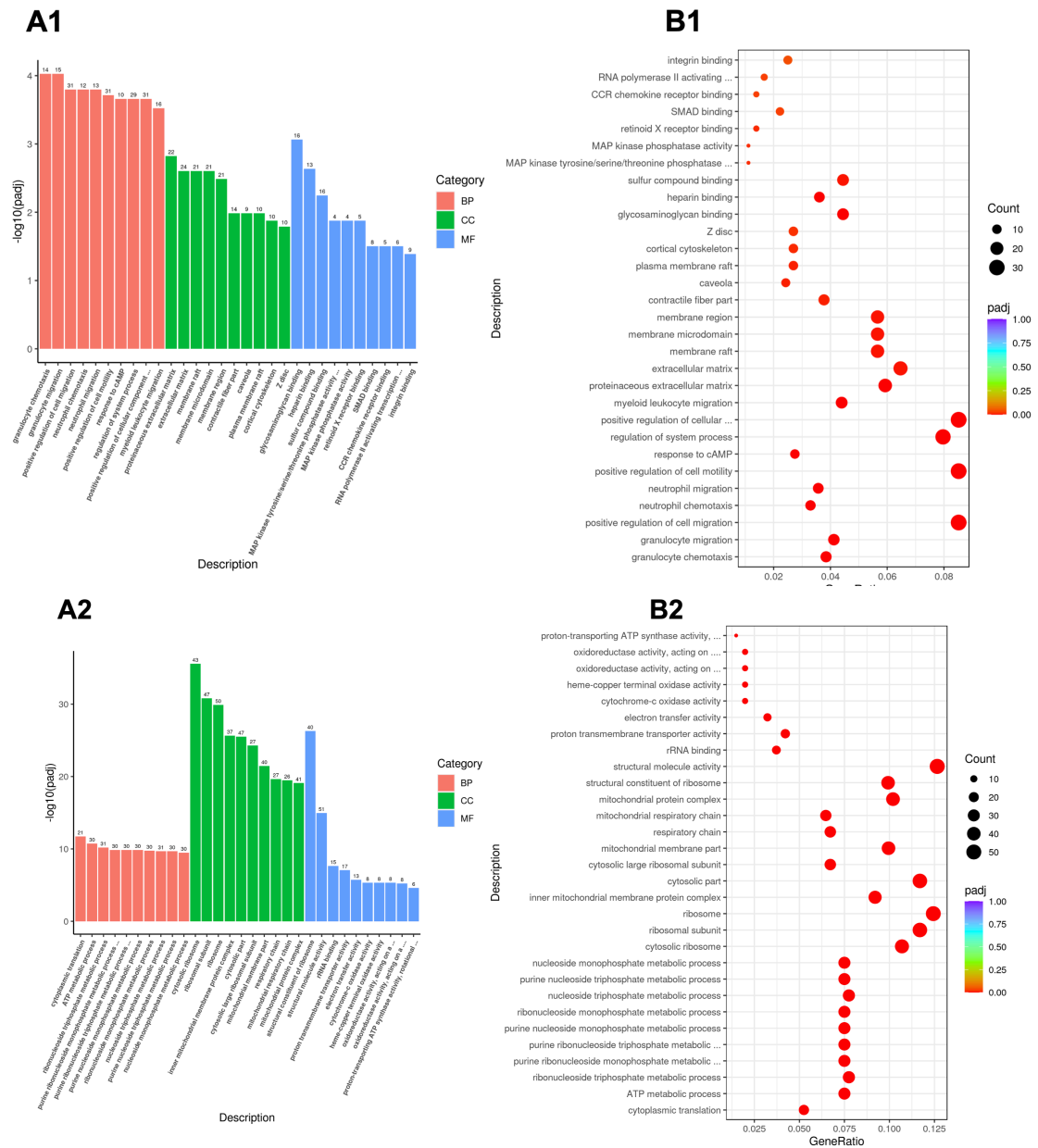


Figure 7.11 GO enrichment Analysis of DEG on pregnant CSE KO vs CSE WT in cardiac tissue. GO of upregulated genes (**A1**) and downregulated genes (**A2**) annotates genes to BP, MF, and CC in a directed acyclic graph structure. Round size represents the gene count of each pathway and the colour of red to purple represents the significance level cut-off at p adjusted of 0.05. This was done with both upregulated DEG (**B1**) and downregulated DEG (**B2**).

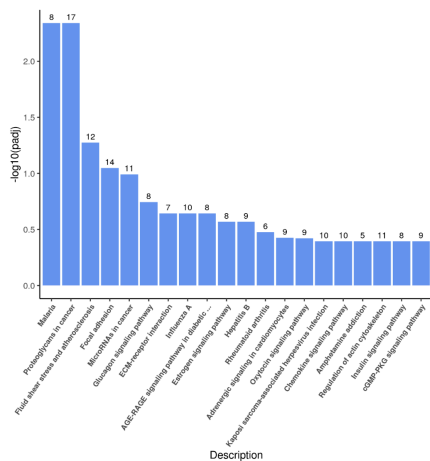
The 5 most markedly upregulated BP terms included granulocyte chemotaxis, muscle tissue development, neutrophil chemotaxis, cardiac muscle tissue development, and cardiac chamber development. In contrast, the top 5 downregulated BP terms featured cytoplasmic translation, ATP metabolic process, ribonucleoside, triphosphate metabolic process, and cell death in response to hydrogen peroxide.

The most prominently upregulated CC terms encompassed proteinaceous extracellular matrix, extracellular matrix, membrane microdomain, membrane raft, and membrane region. Conversely, the top 5 downregulated CC terms cytosolic ribosome, ribosomal subunit, inner mitochondrial membrane protein complex, cytosolic part, and respiratory chain.

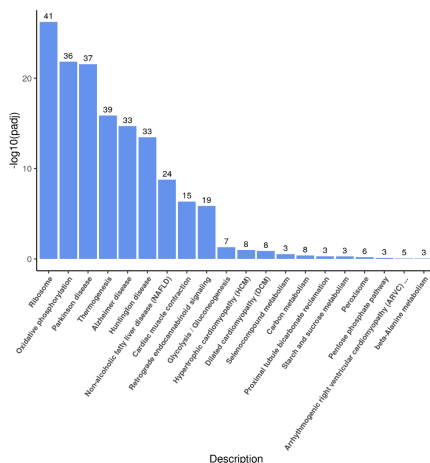
The 5 most notably upregulated MF terms were comprised of glycosaminoglycan binding, heparin binding, MAP kinase tyrosine/serine/threonine phosphatase activity, retinoid X receptor binding, and CCR chemokine receptor binding. On the other hand, the top 5 downregulated structural constituent of ribosome, structural molecule activity, rRNA binding, proton transmembrane transporter activity, and electron transfer activity.

The KEGG analysis (Figure 7.12) revealed 2 significantly upregulated pathways and 10 downregulated pathways. The upregulated pathways (Figure 7.12 A1) consisted of malaria (Figure 7.12 B1) and Proteoglycans in cancer (Figure 7.12 B2). In contrast, the top 5 downregulated pathways (Figure 7.12 A2) featured Ribosome (Figure 7.12 B3), Oxidative phosphorylation (Figure 7.12 B4), Parkinson disease, Thermogenesis, and Alzheimer disease.

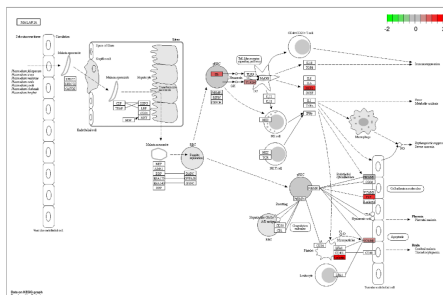
A1
KEGG Pathway of Upregulated Genes



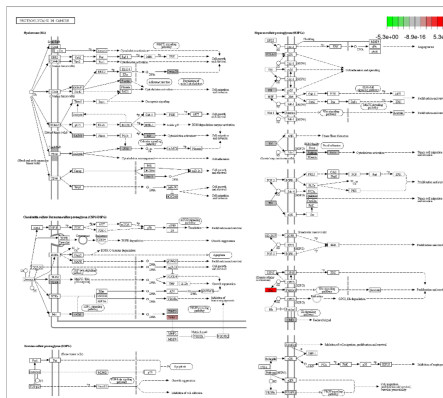
A2
KEGG Pathway of Downregulated Genes



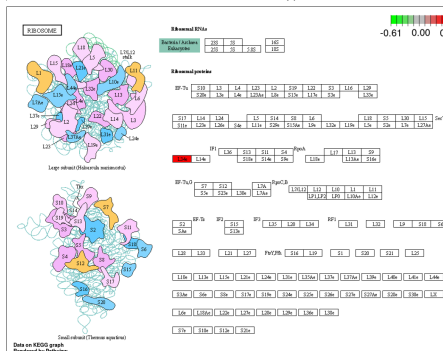
B1



B2



B3



B4

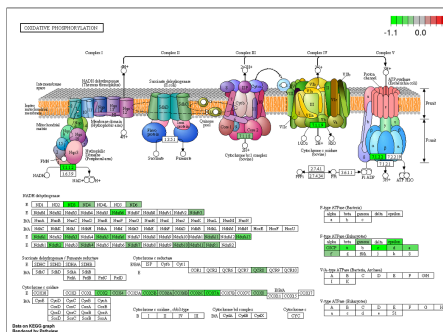


Figure 7.12 KEGG pathway enrichment analysis of DEGs from RNA-seq data.

The bar chart showed the top 20 enriched KEGG pathways of DEG with the p adjusted value cut-off as 0.05. Two significantly upregulated pathways (A1) were features; Malaria (B1) and Proteoglycans in cancer (B2). Ten significantly downregulated pathways (A2) were revealed. The top 2 consisted of Ribosome (B3), and Oxidative phosphorylation (B4).

7.2 Gene expression in pregnant mice overexpressing sFlt-1

sFlt-1 is a soluble form of the vascular endothelial growth factor receptor-1 (VEGFR-1) that plays a critical role in angiogenesis and vascular homeostasis (Gruson et al. 2016b; K. R. Palmer et al. 2017). During pregnancy, sFlt-1 levels increase, particularly in cases of PE, a hypertensive disorder characterized by decreased placental perfusion and endothelial dysfunction (Mustonen & Alitalo 1995; S. Ahmad et al. 2011; Lamarca 2012; Yaling Zhai et al. 2020). An elevated level of sFlt-1 in pregnancy leads to adverse outcomes such as hypertension, proteinuria, and impaired foetal growth, as it can bind and sequester circulating VEGF and PlGF, leading to endothelial dysfunction and vascular damage (Kendall & Thomas 1993; Forsythe et al. 1996; S. Ahmad & Ahmed 2004; Sánchez-Aranguren et al. 2014; Yaling Zhai et al. 2020). Furthermore, recent studies have implied that sFlt-1 levels may remain elevated long-term postpartum, potentially contributing to increased cardiovascular risk in women with a history of PE (Heidrich et al. 2013; Thayaparan et al. 2019; Frost et al. 2021; Khosla et al. 2021; Pittara et al. 2021). Elevated sFlt-1 levels have been related with endothelial dysfunction, arterial stiffness, and impaired diastolic function, highlighting the potential long-term effects of this molecule on cardiovascular health (Amaral et al. 2015; Bokslag et al. 2016; Janzarik et al. 2018; Turbeville & Sasser 2020; DeMartelly et al. 2021; J. Kitt et al. 2021).

In effort to elucidate the genes and pathways implicated in the pathogenesis of PE, mRNA sequencing analysis was conducted on cardiac tissues. We hypothesized that these models would manifest analogous genetic profiles, except for the AdsFlt-1 model in the postpartum period, which was expected to display a distinctive genetic expression pattern. To verify this hypothesis, the mRNA expression profiles in tissues derived from the heart of CSE KO mice, along with heart tissues obtained from AdsFlt-1 mice and their corresponding controls, were performed.

7.2.1 Gene expression in cardiac tissue of AdsFlt-1 vs AdCMV mice in pregnancy

In a similar fashion to the previous section, a comparative study was conducted between the DEG in the LV tissues of AdsFlt-1 pregnant mice and AdCMV pregnant mice. In this study, data from 23,064 DEG identified from pregnant AdsFlt-1 and AdCMV mice, were utilized. Out of these DEGs, only 1165 were found to be significantly expressed ($\log FC > 1$, P value 0.05), with 697 up-regulated genes and 968 down-regulated genes observed on a volcano map (Figure 7.13 A). Red dots on the map represented up-regulated genes, blue dots indicated down-regulated genes, while green dots represented non-significant DEGs. Additionally, a heatmap was generated to display the expression profile of the statistically significant DEGs, where up-regulated genes were depicted in red and down-regulated genes in blue (Figure 7.13 B). Both the heatmap and volcano plot for the DEGs were analysed using Novomagic software and presented in Figure 7.13.

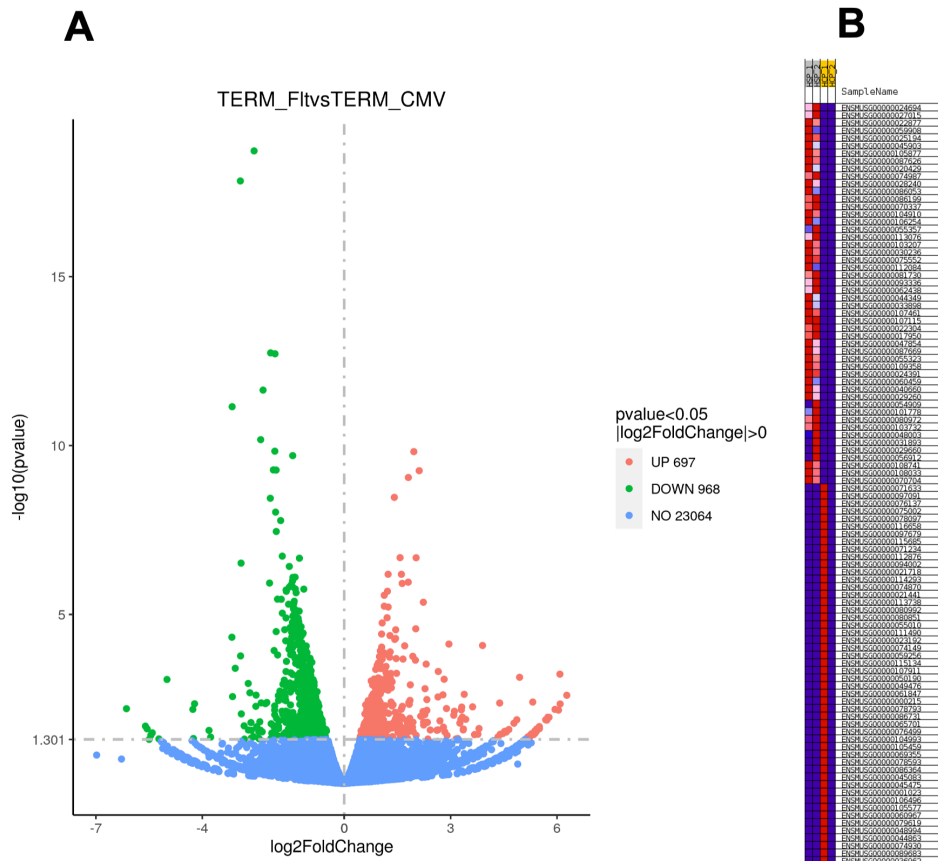


Figure 7.13 The differential expression of genes (DEG) in cardiac tissue of pregnant of AdsFit-1 vs AdCMV pregnant mice, was visually represented by a volcano plot and a heatmap.

The differential expression of genes (DEG) in cardiac tissue of pregnant of AdsFit-1 vs AdCMV pregnant mice, was visually represented by a volcano plot and a heatmap. The volcano plot (A) illustrated up-regulated genes with red dots and down-regulated genes with blue dots. The heatmap (B) depicted up-regulated genes as blue and down-regulated genes as red.

A table with the top 5 most upregulated (table 7.9) DEG and most downregulated DEG (table 7.10) looking at pregnant AdsFit-1 vs AdCMV mice, was recorded.

| Gene ID | Gene Name | Full Name | Adjusted p-value |
|--------------------|-----------|-----------------------------------------------------------|------------------|
| ENSMUSG00000115610 | Gm31251 | predicted gene, 31251 [Source:MGI Symbol;Acc:MGI:5590410] | 0.00089416 |

| | | | |
|--------------------|---------|-----------------------------------------------------------------------------------------------------------------------------------------------|------------|
| ENSMUSG00000016458 | Wt1 | Wilms tumour 1 homolog [Source:MGI Symbol;Acc:MGI:98968] | 4.21E-07 |
| ENSMUSG00000078816 | Prkcg | protein kinase C, gamma [Source:MGI Symbol;Acc:MGI:97597] | 9.28E-05 |
| ENSMUSG00000038587 | Akap12 | A kinase (PRKA) anchor protein (gravin) 12 [Source:MGI Symbol;Acc:MGI:1932576] | 1.66E-07 |
| ENSMUSG00000006403 | Adamts4 | a disintegrin-like and metallopeptidase (reprolysin type) with thrombospondin type 1 motif, 4 [Source:MGI Symbol;Acc:MGI:1339949] | 0.04382682 |

Table 7.9 Table of top 5 upregulated genes with a cut-off at p adjusted of 0.05, ordered in ascending order from the most upregulated gene to the least upregulated gene in pregnant AdsFlt-1 vs AdCMV mice.

| Gene ID | Gene Name | Full Name | Adjusted p-value |
|--------------------|-----------|------------------------------------------------------------------|------------------|
| ENSMUSG00000078922 | Tgtp1 | T cell specific GTPase 1 [Source:MGI Symbol;Acc:MGI:98734] | 1.17E-08 |
| ENSMUSG00000078921 | Tgtp2 | T cell specific GTPase 2 [Source:MGI Symbol;Acc:MGI:3710083] | 7.28E-15 |
| ENSMUSG00000063388 | BC023105 | cDNA sequence BC023105 [Source:MGI Symbol;Acc:MGI:2384767] | 0.00012439 |
| ENSMUSG00000002289 | Angptl4 | angiopoietin-like 4 [Source:MGI Symbol;Acc:MGI:1888999] | 1.88E-15 |
| ENSMUSG00000044338 | Aplnr | apelin receptor [Source:MGI Symbol;Acc:MGI:1346086] | 9.43E-08 |

Table 7.10 Table of top 5 downregulated genes with a cut-off at p adjusted of 0.05, ordered in ascending order from the most downregulated gene to the least downregulated gene in pregnant AdsFlt-1 vs AdCMV mice.

The top 5 upregulated BP terms featured heart process, cardiac muscle hypertrophy, regulation of axon extension, cardiac muscle hypertrophy in response to stress, and heart valve development. The top downregulated terms were constituted of electron transport chain, cytoplasmic translation, mitochondrial respiratory chain complex assembly, oxidative phosphorylation, and mitochondrial respiratory chain complex I assembly.

The top 5 upregulated CC terms featured contractile fibre, myofibril, nuclear speck, Z disc, and cell-substrate junction. The top 5 downregulated terms included ribosome, ribosomal subunit, cytosolic ribosome, mitochondrial protein complex, and inner mitochondrial membrane protein complex.

The five most significantly upregulated MF terms incorporated proximal promoter sequence-specific DNA binding, RNA polymerase II proximal promoter sequence-specific DNA binding, transcription factor functionality, transcription factor interaction, protein binding, and transcription cofactor activity. In contrast, the top five downregulated MF terms involved structural components of the ribosome, rRNA engagement, electron transfer functionality, cytochrome-c oxidase activity, and haem-copper terminal oxidase functionality.

The KEGG analysis (Figure 7.18) revealed 19 significantly upregulated pathways and 18 downregulated pathways. The top 5 upregulated pathways (Figure 7.18 A1) consisted of cGMP-PKG signalling pathway, Insulin resistance, MicroRNAs, Dilated cardiomyopathy (Figure 7.18 B2), and Hypertrophic cardiomyopathy (Figure 7.18 B1). In contrast, the top 5 downregulated pathways (Figure 7.18 A2) featured Cardiac muscle contraction (Figure 7.18 B4), Oxidative phosphorylation (Figure 7.18 B3), Parkinson disease, Thermogenesis, and Huntington disease.

7.2.2 Gene expression in cardiac tissue of AdCMV postpartum vs AdCMV in pregnancy

In a similar fashion to the previous section, a comparative study was carried out between the DEG in the LV tissues of AdsFit-1 pregnant mice and AdCMV pregnant mice. In this study, data from 24,232 DEG identified from AdCMV postpartum and AdCMV pregnant mice were utilized. Out of these 24,232 DEGs, only 544 genes were found to be significantly expressed ($\log FC > 1$, P value 0.05), with 240 up-regulated genes and 304 down-regulated genes observed on a volcano map (Figure 7.19 A). Red dots on the map represented up-regulated genes, blue dots pointed to down-regulated genes, while green dots represented non-significant DEGs. The volcano plot for the DEGs was analysed using Novomagic software and presented in Figure 7.19.

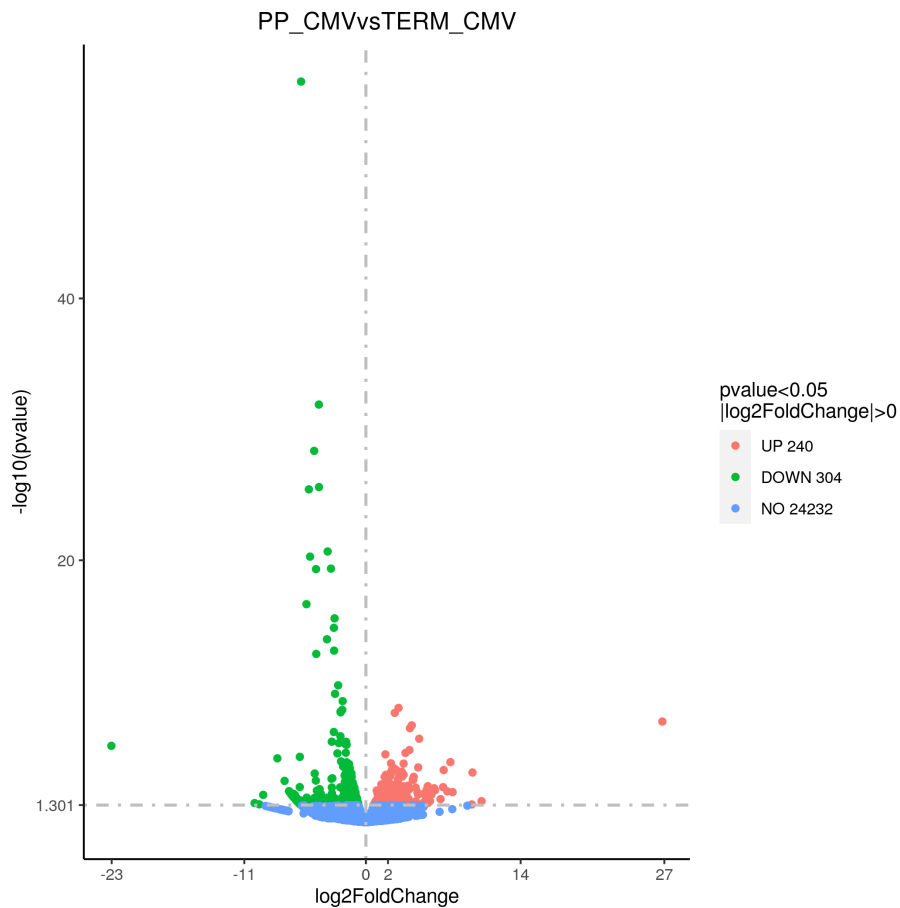


Figure 7.16 The differential expression of genes (DEG) in cardiac tissue of pregnant of AdCMV postpartum vs AdCMV in pregnant mice, was visually represented by a volcano plot.

The volcano plot (A) illustrated up-regulated genes with red dots and down-regulated genes with blue dots.

A table with the top 5 most upregulated (table 7.11) DEG and most downregulated DEG (table 7.12) looking at postpartum AdCMV vs pregnant AdCMV mice, was recorded.

| Gene ID | Gene Name | Full Name | Adjusted P-value |
|--------------------|-----------|-------------------------------------------------------------------------|------------------|
| ENSMUSG00000030046 | Bmp10 | bone morphogenetic protein 10 [Source: MGI Symbol; Acc: MGI:1338820] | 1.48E-05 |

| | | | |
|--------------------|--------|-------------------------------------------------------------------------------|------------|
| ENSMUSG00000020469 | Myl7 | myosin, light polypeptide 7, regulatory [Source:MGI Symbol;Acc:MGI:107495] | 0.04573424 |
| ENSMUSG00000027015 | Cybrd1 | cytochrome b reductase 1 [Source:MGI Symbol;Acc:MGI:2654575] | 0.01011774 |
| ENSMUSG00000044349 | Snhg11 | small nucleolar RNA host gene 11 [Source:MGI Symbol;Acc:MGI:2441845] | 0.03219213 |
| ENSMUSG00000043110 | Lrrn4 | leucine rich repeat neuronal 4 [Source:MGI Symbol;Acc:MGI:2445154] | 0.00025287 |

Table 7.11 Table of top 5 upregulated genes with a cut-off at p adjusted of 0.05, ordered in ascending order from the most upregulated gene to the least upregulated gene in postpartum AdCMV vs pregnant AdCMV mice.

| Gene ID | Gene Name | Full Name | Adjusted P-value |
|--------------------|-----------|-------------------------------------------------------------------------------------------|------------------|
| ENSMUSG00000030851 | Ldhc | lactate dehydrogenase C [Source:MGI Symbol;Acc:MGI:96764] | 0.00073118 |
| ENSMUSG00000032758 | Kap | kidney androgen regulated protein [Source:MGI Symbol;Acc:MGI:96653] | 0.00549447 |
| ENSMUSG00000023034 | Nr4a1 | nuclear receptor subfamily 4, group A, member 1 [Source:MGI Symbol;Acc:MGI:1352454] | 0.00430485 |
| ENSMUSG00000021250 | Fos | FBJ osteosarcoma oncogene [Source:MGI Symbol;Acc:MGI:95574] | 4.66E-53 |
| ENSMUSG00000037868 | Egr2 | early growth response 2 [Source:MGI Symbol;Acc:MGI:95296] | 3.86E-14 |

Table 7.12 Table of top 5 downregulated genes with a cut-off at p adjusted of 0.05, ordered in ascending order from the most downregulated gene to the least downregulated gene in postpartum AdCMV vs pregnant AdCMV mice.

GO analysis (Figure 7.20) was conducted to examine the functional implications of DEG. The upregulated DEG (Figure 7.11 A1) exhibited significant enrichment in 13 BP terms, 5 CC terms, 8 MF terms and the downregulated DEG exhibited significant enrichment in 244 BP terms, 15 CC terms and 23 MF terms.

The top 5 upregulates BP terms consisted of blood coagulation, haemostasis, coagulation, cell-cell adhesion mediated by cadherin, cell surface receptor signalling pathway involved in cell-cell signalling. The top downregulated BP terms included negative regulation of vasculature development, negative regulation of blood vessel morphogenesis, negative regulation of angiogenesis, response to steroid hormone, and ERK1 and ERK2 cascade.

The top 5 upregulated CC terms encompassed plasma membrane protein complex, catenin complex, ion channel complex, transmembrane transporter complex, and transporter complex. The top 5 downregulated CC consisted of ECM, ECM component, proteinaceous extracellular matrix, basement membrane, and complex of collagen trimers.

The top 5 upregulated MF terms were constituted of fibronectin binding, collagen binding, ECM structural constituent, heparan sulphate proteoglycan binding, and heparin binding. The top 5 downregulated MF terms consisted of ECM structural constituent, platelet-derived growth factor binding, ECM structural constituent conferring tensile strength, growth factor binding, and ECM binding.

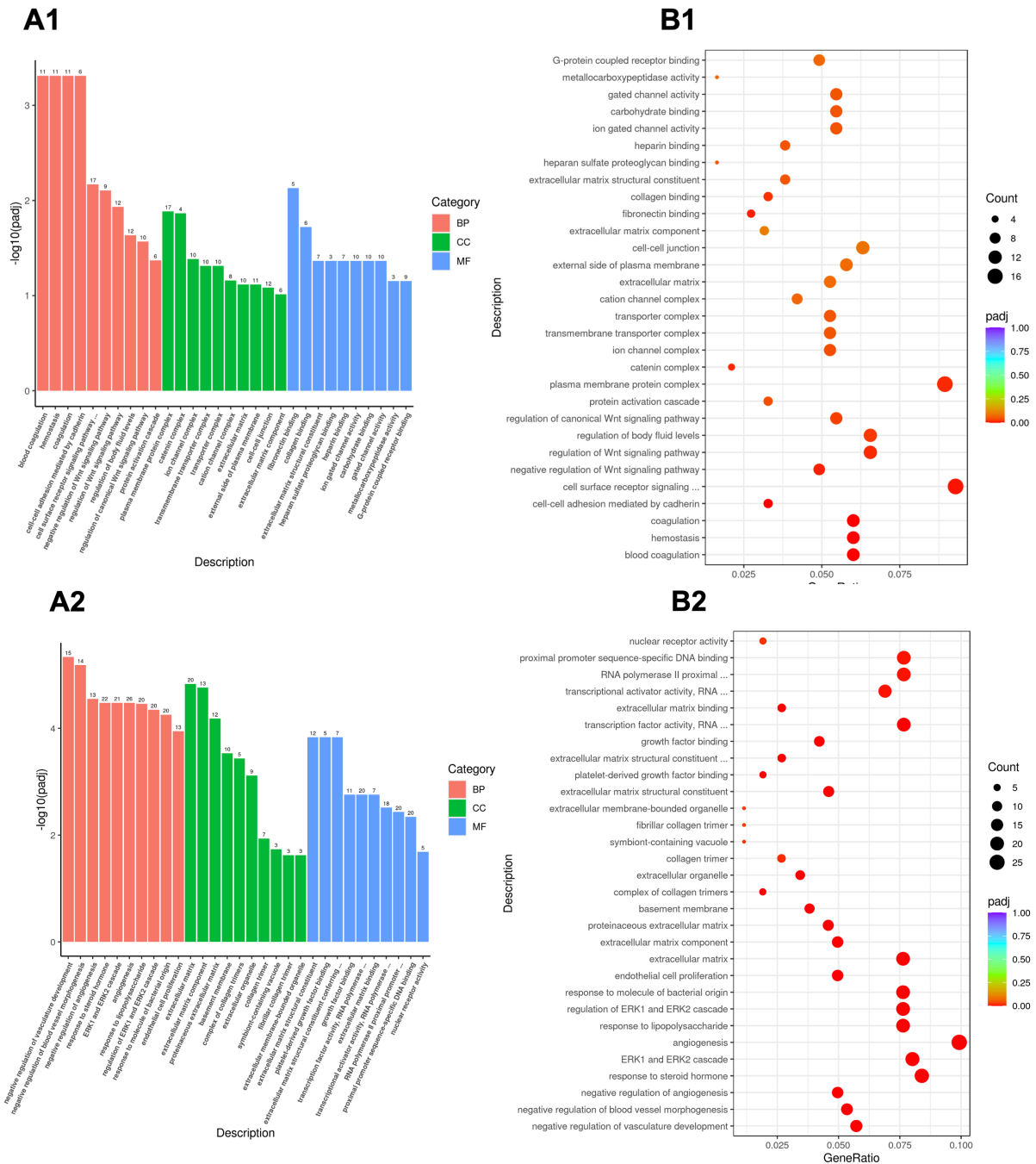


Figure 7.17 GO enrichment Analysis of DEG in cardiac tissue of pregnant of AdCMV postpartum vs AdCMV in pregnant mice.

GO of upregulated genes (**A1**) and downregulated genes (**A2**) annotates genes to BP, MF, and CC in a directed acyclic graph structure. Round size represents the gene count of each pathway and the colour of red to purple represents the significance level cut-off at p adjusted of 0.05. This was done with both upregulated DEG (**B1**) and downregulated DEG (**B2**).

7.2.3 Gene expression in cardiac tissue of AdsFlt-1 postpartum vs AdsFlt-1 mice in pregnancy

A comparative study was conducted between DEG in the LV tissues of postpartum AdsFlt-1 and pregnant AdsFlt-1 mice, utilizing data from 21,695 DEG. Of these 21,695 DEGs, only 3118 genes were found to be significantly expressed ($\log FC > 1$, P value 0.05), with 1295 up-regulated genes and 1823 down-regulated genes observed on a volcano map. The volcano plot (Figure 7.22 A) showcased red dots representing up-regulated genes, blue dots indicating down-regulated genes, and green dots representing non-significant DEGs. A heatmap (Figure 7.22 B) was also generated to display the expression profile of the statistically significant DEGs, where up-regulated genes were depicted in red and down-regulated genes in blue. Both the heatmap and volcano plot for the DEGs were analysed using Novomagic software and presented in Figure 7.22.

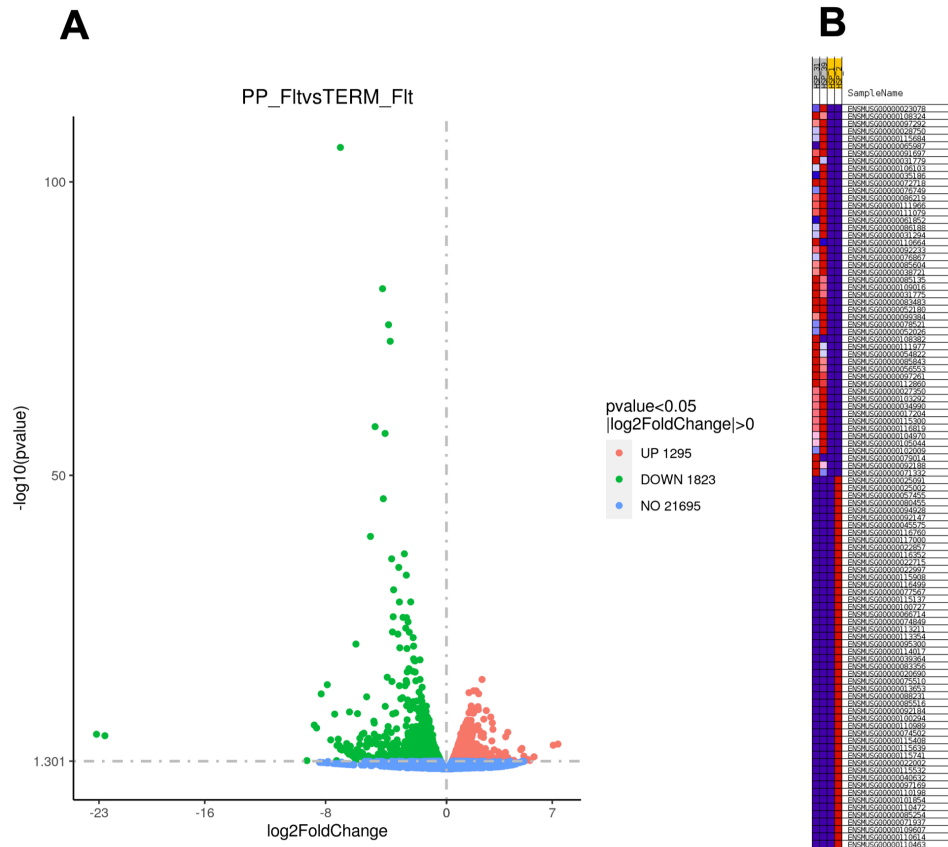


Figure 7.19 The differential expression of genes (DEG) in cardiac tissue of postpartum AdsFit-1 vs AdsFit-1 in pregnant mice, was visually represented by a volcano plot and a heatmap.

The volcano plot (A) illustrated up-regulated genes with red dots and down-regulated genes with blue dots. The heatmap (B) depicted up-regulated genes as blue and down-regulated genes as red.

A table with the top 5 most upregulated (table 7.13) DEG and most downregulated DEG (table 7.14) looking at postpartum AdsFit-1 vs pregnant AdsFit-1 mice, was recorded.

| Gene ID | Gene Name | Full Name | Adjusted P-value |
|--------------------|-----------|--------------------------------------------------------------------------|------------------|
| ENSMUSG00000023078 | Cxcl13 | chemokine (C-X-C motif) ligand 13 [Source:MGI Symbol;Acc:MGI:1888499] | 0.00206306 |

| | | | |
|--------------------|---------|---------------------------------------------------------------|------------|
| ENSMUSG00000108324 | Gm44608 | predicted gene 44608 [Source:MGI Symbol;Acc:MGI:5753184] | 0.00303406 |
| ENSMUSG00000079457 | Gm7609 | predicted pseudogene 7609 [Source:MGI Symbol;Acc:MGI:3644536] | 0.00849665 |
| ENSMUSG00000072769 | Gm10419 | predicted gene 10419 [Source:MGI Symbol;Acc:MGI:3642823] | 0.01277775 |
| ENSMUSG00000051906 | Cd209f | CD209f antigen [Source:MGI Symbol;Acc:MGI:1916392] | 4.51E-05 |

Table 7.13 Table of top 5 upregulated genes with a cut-off at p adjusted of 0.05, ordered in ascending order from the most upregulated gene to the least upregulated gene in postpartum AdsFlt-1 vs pregnant AdsFlt-1 mice.

| Gene ID | Gene Name | Full Name | Adjusted P-value |
|--------------------|-----------|-----------------------------------------------------------------------------------------------|------------------|
| ENSMUSG00000038015 | Prm2 | protamine 2 [Source:MGI Symbol;Acc:MGI:97766] | 8.47E-05 |
| ENSMUSG00000043050 | Tnp2 | transition protein 2 [Source:MGI Symbol;Acc:MGI:98785] | 0.00013498 |
| ENSMUSG00000042985 | Upk3b | uroplakin 3B [Source:MGI Symbol;Acc:MGI:2140882] | 3.85E-06 |
| ENSMUSG00000020609 | Apob | apolipoprotein B [Source:MGI Symbol;Acc:MGI:88052] | 1.02E-05 |
| ENSMUSG00000060807 | Serpina6 | serine (or cysteine) peptidase inhibitor, clade A, member 6 [Source:MGI Symbol;Acc:MGI:88278] | 4.98E-11 |

Table 7.14 Table of top 5 downregulated genes with a cut-off at p adjusted of 0.05, ordered in ascending order from the most downregulated gene to the least downregulated gene in postpartum AdsFlt-1 vs pregnant AdsFlt-1 mice.

GO analysis was completed to identify functional roles of DEG. When comparing postpartum AdsFlt-1 mice with pregnant AdsFlt-1, significantly upregulated DEG (Figure 7.23 A1) were enriched in 136 BP terms, 78 in CC terms, 44 in MF terms, and significantly downregulated DEG were enriched in 840 BP terms, 81 in CC terms, and 93 in MF terms.

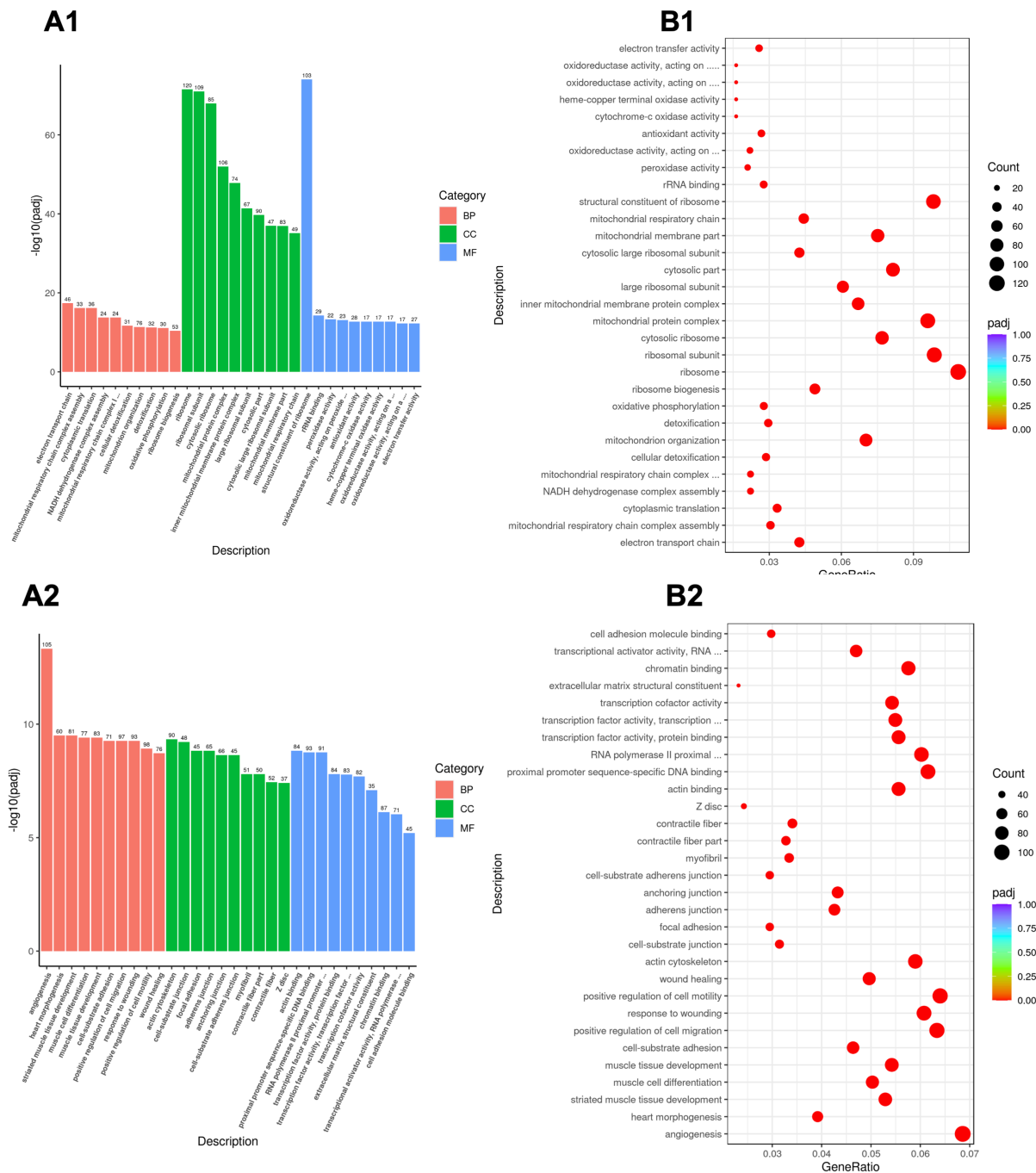


Figure 7.20 GO enrichment Analysis of DEG in cardiac tissue of postpartum AdsFit-1 vs AdsFit-1 in pregnant mice.

GO of upregulated genes (**A1**) and downregulated genes (**A2**) annotates genes to BP, MF, and CC in a directed acyclic graph structure. Round size represents the gene count of each pathway and the colour of red to purple represents the significance level cut-off at p adjusted of 0.05. This was done with both upregulated DEG (**B1**) and downregulated DEG (**B2**).

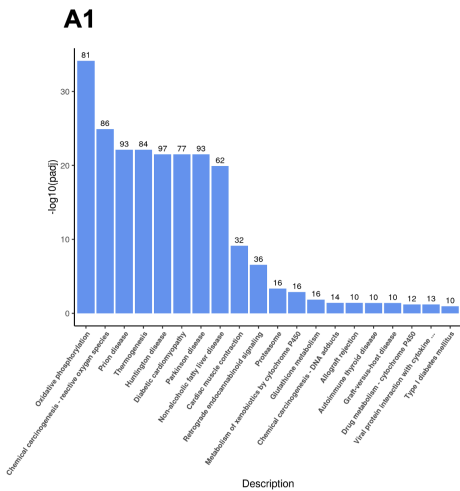
The top 5 upregulated BP terms consisted of electron transport chain, mitochondrial respiratory chain complex assembly, cytoplasmic translation, NADH dehydrogenase complex assembly, and mitochondrial respiratory chain complex I assembly. The top 5 downregulated BP terms involved angiogenesis, heart morphogenesis, striated muscle tissue development, muscle cell differentiation, and muscle tissue development.

The top 5 upregulated CC terms comprised ribosome, ribosomal subunit, cytosolic ribosome, mitochondrial protein complex, and inner mitochondrial membrane protein complex. The top 5 downregulated CC terms consisted of actin cytoskeleton, cell-substrate junction, focal adhesion, cell leading edge, and adherens junction.

The top 5 upregulated MF terms featured structural constituent of ribosome, rRNA binding, peroxidase activity, oxidoreductase activity acting on peroxide as acceptor, and antioxidant activity. The top downregulated MF terms involved actin binding, proximal promoter sequence-specific DNA binding, RNA polymerase II proximal promoter sequence-specific DNA binding, transcription factor functionality, protein binding, and transcription factor functionality and interaction.

KEGG analysis was also undertaken on the cardiac tissues of postpartum AdsFlt-1 vs AdsFlt-1 in pregnant mice and DEG (Figure 7.24 A1) were associated with 17 significantly upregulated pathways and 97 downregulated pathways (Figure 7.24 A2). The top 5 upregulated pathways Oxidative phosphorylation (Figure 7.24 B1), Chemical carcinogenesis - reactive oxygen species (Figure 7.24 B2), Diabetic cardiomyopathy, Parkinson disease and Huntington disease. The top 5 downregulated Focal adhesion (Figure 7.24 B3), ECM-receptor interaction (Figure 7.24 B4), Parathyroid hormone synthesis, secretion, and action, PI3K-Akt signalling pathway, and Proteoglycans in cancer.

KEGG Pathway of Upregulated Genes



KEGG Pathway of Downregulated Genes

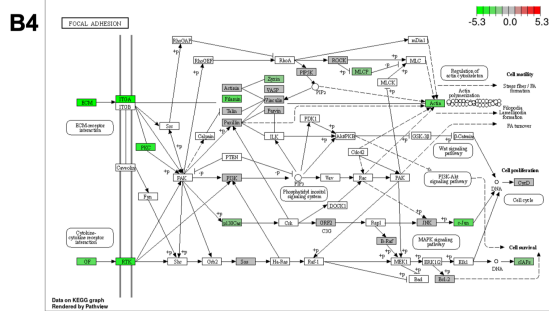
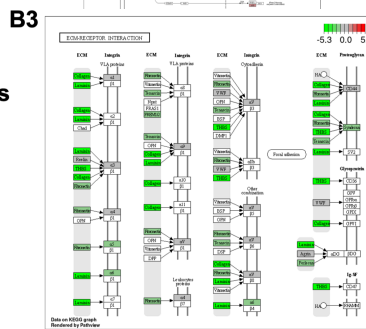
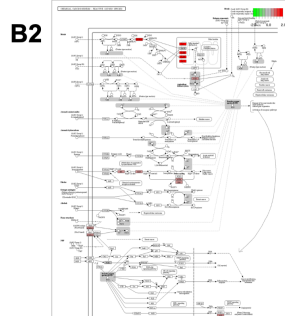
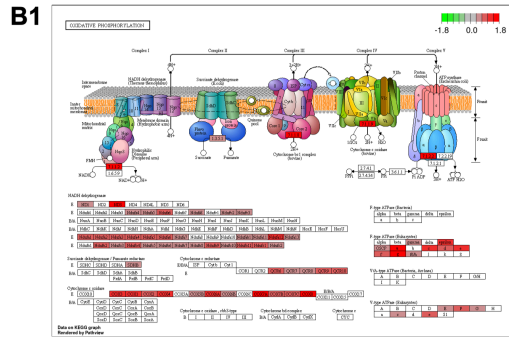
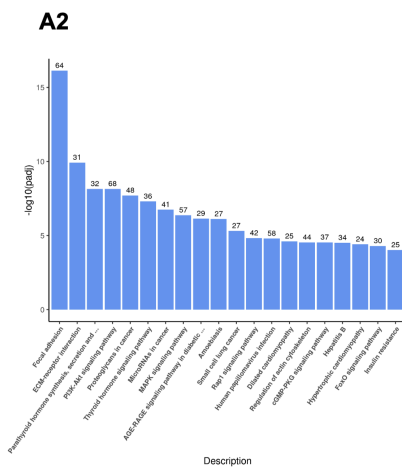


Figure 7.21 KEGG pathway enrichment analysis of DEGs from RNA-seq data of the cardiac tissue in AdsFit-1 postpartum vs AdsFit-1 in pregnant mice.

The bar chart showed the top 20 significantly enriched KEGG pathways of DEG with the p adjusted value cut-off as 0.05. Seventeen upregulated pathways were detected. The top two upregulated DEG (A1) were significantly concomitant with Oxidative phosphorylation (B1) and Chemical carcinogenesis – reactive oxygen species (B2). Ninety-seven significantly downregulated pathways were observed. The top two downregulated pathways (A2) were significantly related with Focal adhesion (B3) and ECM-receptor interaction (B4).

7.2.4 Gene expression in cardiac tissue of postpartum AdsFlt-1 vs AdCMV in mice

In this study, a comparative analysis was performed on DEG in the LV tissues of postpartum AdsFlt-1 and postpartum AdCMV mice utilizing data from 24,251 DEG. Out of these DEGs, only 262 genes were found to be significantly expressed, with 39 up-regulated and 223 down-regulated genes observed on a volcano map. The volcano plot, depicted in Figure 7.25 A, displayed red dots representing up-regulated genes, blue dots indicating down-regulated genes, and green dots representing non-significant DEGs. Additionally, a heatmap was generated to display the expression profile of the statistically significant DEGs, where up-regulated genes were depicted in red and down-regulated genes in blue (Figure 7.25 B). Both the heatmap and volcano plot for the DEGs were analysed using Novomagic software and presented in Figure 7.25.

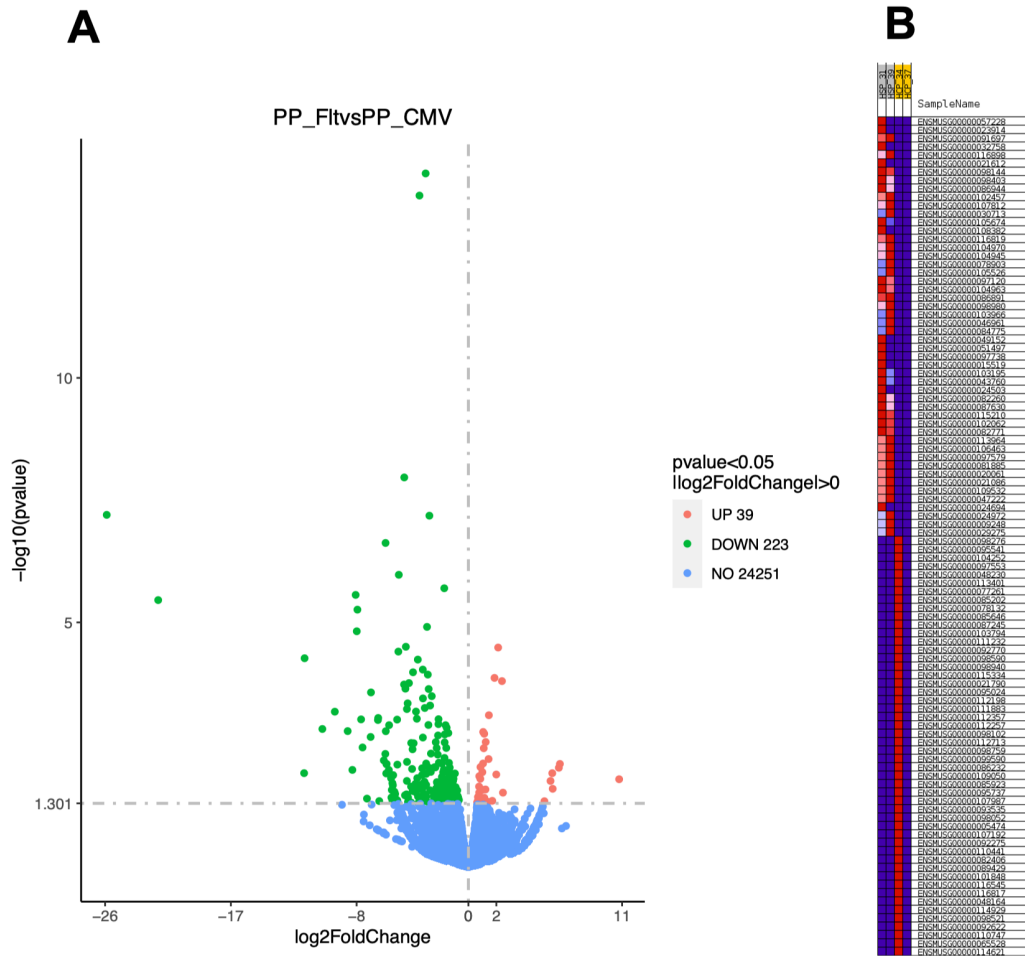


Figure 7.22 The differential expression of genes (DEG) in cardiac tissue of postpartum AdFit-1 vs AdCMV mice, was visually represented by a volcano plot and a heatmap.

The volcano plot (A) illustrated up-regulated genes with red dots and down-regulated genes with blue dots. The heatmap (B) depicted up-regulated genes as blue and down-regulated genes as red.

A table with the top 5 most upregulated (table 7.15) DEG and most downregulated DEG (table 7.16) looking at postpartum AdFit-1 vs AdCMV mice, was recorded.

| Gene ID | Gene Name | Full Name | Adjusted P-value |
|--------------------|-----------|--------------------------------------------------------------------------------------------------|------------------|
| ENSMUSG00000063415 | Cyp26b1 | cytochrome P450, family 26, subfamily b, polypeptide 1 [Source: MGI Symbol; Acc: MGI:2176159] | 0.03881044 |

Table 7.15 Table of upregulated DEG with a cut-off at p adjusted of 0.05, ordered in ascending order from the most upregulated gene to the least upregulated gene in postpartum AdsFit-1 vs AdCMV mice. Only one DEG was significantly upregulated.

| Gene ID | Gene Name | Full Name | Adjusted P-value |
|--------------------|-----------|----------------------------------------------------------------------------|------------------|
| ENSMUSG00000042045 | Sln | sarcolipin [Source: MGI Symbol; Acc: MGI:1913652] | 0.00023459 |
| ENSMUSG00000026347 | Tmem163 | transmembrane protein 163 [Source: MGI Symbol; Acc: MGI:1919410] | 0.0062368 |
| ENSMUSG00000030046 | Bmp10 | bone morphogenetic protein 10 [Source:MGI Symbol;Acc:MGI:1338820] | 0.00542809 |
| ENSMUSG00000042985 | Upk3b | uroplakin 3B [Source:MGI Symbol;Acc:MGI:2140882] | 0.02080121 |
| ENSMUSG00000020469 | Myl7 | myosin, light polypeptide 7, regulatory [Source:MGI Symbol;Acc:MGI:107495] | 0.00889415 |

Table 7.16 Table of downregulated regulated DEG with a cut-off at p adjusted of 0.05, ordered in ascending order from the most downregulated gene to the least downregulated gene in postpartum AdsFit-1 vs AdCMV mice.

GO analysis was undertaken to determine the functional roles of DEG when comparing postpartum AdsFlt-1 and AdCMV mice.

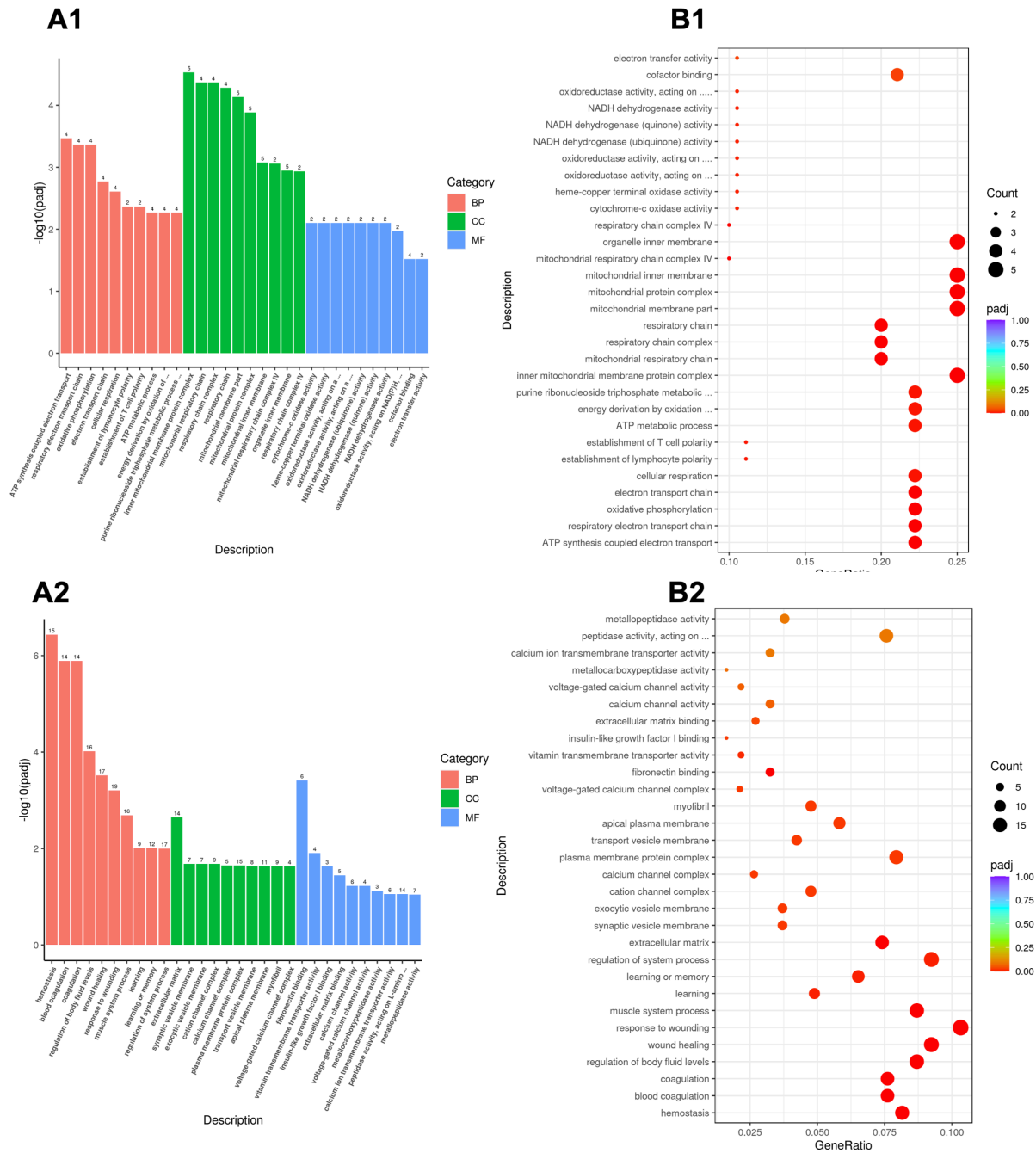


Figure 7.23 GO enrichment Analysis of DEG in cardiac tissue of postpartum AdsFit-1 vs AdCMV mice.

GO of upregulated genes (**A1**) and downregulated genes (**A2**) annotates genes to BP, MF, and CC in a directed acyclic graph structure. Round size represents the gene count of each pathway and the colour of red to purple represents the significance level cut-off at p adjusted of 0.05. This was done with both upregulated DEG (**B1**) and downregulated DEG (**B2**).

When comparing postpartum AdsFlt-1 mice with AdCMV, significantly upregulated DEG (Figure 7.26 A1) were enriched in 27 BP terms, 17 in CC terms, 11 in MF terms, and significantly downregulated DEG were enriched in 26 BP terms, 26 in CC terms, and 4 in MF terms.

The top 5 upregulated BP terms involved ATP synthesis coupled electron transport, respiratory electron transport chain, oxidative phosphorylation, electron transport chain, and cellular respiration. The top 5 downregulated BP terms featured haemostasis, blood coagulation, coagulation, regulation of body fluid levels, and wound healing.

The top 5 upregulated CC terms comprised inner mitochondrial membrane protein complex, mitochondrial respiratory chain, respiratory chain complex, respiratory chain, and mitochondrial membrane part. The top 5 downregulated CC terms consisted of extracellular matrix, synaptic vesicle membrane, exocytic vesicle membrane, cation channel complex, and calcium channel complex.

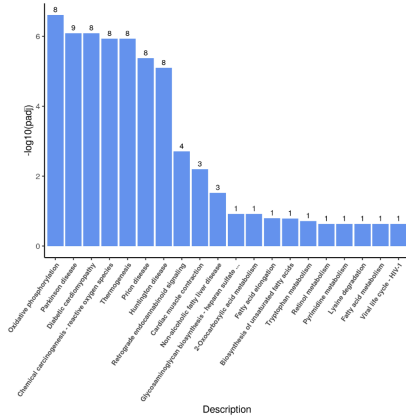
The top 5 upregulated MF terms included cytochrome-c oxidase activity, haem-copper terminal oxidase activity, oxidoreductase activity acting on a haem group of donors with oxygen as acceptor, oxidoreductase activity acting on a haem group of donors, and NADH dehydrogenase (ubiquinone) activity. Conversely, the top 4 downregulated MF terms were fibronectin binding, vitamin transmembrane transporter activity, insulin-like growth factor I binding, and extracellular matrix binding.

KEGG analysis revealed a positive regulation for 10 pathways (Figure 7.27 A1) and a negative regulation for 5 pathways (Figure 7.27 A2). The top 5 upregulated pathways included Oxidative phosphorylation (Figure 7.27 B1), Parkinson disease (Figure 7.27 B2), Diabetic

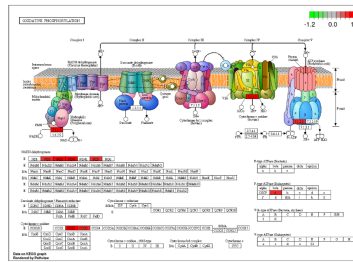
cardiomyopathy, Chemical carcinogenesis - reactive oxygen species, and Thermogenesis. The 5 downregulated pathways were ECM-receptor interaction (Figure 7.27 B3), Dilated cardiomyopathy (Figure 7.27 B4), Hematopoietic cell lineage, Hypertrophic cardiomyopathy, Platelet activation.

KEGG Pathway of Upregulated Genes

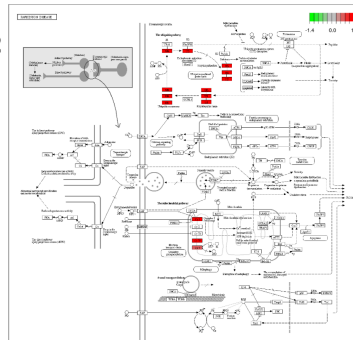
A1



B1

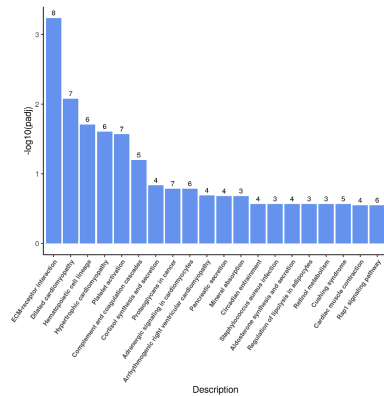


B2

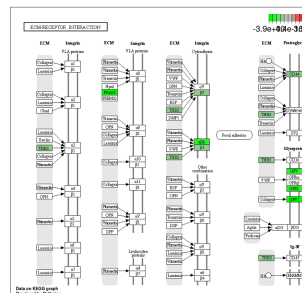


KEGG Pathway of Downregulated Genes

A2



B3



B4

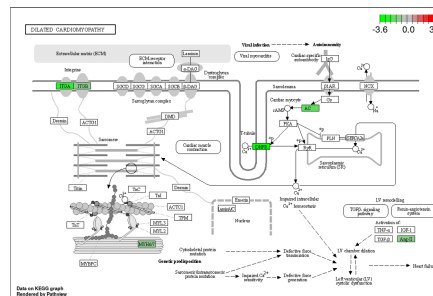


Figure 7.24 KEGG pathway enrichment analysis of DEGs from RNA-seq data in cardiac tissue of postpartum Ad5Flt-1 vs AdCMV mice.

The bar chart showed the top 20 significantly enriched KEGG pathways of DEG with the p adjusted value cut-off as 0.05. Ten significantly upregulated pathways were observed (A1). The top 2 pathways included Oxidative phosphorylation (B1) and Parkinson disease (B2). Five significantly downregulated pathways were seen. The top 2 downregulated pathways (A2) were composed of ECM-receptor interaction (B3) and Dilated cardiomyopathy (B4).

7.2.5 Gene expression in cardiac tissue of AdsFlt-1 postpartum vs pregnant AdCMV mice

This study aimed to perform a comparative analysis on DEG in the LV tissues of postpartum AdsFlt-1 and pregnant AdCMV mice, utilising data from 23,043 DEG. The results showed that only 631 DEGs were significantly expressed, with 150 genes being up-regulated and 481 down-regulated, as observed on a volcano map (Figure 7.28 A). The volcano plot was generated using red dots to indicate up-regulated genes, blue dots to indicate down-regulated genes, and green dots to indicate non-significant DEGs. Furthermore, Novomagic software was used to analyse both the heatmap and volcano plot for the DEGs, where the expression profile of the statistically significant DEGs was depicted in red for up-regulated genes and blue for down-regulated genes (Figure 7.28 B). These findings provide valuable insights into the differential gene expression in postpartum AdsFlt-1 and pregnant AdCMV mice.

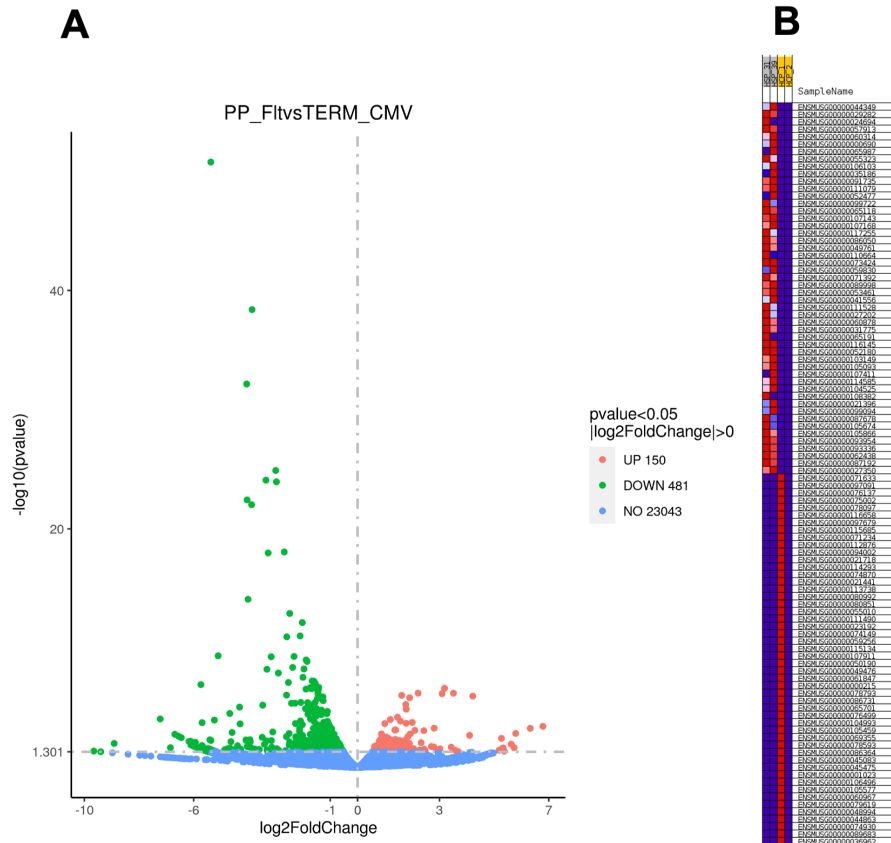


Figure 7.25 The differential expression of genes (DEG) in cardiac tissue of postpartum AdFit-1 vs pregnant AdCMV mice, was visually represented by a volcano plot and a heatmap.

The volcano plot (A) illustrated up-regulated genes with red dots and down-regulated genes with blue dots. The heatmap (B) depicted up-regulated genes as blue and down-regulated genes as red.

A table with the top 5 most upregulated (table 7.17) DEG and most downregulated DEG (table 7.18) looking at postpartum AdFit-1 vs pregnant AdCMV mice, was recorded.

| Gene ID | Gene Name | Full Name | Adjusted P-value |
|--------------------|-----------|-------------------------------------------------------|------------------|
| ENSMUSG00000051906 | Cd209f | CD209f antigen [Source: MGI Symbol; Acc: MGI:1916392] | 0.00039716 |
| ENSMUSG00000053166 | Cdh22 | cadherin 22 [Source: MGI Symbol; Acc: MGI:1341843] | 0.00025382 |

| | | | |
|--------------------|-------|------------------------------------------------------------------------|------------|
| ENSMUSG00000000305 | Cdh4 | cadherin 4 [Source: MGI Symbol; Acc: MGI:99218] | 0.00011584 |
| ENSMUSG00000055489 | Ano5 | anoctamin 5 [Source: MGI Symbol; Acc: MGI:3576659] | 0.00026742 |
| ENSMUSG00000028307 | Aldob | aldolase B, fructose-bisphosphate [Source: MGI Symbol; Acc: MGI:87995] | 0.00025382 |

Table 7.17 Table of upregulated DEG with a cut-off at p adjusted of 0.05, ordered in ascending order from the most upregulated gene to the least upregulated gene in postpartum AdsFit-1 vs pregnant AdCMV mice. Only one DEG was significantly upregulated.

| Gene ID | Gene Name | Full Name | Adjusted P-value |
|--------------------|-----------|-----------------------------------------------------------------------------------------------|------------------|
| ENSMUSG00000042985 | Upk3b | uroplakin 3B [Source:MGI Symbol;Acc:MGI:2140882] | 0.01908989 |
| ENSMUSG00000028341 | Nr4a3 | nuclear receptor subfamily 4, group A, member 3 [Source:MGI Symbol;Acc:MGI:1352457] | 6.47E-05 |
| ENSMUSG00000060807 | Serpina6 | serine (or cysteine) peptidase inhibitor, clade A, member 6 [Source:MGI Symbol;Acc:MGI:88278] | 0.03341233 |
| ENSMUSG00000026628 | Atf3 | activating transcription factor 3 [Source:MGI Symbol;Acc:MGI:109384] | 2.84E-47 |
| ENSMUSG00000028141 | Oaz3 | ornithine decarboxylase antizyme 3 [Source:MGI Symbol;Acc:MGI:1858170] | 0.02290146 |

Table 7.18 Table of downregulated regulated DEG with a cut-off at p adjusted of 0.05, ordered in ascending order from the most downregulated gene to the least downregulated gene in postpartum AdsFit-1 vs pregnant AdCMV mice.

GO analysis was performed to assess the functional implications of DEG in a comparative study between postpartum AdsFit-1 and pregnant AdCMV mice. The results of the analysis implied that only 8 BP terms were significantly upregulated (Figure 7.29 A1). In contrast,

significant downregulation (Figure 7.29 B1) of enrichment in 443 BP terms, 40 CC terms, 34 MF terms were significantly associated with DEG.

The top 5 positively regulated BP terms involved cofactor metabolic process, glucocorticoid secretion, negative regulation of catecholamine secretion, fructose metabolic process, regulation of corticosteroid hormone secretion, and carboxylic acid biosynthetic process. The top 5 negatively regulated BP terms were angiogenesis, extracellular matrix organization, cellular response to interferon-beta, extracellular structure organization, and response to interferon-gamma.

The top 5 negatively regulated CC terms featured proteinaceous extracellular matrix, basement membrane, symbiont-containing vacuole, extracellular membrane-bounded organelle, and negative regulation of angiogenesis.

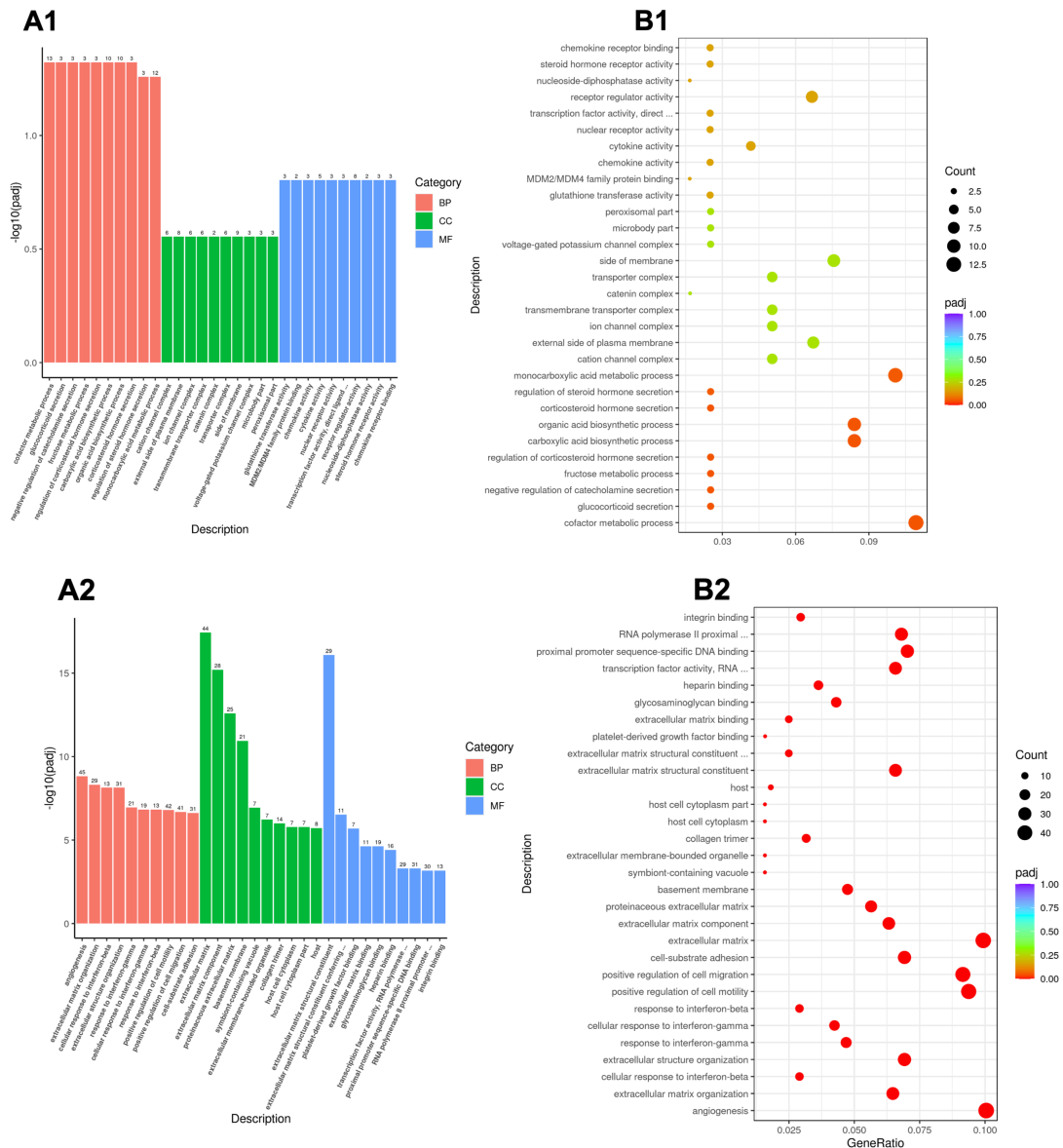


Figure 7.26 GO enrichment Analysis of DEG in cardiac tissue of postpartum Ad5Flt-1 vs pregnant AdCMV mice.

GO of upregulated genes (**A1**) and downregulated genes (**A2**) annotates genes to BP, MF, and CC in a directed acyclic graph structure. Round size represents the gene count of each pathway and the colour of red to purple represents the significance level cut-off at p adjusted of 0.05. This was done with both upregulated DEG (**B1**) and downregulated DEG (**B2**).

The top negatively regulated MF terms constituted extracellular matrix structural constituent, extracellular matrix structural constituent conferring tensile strength, platelet-derived growth factor binding, extracellular matrix binding, and glycosaminoglycan binding.

KEGG Pathway of Upregulated Genes

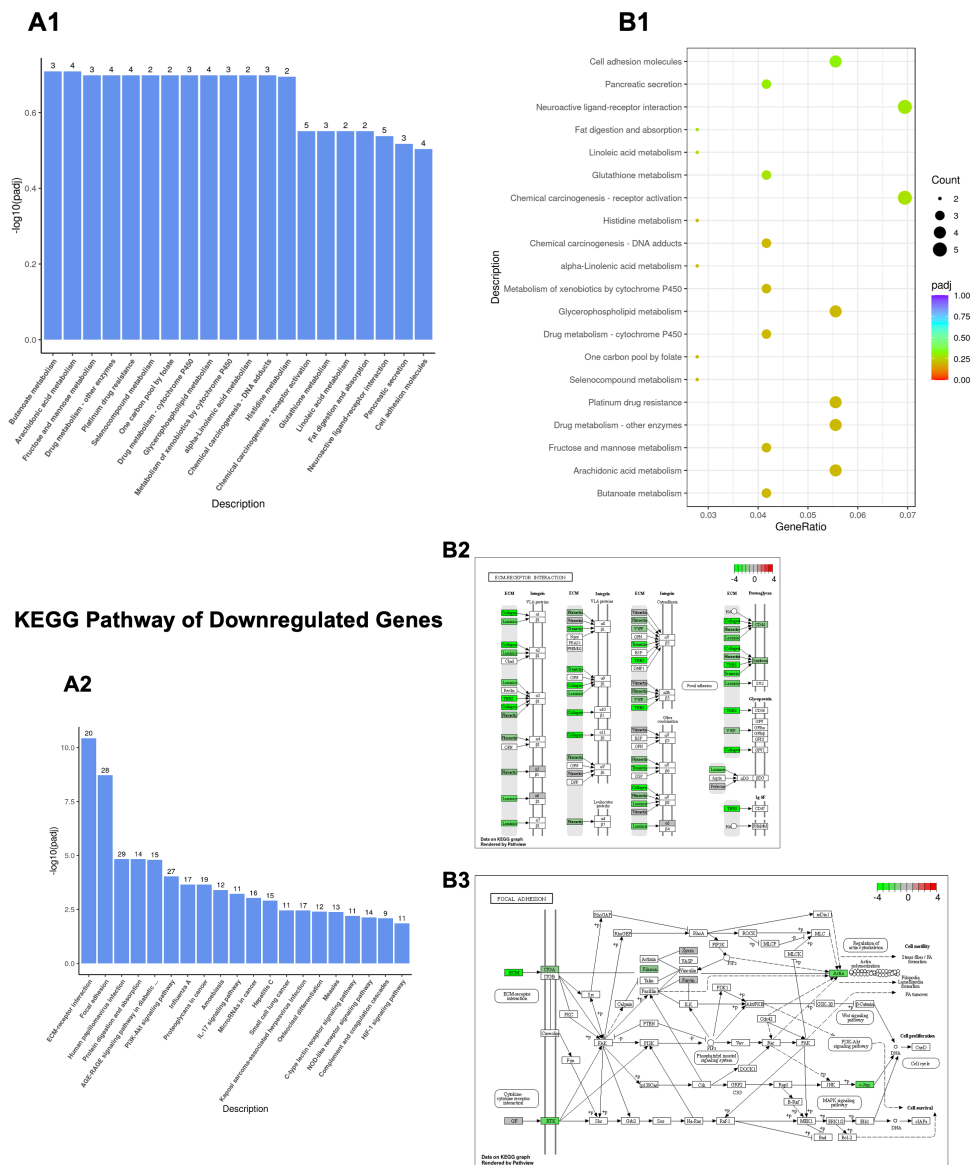


Figure 7.27 KEGG pathway enrichment analysis of DEGs from RNA-seq data in cardiac tissue of postpartum AdsFlt-1 vs pregnant AdCMV mice.

The bar chart showed the top 20 significantly enriched KEGG pathways of DEG with the p adjusted value cut-off as 0.05. The upregulated DEG (A1) were not significantly (B1) associated with any pathway. The downregulated DEG were significantly connected with 26 pathways. The top 2 downregulated pathways were ECM-receptor interaction (B3), and Focal adhesion (B4).

KEGG analysis was carried out on DEG. Curiously, no significant pathways were correlated with upregulated DEG. Contrarily, 26 pathways were correlated with downregulated pathways. The top 5 downregulated pathways entailed ECM-receptor interaction, Focal adhesion, Human papillomavirus infection, Protein digestion and absorption, and AGE-RAGE signalling pathway in diabetic complications.

7.3 Discussion

This chapter investigated the genetic profiles of different PE models, specifically the CSE KO model during pregnancy and the AdsFlt-1 model during pregnancy and postpartum. Different comparisons were made, and each comparison included a full analysis comprised of DEG, GO terms and KEGG pathways. DEG allowed for the identification of genes that were upregulated or downregulated in different PE models and highlighted pregnancy-specific changes in gene expression patterns, which may have implications for cardiac function during pregnancy. Pathway analysis enabled the investigation of the biological pathways and processes enriched among DEG that helped elucidate the functional consequences of altered gene expression in different PE models.

7.3.1 Gene expression in CSE KO in cardiac tissue

7.3.1.1 Pre-gravid profile of CSE KO in cardiac tissue

The genes linked to H₂S deficiency and PE specifically have not been extensively investigated. Our DEG analysis identified that the most affected genes in the cardiac tissue of non-pregnant CSE KO mice compared to CSE WT mice, are in fact related to tissue development, remodelling, cellular signalling, and binding (e.g., ERK1 and ERK2 cascade), membrane structure and components.

The upregulation of genes identified in the present study, such as *Nxpe4*, *Pdzd3*, and *Eif3j1* suggested that H₂S deficiency may affect various cellular processes, including synaptic transmission and protein synthesis (“Brain tissue expression of NXPE4 - Summary - The Human Protein Atlas” n.d.; Y. H. Chen *et al.* 2005; Roos *et al.* 2007; Mebratu & Tesfaigzi 2009; Camilleri *et al.* 2015; Quan *et al.* 2015; Singh & Lin 2015; Buscà *et al.* 2016; Jimenez *et al.* 2017; Tomasovic *et al.* 2020). Likewise, these genes implied that H₂S deficiency may affect the ability of cells to move and migrate, which could have implications for wound healing, tissue repair, and other physiological processes, such as complications of cell signalling and communication with the external environment (Lockhart *et al.* 2011; S. Z. Chen *et al.* 2016).

The upregulated pathways (Staphylococcus aureus infection, Central carbon metabolism in cancer, HIF-1 signalling pathway, and Chagas disease (American trypanosomiasis)) indicated that H₂S deficiency could impair immune response, cellular metabolism, and adaptation to hypoxic conditions, respectively (Toliver-Kinsky *et al.* 2019; Dilek *et al.* 2020; Rahman *et al.* 2020). These findings supported what has been previously reported and highlighted, specifically the role for H₂S in regulating immune responses and cellular processes (Toliver-Kinsky *et al.* 2019; Dilek *et al.* 2020; Rahman *et al.* 2020).

The most down-regulated genes identified were involved in different BP such as protein synthesis (*Rpl29*, *Rpl34*), cell proliferation (*Pcna-ps2*), and cell migration and adhesion

(BC002163 and Gm14085) (Cooper & Ordahl 1985; Wen-Sen Lee et al. 1997; Strzalka & Ziemienowicz 2011; Luo et al. 2012; J. Xu & Shi 2014; Locatelli et al. 2014; Van Den Hoogenhof et al. 2016). Therefore, their downregulation demonstrated that H₂S may play a role in regulating these processes. In particular, the downregulation of genes involved in cell migration and adhesion, which may have implications for immune responses, tissue repair and regeneration, and cancer metastasis (Nishijima *et al.* 2004; Goksu Erol *et al.* 2012; Ohtsuka *et al.* 2013; Toliver-Kinsky *et al.* 2019; Dilek *et al.* 2020; Rahman *et al.* 2020; Saeed *et al.* 2020; Morelli & Sadovsky 2022).

In summary, the DEGs analysis posited that CSE plays an important role in regulating genes involved in major cellular process. Although no significant cardiac dysfunctions were observed in CSE KO non-pregnant mice compared to CSE WT mice, these genes may be implicated in cardiac maladaptation to pregnancy in CSE KO mice.

7.1.1.2 Gene expression profile in pregnancy

7.1.1.2.1 Gene expression profile in the CSE WT

This DEG analysis detected that the most affected genes in the cardiac tissue of CSE WT pregnant mice compared to CSE WT non-pregnant mice, are associated with cofactor metabolism, monocarboxylic acid metabolism, cofactor biosynthesis, tetrapyrrole metabolism, and 2-oxoglutarate metabolism.

The upregulation of genes identified in this study, such as Cyp1a1, Penk, mt-T12, Alas1 and Csdc2 revealed an increase in enkephalin production, protein synthesis, haemoglobin biosynthesis, and RNA splicing in the pregnant heart, potentially serving as protective mechanisms or adaptations to the increased demands of pregnancy (Dhawan et al. 1990; Maines et al. 1990; Puga et al. 1990; Castiglia et al. 1996; Sadlon et al. 1999; Zagon et al. 1999, 2000; Nastasi et al. 2000; Harrison et al. 2001; Y. Kimura et al. 2006; Okano et al. 2010; T. Kato et al. 2010; Sobenin et al. 2012; L. J. C. Wong et al. 2020).

These genes further imply that pregnancy elicits an increase in mitochondrial constituents, including organellar ribosomes, and Tetrapyrroles. Given that mitochondria substantially impact the physiological alterations transpiring during gestation, these components may aid in regulating central cellular processes, thus facilitating the physiological adaptations observed throughout pregnancy (Rodríguez-Cano *et al.* 2020). This could potentially be achieved by enhancing enzyme activity, energy generation, oxygen transport capacity, and providing protection against oxidative stress (Roland-Zejly *et al.* 2011; Kalhan 2016; Broderick *et al.* 2018; Uzun 2019; Rodríguez-Cano *et al.* 2020; Jawaid *et al.* 2021; Gutman & Parrilla 2022).

The upregulated pathways (Metabolism of xenobiotics by cytochrome P450, Chemical carcinogenesis, Drug metabolism - cytochrome P450, Parkinson disease, Glutathione metabolism) imply that the cardiac tissue in pregnant mice undergoes adaptive changes to maintain homeostasis, protect against harmful substances, and ensure proper physiological function during gestation (L. F. Hu *et al.* 2010; Huber *et al.* 2011; Peter Nicholls *et al.* 2013; Bok *et al.* 2021; Gutman & Parrilla 2022),

The most downregulated genes in CSE WT pregnant mice compared to non-pregnant mice, included *Il1b* (Hilbi *et al.* 1997; Sugihara *et al.* 1998; S. Wu *et al.* 2018), *Plaur* (Koh *et al.* 1992; Y. Ye *et al.* 2017; Batiha *et al.* 2022), *Irs2* (Mammarella *et al.* 2000; Lautier *et al.* 2003), and *Cyp26b1* (Koh *et al.* 1992; White *et al.* 2000; Abu-Abed *et al.* 2002; Trofimova-Griffin & Juchau 2002), which denoted decreased inflammation, tissue remodelling, insulin signalling, and atherosclerosis.

Additionally, downregulation of processes such as ossification cellular response to external stimulus, positive regulation of voltage-gated potassium channel activity, leukocyte differentiation, and actin-related structures. The following downregulation reflected that in pregnancy, a shift in resource allocation, altered immune system functioning, and modifications in cellular signalling, neurological development, axonal guidance and structural dynamics takes place (Elkayam & Bitar 2005; Zanardo *et al.* 2006b; Telezhkin *et al.* 2008; Norton *et al.* 2009; Buraei & Yang 2010, 2013; Mistry *et al.* 2011; Patnaik 2018; Squire 2019; Aryan *et al.* 2020; Hsu & Tain 2021; Lewey *et al.* 2021; Pickel *et al.* 2021; C. Pan *et al.* 2022; Morelli & Sadovsky 2022).

The upregulated pathways (Fluid shear stress and atherosclerosis pathway) purport a reduced risk or progression of atherosclerosis and vascular remodelling during pregnancy, which could be beneficial for maintaining healthy blood flow (Ruffolo & Kopia 1986; E. Chung *et al.* 2012; Maymó *et al.* 2012; Q. Sun *et al.* 2018; Mahmood *et al.* 2022).

To summarize, the simultaneous upregulation and downregulation of the mentioned factors, genes and pathways in the heart during a normal pregnancy demonstrate a harmonized response encompassing various physiological adjustments. Adaptations such as enhanced enzymatic activity, energy generation, protein regulation, structural and functional modifications, and changes in intracellular signalling, collaborate to ensure the heart can effectively sustain both the mother and the developing foetus.

7.1.1.2.2 Gene expression profile in the CSE KO

The DEG analysis in the comparison of pregnant CSE KO vs non-pregnant CSE KO, demonstrated that the most upregulated of genes related to cellular regulation, antioxidant defence, and energy metabolism.

The upregulation of genes observed in this study such as Gm3650, Pcn-ps2, Eno1b, Gm14085, and Snca suggests an enhanced cell proliferation in response (PCNA) to the increased demands of pregnancy, an enhanced glycolytic metabolism (Enob1b) in response to the increased energy demands of pregnancy, contributing to the heart's ability to maintain homeostasis despite H₂S deficiency (Feo *et al.* 2000; Gehen *et al.* 2007; Kang *et al.* 2008; Baple *et al.* 2014; I. Huppertz *et al.* 2022). The role of Snca in the heart, especially during pregnancy, remains unclear, but upregulation has been observed in cardiovascular diseases such as atrial fibrillation and stroke (Cronin *et al.* 2009; Tagliaferro & Chiba-Falek 2016; Magistrelli *et al.* 2021).

The cardiac tissue of pregnant CSE KO mice showed combined upregulation in genes related to lipid metabolism, immune responses, inflammation, and cell differentiation, as well as increased antioxidant and peroxidase activity to manage oxidative stress. These changes were not observed in CSE WT pregnant mice, suggesting that the deficiency in H₂S exacerbated oxidative stress in the cardiac tissue of pregnant CSE KO mice (S. A. Smith 2002;

Zanardo et al. 2006b; X. Yang et al. 2011; Mano et al. 2014; K. W. Chung et al. 2018; Yeon Lee et al. 2019).

The upregulated pathways in this study (Fatty acid elongation, Malaria, PPAR signalling pathway) demonstrated alterations in the lipid metabolism, immune response and cellular signalling processes, to potentially compensate for the lack of H₂S (Smith 2002; K. W. Chung et al. 2018). Equally, this could also postulate that an increase in inflammation and cell differentiation is present in pregnant CSE KO mice (Zanardo et al. 2006b; Yeon Lee et al. 2019).

In contrast, the most downregulated genes, such as *Fosb*, *Gm17971*, *Egr2*, *Nr4a1*, and *Egr1*, were associated with muscle organ development, angiogenesis, striated muscle tissue development, and more. Downregulation of these genes further indicate potentially altered regulation of specific target genes during pregnancy (*Fosb*), alterations in cell proliferation and differentiation (*Egr1* & *Egr2*), as well as increased VSMC proliferation, inflammation, susceptibility to atherosclerosis, and higher cardiomyocyte apoptosis (*Nr4a1*), (Heximer et al. 1996; Senali Abayratna Wansa et al. 2002; Baumann et al. 2003; Holmes & Zachary 2004; Kumbrink et al. 2010; S. H. Kim et al. 2010; Kyogoku et al. 2011; Xia Li et al. 2014; Hayashi et al. 2015; Vaiman & Miralles 2016; Gormley et al. 2017; Taefehshokr et al. 2017; Medzikovic et al. 2019). Downregulated pathways (Ribosome, Thermogenesis, Non-alcoholic fatty liver disease (NAFLD), Focal adhesion, and Parkinson disease) purported impairments in various cellular functions such as alterations in protein synthesis, energy expenditure, lipid metabolism, cell-matrix interactions, and cellular maintenance processes in response to the lack of H₂S.

In summary, the comparison of heart function between CSE KO pregnant and non-pregnant mice revealed several key observations. These findings suggested that H₂S deficiency during pregnancy exacerbates oxidative stress and induces adaptive changes in cardiac tissue to attempt to maintain homeostasis and meet the increased demands of pregnancy. Pregnant CSE KO mice exhibited impairments in protein synthesis, energy expenditure, lipid metabolism, cell-matrix interactions, and cellular maintenance.

7.1.1.2.3 Gene expression profile in CSE KO vs CSE WT

This DEG analysis detected that the most affected genes in the cardiac tissue of pregnant CSE KO vs CSE WT mice were associated with cellular signalling and chemotaxis (e.g., neutrophil chemotaxis), cardiac development and function (e.g., cardiac chamber development), ECM and membrane-associated processes, molecular binding and interactions, and Intracellular signalling and enzymatic activities (e.g., MAP kinase).

The top 5 upregulated DEG were *Nxpe4*, *Gm12381*, *Eno1b*, *Cidec*, and *Gm10736* and revealed an increase in lipid (*Cidec*) and energy metabolism (*Eno1b*), synaptic transmission (*Nxpe4*) and protein synthesis (*Gm12381* and *Gm10736*) (“Brain tissue expression of NXPE4 - Summary - The Human Protein Atlas” n.d.; Gupta & Zhang 2005; K. Liu et al. 2009; Karki et al. 2019; X. Meng et al. 2019; Glavan et al. 2021).

Upregulated pathways (Malaria and Proteoglycans in cancer) were mostly involved in cardiac function, involving ECM remodelling, angiogenesis, cell proliferation, and altered immune responses or stress-related processes. This indicated a potential increase in inflammatory and immune response that could lead to tissue damage, fibrosis, and cardiac dysfunction, enhancement in the growth and development of cardiac muscle (K. Miyata *et al.* 1984; Ono *et al.* 1985; Obel *et al.* 1993) (Ono *et al.* 1985; Obel *et al.* 1993; Jordan *et al.* 1999; Higuchi *et al.* 2008).

The most downregulated genes such as *Rpl34*, *BC002163*, *Rab6b*, *Gm1840*, and *Gm6166*, related to protein synthesis (*Gm1840*, and *Gm6166*), ribosomal function (*Rpl34*), metabolic processes (*Rab6b*), cellular stress response (*BC002163*) and cell death. (Opdam *et al.* 2000; Wanschers *et al.* 2008; X. Sun *et al.* 2020; Caponnetto *et al.* 2022; Maloum *et al.* 2022).

Downregulated pathways (Ribosome, Oxidative phosphorylation, Parkinson disease, Thermogenesis, and Alzheimer disease) revealed a decline in protein synthesis, energy production, and stress response mechanisms. These changes could impair the ability of the

heart to adapt to the increased demands of pregnancy and maintain proper function (Rosca & Hoppel 2013; Seo *et al.* 2020; Ramaccini *et al.* 2021; X. Q. Hu & Zhang 2021).

Overall, pregnant CSE KO mice exhibited various changes in the heart's structure, development, signalling, immune response, energy metabolism, protein synthesis, cellular trafficking, and stress responses compared to CSE WT mice. The DEG collectively revealed that the cardiovascular function in CSE KO pregnant mice may be compromised, as evidenced by the upregulation of *Nxpe4* and *SNCA* and the downregulation of *Nr4a1*. The BP, CC, and MF factors alluded to an enhanced inflammatory response, as observed through the upregulation of granulocyte and neutrophil chemotaxis, and potential cardiac tissue remodelling, as supported by the increase in cardiac muscle tissue development. Moreover, diminished protein synthesis and energy production were demonstrated by the downregulation of ribosomal pathways and mitochondrial structures, respectively. Finally, the upregulation of specific pathways further indicated dysfunction in adaptations to pregnancy, as seen by elevated levels of proteoglycans in cancer and the decreased immune response, which was evidenced by an upregulation in malaria-related pathways.

Taken together, these alterations deviate from the typical adaptations observed in a healthy pregnancy and may instead demonstrate maladaptation during pregnancy in CSE KO mice. Nevertheless, it is crucial to emphasize that these interpretations are solely speculative, based on the mRNA findings obtained, and warrant validation through qPCR in order to draw definitive conclusions.

7.3.2 Gene expression in AdsFlt-1

7.3.2.1 Gene expression in AdsFlt-1 in pregnancy

The DEG analysis revealed that the most significantly impacted genes in the cardiac tissue of pregnant AdsFlt-1 mice, as compared to pregnant AdCMV mice, are predominantly associated with aspects of cardiac development and function (e.g., cardiac muscle hypertrophy, heart valve development), cellular structure and organization (e.g., nuclear speck), axon extension and neuronal processes, and transcriptional regulation and molecular interactions.

The observed upregulation of genes, including Gm31251, Wt1, Prkcg, Akap12, and Adamts4, in the current study implies that sFlt-1 overexpression during pregnancy may influence calcium homeostasis and cellular proliferation in cardiac tissue. Additionally, this overexpression appears to impact signalling pathways, encompassing calmodulin-mediated events, prolactin signalling, and interleukin 8 (IL-8) signalling (associated with Prkcg), angiogenesis and vascular dysfunction (linked to Akap12), and cardiac injuries along with inflammasome components in premature membrane ruptures (related to Adamts4) (Coussens et al. 1986; Fields et al. 1988; Lark et al. 1997; Tortorella et al. 1999; Carmona et al. 2001; D. H. Chen et al. 2003; Patel et al. 2003; S. W. Lee et al. 2003; Suri et al. 2007; Wagner et al. 2008; Gelman 2010; Shu et al. 2014; Gökdemir et al. 2016; Qasim & McConnell 2020; Khanam et al. 2022).

The upregulated (cGMP-PKG signalling pathway, Insulin resistance, microRNAs, dilated cardiomyopathy, and hypertrophic cardiomyopathy) pathways indicated structural changes, such as ventricular dilation and impaired systolic function, pathological remodelling and hypertrophy, potentially leading to diastolic dysfunction and increased risk of arrhythmias, cardiac remodelling, stress response, impaired glucose uptake and metabolism, and vascular tone, cell growth, and myocardial relaxation (C. Schannwell et al. 2002; C. M. Schannwell et al. 2003; Roos et al. 2007; Savage et al. 2007; Bernardo et al. 2010; Becker et al. 2011; Inserte & Garcia-Dorado 2015; M. Park et al. 2018; Aryal et al. 2019; Szczerba et al. 2020; Nakamura & Tsujita 2021; Jubaidi et al. 2022; Numata & Takimoto 2022; Cai et al. 2023).

Pregnant AdsFlt-1 mice showed downregulation of genes such as Tgtp1, Tgtp2, BC023105, Angptl4, and Aplnr, related to mitochondrial respiratory chain complex assembly, cytoplasmic translation, oxidative phosphorylation, and ribosome pathways. This included a decrease in Tgtp1 and Tgtp2, which may lead to altered immune responses and inflammation in the heart during pregnancy (Enquobahrie, Abetew, *et al.* 2011; Enquobahrie, Qiu, *et al.* 2011; Berkebile

et al. 2021). Downregulation of *Angptl4* could potentially exacerbate the antiangiogenic consequences observed with sFlt-1 overexpression and lead to a downregulation of lipid metabolism processes (Lei Liu *et al.* 2017; Y. Zhang *et al.* 2020). Additionally, *Aplnr* downregulation may disrupt cardiovascular homeostasis and lead to cellular senescence (Enquobahrie, Qiu, *et al.* 2011; Berkebile *et al.* 2021).

Downregulated pathways (including cardiac muscle contraction, oxidative phosphorylation, Parkinson's disease, thermogenesis, and Huntington's disease) have been implicated in compromised cardiac functionality, diminished blood circulation capacity, decreased ATP synthesis, and impaired cellular energy metabolism ("Mechanism and Contraction Events of Cardiac Muscle Fibers - Medicine LibreTexts" n.d.; A. M. Katz 1967; Douglas S. Kerr 2010; Rosca & Hoppel 2013; Emelyanova *et al.* 2016; Siasos *et al.* 2018; Reicharda & Asosingha 2019; Vasileiou *et al.* 2019; Tabuchi & Sul 2021). Furthermore, these pathways are associated with potential indirect impacts on neurological function, as well as reduced thermogenesis and altered metabolic processes (R. P. Murphy 1979; L. F. Hu *et al.* 2010; Borsche *et al.* 2021; X.-Y. Gao *et al.* 2022). These findings collectively suggest a decline in overall heart function, which may increase the risk of heart failure or other cardiac complications.

In summary, this study demonstrated that sFlt-1 exerts significant adverse effects on pregnancy, particularly regarding cardiac function, even over a short period. Mice injected with sFlt-1 on E10.5 displayed severe consequences by E17.5, as evidenced by impaired heart function. Consequently, the cardiac tissue gene profile of *AdsFlt-1* mice reveals maladaptations and dysfunctions during pregnancy, encompassing cardiac hypertrophy, altered heart valve structure, impaired cellular metabolism, and potential pathological cardiac remodelling and dysfunction.

7.3.3 Gene expression in *AdsFlt-1* postpartum

7.3.3.1 Gene expression in postpartum *AdCMV* vs pregnant *AdCMV*

This DEG analysis revealed that the predominant genes impacted in the cardiac tissue of postpartum AdCMV compared to pregnant AdCMV mice were associated with processes such as coagulation and hemostasis, cellular adhesion and signalling pathways (e.g., ERK1 and ERK2 cascade), membrane-associated and transporter complexes, ECM interactions and binding events, negative regulation of vascular development, responsiveness to hormonal stimuli and growth factors, as well as the constituents and structural organization of the extracellular matrix.

The observed upregulation of specific genes in this study, including *Bmp10*, *Myl7*, *Cybrd1*, *Snhg11*, and *Lrrn4*, suggests that during the postpartum period, several processes are activated: cardiac tissue remodelling and contractility pathways (*Bmp10*), modulation of cardiac muscle contractile properties in response to shifting hemodynamic demands (*Myl7*), alterations in iron homeostasis (*Cybrd1*) or redox equilibrium within the myocardium, which influences oxygen transport and energy production (*Snhg11*), and the reversion to normal morphology and dimensions in instances of physiological hypertrophy (*Lrrn4*) (S. Miyata et al. 2000; A. McKie et al. 2001; A. T. McKie et al. 2002; J. L. Turi et al. 2006; Dorn 2007; Jingyuan Li et al. 2012; Katharina Maria Hillerer et al. 2014; H. Li et al. 2017; R. Li et al. 2017; Rudnicka et al. 2017; Owen et al. 2020; Azbazdar et al. 2021; L. Wang et al. 2021; Ghaemi et al. 2022; J. Sun et al. 2022; Lu Liu et al. 2023). This observation lends further support to the idea that the postpartum period does not induce an instantaneous return of the heart to its pre-pregnancy state; rather, even at 36 weeks postpartum, these physiological alterations continue to transpire.

The upregulated pathways (cytokine-cytokine receptor interaction and ECM-receptor interaction) demonstrate an augmented interplay between cytokines and their corresponding receptors within the cardiac tissue (Pfeffer 2003; Szarka *et al.* 2010; Lockhart *et al.* 2011; S. Z. Chen *et al.* 2016). This enhanced interaction may result in elevated inflammatory or immune responses, as well as facilitate tissue remodelling and repair processes (D A Clark *et al.* 1988; Szarka *et al.* 2010; Raghupathy 2013; Christian & Porter 2014). Consequently, these pathways may play a role in the remodelling and adaptation of cardiac tissue to accommodate the physiological alterations concomitant with the postpartum period.

Conversely, the most downregulated DEGs identified, such as *Ldhc*, *Kap3*, *Nr4a1*, *Fos*, and *Egr2*, were implicated in various cellular processes. These include the conversion of lactate to pyruvate, essential for energy production and maintenance of redox balance (*Ldhc*), influencing cardiac contractility and interference with vital cellular processes (*Kap3*), modulation of diverse cellular events, encompassing inflammation, metabolism, and cell survival (*Nr4a1*), attenuation of stress responses and altered regulation of specific target genes (*Fos*), and eliciting potential anti-inflammatory effects coupled with possible protection against cardiac fibrosis and hypertrophy (*Egr2*) (Takano & Li 1989; Fujioka et al. 1991; Heximer et al. 1996; Senali Abayratna Wansa et al. 2002; Baumann et al. 2003; Holmes & Zachary 2004; Kumbrink et al. 2010; Jaiswar et al. 2011; Hayashi et al. 2015; Vaiman & Miralles 2016; Blakeslee et al. 2017; Taefehshokr et al. 2017; Burwick et al. 2018; Anh et al. 2020; McCowan et al. 2021; H. Tan et al. 2022; Naik & Decock 2022).

Downregulated pathways during the postpartum period (protein digestion and absorption, AGE-RAGE signalling pathway in diabetic complications, fluid shear stress and atherosclerosis, focal adhesion, and thermogenesis) demonstrate a reduction in various molecular processes (Reyat *et al.* 2017). These reductions may lead to diminished protein breakdown and uptake in cardiac tissue, potentially causing alterations in cellular protein turnover and availability (Ishola et al. 2006; Luo et al. 2012; Locatelli et al. 2014; C. Pan et al. 2022). Furthermore, there may be a decreased likelihood of atherosclerotic lesion formation, diminished cell-matrix interactions, and cell signalling events in the heart (James Metcalfe 1963; Rubler *et al.* 1973; Landers *et al.* 2009; Malek *et al.* 2020). Additionally, these downregulated pathways may contribute to an altered metabolic state and energy expenditure within the cardiac tissue during the postpartum period (Herrera & Desoye 2016; Y. Tan *et al.* 2020; Tabuchi & Sul 2021; Batiha *et al.* 2022).

The study supports the notion that the postpartum period involves ongoing physiological alterations in the heart rather than an immediate return to its pre-pregnancy state. These changes contribute to cardiac tissue remodelling and adaptation. Generally, these adaptations

maintain cardiac health during the transition from pregnancy to postpartum. However, some alterations, like the downregulation of KAP3 and factors related to vasculature development, may have potential negative impacts on the heart. In summary, most adaptations observed are necessary for maintaining cardiac health during the postpartum period, but further research is required to understand the implications of potentially detrimental alterations.

7.3.3.2 Gene expression in postpartum AdsFlt-1 vs pregnant AdsFlt-1

In a comparative analysis between postpartum AdsFlt-1 mice and pregnant AsFlt-1 mice, DEG analysis identified that the most affected genes in the cardiac tissue were related to mitochondrial function and energy metabolism, protein synthesis and ribosomes, oxidative stress and antioxidant response, vascular development and tissue morphogenesis, cell adhesion and cellular components, and transcription regulation and binding.

In the current study, the upregulation of specific genes, such as Cxcl13, Gm44608, Gm7609, Gm10419, and Cd209f, demonstrates a connection between sFlt-1 postpartum and heightened immune response, augmented anti-angiogenesis, and activation of inflammatory pathways in these mice (Nhan-Chang *et al.* 2008; Boily-Larouche *et al.* 2012; Muñoz-Fernández *et al.* 2012). These observations could potentially result from prolonged exposure to sFlt-1 or stem from alterations in pathogen recognition or immune cell interactions (Legler *et al.* 1998; Barreiro *et al.* 2006; Vannberg *et al.* 2008; Schuurhof *et al.* 2010).

The upregulated pathways (oxidative phosphorylation, chemical carcinogenesis (reactive oxygen species), diabetic cardiomyopathy, Parkinson's disease, and Huntington's disease), indicate that the postpartum overexpression of sFlt-1 may enhance ATP production for increased energy (Mizukami *et al.* 2004; Spaans *et al.* 2014). However, this could simultaneously elevate ROS levels, leading to oxidative stress and cellular damage (Rosca & Hoppel 2013; Vaka *et al.* 2019; Zhu *et al.* 2022). Consequently, this may contribute to cardiac

dysfunction, augmented inflammation, DNA damage, and cellular injury in cardiac tissue. Furthermore, it may increase the risk of developing cardiac muscle dysfunction, structural abnormalities, and ultimately heart failure in these mice (Neuhaus *et al.* 1999; Montuori *et al.* 2005; Rosca & Hoppel 2013). Additionally, these upregulated pathways may suggest that sFlt-1 impacts cardiac autonomic regulation, affecting heart rate variability and exerting potential effects on cardiac function via altered autonomic regulation or secondary metabolic changes (Roxanne Hastie *et al.* 2019).

In opposition, the most downregulated genes identified, including *Prm2*, *Tnp2*, *Upk3b*, *Apob*, and *Serpina6*, were implicated in various cellular processes and functions. These encompass cellular organization or regulatory mechanisms (*Prm2* and *Upk3b*) (Ingenbleek & Young 1994; Deng *et al.* 2002; Avendaño *et al.* 2009; Cavalcanti *et al.* 2011; Kasak *et al.* 2015; Rogenhofer *et al.* 2017), tissue-specific gene regulation (*Tnp2*) (Morasso *et al.* 1990; Akama *et al.* 1996), cellular differentiation or barrier properties (*Upk3b*) (Receptor *et al.* 1997; Montuori *et al.* 2005), lipid transport and metabolism (*Apob*) (John R Burnett *et al.* 1993; Descamps *et al.* 2003; Y. Wang *et al.* 2010; Wölter *et al.* 2018), as well as corticosteroid homeostasis, potentially influencing stress response and inflammation within the cardiac tissue (*Serpina6*) (Vogeser *et al.* 1999; Nhan-Chang *et al.* 2008; Schäfer *et al.* 2015).

The observed downregulated pathways (Focal adhesion, ECM-receptor interaction, Parathyroid hormone synthesis, secretion, and action, PI3K-Akt signalling pathway, and Proteoglycans in cancer) in postpartum mice overexpressing sFlt-1 imply potential long-term consequences, which may include compromised cell adhesion (S. D. Patel *et al.* 2003; Van Dijk *et al.* 2008; Sweet *et al.* 2018; Malek *et al.* 2020), migration, and signal transduction, subsequently affecting cardiac tissue integrity (Shai *et al.* 2002; Salomon *et al.* 2014; Shabbir *et al.* 2015), remodelling, and overall function (Bisping *et al.* 2006; Jifen Li 2014; Ackermann *et al.* 2017; Meagher *et al.* 2021). Furthermore, these downregulations might disrupt the maintenance of tissue structure, regulation of cellular behaviour, and modulation of signalling pathways. Additionally, alterations in calcium homeostasis (Y. Kim *et al.* 2011; Bu Wang *et al.* 2019; J. Huang *et al.* 2020), blood pressure regulation, and vascular function could be observed. The downregulation of various cellular processes, such as cell survival, growth, and metabolism, may contribute to cardiac hypertrophy (Jifen Li 2014), fibrosis, and impaired function in these mice. Finally, changes in ECM organization, cell adhesion, and signalling

may potentially impact cardiac tissue remodelling and heart function in postpartum mice overexpressing sFlt-1.

In summary, the heart of postpartum mice overexpressing sFlt-1 appears to be significantly affected by the dysregulation of various genes and pathways. The upregulation of specific genes suggests a heightened immune response, anti-angiogenesis, and activation of inflammatory pathways. Additionally, upregulated pathways indicate increased energy production with potential negative consequences, such as oxidative stress and cellular damage, which may contribute to cardiac dysfunction and increased risk of heart failure. On the other hand, downregulated genes and pathways imply potential long-term consequences on cardiac tissue integrity, remodelling, and overall function due to compromised cell adhesion, migration, signal transduction, and alterations in calcium homeostasis, blood pressure regulation, and vascular function. These changes may lead to cardiac hypertrophy, fibrosis, and impaired function in postpartum mice overexpressing sFlt-1. Overall, the observed dysregulation of genes and pathways highlights the complex impact of sFlt-1 overexpression on the heart in postpartum mice, warranting further investigation to better understand the precise consequences and underlying mechanisms.

7.3.3.3 Gene expression in postpartum AdsFlt-1 vs AdCMV

In a comparative analysis between postpartum AdsFlt-1 mice and postpartum AdCMV mice, DEG analysis identified that the most affected genes in the cardiac tissue were related to mitochondrial function and energy metabolism, oxidoreductase activities, hemostasis and coagulation, and ECM and membrane-related processes.

A single significantly upregulated DEG was identified in this study: Cyp26b1, which encodes an enzyme belonging to the cytochrome P450 family. This gene is also involved in the 2Fe-2S iron-sulfur protein adrenodoxin, which may accept electrons from NADPH-dependent adrenodoxin reductase and subsequently reduce cytochrome P450 in the mitochondrial system (Blum et al. 2021). Both adrenodoxin and adrenodoxin reductase are located in the

mitochondrial matrix and exist as soluble substances (Blum *et al.* 2021). Increased expression of Cyp26b1 has been associated with atherosclerotic lesions (Koh *et al.* 1992; White *et al.* 2000; Abu-Abed *et al.* 2002; Trofimova-Griffin & Juchau 2002). Consequently, the long-term effects of sFlt-1 overexpression may be related to the development of atherosclerotic lesions in the heart (Riise *et al.* 2017; Hauge *et al.* 2022). This observation is consistent with previous reports in the literature, which have demonstrated that exposure to significantly elevated levels of sFlt-1 leads to cardiac failure, including atherosclerotic lesions, even after sFlt-1 levels have decreased (Wewers *et al.* 2021; Mauricio *et al.* 2022). This suggests that the damage inflicted upon the heart may be irreversible.

Furthermore, upregulated pathways (Oxidative phosphorylation, Parkinson disease, Diabetic cardiomyopathy, Chemical carcinogenesis - reactive oxygen species, and Thermogenesis) implies a potential enhancement in energy availability for cellular processes. However, this may also result in increased levels of ROS and oxidative stress, potentially leading to cellular damage and contributing to cardiac dysfunction (Navarro-YepesJuliana *et al.* 2014; Alcala *et al.* 2018; Herrock *et al.* 2023). Shared molecular pathways or mechanisms that could influence the heart, such as mitochondrial dysfunction or heightened oxidative stress, are also indicated (Graham J. Burton & Jauniaux 2011; Navarro-YepesJuliana *et al.* 2014; Alcala *et al.* 2018). Moreover, upregulated pathways suggest augmented structural and functional alterations akin to those observed in diabetic cardiomyopathy, encompassing myocardial fibrosis, hypertrophy, and diminished contractile function (Gordon *et al.* 2001; Layland *et al.* 2005; Schmidt & Cammarato 2020). Furthermore, these pathways indicate an elevation in oxidative stress, DNA damage, and cellular injury within cardiac tissue, as well as heightened energy metabolism and heat production.

Conversely, the most down-regulated genes were involved in regulation of muscle thermogenesis and metabolism by reversibly hindering the activity of ATP2A1 and ATP2A2 (Sln), potentially inducing arrhythmias and other cardiac pathologies (M. Pant *et al.* 2016; Bal *et al.* 2021), maintenance zinc homeostasis in the body (Tmem163) (Sanchez *et al.* 2019; Styrpejko & Cuajungco 2021), regulation matrix remodelling-related genes and promoting anti-tumour immunity, which could be favourable for postpartum heart health (Chst4) (Ye *et al.* 2023; "CHST4 carbohydrate sulfotransferase 4 - Gene - NCBI" 2023; "CHST4 - Carbohydrate

sulfotransferase 4 - | UniProtKB | UniProt" n.d.), increased rates of apoptosis in postpartum hearts, which could help reduce the risk of certain cardiovascular diseases (Msln) (Hollevoet *et al.* 2015; Faust *et al.* 2022), modulating epithelial plasticity and TGF- β 1-induced epithelial dedifferentiation, as well as regulating spermatogenesis (Bnc1) (Feuerborn *et al.* 2015; J. Y. Li *et al.* 2020; Liang *et al.* 2022)

The downregulated pathways (ECM-receptor interaction, Dilated cardiomyopathy, Hematopoietic cell lineage, Hypertrophic cardiomyopathy, and Platelet activation) demonstrated that sFlt-1 may influence alterations in molecular mechanisms regulating cardiac remodelling could also result in other consequences on cardiac function (Ferreira *et al.* 2021). Additionally, these pathways could influence blood supply, oxygen delivery, and the heart's ability to meet postpartum demands by impacting the production, differentiation, and function of blood cells (Gerbasi *et al.* 1990; Cullen 2013; Liberto & Nall 2017; Marcin & Berry 2018; Bell *et al.* 2023; Butt *et al.* 2023; Hofer *et al.* 2023). Furthermore, downregulation may signify changes in regulatory mechanisms governing cardiac growth and remodelling, potentially affecting overall cardiac function. Lastly, these pathways could influence the risk of thrombus formation and associated complications while hindering the normal haemostatic response to vascular injury, potentially impacting the heart's capacity for recovery from deterioration.

In conclusion, the comparative analysis between postpartum AdsFlt-1 mice and postpartum AdCMV mice revealed that sFlt-1 overexpression significantly affects genes related to mitochondrial function, energy metabolism, oxireductase activities, hemostasis, coagulation, and ECM and membrane-related processes in cardiac tissue. The upregulation of Cyp26b1, which is correlated with atherosclerotic lesions, implied that sFlt-1 overexpression may cause irreversible damage to the heart. Upregulated pathways indicated potential enhancements in energy availability but also potential negative consequences, such as increased ROS levels, oxidative stress, cellular damage, and cardiac dysfunction. Conversely, downregulated pathways suggested alterations in molecular mechanisms regulating cardiac remodelling, blood supply, oxygen delivery, and the heart's ability to meet postpartum demands. These

changes may affect overall cardiac function and the heart's capacity for recovery from damage.

7.3.3.4 Gene expression in postpartum AdsFlt-1 and pregnant AdCMV

This DEG analysis identified that the most affected genes in the cardiac tissue of postpartum AdsFlt-1 mice compared to pregnant AdCMV mice, are related to metabolic processes, hormone secretion regulation, cell motility and migration, ECM components and structure, transcription and DNA binding, response to external factors, and angiogenesis.

The upregulation of genes observed in this study, including Cd209f, Cdh22, Cdh4, Ano5, and Aldob, indicates that mice exposed to elevated sFlt-1 levels during pregnancy may exhibit enhanced immune responses or altered cell adhesion (Cd209f). Additionally, potential modifications in cell adhesion, communication, and tissue organization within the postpartum heart could influence its structure and function (Cdh22 and Cdh4). Furthermore, changes in ion channel activity might affect the electrical properties of cardiac cells, thereby impacting overall heart function (Ano5). Lastly, upregulation of Aldob suggests increased energy production via fructose metabolism in the postpartum heart; however, this could also result in altered metabolic processes that may affect cardiac function and stress response.

Curiously, no upregulated pathways were associated with postpartum AdsFlt-1 mice when compared to pregnant AdCMV mice.

Nevertheless, the most downregulated genes in this study were found to be associated with alterations in membrane-associated proteins (Upk3b) (Receptor *et al.* 1997; Montuori *et al.* 2005; Rudat *et al.* 2014), which could potentially impact the structure and function of cardiac cells (Nr4a3) (Hayashi *et al.* 2015; Medzikovic *et al.* 2019; Paredes *et al.* 2021). Additionally, these downregulated genes may influence the transcriptional regulation of target genes, resulting in modified cellular responses (Nr4a3) (Hayashi *et al.* 2015; Medzikovic *et al.* 2019; Paredes *et al.* 2021). Furthermore, changes in cortisol transport and availability due to the downregulation of Serpina6 could potentially affect stress response and hormone regulation (Vogeser *et al.* 1999; Gennari-Moser *et al.* 2011; Schäfer *et al.* 2015). The downregulation of Atf3 may have implications for the regulation of stress response, apoptosis, and cell survival, as well as the progression and stability of atherosclerotic plaques (B. P. Chen *et al.* 1996; S.

D. Bailey *et al.* 2010). Furthermore, Atf3 may influence the structural stability of atherosclerotic plaques by modulating the inflammatory response, thus participating in the regulation of atherosclerotic progression (Peng *et al.* 2021). Lastly, alterations in polyamine levels and cellular growth regulation, potentially influencing cardiac cell proliferation, could be a consequence of the downregulation of Oaz3 (Y. Liu *et al.* 2019; Huttlin *et al.* 2021).

The downregulated pathways (Human papillomavirus infection, Focal adhesion, PI3K-Akt signalling pathway, ECM-receptor interaction, and Proteoglycans in cancer) suggest that sFlt-1 may decrease susceptibility to viral infections or modulate the immune response, leading to alterations in cardiac cell interactions and compromised signal transduction. Additionally, sFlt-1 could potentially influence a range of cellular processes, including cell growth, proliferation, survival, and metabolism. Furthermore, sFlt-1 may affect cell adhesion, migration, and communication among cardiac cells, as well as alter cellular behaviour and communication, which could ultimately impact cardiac function.

In postpartum AdsFlt-1 mice compared to pregnant AdCMV mice revealed that the most affected genes are associated with metabolic processes, hormone secretion regulation, cell motility and migration, ECM components and structure, transcription and DNA binding, response to external factors, and angiogenesis. The upregulation and downregulation of specific genes suggest that elevated sFlt-1 levels during pregnancy may lead to alterations in immune response, cell adhesion, communication, tissue organization, ion channel activity, and energy production via fructose metabolism, potentially affecting cardiac function and stress response. Furthermore, the downregulated pathways indicate that sFlt-1 could modulate susceptibility to viral infections, immune responses, signal transduction, cellular processes (such as growth, proliferation, survival, and metabolism), cell adhesion, migration, communication, and cellular behaviour. These changes could ultimately impact the overall structure, function, and adaptability of the postpartum heart. However, further research is needed to elucidate the precise effects of these differentially expressed genes and pathways on cardiac function and health in the context of postpartum mice overexpressing sFlt-1.

7.4 Conclusion

7.4.1 CSE KO and pregnancy

In conclusion, the gene expression profiles in CSE KO mice suggest that CSE plays a critical role in regulating genes involved in major cellular processes. Although no significant cardiac dysfunctions were observed in non-pregnant CSE KO mice compared to WT mice, these genes may contribute to cardiac maladaptation during pregnancy in CSE KO mice. The comparison of heart function between pregnant and non-pregnant CSE KO mice indicated that H₂S deficiency during pregnancy exacerbates oxidative stress and induces adaptive changes in cardiac tissue. These changes include impairments in protein synthesis, energy expenditure, lipid metabolism, cell-matrix interactions, and cellular maintenance. When comparing the gene expression profiles in CSE KO mice to those in CSE WT mice, the observed alterations deviate from the typical adaptations seen in a healthy pregnancy, suggesting potential maladaptation during pregnancy in CSE KO mice. However, it is essential to emphasize that these interpretations are speculative, based on the mRNA findings obtained, and require validation through qPCR to draw definitive conclusions.

7.4.1.1 Short-term impact of sFlt-1 on pregnancy

In conclusion, this study highlights that overexpression of sFlt-1 during pregnancy has considerable negative effects on cardiac function, even within a short timeframe. Mice injected with sFlt-1 at E10.5 exhibited severe consequences by E17.5, manifested through compromised heart function. As a result, the gene profile of cardiac tissue in AdsFlt-1 mice reveals maladaptations and dysfunctions during pregnancy, including cardiac hypertrophy, altered heart valve structure, impaired cellular metabolism, and potential pathological cardiac remodelling and dysfunction.

7.4.1.2 Long-term effect of sFlt-1 on cardiac function and postpartum reversal

In conclusion, the overexpression of sFlt-1 during pregnancy has significant effects on gene expression and various pathways in cardiac tissue both during the postpartum period and potentially in the long term. The dysregulation of genes observed in postpartum mice overexpressing sFlt-1 is associated with heightened immune response, anti-angiogenesis, activation of inflammatory pathways, compromised cell adhesion, migration, signal

transduction, and alterations in calcium homeostasis, blood pressure regulation, and vascular function. These changes may lead to cardiac hypertrophy, fibrosis, impaired function, and potentially irreversible damage to the heart. The upregulation of specific genes and pathways suggests potential enhancements in energy availability but also potential negative consequences, such as increased ROS levels, oxidative stress, cellular damage, and cardiac dysfunction. Conversely, downregulated pathways imply alterations in molecular mechanisms regulating cardiac remodelling, blood supply, oxygen delivery, and the heart's ability to meet postpartum demands, which may affect overall cardiac function and the heart's capacity for recovery from damage. Overall, the complex impact of sFlt-1 overexpression on the heart in postpartum mice warrants further investigation to better understand the precise consequences and underlying mechanisms. A deeper understanding of these differentially expressed genes and pathways will help elucidate the long-term effects of sFlt-1 overexpression on cardiac function and health in the context of postpartum mice.

In summary, both CSE KO and AdsFlt-1 models demonstrate maladaptations during pregnancy, but they present distinct differences in the genes and pathways involved. Further research is needed to fully understand the underlying mechanisms and potential therapeutic strategies for improving cardiac health during pregnancy and the postpartum period.

7.5 Limitations

This study successfully identified significant differences in gene expression profiles between PE models and control groups. Nonetheless, it is crucial to acknowledge that these findings are based on mRNA data, which calls for validation through qPCR to enable definitive conclusions and the potential for candidate genes identification for PE diagnosis and long-term predictions. Additionally, while the AdsFlt-1 model incorporated postpartum profiles, such data was lacking for the CSE KO model, highlighting the need for future studies to include this postpartum aspect.

Prior to time-mating mRNA profiles of mice injected with AdsFlt-1 and AdCMV, respectively, should be assessed for a more comprehensive and robust analysis. This approach would allow for a comparison of the effects of AdsFlt-1 prior to pregnancy versus during pregnancy and would also help determine whether AdCMV has any impact on normal cardiovascular functions in pre-gravid states.

In light of recent literature presenting mixed conclusions regarding cardiovascular disease risk/prevention following lactation postpartum, and articles indicating that cardiac hypertrophy may be exacerbated by lactation, it would be valuable to conduct parallel studies investigating both CSE KO and AdsFlt-1 mice postpartum. This approach would help ascertain whether the observed effects in mice postpartum are indeed exacerbated by the PE model or if they are consequences of the additional pressure exerted by lactation.

Lastly, to obtain a more detailed understanding of the postpartum period, it is advisable to include multiple time points in future investigations. For instance, assessments every two weeks up until six months could provide valuable insights into the dynamic changes occurring during this critical phase. This timeframe aligns with the point at which most literature reports the adaptations to pregnancy have reverted to pre-gravid levels, offering a comprehensive evaluation of PE models and controls.

Chapter 8

General Discussion And Conclusions

8. General Discussion and Conclusions

Pregnancy significantly impacts the cardiovascular, hormonal, and metabolic systems of the human body, serving as a natural stress test that can reveal underlying heart disease. Cardiovascular disease is the leading non-obstetric cause of death during pregnancy and postpartum. Women with a history of PE face an increased risk of future cardiovascular disease and stroke. Understanding cardiac structure and function during pregnancy is crucial for early detection and intervention to prevent complications such as PE, or even long-term CVD risk. This study's primary aim was to examine cardiovascular adaptation in normal pregnancies and PE murine models and assess both the short-term and the long-term impact of PE on cardiovascular functions.

8.1 Summary of findings

8.1.1 sFlt-1 effects on Cardiovascular functions

Angiogenic imbalance is linked to PE development through inhibition of pro-angiogenic VEGF and PlGF, causing endothelial dysfunction (S. E. Maynard, Min, Merchan, Lim, Li, Mondal, Libermann, Morgan, et al. 2003; Ramma & Ahmed 2011b). It has been widely established that placental sFlt-1, an antagonist of VEGF, causes endothelial damage in prenatal diseases (Sugimoto et al. 2003b; Fan et al. 2014; Walentowicz-Sadlecka, Domaracki, Sadlecki, Siodmiak, Grabiec, Walentowicz, Moliz, Odrowaz-Sypniewska, et al. 2019; Yaling Zhai et al. 2020). Indeed, sFlt-1 is a multifaceted molecule that has been implicated in various diseases and biological functions (Scheufler et al. 2003; Gruson et al. 2016b; Yaling Zhai et al. 2020; Verlohren et al. 2022). Notwithstanding, sFlt-1 has been getting considerable attention in the context of PE, sFlt-1 has also been associated with cardiac failure (Ky et al. 2011b; Gruson et al. 2016b), inhibition of cardiac mitochondrial activity (Sánchez-Aranguren *et al.* 2018; Sanchez-Aranguren, Rezai, *et al.* 2020), and an increased risk of gestational diabetes (Walentowicz-Sadlecka, Domaracki, Sadlecki, Siodmiak, Grabiec, Walentowicz, Moliz, Odrowaz-Sypniewska, et al. 2019). Intriguingly, these factors have been identified as either risk factors for PE or consequences following a PE pregnancy.

This convergence of associations emphasises the potential of sFlt-1 as a valuable marker for investigating the complex pathophysiology of PE, thereby contributing to a more comprehensive understanding of this condition. Thus, given the presence of elevated sFlt-1 levels in numerous studies evaluating the potential use of a sFlt-1:PIGF ratio as both a predictive and diagnostic tool for PE risk (V. Pant et al. 2019; Quezada et al. 2020; Ohkuchi et al. 2021; W. Chen et al. 2022), the two initial studies in this thesis sought to examine sFlt-1 levels specifically during pregnancy (chapter 4) and the postpartum period (chapter 5).

8.1.1.1 Short-term effects

In the current study, we first used a well-established murine PE model, the AdsFlt-1 induced PE model. We found that overexpression of sFlt-1 during pregnancy, induced PE-like symptoms in mice (chapter 4), and this was associated with cardiovascular maladaptations to pregnancy.

Studies on PE have extensively demonstrated the presence of cardiovascular abnormalities both during PE (Valdés 2017; Foo *et al.* 2018; Perry *et al.* 2018; Youssef & Crispi 2020) and before its onset (Mousa *et al.* 2012; Kaartokallio *et al.* 2014; Morgan *et al.* 2018). However, the most noteworthy finding of this study (Chapter 4) is that 7-day exposure to sFlt-1 (from E10.5 until cardiovascular assessment during pregnancy at E17.5) led to serious systolic, diastolic, and left ventricular dysfunctions.

Various PE models have been employed to investigate the pathogenesis of PE. sFlt-1 overexpression model is one of the commonly used PE models. Maynard et al. (2003) were the first to use AdsFlt-1 to induce elevated sFlt-1 expression and PE symptoms during pregnancy in rat. (S. E. Maynard, Min, Merchan, Lim, Li, Mondal, Libermann, Morgan, et al. 2003). Vogtmann et al. 2019, created transgenic inducible humansFLT1/reverse tetracycline-controlled transactivator (hsFLT1/rtTA) mice, which can produce high levels of hsFLT1 throughout pregnancy in dams (Vogtmann *et al.* 2019). When the expression of hsFlt-1 was induced at E10.5, an increase in circulating sFlt-1 and MAP was observed (Vogtmann *et al.* 2021).

Nevertheless, despite the contribution of numerous animal models to the understanding of PE's biological disruptions and molecular mechanisms (G. Yang et al. 2008b; Bytautiene et al. 2010; Szalai et al. 2015a; Vogtmann et al. 2021), their physiological relevance and cross-model comparability can be limited. Previous sFlt-1 overexpression PE models often lacked echocardiographic assessments, impeding human comparisons (S. E. Maynard, Min, Merchan, Lim, Li, Mondal, Libermann, Morgan, et al. 2003; Vogtmann et al. 2019).

On the other hand, echocardiographic analysis is an essential tool that should not be overlooked, as echocardiographic markers are vital for early detection, management of PE in women, and can predict cardiac morbidity and mortality by evaluating target organ damage, such as left ventricular mass and relative wall thickness (Meyers *et al.* 2007; Preeclampsia Foundation 2022).

Expanding beyond echocardiographic evaluations (Chapter 4), which have been widely employed in cardiovascular studies, the current study also investigated gene expression profiles associated with sFlt-1 overexpression during pregnancy and PE (Chapter 7). Gene analysis suggested that sFlt-1 overexpression influenced calcium homeostasis, cellular proliferation, and multiple signalling pathways within cardiac tissue (chapter 7). Additionally, it also pointed to a potentially disrupted mitochondrial function, disrupted metabolism, failed immune response, disrupted angiogenesis, cardiovascular homeostasis, potentially leading to dilated cardiomyopathy and hypertrophic cardiomyopathy. These alterations could potentially culminate to detrimental effects on structural modifications, energy metabolism, and impaired cardiac functionality. The results in the gene analysis confirmed the earlier indications of dysfunctions seen in the echocardiographic measurements during a short exposure to elevated levels of sFlt-1. Nevertheless, it is important to note that the mRNA gene analysis has not been validated through qPCR to draw definitive conclusions and can only be interpreted in a speculative manner.

In summary, this investigation revealed that even a brief exposure duration to sFlt-1 substantially affects cardiovascular function. The findings underscore the necessity for additional research to examine the relationship between varying sFlt-1 exposure times and their implications for cardiovascular health. For instance, future studies could explore whether a single day or two of exposure to elevated sFlt-1 levels during pregnancy is sufficient to detect the initial manifestations of cardiovascular dysfunction.

8.1.1.2 Long-term effects

While cardiovascular dysfunctions and maladaptation have widely been recognized in PE (Ducray *et al.* 2011; Sones & Davisson 2016; Jing Huai *et al.* 2018), very scarce literature focuses specifically on the sFlt-1 levels and their effect in the aftermath of PE. Investigating the long-term effects of PE is crucial, as recent research spanning the past 5 to 7 years has unveiled numerous risks associated with the condition (Escouto *et al.* 2018; Hauspurg *et al.* 2019; Mcgrath *et al.* 2020; Beckett *et al.* 2023). These risks range from cardiovascular diseases, such as cardiomyopathy (Behrens *et al.* 2019; Moolla *et al.* 2022; Aranda & McFarland 2023; Mubarik *et al.* 2023), to increased susceptibility to cerebrovascular diseases including Alzheimer's, Parkinson's, and Huntington's disease (L. F. Hu *et al.* 2010; Fujita *et al.* 2014; Kalaria 2016; Wright *et al.* 2016; F. Zhou *et al.* 2021).

An in-depth understanding of the postpartum reverse cardiovascular adaptations in normal versus abnormal pregnancies is essential to prevent persistent sequelae following a pregnancy complicated by PE (Ferreira *et al.* 2021; Vasconcelos *et al.* 2023). By addressing the underlying mechanisms connecting postpartum risks in women with a history of PE to various cardiovascular and cerebrovascular disorders, potential therapeutic targets and strategies to prevent the long-term consequences of PE could be developed (Evans *et al.* 2011a; F. Wu *et al.* 2018; Markovitz *et al.* 2019; Reddy *et al.* 2019; Bokslag *et al.* 2020; Shaaban *et al.* 2021; Beckett *et al.* 2023). Therefore, the second study in this thesis (chapter 5), sought to assess the reversal adaptations from pregnancy to postpartum in sFlt-1 overexpressing mice, while also scrutinizing the gene expression postpartum.

In the present study (chapter 5), through monitoring cardiac function during pregnancy and postpartum via echocardiography, we found that sFlt-1 overexpression led to long-term impacts on cardiac function, manifesting as systolic, diastolic and structural anomalies, potentially causing irreversible damage to the cardiovascular system. This demonstrated that exposure to sFlt-1 during pregnancy not only contributes to the development of PE symptoms during pregnancy in the short-term but also potentially causes irreversible damage to the cardiovascular system, as well as persistent deterioration of cardiac function. The irreversible and persistent degeneration observed in PE extends beyond cardiac function, impacting other organs as well (Hooijschuur *et al.* 2019; Yijun Yang *et al.* 2021; Fulghum *et al.* 2022). For

instance, studies have reported long-term alterations in cerebral white and grey matter following PE (Siepmann *et al.* 2017), as well as enduring hippocampal vascular dysfunction and memory impairment (Brussé *et al.* 2008; Johnson & Cipolla 2017; Johnson *et al.* 2021, 2022).

Postpartum structural and hemodynamic alterations, such as physiological hypertrophy, are observed in normal pregnancies; however, in PE cases, structural complications and myocardial damage have been shown to persist up to 10 years post-delivery (Karen Melchiorre, Sutherland, Liberati, *et al.* 2011; Castleman *et al.* 2016; DeMartelly *et al.* 2021).

In line with structural abnormal adaptations observed in the postpartum period, gene expression analysis of the cardiac tissues of AdsFlt-1 mice when compared to AdCMV mice (chapter 7), pointed to sFlt-1 overexpression impacting genes in cardiac tissue related to mitochondrial function, haemostasis, coagulation, ECM and membrane-related processes. Moreover, the gene analysis implicated increased risks for the development of Parkinson disease, atherosclerotic lesions, diabetic cardiomyopathy as well as disruptions in proper cardiac remodelling. Reiterating, it is important to note that the mRNA gene analysis has not been validated through qPCR to draw definitive conclusions and can only be interpreted in a speculative manner.

Overall, this study confirmed the long-term irreversible effects associated with a brief exposure to elevated sFlt-1 levels. However, a major limitation of this study was the absence of cardiovascular assessment during the lactation period, which has been associated with cardiac hypertrophy and altered cardiac reverse remodelling (Katharina M. Hillerer *et al.* 2014; Countouris *et al.* 2016; Hyatt *et al.* 2017). Hence, further research incorporating measurements of cardiovascular function in this sFlt-1 model in lactating mice and non-lactating mice, as well as lactating in different intervals should be conducted to understand more clearly the effects of lactation postpartum on the cardiovascular system.

8.1.2 The role of CSE on cardiovascular adaptations to pregnancy

H₂S plays a key role in cardiovascular function, immune hemostasis regulation, promoting vasodilation and its decrease has been linked to cardiovascular disease (Wen et al. 2018; Zhen Li et al. 2018; Banqin Wang et al. 2020; Hsu & Tain 2021). In fact, a decrease in the H₂S producing CSE enzyme, has been shown in both the placenta of women with PE (K. Wang *et al.* 2013) and the villous cytotrophoblast of women developing recurrent spontaneous abortion (Banqin Wang et al. 2020). Thus, CSE/H₂S has been identified as a potential protective pathway mechanism (A. Ahmed & Ramma 2015b). While it has been shown that decreased CSE is linked to PE and that CSE plays a role in the mitochondrial function, associated with PE, the specific reasons behind this have not yet fully been elucidated (Untereiner, Fu, et al. 2016; Toliver-Kinsky et al. 2019; Banqin Wang et al. 2020). Thus, to attempt to gain a better understanding in of the underlying mechanisms of CSE specifically during pregnancy, this study (chapter 6) sought to assess the mitochondrial functions and adaptations observed in normotensive pregnancies with those seen in CSE KO models.

Echocardiography assessment delineated various maladaptations of cardiac function and structure between CSE KO and CSE WT mice during pregnancy (chapter 6). Another significant aspect is that several of the disparities between CSE KO and CSE WT mice were observed in the pre-pregnancy state, suggesting that cardiovascular dysfunctions more likely occur prior to pregnancy but could be exacerbated and revealed more distinctively during pregnancy (chapter 6).

H₂S is associated with cardiac mitochondria through its various functions such as the maintenance of cardiac function, ROS production and regulation, calcium homeostasis, fatty acid metabolism and apoptosis regulation (Stark & Roden 2007; Di Lisa & Scorrano 2012; Reicharda & Asosingha 2019; Vasileiou *et al.* 2019). Furthermore, a downregulation of H₂S has been linked to mitochondrial dysfunction (Gerő *et al.* 2016; Karwi *et al.* 2017; Sanchez-Aranguren, Ahmad, *et al.* 2020; Sanchez-Aranguren, Rezai, *et al.* 2020). Therefore, cardiac mtDNA levels were measured in the cardiac tissue of CSE KO and CSE WT mice during pre-gravid and pregnancy states. This study revealed an decrease in relative mtDNA levels in pregnant CSE KO mice when compared to both pregnant and non-pregnant levels of CSE WT mice, suggesting that CSE/H₂S pathway is important in regulating mitochondrial biogenesis

during pregnancy, and dysregulation of this pathway may impair mitochondrial function and subsequently results in cardiovascular dysfunction in PE.

Strikingly, when looking at the gene profiles in the cardiac tissues of pre-pregnant states, CSE KO seemed to influence the dysregulation of major cellular processes. However, in the pregnant state gene expression profiles in the cardiac tissues of CSE KO mice when compared to CSE WT mice showed a notable difference on heart's structure, development, signalling, immune response, energy metabolism, protein synthesis, cellular trafficking, and stress responses. Furthermore, CSE KO seemed to suggest a disrupted protein synthesis, energy production, and stress response mechanisms, ultimately pointing to dysfunctions in the mitochondria. Yet again, it is important to note that the mRNA gene analysis has not been validated through qPCR to draw definitive conclusions and can only be interpreted in a speculative manner.

In summary, in conjunction with the echocardiographic assessments, the mtDNA levels observed and the gene expression analysis, CSE KO seemed to cause cardiac and mitochondrial dysfunctions in the pre-gravid state already and to further exacerbate and ultimately fail the stress test imposed by cardiovascular needs during pregnancy.

8.2 Conclusions and Future Work

In conclusion, the work presented in this thesis examined two distinct models of PE and identified cardiac systolic, diastolic and structural dysfunctions associated with this pregnancy disease. The AdsFlt-1 model demonstrated persistent effects on cardiovascular function and potential neurological implications after a brief exposure to elevated levels of sFlt-1, while the CSE KO model underlined the importance of H₂S even prior to pregnancy. These models albeit completely different may further help navigating the understanding of the complex pathophysiology underlying PE. Nevertheless, it is crucial to emphasize that both models only investigate specific hypotheses related to the complexity of PE and do not fully encapsulate the still elusive aetiology behind PE. This study highlighted the multifaceted and complex nature of PE, encompassing cardiovascular and genetic factors.

8.3 Limitations

The major limitation of the work described in this thesis, is the lack of mRNA data validation using qPCR and the lack of immunohistochemistry of the cardiac tissue. To obtain a more comprehensive understanding of these models, validation of mRNA data should be conducted as this would allow for a more definitive conclusion rather than a speculation. Moreover, although this work focused on the cardiovascular aspects of PE, it is important to note that gene expression analysis pointed to several neurological dysfunctions that warrant further investigations, in both of these models. Alongside the validation of these genes, further analysis and identification of these genes could present both a diagnostic genetic profile as well as a potential therapeutic target for PE.

Immunohistochemical analysis should be performed on cardiac tissues specifically to pinpoint whether the structural and vascular changes observed in the echocardiographic assessments can be recapitulated visually. Additionally, following on from the observations of the mRNA analysis immunohistochemical analysis should also be performed and paired with electrophysiology to look at the neurological function.

Albeit that mtDNA levels were investigated in CSE KO, research has shown that its increase or decrease is not always a marker for efficient mitochondria function. Thus, using high-resolution respirometry or fluorescence-based assays to measure parameters such as mitochondrial calcium, superoxide, mitochondrial permeability transition, and membrane potential would aid in the determination of the mtDNA function. MtDNA levels were only explored in the CSE KO model, nevertheless, according to the evidence supporting mitochondrial involvement seen on both the CSE KO model and the gene expression analysis, this emphasizes the need for the assessment of mitochondrial functions in the sFlt-1 model as well.

Future research is necessary to explore the relationship between varying sFlt-1 exposure durations and their consequences for cardiovascular health. For instance, studies could explore whether short-term exposure (of 12 hours or 2 days) to elevated sFlt-1 levels during pregnancy is enough to detect early signs of cardiovascular dysfunction. In parallel, different timepoints for exposure should also be investigated. For example, studies could also explore

whether more severe effects in the cardiovascular function are seen when elevated sFlt-1 exposure starts at E16.5 versus E.10.5. Moreover, further research should examine the influence of lactation on cardiovascular function in individuals with a history of PE.

Finally, the postpartum effects of the CSE KO model warrant investigation. It would be valuable to determine whether the cardiovascular maladaptations observed during pregnancy revert to the pre-gravid state, persist permanently, or result in a distinct phenotype. This could suggest that pregnancy not only causes irreversible damage but also significantly alters the cardiovascular phenotype.

9. References

- A. K. Pandey, A. Das, C. Srinivas, M. S. Babu, Y. Himabindu, A. Kumar & G. Bhawani, 2010. Maternal Myocardial Performance in Various Stages of Pregnancy and Post-Partum. *Research Journal of Cardiology*, **3**, 9–16.
- Aardenburg, R., Spaanderman, M.E., Courtar, D.A., Eijndhoven, H.W. Van, Leeuw, P.W. De & Peeters, L.L., 2005. A Subnormal Plasma Volume in Formerly Preeclamptic Women Is Associated With a Low Venous Capacitance. *Journal of the Society of Gynecological Investigations*, **12**, 107–111.
- Abe, K. & Kimura, H., 1996. The Possible Role of Hydrogen Sulfide as an Endogenous Neuromodulator. *The Journal of Neuroscience*, **76**, 1066.
- Abe, K. & Kimura, H., 1996. The Possible Role of Hydrogen Sulfide as an Endogenous Neuromodulator. *The Journal of Neuroscience*, Vol. 76.
- Abu-Abed, S., MacLean, G., Fraulob, V., Chambon, P., Petkovich, M. & Dollé, P., 2002. Differential expression of the retinoic acid-metabolizing enzymes CYP26A1 and CYP26B1 during murine organogenesis. *Mech Dev*, **110**, 173–177, Elsevier Ireland Ltd. doi:10.1016/S0925-4773(01)00572-X
- Ackermann, M.A., Petrosino, J.M., Manring, H.R., Wright, P., Shettigar, V., Kilic, A., Janssen, P.M.L., *et al.*, 2017. TGF- β 1 affects cell-cell adhesion in the heart in an NCAM1-dependent mechanism. *J Mol Cell Cardiol*, **112**, 49, NIH Public Access. doi:10.1016/J.YJMCC.2017.08.015
- ACOG, 2020. American College of Obstetricians and Gynecologists. *Gestational Hypertension and Preeclampsia*. Retrieved June 22, 2023, from https://scholar.google.com/scholar_lookup?journal=Obstet+Gynecol&title=Clinical+management+guidelines+for+obstetrician-gynecologists.+Gestational+hypertension+and+preeclampsia&volume=133&publication_year=2019&pages=e1-e25&

- Acosta-Sison, H., 1956. The relationship of hydatidiform mole to pre-eclampsia and eclampsia: A study of 85 cases. *Am J Obstet Gynecol*, **71**, 1279–1282, Mosby. doi:10.1016/0002-9378(56)90437-9
- Adeyeye, V.O., Balogun, M.O., Adebayo, R.A., Makinde, O.N., Akinwusi, P.O., Ajayi, E.A., Ogunyemi, S.A., *et al.*, 2016. Echocardiographic assessment of cardiac changes during normal pregnancy among Nigerians. *Clin Med Insights Cardiol*, **10**, 157–162, Libertas Academica Ltd. doi:10.4137/CMC.S40191
- Adhikari, S. & Bhatia, M., 2008. H₂S-induced pancreatic acinar cell apoptosis is mediated via JNK and p38 MAP kinase. *J Cell Mol Med*, **12**, 1374–1383, J Cell Mol Med. doi:10.1111/J.1582-4934.2008.00318.X
- Agarwal, A., Tvrda, E. & Mulgund, A., 2015. Oxidative Stress in Preeclampsia. in *The Handbook of Fertility: Nutrition, Diet, Lifestyle and Reproductive Health*, pp. 283–290, ed. Watson, R.R.W. doi:10.1016/B978-0-12-800872-0.00026-3
- Ahmad, A., Olah, G., Szczesny, B., Wood, M.E., Whiteman, M. & Szabo, C., 2016. AP39, A Mitochondrially Targeted Hydrogen Sulfide Donor, Exerts Protective Effects in Renal Epithelial Cells Subjected to Oxidative Stress in Vitro and in Acute Renal Injury in Vivo. *Shock*, **45**, 88–97, Shock. doi:10.1097/SHK.0000000000000478
- Ahmad, S. & Ahmed, A., 2004. Elevated Placental Soluble Vascular Endothelial Growth Factor Receptor-1 Inhibits Angiogenesis in Preeclampsia. *Circ Res*, **95**, 884–891, Lippincott Williams & Wilkins. doi:10.1161/01.RES.0000147365.86159.f5
- Ahmad, S., Hewett, P.W., Al-Ani, B., Sissaoui, S., Fujisawa, T., Cudmore, M.J. & Ahmed, A., 2011. Autocrine activity of soluble Flt-1 controls endothelial cell function and angiogenesis. *Vasc Cell*, **3**, 1–8. doi:10.1186/2045-824X-3-15
- Ahmad, S., Wang, K., Egginton, S., Hewett, P.W. & Ahmed, A., 2015. Hydrogen sulphide rescues preeclampsia-like phenotype aggravated by high sFlt-1 in placenta growth factor (PlGF) deficiency. *Nitric Oxide*, **47**, S27–S28. doi:10.1016/j.niox.2015.02.066
- Ahmed, A., 1997. Heparin-binding angiogenic growth factors in pregnancy. *Placenta*, **18**, 215–258, Elsevier BV. doi:10.1016/s0143-4004(97)80091-4

- Ahmed, A., Rahman, M., Zhang, X., Acevedo, C.H., Nijjar, S., Rushton, I., Bussolati, B., *et al.*, 2000. Induction of Placental Heme Oxygenase-1 Is Protective Against TNF-induced Cytotoxicity and Promotes Vessel Relaxation. *Molecular Medicine*, **6**, 391–409.
- Ahmed, A. & Ramma, W., 2015. Unravelling the theories of pre-eclampsia: Are the protective pathways the new paradigm? *Br J Pharmacol*, John Wiley and Sons Inc. doi:10.1111/bph.12977
- Ahmed, A. & Ramma, W., 2015. Unravelling the theories of pre-eclampsia: Are the protective pathways the new paradigm? *Br J Pharmacol*, John Wiley and Sons Inc. doi:10.1111/bph.12977
- Ahmed, R., Dunford, J., Mehran, R., Robson, S. & Kunadian, V., 2014, May 13. Pre-eclampsia and future cardiovascular risk among women: A review. *J Am Coll Cardiol*, Elsevier USA. doi:10.1016/j.jacc.2014.02.529
- Akahoshi, N., Handa, H., Takemoto, R., Kamata, S., Yoshida, M., Onaka, T. & Ishii, I., 2019. Preeclampsia-Like Features and Partial Lactation Failure in Mice Lacking Cystathionine γ -Lyase-An Animal Model of Cystathioninuria. *Int J Mol Sci*. doi:10.3390/ijms20143507
- Akama, K., Sato, H., Furihata-Yamauchi, M., Komatsu, Y., Tobita, T. & Nakano, M., 1996. Interaction of nucleosome core DNA with transition proteins 1 and 3 from boar late spermatid nuclei. *J Biochem*, **119**, 448–455, Oxford University Press. doi:10.1093/oxfordjournals.jbchem.a021262
- Akçay, M. & Özdemir, A.Z., 2021. Effect of supraphysiological estrogen levels on arterial stiffness and hemodynamic parameters. *Anatol J Cardiol*, **25**, 346–351, Turkish Society of Cardiology. doi:10.14744/AnatolJCardiol.2020.38890
- Alcala, M., Gutierrez-Vega, S., Castro, E., Guzman-Gutiérrez, E., Ramos-Álvarez, M.P. & Viana, M., 2018. Antioxidants and oxidative stress: Focus in obese pregnancies. *Front Physiol*, **9**, 1–10. doi:10.3389/fphys.2018.01569
- Alexander, B.T., Cockrell, K.L., Massey, M.B., Bennett, W.A. & Granger, J.P., 2002. Tumor Necrosis Factor-Induced Hypertension in Pregnant Rats Results in Decreased Renal

- Neuronal Nitric Oxide Synthase Expression. *Am J Hypertens*, **15**, 170–175. Retrieved from <https://academic.oup.com/ajh/article-abstract/15/2/170/95151>
- Alhakak, A.S., Brainin, P., Møgelvang, R., Jensen, G.B., Jensen, J.S. & Biering-Sørensen, T., 2020. The cardiac isovolumetric contraction time is an independent predictor of incident atrial fibrillation and adverse outcomes following first atrial fibrillation event in the general population. *Eur Heart J Cardiovasc Imaging*, **21**, 49–57, Oxford University Press. doi:10.1093/ehjci/jez059
- Allison, S.J., 2013, July. Diabetes: Pre-eclampsia: Association with increased risk of diabetes. *Nat Rev Nephrol*. doi:10.1038/nrneph.2013.96
- Amaral, L.M., Cunningham, M.W., Jr, Cornelius, D.C. & LaMarca, B., 2015. Preeclampsia: long-term consequences for vascular health. *Vasc Health Risk Manag*, **11**, 403, Dove Press. doi:10.2147/VHRM.S64798
- Ambia, A.M., Morgan, J.L., Wells, C.E., Roberts, S.W., Sanghavi, M., Nelson, D.B. & Cunningham, F.G., 2018. Perinatal outcomes associated with abnormal cardiac remodeling in women with treated chronic hypertension. *Am J Obstet Gynecol*, **218**, 519.e1-519.e7, Mosby. doi:10.1016/J.AJOG.2018.02.015
- Amraoui, F., Lahsinoui, H.H., Vogt, L., Post, J. Van Der, Peters, S., Afink, G., Ris-Stalpers, C., *et al.*, 2014. sFlt-1 Elevates Blood Pressure by Augmenting Endothelin-1-Mediated Vasoconstriction in Mice. *PLoS One*, **9**, 1–7. doi:10.1371/journal.pone.0091897
- Andersen, M.D., Alstrup, A.K.O., Duvald, C.S., Mikkelsen, E.F.R., Vendelbo, M.H., Ovesen, P.G., Pedersen, M., *et al.*, 2018. Animal Models of Fetal Medicine and Obstetrics. *Experimental Animal Models of Human Diseases - An Effective Therapeutic Strategy*, IntechOpen. doi:10.5772/INTECHOPEN.74038
- Andres, A.M., Stotland, A., Queliconi, B.B. & Gottlieb, R.A., 2015. A time to reap, a time to sow: Mitophagy and biogenesis in cardiac pathophysiology. *J Mol Cell Cardiol*, **78**, 62–72, Elsevier. doi:10.1016/J.YJMCC.2014.10.003
- Andrikos, A., Andrikos, D., Schmidt, B., Birdir, C., Kimmig, R., Gellhaus, A. & Köninger, A., 2022. Course of the sFlt-1/PIGF ratio in fetal growth restriction and correlation with

- biometric measurements, feto-maternal Doppler parameters and time to delivery. *Arch Gynecol Obstet*, **305**, 597–605, Springer Science and Business Media Deutschland GmbH. doi:10.1007/s00404-021-06186-5
- Anh, T.N. Van, Hao, T.K. & Hoang, H.H., 2020. The Role of Plasma Lactate Dehydrogenase Testing in the Prediction of Severe Conditions in Newborn Infants: A Prospective Study. *Res Rep Neonatol*, **10**, 31–35, Dove Press. doi:10.2147/RRN.S254500
- Apicella, C., Ruano, C.S.M., Méhats, C., Miralles, F. & Vaiman, D., 2019. The Role of Epigenetics in Placental Development and the Etiology of Preeclampsia. *Int J Mol Sci*, **20**, 2837. doi:10.3390/ijms20112837
- Aranda, R. & McFarland, J., 2023. Peripartum Cardiomyopathy. *American Heart Association*. Retrieved June 15, 2023, from <https://www.heart.org/en/health-topics/cardiomyopathy/what-is-cardiomyopathy-in-adults/peripartum-cardiomyopathy-ppcm>
- Arngrímsson, R., Sigurðardóttir, S., Frigge, M.L., Bjarnadóttir, R.I., Jónsson, T., Stefánsson, H., Baldursdóttir, Á., *et al.*, 1999. A genome-wide scan reveals a maternal susceptibility locus for pre-eclampsia on chromosome 2p13. *Hum Mol Genet*, **8**, 1799–1805, Hum Mol Genet. doi:10.1093/HMG/8.9.1799
- Aryal, B., Price, N.L., Suarez, Y. & Fernández-Hernando, C., 2019, August 1. ANGPTL4 in Metabolic and Cardiovascular Disease. *Trends Mol Med*, Elsevier Ltd. doi:10.1016/j.molmed.2019.05.010
- Aryan, L., Medzikovic, L., Umar, S. & Eghbali, M., 2020. Pregnancy-associated cardiac dysfunction and the regulatory role of microRNAs. *Biology of Sex Differences 2020 11:1*, **11**, 1–17, BioMed Central. doi:10.1186/S13293-020-00292-W
- Atakul, T., 2019. Serum levels of angiogenic factors distinguish between women with preeclampsia and normotensive pregnant women but not severity of preeclampsia in an obstetric center in Turkey. *Medical Science Monitor*, **25**, 6924–6931. doi:10.12659/MSM.915092

- Atkinson, K.R., Blumenstein, M., Black, M.A., Wu, S.H., Kasabov, N., Taylor, R.S., Cooper, G.J.S., *et al.*, 2009. An altered pattern of circulating apolipoprotein E3 isoforms is implicated in preeclampsia. *J Lipid Res*, **50**, 71–80, *J Lipid Res*. doi:10.1194/JLR.M800296-JLR200
- Atuk, F.A., Binti, J. & Basuni, M., 2018. Molar pregnancy with normal viable fetus presenting with severe pre-eclampsia: a case report. *J Med Case Rep*, **12**. doi:10.1186/s13256-018-1689-9
- Avendaño, C., Franchi, A., Jones, E. & Oehninger, S., 2009. Pregnancy-specific {beta}-1-glycoprotein 1 and human leukocyte antigen-E mRNA in human sperm: differential expression in fertile and infertile men and evidence of a possible functional role during early development. *Hum Reprod*, **24**, 270–277, *Hum Reprod*. doi:10.1093/HUMREP/DEN381
- Avni, B., Frenkel, G., Shahar, L., Golik, A., Sherman, D. & Dishy, V., 2010. Aortic stiffness in normal and hypertensive pregnancy. *Blood Press*, **19**, 11–15, *Blood Press*. doi:10.3109/08037050903464535
- Ayansina, D., Black, C., Hall, S.J., Marks, A., Millar, C., Prescott, G.J., Wilde, K., *et al.*, 2016. Long term effects of gestational hypertension and pre-eclampsia on kidney function: Record linkage study. *Pregnancy Hypertens*, **6**, 344–349, Elsevier B.V. doi:10.1016/j.preghy.2016.08.231
- Azbazdar, Y., Karabicici, M., Erdal, E. & Ozhan, G., 2021. Regulation of Wnt Signaling Pathways at the Plasma Membrane and Their Misregulation in Cancer. *Front Cell Dev Biol*, **9**, 1–14, Frontiers Media S.A. doi:10.3389/FCELL.2021.631623/BIBTEX
- Bachmayer, N., Rafik Hamad, R., Liszka, L., Bremme, K. & Sverremark-Ekström, E., 2006. Aberrant Uterine Natural Killer (NK)-Cell Expression and Altered Placental and Serum Levels of the NK-Cell Promoting Cytokine Interleukin-12 in Pre-Eclampsia. *American Journal of Reproductive Immunology*, **56**, 292–301, John Wiley & Sons, Ltd. doi:10.1111/j.1600-0897.2006.00429.x

- Bailey, J., Shaw, A., Fischer, R., Ryan, B.J., Kessler, B.M., Mccullagh, J., Wade-Martins, R., *et al.*, 2017. A novel role for endothelial tetrahydrobiopterin in mitochondrial redox balance. *Free Radic Biol Med*, **104**, 214–225. doi:10.1016/j.freeradbiomed.2017.01.012
- Bailey, S.D., Xie, C., Do, R., Montpetit, A., Diaz, R., Mohan, V., Keavney, B., *et al.*, 2010. Variation at the NFATC2 locus increases the risk of thiazolidinedione-induced edema in the Diabetes REduction Assessment with ramipril and rosiglitazone Medication (DREAM) study. *Diabetes Care*, **33**, 2250–2253, Diabetes Care. doi:10.2337/DC10-0452
- Bal, N.C., Gupta, S.C., Pant, M., Sopariwala, D.H., Gonzalez-Escobedo, G., Turner, J., Gunn, J.S., *et al.*, 2021. Is Upregulation of Sarcolipin Beneficial or Detrimental to Muscle Function? *Front Physiol*, **12**, 1–9, Frontiers Media S.A. doi:10.3389/FPHYS.2021.633058/FULL
- Balan, S., Ohnishi, T., Watanabe, A., Ohba, H., Iwayama, Y., Toyoshima, M., Hara, T., *et al.*, 2020. Role of an atypical cadherin gene, Cdh23 in prepulse inhibition and its implication in schizophrenia. *bioRxiv*, **47**, 1190–1200, Cold Spring Harbor Laboratory. doi:10.1101/2020.10.29.360180
- Bamfo, J.E.A.K., Kametas, N.A., Nicolaidis, K.H. & Chambers, J.B., 2007. Maternal left ventricular diastolic and systolic long-axis function during normal pregnancy. *European Journal of Echocardiography*, **8**, 360–368. doi:10.1016/j.euje.2006.12.004
- Bányász, I., Bokodi, G., Vannay, Á., Szébeni, B., Treszl, A., Vásárhelyi, B., Tulassay, T., *et al.*, 2006. Genetic polymorphisms of vascular endothelial growth factor and angiopoietin 2 in retinopathy of prematurity. *Curr Eye Res*, **31**, 685–690, Curr Eye Res. doi:10.1080/02713680600801123
- Baple, E.L., Chambers, H., Cross, H.E., Fawcett, H., Nakazawa, Y., Chioza, B.A., Harlalka, G. V., *et al.*, 2014. Hypomorphic PCNA mutation underlies a human DNA repair disorder. *J Clin Invest*, **124**, 3137–3146, J Clin Invest. doi:10.1172/JCI74593
- Barneo-Caragol, C., Martínez-Morillo, E., Rodríguez-González, S., Lequerica-Fernández, P., Vega-Naredo, I. & Álvarez, F. V., 2019. Increased serum strontium levels and altered oxidative stress status in early-onset preeclampsia. *Free Radic Biol Med*, **138**, 1–9, Elsevier B.V. doi:10.1016/j.freeradbiomed.2019.05.001

- Barreiro, L.B., Neyrolles, O., Babb, C.L., Tailleux, L., Quach, H., McElreavey, K., Helden, P.D. Van, *et al.*, 2006. Promoter variation in the DC-SIGN-encoding gene CD209 is associated with tuberculosis. *PLoS Med*, **3**, 0230–0235, *PLoS Med*. doi:10.1371/JOURNAL.PMED.0030020
- Baskar, R., Li, L. & Moore, P.K., 2007. Hydrogen sulfide-induces DNA damage and changes in apoptotic gene expression in human lung fibroblast cells. *FASEB J*, **21**, 247–255, *FASEB J*. doi:10.1096/FJ.06-6255COM
- Batiha, G.E.S., Al-kuraishy, H.M., Al-Maiahy, T.J., Al-Buhadily, A.K., Saad, H.M., Al-Gareeb, A.I. & Simal-Gandara, J., 2022. Plasminogen activator inhibitor 1 and gestational diabetes: the causal relationship. *Diabetol Metab Syndr*, **14**, 1–6, BioMed Central Ltd. doi:10.1186/S13098-022-00900-2/FIGURES/3
- Bauer, S.T. & Cleary, K.L., 2009. Cardiopulmonary complications of pre-eclampsia. *Semin Perinatol*, **33**, 158–165, *Semin Perinatol*. doi:10.1053/J.SEMPERI.2009.02.008
- Baumann, S., Hess, J., Eichhorst, S.T., Krueger, A., Angel, P., Krammer, P.H. & Kirchhoff, S., 2003. An unexpected role for FosB in activation-induced cell death of T cells. *Oncogene*, **22**, 1333–1339, *Oncogene*. doi:10.1038/SJ.ONC.1206126
- Becker, J.R., Deo, R.C., Werdich, A.A., Panàková, D., Coy, S. & MacRae, C.A., 2011. Human cardiomyopathy mutations induce myocyte hyperplasia and activate hypertrophic pathways during cardiogenesis in zebrafish. *DMM Disease Models and Mechanisms*, **4**, 400–410. doi:10.1242/dmm.006148
- Beckett, A.G., McFadden, M.D. & Warrington, J.P., 2023. Preeclampsia history and postpartum risk of cerebrovascular disease and cognitive impairment: Potential mechanisms. *Front Physiol*, *Frontiers Media S.A.* doi:10.3389/fphys.2023.1141002
- Behrens, I., Basit, S., Lykke, J.A., Ranthe, M.F., Wohlfahrt, J., Bundgaard, H., Melbye, M., *et al.*, 2019. Hypertensive disorders of pregnancy and peripartum cardiomyopathy: A nationwide cohort study. *PLoS One*, **14**, 1–12, *PLoS One*. doi:10.1371/JOURNAL.PONE.0211857

- Bell, S.F., Lucy De Lloyd, |, Preston, N. & Collins, P.W., 2023. Managing the coagulopathy of postpartum hemorrhage: an evolving role for viscoelastic hemostatic assays. *J Thromb Haemostat*, **5**, 1–14. doi:10.1016/j.jtha.2023.03.029
- Bellamy, L., Casas, J.-P., Hingorani, A.D. & Williams, D.J., 2007. Pre-eclampsia and risk of cardiovascular disease and cancer in later life: systematic review and meta-analysis. *BMJ*. doi:10.1136/bmj.39335.385301.BE
- Bello, N., Rendon, I.S.H. & Arany, Z., 2013. The Relationship Between Pre-Eclampsia and Peripartum Cardiomyopathy: A Systematic Review and Meta-Analysis. *J Am Coll Cardiol*, **62**, 1715–1723, American College of Cardiology Foundation Washington, D.C. doi:10.1016/J.JACC.2013.08.717
- Bergmann, A., Ahmad, S., Cudmore, M., Gruber, A.D., Wittschen, P., Lindenmaier, W., Christofori, G., *et al.*, 2010. Reduction of circulating soluble Flt-1 alleviates preeclampsia-like symptoms in a mouse model. *J Cell Mol Med*, **14**, 1857–1867. doi:10.1111/j.1582-4934.2009.00820.x
- Berkebile, Z.W., Putri, D.S., Abrahante, J.E., Seelig, D.M., Schleiss, M.R. & Bierle, C.J., 2021. The Placental Response to Guinea Pig Cytomegalovirus Depends Upon the Timing of Maternal Infection. *Front Immunol*, **12**, 1–21, Front Immunol. doi:10.3389/FIMMU.2021.686415
- Bernardo, B.C., Weeks, K.L., Pretorius, L. & McMullen, J.R., 2010. Molecular distinction between physiological and pathological cardiac hypertrophy: Experimental findings and therapeutic strategies. *Pharmacol Ther*, **128**, 191–227. doi:10.1016/j.pharmthera.2010.04.005
- Billieux, M.-H., Petignat, P., Fior, A., Mhawech, P., Blouin, J.-L., Dahoun, S. & Vassilakos, P., 2004. Pre-eclampsia and peripartum cardiomyopathy in molar pregnancy: clinical implication for maternally imprinted genes. *Ultrasound in Obstetrics and Gynecology*, **23**, 398–401, John Wiley & Sons, Ltd. doi:10.1002/uog.1015
- Bilodeau, J.F., 2014. Review: Maternal and placental antioxidant response to preeclampsia – Impact on vasoactive eicosanoids. *Placenta*, **35**, S32–S38, W.B. Saunders. doi:10.1016/J.PLACENTA.2013.11.013

- Bisping, E., Ikeda, S., Kong, S.W., Tarnavski, O., Bodyak, N., McMullen, J.R., Rajagopal, S., *et al.*, 2006. Gata4 is required for maintenance of postnatal cardiac function and protection from pressure overload-induced heart failure. *Proc Natl Acad Sci U S A*, **103**, 14471–14476, National Academy of Sciences. doi:10.1073/PNAS.0602543103/SUPPL_FILE/02543TABLE5.PDF
- Blackstone, E. & Roth, M.B., 2007. Suspended Animation-Like State Protects Mice From Lethal Hypoxia. *Shock*, **27**, 370–372. doi:10.1097/SHK.0b013e31802e27a0
- Blakeslee, W.W., Lin, Y.H., Stratton, M.S., Tatman, P.D., Hu, T., Ferguson, B.S. & McKinsey, T.A., 2017. Class I HDACs control a JIP1-dependent pathway for kinesin-microtubule binding in cardiomyocytes. *J Mol Cell Cardiol*, **112**, 74–82, Academic Press. doi:10.1016/j.yjmcc.2017.09.002
- Blum, M., Chang, H.Y., Chuguransky, S., Grego, T., Kandasamy, S., Mitchell, A., Nuka, G., *et al.*, 2021. The InterPro protein families and domains database: 20 years on. *Nucleic Acids Res*, **49**, D344–D354, Oxford University Press. doi:10.1093/NAR/GKAA977
- Boeldt, D.S. & Bird, I.M., 2017. Vascular adaptation in pregnancy and endothelial dysfunction in preeclampsia. *Journal of Endocrinology*, BioScientifica Ltd. doi:10.1530/JOE-16-0340
- Boily-Larouche, G., Milev, M.P., Zijenah, L.S., Labbé, A.C., Zannou, D.M., Humphrey, J.H., Ward, B.J., *et al.*, 2012. Naturally-occurring genetic variants in human DC-SIGN increase HIV-1 capture, cell-transfer and risk of mother-to-child transmission. *PLoS One*, **7**, 1–11, PLoS One. doi:10.1371/JOURNAL.PONE.0040706
- Bok, R., Guerra, D.D., Lorca, R.A., Wennersten, S.A., Harris, P.S., Rauniyar, A.K., Stabler, S.P., *et al.*, 2021. Cystathionine γ -lyase promotes estrogen-stimulated uterine artery blood flow via glutathione homeostasis. *Redox Biol*, **40**, 1–15, Redox Biol. doi:10.1016/J.REDOX.2020.101827
- Bokslag, A., Fons, A.B., Zeveerijn, L.J., Teunissen, P.W. & Groot, C.J.M. de, 2020. Maternal recall of a history of early-onset preeclampsia, late-onset preeclampsia, or gestational hypertension: a validation study. *Hypertens Pregnancy*, **39**, 444–450, Taylor and Francis Ltd. doi:10.1080/10641955.2020.1818090

- Bokslag, A., Teunissen, P.W., Franssen, C., Kesteren, F. van, Kamp, O., Ganzevoort, J.W., Paulus, W.J., *et al.*, 2017. Increased cardiovascular risk 9-16 years after early onset preeclampsia. *Am J Obstet Gynecol*, Vol. 216, Elsevier BV. doi:10.1016/j.ajog.2016.11.953
- Bokslag, A., Teunissen, P.W., Franssen, C., Kesteren, F. van, Kamp, O., Ganzevoort, W., Paulus, W.J., *et al.*, 2017. Effect of early-onset preeclampsia on cardiovascular risk in the fifth decade of life. *Am J Obstet Gynecol*, **216**, 523.e1-523.e7, Mosby Inc. doi:10.1016/j.ajog.2017.02.015
- Bokslag, A., Weissenbruch, M. van, Mol, B.W. & Groot, C.J.M. de, 2016, November 1. Preeclampsia; short and long-term consequences for mother and neonate. *Early Hum Dev*, Elsevier Ireland Ltd. doi:10.1016/j.earlhumdev.2016.09.007
- Booz, G.W., Kennedy, D., Bowling, M., Robinson, T., Azubuike, D., Fisher, B., Brooks, K., *et al.*, 2021. Angiotensin II type 1 receptor agonistic autoantibody blockade improves postpartum hypertension and cardiac mitochondrial function in rat model of preeclampsia. *Biol Sex Differ*, **12**, BioMed Central Ltd. doi:10.1186/s13293-021-00396-x
- Borges, V.T.M., Zanati, S.G., Peraçoli, M.T.S., Poiati, J.R., Romão-Veiga, M., Peraçoli, J.C. & Thilaganathan, B., 2018. Maternal left ventricular hypertrophy and diastolic dysfunction and brain natriuretic peptide concentration in early- and late-onset pre-eclampsia. *Ultrasound in Obstetrics and Gynecology*, **51**, 519–523, John Wiley and Sons Ltd. doi:10.1002/uog.17495
- Borghetti, G., Lewinski, D. Von, Eaton, D.M., Sourij, H., Houser, S.R. & Wallner, M., 2018, October 30. Diabetic cardiomyopathy: Current and future therapies. Beyond glycemic control. *Front Physiol*, Frontiers Media S.A. doi:10.3389/fphys.2018.01514
- Borghi, C., Degli Esposti, D., Immordino, V., Cassani, A., Boschi, S., Bovicelli, L. & Ambrosini, E., 2000. Relationship of systemic hemodynamics, left ventricular structure and function, and plasma natriuretic peptide concentrations during pregnancy complicated by preeclampsia. *American Journal Obstetric Gynecology*, **183**, 140–147.
- Borghi, C., Francesco, A., Cicero, G., Degli Esposti, D., Immordino, V., Bacchelli, S., Rizzo, N., *et al.*, 2011. Hemodynamic and neurohumoral profile in patients with different types

of hypertension in pregnancy. *Intern Emerg Med*, **6**, 227–234. doi:10.1007/s11739-010-0483-5

Borsche, M., Pereira, S.L., Klein, C. & Grünewald, A., 2021. Mitochondria and Parkinson's Disease: Clinical, Molecular, and Translational Aspects. *J Parkinsons Dis*, **11**, 45–60, J Parkinsons Dis. doi:10.3233/JPD-201981

Bos, E.M., Goor, H. Van, Joles, J.A., Whiteman, M., Leuvenink, H.G.D. & Goor, D.H. Van, 2015. Hydrogen sulfide: physiological properties and therapeutic potential in ischaemia. *Br J Pharmacol*, **172**, 1479–1493. doi:10.1111/bph.2015.172.issue-6

Bosio, P.M., McKenna, P.J., Conroy, R. & O'Herlihy, C., 1999. Maternal central hemodynamics in hypertensive disorders of pregnancy. *Obstetrics & Gynecology*, **94**, 978–984, No longer published by Elsevier. doi:10.1016/S0029-7844(99)00430-5

Bozkurt, B., Colvin, M., Cook, J., Cooper, L.T., Deswal, A., Fonarow, G.C., Francis, G.S., *et al.*, 2016. Current Diagnostic and Treatment Strategies for Specific Dilated Cardiomyopathies: A Scientific Statement From the American Heart Association. *Circulation*, **134**, e579–e646, Lippincott Williams & Wilkins Hagerstown, MD . doi:10.1161/CIR.0000000000000455

Brain tissue expression of NXPE4 - Summary - The Human Protein Atlas, (n.d.). *The human protein Atlas*. Retrieved June 10, 2023, from <https://www.proteinatlas.org/ENSG00000137634-NXPE4/brain>

Brainard, A.M., Korovkina, V.P. & England, S.K., 2007. Potassium channels and uterine function. *Semin Cell Dev Biol*, **18**, 339, NIH Public Access. doi:10.1016/J.SEMCDB.2007.05.008

Brennecke, S.P., Gude, N.M., Iulio, J.L. Di & King, R.G., 1997. Reduction of placental nitric oxide synthase activity in pre-eclampsia. *Clin Sci (Lond)*, **93**, 51–55, Clin Sci (Lond). doi:10.1042/CS0930051

Brenner, B., 2002. Thrombophilia and pregnancy loss. *Thromb Res*, **108**, 197–202, Elsevier Ltd. doi:10.1016/S0049-3848(02)00390-0

- Broderick, T.L., Cusimano, F.A., Carlson, C. & Babu, J.R., 2018. Biosynthesis of the Essential Fatty Acid Oxidation Cofactor Carnitine Is Stimulated in Heart and Liver after a Single Bout of Exercise in Mice. *J Nutr Metab*, **2018**, 1–7, J Nutr Metab. doi:10.1155/2018/2785090
- Brosens, I., 1964. A Study of The Spiral Arteries Of The Decidua Basalis In Normotensive And Hypertensive Pregnancies. *BJOG*, **71**, 222–230, John Wiley & Sons, Ltd. doi:10.1111/j.1471-0528.1964.tb04270.x
- Brosens, I.A., 1972. The role of the spiral arteries in the pathogenesis of preeclampsia. *Obstet Gynecol Annu*, 177–190.
- Brown, C.E., Casey, H., Dominiczak, A.F., Kerr, S., Campbell, A. & Delles, C., 2023. Impact of preeclampsia on cardiovascular events: An analysis of the Generation Scotland: Scottish family health study. *Journal of Human Hypertension* 2023, 1–7, Nature Publishing Group. doi:10.1038/s41371-023-00812-2
- Brown, D.A., Perry, J.B., Allen, M.E., Sabbah, H.N., Stauffer, B.L., Shaikh, S.R., Cleland, J.G.F., *et al.*, 2017. Mitochondrial function as a therapeutic target in heart failure. *Nat Rev Cardiol*, **14**, 250, NIH Public Access. doi:10.1038/NRCARDIO.2016.203
- Brown, D.W., Dueker, N., Jamieson, D.J., Cole, J.W., Wozniak, M.A., Stern, B.J., Giles, W.H., *et al.*, 2006. Preeclampsia and the Risk of Ischemic Stroke Among Young Women. *Stroke*, **37**, 1055–1059. doi:10.1161/01.STR.0000206284.96739.ee
- Brown, M. A., Zammit, V.C. & Lowe, S.A., 1989. Capillary Permeability and Extracellular Fluid Volumes in Pregnancy-Induced Hypertension. *Clin Sci*, **77**, 599–604, Portland Press. doi:10.1042/CS0770599
- Brown, Mark A., Magee, L.A., Kenny, L.C., Karumanchi, S.A., McCarthy, F.P., Saito, S., Hall, D.R., *et al.*, 2018, July 1. Hypertensive disorders of pregnancy: ISSHP classification, diagnosis, and management recommendations for international practice. *Hypertension*, Lippincott Williams and Wilkins. doi:10.1161/HYPERTENSIONAHA.117.10803
- Browne, V.A., Julian, C.G., Toledo-Jaldin, L., Cioffi-Ragan, D., Vargas, E. & Moore, L.G., 2015, March 5. Uterine artery blood flow, fetal hypoxia and fetal growth. *Philosophical*

Transactions of the Royal Society B: Biological Sciences, Royal Society of London.
doi:10.1098/rstb.2014.0068

Brussé, I., Duvekot, J., Jongerling, J., Steegers, E. & Koning, I. De, 2008. Impaired maternal cognitive functioning after pregnancies complicated by severe pre-eclampsia: A pilot case-control study. *Acta Obstet Gynecol Scand*, **87**, 408–412.
doi:10.1080/00016340801915127

Bunik, V., Kaehne, T., Degtyarev, D., Shcherbakova, T. & Reiser, G., 2008. Novel isoenzyme of 2-oxoglutarate dehydrogenase is identified in brain, but not in heart. *FEBS J*, **275**, 4990–5006, FEBS J. doi:10.1111/J.1742-4658.2008.06632.X

Buraei, Z. & Yang, J., 2010, October. The β subunit of voltage-gated Ca^{2+} channels. *Physiol Rev*. doi:10.1152/physrev.00057.2009

Buraei, Z. & Yang, J., 2013, July. Structure and function of the β subunit of voltage-gated Ca^{2+} channels. *Biochim Biophys Acta Biomembr*. doi:10.1016/j.bbamem.2012.08.028

Burbank, F., 2009. *Hemodynamic Changes in the Uterus and its Blood Vessels in Pregnancy** †. (E. Palacios-Jaraquemada, Ed.), 1st ed., Wheatmark. Retrieved from www.glowm.com

Burbank, Fred., 2009. *Fibroids, menstruation, childbirth and evolution : the fascinating story of uterine blood vessels*, Vol. 22, Wheatmark.

Burgess, A., McDowell, W. & Ebersold, S., 2019. Association between Lactation and Postpartum Blood Pressure in Women with Preeclampsia. *MCN The American Journal of Maternal/Child Nursing*, **44**, 86–93, Lippincott Williams and Wilkins.
doi:10.1097/NMC.0000000000000502

Burke, S.D. & Ananth Karumanchi, S., 2013. Spiral artery remodeling in preeclampsia revisited. *Hypertension*, **62**, 1013–1014. doi:10.1161/HYPERTENSIONAHA.113.02049

Burke, S.D., Barrette, V.F., Bianco, J., Thorne, J.G., Yamada, A.T., Pang, S.C., Adams, M.A., *et al.*, 2010. Spiral arterial remodeling is not essential for normal blood pressure regulation in pregnant mice. *Hypertension*, **55**, 729–737, PMC Canada manuscript submission. doi:10.1161/HYPERTENSIONAHA.109.144253

- Burke, S.D., Barrette, V.F., Carter, A.L., Gravel, J., Adams, M.A. & Croy, B.A., 2011. Cardiovascular adaptations of pregnancy in T and B cell-deficient mice. *Biol Reprod*, **85**, 605–614. doi:10.1095/biolreprod.111.092668
- Burton, G. J., Woods, A.W., Jauniaux, E. & Kingdom, J.C.P., 2009. Rheological and Physiological Consequences of Conversion of the Maternal Spiral Arteries for Uteroplacental Blood Flow during Human Pregnancy. *Placenta*, **30**, 473–482, W.B. Saunders. doi:10.1016/j.placenta.2009.02.009
- Burton, Graham J & Jauniaux, E., 2004. Placental Oxidative Stress: From Miscarriage to Preeclampsia. *J Soc Gynecol Investig*, **11**, 342–352.
- Burton, Graham J. & Jauniaux, E., 2011. Oxidative stress. *Best Pract Res Clin Obstet Gynaecol*, **25**, 287–299. doi:10.1016/j.bpobgyn.2010.10.016
- Burton, Graham J. & Jauniaux, E., 2018. Pathophysiology of placental-derived fetal growth restriction. *Am J Obstet Gynecol*, **218**, S745–S761, Mosby Inc. doi:10.1016/J.AJOG.2017.11.577/ATTACHMENT/D00A3DED-0031-41F4-B91C-23836CE91FDF/MMC6.MP4
- Burton, Graham J. & Jauniaux, E., 2018. Pathophysiology of placental-derived fetal growth restriction. *Am J Obstet Gynecol*, **218**, S745–S761, Mosby Inc. doi:10.1016/j.ajog.2017.11.577
- Burton, J.G., Redman, C.W., Roberts, J.M. & Moffett, A., 2019. Pre-eclampsia: pathophysiology and clinical implications. *BMJ*, **366**. doi:10.1136/bmj.l2381
- Burton, P.R., Clayton, D.G., Cardon, L.R., Craddock, N., Deloukas, P., Duncanson, A., Kwiatkowski, D.P., *et al.*, 2007. Genome-wide association study of 14,000 cases of seven common diseases and 3,000 shared controls. *Nature*, **447**, 661–678, Nature. doi:10.1038/NATURE05911
- Burwick, R.M., Rincon, M., Beeraka, S.S., Gupta, M. & Feinberg, B.B., 2018. Evaluation of hemolysis as a severe feature of preeclampsia. *Hypertension*, **72**, 460–465, Lippincott Williams and Wilkins. doi:10.1161/HYPERTENSIONAHA.118.11211

- Buscà, R., Pouysségur, J. & Lenormand, P., 2016. ERK1 and ERK2 map kinases: Specific roles or functional redundancy? *Front Cell Dev Biol*, **4**, 195438, Frontiers Media S.A. doi:10.3389/FCELL.2016.00053/BIBTEX
- Busch, A.W.U. & Montgomery, B.L., 2015. Interdependence of tetrapyrrole metabolism, the generation of oxidative stress and the mitigative oxidative stress response. *Redox Biol*, **4**, 271, Elsevier. doi:10.1016/J.REDOX.2015.01.010
- Bushnell, C. & Chireau, M., 2011. Preeclampsia and stroke: Risks during and after pregnancy. *Stroke Res Treat*. doi:10.4061/2011/858134
- Butt, A.L., Bouvette, S., Kulesus, K. & Tanaka, K.A., 2023. Randomised trials to improve haemostasis management for postpartum haemorrhage. Comment on Br J Anaesth 2023; 130: 165–74. *Br J Anaesth*, **130**, 165–174, Elsevier BV. doi:10.1016/j.bja.2023.02.011
- Bytautiene, E., Lu, F., Tamayo, E.H., Hankins, G.D.V., Longo, M., Kublickiene, K. & Saade, G.R., 2010. Long-term maternal cardiovascular function in a mouse model of sFlt-1-induced preeclampsia. *Am J Physiol Heart Circ Physiol*, **298**, 189–193, Am J Physiol Heart Circ Physiol. doi:10.1152/AJPHEART.00792.2009
- Cai, Z., Wu, C., Xu, Y., Cai, J., Zhao, M. & Zu, L., 2023. The NO-cGMP-PKG Axis in HFpEF: From Pathological Mechanisms to Potential Therapies. *Aging Dis*, **14**, 46–62, Aging and Disease. doi:10.14336/AD.2022.0523
- Camilleri, M., Carlson, P., Acosta, A. & Busciglio, I., 2015. Colonic mucosal gene expression and genotype in irritable bowel syndrome patients with normal or elevated fecal bile acid excretion. *Am J Physiol Gastrointest Liver Physiol*, **309**, G10–G20, American Physiological Society. doi:10.1152/AJPGI.00080.2015
- Campbell, D.M. & MacGillivray, I., 1972. COMPARISON OF MATERNAL RESPONSE IN FIRST AND SECOND PREGNANCIES IN RELATION TO BABY WEIGHT. *BJOG*, **79**, 684–693. doi:10.1111/j.1471-0528.1972.tb12901.x

- Candela, J., Wang, R. & White, C., 2017. Microvascular endothelial dysfunction in obesity is driven by macrophage-dependent hydrogen sulfide depletion. *Arterioscler Thromb Vasc Biol*, **37**, 889–899. doi:10.1161/ATVBAHA.117.309138
- Canto, P., Canto-Cetina, T., Juárez-Velázquez, R., Rosas-Vargas, H., Rangel-Villalobos, H., Canizalez-Quinteros, S., Velázquez-Wong, A.C., *et al.*, 2008. Methylenetetrahydrofolate reductase C677T and glutathione S-transferase P1 A313G are associated with a reduced risk of preeclampsia in Maya-Mestizo women. *Hypertens Res*, **31**, 1015–1019, Hypertens Res. doi:10.1291/HYPRES.31.1015
- Capeless, E.L. & Clapp, J.F., 1991. When do cardiovascular parameters return to their preconception values? *American Journal of Obstetrics and Gynecology*, **165**, 883–886.
- Caponnetto, A., Battaglia, R., Ferrara, C., Vento, M.E., Borzi, P., Paradiso, M., Scollo, P., *et al.*, 2022. Down-regulation of long non-coding RNAs in reproductive aging and analysis of the lncRNA-miRNA-mRNA networks in human cumulus cells. *J Assist Reprod Genet*, **39**, 919–931, J Assist Reprod Genet. doi:10.1007/S10815-022-02446-8
- Carla Van Oppen, A.C., Tweel, I. Van Der, Johan Alsbach, G.P., Heethaar, R.M. & Bruinse, H.W., 1996. A Longitudinal Study of Maternal Hemodynamics During Normal Pregnancy From the Departments of Obstetrics and. *Obstetric Gynecology*, **88**, 40–46.
- Carmona, R., González-Iriarte, M., Pérez-Pomares, J.M. & Muñoz-Chápuli, R., 2001. Localization of the Wilm's tumour protein WT1 in avian embryos. *Cell Tissue Res*, **303**, 173–186, Cell Tissue Res. doi:10.1007/S004410000307
- Carson, R.J. & Konje, J.C., 2014. Role of hydrogen sulfide in the female reproductive tract. *Expert Rev Obstet Gynecol*, **5**, 203–213, Taylor & Francis. doi:10.1586/EOG.10.5
- Carter, A.M., 2020. Animal models of human pregnancy and placentation: alternatives to the mouse. *Society for Reproduction and Fertility*, **160**, R129–R143. doi:10.1530/REP-20-0354
- Cartwright, J.E., Fraser, R., Leslie, K., Wallace, A.E. & James, J.L., 2010. Remodelling at the maternal-fetal interface: Relevance to human pregnancy disorders. *Reproduction*, **140**, 803–813. doi:10.1530/REP-10-0294

- Castellani, C.A., Longchamps, R.J., Sumpter, J.A., Newcomb, C.E., Lane, J.A., Grove, M.L., Bressler, J., *et al.*, 2020. Mitochondrial DNA copy number can influence mortality and cardiovascular disease via methylation of nuclear DNA CpGs. *Genome Med*, **12**, 1–17, BioMed Central Ltd. doi:10.1186/S13073-020-00778-7/FIGURES/5
- Castiglia, D., Scaturro, M., Nastasi, T., Cestelli, A. & Liegro, I. Di, 1996. PIPPin, a putative RNA-binding protein specifically expressed in the rat brain. *Biochem Biophys Res Commun*, **218**, 390–394, Biochem Biophys Res Commun. doi:10.1006/BBRC.1996.0068
- Castleman, J.S., Ganapathy, R., Taki, F., Lip, G.Y.H., Steeds, R.P. & Kotecha, D., 2016. Echocardiographic Structure and Function in Hypertensive Disorders of Pregnancy: A Systematic Review. *Circ Cardiovasc Imaging*, **9**, Lippincott Williams and Wilkins. doi:10.1161/CIRCIMAGING.116.004888
- Castleman, J.S., Shantsila, A., Brown, R.A., Shantsila, E. & Lip, G.Y.H., 2023. Altered cardiac and vascular stiffness in pregnancy after a hypertensive pregnancy. *J Hum Hypertens*, **37**, 189–196, Springer Nature. doi:10.1038/s41371-022-00662-4
- Cavalcanti, M.C.O., Steilmann, C., Failing, K., Bergmann, M., Kliesch, S., Weidner, W. & Steger, K., 2011. Apoptotic gene expression in potentially fertile and subfertile men. *Mol Hum Reprod*, **17**, 415–420, Mol Hum Reprod. doi:10.1093/MOLEHR/GAR011
- Cester, N., Staffolani, R., Rabini, R.A., Magnanelli, R., Salvolini, E., Galassi, R., Mazzanti, L., *et al.*, 1994. Pregnancy induced hypertension: a role for peroxidation in microvillus plasma membranes. *Mol Cell Biochem*, **131**, 151–155, Kluwer Academic Publishers. doi:10.1007/BF00925951
- Chaiworapongsa, T., Romero, R., Espinoza, J., Bujold, E., Mee Kim, Y., Gonçalves, L.F., Gomez, R., *et al.*, 2004. Evidence supporting a role for blockade of the vascular endothelial growth factor system in the pathophysiology of preeclampsia: Young Investigator Award. *Am J Obstet Gynecol*, Vol. 190, pp. 1541–1547, Mosby Inc. doi:10.1016/j.ajog.2004.03.043
- Chaiworapongsa, T., Romero, R., Kim, Y.M., Kim, G.J., Kim, M.R., Espinoza, J., Bujold, E., *et al.*, 2005. Plasma soluble vascular endothelial growth factor receptor-1 concentration is

elevated prior to the clinical diagnosis of pre-eclampsia. *Journal of Maternal-Fetal and Neonatal Medicine*, **17**, 3–18, Taylor & Francis. doi:10.1080/14767050400028816

Chakraborty, P.K., Murphy, B., Mustafi, S.B., Dey, A., Xiong, X., Rao, G., Naz, S., *et al.*, 2018. Cystathionine β -synthase regulates mitochondrial morphogenesis in ovarian cancer. *FASEB J*, **32**, 4145–4157, FASEB J. doi:10.1096/FJ.201701095R

Chatterjee, M., Campo, M. Del, Morrema, T.H.J., Waal, M. De, Flier, W.M. Van Der, Hoozemans, J.J.M. & Teunissen, C.E., 2018. Contactin-2, a synaptic and axonal protein, is reduced in cerebrospinal fluid and brain tissue in Alzheimer's disease. *Alzheimers Res Ther*, **10**, BioMed Central Ltd. doi:10.1186/s13195-018-0383-x

Chauhan, G. & Tadi, P., 2022, November 14. Physiology, Postpartum Changes. *StatPearls*, StatPearls Publishing. Retrieved June 17, 2023, from <https://www.ncbi.nlm.nih.gov/books/NBK555904/>

Che, C., Dudick, K. & Shoemaker, R., 2019. Cardiac hypertrophy with obesity is augmented after pregnancy in C57BL/6 mice. *Biol Sex Differ*, **10**, BioMed Central Ltd. doi:10.1186/s13293-019-0269-z

Chechko, N., Dukart, J., Tchaikovski, S., Enzensberger, C., Neuner, I. & Stickel, S., 2022. The expectant brain-pregnancy leads to changes in brain morphology in the early postpartum period. *Cereb Cortex*, **32**, 4025–4038, NLM (Medline). doi:10.1093/cercor/bhab463

Chen, B.P., Wolfgang, C.D. & Hai, T., 1996. Analysis of ATF3, a transcription factor induced by physiological stresses and modulated by gadd153/Chop10. *Mol Cell Biol*, **16**, 1157–1168, Mol Cell Biol. doi:10.1128/MCB.16.3.1157

Chen, D., Wang, H., Huang, H. & Dong, M., 2008. Vascular endothelial growth factor attenuates Nw-Nitro-L-arginine methyl ester-induced preeclampsia-like manifestations in rats. *Clin Exp Hypertens*, **30**, 606–615, Taylor & Francis. doi:10.1080/10641960802443118

Chen, D.-B. & Zheng, J., 2013. Regulation of Placental Angiogenesis.

- Chen, D.H., Brkanac, Z., Verlinde, C.L.M.J., Tan, X.J., Bylenok, L., Nochlin, D., Matsushita, M., *et al.*, 2003. Missense mutations in the regulatory domain of PKC gamma: a new mechanism for dominant nonepisodic cerebellar ataxia. *Am J Hum Genet*, **72**, 839–849, Am J Hum Genet. doi:10.1086/373883
- Chen, J.Z.J., Sheehan, P.M., Brennecke, S.P. & Keogh, R.J., 2012, February 26. Vessel remodelling, pregnancy hormones and extravillous trophoblast function. *Mol Cell Endocrinol*. doi:10.1016/j.mce.2011.10.014
- Chen, S.Z., Ning, L.F., Xu, X., Jiang, W.Y., Xing, C., Jia, W.P., Chen, X.L., *et al.*, 2016. The MIR-181d-regulated metalloproteinase Adamts1 enzymatically impairs adipogenesis via ECM remodeling. *Cell Death Differ*, **23**, 1778–1791, Nature Publishing Group. doi:10.1038/cdd.2016.66
- Chen, W., Wei, Q., Liang, Q., Song, S. & Li, J., 2022. Diagnostic capacity of sFlt-1/PIGF ratio in fetal growth restriction: A systematic review and meta-analysis. *Placenta*, **127**, 37–42, W.B. Saunders Ltd. doi:10.1016/j.placenta.2022.07.020
- Chen, X., Jhee, K.H. & Kruger, W.D., 2004. Production of the neuromodulator H₂S by cystathionine beta-synthase via the condensation of cysteine and homocysteine. *J Biol Chem*, **279**, 52082–52086, J Biol Chem. doi:10.1074/JBC.C400481200
- Chen, Y.H., Yao, W.Z., Geng, B., Ding, Y.L., Lu, M., Zhao, M.W. & Tang, C.S., 2005. Endogenous hydrogen sulfide in patients with COPD. *Chest*, **128**, 3205–3211, Chest. doi:10.1378/CHEST.128.5.3205
- Chesley, L.C., Annitto, J.E. & Cosgrove, R.A., 1968. The familial factor in toxemia of pregnancy. *Obstetrics Gynecol.*, **32**, 303–311. doi:10.1038/ki.1980.131
- Cheung, S.H. & Lau, J.Y.W., 2018. Hydrogen sulfide mediates athero-protection against oxidative stress via S-sulfhydration. *PLoS One*, **13**, PLoS One. doi:10.1371/JOURNAL.PONE.0194176
- Cho, G.J., Jung, U.S., Sim, J.Y., Lee, Y.J., Bae, N.Y., Choi, H.J., Park, J.H., *et al.*, 2019. Is preeclampsia itself a risk factor for the development of metabolic syndrome after

delivery? *Obstet Gynecol Sci*, **62**, 233–241, Korean Society of Obstetrics and Gynecology. doi:10.5468/ogs.2019.62.4.233

Christensen, M., Kronborg, C.S., Eldrup, N., Rossen, N.B. & Knudsen, U.B., 2016. Preeclampsia and cardiovascular disease risk assessment - Do arterial stiffness and atherosclerosis uncover increased risk ten years after delivery? *Pregnancy Hypertens*, **6**, 110–114, Elsevier B.V. doi:10.1016/j.preghy.2016.04.001

Christian, L.M. & Porter, K., 2014. Longitudinal Changes in Serum Proinflammatory Markers across Pregnancy and Postpartum: Effects of Maternal Body Mass Index. *Cytokine*, **70**, 140, NIH Public Access. doi:10.1016/J.CYTO.2014.06.018

CHST4 - Carbohydrate sulfotransferase 4 - | UniProtKB | UniProt, (n.d.). *UniProt*. Retrieved June 13, 2023, from <https://www.uniprot.org/uniprotkb/Q8NCG5/entry>

CHST4 carbohydrate sulfotransferase 4 - Gene - NCBI, 2023, May. *National Library of Medicine*. Retrieved June 13, 2023, from <https://www.ncbi.nlm.nih.gov/gene/10164>

Chung, E. & Leinwand, L.A., 2014. Pregnancy as a Cardiac Stress Model. *Cardiovasc Res*, **101**, 561–570. doi:10.1093/cvr/cvu013

Chung, E., Yeung, F. & Leinwand, L.A., 2012. Akt and MAPK signaling mediate pregnancy-induced cardiac adaptation. *J Appl Physiol (1985)*, **112**, 1564–1575, *J Appl Physiol (1985)*. doi:10.1152/JAPPLPHYSIOL.00027.2012

Chung, K.W., Lee, E.K., Lee, M.K., Oh, G.T., Yu, B.P. & Chung, H.Y., 2018. Impairment of PPAR α and the Fatty Acid Oxidation Pathway Aggravates Renal Fibrosis during Aging. *J Am Soc Nephrol*, **29**, 1223–1237, *J Am Soc Nephrol*. doi:10.1681/ASN.2017070802

Ciftci, F.C., Caliskan, M., Ciftci, O., Gullu, H., Uckuyu, A., Toprak, E. & Yanik, F., 2014. Impaired coronary microvascular function and increased intima-media thickness in preeclampsia. *Journal of the American Society of Hypertension*, **8**, 820–826, Elsevier Ireland Ltd. doi:10.1016/j.jash.2014.08.012

- Cikes, M. & Solomon, S.D., 2016, June 1. Beyond ejection fraction: An integrative approach for assessment of cardiac structure and function in heart failure. *Eur Heart J*, Oxford University Press. doi:10.1093/eurheartj/ehv510
- Cindrova-Davies, T., Herrera, E.A., Niu, Y., Kingdom, J., Giussani, D.A. & Burton, G.J., 2013. Reduced Cystathionine γ -Lyase and Increased miR-21 Expression Are Associated with Increased Vascular Resistance in Growth-Restricted Pregnancies: Hydrogen Sulfide as a Placental Vasodilator. *Am J Pathol*, **182**, 1448–1458, Elsevier. doi:10.1016/J.AJPAT.2013.01.001
- Clapp, J.F. & Capeless, E., 1997. Cardiovascular Function Before, During, and After the First and Subsequent Pregnancies. *American Journal of Cardiology*, **80**, 1469–1473.
- Crossen, J.S., Morris, R.K., Riet, G. Ter, Mol, B.W.J., Post, J.A.M. Van Der, Coomarasamy, A., Zwinderman, A.H., *et al.*, 2008. Use of uterine artery Doppler ultrasonography to predict pre-eclampsia and intrauterine growth restriction: a systematic review and bivariable meta-analysis. *CMAJ: Canadian Medical Association Journal*, **178**, 701, Canadian Medical Association. doi:10.1503/CMAJ.070430
- Coelho-Santos, V. & Shih, A.Y., 2020. Postnatal development of cerebrovascular structure and the neuroglial unit. *Wiley Interdiscip Rev Dev Biol*, **9**, 363–340, Wiley-Blackwell. doi:10.1002/WDEV.363
- Colhoun, H.M., McKeigue, P.M. & Smith, G.D., 2003. Problems of reporting genetic associations with complex outcomes. *Lancet*, **361**, 865–872, Elsevier B.V. doi:10.1016/S0140-6736(03)12715-8
- Collinot, H., Marchiol, C., Lagoutte, I., Lager, F., Siauve, N., Autret, G., Balvay, D., *et al.*, 2018. Preeclampsia induced by STOX1 overexpression in mice induces intrauterine growth restriction, abnormal ultrasonography and BOLD MRI signatures. *J Hypertens*, **36**, 1399–1406, Lippincott Williams and Wilkins. doi:10.1097/HJH.0000000000001695
- Conde-Agudelo, A., Romero, R., Kusanovic, J.P. & Hassan, S.S., 2011. Supplementation with vitamins C and e during pregnancy for the prevention of preeclampsia and other adverse maternal and perinatal outcomes: A systematic review and metaanalysis. *Am J Obstet Gynecol*, **204**, 503.e1-503.e12, Mosby Inc. doi:10.1016/j.ajog.2011.02.020

- Cong, J., Fan, T., Yang, X., Squires, J.W., Cheng, G., Zhang, L. & Zhang, Z., 2015. Structural and functional changes in maternal left ventricle during pregnancy: A three-dimensional speckle-tracking echocardiography study. *Cardiovasc Ultrasound*, **13**, BioMed Central Ltd. doi:10.1186/1476-7120-13-6
- Cooper, T.A. & Ordahl, C.P., 1985. A single cardiac troponin T gene generates embryonic and adult isoforms via developmentally regulated alternate splicing. *J Biol Chem*, **160**, 11140–11148. doi:10.1126/science.6095446
- Coroyannakis, C. & Khalil, A., 2019. Management of Hypertension in the Obese Pregnant Patient. *Curr Hypertens Rep*, **21**, 1–7, Current Hypertension Reports. doi:10.1007/s11906-019-0927-x LK -
<http://sfx.library.uu.nl/utrecht?sid=EMBASE&issn=15343111&id=doi:10.1007%2Fs11906-019-0927-x&title=Management+of+Hypertension+in+the+Obese+Pregnant+Patient&stitle=Curr.+Hypertens.+Rep.&title=Current+Hypertension+Reports&volume=21&issue=3&page=&epage=&aualast=Coroyannakis&aufirst=Christina&aunit=C.&aufull=Coroyannakis+C.&coden=CHRUC&isbn=&pages=-&date=2019&aunit1=C&aunitm=>
- Costa, L.E., Boveris, A., Koch, O.R. & Taquini, A.C., 1988. Liver and heart mitochondria in rats submitted to chronic hypobaric hypoxia. *Am J Physiol Cell Physiol*, **255**, American Physiological Society Bethesda, MD . doi:10.1152/ajpcell.1988.255.1.c123
- Countouris, M.E., Schwarz, E.B., Rossiter, B.C., Althouse, A.D., Berlacher, K.L., Jeyabalan, A. & Catov, J.M., 2016. Effects of lactation on postpartum blood pressure among women with gestational hypertension and preeclampsia. *Am J Obstet Gynecol*, **215**, 241.e1-241.e8, Mosby Inc. doi:10.1016/j.ajog.2016.02.046
- Coussens, L., Parker, P.J., Rhee, L., Yang-Feng, T.L., Chen, E., Waterfield, M.D., Francke, U., *et al.*, 1986. Multiple, distinct forms of bovine and human protein kinase C suggest diversity in cellular signaling pathways. *Science*, **233**, 859–866, Science. doi:10.1126/SCIENCE.3755548

- Cox, B., Leavey, K., Nosi, U., Wong, F. & Kingdom, J., 2015. Placental transcriptome in development and pathology: expression, function, and methods of analysis. *Am J Obstet Gynecol*, **213**, S138–S151, Elsevier. doi:10.1016/J.AJOG.2015.07.046
- Craici, I., Wagner, S. & Garovic, V.D., 2008. Preeclampsia and future cardiovascular risk: formal risk factor or failed stress test? *Ther Adv Cardiovasc Dis*, **2**, 249–59, SAGE PublicationsSage UK: London, England. doi:10.1177/1753944708094227
- Crichton, R.R., 2012. Biological Ligands for Metal Ions. *Biological Inorganic Chemistry*, **3**, 69–89, Elsevier. doi:10.1016/B978-0-444-53782-9.00004-8
- Cronin, K.D., Ge, D., Manninger, P., Linnertz, C., Rossoshek, A., Orrison, B.M., Bernard, D.J., *et al.*, 2009. Expansion of the Parkinson disease-associated SNCA-Rep1 allele upregulates human α -synuclein in transgenic mouse brain. *Hum Mol Genet*, **18**, 3274–3285. doi:10.1093/hmg/ddp265
- Cronqvist, T., Saljé, K., Familiarì, M., Guller, S., Schneider, H., Gardiner, C., Sargent, I.L., *et al.*, 2014. Syncytiotrophoblast vesicles show altered micro-RNA and haemoglobin content after ex-vivo perfusion of placentas with haemoglobin to mimic preeclampsia. *PLoS One*, **9**, Public Library of Science. doi:10.1371/journal.pone.0090020
- Cross, S.N., Ratner, E., Rutherford, T.J., Schwartz, P.E. & Norwitz, E.R., 2012. Bevacizumab-Mediated Interference With VEGF Signaling Is Sufficient to Induce a Preeclampsia-Like Syndrome in Nonpregnant Women. *Rev Obstet Gynecol*, **5**, 1–8. doi:10.3909/riog0179
- Cui, Y., Wang, W., Dong, N., Lou, J., Srinivasan, D.K., Cheng, W., Huang, X., *et al.*, 2013. Role of Corin in Trophoblast Invasion and Uterine Spiral Artery Remodeling in Pregnancy. *Nature*, **484**, 246–250. doi:10.1038/nature10897
- Cullen, A., 2013. Platelet margination in postpartum haemorrhage. *BJA: British Journal of Anaesthesia*, **110**, 1052–1053, Oxford Academic. doi:10.1093/BJA/AET136
- D A Clark, G Chaouat, P C Arck, H W Mittrucker & G A Levy, 1988. Cytokine-dependent abortion in CBA x DBA/2 mice is mediated by the procoagulant fgl2 prothrombinase . *Journal of Immunology*, **15**, 545–549, Wiley. doi:10.1111/j.1600-0897.2004.00237.x

- Dai, C., Li, Q., May, H.I., Li, C., Zhang, G., Sharma, G., Sherry, A.D., *et al.*, 2020. Lactate Dehydrogenase A Governs Cardiac Hypertrophic Growth in Response to Hemodynamic Stress. *Cell Rep*, **32**, Elsevier B.V. doi:10.1016/j.celrep.2020.108087
- Dai, W., Xu, L., Yu, X., Zhang, G., Guo, H., Liu, H., Song, G., *et al.*, 2020. OGDHL silencing promotes hepatocellular carcinoma by reprogramming glutamine metabolism. *J Hepatol*, **72**, 909–923, J Hepatol. doi:10.1016/J.JHEP.2019.12.015
- Dalmáz, C.A., Santos, K.G., Botton, M.R., Tedoldi, C.L. & Roisenberg, I., 2006. Relationship between polymorphisms in thrombophilic genes and preeclampsia in a Brazilian population. *Blood Cells Mol Dis*, **37**, 107–110, Blood Cells Mol Dis. doi:10.1016/J.BCMD.2006.07.005
- Danzmann, L.C., Bodanese, L.C., Köhler, I. & Torres, M.R., 2008. Left atrioventricular remodeling in the assessment of the left ventricle diastolic function in patients with heart failure: A review of the currently studied echocardiographic variables. *Cardiovasc Ultrasound*, **6**, 1–13. doi:10.1186/1476-7120-6-56
- Das, E., Singh, V., Agrawal, S. & Pati, S.K., 2022. Prediction of Preeclampsia Using First-Trimester Uterine Artery Doppler and Pregnancy-Associated Plasma Protein-A (PAPP-A): A Prospective Study in Chhattisgarh, India. *Cureus*, **14**, 1–10. doi:10.7759/cureus.22026
- Dathan-Stumpf, A., Rieger, A., Verlohren, S., Wolf, C. & Stepan, H., 2022. sFlt-1/PIGF ratio for prediction of preeclampsia in clinical routine: A pragmatic real-world analysis of healthcare resource utilisation. *PLoS One*, **17**, Public Library of Science. doi:10.1371/journal.pone.0263443
- Datta, S., Kodali, B.S. & Segal, S., 2010. Maternal Physiological Changes During Pregnancy, Labor, and the Postpartum Period. in *Obstetric Anesthesia Handbook*, pp. 1–14, Springer New York. doi:10.1007/978-0-387-88602-2_1
- Datta, S., Kodali, S.B. & Segal, S., 2010. *Obstetric Anesthesia Handbook*. (Springer, Ed.), 5th ed., Vol. 5, Springer Science Business Media. doi:10.1007/978-0-387-88602-2_1

- Dayan, N. & Nerenberg, K., 2019, June 1. Postpartum Cardiovascular Prevention: The Need for a National Health Systems-Based Strategy. *Canadian Journal of Cardiology*, Elsevier Inc. doi:10.1016/j.cjca.2019.04.004
- DeMartelly, V.A., Dreixler, J., Tung, A., Mueller, A., Heimberger, S., Fazal, A.A., Naseem, H., *et al.*, 2021. Long-term postpartum cardiac function and its association with preeclampsia. *J Am Heart Assoc*, **10**, 1–9, American Heart Association Inc. doi:10.1161/JAHA.120.018526
- Dempster, S., Harper, S., Moses, J.E. & Dreveny, I., 2014. Structural characterization of the apo form and NADH binary complex of human lactate dehydrogenase. *Acta Crystallogr D Biol Crystallogr*, **70**, 1484–1490, International Union of Crystallography. doi:10.1107/S1399004714005422
- Deng, F.M., Liang, F.X., Tu, L., Resing, K.A., Hu, P., Supino, M., Andrew Hu, C.C., *et al.*, 2002. Uroplakin IIIb, a urothelial differentiation marker, dimerizes with uroplakin Ib as an early step of urothelial plaque assembly. *J Cell Biol*, **159**, 685–694, J Cell Biol. doi:10.1083/JCB.200204102
- Denney, J.M., Bird, C., Gendron-Fitzpatrick, A., Sampene, E., Bird, I.M. & Shah, D.M., 2016. Renin-angiotensin system transgenic mouse model recapitulates pathophysiology similar to human preeclampsia with renal injury that may be mediated through VEGF. *American Journal of Physiology-Renal Physiology*, **312**, F445–F455. doi:10.1152/ajprenal.00108.2016
- Dennis, A.T. & Castro, J.M., 2014. Transthoracic echocardiography in women with treated severe pre-eclampsia. *Anaesthesia*, **69**, 436–444. doi:10.1111/anae.12623
- Desai, D.K., Moodley, J. & Naidoo, D.P., 2004. Echocardiographic assessment of cardiovascular hemodynamics in normal pregnancy. *Obstetrics and Gynecology*, **104**, 20–29. doi:10.1097/01.AOG.0000128170.15161.1d
- Descamps, O.S., Bruniaux, M., Guilmot, P.F., Tonglet, R. & Heller, F.R., 2005. Lipoprotein metabolism of pregnant women is associated with both their genetic polymorphisms and those of their newborn children. *J Lipid Res*, **46**, 2405–2414, J Lipid Res. doi:10.1194/JLR.M500223-JLR200

- Descamps, O.S., Gilbeau, J.P., Luwaert, R. & Heller, F.R., 2003. Impact of genetic defects on coronary atherosclerosis in patients suspected of having familial hypercholesterolaemia. *Eur J Clin Invest*, **33**, 1–9, Eur J Clin Invest. doi:10.1046/J.1365-2362.2003.01094.X
- Despanie, J., Dhandhukia, J.P., Hamm-Alvarez, S.F. & MacKay, J.A., 2016. Elastin-like polypeptides: Therapeutic applications for an emerging class of nanomedicines. *Journal of Controlled Release*, **240**, 93–108, Elsevier B.V. doi:10.1016/j.jconrel.2015.11.010
- DeVore, G.R. & Polanco, B., 2023. Assessing maternal cardiac function by obstetricians: technique and reference ranges. *Am J Obstet Gynecol*, Elsevier Inc. doi:10.1016/j.ajog.2023.01.003
- Dhawan, A., Parmar, D., Das, M. & Seth, P.K., 1990. Cytochrome P-450 dependent monooxygenases in neuronal and glial cells: inducibility and specificity. *Biochem Biophys Res Commun*, **170**, 441–447, Biochem Biophys Res Commun. doi:10.1016/0006-291X(90)92111-C
- Dijk, A. Van, Niessen, H.W.M., Ursem, W., Twisk, J.W.R., Visser, F.C. & Milligen, F.J. Van, 2008. Accumulation of fibronectin in the heart after myocardial infarction: a putative stimulator of adhesion and proliferation of adipose-derived stem cells. *Cell Tissue Res*, **332**, 298, Springer. doi:10.1007/S00441-008-0573-0
- Dilek, N., Papapetropoulos, A., Toliver-Kinsky, T. & Szabo, C., 2020. Hydrogen sulfide: An endogenous regulator of the immune system. *Pharmacol Res*, **161**, 1–21, Academic Press. doi:10.1016/J.PHRS.2020.105119
- Doganlar, Z.B., Güçlü, H., Öztopuz, Ö., Türkön, H., Dogan, A., Uzun, M. & Doganlar, O., 2019. The role of melatonin in oxidative stress, DNA damage, apoptosis and angiogenesis in fetal eye under preeclampsia and melatonin deficiency stress. *Curr Eye Res*, **0**, 1–13, Taylor & Francis. doi:10.1080/02713683.2019.1619778
- Dorn, G.W., 2007. The Fuzzy Logic of Physiological Cardiac Hypertrophy. *Hypertension*, **49**, 962–970, Lippincott Williams & Wilkins. doi:10.1161/HYPERTENSIONAHA.106.079426

- Douglas S. Kerr, 2010. Treatment of mitochondrial electron transport chain disorders: a review of clinical trials over the past decade. *Mol Genet Metab*, **99**, Mol Genet Metab. doi:10.1016/J.YMGME.2009.11.005
- Du, X.-J., Cole, T.J., Tennis, N., Gao, X.-M., Köntgen, F., Kemp, B.E. & Heierhorst, J., 2002. Impaired Cardiac Contractility Response to Hemodynamic Stress in S100A1-Deficient Mice. *Mol Cell Biol*, **22**, 2821–2829, Informa UK Limited. doi:10.1128/mcb.22.8.2821-2829.2002
- Dual, S.A. & Schmid Daners, M., 2022. Intelligent Systems and Smart Devices for the Continuous Monitoring of Cardiac Hemodynamics. *Advances in Cardiovascular Technology*, 489–500, Elsevier. doi:10.1016/B978-0-12-816861-5.00007-1
- Ducray, J.F., Naicker, T. & Moodley, J., 2011. Pilot study of comparative placental morphometry in pre-eclamptic and normotensive pregnancies suggests possible maladaptations of the fetal component of the placenta. *European Journal of Obstetrics and Gynecology and Reproductive Biology*, **156**, 29–34, Elsevier Ireland Ltd. doi:10.1016/j.ejogrb.2010.12.038
- Dunsworth, H.M., Warrener, A.G., Deacon, T., Ellison, P.T. & Pontzer, H., 2012. Metabolic hypothesis for human altriciality. *Proc Natl Acad Sci U S A*, **109**, 15212–15216, National Academy of Sciences. doi:10.1073/pnas.87.6.2324
- Duvekot, J.J., Cheriex, E.C., Pieters, F.A.A., Menheere, P.P.C.A. & Peeters, L.L.H., 1993. Early pregnancy changes in hemodynamics and volume homeostasis are consecutive adjustments triggered by a primary fall in systemic vascular tone. *Journal of Obstetric Gynecology*, **169**, 1382–1392.
- Duvekot, J.J., Cheriex, E.C., Pieters, F.A.A., Menheere, P.P.C.A., Schouten, H.J.A. & Peeters, L.L.H., 1995. Maternal Volume Homeostasis in Early Pregnancy in Relation to Fetal Growth Restriction. *Journal of Obstetrics & Gynecology*, **85**, 361–368.
- Duvekot, J.J. & Peeters, L.L.H., 1994. Maternal cardiovascular hemodynamic adaptation to pregnancy. *Obstet Gynecol Surv*, **49**, S1–S14, Obstet Gynecol Surv. doi:10.1097/00006254-199412011-00001

- Dypvik, J., Larsen, S., Haavaldsen, C., Jukic, A.M., Vatten, L.J. & Eskild, A., 2017. Placental weight in the first pregnancy and risk for preeclampsia in the second pregnancy: A population-based study of 186 859 women. *European Journal of Obstetrics and Gynecology and Reproductive Biology*, **214**, 184–189, Elsevier Ireland Ltd. doi:10.1016/j.ejogrb.2017.05.010
- Easterling, T., Benedetti, T., Schmucker, B. & Millard, S., 1990. Maternal Hemodynamics in Normal and Preeclamptic Pregnancies...: Obstetrics & Gynecology. *Obstetrics & Gynecology*, **76**, 1061–1069. Retrieved from https://journals.lww.com/greenjournal/Abstract/1990/12000/Maternal_Hemodynamics_in_Normal_and_Preeclamptic.14.aspx
- Eddy, A.C., Bidwell Iii, G.L. & George, E.M., 2018. Pro-angiogenic therapeutics for preeclampsia. *Biol Sex Differ*. doi:10.1186/s13293-018-0195-5
- Eder, D.J. & Mcdonald, M.T., 1987. A role for brain angiotensin II in experimental pregnancy-induced hypertension in laboratory rats. *Hypertens Pregnancy*, **B6**, 431–451, Informa Healthcare. doi:10.3109/10641958709023492
- Eghbal, M.A., Pennefather, P.S. & O'Brien, P.J., 2004. H₂S cytotoxicity mechanism involves reactive oxygen species formation and mitochondrial depolarisation. *Toxicology*, **203**, 69–76, Toxicology. doi:10.1016/j.tox.2004.05.020
- Eghbali, M., Deva, R., Alioua, A., Minosyan, T.Y., Ruan, H., Wang, Y., Toro, L., *et al.*, 2005. Molecular and functional signature of heart hypertrophy during pregnancy. *Circ Res*, **96**, 1208–1216. doi:10.1161/01.RES.0000170652.71414.16/FORMAT/EPUB
- Ehler, E., 2018. Actin-associated proteins and cardiomyopathy—the ‘unknown’ beyond troponin and tropomyosin. *Biophys Rev*, **10**, 1128, Springer. doi:10.1007/S12551-018-0428-1
- Elkayam, U. & Bitar, F., 2005. Valvular Heart Disease and Pregnancy: Part II: Prosthetic Valves. *J Am Coll Cardiol*, **46**, 403–410, Elsevier. doi:10.1016/J.JACC.2005.02.087
- Elliot, M.G., 2016. Oxidative stress and the evolutionary origins of preeclampsia. *J Reprod Immunol*, **114**, 75–80, Elsevier Ireland Ltd. doi:10.1016/j.jri.2016.02.003

- Elrod, J.W., Calvert, J.W., Morrison, J., Doeller, J.E., Kraus, D.W., Tao, L., Jiao, X., *et al.*, 2007. Hydrogen sulfide attenuates myocardial ischemia-reperfusion injury by preservation of mitochondrial function. *PNAS*, **104**, 15560–15565.
- Emelyanova, L., Ashary, Z., Cosic, M., Negmadjanov, U., Ross, G., Rizvi, F., Olet, S., *et al.*, 2016. Selective downregulation of mitochondrial electron transport chain activity and increased oxidative stress in human atrial fibrillation. *Am J Physiol Heart Circ Physiol*, **311**, H54–H63, *Am J Physiol Heart Circ Physiol*. doi:10.1152/AJPHEART.00699.2015
- English, F.A., Kenny, L.C. & Mccarthy, F.P., 2015. Risk Factors and effective management of preeclampsia. *Integr Blood Press Control*, **8**, 7–12. doi:10.2147/IBPC.S50641
- Enquobahrie, D.A., Abetew, D.F., Sorensen, T.K., Willoughby, D., Chidambaram, K. & Williams, M.A., 2011. Placental microRNA expression in pregnancies complicated by preeclampsia. *Am J Obstet Gynecol*, **204**, 178.e12-178.e21, Elsevier Inc. doi:10.1016/j.ajog.2010.09.004
- Enquobahrie, D.A., Qiu, C., Muhie, S.Y. & Williams, M.A., 2011. Maternal peripheral blood gene expression in early pregnancy and preeclampsia. *Int J Mol Epidemiol Genet*, **2**, 94, e-Century Publishing Corporation. Retrieved from /pmc/articles/PMC3077242/
- Erusalimsky, J.D., 2009. Vascular endothelial senescence: From mechanisms to pathophysiology. *J Appl Physiol*, **106**, 326–332. doi:10.1152/jappphysiol.91353.2008
- Escouto, D.C., Green, A., Kurlak, L., Walker, K., Loughna, P., Chappell, L., Broughton Pipkin, F., *et al.*, 2018. Postpartum evaluation of cardiovascular disease risk for women with pregnancies complicated by hypertension. *Pregnancy Hypertens*, **13**, 218–224, Elsevier B.V. doi:10.1016/j.preghy.2018.06.019
- Estensen, M.E., Beitnes, J.O., Grindheim, G., Aaberge, L., Smiseth, O.A., Henriksen, T. & Aakhus, S., 2013. Altered maternal left ventricular contractility and function during normal pregnancy. *Ultrasound in Obstetrics and Gynecology*, **41**, 659–666. doi:10.1002/uog.12296

- Evans, C.S., Gooch, L., Flotta, D., Lykins, D., Powers, R.W., Landsittel, D., Roberts, J.M., *et al.*, 2011. Cardiovascular system during the postpartum state in women with a history of preeclampsia. *Hypertension*, **58**, 57–62. doi:10.1161/HYPERTENSIONAHA.111.173278
- Evans, C.S., Gooch, L., Flotta, D., Lykins, D., Powers, R.W., Landsittel, D., Roberts, J.M., *et al.*, 2011. Cardiovascular system during the postpartum state in women with a history of preeclampsia. *Hypertension*, **58**, 57–62, Magee-Womens Hospital. doi:10.1161/HYPERTENSIONAHA.111.173278
- Everett, T.R., Mahendru, A.A., McEniery, C.M., Wilkinson, I.B. & Lees, C.C., 2012. Raised uterine artery impedance is associated with increased maternal arterial stiffness in the late second trimester. *Placenta*, **33**, 572–577, Placenta. doi:10.1016/J.PLACENTA.2012.04.001
- F Hytten, 1985. Blood volume changes in normal pregnancy. *Clinical Haematology*, **14**, 601–612.
- F J Dagher, J H Lyons, D C Finlayson, J Shamsai & F D Moore, 1965. Blood volume measurement: a critical study prediction of normal values: controlled measurement of sequential changes: choice of a bedside method. *Advanced Surgery*, **1**, 69–109.
- Fabbro, D., D'Elia, A. V., Spizzo, R., Driul, L., Barillari, G., Loreto, C. Di, Marchesoni, D., *et al.*, 2003. Association between plasminogen activator inhibitor 1 gene polymorphisms and preeclampsia. *Gynecol Obstet Invest*, **56**, 17–22, Gynecol Obstet Invest. doi:10.1159/000072326
- Falco, M.L., Sivanathan, J., Laoreti, A., Thilaganathan, B. & Khalil, A., 2017. Placental histopathology associated with pre-eclampsia: systematic review and meta-analysis. *Ultrasound in Obstetrics & Gynecology*, **50**, 295–301, John Wiley and Sons Ltd. doi:10.1002/uog.17494
- Fan, X., Rai, A., Kambham, N., Sung, J.F., Singh, N., Petitt, M., Dhal, S., *et al.*, 2014. Endometrial VEGF induces placental sFLT1 and leads to pregnancy complications. *Journal of Clinical Investigation*, **124**, 4941–4952, American Society for Clinical Investigation. doi:10.1172/JCI76864

- Fatmeh, J. & Farahnaz, C., 2018. Seasonal variation in the prevalence of preeclampsia. *Journal of Family Medicine*, **6**, 766–769. Retrieved from 10.4103/jfmpc.jfmpc_132_17
- Faust, J.R., Hamill, D., Kolb, E.A., Gopalakrishnapillai, A. & Barwe, S.P., 2022. Mesothelin: An Immunotherapeutic Target beyond Solid Tumors. *Cancers 2022*, Vol. 14, Page 1550, **14**, 1556, Multidisciplinary Digital Publishing Institute. doi:10.3390/CANCERS14061550
- Feher, J., 2012. The Heart as a Pump. *Quantitative Human Physiology*, 446–454, Elsevier. doi:10.1016/B978-0-12-382163-8.00047-5
- Feo, S., Arcuri, D., Piddini, E., Passantino, R. & Giallongo, A., 2000. ENO1 gene product binds to the c-myc promoter and acts as a transcriptional repressor: relationship with Myc promoter-binding protein 1 (MBP-1). *FEBS Lett*, **473**, 47–52, FEBS Lett. doi:10.1016/S0014-5793(00)01494-0
- Ferreira, A.F., Azevedo, M.J., Proenca, T., Saraiva, F.A., Machado, A.P., Sousa, C., Sampaio Maia, B., *et al.*, 2021. Cardiac remodelling and reverse remodelling in pregnant women: what can be expected? *Eur Heart J*, **42**, 2904. Retrieved from https://academic.oup.com/eurheartj/article/42/Supplement_1/ehab724.2904/6392460
- Feuerborn, A., Mathow, D., Srivastava, P.K., Gretz, N. & Gröne, H.J., 2015. Basonuclin-1 modulates epithelial plasticity and TGF- β 1-induced loss of epithelial cell integrity. *Oncogene*, **34**, 1185–1195, Nature Publishing Group. doi:10.1038/onc.2014.54
- Fields, A.P., Bednarik, D.P., Hess, A. & Stratford May, W., 1988. Human immunodeficiency virus induces phosphorylation of its cell surface receptor. *Nature*, **333**, 278–280, Nature. doi:10.1038/333278A0
- Fillmore, N., Mori, J. & Lopaschuk, G.D., 2014. Mitochondrial fatty acid oxidation alterations in heart failure, ischaemic heart disease and diabetic cardiomyopathy. *Br J Pharmacol*, **171**, 2090, Wiley-Blackwell. doi:10.1111/BPH.12475
- Fok, W.Y., Chan, L.Y., Wong, J.T., Yu, C.M. & Lau, T.K., 2006. Left ventricular diastolic function during normal pregnancy: Assessment by spectral tissue Doppler imaging. *Ultrasound in Obstetrics and Gynecology*, **28**, 789–793. doi:10.1002/uog.3849

- Foo, F.L., Mahendru, A.A., Masini, G., Fraser, A., Cacciatore, S., MacIntyre, D.A., McEniery, C.M., *et al.*, 2018. Association Between Prepregnancy Cardiovascular Function and Subsequent Preeclampsia or Fetal Growth Restriction. *Hypertension*, **72**, 442–450, Lippincott Williams & Wilkins Hagerstown, MD . doi:10.1161/HYPERTENSIONAHA.118.11092
- Ford, J., Iii, C. & Capeless, E., 1997. Cardiovascular Function Before, During, and After the First and Subsequent Pregnancies. *by Excerpta Medica, Inc*, Vol. 80.
- Forrest, M., Bourgeois, S., Pichette, É., Caughlin, S., Kuate Defo, A., Hales, L., Labos, C., *et al.*, 2022. Arterial stiffness measurements in pregnancy as a predictive tool for hypertensive disorders of pregnancy and preeclampsia: Protocol for a systematic review and meta-analysis. *Eur J Obstet Gynecol Reprod Biol X*, **13**, Elsevier Ireland Ltd. doi:10.1016/j.eurox.2022.100141
- Forsythe, J.A., Jiang, B.H., Iyer, N. V, Agani, F., Leung, S.W., Koos, R.D. & Semenza, G.L., 1996. Activation of vascular endothelial growth factor gene transcription by hypoxia-inducible factor 1. *Mol Cell Biol*, **16**, 4604–4613, American Society for Microbiology. doi:10.1128/mcb.16.9.4604
- Foster, E., Sharma, G.K., Carson, M. & Blissett, S., 2019. Peripartum (Postpartum) Cardiomyopathy (PPCM). *eMedicine*. Retrieved June 15, 2023, from <https://emedicine.medscape.com/article/153153-overview>
- Fox, H. & Elston, C.W., 1978. *Pathology of the placenta. Major Probl Pathol*, Vol. 7.
- Frost, A.L., Suriano, K., Aye, C.Y.L., Leeson, P. & Lewandowski, A.J., 2021, May 31. The Immediate and Long-Term Impact of Preeclampsia on Offspring Vascular and Cardiac Physiology in the Preterm Infant. *Front Pediatr*, Frontiers Media S.A. doi:10.3389/fped.2021.625726
- Fu, M., Zhang, W., Wu, L., Yang, G., Li, H. & Wang, R., 2012. Hydrogen sulfide (H₂S) metabolism in mitochondria and its regulatory role in energy production. *Proc Natl Acad Sci U S A*, **109**, 2943–2948, National Academy of Sciences. doi:10.1073/PNAS.1115634109/SUPPL_FILE/PNAS.201115634SI.PDF

- Fujioka, H., Kaibuchi, K., Kikuchi, A., Kawata, M., Sasaki, T. & Yamamoto, T., 1991. Transforming and c-fos promoter/enhancer-stimulating activities of a GDP/GTP exchange protein for small GTP-binding proteins. *Princess Takamatsu Symp*, **22**, 197–204.
- Fujita, K.A., Ostaszewski, M., Matsuoka, Y., Ghosh, S., Glaab, E., Trefois, C., Crespo, I., *et al.*, 2014. Integrating Pathways of Parkinson's Disease in a Molecular Interaction Map. *Mol Neurobiol*, **49**, 88–102, Humana Press Inc. doi:10.1007/s12035-013-8489-4
- Fulghum, K.L., Smith, J.B., Chariker, J., Garrett, L.F., Brittan, K.R., Lorkiewicz, P., McNally, L.A., *et al.*, 2022. Metabolic signatures of pregnancy-induced cardiac growth. *Am J Physiol Heart Circ Physiol*, **323**, 1–56, Am J Physiol Heart Circ Physiol. doi:10.1152/AJPHEART.00105.2022
- Gammill, H.S., Chettier, R., Brewer, A., Roberts, J.M., Shree, R., Tsigas, E. & Ward, K., 2018. Cardiomyopathy and Preeclampsia: Shared Genetics? *Circulation*, **138**, 2359–2366, Lippincott Williams and Wilkins. doi:10.1161/CIRCULATIONAHA.117.031527
- Gao, X.-Y., Yang, T., Gu, Y. & Sun, X.-H., 2022. Mitochondrial Dysfunction in Parkinson's Disease: From Mechanistic Insights to Therapy. *Front Aging Neurosci*, **14**, 1–17, Frontiers Media SA. doi:10.3389/FNAGI.2022.885500
- Garovic, V.D. & August, P., 2013, April. Preeclampsia and the future risk of hypertension: The pregnant evidence. *Curr Hypertens Rep*, *Curr Hypertens Rep*. doi:10.1007/s11906-013-0329-4
- Garovic, V.D., Bailey, K.R., Boerwinkle, E., Hunt, S.C., Weder, A.B., Curb, D., Mosley, T.H., *et al.*, 2010. Hypertension in pregnancy as a risk factor for cardiovascular disease later in life. *J Hypertens*, **28**, 826–833, Lippincott Williams and Wilkins. doi:10.1097/HJH.0b013e3283335c29a
- Garrido-Gimenez, C., Mendoza, M., Cruz-Lemini, M., Galian-Gay, L., Sanchez-Garcia, O., Granato, C., Rodriguez-Sureda, V., *et al.*, 2020. Angiogenic Factors and Long-Term Cardiovascular Risk in Women That Developed Preeclampsia during Pregnancy. *Hypertension*, 1808–1816, Lippincott Williams and Wilkins. doi:10.1161/HYPERTENSIONAHA.120.15830

- Gebara, N., Correia, Y., Wang, K. & Bussolati, B., 2021. Angiogenic Properties of Placenta-Derived Extracellular Vesicles in Normal Pregnancy and in Preeclampsia. *Int J Mol Sci*, **22**, Int J Mol Sci. doi:10.3390/IJMS22105402
- Gehen, S.C., Vitiello, P.F., Bambara, R.A., Keng, P.C. & O'Reilly, M.A., 2007. Downregulation of PCNA potentiates p21-mediated growth inhibition in response to hyperoxia. *Am J Physiol Lung Cell Mol Physiol*, **292**, 716–724, Am J Physiol Lung Cell Mol Physiol. doi:10.1152/AJPLUNG.00135.2006
- Gelman, I.H., 2010. Emerging roles for SSeCKS/Gravin/AKAP12 in the control of cell proliferation, cancer malignancy, and barrierogenesis. *Genes Cancer*, **1**, 1147–1156, SAGE Publications Inc. doi:10.1177/1947601910392984/ASSET/IMAGES/LARGE/10.1177_1947601910392984-FIG4.JPEG
- Gennari-Moser, C., Khankin, E. V., Schüller, S., Escher, G., Frey, B.M., Portmann, C.B., Baumann, M.U., *et al.*, 2011. Regulation of placental growth by aldosterone and cortisol. *Endocrinology*, **152**, 263–271. doi:10.1210/en.2010-0525
- George, E.M., Liu, H., Robinson, G.B.G. & Bidwell, G.L., 2014. A Polypeptide Drug Carrier for Maternal Delivery and Prevention of Fetal Exposure. *J Drug Target*, **22**, 935–947. doi:10.3109/1061186X.2014.950666
- George, E.M., Liu, H., Robinson, G.G., Mahdi, F., Perkins, E. & Bidwell, G.L., 2015. Growth factor purification and delivery systems (PADS) for therapeutic angiogenesis. *Vasc Cell*, **7**, 8, BioMed Central Ltd. doi:10.1186/s13221-014-0026-3
- Gerbasi, F.R., Bottoms, S., Farag, A. & Mammen, E.F., 1990. Changes in hemostasis activity during delivery and the immediate postpartum period. *Am J Obstet Gynecol*, **162**, 1158–1163, Mosby. doi:10.1016/0002-9378(90)90006-S
- Gerhardt, A., Goecke, T.W., Beckmann, M.W., Wagner, K.J., Tutschek, B., Willers, R., Bender, H.G., *et al.*, 2005. The G20210A prothrombin-gene mutation and the plasminogen activator inhibitor (PAI-1) 5G/5G genotype are associated with early onset of severe preeclampsia. *J Thromb Haemost*, **3**, 686–691, J Thromb Haemost. doi:10.1111/J.1538-7836.2005.01226.X

- Gerhardt, G.S., Peters, W.H.M., Hillermann, R., Odendaal, H.J., Carelse-Tofa, K., Raijmakers, M.T.M. & Steegers, E.A.P., 2004. Maternal and fetal single nucleotide polymorphisms in the epoxide hydrolase and glutathione S-transferase P1 genes are not associated with pre-eclampsia in the Coloured population of the Western Cape, South Africa. *J Obstet Gynaecol*, **24**, 866–872, J Obstet Gynaecol. doi:10.1080/01443610400018841
- Gerő, D., Torregrossa, R., Perry, A., Waters, A., Le-Trionnaire, S., Whatmore, J.L., Wood, M., *et al.*, 2016. The novel mitochondria-targeted hydrogen sulfide (H₂S) donors AP123 and AP39 protect against hyperglycemic injury in microvascular endothelial cells in vitro. *Pharmacol Res*, **113**, 186–198, Pharmacol Res. doi:10.1016/J.PHRS.2016.08.019
- Geva, T., Mauer, M.B., Striker, L., Kirshon, B., Pivarnik, J.M. & Houston, E., 1997. Effects of physiologic load of pregnancy on left ventricular contractility and remodeling. *Am Heart J*, Vol. 133, pp. 53–60.
- Ghaemi, M.S., Tarca, A.L., Romero, R., Stanley, N., Fallahzadeh, R., Tanada, A., Culos, A., *et al.*, 2022. Proteomic signatures predict preeclampsia in individual cohorts but not across cohorts – implications for clinical biomarker studies. *J Matern Fetal Neonatal Med*, **35**, 5628, NIH Public Access. doi:10.1080/14767058.2021.1888915
- Gigante, B., Morlino, G., Gentile, M.T., Persico, M.G. & Falco, S. De, 2006. Plgf / eNos / mice show defective angiogenesis associated with increased oxidative stress in response to tissue ischemia. *The FASEB Journal*, **20**, 970–979. doi:10.1096/fj.05-4481fje
- Gilbert, J.S., Babcock, S.A. & Granger, J.P., 2007. Hypertension Produced by Reduced Uterine Perfusion in Pregnant Rats Is Associated With Increased Soluble Fms-Like Tyrosine Kinase-1 Expression. *Pregnancy Hypertens*, **50**, 1142–1147. doi:10.1161/HYPERTENSIONAHA.107.096594
- Gilbert, J.S., Verzwylt, J., Colson, D., Arany, M., Ananth Karumanchi, S. & Granger, J.P., 2010. Recombinant VEGF 121 infusion lowers blood pressure and improves renal function in rats with placental ischemia-induced hypertension. *Hypertension*, **55**, 380–385. doi:10.1161/HYPERTENSIONAHA.109.141937
- Gilson, G. 1, Samaan, S., Crawford, M.H., Qualls, C.R. & Curet, L.B., 1997. Changes in Hemodynamics, Ventricular Remodeling, and Ventricular Contractility During Normal

- Pregnancy: A Longitudinal Study. *The American College of Obstetricians and Gynecologists*, **89**, 957–962.
- Gimbrone, M.A. & García-Cardena, G., 2016. Endothelial Cell Dysfunction and the Pathobiology of Atherosclerosis. *Circ Res*, **118**, 620–636, *Circ Res*. doi:10.1161/CIRCRESAHA.115.306301
- Giorgione, V., Khalil, A., O'driscoll, J. & Thilaganathan, B., 2023. Postpartum Cardiovascular Function In Patients With Hypertensive Disorders Of Pregnancy: A Longitudinal Study. *Am J Obstet Gynecol*, Elsevier BV. doi:10.1016/j.ajog.2023.03.019
- Giorgione, V., Khalil, A., O'driscoll, J. & Thilaganathan, B., 2023. Postpartum cardiovascular function in patients with hypertensive disorders of pregnancy: a longitudinal study. *American Journal of Obstetrics & Gynaecology*, 1–15. doi:10.1016/j.ajog.2023.03.019
- Glavan, D., Gheorman, V., Gresita, A., Hermann, D.M., Udristoiu, I. & Popa-Wagner, A., 2021. Identification of transcriptome alterations in the prefrontal cortex, hippocampus, amygdala and hippocampus of suicide victims. *Sci Rep*, **11**, 18867, Nature Publishing Group. doi:10.1038/S41598-021-98210-6
- Goffart, S., Kleist-Retzow, J.C. Von & Wiesner, R.J., 2004. Regulation of mitochondrial proliferation in the heart: Power-plant failure contributes to cardiac failure in hypertrophy. *Cardiovasc Res*, **64**, 198–207, Oxford Academic. doi:10.1016/J.CARDIORES.2004.06.030/2/64-2-198-FIG2.GIF
- Gökdemir, İ.E., Evliyaoğlu, Ö. & Çoşkun, B., 2016. The role of ADAMTS genes in preeclampsia. *Turk J Obstet Gynecol*, **13**, 153, Turkish Society of Obstetrics and Gynecology. doi:10.4274/TJOD.57701
- Gokina, N.I., Fairchild, R.I., Bishop, N.M., Dawson, T.E., Prakash, K. & Bonney, E.A., 2021. Kinetics of Postpartum Mesenteric Artery Structure and Function Relative to Pregnancy and Lactation in Mice. *Reproductive Sciences*, **28**, 1200–1215. doi:10.1007/s43032-020-00402-4/Published
- Goksu Erol, A.Y., Nazli, M. & Yildiz, S.E., 2012. Significance of platelet endothelial cell adhesion molecule-1 (PECAM-1) and intercellular adhesion molecule-1 (ICAM-1)

- expressions in preeclamptic placentae. *Endocrine*, **42**, 125–131, Springer. doi:10.1007/s12020-012-9644-9
- Goldsmith, L.T. & Weiss, G., 2009. Relaxin in human pregnancy. *Ann N Y Acad Sci*, Vol. 1160, pp. 130–135, Blackwell Publishing Inc. doi:10.1111/j.1749-6632.2008.03800.x
- Gordon, A.M., Regnier, M. & Homsher, E., 2001. Skeletal and cardiac muscle contractile activation: Tropomyosin 'rocks and rolls'. *News in Physiological Sciences*, **16**, 49–55, American Physiological Society. doi:10.1152/PHYSIOLOGYONLINE.2001.16.2.49/ASSET/IMAGES/MEDIUM/015106A.JPG
- Gormley, M., Ona, K., Kapidzic, M., Garrido-Gomez, T., Zdravkovic, T. & Fisher, S.J., 2017. Preeclampsia: novel insights from global RNA profiling of trophoblast subpopulations. *Am J Obstet Gynecol*, **217**, 200.e1-200.e17, Mosby. doi:10.1016/j.AJOG.2017.03.017
- Gourvas, V., Soultzis, N., Konstantinidou, A., Dalpa, E., Koukoura, O., Koutroulakis, D., Spandidos, D.A., *et al.*, 2014. Reduced ANXA5 mRNA and protein expression in pregnancies complicated by preeclampsia. *Thromb Res*, **133**, 495–500. doi:10.1016/j.thromres.2013.12.027
- Graves, S.W., Seely, E.W. & Williams, G.H., 1993. Genes, phenotypes and hypertensive pregnancies. *Nat Genet*, **4**, 7–8. doi:10.1038/ng0593-7
- Gruson, D., Hermans, M.P., Ferracin, B., Ahn, S.A. & Rousseau, M.F., 2016. Sflt-1 in heart failure: relation with disease severity and biomarkers. *Scand J Clin Lab Invest*, **76**, 411–416, Scand J Clin Lab Invest. doi:10.1080/00365513.2016.1190863
- Gruson, D., Hermans, M.P., Ferracin, B., Ahn, S.A. & Rousseau, M.F., 2016. Sflt-1 in heart failure: relation with disease severity and biomarkers. *Scand J Clin Lab Invest*, **76**, 411–416, Taylor and Francis Ltd. doi:10.1080/00365513.2016.1190863
- Guedes-Martins, L., Cunha, A., Saraiva, J., Gaio, R., Macedo, F. & Almeida, H., 2014. Internal iliac and uterine arteries Doppler ultrasound in the assessment of normotensive and chronic hypertensive pregnant women. *Sci Rep*, **4**, Nature Publishing Group. doi:10.1038/srep03785

- Guedes-Martins, L., Gaio, A.R., Saraiva, J., Cunha, A., Macedo, F. & Almeida, H., 2015. Uterine artery impedance during the first eight postpartum weeks. *Sci Rep*, **5**, 8786–8798, Nature Publishing Group. doi:10.1038/SREP08786
- Gupta, K. & Zhang, J., 2005, April. Angiogenesis: A curse or cure? *Postgrad Med J*. doi:10.1136/pgmj.2004.023309
- Gutgesell, A., Ringseis, R., Schmidt, E., Brandsch, C., Stangl, G.I. & Eder, K., 2009. Downregulation of peroxisome proliferator-activated receptor α and its coactivators in liver and skeletal muscle mediates the metabolic adaptations during lactation in mice. *J Mol Endocrinol*, **43**, 241–250, Society for Endocrinology. doi:10.1677/JME-09-0064
- Gutman, J. & Parrilla, A., 2022. Role of glutathione in the pathophysiology of pre-eclampsia: implications for nutritional intervention. *Gutman and Parrilla*, **1**, 23. doi:10.1097/PN9.0000000000000023
- Gyselaers, W., Mullens, W., Tomsin, K., Mesens, T. & Peeters, L., 2011, August. Role of dysfunctional maternal venous hemodynamics in the pathophysiology of pre-eclampsia: A review. *Ultrasound in Obstetrics and Gynecology*. doi:10.1002/uog.9061
- Gyselaers, W., Mullens, W., Tomsin, K., Mesens, T. & Peeters, L., 2011. Role of dysfunctional maternal venous hemodynamics in the pathophysiology of pre-eclampsia: a review. *Ultrasound Obstet Gynecol*, **38**, 123–129. doi:10.1002/uog.9061
- Haas, S. de, Spaanderman, M.E.A., Kuijk, S.M.J. van, Drongelen, J. van, Mohseni, Z., Jorissen, L. & Ghossein-Doha, C., 2021. Adaptation of left ventricular diastolic function to pregnancy: a systematic review and meta-analysis. *J Hypertens*, **39**, 1934–1941, NLM (Medline). doi:10.1097/HJH.0000000000002886
- Hagmann, H., Thadhani, R., Benzing, T., Karumanchi, S.A. & Stepan, H., 2012. The promise of angiogenic markers for the early diagnosis and prediction of preeclampsia. *Clin Chem*, **58**, 837–845, Clin Chem. doi:10.1373/CLINCHEM.2011.169094
- Hahn, S. & Holzgreve, W., 2002. Fetal cells and cell-free fetal DNA in maternal blood: new insights into pre-eclampsia. *Hum Reprod Update*, **8**, 501–508. Retrieved from <https://academic.oup.com/humupd/article-abstract/8/6/501/718644>

- Hale, S.A., Sobel, B., Benvenuto, A., Schonberg, A., Badger, G.J. & Bernstein, I.M., 2012. Coagulation and fibrinolytic system protein profiles in women with normal pregnancies and pregnancies complicated by hypertension. *Pregnancy Hypertens*, **2**, 152–157. doi:10.1016/j.preghy.2012.01.004
- Hall, M.E., George, E.M. & Granger, J.P., 2011. The Heart During Pregnancy. *Rev Esp Cardiol*, **64**, 1045, NIH Public Access. doi:10.1016/J.RECESP.2011.07.009
- Hallum, S., Basit, S., Kamper-Jørgensen, M., Sehested, T.S.G. & Boyd, H.A., 2023. Risk and trajectory of premature ischaemic cardiovascular disease in women with a history of pre-eclampsia: a nationwide register-based study. *Eur J Prev Cardiol*, Oxford University Press (OUP). doi:10.1093/EURJPC/ZWAD003
- Hamad, R.R., Larsson, A., Pernow, J., Bremme, K. & Eriksson, M.J., 2009. Assessment of left ventricular structure and function in preeclampsia by echocardiography and cardiovascular biomarkers. *J Hypertens*, **27**, 2257–2264, Lippincott Williams and Wilkins. doi:10.1097/HJH.0B013E3283300541
- Hamza, A., Gerlinger, C., Radosa, J., Solomayer, E.F., Hagmann, J., Sester, U., Bohle, R., *et al.*, 2019. Pilot study: placental biomarker predictive capability (sFit-1, PIGF and their ratio) of postpartum maternal outcome. *Arch Gynecol Obstet*, **299**, 1557–1566, Springer Verlag. doi:10.1007/S00404-019-05128-6/TABLES/4
- Hansson, S.R., Nääv, Å. & Erlandsson, L., 2015. Oxidative stress in preeclampsia and the role of free fetal hemoglobin. *Front Physiol*, **6**, 1–11, Frontiers Media S.A. doi:10.3389/fphys.2014.00516
- Haram, K., Mortensen, J.H., Myking, O., Magann, E.F. & Morrison, J.C., 2019. The Role of Oxidative Stress, Adhesion Molecules and Antioxidants in Preeclampsia. *Curr Hypertens Rev*, **15**, 105–112. doi:10.2174/1573402115666190119163942
- Harmelink, C., Peng, Y., DeBenedittis, P., Chen, H., Shou, W. & Jiao, K., 2013. Myocardial Mycn is essential for mouse ventricular wall morphogenesis. *Dev Biol*, **373**, 53–63, Academic Press Inc. doi:10.1016/j.ydbio.2012.10.005

- Harrison, M.B., Kumar, S., Hubbard, C.A. & Trugman, J.M., 2001. Early changes in neuropeptide mRNA expression in the striatum following reserpine treatment. *Exp Neurol*, **167**, 321–328. doi:10.1006/exnr.2000.7555
- Hastie, R. & Lappas, M., 2014. The effect of pre-existing maternal obesity and diabetes on placental mitochondrial content and electron transport chain activity. *Placenta*, **35**, 673–683, W.B. Saunders Ltd. doi:10.1016/j.placenta.2014.06.368
- Hastie, Roxanne, Brownfoot, F.C., Pritchard, N., Hannan, N.J., Cannon, P., Nguyen, V., Palmer, K., *et al.*, 2019. EGFR (Epidermal Growth Factor Receptor) Signaling and the Mitochondria Regulate sFlt-1 (Soluble FMS-Like Tyrosine Kinase-1) Secretion. *Hypertension*, **73**, 659–670, Lippincott Williams and Wilkins. doi:10.1161/HYPERTENSIONAHA.118.12300
- Haug, E.B., Horn, J., Markovitz, A.R., Fraser, A., Klykken, B., Dalen, H., Vatten, L.J., *et al.*, 2019. Association of Conventional Cardiovascular Risk Factors With Cardiovascular Disease After Hypertensive Disorders of Pregnancy: Analysis of the Nord-Trøndelag Health Study. *JAMA Cardiol*, **4**, 628–635, JAMA Cardiol. doi:10.1001/JAMACARDIO.2019.1746
- Hauge, M.G., Damm, P., Kofoed, K.F., Ersbøll, A.S., Johansen, M., Sigvardsen, P.E., Møller, M.B., *et al.*, 2022. Early Coronary Atherosclerosis in Women With Previous Preeclampsia. *J Am Coll Cardiol*, **79**, 2310–2321, J Am Coll Cardiol. doi:10.1016/J.JACC.2022.03.381
- Hauspurg, A., Countouris, M.E., Jeyabalan, A., Hubel, C.A., Roberts, J.M., Schwarz, E.B. & Catov, J.M., 2019. Risk of hypertension and abnormal biomarkers in the first year postpartum associated with hypertensive disorders of pregnancy among overweight and obese women. *Pregnancy Hypertens*, **15**, 1–6, Elsevier B.V. doi:10.1016/j.preghy.2018.10.009
- Hausvater, A., Giannone, T., Sandoval, Y.H.G., Doonan, R.J., Antonopoulos, C.N., Matsoukis, I.L., Petridou, E.T., *et al.*, 2012. The association between preeclampsia and arterial stiffness. *J Hypertens*, **30**, 17–33, Lippincott Williams and Wilkins. doi:10.1097/HJH.0B013E32834E4B0F

- Havenon, A. De, Delic, A., Stulberg, E., Sheibani, N., Stoddard, G., Hanson, H. & Theilen, L., 2021. Association of Preeclampsia with Incident Stroke in Later Life among Women in the Framingham Heart Study. *JAMA Netw Open*, American Medical Association. doi:10.1001/jamanetworkopen.2021.5077
- Hayashi, Y., Lai, L., Kim, M.H., Leone, T.C., Vega, R.B. & Kelly, D.P., 2015. The Nuclear Receptor NR4A1 Regulates Transcriptional Programs Involved in Cardiac Fuel Metabolism and Hypertrophic Growth. *Circulation*, **132**, 1–24, Lippincott Williams & Wilkins Hagerstown, MD . doi:10.1161/CIRC.132.SUPPL_3.12289
- He, L., Wang, Z. & Sun, Y., 2004. Reduced amount of cytochrome c oxidase subunit I messenger RNA in placentas from pregnancies complicated by preeclampsia. *Acta Obstet Gynecol Scand*, **83**, 144–148, John Wiley & Sons, Ltd. doi:10.1111/j.0001-6349.2004.00345.x
- Healthwise Staff, 2019. Heart Failure With Reduced Ejection Fraction (Systolic Heart Failure) | UW Health | Madison, WI. Retrieved April 29, 2020, from <https://www.uwhealth.org/health/topic/special/heart-failure-with-reduced-ejection-fraction-systolic-heart-failure/tx4090abc.html>
- Heidrich, M.-B., Wenzel, D., Kaisenberg, C.S. Von, Schippert, C. & Versen-Höynck, F.M. Von, 2013. Preeclampsia and long-term risk of cardiovascular disease: what do obstetrician-gynecologists know? *BMC Pregnancy Childbirth*. doi:10.1186/1471-2393-13-61
- Hemant Suryawanshi, Pavel Morozov, Alexander Straus, Nicole Sahasrabudhe, Klaas E. A. Max, Aitor Garzia, Manjunath Kustagi, *et al.*, 2018. A single-cell survey of the human first-trimester placenta and decidua. *Sci Adv*, **4**, eaau4788. doi:10.1126/sciadv.aau4788
- Herrera, E. & Desoye, G., 2016. Maternal and fetal lipid metabolism under normal and gestational diabetic conditions. *Horm Mol Biol Clin Investig*, **26**, 109–127, Walter de Gruyter GmbH. doi:10.1515/HMBCI-2015-0025/ASSET/GRAPHIC/J_HMBCI-2015-0025_FIG_002.JPG
- Herrock, O., Deer, E. & LaMarca, B., 2023. Setting a stage: Inflammation during preeclampsia and postpartum. *Front Physiol*, **14**, 1–15, Frontiers Media S.A. doi:10.3389/FPHYS.2023.1130116/BIBTEX

- Hertig, A., Berkane, N., Lefevre, G., Toumi, K., Marti, H.-P., Capeau, J., Uzan, S., *et al.*, 2004. Maternal Serum sFlt1 Concentration Is an Early and Reliable Predictive Marker of Preeclampsia. *Clin Chem*, **50**, 1702–1703, Oxford Academic. doi:10.1373/clinchem.2004.036715
- Hertig, A.T., Rock, J. & Adams, E.C., 1956. A description of 34 human ova within the first 17 days of development. *American Journal of Anatomy*, **98**, 435–493, John Wiley & Sons, Ltd. doi:10.1002/aja.1000980306
- Heximer, S.P., Cristillo, A.D., Russell, L. & Forsdyke, D.R., 1996. Sequence analysis and expression in cultured lymphocytes of the human FOSB gene (G0S3). *DNA Cell Biol*, **15**, 1025–1038, DNA Cell Biol. doi:10.1089/DNA.1996.15.1025
- Hibbard, J.U., Korcarz, C.E., Nendaz, G.G., Lindheimer, M.D., Lang, R.M. & Shroff, S.G., 2005. The arterial system in pre-eclampsia and chronic hypertension with superimposed pre-eclampsia. *BJOG*, **112**, 897–903, John Wiley & Sons, Ltd. doi:10.1111/J.1471-0528.2005.00600.X
- Hilfiker-Kleiner, D. & Sliwa, K., 2014. Pathophysiology and epidemiology of peripartum cardiomyopathy. *Nat Rev Cardiol*, **11**, 364–370, Nat Rev Cardiol. doi:10.1038/NRCARDIO.2014.37
- Hill, B.C., Woon, T.C., Nicholls, P., Peterson, J., Greenwood, C. & Thomson, A.J., 1984. Interactions of sulphide and other ligands with cytochrome c oxidase. An electron-paramagnetic-resonance study. *Biochemical Journal*, **224**, 591–600, Portland Press. doi:10.1042/BJ2240591
- Hillner, Katharina M., Neumann, I.D., Couillard-Despres, S., Aigner, L. & Slattery, D.A., 2014. Lactation-induced reduction in hippocampal neurogenesis is reversed by repeated stress exposure. *Hippocampus*, **24**, 673–683, Hippocampus. doi:10.1002/HIPO.22258
- Hillner, Katharina Maria, Jacobs, V.R., Fischer, T. & Aigner, L., 2014. The maternal brain: An organ with peripartal plasticity. *Neural Plast*, **2014**, 1–20, Hindawi Publishing Corporation. doi:10.1155/2014/574159

- Hiratsuka, S., Maru, Y., Okada, A., Seiki, M., Noda, T. & Shibuya, M., 2001. Involvement of Flt-1 Tyrosine Kinase (Vascular Endothelial Growth Factor Receptor-1) in Pathological Angiogenesis 1. *Cancer Res*, Vol. 61. Retrieved from <http://aacrjournals.org/cancerres/article-pdf/61/3/1207/3252010/ch030101207p.pdf>
- Hoeben, A., Landuyt, B., Highley, M., Wildiers, H., Oosterom, A.T. Van & Bruijn, E.A., 2004. Vascular Endothelial Growth Factor and Angiogenesis. in *Pharmacological Reviews*, Vol. 56, pp. 549–580. doi:10.1124/pr.56.4.3.549
- Hofer, S., Blaha, J., Collins, P.W., Ducloy-Bouthors, A.S., Guasch, E., Labate, F., Lança, F., *et al.*, 2023. Haemostatic support in postpartum haemorrhage: A review of the literature and expert opinion. *Eur J Anaesthesiol*, **40**, 38, Wolters Kluwer Health. doi:10.1097/EJA.0000000000001744
- Holland, O., Dekker Nitert, M., Gallo, L.A., Vejzovic, M., Fisher, J.J. & Perkins, A. V., 2017. Review: Placental mitochondrial function and structure in gestational disorders. *Placenta*, **54**, 2–9, W.B. Saunders Ltd. doi:10.1016/j.placenta.2016.12.012
- Hollevoet, K., Mason-Osann, E., Müller, F. & Pastan, I., 2015. Methylation-Associated Partial Down-Regulation of Mesothelin Causes Resistance to Anti-Mesothelin Immunotoxins in a Pancreatic Cancer Cell Line. *PLoS One*, **10**, 122462–122473, PLOS. doi:10.1371/JOURNAL.PONE.0122462
- Holmes, D.I.R. & Zachary, I., 2004. Placental growth factor induces FosB and c-Fos gene expression via Flt-1 receptors. *FEBS Lett*, **557**, 93–98, Elsevier. doi:10.1016/S0014-5793(03)01452-2
- Holwerda, K. M., Bos, E.M., Rajakumar, A., Ris-Stalpers, C., Pampus, M.G. Van, Timmer, A., Erwich, J.J.H.M., *et al.*, 2012. Hydrogen sulfide producing enzymes in pregnancy and preeclampsia. *Placenta*, **33**, 518–521, W.B. Saunders. doi:10.1016/j.placenta.2012.02.014
- Holwerda, Kim M., Burke, S.D., Faas, M.M., Zsengeller, Z., Stillman, I.E., Kang, P.M., Goor, H. Van, *et al.*, 2014. Hydrogen Sulfide attenuates sFlt1-induced hypertension and renal damage by upregulating vascular endothelial growth factor. *Journal of the American Society of Nephrology*, **25**, 717–725. doi:10.1681/ASN.2013030291

- Honigberg, M.C., 2021, December 7. Understanding Heart Failure in Women With Preeclampsia: A Call for Prevention. *J Am Coll Cardiol*, Elsevier Inc. doi:10.1016/j.jacc.2021.09.1361
- Honigberg, M.C. & Givertz, M.M., 2019. Peripartum cardiomyopathy. *BMJ*, **364**, 1–14, British Medical Journal Publishing Group. doi:10.1136/BMJ.K5287
- Hoogenhof, M.M.G. Van Den, Pinto, Y.M. & Creemers, E.E., 2016. RNA Splicing: Regulation and Dysregulation in the Heart. *Circ Res*, **118**, 454–468, Circ Res. doi:10.1161/CIRCRESAHA.115.307872
- Hooijschuur, M.C.E., Ghossein-Doha, C., Kroon, A.A., Leeuw, P.W. De, Zandbergen, A.A.M., Kuijk, S.M.J. Van & Spaanderman, M.E.A., 2019. Metabolic syndrome and preeclampsia. *Ultrasound in Obstetrics and Gynecology*, **54**, 64–71, John Wiley and Sons Ltd. doi:10.1002/uog.20126
- Hsu, C.N. & Tain, Y.L., 2021. Preventing Developmental Origins of Cardiovascular Disease: Hydrogen Sulfide as a Potential Target? *Antioxidants*, **10**, 1–19, Multidisciplinary Digital Publishing Institute (MDPI). doi:10.3390/ANTIOX10020247
- Hu, J., Zhang, J. & Zhu, B., 2019. Protective effect of metformin on a rat model of lipopolysaccharide-induced preeclampsia. *Fundam Clin Pharmacol*, **33**, 649–658. doi:10.1111/fcp.12501
- Hu, L.F., Lu, M., Tiong, C.X., Dawe, G.S., Hu, G. & Bian, J.S., 2010. Neuroprotective effects of hydrogen sulfide on Parkinson's disease rat models. *Aging Cell*, **9**, 135–146, Aging Cell. doi:10.1111/J.1474-9726.2009.00543.X
- Hu, X., Zhang, L., Nayak, R., Stevenson, D.K. & Longo, L.D., 2021. Uteroplacental Circulation in Normal Pregnancy and Preeclampsia: Functional Adaptation and Maladaptation. *International Journal of Molecular Sciences 2021, Vol. 22, Page 8622*, **22**, 8635, Multidisciplinary Digital Publishing Institute. doi:10.3390/IJMS22168622
- Hu, X.Q. & Zhang, L., 2021. Hypoxia and Mitochondrial Dysfunction in Pregnancy Complications. *Antioxidants 2021, Vol. 10, Page 405*, **10**, 415, Multidisciplinary Digital Publishing Institute. doi:10.3390/ANTIOX10030405

- Huang, G., Chen, Y., Lu, H. & Cao, X., 2007. Coupling mitochondrial respiratory chain to cell death: An essential role of mitochondrial complex I in the interferon- β and retinoic acid-induced cancer cell death. *Cell Death Differ*, **14**, 327–337. doi:10.1038/sj.cdd.4402004
- Huang, J., Zheng, L., Wang, F., Su, Y., Kong, H. & Xin, H., 2020. Mangiferin ameliorates placental oxidative stress and activates PI3K/Akt/mTOR pathway in mouse model of preeclampsia. *Arch Pharm Res*, **43**, 233–241. doi:10.1007/s12272-020-01220-7
- Hubel, C.A., 1999. Oxidative Stress in the Pathogenesis of Preeclampsia. *Proceedings of the Society for Experimental Biology and Medicine*, **222**, 222–235, John Wiley & Sons, Ltd. doi:10.1046/J.1525-1373.1999.D01-139.X
- Hubel, C.A., Roberts, J.M. & Ferrell, R.E., 1999. Association of pre-eclampsia with common coding sequence variations in the lipoprotein lipase gene. *Clin Genet*, **56**, 289–296, Clin Genet. doi:10.1034/J.1399-0004.1999.560406.X
- Huber, H.J., Dussmann, H., Kilbride, S.M., Rehm, M. & Prehn, J.H.M., 2011. Glucose metabolism determines resistance of cancer cells to bioenergetic crisis after cytochrome-c release. *Mol Syst Biol*. doi:10.1038/msb.2011.2
- Hunter, S. & Robson, S.C., 1992. Adaptation of the maternal heart in pregnancy. *Br Heart J*, Vol. 68.
- Hunter, S. & Robson, S.C., 1992. Adaptation of the maternal heart in pregnancy. *Heart*, **68**, 540–543, BMJ Publishing Group. doi:10.1136/hrt.68.12.540
- Huppertz, B., 2008. Placental Origins of Preeclampsia. *Hypertension*, **51**, 970–975. doi:10.1161/HYPERTENSIONAHA.107.107607
- Huppertz, I., Perez-Perri, J.I., Mantas, P., Sekaran, T., Schwarzl, T., Russo, F., Ferring-Appel, D., *et al.*, 2022. Riboregulation of Enolase 1 activity controls glycolysis and embryonic stem cell differentiation. *Mol Cell*, **82**, 2666-2680.e11, Mol Cell. doi:10.1016/J.MOLCEL.2022.05.019

- Hutchens, J., Frawley, J. & Sullivan, E.A., 2022. Cardiac disease in pregnancy and the first year postpartum: a story of mental health, identity and connection. *BMC Pregnancy Childbirth*, **22**, BioMed Central Ltd. doi:10.1186/s12884-022-04614-1
- Huttlin, E.L., Bruckner, R.J., Navarrete-Perea, J., Cannon, J.R., Baltier, K., Gebreab, F., Gygi, M.P., *et al.*, 2021. Dual proteome-scale networks reveal cell-specific remodeling of the human interactome. *Cell*, **184**, 3040, Cell. doi:10.1016/J.CELL.2021.04.011
- Hyatt, H.W., Zhang, Y., Hood, W.R. & Kavazis, A.N., 2017. Lactation has persistent effects on a mother's metabolism and mitochondrial function. *Sci Rep*, **7**, 17118–17129, Nature Publishing Group. doi:10.1038/S41598-017-17418-7
- Iemitsu, M., Maeda, S., Otsuki, T., Sugawara, J., Kuno, S., Ajisaka, R. & Matsuda, M., 2008. Arterial stiffness, physical activity, and atrial natriuretic Peptide gene polymorphism in older subjects. *Hypertens Res*, **31**, 767–774, Hypertens Res. doi:10.1291/HYPRES.31.767
- Ikeda, K., Marutani, E., Hirai, S., Wood, M.E., Whiteman, M. & Ichinose, F., 2015. Mitochondria-targeted hydrogen sulfide donor AP39 improves neurological outcomes after cardiac arrest in mice. *Nitric Oxide*, **49**, 90–96, Nitric Oxide. doi:10.1016/J.NIOX.2015.05.001
- Iman Gurnadi, J., Mose, J., Handono, B., Satari, M.H., Deborah Anwar, A., Nanda Fauziah, P., Yogi Pramartira, A., *et al.*, 2015. Difference of concentration of placental soluble fms-like tyrosine kinase-1(sFlt-1), placental growth factor (PlGF), and sFlt-1/PlGF ratio in severe preeclampsia and normal pregnancy. *BMC Res Notes*, **8**, 1–5. doi:10.1186/s13104-015-1506-0
- Ingenbleek, Y. & Young, V., 1994. Transthyretin (prealbumin) in health and disease: nutritional implications. *Annu Rev Nutr*, **14**, 495–533, Annu Rev Nutr. doi:10.1146/ANNUREV.NU.14.070194.002431
- Inoue, I., Rohrwasser, A., Helin, C., Jeunemaitre, X., Crain, P., Bohlender, J., Lifton, R.P., *et al.*, 1995. A mutation of angiotensinogen in a patient with preeclampsia leads to altered kinetics of the renin-angiotensin system. *J Biol Chem*, **270**, 11430–11436, J Biol Chem. doi:10.1074/JBC.270.19.11430

- Inserte, J. & Garcia-Dorado, D., 2015. The cGMP/PKG pathway as a common mediator of cardioprotection: translatability and mechanism. *Br J Pharmacol*, **172**, 2009, Wiley-Blackwell. doi:10.1111/BPH.12959
- IPLACENTA, (n.d.). Retrieved April 10, 2020, from <https://www.iplacenta.eu/about.html>
- Irgens, H., Reisaeter, L., Irgens, L.M. & Lie, R.T., 2001. Long term mortality of mothers and fathers after pre-eclampsia: population based cohort study. *BMJ*, **315**, 21–25.
- Isermann, B., Sood, R., Pawlinski, R., Zogg, M., Kalloway, S., Degen, J.L., Mackman, N., *et al.*, 2003. The thrombomodulin-protein C system is essential for the maintenance of pregnancy. *Nat Med*, **9**, 331–337, Nat Med. doi:10.1038/NM825
- Ishihara, N., Eura, Y. & Mihara, K., 2004. Mitofusin 1 and 2 play distinct roles in mitochondrial fusion reactions via GTPase activity. *J Cell Sci*, **117**, 6535–6546, J Cell Sci. doi:10.1242/JCS.01565
- Ishihara, N., Fujita, Y., Oka, T. & Mihara, K., 2006. Regulation of mitochondrial morphology through proteolytic cleavage of OPA1. *EMBO J*, **25**, 2966–2977, EMBO J. doi:10.1038/SJ.EMBOJ.7601184
- Ishola, D.A., Giezen, D.M. van der, Hahnel, B., Goldschmeding, R., Kriz, W., Koomans, H.A. & Joles, J.A., 2006. In mice, proteinuria and renal inflammatory responses to albumin overload are strain-dependent. *Nephrology Dialysis Transplantation*, **21**, 591–597, Oxford Academic. doi:10.1093/NDT/GFI303
- Iyer, S., Leonidas, D.D., Swaminathan, G.J., Maglione, D., Battisti, M., Tucci, M., Persico, M.G., *et al.*, 2001. The Crystal Structure of Human Placenta Growth Factor-1 (PlGF-1), an Angiogenic Protein, at 2.0 Å Resolution. *Journal of Biological Chemistry*, **276**, 12153–12161, American Society for Biochemistry and Molecular Biology. doi:10.1074/jbc.M008055200
- J. D. Boyd & W. J. Hamilton. Heffer, 1970. The human placenta. *Teratology*, **8**, 365, Wiley. doi:10.1002/tera.1420080118

- J Jose, 1993. Mitral valve area by colour flow imaging - PubMed. *Indian Heart J*, **45**, 41–43. Retrieved from <https://pubmed.ncbi.nlm.nih.gov/8365739/>
- Jaiswar, S.P., Amrit, G., Rekha, S., Natu, S.N. & Mohan, S., 2011. Lactic dehydrogenase: A biochemical marker for preeclampsia-eclampsia. *Journal of Obstetrics and Gynecology of India*, **61**, 645–648, Springer. doi:10.1007/S13224-011-0093-9/TABLES/4
- James Metcalfe, 1963. The Maternal Heart in the postpartum period. *Am J Cardiol*, 439–440.
- Jansson, T. & Powell, T.L., 2006. Human Placental Transport in Altered Fetal Growth: Does the Placenta Function as a Nutrient Sensor? - A Review. *Placenta*, **27**, 91–97, W.B. Saunders. doi:10.1016/j.placenta.2005.11.010
- Janzarik, W.G., Janzarik, W.G., Gerber, A.K., Reinhard, M., Markfeld-Erol, F., Gerber, A.K., Sommerlade, L., *et al.*, 2018. No long-term impairment of cerebral autoregulation after preeclampsia. *Pregnancy Hypertens*, **13**, 171–173, Elsevier B.V. doi:10.1016/j.preghy.2018.06.009
- Jauniaux, E., Watson, A.L., Hempstock, J., Bao, Y.P., Skepper, J.N. & Burton, G.J., 2000. Onset of maternal arterial blood flow and placental oxidative stress. A possible factor in human early pregnancy failure. *Am J Pathol*, **157**, 2111–2122, Am J Pathol. doi:10.1016/S0002-9440(10)64849-3
- Jawaid, S., Strainic, J.P., Kim, J., Ford, M.R., Thrane, L., Karunamuni, G.H., Sheehan, M.M., *et al.*, 2021. Glutathione Protects the Developing Heart from Defects and Global DNA Hypomethylation Induced by Prenatal Alcohol Exposure. *Alcohol Clin Exp Res*, **45**, 78, NIH Public Access. doi:10.1111/ACER.14511
- Jeney, V., Komódi, E., Nagy, E., Zarjou, A., Vercellotti, G.M., Eaton, J.W., Balla, G., *et al.*, 2009. Suppression of hemin-mediated oxidation of low-density lipoprotein and subsequent endothelial reactions by hydrogen sulfide (H₂S). *Free Radic Biol Med*, **46**, 616–623, Free Radic Biol Med. doi:10.1016/J.FREERADBIOMED.2008.11.018
- Ježek, P., Plecítá-Hlavatá, L., Smolková, K. & Rossignol, R., 2010. Distinctions and similarities of cell bioenergetics and the role of mitochondria in hypoxia, cancer, and embryonic

- development. *Int J Biochem Cell Biol*, **42**, 604–622, Pergamon. doi:10.1016/J.BIOCEL.2009.11.008
- Jia, G., Aroor, A.R., Jia, C. & Sowers, J.R., 2019, July 1. Endothelial cell senescence in aging-related vascular dysfunction. *Biochim Biophys Acta Mol Basis Dis*, Elsevier B.V. doi:10.1016/j.bbadis.2018.08.008
- Jia, G., Hill, M.A. & Sowers, J.R., 2018, February 1. Diabetic cardiomyopathy: An update of mechanisms contributing to this clinical entity. *Circ Res*, Lippincott Williams and Wilkins. doi:10.1161/CIRCRESAHA.117.311586
- Jiang, Z., Zou, Y., Ge, Z., Zuo, Q., Huang, S.Y. & Sun, L., 2015. A role of sFlt-1 in oxidative stress and apoptosis in human and mouse pre-eclamptic trophoblasts. *Biol Reprod*, **93**, Society for the Study of Reproduction. doi:10.1095/biolreprod.114.126227
- Jimenez, M., Gil, V., Martinez-Cutillas, M., Mañé, N. & Gallego, D., 2017. Hydrogen sulphide as a signalling molecule regulating physiopathological processes in gastrointestinal motility. *Br J Pharmacol*, **174**, 2817, Wiley-Blackwell. doi:10.1111/BPH.13918
- Jing Huai, Zi Yang, Yan-Hong Yi & Guan-Jiao Wang, 2018. Different Effects of Pravastatin on Preeclampsia-like Symptoms in Different Mouse Models. *Chin Med J (Engl)*, **131**, 461–471. Retrieved from <https://www.ncbi.nlm.nih.gov/pmc/articles/PMC5830832/pdf/CMJ-131-461.pdf>
- Jingyuan Li, Soban Umar, Marjan Amjedi, Andrea Iorga, Salil Sharma, Rangarajan D Nadadur, Vera Regitz-Zagrosek, *et al.*, 2012. New frontiers in heart hypertrophy during pregnancy. *Am J Cardiovasc Dis*, **2**, 192–207. Retrieved from www.AJCD.us
- Jingyuan Li, Soban Umar, Marjan Amjedi, Andrea Iorga, Salil Sharma, Rangarajan D Nadadur, Vera Regitz-Zagrosek, *et al.*, 2012. Pregnancy-induced physiological heart hypertrophy. *Am J Cardiovasc Dis*, **3**, 192–207. Retrieved from www.AJCD.us
- Johansson, M.C., Barasa, A., Basic, C., Nyberg, G. & Schaufelberger, M., 2021. Increased arterial stiffness and reduced left ventricular long-axis function in patients recovered from peripartum cardiomyopathy. *Clin Physiol Funct Imaging*, **41**, 102, Wiley-Blackwell. doi:10.1111/CPF.12671

- John H Fowler & Donald J Nash, 1968. Erythropoiesis in the Spleen and Bone Marrow of the Pregnant Mouse'. *Dev Biol*, **18**, 331–353.
- John R Burnett, Amanda J Hooper, Margaret P Adam & Ghayda M Mirzaa, 1993. APOB-Related Familial Hypobetalipoproteinemia - PubMed, Seattle . Retrieved from <https://pubmed.ncbi.nlm.nih.gov/33983694/>
- Johnson, A.C. & Cipolla, M.J., 2017. Altered hippocampal arteriole structure and function in a rat model of preeclampsia: Potential role in impaired seizure-induced hyperemia. *Journal of Cerebral Blood Flow and Metabolism*, **37**, 2857–2869, SAGE Publications Ltd. doi:10.1177/0271678X16676287/ASSET/IMAGES/LARGE/10.1177_0271678X16676287-FIG7.JPG
- Johnson, A.C., Li, Z., Orfila, J.E., Herson, P.S. & Cipolla, M.J., 2021. Hippocampal network dysfunction as a mechanism of early-onset dementia after preeclampsia and eclampsia. *Prog Neurobiol*, **199**, Elsevier Ltd. doi:10.1016/j.pneurobio.2020.101938
- Johnson, A.C., Tremble, S.M. & Cipolla, M.J., 2022. Experimental Preeclampsia Causes Long-Lasting Hippocampal Vascular Dysfunction and Memory Impairment. *Front Physiol*, **13**, 1–23, Frontiers Media SA. doi:10.3389/FPHYS.2022.889918
- Jones, C.J.P. & Fox, H., 1980. An ultrastructural and ultrahistochemical study of the human placenta in maternal pre-eclampsia. *Placenta*, **1**, 61–76, W.B. Saunders. doi:10.1016/S0143-4004(80)80016-6
- Jovin, I.S., Ebisu, K., Liu, Y.H., Finta, L.A., Oprea, A.D., Brandt, C.A., Dziura, J., *et al.*, 2013. Left Ventricular Ejection Fraction and Left Ventricular End-Diastolic Volume in Patients With Diastolic Dysfunction. *Congestive Heart Failure*, **19**, 130–134. doi:10.1111/CHF.12013/ABSTRACT
- Jubaidi, F.F., Zainalabidin, S., Taib, I.S., Abdul Hamid, Z., Mohamad Anuar, N.N., Jalil, J., Mohd Nor, N.A., *et al.*, 2022. The Role of PKC-MAPK Signalling Pathways in the Development of Hyperglycemia-Induced Cardiovascular Complications. *International Journal of Molecular Sciences* 2022, Vol. 23, Page 8582, **23**, 8582, Multidisciplinary Digital Publishing Institute. doi:10.3390/IJMS23158582

- Jukic, A.M., Baird, D.D., Weinberg, C.R., McConnaughey, D.R. & Wilcox, A.J., 2013. Length of human pregnancy and contributors to its natural variation. *Human Reproduction*, **28**, 2848–2855, Oxford University Press. doi:10.1093/humrep/det297
- Jukic, A.M., Baird, D.D., Weinberg, C.R., McConnaughey, D.R. & Wilcox, A.J., 2013. Length of human pregnancy and contributors to its natural variation. *Human Reproduction*, **28**, 2848–2855, Oxford University Press. doi:10.1093/humrep/det297
- Kaartokallio, T., Klemetti, M.M., Timonen, A., Uotila, J., Heinonen, S., Kajantie, E., Kere, J., *et al.*, 2014. Microsatellite polymorphism in the heme oxygenase-1 promoter is associated with nonsevere and late-onset preeclampsia. *Hypertension*, **64**, 172–177, Lippincott Williams and Wilkins. doi:10.1161/HYPERTENSIONAHA.114.03337
- Kaihura, C., Savvidou, M.D., Anderson, J.M., McEniery, C.M. & Nicolaides, K.H., 2009. Maternal arterial stiffness in pregnancies affected by preeclampsia. *Am J Physiol Heart Circ Physiol*, **297**, H759–H764, Am J Physiol Heart Circ Physiol. doi:10.1152/AJPHEART.01106.2008
- Kajantie, E., Thornburg, K., Eriksson, J.G., Osmond, L. & Barker, D.J.P., 2010. In preeclampsia, the placenta grows slowly along its minor axis. *Int J Dev Biol*, **54**, 469–473, UPV/EHU Press. doi:10.1387/ijdb.082833ek
- Kalafat, E., Laoreti, A., Khalil, A., Silva Costa, F. Da & Thilaganathan, B., 2018. Ophthalmic artery Doppler for prediction of pre-eclampsia: systematic review and meta-analysis. *Ultrasound in Obstetrics & Gynecology*, **51**, 731–737, John Wiley & Sons, Ltd. doi:10.1002/UOG.19002
- Kalaria, R.N., 2016, May 1. Neuropathological diagnosis of vascular cognitive impairment and vascular dementia with implications for Alzheimer's disease. *Acta Neuropathol*, Springer Verlag. doi:10.1007/s00401-016-1571-z
- Kalhan, S.C., 2016. One Carbon Metabolism in Pregnancy: Impact on Maternal, Fetal and Neonatal Health. *Mol Cell Endocrinol*, **435**, 60, NIH Public Access. doi:10.1016/J.MCE.2016.06.006

- Kametas, N.A., McAuliffe, F., Hancock, J., Chambers, J. & Nicolaides, K.H., 2001. Maternal left ventricular mass and diastolic function during pregnancy. *Ultrasound in Obstetrics and Gynecology*, **18**, 460–466. doi:10.1046/j.0960-7692.2001.00573.x
- Kang, H.J., Jung, S.K., Kim, S.J. & Chung, S.J., 2008. Structure of human alpha-enolase (hENO1), a multifunctional glycolytic enzyme. *Acta Crystallogr D Biol Crystallogr*, **64**, 651–657, *Acta Crystallogr D Biol Crystallogr*. doi:10.1107/S0907444908008561
- Karki, S., Farb, M.G., Sharma, V.M., Jash, S., Zizza, E.J., Hess, D.T., Carmine, B., *et al.*, 2019. Fat-Specific Protein 27 Regulation of Vascular Function in Human Obesity. *Journal of the American Heart Association: Cardiovascular and Cerebrovascular Disease*, **8**, 1–16, Wiley-Blackwell. doi:10.1161/JAHA.118.011431
- Karumanchi, S.A. & Levine, R.J., 2010. How does smoking reduce the risk of preeclampsia? *Hypertension*, **55**, 1100–1101, Howard Hughes Medical Institute. doi:10.1161/HYPERTENSIONAHA.109.148973
- Karwi, Q.G., Bornbaum, J., Boengler, K., Torregrossa, R., Whiteman, M., Wood, M.E., Schulz, R., *et al.*, 2017. AP39, a mitochondria-targeting hydrogen sulfide (H₂S) donor, protects against myocardial reperfusion injury independently of salvage kinase signalling. *Br J Pharmacol*, **174**, 287–301, *Br J Pharmacol*. doi:10.1111/BPH.13688
- Kasak, L., Rull, K., Vaas, P., Teesalu, P. & Laan, M., 2015. Extensive load of somatic CNVs in the human placenta. *Sci Rep*, **5**, 8342–8346, *Sci Rep*. doi:10.1038/SREP08342
- Kasula Sunanda, Beeram Sumalatha, Janapati Ramakrishna & Garre Indrani, 2017. Structural and Functional Changes in Maternal Heart during Pregnancy: An Echocardiographic Study. *Indian J Cardiovasc Dis Women WINCARS*, **02**, 072–076, Scientific Scholar. doi:10.1055/s-0038-1624065
- Katie Delach, 2016. The Placenta: Our Least Understood Organ. *Penn Medicine News*. Retrieved July 15, 2019, from <https://www.pennmedicine.org/news/news-blog/2016/january/the-placenta-our-least-underst>
- Kato, M., Dote, K., Sasaki, S., Goto, K., Takemoto, H., Habara, S. & Hasegawa, D., 2005. Myocardial performance index for assessment of left ventricular outcome in successfully

- recanalised anterior myocardial infarction. *Heart*, **91**, 583, BMJ Publishing Group. doi:10.1136/HRT.2004.035758
- Kato, T., Nishigaki, Y., Noguchi, Y., Ueno, H., Hosoya, H., Ito, T., Kimura, Y., *et al.*, 2010. Extensive and rapid screening for major mitochondrial DNA point mutations in patients with hereditary hearing loss. *J Hum Genet*, **55**, 147–154, J Hum Genet. doi:10.1038/JHG.2009.143
- Kattah, A., 2020, November 1. Preeclampsia and Kidney Disease: Deciphering Cause and Effect. *Curr Hypertens Rep*, Springer. doi:10.1007/s11906-020-01099-1
- Katz, A.M., 1967. Regulation of Cardiac Muscle Contractility. *J Gen Physiol*, **50**, 185–196. Retrieved from <http://rupress.org/jgp/article-pdf/50/6/185/1244175/185.pdf>
- Katz, R., Karlner, J.S. & Resnik, R., 1978. Effects of a Natural Volume Overload State (Pregnancy) on Left Ventricular Performance in Normal Human Subjects. *Circulation*, **58**, 434–441. Retrieved from <http://ahajournals.org>
- Kawahara, T., Yamagishi, M., Mitani, M., Nakatani, S., Beppu, S., Nagata, S. & Miyatake, K., 1991. Application of Doppler Color Flow Imaging to Determine Valve Area in Mitral Stenosis. *J Am Coll Cardiol*, **18**, 85–92. doi:10.1016/S0735-1097(10)80223-2
- Kazma, J.M., Anker, J. van den, Allegaert, K., Dallmann, A. & Ahmadzia, H.K., 2020, August 1. Anatomical and physiological alterations of pregnancy. *J Pharmacokinet Pharmacodyn*, Springer. doi:10.1007/s10928-020-09677-1
- Kendall, R.L. & Thomas, K.A., 1993. Inhibition of vascular endothelial cell growth factor activity by an endogenously encoded soluble receptor. *Proc Natl Acad Sci U S A*, **90**, 10705–10709, National Academy of Sciences. doi:10.1073/pnas.90.22.10705
- Kendall, R.L. & Thomas, K.A., 1993. Inhibition of vascular endothelial cell growth factor activity by an endogenously encoded soluble receptor. *Proc Natl Acad Sci U S A*, **90**, 10705–10709, National Academy of Sciences. doi:10.1073/pnas.90.22.10705
- Kepley, J., Bates, K. & Shamim, M., 2022. Physiology, Maternal Changes. *StatPearls*, 1–4. Retrieved from <https://www.ncbi.nlm.nih.gov/books/NBK539766/?report=printable>

- Khalil, A., Akolekar, R., Syngelaki, A., Elkhoul, M. & Nicolaides, K.H., 2012. Maternal hemodynamics at 11-13 weeks' gestation and risk of pre-eclampsia. *Ultrasound in Obstetrics & Gynecology*, **40**, 28–34, John Wiley & Sons, Ltd. doi:10.1002/uog.11183
- Khan, S.G., Melikian, N., Mushemi-Blake, S., Dennes, W., Jouhra, F., Monaghan, M. & Shah, A.M., 2016. Physiological Reduction in Left Ventricular Contractile Function in Healthy Postpartum Women: Potential Overlap with Peripartum Cardiomyopathy. *PLoS One*, **11**, 147074–147089, PLOS. doi:10.1371/JOURNAL.PONE.0147074
- Khanam, R., Sengupta, A., Mukhopadhyay, D. & Chakraborty, S., 2022. Identification of Adamts4 as a novel adult cardiac injury biomarker with therapeutic implications in patients with cardiac injuries. *Scientific Reports 2022 12:1*, **12**, 1–15, Nature Publishing Group. doi:10.1038/s41598-022-13918-3
- Khandoker, A.H., Marzbanrad, F., Kimura, Y., Nuaimi, S. Al & Palaniswami, M., 2016. Assessing the development of fetal myocardial function by a novel Doppler myocardial performance index. *Proceedings of the Annual International Conference of the IEEE Engineering in Medicine and Biology Society, EMBS*, Vol. 2016-October, pp. 3753–3756, Institute of Electrical and Electronics Engineers Inc. doi:10.1109/EMBC.2016.7591544
- Khong, S.L., Kane, S.C., Brennecke, S.P. & Silva Costa, F. Da, 2015. First-Trimester Uterine Artery Doppler Analysis in the Prediction of Later Pregnancy Complications. *Hindawi Publishing Corporation*, **679**, 1–10. doi:10.1155/2015/679730
- Khong, T.Y., Wolf, F., Robertson, W.B. & Brosens, I., 1986. Inadequate maternal vascular response to placentation in pregnancies complicated by pre-eclampsia and by small-for-gestational age infants. *BJOG*, **93**, 1049–1059, John Wiley & Sons, Ltd. doi:10.1111/j.1471-0528.1986.tb07830.x
- Khosla, K., Heimberger, S., Nieman, K.M., Tung, A., Shahul, S., Staff, A.C. & Rana, S., 2021, October 1. Long-Term Cardiovascular Disease Risk in Women After Hypertensive Disorders of Pregnancy: Recent Advances in Hypertension. *Hypertension*, Lippincott Williams and Wilkins. doi:10.1161/HYPERTENSIONAHA.121.16506
- Kim, S., Lim, H.J., Kim, J.R., Oh, K.J., Hong, J.S. & Suh, J.W., 2020. Longitudinal change in arterial stiffness after delivery in women with preeclampsia and normotension: a

- prospective cohort study. *BMC Pregnancy Childbirth*, **20**, 685–672, BioMed Central. doi:10.1186/S12884-020-03374-0
- Kim, S.H., Song, J.Y., Joo, E.J., Lee, K.Y., Ahn, Y.M. & Kim, Y.S., 2010. EGR3 as a potential susceptibility gene for schizophrenia in Korea. *Am J Med Genet B Neuropsychiatr Genet*, **153B**, 1355–1360, Am J Med Genet B Neuropsychiatr Genet. doi:10.1002/AJMG.B.31115
- Kim, S.M. & Ye, S.Y., 2021. Evaluation of the fetal left ventricular myocardial performance index (Mpi) by using an automated measurement of doppler signals in normal pregnancies. *Diagnostics*, **11**, MDPI AG. doi:10.3390/diagnostics11020358
- Kim, Y., Hollenbaugh, J.A., Kim, D.-H. & Kim, B., 2011. Novel PI3K/Akt Inhibitors Screened by the Cytoprotective Function of Human Immunodeficiency Virus Type 1 Tat. (D.-Y. Jin, Ed.) *PLoS One*, **6**, e21781, Public Library of Science. doi:10.1371/journal.pone.0021781
- Kim, Y.J., Williamson, R.A., Chen, K., Smith, J.L., Murray, J.C. & Merrill, D.C., 2001. Lipoprotein lipase gene mutations and the genetic susceptibility of preeclampsia. *Hypertension*, **38**, 992–996, Hypertension. doi:10.1161/HY1101.093105
- Kimura, H., 2014. Production and physiological effects of hydrogen sulfide. *Antioxid Redox Signal*, **20**, 783–793, Mary Ann Liebert, Inc. doi:10.1089/ars.2013.5309
- Kimura, Y., Dargusch, R., Schubert, D. & Kimura, H., 2006. Hydrogen sulfide protects HT22 neuronal cells from oxidative stress. *Antioxid Redox Signal*, **8**, 661–670, Antioxid Redox Signal. doi:10.1089/ARS.2006.8.661
- King, A.L., Polhemus, D.J., Bhushan, S., Otsuka, H., Kondo, K., Nicholson, C.K., Bradley, J.M., *et al.*, 2014. Hydrogen sulfide cytoprotective signaling is endothelial nitric oxide synthase-nitric oxide dependent. *Proc Natl Acad Sci U S A*, **111**, 3182–3187, National Academy of Sciences. doi:10.1073/PNAS.1321871111/SUPPL_FILE/PNAS.201321871SI.PDF
- Kirkinen P, D.J., Baumann H, J., Huch, A. & Huch, R., 1988. Postpartum blood flow velocity waveforms of the uterine arteries - PubMed. *J Reprod Med*, **33**, 745–748. Retrieved from <https://pubmed.ncbi.nlm.nih.gov/3050078/>

- Kitt, J., Frost, A. & Leeson, P., 2021. Preeclampsia and the Brain - A Long-term View. *JAMA Netw Open*, American Medical Association. doi:10.1001/jamanetworkopen.2021.5364
- Kitt, J.A., Fox, R.L., Cairns, A.E., Mollison, J., Burchert, H.H., Kenworthy, Y., McCourt, A., *et al.*, 2021. Short-Term Postpartum Blood Pressure Self-Management and Long-Term Blood Pressure Control: A Randomized Controlled Trial. *Hypertension*, **78**, 469–479, Lippincott Williams and Wilkins. doi:10.1161/HYPERTENSIONAHA.120.17101
- Knight, M., Redman, C.W.G., Linton, E.A. & Sargent, I.L., 1998. Shedding of syncytiotrophoblast microvilli into the maternal circulation in pre-eclamptic pregnancies. *BJOG*, **105**, 632–640. doi:10.1111/j.1471-0528.1998.tb10178.x
- Knöfler, M., Haider, S., Saleh, L., Pollheimer, J., Gamage, T.K.J.B. & James, J., 2019. Human placenta and trophoblast development: key molecular mechanisms and model systems. *Cellular and Molecular Life Sciences* 2019 76:18, **76**, 3479–3496, Springer. doi:10.1007/S00018-019-03104-6
- Kodogo, V., Azibani, F. & Sliwa, K., 2019, August 1. Role of pregnancy hormones and hormonal interaction on the maternal cardiovascular system: a literature review. *Clinical Research in Cardiology*, Dr. Dietrich Steinkopff Verlag GmbH and Co. KG. doi:10.1007/s00392-019-01441-x
- Koga, K., Osuga, Y., Yoshino, O., Hirota, Y., Ruimeng, X., Hirata, T., Takeda, S., *et al.*, 2003. Elevated serum soluble vascular endothelial growth factor receptor 1 (sVEGFR-1) levels in women with preeclampsia. *The Journal of Clinical Endocrinology & Metabolism*, **88**, 2348–2351. doi:10.1210/jc.2002-021942
- Koh, C.L.S., Viegas, O.A.C., Yuen, R., Chua, S.E., Ng, B.L. & Ratnam, S.S., 1992. Plasminogen activators and inhibitors in normal late pregnancy, postpartum and in the postnatal period. *International Journal of Gynecology and Obstetrics*, **38**, 9–18. doi:10.1016/0020-7292(92)90723-V
- Kohli, S., Ranjan, S., Hoffmann, J., Kashif, M., Daniel, E.A., Al-Dabet, M.M., Bock, F., *et al.*, 2016. Maternal extracellular vesicles and platelets promote preeclampsia via inflammasome activation in trophoblasts. *Blood*, **128**, 2153–2164, American Society of Hematology. doi:10.1182/blood-2016-03-705434

- Kondo, K., Bhushan, S., King, A.L., Prabhu, S.D., Hamid, T., Koenig, S., Murohara, T., *et al.*, 2013. H₂S protects against pressure overload-induced heart failure via upregulation of endothelial nitric oxide synthase. *Circulation*, **127**, 1116–1127. doi:10.1161/CIRCULATIONAHA.112.000855
- Konukoglu, D. & Uzun, H., 2017. Endothelial Dysfunction and Hypertension. *Adv Exp Med Biol*, **956**, 511–540, Adv Exp Med Biol. doi:10.1007/5584_2016_90
- Kristensen, J.H., Basit, S., Wohlfahrt, J., Damholt, M.B. & Boyd, H.A., 2019. Pre-eclampsia and risk of later kidney disease: Nationwide cohort study. *BMJ (Online)*, **365**, BMJ Publishing Group. doi:10.1136/bmj.l1516
- Kristoffersen, K. & Jørgensen, F.S., 1970. A Case of Hydatidiform Mole with Severe Preeclampsia and Severe Disturbances in Thyroid Function. *Acta Obstet Gynecol Scand*, **49**, 119–123. doi:10.3109/00016347009158041
- Kroll, J. & Waltenberger, J., 2000. Regulation of endothelial function and angiogenesis by vascular endothelial growth factor-A (VEGF-A). *Z Kardiol*, **89**, 206–218. doi:10.1007/s003920050472
- Kruger, W.D., 2017. Cystathionine β -synthase Deficiency: Of Mice and Men. *Mol Genet Metab*, **121**, 205, NIH Public Access. doi:10.1016/J.YMGME.2017.05.011
- Kuć, A., Kubik, D., Męcik-Kronenberg, T., Kościelecka, K. & Szymanek, W., 2022. The Relationship Between Peripartum Cardiomyopathy and Preeclampsia – Pathogenesis, Diagnosis and Management. *J Multidiscip Healthc*, **15**, 867, Dove Press. doi:10.2147/JMDH.S357872
- Kulandavelu, S., Qu, D. & Adamson, S.L., 2006. Cardiovascular function in mice during normal pregnancy and in the absence of endothelial NO synthase. *Hypertension*, **47**, 1175–1182. doi:10.1161/01.HYP.0000218440.71846.db
- Kumar, V., Aneesh Kumar, A., Sanawar, R., Jaleel, A., Santhosh Kumar, T.R. & Kartha, C.C., 2019. Chronic Pressure Overload Results in Deficiency of Mitochondrial Membrane Transporter ABCB7 Which Contributes to Iron Overload, Mitochondrial Dysfunction,

Metabolic Shift and Worsens Cardiac Function. *Sci Rep*, **9**, 1–21, Nature Publishing Group. doi:10.1038/S41598-019-49666-0

Kumbrink, J., Kirsch, K.H. & Johnson, J.P., 2010. EGR1, EGR2, and EGR3 activate the expression of their coregulator NAB2 establishing a negative feedback loop in cells of neuroectodermal and epithelial origin. *J Cell Biochem*, **111**, 217, NIH Public Access. doi:10.1002/JCB.22690

Ky, B., French, B., Ruparel, K., Sweitzer, N.K., Fang, J.C., Levy, W.C., Sawyer, D.B., *et al.*, 2011. The Vascular Marker Soluble Fms-Like Tyrosine Kinase 1 Is Associated With Disease Severity and Adverse Outcomes in Chronic Heart Failure. *J Am Coll Cardiol*, **58**, 386–394, Elsevier. doi:10.1016/J.JACC.2011.03.032

Ky, B., French, B., Ruparel, K., Sweitzer, N.K., Fang, J.C., Levy, W.C., Sawyer, D.B., *et al.*, 2011. The Vascular Marker Soluble Fms-like Tyrosine Kinase 1 is Associated with Disease Severity and Adverse Outcomes in Chronic Heart Failure. *J Am Coll Cardiol*, **58**, 394, NIH Public Access. doi:10.1016/J.JACC.2011.03.032

Kyogoku, C., Yanagi, M., Nishimura, K., Sugiyama, D., Morinobu, A., Fukutake, M., Maeda, K., *et al.*, 2011. Association of calcineurin A gamma subunit (PPP3CC) and early growth response 3 (EGR3) gene polymorphisms with susceptibility to schizophrenia in a Japanese population. *Psychiatry Res*, **185**, 16–19, Psychiatry Res. doi:10.1016/J.PSYCHRES.2009.11.003

L D Longo, 1983. Maternal blood volume and cardiac output during pregnancy- a hypothesis of endocrinologic control. *American Journal of Physiology*, **245**.

Laasanen, J., Romppanen, E.L., Hiltunen, M., Helisalml, S., Mannermaa, A., Punnonen, K. & Heinonen, S., 2002. Two exonic single nucleotide polymorphisms in the microsomal epoxide hydrolase gene are jointly associated with preeclampsia. *Eur J Hum Genet*, **10**, 569–573, Eur J Hum Genet. doi:10.1038/SJ.EJHG.5200849

LaFee, S., 2014, November 19. Of Mice, Not Men. *Catalog of mouse functional genome pinpoints similarities and some significant differences*. Retrieved December 23, 2022, from <https://health.ucsd.edu/news/releases/pages/2014-11-19-mouse-and-human-genome.aspx>

- Lain, K.Y. & Roberts, J.M., 2002. Contemporary concepts of the pathogenesis and management of preeclampsia. *J Am Med Assoc*, **287**, 3183–3186. doi:10.1001/jama.287.24.3183
- Lamarca, B., 2012. Endothelial dysfunction; an important mediator in the Pathophysiology of Hypertension during Preeclampsia. *Minerva Ginecol*, **64**, 309, NIH Public Access. Retrieved from /pmc/articles/PMC3796355/
- Lambert, G., Brichant, J.F., Hartstein, G., Bonhomme, V. & Dewandre, P.Y., 2014. Preeclampsia : an update. *Acta Anaesthesiol*, **65**, 137–149.
- Lander, E. & Kruglyak, L., 1995. Genetic dissection of complex traits: guidelines for interpreting and reporting linkage results. *Nat Genet*, **11**, 241–247, Nat Genet. doi:10.1038/NG1195-241
- Landers, J.E., Melki, J., Meininger, V., Glass, J.D., Berg, L.H. Van Den, Es, M.A. Van, Sapp, P.C., *et al.*, 2009. Reduced expression of the Kinesin-Associated Protein 3 (KIFAP3) gene increases survival in sporadic amyotrophic lateral sclerosis. *Proc Natl Acad Sci U S A*, **106**, 9004–9009, National Academy of Sciences. doi:10.1073/PNAS.0812937106/SUPPL_FILE/0812937106SI.PDF
- Lang, R.M., Pridjian, G., Feldman, T., Neumann, A., Lindheimer, M. & Borow, K.M., 1991. Left ventricular mechanics in preeclampsia. *Am Heart J*, **121**, 1768–1775, Am Heart J. doi:10.1016/0002-8703(91)90024-C
- Lark, M.W., Bayne, E.K., Flanagan, J., Harper, C.F., Hoerrner, L.A., Hutchinson, N.I., Singer, I.I., *et al.*, 1997. Aggrecan degradation in human cartilage. Evidence for both matrix metalloproteinase and aggrecanase activity in normal, osteoarthritic, and rheumatoid joints. *J Clin Invest*, **100**, 93–106, J Clin Invest. doi:10.1172/JCI119526
- Lattuada, D., Colleoni, F., Martinelli, A., Garretto, A., Magni, R., Radaelli, T. & Cetin, I., 2008. Higher Mitochondrial DNA Content in Human IUGR Placenta. *Placenta*, **29**, 1029–1033. doi:10.1016/j.placenta.2008.09.012
- Lauboeck, H., 1980. Echocardiographic study of the isovolumetric contraction time. *J Biomed Eng*, **2**, 281–284, J Biomed Eng. doi:10.1016/0141-5425(80)90121-1

- Lavie, A., Ram, M., Lev, S., Blecher, Y., Amikam, U., Shulman, Y., Avnon, T., *et al.*, 2018. Maternal cardiovascular hemodynamics in normotensive versus preeclamptic pregnancies: A prospective longitudinal study using a noninvasive cardiac system (NICaS™). *BMC Pregnancy Childbirth*, **18**, BioMed Central Ltd. doi:10.1186/s12884-018-1861-7
- Layland, J., Solaro, R.J. & Shah, A.M., 2005. Regulation of cardiac contractile function by troponin I phosphorylation. *Cardiovasc Res*, **66**, 12–21, *Cardiovasc Res*. doi:10.1016/J.CARDIORES.2004.12.022
- Leal, C.R.V., Costa, L.B., Ferreira, G.C., Ferreira, A. de M., Reis, F.M. & Simões e Silva, A.C., 2022. Renin-angiotensin system in normal pregnancy and in preeclampsia: A comprehensive review. *Pregnancy Hypertens*, **28**, 15–20, Elsevier. doi:10.1016/J.PREGHY.2022.01.011
- Lee, H.C. & Wei, Y.H., 2000. Mitochondrial Role in Life and Death of the Cell. *J Biomed Sci*, **7**, 2–15, S. Karger AG. doi:10.1159/000025424
- Lee, H.M., Greeley, G.H. & Englander, E.W., 2007. Sustained hypoxia modulates mitochondrial DNA content in the neonatal rat brain. *Free Radic Biol Med*, **44**, 807–814. doi:10.1016/j.freeradbiomed.2007.11.005
- Lee, S.M., Jun, J.K., Sung, S.J., Choo, S. Il, Cho, J.Y., Yang, H.J., Park, C.-W., *et al.*, 2016. Uterine artery pulsatility index in hypertensive pregnancies: When does the index normalize in the puerperium? *Obstet Gynecol Sci*, **59**, 469, Korean Society of Obstetrics and Gynecology. doi:10.5468/OGS.2016.59.6.463
- Lee, S.W., Kim, W.J., Choi, Y.K., Song, H.S., Son, M.J., Gelman, I.H., Kim, Y.J., *et al.*, 2003. SSeCKS regulates angiogenesis and tight junction formation in blood-brain barrier. *Nature Medicine* 2003 9:7, **9**, 900–906, Nature Publishing Group. doi:10.1038/nm889
- Legler, D.F., Loetscher, M., Roos, R.S., Clark-Lewis, I., Baggiolini, M. & Moser, B., 1998. B cell-attracting chemokine 1, a human CXC chemokine expressed in lymphoid tissues, selectively attracts B lymphocytes via BLR1/CXCR5. *J Exp Med*, **187**, 655–660, *J Exp Med*. doi:10.1084/JEM.187.4.655

- Leon, L.J., McCarthy, F.P., Direk, K., Gonzalez-Izquierdo, A., Prieto-Merino, D., Casas, J.P. & Chappell, L., 2019. Preeclampsia and Cardiovascular Disease in a Large UK Pregnancy Cohort of Linked Electronic Health Records: A CALIBER Study. *Circulation*, **140**, 1050–1060, Circulation. doi:10.1161/CIRCULATIONAHA.118.038080
- Levine, R.J., Maynard, S.E., Qian, C., Lim, K.-H., England, L.J., Yu, K.F., Schisterman, E.F., *et al.*, 2005. Circulating Angiogenic Factors and the Risk of Preeclampsia. *Survey of Anesthesiology*, **49**, 14–15. doi:10.1097/01.sa.0000151206.53344.39
- Lewey, J., Andrade, L. & Levine, L.D., 2021. Valvular Heart Disease in Pregnancy. *Cardiol Clin*, **39**, 161, NIH Public Access. doi:10.1016/J.CCL.2020.09.010
- Li, F., Xie, Y., Wu, Y., He, M., Yang, M., Fan, Y., Li, X., *et al.*, 2019. HSP20 Exerts a Protective Effect on Preeclampsia by Regulating Function of Trophoblast Cells Via Akt Pathways. *Reproductive Sciences*, **26**, 961–971. doi:10.1177/1933719118802057
- Li, H., Mani, S., Wu, L., Fu, M., Shuang, T., Xu, C. & Wang, R., 2017. The interaction of estrogen and CSE/H2S pathway in the development of atherosclerosis. *Am J Physiol Heart Circ Physiol*, **312**, H406–H414, American Physiological Society. doi:10.1152/AJPHEART.00245.2016/ASSET/IMAGES/LARGE/ZH40021721500006.JPEG
- Li, Jifen, 2014. Alterations in cell adhesion proteins and cardiomyopathy. *World J Cardiol*, **6**, 313, Baishideng Publishing Group Inc. doi:10.4330/WJC.V6.I5.304
- Li, Jing, LaMarca, B. & Reckelhoff, J.F., 2012. A model of preeclampsia in rats: The reduced uterine perfusion pressure (RUPP) model. *Am J Physiol Heart Circ Physiol*, **303**, H1, American Physiological Society. doi:10.1152/ajpheart.00117.2012
- Li, J.Y., Liu, Y.F., Xu, H.Y., Zhang, J.Y., Lv, P.P., Liu, M.E., Ying, Y.Y., *et al.*, 2020. Basonuclin 1 deficiency causes testicular premature aging: BNC1 cooperates with TAF7L to regulate spermatogenesis. *J Mol Cell Biol*, **12**, 71–83, Oxford Academic. doi:10.1093/JMCB/MJZ035

- Li, L., Zhao, G.D., Shi, Z., Qi, L.L., Zhou, L.Y. & Fu, Z.X., 2016, November 1. The Ras/Raf/MEK/ERK signaling pathway and its role in the occurrence and development of HCC (Review). *Oncol Lett*, Spandidos Publications. doi:10.3892/ol.2016.5110
- Li, R., Fang, J., Huo, B., Su, Y.S., Wang, J., Liu, L.G., Hu, M., *et al.*, 2017. Leucine-rich repeat neuronal protein 4 (LRRN4) potentially functions in dilated cardiomyopathy. *Int J Clin Exp Pathol*, **10**, 9933, e-Century Publishing Corporation. Retrieved from /pmc/articles/PMC6965904/
- Li, S. & Yang, G., 2015. Hydrogen Sulfide Maintains Mitochondrial DNA Replication via Demethylation of TFAM. *Antioxid Redox Signal*, **23**, 630–642, Antioxid Redox Signal. doi:10.1089/ARS.2014.6186
- Li, Xia, Ma, Y.T., Xie, X., Yang, Y.N., Ma, X., Zheng, Y.Y., Pan, S., *et al.*, 2014. Association of Egr3 genetic polymorphisms and coronary artery disease in the Uygur and Han of China. *Lipids Health Dis*, **13**, 92, BioMed Central. doi:10.1186/1476-511X-13-84
- Li, Xiaomei, Liu, L., Whitehead, C., Li, J., Thierry, B., Le, T.D. & Winter, M., 2022. Identifying preeclampsia-associated genes using a control theory method. *Brief Funct Genomics*, **21**, 296–309, Oxford University Press. doi:10.1093/bfpg/elac006
- Li, Zhen, Polhemus, D.J. & Lefer, D.J., 2018. Evolution of Hydrogen Sulfide Therapeutics to Treat Cardiovascular Disease. *Circ Res*, **123**, 590–600, Circ Res. doi:10.1161/CIRCRESAHA.118.311134
- Li, Zhihe, Zhang, Y., Ying Ma, J., Kapoun, A.M., Shao, Q., Kerr, I., Lam, A., *et al.*, 2007. Recombinant Vascular Endothelial Growth Factor 121 Attenuates Hypertension and Improves Kidney Damage in a Rat Model of Preeclampsia. *Hypertension*, **50**, 686–692. doi:10.1161/HYPERTENSIONAHA.107.092098
- Liang, Z.Q., Zhong, L.Y., Li, J., Shen, J.H., Tu, X.Y., Zhong, Z.H., Zeng, J.J., *et al.*, 2022. Clinicopathological significance and underlying molecular mechanism of downregulation of basoenuclin 1 expression in ovarian carcinoma. *Exp Biol Med (Maywood)*, **247**, 106–119, Exp Biol Med (Maywood). doi:10.1177/15353702211052036

- Libanoff, A.J. & Rodbard, S., 1968. Atrioventricular Pressure Half-Time Measure of Mitral Valve Orifice Area. *Circulation*, **38**, 144–150. Retrieved from <http://ahajournals.org>
- Libby, G., Murphy, D.J., McEwan, N.F., Greene, S.A., Forsyth, J.S., Chien, P.W. & Morris, A.D., 2007. Pre-eclampsia and the later development of type 2 diabetes in mothers and their children: An intergenerational study from the Walker cohort. *Diabetologia*, **50**, 523–530. doi:10.1007/s00125-006-0558-z
- Liberto, R. & Nall, R., 2017. Blood Clots After Birth: Symptoms, Treatment, and More. *Healthline*. Retrieved June 13, 2023, from https://www.healthline.com/health/pregnancy/blood-clots-after-birth#TOC_TITLE_HDR_1
- Libiad, M., Vitvitsky, V., Bostelaar, T., Bak, D.W., Lee, H.J., Sakamoto, N., Fearon, E., *et al.*, 2019. Hydrogen sulfide perturbs mitochondrial bioenergetics and triggers metabolic reprogramming in colon cells. *J Biol Chem*, **294**, 12077–12090, *J Biol Chem*. doi:10.1074/JBC.RA119.009442
- Lima, F., Nie, L., Yang, J., Owens, A., Dianati-Maleki, N., Avila, C. & Stergiopoulos, K., 2019. Postpartum Cardiovascular Outcomes Among Women With Heart Disease from A Nationwide Study. *American Journal of Cardiology*, **123**, 2006–2014, Elsevier Inc. doi:10.1016/j.amjcard.2019.03.012
- Lin, J. & August, P., 2005. Genetic thrombophilias and preeclampsia: a meta-analysis. *Obstetrics and gynecology*, **105**, 182–192, *Obstet Gynecol*. doi:10.1097/01.AOG.0000146250.85561.E9
- Lisa, F. Di & Scorrano, L., 2012. Mitochondrial Morphology and Function. *Muscle: Fundamental Biology and Mechanisms of Disease*, **1–2**, 217–229, Elsevier. doi:10.1016/B978-0-12-381510-1.00017-X
- Liu, K., Zhou, S., Kim, J.Y., Tillison, K., Majors, D., Rearick, D., Lee, J.H., *et al.*, 2009. Functional analysis of FSP27 protein regions for lipid droplet localization, caspase-dependent apoptosis, and dimerization with CIDEA. *Am J Physiol Endocrinol Metab*, **297**, E1395–E1413, *Am J Physiol Endocrinol Metab*. doi:10.1152/AJPENDO.00188.2009

- Liu, Lei, Zhuang, X., Jiang, M., Guan, F., Fu, Q. & Lin, J., 2017. ANGPTL4 mediates the protective role of PPAR γ activators in the pathogenesis of preeclampsia. *Cell Death Dis*, **8**, 3054–3063, Cell Death Dis. doi:10.1038/CDDIS.2017.419
- Liu, Lu, Yang, X., Zhang, J., Jiang, W., Hou, T., Zong, Y., Bai, H., *et al.*, 2023. Long non-coding RNA SNHG11 regulates the Wnt/ β -catenin signaling pathway through rho/ROCK in trabecular meshwork cells. *FASEB J*, **37**, 22873–22889, FASEB J. doi:10.1096/FJ.202201733RRR
- Liu, M., Lv, J., Pan, Z., Wang, D., Zhao, L. & Guo, X., 2022. Mitochondrial dysfunction in heart failure and its therapeutic implications. *Front Cardiovasc Med*, **9**, Frontiers Media SA. doi:10.3389/FCVM.2022.945142
- Liu, N., Wu, J., Zhang, L., Gao, Z., Sun, Y., Yu, M., Zhao, Y., *et al.*, 2017. Hydrogen Sulphide modulating mitochondrial morphology to promote mitophagy in endothelial cells under high-glucose and high-palmitate. *J Cell Mol Med*, **21**, 3190–3203, J Cell Mol Med. doi:10.1111/JCMM.13223
- Liu, X., Zhao, W., Liu, H., Kang, Y., Ye, C., Gu, W., Hu, R., *et al.*, 2016. Developmental and Functional Brain Impairment in Offspring from Preeclampsia-Like Rats. *Mol Neurobiol*, **53**, 1009–1019. doi:10.1007/s12035-014-9060-7
- Liu, Y., Li, J., Ma, Z., Zhang, J., Wang, Y., Yu, Z., Lin, X., *et al.*, 2019. Oncogenic functions of protein kinase D2 and D3 in regulating multiple cancer-related pathways in breast cancer. *Cancer Med*, **8**, 729–741, Cancer Med. doi:10.1002/CAM4.1938
- Locatelli, J., Assis, L.V.M. De & Isoldi, M.C., 2014. Calcium handling proteins: structure, function, and modulation by exercise. *Heart Fail Rev*, **19**, 207–225, Heart Fail Rev. doi:10.1007/S10741-013-9373-Z
- Lockhart, M., Wirrig, E., Phelps, A. & Wessels, A., 2011. Extracellular Matrix and Heart Development. *Birth Defects Res A Clin Mol Teratol*, **91**, 550, NIH Public Access. doi:10.1002/BDRA.20810
- Logue, O.C., Fakhri, ;, Chapman, ;, Heather, George, E.M. & Bidwell, G.L., 2017. A Maternally Sequestered, Biopolymer-Stabilized Vascular Endothelial Growth Factor (VEGF)

- Chimera for Treatment of Preeclampsia. *J Am Heart Assoc*, **6**, 1–15. doi:10.1161/JAHA.117.007216
- Lopes van Balen, V. A., Gansewinkel, T.A.G. van, Haas, S. de, Kuijk, S.M.J. van, Drongelen, J. van, Ghossein-Doha, C. & Spaanderman, M.E.A., 2017. Physiological adaptation of endothelial function to pregnancy: systematic review and meta-analysis. *Ultrasound in Obstetrics & Gynecology*, **50**, 697–708, John Wiley & Sons, Ltd. doi:10.1002/UOG.17431
- Lopes van Balen, Veronica Agatha, Spaan, J.J., Cornelis, T. & Spaanderman, M.E.A., 2017. Prevalence of chronic kidney disease after preeclampsia. *J Nephrol*, **30**, 403–409, Springer New York LLC. doi:10.1007/s40620-016-0342-1
- López-Jaramillo, P., Díaz, L.A., Pardo, A., Parra, G., Jaimes, H. & Chaudhuri, G., 2004. Estrogen therapy increases plasma concentrations of nitric oxide metabolites in postmenopausal women but increases flow-mediated vasodilation only in younger women. *Fertil Steril*, **82**. doi:10.1016/j.fertnstert.2004
- Lorenz-Meyer, L.A., Frank, L., Sroka, D., Busjahn, A., Henrich, W. & Verlohren, S., 2022. Correlation between placental weight and angiogenic markers sFlt-1 and PlGF in women with preeclampsia and fetal growth restriction. *Pregnancy Hypertens*, **28**, 149–155, Elsevier B.V. doi:10.1016/j.preghy.2022.04.002
- Lu, F., Longo, M., Tamayo, E., Maner, W., Al-Hendy, A., Anderson, G.D., Hankins, G.D.V., *et al.*, 2007. The effect of over-expression of sFlt-1 on blood pressure and the occurrence of other manifestations of preeclampsia in unrestrained conscious pregnant mice. *Am J Obstet Gynecol*, **196**, 396.e1-396.e7, Mosby Inc. doi:10.1016/j.ajog.2006.12.024
- Lu, J., Sharma, L.K. & Bai, Y., 2009. Implications of mitochondrial DNA mutations and mitochondrial dysfunction in tumorigenesis. *Cell Research 2009 19:7*, **19**, 802–815, Nature Publishing Group. doi:10.1038/cr.2009.69
- Luewan, S., Fuanglada Tongprasert, Kasemsri Srisupundit, Kuntharee Traisisilp & Theera Tongsong, 2014. Reference ranges of myocardial performance index from 12 to 40 weeks of gestation. *Arch Gynecol Obstetrics*, **290**, 859–865. doi:10.1007/s00404-014-3288-3

- Lund, C.J., Donovan, J.C. & York, N., 1967. Blood volume during pregnancy: Significance of plasma and red cell volumes. *American Journal of Obstetric Gynecology*, **98**, 394–403.
- Luo, R., Akpan, I.O., Hayashi, R., Sramko, M., Barr, V., Shiba, Y. & Randazzo, P.A., 2012. GTP-binding protein-like domain of AGAP1 is protein binding site that allosterically regulates ArfGAP protein catalytic activity. *Journal of Biological Chemistry*, **287**, 17176–17185. doi:10.1074/jbc.M111.334458
- Lyll, F., 2002. The human placental bed revisited. *Placenta*, **23**, 555–562, W.B. Saunders Ltd. doi:10.1053/plac.2002.0850
- Ma, L.N., Huang, X.B., Muyayalo, K.P., Mor, G. & Liao, A.H., 2020. Lactic Acid: A Novel Signaling Molecule in Early Pregnancy? *Front Immunol*, **11**, 1–12, Frontiers Media SA. doi:10.3389/FIMMU.2020.00279
- Madron, Éric de, 2015. *Clinical Echocardiography of the Dog and the Cat*. (Éric, de Madron, V. Chetboul & C. Bussadori, Eds.) *Clinical Echocardiography of the Dog and Cat*, 1st ed., Vol. 9, Elsevier Masson. doi:10.1016/B978-0-323-31650-7.00009-0
- Magann, E.F., Bass, J.D., Chauhan, S.P., Perry, K.G., Morrison, J.C. & Martin, J.N., 1994. Accelerated Recovery From Severe Preeclampsia: Uterine Curettage Versus Nifedipine. *J Soc Gynecol Investig*, **1**, 210–214. doi:10.1177/107155769400100306
- Magistrelli, L., Contaldi, E. & Comi, C., 2021. The Impact of SNCA Variations and Its Product Alpha-Synuclein on Non-Motor Features of Parkinson's Disease. *Life*, **11**, 804–813, Multidisciplinary Digital Publishing Institute (MDPI). doi:10.3390/LIFE11080804
- Maglione, D., Guerriero, V., Viglietto, G., Delli-Bovit, P. & Graziella Persico, M., 1991. Isolation of a human placenta cDNA coding for a protein related to the vascular permeability factor (growth factors/cancer/angiogenesis/protein processing). *Proc. Natl. Acad. Sci. USA*, **88**, 9267–9271.
- Magon, N. & Kumar, P., 2012. Hormones in pregnancy. *Nigerian Medical Journal*, **53**, 179, Medknow. doi:10.4103/0300-1652.107549

- Mahendru, A.A., Everett, T.R., Wilkinson, I.B., Lees, C.C. & McEniery, C.M., 2014. A longitudinal study of maternal cardiovascular function from preconception to the postpartum period. *J Hypertens*, **32**, 849–856, Lippincott Williams and Wilkins. doi:10.1097/HJH.0000000000000090
- Maheu-Cadotte, M.-A., Pépin, C., Lavallée, A., Hupé, C., Mailhot, T., Duchaine, C. & Fontaine, G., 2019. Gestational Hypertension, Preeclampsia, and Peripartum Cardiomyopathy: A Clinical Review. *Am J Nurs*, **119**, 41. doi:10.1097/01.NAJ.0000605356.14571.89
- Mahmood, A., Ahmed, K. & Zhang, Y., 2022. β -Adrenergic Receptor Desensitization/Down-Regulation in Heart Failure: A Friend or Foe? *Front Cardiovasc Med*, **9**, 952702, Frontiers Media SA. doi:10.3389/FCVM.2022.925692
- Maines, M.D., Sluss, P.M. & Iscan, M., 1990. Cis-platinum-mediated decrease in serum testosterone is associated with depression of luteinizing hormone receptors and cytochrome p-450scc in rat testis. *Endocrinology*, **126**, 2398–2406. doi:10.1210/endo-126-5-2398
- Makris, A, Thornton, C., Thompson, J., Thomson, S., Martin, R., Ogle, R., Waugh, R., *et al.*, 2007. Uteroplacental ischemia results in proteinuric hypertension and elevated sFLT-1. *Kidney Int*, **71**, 977–984. doi:10.1038/sj.ki.5002175
- Makris, Angela, Yeung, K.R., Lim, S.M., Sunderland, N., Heffernan, S., Thompson, J.F., Iliopoulos, J., *et al.*, 2016. Placental growth factor reduces blood pressure in a uteroplacental ischemia model of preeclampsia in non-human primates Europe PMC Funders Group. *Hypertension*, **67**, 1263–1272. doi:10.1161/HYPERTENSIONAHA.116.07286
- Malek, N., Mrówczyńska, E., Michrowska, A., Mazurkiewicz, E., Pavlyk, I. & Mazur, A.J., 2020. Knockout of ACTB and ACTG1 with CRISPR/Cas9(D10A) Technique Shows that Non-Muscle β and γ Actin Are Not Equal in Relation to Human Melanoma Cells' Motility and Focal Adhesion Formation. *Int J Mol Sci*, **21**. doi:https://doi.org/10.3390/ijms21082746
- Malhamé, I., Dayan, N., Moura, C.S., Samuel, M., Vinet, E. & Pilote, L., 2019. Peripartum cardiomyopathy with co-incident preeclampsia: A cohort study of clinical risk factors and

- outcomes among commercially insured women. *Pregnancy Hypertens*, **17**, 82–88, Elsevier. doi:10.1016/J.PREGHY.2019.05.014
- Maloum, Z., Ramezani, S., Taheri, M., Ghafouri-Fard, S. & Shirvani-Farsani, Z., 2022. Downregulation of long non-coding RNAs in patients with bipolar disorder. *Sci Rep*, **12**, 1–7, Nature Publishing Group. doi:10.1038/s41598-022-11674-y
- Mandavilli, A., 2018. The Placenta, an Afterthought No Longer - The New York Times. Retrieved April 8, 2020, from <https://www.nytimes.com/2018/12/03/health/placenta-pregnancy-health.html>
- Mandò, C., Palma, C. De, Stampalija, T., Anelli, G.M., Figus, M., Novielli, C., Parisi, F., *et al.*, 2014. Placental mitochondrial content and function in intrauterine growth restriction and preeclampsia. *American Journal of Physiology-Endocrinology and Metabolism*, **306**, E404–E413, American Physiological Society Bethesda, MD. doi:10.1152/ajpendo.00426.2013
- Maneerattanasuporn, T., 2017. Maternal Diabetes, Related Biomarkers and Genes, and Risk of Maternal Diabetes, Related Biomarkers and Genes, and Risk of Orofacial Clefts Orofacial Clefts. *Nutrition Commons*, 5–10. Retrieved from <https://digitalcommons.usu.edu/etd/6215>
- Mano, Y., Kotani, T., Ito, M., Nagai, T., Ichinohashi, Y., Yamada, K., Ohno, K., *et al.*, 2014. Maternal molecular hydrogen administration ameliorates rat fetal hippocampal damage caused by in utero ischemia–reperfusion. *Free Radic Biol Med*, **69**, 324–330, Pergamon. doi:10.1016/J.FREERADBIOMED.2014.01.037
- Marcin, J. & Berry, J., 2018, July 1. Postpartum blood clots and bleeding: What to expect. *Medical News Today*, Lippincott Williams and Wilkins. doi:10.1056/NEJMOMA1311485
- Marcolan Quitete, C.M., Marcolan Salvany, A., Andrade Martins, W. De & Mesquita, E.T., 2015. Left ventricular remodeling and diastolic function in chronic hypertensive pregnant women. *Pregnancy Hypertens*, **5**, 187–192, Elsevier. doi:10.1016/j.preghy.2015.01.007
- Markovitz, A.R., Stuart, J.J., Horn, J., Williams, P.L., Rimm, E.B., Missmer, S.A., Tanz, L.J., *et al.*, 2019. Does pregnancy complication history improve cardiovascular disease risk

prediction? Findings from the HUNT study in Norway. *Eur Heart J*, **40**, 1113–1120, Eur Heart J. doi:10.1093/EURHEARTJ/EHY863

Marschalek, J., Wohlrab, P., Ott, J., Wojta, J., Speidl, W., Klein, K.U., Kiss, H., *et al.*, 2018. Maternal serum mitochondrial DNA (mtDNA) levels are elevated in preeclampsia – A matched case-control study. *Pregnancy Hypertens*, **14**, 195–199, Elsevier. doi:10.1016/J.PREGHY.2018.10.003

Mashini, I.S., Albazzaz, S.J., Fadel, H.E., Abdulla, A.M., Hadi, H.A., Harp, R. & Devoe, L.D., 1987. Serial noninvasive evaluation of cardiovascular hemodynamics during pregnancy. *American Journal of Obstetrics*, **156**, 1208–1213.

Matsuo, K., Kooshesh, S., Dinc, M., Sun, C.C.J., Kimura, T. & Baschat, A.A., 2007. Late postpartum eclampsia: report of two cases managed by uterine curettage and review of the literature. *Am J Perinatol*, **24**, 257–266, Am J Perinatol. doi:10.1055/S-2007-976548

Matsuzawa, Y., Kwon, T.G., Lennon, R.J., Lerman, L.O. & Lerman, A., 2015. Prognostic Value of Flow-Mediated Vasodilation in Brachial Artery and Fingertip Artery for Cardiovascular Events: A Systematic Review and Meta-Analysis. *J Am Heart Assoc*, **4**, 1–17, John Wiley and Sons Inc. doi:10.1161/JAHA.115.002270

Mauricio, R., Singh, K., Sanghavi, M., Ayers, C.R., Rohatgi, A., Vongpatanasin, W., Lemos, J.A. de, *et al.*, 2022. Soluble Fms-like tyrosine kinase-1 (sFlt-1) is associated with subclinical and clinical atherosclerotic cardiovascular disease: The Dallas Heart Study. *Atherosclerosis*, **346**, 46–52, Atherosclerosis. doi:10.1016/J.ATHEROSCLEROSIS.2022.02.026

Mayhan, W.G., Faraci, F.M. & Heistad, D.D., 1988. Effects of vasodilatation and acidosis on the blood-brain barrier. *Microvasc Res*, **35**, 179–192, Academic Press. doi:10.1016/0026-2862(88)90061-1

Maymó, J.L., Pérez Pérez, A., Maskin, B., Dueñas, J.L., Calvo, J.C., Sánchez Margalet, V. & Varone, C.L., 2012. The Alternative Epac/cAMP Pathway and the MAPK Pathway Mediate hCG Induction of Leptin in Placental Cells. *PLoS One*, **7**, e46223, Public Library of Science. doi:10.1371/JOURNAL.PONE.0046216

- Maynard, S., Epstein, F.H. & Ananth Karumanchi, S., 2008. Preeclampsia and Angiogenic Imbalance. *Annu Rev Med*, **59**, 61–78. doi:10.1146/annurev.med.59.110106.214058
- Maynard, S.E., Min, J., Merchan, J., Lim, K.-H., Li, J., Mondal, S., Libermann, T.A., Morgon, J.P., *et al.*, 2003. Excess placental soluble fms-like tyrosine kinase 1 (sFlt1) may contribute to endothelial dysfunction hypertension, and proteinuria in preeclampsia. *Journal of Clinical Investigation*, **111**, 649–58. doi:10.1172/JCI200317189.
- Maynard, S.E., Min, J.Y., Merchan, J., Lim, K.H., Li, J., Mondal, S., Libermann, T.A., Morgan, J.P., *et al.*, 2003. Excess placental soluble fms-like tyrosine kinase 1 (sFlt1) may contribute to endothelial dysfunction hypertension, and proteinuria in preeclampsia. *Journal of Clinical Investigation*, **111**, 649–658, The American Society for Clinical Investigation. doi:10.1172/JCI17189
- McAninch, D., Roberts, C.T. & Bianco-Miotto, T., 2017. Mechanistic Insight into Long Noncoding RNAs and the Placenta. *International Journal of Molecular Sciences 2017*, Vol. 18, Page 1371, **18**, 1387, Multidisciplinary Digital Publishing Institute. doi:10.3390/IJMS18071371
- McCowan, J., Kirkwood, P.M., Fercoq, F., T'Jonck, W., Mawer, C.M., Cunningham, R., Mirchandani, A.S., *et al.*, 2021. The transcription factor EGR2 is indispensable for tissue-specific imprinting of alveolar macrophages in health and tissue repair. *bioRxiv*, **4**, Cold Spring Harbor Laboratory. doi:10.1101/2021.05.06.442095
- Mcgrath, C., Pudwell, J., Pienaar, M., Pienaar, E. & Smith, G., 2020. Postpartum Cardiovascular Risk Screening In A Northern Community Clinic Vs. A Tertiary Centre Clinic. *Journal of Obstetrics and Gynaecology Canada*, **42**, 682. doi:10.1016/j.jogc.2020.02.067
- McKie, A., Barrow, D., Latunde-Dada, G.O., Rolfs, A., Sager, G., Mudaly, E., Mudaly, M., *et al.*, 2001. An iron-regulated ferric reductase associated with the absorption of dietary iron. *Science*, **291**, 1755–1759, Science. doi:10.1126/SCIENCE.1057206
- McKie, A.T., Latunde-Dada, G.O., Miret, S., McGregor, J.A., Anderson, G.J., Vulpe, C.D., Wrigglesworth, J.M., *et al.*, 2002. Molecular evidence for the role of a ferric reductase in

iron transport. *Biochem Soc Trans*, **30**, 722–724, Biochem Soc Trans. doi:10.1042/BST0300722

Meagher, P.B., Lee, X.A., Lee, J., Visram, A., Friedberg, M.K. & Connelly, K.A., 2021. Cardiac Fibrosis: Key Role of Integrins in Cardiac Homeostasis and Remodeling. *Cells* **2021**, Vol. *10*, Page 770, **10**, 788, Multidisciplinary Digital Publishing Institute. doi:10.3390/CELLS10040770

Meah, V.L., Cockcroft, J.R., Backx, K., Shave, R. & Stöhr, E.J., 2016. Cardiac output and related haemodynamics during pregnancy: A series of meta-analyses. *Heart*, **102**, 518–526, BMJ Publishing Group. doi:10.1136/heartjnl-2015-308476

Mebratu, Y. & Tesfaigzi, Y., 2009. How ERK1/2 Activation Controls Cell Proliferation and Cell Death Is Subcellular Localization the Answer? *Cell Cycle*, **8**, 1168, NIH Public Access. doi:10.4161/CC.8.8.8147

Mechanism and Contraction Events of Cardiac Muscle Fibers - Medicine LibreTexts, (n.d.). *Cardiac Muscle Tissue*. Retrieved June 6, 2023, from [https://med.libretexts.org/Bookshelves/Anatomy_and_Physiology/Anatomy_and_Physiology_\(Boundless\)/17%3A_Cardiovascular_System%3A_The_Heart/17.3%3A_Cardiac_Muscle_Tissue/17.3A%3A_Mechanism_and_Contraction_Events_of_Cardiac_Muscle_Fibers](https://med.libretexts.org/Bookshelves/Anatomy_and_Physiology/Anatomy_and_Physiology_(Boundless)/17%3A_Cardiovascular_System%3A_The_Heart/17.3%3A_Cardiac_Muscle_Tissue/17.3A%3A_Mechanism_and_Contraction_Events_of_Cardiac_Muscle_Fibers)

Medica, I., Kastrin, A. & Peterlin, B., 2007. Genetic polymorphisms in vasoactive genes and preeclampsia: a meta-analysis. *Eur J Obstet Gynecol Reprod Biol*, **131**, 115–126, Eur J Obstet Gynecol Reprod Biol. doi:10.1016/J.EJOGRB.2006.10.005

Medina-Bastidas, D., Guzmán-Huerta, M., Borboa-Olivares, H., Ruiz-Cruz, C., Parra-Hernández, S., Flores-Pliego, A., Salido-Guadarrama, I., *et al.*, 2020. Placental Microarray Profiling Reveals Common mRNA and lncRNA Expression Patterns in Preeclampsia and Intrauterine Growth Restriction. *International Journal of Molecular Sciences Article Int. J. Mol. Sci*, **21**, 121–3618. doi:10.3390/ijms21103597

Medzikovic, L., Vries, C.J.M. de & Waard, V. de, 2019. NR4A nuclear receptors in cardiac remodeling and neurohormonal regulation. *Trends Cardiovasc Med*, **29**, 429–437, Trends Cardiovasc Med. doi:10.1016/J.TCM.2018.11.015

- Mehendale, R., Hibbard, J., Fazleabas, A. & Leach, R., 2007. Placental angiogenesis markers sFlt-1 and PIGF: response to cigarette smoke. *Am J Obstet Gynecol*, **197**, e1–e5. doi:10.1016/j.ajog.2007.06.025
- Melchiorre, K., Sutherland, G., Sharma, R., Nanni, M. & Thilaganathan, B., 2013. Mid-gestational maternal cardiovascular profile in preterm and term pre-eclampsia: a prospective study. *BJOG*, **120**, 496–504, John Wiley & Sons, Ltd. doi:10.1111/1471-0528.12068
- Melchiorre, K., Sutherland, G., Sharma, R., Nanni, M. & Thilaganathan, B., 2013. Mid-gestational maternal cardiovascular profile in preterm and term pre-eclampsia: a prospective study. *BJOG*, **120**, 496–504, John Wiley & Sons, Ltd. doi:10.1111/1471-0528.12068
- Melchiorre, Karen, Sharma, R., Khalil, A. & Thilaganathan, B., 2016. Maternal Cardiovascular Function in Normal Pregnancy: Evidence of Maladaptation to Chronic Volume Overload. *Hypertension*, **67**, 754–62, Lippincott Williams and Wilkins. doi:10.1161/HYPERTENSIONAHA.115.06667
- Melchiorre, Karen, Sharma, R., Khalil, A. & Thilaganathan, B., 2016. Maternal cardiovascular function in normal pregnancy: Evidence of maladaptation to chronic volume overload. *Hypertension*, **67**, 754–762, Lippincott Williams and Wilkins. doi:10.1161/HYPERTENSIONAHA.115.06667/-/DC1
- Melchiorre, Karen, Sharma, R. & Thilaganathan, B., 2012. Cardiac structure and function in normal pregnancy. *Curr Opin Obstet Gynecol*, **24**, 413–421. doi:10.1097/GCO.0b013e328359826f
- Melchiorre, Karen, Sharma, R. & Thilaganathan, B., 2014. Cardiovascular implications in preeclampsia: An overview. *Circulation*, **130**, 703–714. doi:10.1161/CIRCULATIONAHA.113.003664
- Melchiorre, Karen, Sutherland, G.R., Baltabaeva, A., Liberati, M. & Thilaganathan, B., 2011. Maternal cardiac dysfunction and remodeling in women with preeclampsia at term. *Hypertension*, **57**, 85–93, Lippincott Williams & Wilkins Hagerstown, MD. doi:10.1161/HYPERTENSIONAHA.110.162321

- Melchiorre, Karen, Sutherland, G.R., Baltabaeva, A., Liberati, M. & Thilaganathan, B., 2011. Maternal Cardiac Dysfunction and Remodeling in Women With Preeclampsia at Term. *Hypertension*, **57**, 85–93, Lippincott Williams & Wilkins Hagerstown, MD. doi:10.1161/HYPERTENSIONAHA.110.162321
- Melchiorre, Karen, Sutherland, G.R., Liberati, M. & Thilaganathan, B., 2011. Preeclampsia is associated with persistent postpartum cardiovascular impairment. *Hypertension*, **58**, 709–715. doi:10.1161/HYPERTENSIONAHA.111.176537
- Melchiorre, Karen, Sutherland, G.R., Watt-Coote, I., Liberati, M. & Thilaganathan, B., 2012. Severe myocardial impairment and chamber dysfunction in preterm preeclampsia. *Hypertens Pregnancy*, **31**, 454–471, Taylor & Francis. doi:10.3109/10641955.2012.697951
- Meng, G., Liu, J., Liu, S., Song, Q., Liu, L., Xie, L., Han, Y., *et al.*, 2018. Hydrogen sulfide pretreatment improves mitochondrial function in myocardial hypertrophy via a SIRT3-dependent manner. *Br J Pharmacol*, **175**, 1126–1145, Br J Pharmacol. doi:10.1111/BPH.13861
- Meng, X., McGraw, C.M., Wang, W., Jing, J., Yeh, S.Y., Wang, L., Lopez, J., *et al.*, 2019. Neurexophilin4 is a selectively expressed α -neurexin ligand that modulates specific cerebellar synapses and motor functions. *Elife*, **8**, 1–28, eLife Sciences Publications, Ltd. doi:10.7554/ELIFE.46773
- Mesa, A., Jessurun, C., Hernandez, A., Adam, K., Brown, D., Vaughn, W.K. & Wilansky, S., 1999. Left Ventricular Diastolic Function in Normal Human Pregnancy. *Circulation*, **99**, 511–517, Lippincott Williams and Wilkins. doi:10.1161/01.CIR.99.4.511
- Meyer, D.E. & Chilkoti, A., 1999. Purification of recombinant proteins by fusion with thermally-responsive polypeptides. *Nat Biotechnol*, **17**, 1112–1115, Nature Publishing Group. doi:10.1038/15100
- Meyers, K.J., Mosley, T.H., Fox, E., Boerwinkle, E., Arnett, D.K., Devereux, R.B. & Kardia, S.L.R., 2007. Genetic variations associated with echocardiographic left ventricular traits in hypertensive blacks. *Hypertension*, **49**, 992–999, Hypertension. doi:10.1161/HYPERTENSIONAHA.106.081265

- Miao, L., Shen, X., Whiteman, M., Xin, H., Shen, Y., Xin, X., Moore, P.K., *et al.*, 2016. Hydrogen Sulfide Mitigates Myocardial Infarction via Promotion of Mitochondrial Biogenesis-Dependent M2 Polarization of Macrophages. *Antioxid Redox Signal*, **25**, 268–281, Antioxid Redox Signal. doi:10.1089/ARS.2015.6577
- Miller, E.C., 2019. Preeclampsia and Cerebrovascular Disease: The Maternal Brain at Risk. *Hypertension*, **74**, 5–13. doi:10.1161/HYPERTENSIONAHA.118.11513
- Miller, E.C., Miltiades, A., Pimentel-Soler, N., Booker, W.A., Landau-Cahana, R., Marshall, R.S., D’Alton, M.E., *et al.*, 2021. Cardiovascular and cerebrovascular health after pre-eclampsia: The Motherhealth prospective cohort study protocol. *BMJ Open*, **11**, 1–6. doi:10.1136/bmjopen-2020-043052
- Minamishima, S., Bougaki, M., Sips, P.Y., Yu, J. De, Minamishima, Y.A., Elrod, J.W., Lefer, D.J., *et al.*, 2009. Hydrogen Sulfide Improves Survival After Cardiac Arrest and Cardiopulmonary Resuscitation via a Nitric Oxide Synthase 3–Dependent Mechanism in Mice. *Circulation*, **120**, 888–896, Lippincott Williams & Wilkins. doi:10.1161/CIRCULATIONAHA.108.833491
- Miquerol, L., Langille, B.L. & Nagy, A., 2000. Embryonic development is disrupted by modest increases in vascular endothelial growth factor gene expression. *Development*, 3941–3946. doi:doi.org/10.1242/dev.127.18.3941
- Mistry, H.D., McCallum, L.A., Kurlak, L.O., Greenwood, I.A., Pipkin, F.B. & Tribe, R.M., 2011. Novel expression and regulation of voltage-dependent potassium channels in placentas from women with preeclampsia. *Hypertension*, **58**, 497–504, Lippincott Williams & Wilkins Hagerstown, MD. doi:10.1161/HYPERTENSIONAHA.111.173740
- Miyata, K., Kawakami, K., Onimaru, T., Baba, Y., Ono, S., Hokonohara, M., Yoshinaga, M., *et al.*, 1984. Circulation Immune Complexes and Granulocytes Chemotaxis in Kawasaki Disease: THE 8TH CONFERENCE ON PREVENTION FOR RHEUMATIC FEVER AND RHEUMATIC HEART DISEASE. *Jpn Circ J*, **48**, 1350–1353, The Japanese Circulation Society. doi:10.1253/JCJ.48.1350

- Miyata, S., Minobe, W., Bristow, M.R. & Leinwand, L.A., 2000. Myosin Heavy Chain Isoform Expression in the Failing and Nonfailing Human Heart. *Circ Res*, **86**, 386–390, Lippincott Williams & Wilkins. doi:10.1161/01.RES.86.4.386
- Mizukami, Y., Iwamatsu, A., Aki, T., Kimura, M., Nakamura, K., Nao, T., Okusa, T., *et al.*, 2004. ERK1/2 regulates intracellular ATP levels through alpha-enolase expression in cardiomyocytes exposed to ischemic hypoxia and reoxygenation. *J Biol Chem*, **279**, 50120–50131, J Biol Chem. doi:10.1074/JBC.M402299200
- Módis, K., Coletta, C., Erdélyi, K., Papapetropoulos, A. & Szabo, C., 2013. Intramitochondrial hydrogen sulfide production by 3-mercaptopyruvate sulfurtransferase maintains mitochondrial electron flow and supports cellular bioenergetics. *The FASEB Journal*, **27**, 601–611, John Wiley & Sons, Ltd. doi:10.1096/FJ.12-216507
- Mohamad, M.A., Manzor, N.F.M., Zulkifli, N.F., Zainal, N., Hayati, A.R. & Asnawi, A.W.A., 2020. A Review of Candidate Genes and Pathways in Preeclampsia—An Integrated Bioinformatical Analysis. *Biology (Basel)*, **9**, 83, Multidisciplinary Digital Publishing Institute (MDPI). doi:10.3390/BIOLOGY9040062
- Mol, B.W.J., Roberts, C.T., Thangaratinam, S., Magee, L.A., Groot, C.J.M. De & Hofmeyr, G.J., 2016. Pre-eclampsia. *The Lancet*, Vol. 387, pp. 999–1011, Lancet Publishing Group. doi:10.1016/S0140-6736(15)00070-7
- Mone, S.M., Sanders, S.P. & Colan, S.D., 1996. Control mechanisms for physiological hypertrophy of pregnancy. *Circulation*, **94**, 667–672, Lippincott Williams and Wilkins. doi:10.1161/01.CIR.94.4.667
- Monika Sanghavi & John D. Rutherford, 2014. Cardiovascular Management in Pregnancy. *Circulation*, **130**, 1003–1008. doi:10.1161/CIRCULATIONAHA.114.009029
- Montuori, N., Visconte, V., Rossi, G. & Ragno, P., 2005. Soluble and cleaved forms of the urokinase-receptor: degradation products or active molecules? *Thromb Haemost*, **93**, 192–198, Thromb Haemost. doi:10.1160/TH04-09-0580

- Moolla, M., Mathew, A., John, K., Yogasundaram, H., Alhumaid, W., Campbell, S. & Windram, J., 2022. Outcomes of pregnancy in women with hypertrophic cardiomyopathy: A systematic review ☆. *Int J Cardiol*, **359**, 54–60. doi:10.1016/j.ijcard.2022.04.034
- Morasso, M.I., Rieber, M.S., Gil, F. & Rieber, M., 1990. Cell adhesion regulates melanoma specific differentiation and interactions with the 3' region of the tyrosinase gene. *Biochem Biophys Res Commun*, **172**, 638–645, Biochem Biophys Res Commun. doi:10.1016/0006-291X(90)90722-Y
- Morelli, A.E. & Sadovsky, Y., 2022. Extracellular vesicles and immune response during pregnancy: A balancing act*. *Immunol Rev*, **308**, 105–122, John Wiley & Sons, Ltd. doi:10.1111/IMR.13074
- Morgan, H.L., Butler, E., Ritchie, S., Herse, F., Dechend, R., Beattie, E., McBride, M.W., *et al.*, 2018. Modeling superimposed preeclampsia using ang II (angiotensin II) infusion in pregnant stroke-prone spontaneously hypertensive rats. *Hypertension*, **72**, 208–218, Lippincott Williams and Wilkins. doi:10.1161/HYPERTENSIONAHA.118.10935
- Mosca, L., Benjamin, E.J., Berra, K., Bezanson, J.L., Dolor, R.J., Lloyd-Jones, D.M., Newby, L.K., *et al.*, 2011. Effectiveness-based guidelines for the prevention of cardiovascular disease in women--2011 update: a guideline from the american heart association. *Circulation*, **123**, 1243–1262, Circulation. doi:10.1161/CIR.0B013E31820FAAF8
- Moser, G., Guettler, J., Forstner, D. & Gauster, M., 2019. Maternal Platelets of the Human Placenta: Friend or Foe? *Int J Mol Sci*, **20**. doi:10.3390/ijms20225639
- Moses, E.K., Lade, J.A., Guo, G., Wilton, A.N., Grehan, M., Freed, K., Borg, A., *et al.*, 2000. A genome scan in families from Australia and New Zealand confirms the presence of a maternal susceptibility locus for pre-eclampsia, on chromosome 2. *Am J Hum Genet*, **67**, 1581–1585, Am J Hum Genet. doi:10.1086/316888
- Most, P., Bernotat, J., Ehlermann, P., Pleger, S.T., Reppel, M., Bö, M., Niroomand, F., *et al.*, 2001. S100A1: A regulator of myocardial contractility. *PNAS*, **98**, 13889–13894. Retrieved from www.pnas.org/cgi/doi/10.1073/pnas.241393598

- Mostafavi, A., Tase, Y., Id, Z., Id, N. & Tabatabaei, A., 2019. Comparison of left ventricular systolic function by 2D speckle-tracking echocardiography between normal pregnant women and pregnant women with preeclampsia. *J Cardiovasc Thorac Res*, **11**, 309–313. doi:10.15171/jcvtr.2019.50
- Mousa, A.A., Strauss, J.F. & Walsh, S.W., 2012. Reduced methylation of the thromboxane synthase gene is correlated with its increased vascular expression in preeclampsia. *Hypertension*, **59**, 1249–1255, Lippincott Williams & Wilkins Hagerstown, MD. doi:10.1161/HYPERTENSIONAHA.111.188730
- Mu Junwu & Lee, S.A., 2006. Developmental changes in hemodynamics of uterine artery, utero- and umbilicoplacental, and vitelline circulations in mouse throughout gestation. *American Journal of Physiology-Heart and Circulatory Physiology*, **291**, H1421–H1428. doi:10.1152/ajpheart.00031.2006
- Mubarik, A., Chippa, V. & Iqbal, A.M., 2023. Postpartum Cardiomyopathy. *Appl Radiol*, **41**, 25–26, StatPearls Publishing. doi:10.37549/ar1956
- Muellner, M.K., Schreier, S.M., Laggner, H., Hermann, M., Esterbauer, H., Exner, M., Gmeiner, B.M.K., *et al.*, 2009. Hydrogen sulfide destroys lipid hydroperoxides in oxidized LDL. *Biochem J*, **420**, 277–281, Biochem J. doi:10.1042/BJ20082421
- Muhr et al. 2022_Embryology, Gastrulation - StatPearls - NCBI Bookshelf, (n.d.).
- Mulder, E.G., Haas, S. de, Mohseni, Z., Schartmann, N., Abo Hasson, F., Alsadah, F., Kuijk, S.M.J. van, *et al.*, 2022. Cardiac output and peripheral vascular resistance during normotensive and hypertensive pregnancy – a systematic review and meta-analysis. *BJOG*, **129**, 696–707, John Wiley and Sons Inc. doi:10.1111/1471-0528.16678
- Mulic-Lutvica, A., Eurenus, K. & Axelsson, O., 2007. Longitudinal study of Doppler flow resistance indices of the uterine arteries after normal vaginal delivery. *Acta Obstet Gynecol Scand*, **86**, 1207–1214, Acta Obstet Gynecol Scand. doi:10.1080/00016340701621569
- Muñoz-Fernández, R., Prados, A., Leno-Durán, E., Blázquez, A., García-Fernández, J.R., Ortiz-Ferrón, G. & Olivares, E.G., 2012. Human decidual stromal cells secrete C-X-C

motif chemokine 13, express B cell-activating factor and rescue B lymphocytes from apoptosis: distinctive characteristics of follicular dendritic cells. *Hum Reprod*, **27**, 2775–2784, Hum Reprod. doi:10.1093/HUMREP/DES198

Murata, K., Saito, C., Ishida, J., Hamada, J., Sugiyama, F., Yagami, K.I. & Fukamizu, A., 2013. Effect of Lactation on Postpartum Cardiac Function of Pregnancy-Associated Hypertensive Mice. *Endocrinology*, **154**, 597–602, Oxford Academic. doi:10.1210/EN.2012-1789

Murphy, E., Ardehali, H., Balaban, R.S., DiLisa, F., Dorn, G.W., Kitsis, R.N., Otsu, K., *et al.*, 2016. Mitochondrial Function, Biology, and Role in Disease: A Scientific Statement From the American Heart Association. *Circ Res*, **118**, 1960–1991, Circ Res. doi:10.1161/RES.000000000000104

Murphy, R.P., 1979. Parkinsonism after traumatic childbirth The operation and postoperative period were uneventful until the. *J Neurol Neurosurg Psychiatry*, **42**, 384–385. doi:10.1136/jnnp.42.4.384

Mustafa, A.K., Sikka, G., Gazi, S.K., Stepan, J., Jung, S.M., Bhunia, A.K., Barodka, V.M., *et al.*, 2011. Hydrogen sulfide as endothelium-derived hyperpolarizing factor sulfhydrates potassium channels. *Circ Res*, **109**, 1259–1268. doi:10.1161/CIRCRESAHA.111.240242

Mustonen, T. & Alitalo, K., 1995. Endothelial receptor tyrosine kinases involved in angiogenesis. *Journal of Cell Biology*, **129**, 895–898, Rockefeller University Press. doi:10.1083/jcb.129.4.895

Muthyala, T., Mehrotra, S., Sikka, P. & Suri, V., 2016. Maternal cardiac diastolic dysfunction by doppler echocardiography in women with preeclampsia. *Journal of Clinical and Diagnostic Research*, **10**, QC01–QC03, Journal of Clinical and Diagnostic Research. doi:10.7860/JCDR/2016/17840.8220

Mutter, W.P. & Karumanchi, S.A., 2008. Molecular mechanisms of preeclampsia. *Microvasc Res*, **75**, 1–8. doi:10.1016/j.mvr.2007.04.009

Mutter, W.P. & Karumanchi, S.A., 2008, January. Molecular mechanisms of preeclampsia. *Microvasc Res*. doi:10.1016/j.mvr.2007.04.009

- Mütze, S., Rudnik-Schöneborn, S., Zerres, K. & Rath, W., 2008. Genes and the preeclampsia syndrome. *J Perinat Med*, **36**, 38–58, J Perinat Med. doi:10.1515/JPM.2008.004
- Myatt, L. & Cui, X., 2004. Oxidative stress in the placenta. *Histochem Cell Biol*, **122**, 369–382. doi:10.1007/s00418-004-0677-x
- Myatt, L. & Cui, X., 2004. Oxidative stress in the placenta. *Histochem Cell Biol*, **122**, 369–382, Springer. doi:10.1007/S00418-004-0677-X/FIGURES/6
- Myatt, L. & Powell, T., 2010. Maternal adaptations to pregnancy and the role of the placenta. in *Maternal-Fetal Nutrition During Pregnancy and Lactation*, pp. 1–11, Cambridge University Press. doi:10.1017/CBO9780511674792.001
- Myredal, A., Gan, L.M., Osika, W., Friberg, P. & Johansson, M., 2010. Increased intima thickness of the radial artery in individuals with prehypertension and hypertension. *Atherosclerosis*, **209**, 147–151, Elsevier. doi:10.1016/J.ATHEROSCLEROSIS.2009.09.017
- Naeh, A., Berezowsky, A., Yaniv, S.S., Berger, H., Agrawal, S. & Ray, J.G., 2022. Persistence of abnormal uterine artery flow postpartum: Case-control study. *Pregnancy Hypertens*, **29**, 21–22, Elsevier. doi:10.1016/J.PREGHY.2022.05.010
- Nagueh, S.F., Smiseth, O.A., Appleton, C.P., Byrd, B.F., Dokainish, H., Edvardsen, T., Flachskampf, F.A., *et al.*, 2016. Recommendations for the Evaluation of Left Ventricular Diastolic Function by Echocardiography: An Update from the American Society of Echocardiography and the European Association of Cardiovascular Imaging. *Journal of the American Society of Echocardiography*, **29**, 277–314, Mosby Inc. doi:10.1016/j.echo.2016.01.011
- Naik, A. & Decock, J., 2022. Targeting of lactate dehydrogenase C dysregulates the cell cycle and sensitizes breast cancer cells to DNA damage response targeted therapy. *Mol Oncol*, **16**, 885–903, Mol Oncol. doi:10.1002/1878-0261.13024
- Nakamura, T. & Tsujita, K., 2021. Current trends and future perspectives for heart failure treatment leveraging cGMP modifiers and the practical effector PKG. *J Cardiol*, **78**, 261–268, Elsevier. doi:10.1016/J.JJCC.2021.03.004

- Namugowa, A., Iputo, J., Wandabwa, J., Meeme, A., Buga, G.A.B., Abura, S. & Stofile, Y.Y., 2019. Arterial stiffness in women previously with preeclampsia from a semi-rural region of South Africa. *Clin Exp Hypertens*, **41**, 36–43, Clin Exp Hypertens. doi:10.1080/10641963.2018.1441858
- Nastasi, T., Muzi, P., Beccari, S., Bellafore, M., Dolo, V., Bologna, M., Cestelli, A., *et al.*, 2000. Specific neurons of brain cortex and cerebellum are PIPPin positive. *Neuroreport*, **11**, 2233–2236, Neuroreport. doi:10.1097/00001756-200007140-00034
- Navarro-YepesJuliana, BurnsMichaela, AnandhanAnnadurai, KhalimonchukOleh, Maria, del R., Quintanilla-VegaBetzabet, PappaAglaiia, *et al.*, 2014. Oxidative Stress, Redox Signaling, and Autophagy: Cell Death Versus Survival. <https://home.liebertpub.com/ars>, Mary Ann Liebert, Inc. 140 Huguenot Street, 3rd Floor New Rochelle, NY 10801 USA . doi:10.1089/ARS.2014.5837
- Neuhaus, H., Rosen, V. & Thies, R.S., 1999. Heart specific expression of mouse BMP-10 a novel member of the TGF- β superfamily. *Mech Dev*, **80**, 181–184, Mech Dev. doi:10.1016/S0925-4773(98)00221-4
- Neuman, R.I., Figaroa, A.M.J., Nieboer, D., Saleh, L., Verdonk, K., Danser, A.H.J., Duvekot, H.J.J., *et al.*, 2021. Angiogenic markers during preeclampsia: Are they associated with hypertension 1 year postpartum? *Pregnancy Hypertens*, **23**, 116–122, Elsevier. doi:10.1016/J.PREGHY.2020.11.011
- Ngene, N.C. & Moodley, J., 2020. Postpartum blood pressure patterns in severe preeclampsia and normotensive pregnant women following abdominal deliveries: a cohort study. *Journal of Maternal-Fetal and Neonatal Medicine*, **33**, 3152–3162, Taylor and Francis Ltd. doi:10.1080/14767058.2019.1569621
- Nhan-Chang, C.L., Romero, R., Kusanovic, J.P., Gotsch, F., Edwin, S.S., Erez, O., Mittal, P., *et al.*, 2008. A role for CXCL13 (BCA-1) in pregnancy and intra-amniotic infection/inflammation. *J Matern Fetal Neonatal Med*, **21**, 763–775, J Matern Fetal Neonatal Med. doi:10.1080/14767050802244946
- Nicholls, P. & Kim, J.K., 1982. Sulphide as an inhibitor and electron donor for the cytochrome c oxidase system. *Can J Biochem*, **60**, 613–623, Can J Biochem. doi:10.1139/O82-076

- Nicholls, Peter, Marshall, D.C., Cooper, C.E. & Wilson, M.T., 2013. Sulfide inhibition of and metabolism by cytochrome c oxidase. *Biochem Soc Trans*, **41**, 1312–1316, Biochem Soc Trans. doi:10.1042/BST20130070
- Nicholson, C.K. & Calvert, J.W., 2010. Hydrogen sulfide and ischemia–reperfusion injury. *Pharmacol Res*, **62**, 289–297, Academic Press. doi:10.1016/J.PHRS.2010.06.002
- Nishijima, K., Kiryu, J., Tsujikawa, A., Miyamoto, K., Honjo, M., Tanihara, H., Nonaka, A., *et al.*, 2004. Platelets Adhering to the Vascular Wall Mediate Postischemic Leukocyte–Endothelial Cell Interactions in Retinal Microcirculation. *Invest Ophthalmol Vis Sci*, **45**, 977–984, The Association for Research in Vision and Ophthalmology. doi:10.1167/IOVS.03-0526
- Noback, C.R., 1946. Placentation and angiogenesis in the amnion of a baboon (*Papio papio*). *Anat Rec*, **94**, 553–567, John Wiley & Sons, Ltd. doi:10.1002/ar.1090940402
- Norton, M.T., Fortner, K.A., Bizargity, P. & Bonney, E.A., 2009. Pregnancy alters the proliferation and apoptosis of mouse splenic erythroid lineage cells and leukocytes. *Biol Reprod*, **81**, 457–464. doi:10.1095/biolreprod.109.076976
- Nouri, F.S., Wang, X., Chen, X. & Hatefi, A., 2015. Reducing the Visibility of the Vector/DNA Nanocomplexes to the Immune System by Elastin-Like Peptides. *Pharm Res*, **32**, 3018–3028. doi:10.1007/s11095-015-1683-5
- Novelli, G.P., Vasapollo, B., Gagliardi, G., Tiralongo, G.M., Pisani, I., Manfellotto, D., Giannini, L., *et al.*, 2012. Left ventricular midwall mechanics at 24 weeks' gestation in high-risk normotensive pregnant women: relationship to placenta-related complications of pregnancy. *Ultrasound Obstet Gynecol*, **39**, 430–437. doi:10.1002/uog.10089
- Numata, G. & Takimoto, E., 2022. Cyclic GMP and PKG Signaling in Heart Failure. *Front Pharmacol*, **13**, 1–12, Frontiers Media S.A. doi:10.3389/FPHAR.2022.792798/BIBTEX
- O. Adeyeye¹, V., M. O. Balogun², R. A. Adebayo², O. N. Makinde³, P. O. Akinwusi⁴, E. A. Ajayi⁵, S. A. Ogunyemi², *et al.*, 2016. Echocardiographic Assessment of Cardiac Changes During Normal Pregnancy Among Nigerians. *Clin Med Insights Cardiol*, **10**,

<https://www.ncbi.nlm.nih.gov/pmc/articles/PMC5015814/pdf/cmc-10-2016-157.pdf>

- Obel, N., Andersen, P.L. & Andersen, H.R., 1993. Preserved oxidative activity and chemotaxis of circulating neutrophils in patients with acute myocardial infarction. *Eur Heart J*, **14**, 790–794, *Eur Heart J*. doi:10.1093/EURHEARTJ/14.6.790
- Ocaña, O.H., Coskun, H., Minguillón, C., Murawala, P., Tanaka, E.M., Galcerán, J., Muñoz-Chápuli, R., *et al.*, 2017. A right-handed signalling pathway drives heart looping in vertebrates. *Nature*, **549**, 90, Europe PMC Funders. doi:10.1038/NATURE23454
- Oehm, E., Hetzel, A., Els, T., Berlis, A., Keck, C., Will, H.G. & Reinhard, M., 2006. Cerebral hemodynamics and autoregulation in reversible posterior leukoencephalopathy syndrome caused by pre-eclampsia. *Cerebrovascular Diseases*, **22**, 204–208. doi:10.1159/000093810
- Ohkuchi, A., Saito, S., Yamamoto, T., Minakami, H., Masuyama, H., Kumasawa, K., Yoshimatsu, J., *et al.*, 2021. Short-term prediction of preeclampsia using the sFlt-1/PIGF ratio: a subanalysis of pregnant Japanese women from the PROGNOSIS Asia study. *Hypertension Research*, **44**, 813–821, Springer Nature. doi:10.1038/s41440-021-00629-x
- Ohta, K., Kobashi, G., Hata, A., Yamada, H., Minakami, H., Fujimoto, S., Kondo, K., *et al.*, 2003. Association between a variant of the glutathione S-transferase P1 gene (GSTP1) and hypertension in pregnancy in Japanese: interaction with parity, age, and genetic factors. *Semin Thromb Hemost*, **29**, 653–659, *Semin Thromb Hemost*. doi:10.1055/S-2004-815636
- Ohtsuka, M., Sasaki, K. ichiro, Ueno, T., Seki, R., Nakayoshi, T., Koiwaya, H., Toyama, Y., *et al.*, 2013. Platelet-derived microparticles augment the adhesion and neovascularization capacities of circulating angiogenic cells obtained from atherosclerotic patients. *Atherosclerosis*, **227**, 275–282, *Atherosclerosis*. doi:10.1016/j.atherosclerosis.2013.01.040
- Okano, S., Zhou, L., Kusaka, T., Shibata, K., Shimizu, K., Gao, X., Kikuchi, Y., *et al.*, 2010. Indispensable function for embryogenesis, expression and regulation of the nonspecific

form of the 5-aminolevulinate synthase gene in mouse. *Genes to Cells*, **15**, 77–89, John Wiley & Sons, Ltd. doi:10.1111/J.1365-2443.2009.01366.X

Oloyede, O.A. & Iketubosin, F., 2013. Uterine artery Doppler study in second trimester of pregnancy. *Pan African Medical Journal*, **15**. doi:10.11604/pamj.2013.15.87.2321

Omeroglu, I., Golbasi, H., Bayraktar, B., Golbasi, C., Yildirim Karaca, S., Demircan, T. & Ekin, A., 2023. Modified myocardial performance index for evaluation of fetal heart function and perinatal outcomes in intrahepatic pregnancy cholestasis. *International Journal of Cardiovascular Imaging*, **39**, 907–914, Springer Science and Business Media B.V. doi:10.1007/S10554-022-02789-4/METRICS

Ono, S., Onimaru, T., Kawakami, K., Hokonohara, M. & Miyata, K., 1985. Impaired granulocyte chemotaxis and increased circulating immune complexes in Kawasaki disease. *J Pediatr*, **106**, 567–570, Mosby. doi:10.1016/S0022-3476(85)80073-1

Opdam, F.J.M., Echard, A., Croes, H.J.E., Hurk, J.A.J.M. van den, Vorstenbosch, R.A. van de, Ginsel, L.A., Goud, B., *et al.*, 2000. The small GTPase Rab6B, a novel Rab6 subfamily member, is cell-type specifically expressed and localised to the Golgi apparatus. *J Cell Sci*, **113 (Pt 15)**, 2725–2735, J Cell Sci. doi:10.1242/JCS.113.15.2725

O'Shaughnessy, K.M., Ferraro, F., Fu, B., Downing, S. & Morris, N.H., 2000. Identification of monozygotic twins that are concordant for preeclampsia. *Am J Obstet Gynecol*, **182**, 1156–1157, Am J Obstet Gynecol. doi:10.1067/MOB.2000.105429

Osol, G., Ko, N.L. & Mandalà, M., 2019, February 10. Plasticity of the Maternal Vasculature during Pregnancy. *Annu Rev Physiol*, Annual Reviews Inc. doi:10.1146/annurev-physiol-020518-114435

Ossada, V., Jank, A. & Stepan, H., 2016. The impact of uterine curettage postpartum on maternal sFlt-1 concentration. *J Perinat Med*, **44**, 351–354, J Perinat Med. doi:10.1515/JPM-2015-0104

Ottanelli, S., Simeone, S., Serena, C., Rambaldi, M.P., Villanucci, A., Tavella, K., Amunni, G., *et al.*, 2012. PP120. Hydatidiform mole as a cause of eclampsia in the first trimester: A

case report. *Pregnancy Hypertension: An International Journal of Women's Cardiovascular Health*, **2**, 304, Elsevier BV. doi:10.1016/j.preghy.2012.04.231

Otto, C., 2021. *The Practice of Clinical Echocardiography*. (Matthew Alan Colna, Ed.) *ECG & ECHO Learning*, 6th ed., Vol. 1, Elsevier.

Owen, N.E., Alexander, G.J., Sen, S., Bunclark, K., Polwarth, G., Pepke-Zaba, J., Davenport, A.P., *et al.*, 2020. Reduced circulating BMP10 and BMP9 and elevated endoglin are associated with disease severity, decompensation and pulmonary vascular syndromes in patients with cirrhosis. *EBioMedicine*, **56**, 1–17, Elsevier. doi:10.1016/J.EBIOM.2020.102794

P. Kamoun, 2004. Endogenous production of hydrogen sulfide in mammals. *Amino Acids*, **26**, 243–254. doi:10.1007/s00726-004-0072-x

Palmer, K. R., Tong, S. & Kaitu'u-Lino, T.J., 2017. Placental-specific sFLT-1: Role in pre-eclamptic pathophysiology and its translational possibilities for clinical prediction and diagnosis. *Mol Hum Reprod*, **23**, 69–78. doi:10.1093/molehr/gaw077

Palmer, Kirsten R., Kaitu'u-Lino, T.J., Hastie, R., Hannan, N.J., Ye, L., Binder, N., Cannon, P., *et al.*, 2015. Placental-Specific sFLT-1 e15a Protein Is Increased in Preeclampsia, Antagonizes Vascular Endothelial Growth Factor Signaling, and Has Antiangiogenic Activity. *Hypertension*, **66**, 1251–1259, Lippincott Williams and Wilkins. doi:10.1161/HYPERTENSIONAHA.115.05883

Palmer, Kirsten R, Tong, S., Tuohey, L., Cannon, P., Ye, L., Hannan, N.J., Brownfoot, F.C., *et al.*, 2016. Jumonji Domain Containing Protein 6 Is Decreased in Human Preeclamptic Placentas and Regulates sFLT-1 Splice Variant Production 1. *Biol Reprod*, **94**, 59–60. doi:10.1095/biolreprod.115.134460

Pan, C., Wang, S., Liu, C. & Ren, Z., 2022, November 1. Actin-Binding Proteins in Cardiac Hypertrophy. *Cells*, MDPI. doi:10.3390/cells11223566

Pan, H., Xie, X., Chen, D., Zhang, J., Zhou, Y. & Yang, G., 2014. Protective and biogenesis effects of sodium hydrosulfide on brain mitochondria after cardiac arrest and

- resuscitation. *Eur J Pharmacol*, **741**, 74–82, *Eur J Pharmacol*. doi:10.1016/J.EJPHAR.2014.07.037
- Pan, L.L., Liu, X.H., Gong, Q.H., Wu, D. & Zhu, Y.Z., 2011. Hydrogen sulfide attenuated tumor necrosis factor- α -induced inflammatory signaling and dysfunction in vascular endothelial cells. *PLoS One*, **6**. doi:10.1371/journal.pone.0019766
- Pant, M., Bal, N.C. & Periasamy, M., 2016. Sarcolipin: a key thermogenic and metabolic regulator in skeletal muscle. *Trends Endocrinol Metab*, **27**, 892, NIH Public Access. doi:10.1016/J.TEM.2016.08.006
- Pant, V., Yadav, B.K. & Sharma, J., 2019. A cross sectional study to assess the sFlt-1:PIGF ratio in pregnant women with and without preeclampsia. *BMC Pregnancy Childbirth*, **19**, 1–8, BioMed Central Ltd. doi:10.1186/S12884-019-2399-Z/TABLES/4
- Papa Gobbi, R., Magnarelli, G. & Rovedatti, M.G., 2018. Susceptibility of placental mitochondria to oxidative stress. *Birth Defects Res*, **110**, 1228–1232. doi:10.1002/bdr2.1377
- Papaoannou, T.G., Protogerou, A.D., Stergiopoulos, N., Vardoulis, O., Stefanadis, C., Safar, M. & Blacher, J., 2014. Total arterial compliance estimated by a novel method and all-cause mortality in the elderly: the PROTEGER study. *Age (Omaha)*, **36**, 1555–1563. doi:10.1007/s11357-014-9661-0
- Papapetropoulos, A., Pyriochou, A., Altaany, Z., Yang, G., Marazioti, A., Zhou, Z., Jeschke, M.G., *et al.*, 2009. Hydrogen sulfide is an endogenous stimulator of angiogenesis. *PNAS*, **106**, 21972–21977. Retrieved from www.pnas.org/cgi/content/full/
- Papazoglu, D., Galazios, G., Koukourakis, M.I., Panagopoulos, I., Kontomanolis, E.N., Papatheodorou, K. & Maltezos, E., 2004. Vascular endothelial growth factor gene polymorphisms and pre-eclampsia. *Mol Hum Reprod*, **10**, 321–324, *Mol Hum Reprod*. doi:10.1093/MOLEHR/GAH048
- Paranavitana, L., Walker, M., Chandran, A.R., Milligan, N., Shinar, S., Whitehead, C.L., Hobson, S.R., *et al.*, 2021. Sex differences in uterine artery Doppler during gestation in

- pregnancies complicated by placental dysfunction. *Biol Sex Differ*, **12**, 1–6, BioMed Central Ltd. doi:10.1186/S13293-021-00362-7/FIGURES/2
- Paredes, A., Santos-clemente, R. & Ricote, M., 2021. Untangling the Cooperative Role of Nuclear Receptors in Cardiovascular Physiology and Disease. *Int J Mol Sci*, **22**, 7775–7787, Multidisciplinary Digital Publishing Institute (MDPI). doi:10.3390/IJMS22157775
- Park, J.E., Chen, H.H., Winer, J., HouckS, K.A. & Ferrara, N., 1994. Potentiation Of Vascular Endothelial Growth Factor Bioactivity, In Vitro And In Vivo, And High Affinity Binding To Flt-1 But Not To Flk-L/Kdr*. *J Biol Chem*, **269**, 3590–3592. doi:10.1007/978-3-662-46875-3_4588
- Park, M., Sandner, P. & Krieg, T., 2018. cGMP at the centre of attention: emerging strategies for activating the cardioprotective PKG pathway. *Basic Res Cardiol*, **113**, 1–7, Dr. Dietrich Steinkopff Verlag GmbH and Co. KG. doi:10.1007/S00395-018-0679-9/FIGURES/1
- Parks, W.T., 2017. Manifestations of Hypoxia in the Second and Third Trimester Placenta. *Birth Defects Res*, **109**, 1345–1357, Birth Defects Res. doi:10.1002/BDR2.1143
- Patel, P., Vatish, M., Heptinstall, J., Wang, R. & Carson, R.J., 2009. The endogenous production of hydrogen sulphide in intrauterine tissues. *Reproductive Biology and Endocrinology*, **7**, 1–9. doi:10.1186/1477-7827-7-10
- Patel, S.D., Chen, C.P., Bahna, F., Honig, B. & Shapiro, L., 2003. Cadherin-mediated cell–cell adhesion: sticking together as a family. *Curr Opin Struct Biol*, **13**, 690–698, Elsevier Current Trends. doi:10.1016/J.SBI.2003.10.007
- Pathak, S., Sebire, N.J., Hook, L., Hackett, G., Murdoch, E., Jessop, F. & Lees, C., 2011. Relationship between placental morphology and histological findings in an unselected population near term. *Virchows Archiv*, **459**, 11–20, Springer. doi:10.1007/s00428-011-1061-6
- Patnaik, A.N., 2018. Structural Heart Diseases during Pregnancy: Part 1-Valvular Heart Diseases. *Indian J Cardiovasc Dis Women*, **3**, 108–114. doi:10.1055/s-0038-1676549

- Paul, B.D. & Snyder, S.H., 2012. H₂S signalling through protein sulfhydration and beyond. *Nature Reviews Molecular Cell Biology* 2012 13:8, **13**, 499–507, Nature Publishing Group. doi:10.1038/nrm3391
- Peavey, M.C., Wu, S.-P., Li, R., Liu, J., Emery, O.M., Wang, T., Zhou, L., *et al.*, 2021. Progesterone receptor isoform B regulates the O_{xtr}-Plcl2-Trpc3 pathway to suppress uterine contractility. *PNAS*, **118**, 1–12. doi:10.1073/pnas.2011643118/-/DCSupplemental
- Pedroso, M.A., Palmer, K.R., Hodges, R.J., Silva Costa, F. Da & Rolnik, D.L., 2018. Uterine Artery Doppler in Screening for Preeclampsia and Fetal Growth Restriction Doppler das artérias uterinas no rastreamento para pré-eclâmpsia e restrição do crescimento fetal. *Rev Bras Ginecol Obstet*, **40**, 287–293. doi:10.1055/s-0038-1660777
- Peng, J., Le, C.Y., Xia, B., Wang, J.W., Liu, J.J., Li, Z., Zhang, Q.J., *et al.*, 2021. Research on the correlation between activating transcription factor 3 expression in the human coronary artery and atherosclerotic plaque stability. *BMC Cardiovasc Disord*, **21**, BMC Cardiovasc Disord. doi:10.1186/S12872-021-02161-9
- Pennington, K.A., Schlitt, J.M., Jackson, D.L., Schulz, L.C. & Schust, D.J., 2012. Preeclampsia: multiple approaches for a multifactorial disease. *Dis Model Mech*, **5**, 9–18. doi:10.1242/dmm.008516
- Perales, A., Delgado, J.L., la Calle, M. de, García-Hernández, J.A., Escudero, A.I., Campillos, J.M., Sarabia, M.D., *et al.*, 2017. sFlt-1/PIGF for prediction of early-onset pre-eclampsia: STEPS (Study of Early Pre-eclampsia in Spain). *Ultrasound in Obstetrics and Gynecology*, **50**, 373–382, John Wiley and Sons Ltd. doi:10.1002/uog.17373
- Perkins, A. V., 2006. Endogenous anti-oxidants in pregnancy and preeclampsia. *Aust N Z J Obstet Gynaecol*, **46**, 77–83, Aust N Z J Obstet Gynaecol. doi:10.1111/J.1479-828X.2006.00532.X
- Perry, H., Khalil, A. & Thilaganathan, B., 2018, November 1. Preeclampsia and the cardiovascular system: An update. *Trends Cardiovasc Med*, Elsevier Inc. doi:10.1016/j.tcm.2018.04.009

- Persico, M.G., Vincenti, V. & DiPalma, T., 1999. Structure, expression and receptor-binding properties of placenta growth factor (PlGF). *Curr Top Microbiol Immunol*, **237**, 31–70, Springer, Berlin, Heidelberg. doi:10.1007/978-3-642-59953-8_2
- Peter, I., Kelley-Hedgpeth, A., Huggins, G.S., Housman, D.E., Mendelsohn, M.E., Vita, J.A., Vasan, R.S., *et al.*, 2009. Association between arterial stiffness and variations in oestrogen-related genes. *J Hum Hypertens*, **23**, 636–644. doi:10.1038/jhh.2009.1
- Pfeffer, K., 2003. Biological functions of tumor necrosis factor cytokines and their receptors. *Cytokine Growth Factor Rev*, **14**, 185–191. doi:10.1016/S1359-6101(03)00022-4
- Pickel, S., Cruz-Garcia, Y., Bandleon, S., Barkovits, K., Heindl, C., Völker, K., Abeßer, M., *et al.*, 2021. The β 2-Subunit of Voltage-Gated Calcium Channels Regulates Cardiomyocyte Hypertrophy. *Front Cardiovasc Med*, **8**, Frontiers Media SA. doi:10.3389/fcvm.2021.704657
- Pijnenborg, R., Vercruyse, L. & Hanssens, M., 2006. The Uterine Spiral Arteries In Human Pregnancy: Facts and Controversies. *Placenta*. doi:10.1016/j.placenta.2005.12.006
- Pittara, T., Vyrides, A., Lamnisis, D. & Giannakou, K., 2021. Pre-eclampsia and long-term health outcomes for mother and infant: an umbrella review. *BJOG*, Blackwell Publishing Ltd. doi:10.1111/1471-0528.16683
- Poidatz, D., Santos, E. Dos, Duval, F., Moindjie, H., Serazin, V., Vialard, F., Mazancourt, P. De, *et al.*, 2015. Involvement of estrogen-related receptor- γ and mitochondrial content in intrauterine growth restriction and preeclampsia. *Fertil Steril*, **104**, 483–490, Elsevier Inc. doi:10.1016/j.fertnstert.2015.05.005
- Polhemus, D.J., Kondo, K., Bhushan, S., Bir, S.C., Kevil, C.G., Murohara, T., Lefer, D.J., *et al.*, 2013. Hydrogen sulfide attenuates cardiac dysfunction after heart failure via induction of angiogenesis. *Circ Heart Fail*, **6**, 1077–1086. doi:10.1161/CIRCHEARTFAILURE.113.000299
- Poole, A.T., Vincent, K.L., Olson, G.L., Patrikeev, I., Saade, G.R., Stuebe, A. & Bytautiene, E., 2014. Effect of lactation on maternal postpartum cardiac function and adiposity: a

- murine model. *Am J Obstet Gynecol*, **211**, 424.e1-424.e7, Mosby. doi:10.1016/J.AJOG.2014.06.004
- Porto, L.B., Brandão, A.H.F., Leite, H.V. & Cabral, A.C.V., 2017. Longitudinal evaluation of uterine perfusion, endothelial function and central blood flow in early onset preeclampsia. *Pregnancy Hypertens*, **10**, 161–164, Elsevier. doi:10.1016/J.PREGHY.2017.08.005
- Possomato-Vieira, J.S. & Khalil, R.A., 2016. Mechanisms of Endothelial Dysfunction in Hypertensive Pregnancy and Preeclampsia. *Adv Pharmacol*, **77**, 361–431. doi:10.1016/bs.apha.2016.04.008
- Possomato-Vieira, J.S. & Khalil, R.A., 2016. Mechanisms of Endothelial Dysfunction in Hypertensive Pregnancy and Preeclampsia. *Adv Pharmacol*, **77**, 361–431. doi:10.1016/bs.apha.2016.04.008
- Poston, L., Igosheva, N., Mistry, H.D., Seed, P.T., Shennan, A.H., Rana, S., Karumanchi, A., *et al.*, 2011. Role of oxidative stress and antioxidant supplementation in pregnancy disorders 1-4. *Am J Clin Nutr*, **94**. doi:10.3945/ajcn.110.001156
- Powers, R.W., Roberts, J.M., Cooper, K.M., Gallaher, M.J., Frank, M.P., Harger, G.F. & Ness, R.B., 2005. Maternal serum soluble fms-like tyrosine kinase 1 concentrations are not increased in early pregnancy and decrease more slowly postpartum in women who develop preeclampsia. *Am J Obstet Gynecol*, **193**, 185–191, Elsevier. doi:10.1016/j.ajog.2004.11.038
- Preeclampsia Foundation, 2022. No Time To Wait: Women Need Accurate Tests For Preeclampsia, Now. Retrieved June 4, 2023, from <https://www.preeclampsia.org/biomarkers>
- Prins, J.R., Hoorn, M.L.P. van der, Keijser, R., Ris-Stalpers, C., Beelen, E. van, Afink, G.B., Claas, F.H.J., *et al.*, 2016. Higher decidual EBI3 and HLA-G mRNA expression in preeclampsia: Cause or consequence of preeclampsia. *Hum Immunol*, **77**, 68–70, Elsevier Inc. doi:10.1016/j.humimm.2015.10.004

- Puga, A., Raychaudhuri, B., Salata, K., Zhang, Y.H. & Nebert, D.W., 1990. Stable expression of mouse Cyp1a1 and human CYP1A2 cDNAs transfected into mouse hepatoma cells lacking detectable P450 enzyme activity. *DNA Cell Biol*, **9**, 425–436, DNA Cell Biol. doi:10.1089/DNA.1990.9.425
- Qasim, H. & McConnell, B.K., 2020. Akap12 signaling complex: Impacts of compartmentalizing camp-dependent signaling pathways in the heart and various signaling systems. *J Am Heart Assoc*, **9**, 1–25, American Heart Association Inc. doi:10.1161/JAHA.120.016615
- Qiao, P., Zhao, F., Liu, M., Gao, D., Zhang, H. & Yan, Y., 2017. Hydrogen sulfide inhibits mitochondrial fission in neuroblastoma N2a cells through the Drp1/ERK1/2 signaling pathway. *Mol Med Rep*, **16**, 971–977, Mol Med Rep. doi:10.3892/MMR.2017.6627
- Qiao, P., Zhao, F., Liu, M., Gao, D., Zhang, H. & Yan, Y., 2017. Hydrogen sulfide inhibits mitochondrial fission in neuroblastoma N2a cells through the Drp1/ERK1/2 signaling pathway. *Mol Med Rep*, **16**, 971–977, Mol Med Rep. doi:10.3892/MMR.2017.6627
- Qiu, C., Hevner, K., Abetew, D., Sedensky, M., Morgan, P., Enquobahrie, D.A. & Williams, M.A., 2013. Mitochondrial DNA Copy Number and Oxidative DNA Damage in Placental Tissues from Gestational Diabetes and Control Pregnancies: A Pilot Study. *Clin Lab*, **59**, 655, NIH Public Access.
- Qiu, C., Hevner, K., Enquobahrie, D.A. & Williams, M.A., 2012. A case-control study of maternal blood mitochondrial DNA copy number and preeclampsia risk. *Int J Mol Epidemiol Genet*, **3**, 237, e-Century Publishing Corporation.
- Quan, X., Luo, H., Liu, Y., Xia, H., Chen, W. & Tang, Q., 2015. Hydrogen Sulfide Regulates the Colonic Motility by Inhibiting Both L-Type Calcium Channels and BKCa Channels in Smooth Muscle Cells of Rat Colon. *PLoS One*, **10**, e0121331, Public Library of Science. doi:10.1371/JOURNAL.PONE.0121331
- Quezada, M.S., Rodríguez-Calvo, J., Villalaín, C., Gómez-Arriaga, P.I., Galindo, A. & Herraiz, I., 2020. sFlt-1/PIGF ratio and timing of delivery in early-onset fetal growth restriction with antegrade umbilical artery flow. *Ultrasound in Obstetrics and Gynecology*, **56**, 549–556, John Wiley and Sons Ltd. doi:10.1002/uog.21949

- Quitterer, U. & Abdalla, S., 2021. Pathological AT1R-B2R Protein Aggregation and Preeclampsia. *Cells*, **10**, 2609–2621, Multidisciplinary Digital Publishing Institute (MDPI). doi:10.3390/CELLS10102609
- Quitterer, U., Fu, X., Pohl, A., Bayoumy, K.M. & Langer, A., 2019. Beta-Arrestin1 Prevents Preeclampsia by Downregulation of Mechanosensitive AT1-B2 Receptor Heteromers. *Cell*, **176**, 318–333. doi:10.1016/j.cell.2018.10.050
- Rafeeina, A., Tabandeh, A., Khajeniazi, S. & Marjani, A., 2014. Metabolic Syndrome in Preeclampsia Women in Gorgan. *Open Biochem J*, **8**, 94–99.
- Raghupathy, R., 2013. Cytokines as key players in the pathophysiology of preeclampsia. *Medical Principles and Practice*, **22**, 8–19. doi:10.1159/000354200
- Rahman, M.A., Cumming, B.M., Addicott, K.W., Pacl, H.T., Russell, S.L., Nargan, K., Naidoo, T., *et al.*, 2020. Hydrogen sulfide dysregulates the immune response by suppressing central carbon metabolism to promote tuberculosis. *Proc Natl Acad Sci U S A*, **117**, 6663–6674, NLM (Medline). doi:10.1073/PNAS.1919211117/SUPPL_FILE/PNAS.1919211117.SAPP.PDF
- Ramaccini, D., Montoya-Urbe, V., Aan, F.J., Modesti, L., Potes, Y., Wieckowski, M.R., Krga, I., *et al.*, 2021. Mitochondrial Function and Dysfunction in Dilated Cardiomyopathy. *Front Cell Dev Biol*, **8**, 624227, Frontiers Media S.A. doi:10.3389/FCELL.2020.624216/BIBTEX
- Ramadan, H., Rana, S., Mueller, A., Medvedofsky, D., Nizamuddin, J., Bajracharya, S., Salahuddin, S., *et al.*, 2016. Myocardial performance index and anti angiogenic factors among women with preeclampsia: Hemodynamics. *Pregnancy Hypertension: An International Journal of Women's Cardiovascular Health*, **6**, 180, Elsevier. doi:10.1016/J.PREGHY.2016.08.087
- Ramma, W. & Ahmed, A., 2011. Is inflammation the cause of pre-eclampsia? *Biochem Soc Trans*, Vol. 39, pp. 1619–1627, Portland Press. doi:10.1042/BST20110672
- Ramma, W. & Ahmed, A., 2011. Is inflammation the cause of pre-eclampsia? *Biochem Soc Trans*, Vol. 39, pp. 1619–1627, Portland Press. doi:10.1042/BST20110672

- Ramma, W. & Ahmed, A., 2014. Therapeutic potential of statins and the induction of heme oxygenase-1 in preeclampsia. *J Reprod Immunol*, **101–102**, 153–160, Elsevier Ireland Ltd. doi:10.1016/j.jri.2013.12.120
- Rana, S., Hacker, M.R., Modest, A.M., Salahuddin, S., Lim, K.H., Verlohren, S., Perschel, F.H., *et al.*, 2012. Circulating angiogenic factors and risk of adverse maternal and perinatal outcomes in twin pregnancies with suspected preeclampsia. *Hypertension*, **60**, 451–458. doi:10.1161/HYPERTENSIONAHA.112.195065
- Rana, S., Lemoine, E., Granger, J.P. & Karumanchi, S.A., 2019. Preeclampsia. *Circ Res*, **124**, 1094–1112, Lippincott Williams and Wilkins. doi:10.1161/CIRCRESAHA.118.313276
- Ray, J.G., Vermeulen, M.J., Schull, M.J. & Redelmeier, D.A., 2005. Cardiovascular health after maternal placental syndromes (CHAMPS): population-based retrospective cohort study. *Lancet*, **366**, 1797–1803, Lancet. doi:10.1016/S0140-6736(05)67726-4
- Receptor, A., Plesner, T., Behrendt, N. & Ploug, M., 1997. Structure, Function and Expression on Blood and Bone Marrow Cells of the Urokinase-Type Plasminogen. *Stem Cells*, **15**, 398–408. Retrieved from <https://academic.oup.com/stmcls/article/15/6/398/6390963>
- Reddy, M., Wright, L., Rolnik, D.L., Li, W., Mol, B.W., Gerche, A. La, SilvaCosta, F. da, *et al.*, 2019. Evaluation of Cardiac Function in Women With a History of Preeclampsia: A Systematic Review and Meta-Analysis. *J Am Heart Assoc*, **8**. doi:10.1161/JAHA.119.013545
- Redman, C.W.G., 2011. Preeclampsia: A multi-stress disorder. *Revue de Medecine Interne*, **32**, 41–44. doi:10.1016/j.revmed.2011.03.331
- Redman, C.W.G. & Sargent, I.L., 2008. Circulating Microparticles in Normal Pregnancy and Pre-Eclampsia. *Placenta*, **29**, 73–77. doi:10.1016/j.placenta.2007.11.016
- Reekum, R. Van, David, F.R.C.P.C., Streiner, L., Psych, C., David, K. & Conn, M.B., 2001. Applying Bradford Hill's Criteria for Causation to Neuropsychiatry: Challenges and Opportunities. *J Neuropsychiatry Clin Neurosci*, **13**, 318–325.

- Rees, D.D., Palmer, R.M.J., Schulz, R., Hodson, H.F. & Moncada, S., 1990. Characterization of three inhibitors of endothelial nitric oxide synthase in vitro and in vivo . *Br. J. Pharmacol*, **101**, 746–752.
- Reicharda, A. & Asosingha, K., 2019. The Role of Mitochondria in Angiogenesis. *Mol Biol Rep*, **46**, 1393–1400. doi:10.1007/s11033-018-4488-x.
- Remien, K. & Majmundar, S.H., 2022. Physiology, Fetal Circulation. *StatPearls*, StatPearls Publishing. Retrieved from <https://www.ncbi.nlm.nih.gov/books/NBK539710/>
- Reyat, J.S., Chimen, M., Noy, P.J., Szyroka, J., Rainger, G.E. & Tomlinson, M.G., 2017. ADAM10-Interacting Tetraspanins Tspan5 and Tspan17 Regulate VE-Cadherin Expression and Promote T Lymphocyte Transmigration. *The Journal of Immunology*, **199**, 666–676, The American Association of Immunologists. doi:10.4049/jimmunol.1600713
- Rezk, M., Grasegger, L., Brandstetter, N., Pol-Edern, L.R., Stelzl, P., Oppelt, P. & Arbeithuber, B., 2022. Biomarker screening in preeclampsia: an RNA-sequencing approach based on data from multiple studies. *J Hypertens*, **40**, 2022–2036, J Hypertens. doi:10.1097/HJH.0000000000003226
- Rhee, J., Shahul, S., Mitchell, J., Powe, C., Mahmood, F., Hamar, B., Hess, P., *et al.*, 2011. Myocardial performance index in preeclampsia. *Am J Obstet Gynecol*, **204**, S159. doi:10.1016/j.ajog.2010.10.408
- Ridder, A., Giorgione, V., Khalil, A. & Thilaganathan, B., 2019. Preeclampsia: The Relationship between Uterine Artery Blood Flow and Trophoblast Function. *Int J Mol Sci*, **20**, 3263, MDPI AG. doi:10.3390/ijms20133263
- Ridder, A., Giorgione, V., Khalil, A. & Thilaganathan, B., 2019. Molecular Sciences Preeclampsia: The Relationship between Uterine Artery Blood Flow and Trophoblast Function. *Int J Mol Sci*, **20**, 1–14. doi:10.3390/ijms20133263
- Riise, H.K.R., Sulo, G., Tell, G.S., Igland, J., Nygård, O., Vollset, S.E., Iversen, A.C., *et al.*, 2017. Incident coronary heart disease after Preeclampsia: Role of reduced fetal growth,

- preterm delivery, and parity. *J Am Heart Assoc*, **6**, 1–18, John Wiley and Sons Inc. doi:10.1161/JAHA.116.004158
- Roberts, D.J. & Post, M.D., 2008, December 1. The placenta in pre-eclampsia and intrauterine growth restriction. *J Clin Pathol*, BMJ Publishing Group. doi:10.1136/jcp.2008.055236
- Roberts, James, 1998. Endothelial Dysfunction in Preeclampsia. *Semin Reprod Med*, **16**, 5–15, Thieme Medical Publishers, Inc. doi:10.1055/s-2007-1016248
- Roberts, Jim, 2007. Pre-eclampsia a two-stage disorder: What is the linkage? are there directed fetal/placental signals? in *Pre-Eclampsia: Etiology and Clinical Practice*, pp. 183–194, Cambridge University Press. doi:10.1017/CBO9780511545634.013
- Roberts, J.M., 2014. Pathophysiology of ischemic placental disease. *Semin Perinatol*, **38**, 139–145, W.B. Saunders. doi:10.1053/J.SEMPERI.2014.03.005
- Roberts, J.M. & Escudero, C., 2012. The placenta in preeclampsia. *Pregnancy Hypertens*, **2**, 72–83. doi:10.1016/j.preghy.2012.01.001
- Roberts, J.M. & Gammill, H.S., 2005. Preeclampsia Recent Insights Preeclampsia: A Two-Stage Disorder. *Hypertension*, **46**, 1243–1249. doi:10.1161/01.HYP.0000188408.49896.c5
- Roberts, J.M., Taylor, R.N., Musci, T.J., Rodgers, G.M., Hubel, C.A. & McLaughlin, M.K., 1989. Preeclampsia: An endothelial cell disorder. *Am J Obstet Gynecol*, **161**, 1200–1204, Elsevier. doi:10.1016/0002-9378(89)90665-0
- Roberts, V.H.J., Lo, J.O., Lewandowski, K.S., Blundell, P., Grove, K.L., Kroenke, C.D., Sullivan, E.L., *et al.*, 2018. Adverse Placental Perfusion and Pregnancy Outcomes in a New Nonhuman Primate Model of Gestational Protein Restriction. *Reproductive Sciences*, **25**, 110–119, SAGE Publications Inc. doi:10.1177/1933719117704907
- Robertson, W., Brosens, I. & Dixon, H., 1973. Placental bed vessels. *Am J. Obstet Gynecol.* doi:10.1016/0002-9378(73)90655-8

- Robertson, W.B., Brosens, I. & Dixon, H.G., 1967. The pathological response of the vessels of the placental bed to hypertensive pregnancy. *J Pathol Bacteriol*, **93**, 581–592, John Wiley & Sons, Ltd. doi:10.1002/path.1700930219
- Robson, A., Harris, L.K., Innes, B.A., Lash, G.E., Aljunaidy, M.M., Aplin, J.D., Baker, P.N., *et al.*, 2012. Uterine natural killer cells initiate spiral artery remodeling in human pregnancy. *FASEB Journal*, **26**, 4876–4885, Federation of American Societies for Experimental Biology Bethesda, MD, USA. doi:10.1096/fj.12-210310
- Robson, S.C., Dunlop W., Moore, M. & Hunter, S., 1987. Combined Doppler and echocardiographic measurement of cardiac output: theory and application in pregnancy. *BJOG*, **94**, 1014–1027. doi:10.1111/j.1471-0528.1987.tb02285.x
- Robson, S.C., Hunter, S., Boys, R.J. & Dunlop, W., 1989. Serial study of factors influencing changes in cardiac output during human pregnancy. *Am J Physiol Heart Circ Physiol*, **256**. doi:10.1152/ajpheart.1989.256.4.h1060
- Rodgers, G.M., Taylor, R.N. & Roberts, J.M., 1988. Preeclampsia is associated with a serum factor cytotoxic to human endothelial cells. *Am J Obstet Gynecol*, **159**, 908–914, Elsevier. doi:10.1016/S0002-9378(88)80169-8
- Rodríguez-Cano, A.M., Calzada-Mendoza, C.C., Estrada-Gutierrez, G., Mendoza-Ortega, J.A. & Perichart-Perera, O., 2020. Nutrients, Mitochondrial Function, and Perinatal Health. *Nutrients*, **12**, 1–19, Multidisciplinary Digital Publishing Institute (MDPI). doi:10.3390/NU12072166
- Rogenhofer, N., Ott, J., Pilatz, A., Wolf, J., Thaler, C.J., Windischbauer, L., Schagdarsurengin, U., *et al.*, 2017. Unexplained recurrent miscarriages are associated with an aberrant sperm protamine mRNA content. *Hum Reprod*, **32**, 1574–1582, Hum Reprod. doi:10.1093/HUMREP/DEX224
- Roland-Zejly, L., Moisan, V., St-Pierre, I. & Bilodeau, J.F., 2011. Altered placental glutathione peroxidase mRNA expression in preeclampsia according to the presence or absence of labor. *Placenta*, **32**, 161–167. doi:10.1016/j.placenta.2010.11.005

- Rolnik, D.L., Wright, D., Poon, L.C.Y., Syngelaki, A., O’Gorman, N., Paco Matallana, C. de, Akolekar, R., *et al.*, 2017. ASPRE trial: performance of screening for preterm pre-eclampsia. *Ultrasound in Obstetrics & Gynecology*, **50**, 492–495, John Wiley & Sons, Ltd. doi:10.1002/UOG.18816
- Romero, R., Kusanovic, J.P., Chaiworapongsa, T. & Hassan, S.S., 2011. Placental bed disorders in preterm labor, preterm PROM, spontaneous abortion and abruptio placentae. *Best Pract Res Clin Obstet Gynaecol*, **25**, 313–327, Elsevier Ltd. doi:10.1016/j.bpobgyn.2011.02.006
- Roos, K.P., Jordan, M.C., Fishbein, M.C., Ritter, M.R., Friedlander, M., Chang, H.C., Rahgozar, P., *et al.*, 2007. Hypertrophy and Heart Failure in Mice Overexpressing the Cardiac Sodium-Calcium Exchanger. *J Card Fail*, **13**, 329, NIH Public Access. doi:10.1016/J.CARDFAIL.2007.01.004
- Rosca, M.G. & Hoppel, C.L., 2013. Mitochondrial dysfunction in heart failure. *Heart Fail Rev*, **18**, 1–20. doi:10.1007/s10741-012-9340-0
- Rovinsky, J.J. & Jaffin, H., 1965. Cardiovascular hemodynamics in pregnancy II. Cardiac output and left ventricular work in multiple pregnancy. *American Journal of Obstetric Gynecology*, **93**, 1–15.
- Rubler, S., Schneebaum, R. & Hammer, N., 1973. Systolic time intervals in pregnancy and the postpartum period. *Am Heart J*, **86**, 182–188.
- Rudat, C., Grieskamp, T., Hr, C.R., Airik, R., Wrede, C., Hegermann, J., Herrmann, B.G., *et al.*, 2014. Upk3b is dispensable for development and integrity of urothelium and mesothelium. *PLoS One*, **9**, 1–10, Public Library of Science. doi:10.1371/JOURNAL.PONE.0112112
- Rudnicka, A., Woziwodzka, A., Wróblewska, A., Rybicka, M., Bielawski, K.P., Sikorska, K. & Bernat, A., 2017. Analysis of polymorphism and hepatic expression of duodenal cytochrome b in chronic hepatitis C. *J Gastroenterol Hepatol*, **32**, 482–486, J Gastroenterol Hepatol. doi:10.1111/JGH.13495

- Rudov, A., Balduini, W., Carloni, S., Perrone, S., Buonocore, G. & Albertini, M.C., 2014. Involvement of miRNAs in Placental Alterations Mediated by Oxidative Stress. *Oxid Med Cell Longev*, 1–7. doi:10.1155/2014/103068
- Ruffolo, R.R. & Kopia, G.A., 1986. Importance of receptor regulation in the pathophysiology and therapy of congestive heart failure. *Am J Med*, **80**, 67–72, Elsevier. doi:10.1016/0002-9343(86)90148-8
- Sadlon, T.J., Dell’Oso, T., Surinya, K.H. & May, B.K., 1999. Regulation of erythroid 5-aminolevulinic synthase expression during erythropoiesis. *Int J Biochem Cell Biol*, **31**, 1153–1167, Int J Biochem Cell Biol. doi:10.1016/S1357-2725(99)00073-4
- Saeed, M.B., Record, J. & Westerberg, L.S., 2020. Two sides of the coin: Cytoskeletal regulation of immune synapses in cancer and primary immune deficiencies. in *International Review of Cell and Molecular Biology*, Vol. 356, pp. 1–97, Elsevier Inc. doi:10.1016/bs.ircmb.2020.06.001
- Salas, S.P., Marshall, G., Gutiérrez, B.L. & Rosso, P., 2006. Time Course of Maternal Plasma Volume and Hormonal Changes in Women With Preeclampsia or Fetal Growth Restriction. *Hypertension*, **47**, 203–208. doi:10.1161/01.HYP.0000200042.64517.19
- Salomon, C., Torres, M.J., Kobayashi, M., Scholz-Romero, K., Sobrevia, L., Dobierzewska, A., Illanes, S.E., *et al.*, 2014. A gestational profile of placental exosomes in maternal plasma and their effects on endothelial cell migration. *PLoS One*, **9**. doi:10.1371/journal.pone.0098667
- Salvo, T.G. Di, Yang, K.C., Brittain, E., Absi, T., Maltais, S. & Hemnes, A., 2015. Right ventricular myocardial biomarkers in human heart failure. *J Card Fail*, **21**, 398–411, Churchill Livingstone Inc. doi:10.1016/j.cardfail.2015.02.005
- Sammar, M., Nisemblat, S., Fleischfarb, Z., Golan, A., Sadan, O., Meiri, H., Huppertz, B., *et al.*, 2011. Placenta-bound and body fluid PP13 and its mRNA in normal pregnancy compared to preeclampsia, HELLP and preterm delivery. *Placenta*, **32**. doi:10.1016/j.placenta.2010.09.006

- Sanchez, V.B., Ali, S., Escobar, A. & Cuajungco, M.P., 2019. Transmembrane 163 (TMEM163) protein effluxes zinc. *Arch Biochem Biophys*, **677**, 1–3, Academic Press Inc. doi:10.1016/J.ABB.2019.108166
- Sanchez-Aranguren, L.C., Ahmad, S., Dias, I.H.K., Alzahrani, F.A., Rezai, H., Wang, K. & Asif Ahmed, 2020. Bioenergetic effects of hydrogen sulfide suppress soluble Flt-1 and soluble endoglin in cystathionine gamma-lyase compromised endothelial cells. *Nature*, **10**, 1–11. doi:10.1038/s41598-020-72371-2
- Sánchez-Aranguren, L.C., Espinosa-González, C.T., González-Ortiz, L.M., Sanabria-Barrera, S.M., Riaño-Medina, C.E., Nuñez, A.F., Ahmed, A., *et al.*, 2018. Soluble Fms-like tyrosine kinase-1 alters cellular metabolism and mitochondrial bioenergetics in preeclampsia. *Front Physiol*, **9**, 1–13. doi:10.3389/fphys.2018.00083
- Sánchez-Aranguren, L.C., Prada, C.E., Riaño-Medina, C.E., Lopez, M., Pandey, D. & Health, G., 2014. Endothelial dysfunction and preeclampsia: role of oxidative stress Preeclampsia: A disorder of global impact. *Front Physiol*, **5**. doi:10.3389/fphys.2014.00372
- Sanchez-Aranguren, L.C., Rezai, H., Ahmad, S., Alzahrani, F.A., Sparatore, A., Wang, K. & Ahmed, A., 2020. MZe786 Rescues Cardiac Mitochondrial Activity in High sFlt-1 and Low HO-1 Environment. *Antioxidants*, **9**, 1–16, Multidisciplinary Digital Publishing Institute (MDPI). doi:10.3390/ANTIOX9070598
- Sandoo, A., Veldhuijzen Van Zanten, J.J.C.S., Metsios, G.S., Carroll, D. & Kitas, G.D., 2010. The Endothelium and Its Role in Regulating Vascular Tone. *Open Cardiovasc Med J*, Vol. 4.
- Sanghavi, M. & Rutherford, J.D., 2014. Cardiovascular physiology of pregnancy. *Circulation*, **130**, 1003–1008, Lippincott Williams and Wilkins. doi:10.1161/CIRCULATIONAHA.114.009029
- Santel, A. & Fuller, M.T., 2001. Control of mitochondrial morphology by a human mitofusin. *J Cell Sci*, **114**, 867–874, J Cell Sci. doi:10.1242/JCS.114.5.867

- Sarhaddi, F., Azimi, I., Axelin, A., Niela-Vilen, H., Liljeberg, P. & Rahmani, A.M., 2022. Trends in Heart Rate and Heart Rate Variability During Pregnancy and the 3-Month Postpartum Period: Continuous Monitoring in a Free-living Context. *JMIR Mhealth Uhealth*, **10**, JMIR Publications Inc. doi:10.2196/33458
- Sarhaddi, F., Azimi, I., Axelin, A., Niela-Vilen, H., Liljeberg, P. & Rahmani, A.M., 2022. Trends in Heart Rate and Heart Rate Variability During Pregnancy and the 3-Month Postpartum Period: Continuous Monitoring in a Free-living Context. *JMIR Mhealth Uhealth*, **10**, 33458–233469, JMIR Publications Inc. doi:10.2196/33458
- Sattar, N. & Greer, I.A., 2002. Pregnancy complications and maternal cardiovascular risk: opportunities for intervention and screening? *BMJ*, **325**, 157–160, BMJ. doi:10.1136/BMJ.325.7356.157
- Savage, D.B., Petersen, K.F. & Shulman, G.I., 2007. Disordered Lipid Metabolism and the Pathogenesis of Insulin Resistance. *Physiol Rev*, **87**, 520, NIH Public Access. doi:10.1152/PHYSREV.00024.2006
- Savu, O., Jurcuț, R., Giușcă, S., Mieghem, T. van, Gussi, I., Popescu, B.A., Ginghină, C., *et al.*, 2012. Morphological and functional adaptation of the maternal heart during pregnancy. *Circ Cardiovasc Imaging*, **5**, 289–97, Lippincott Williams & Wilkins Hagerstown, MD . doi:10.1161/CIRCIMAGING.111.970012
- Schäfer, H.H., Gebhart, V.M., Hertel, K. & Jirikowski, G.F., 2015. Expression of corticosteroid-binding globulin CBG in the human heart. *Horm Metab Res*, **47**, 596–599, Horm Metab Res. doi:10.1055/S-0034-1389957
- Schannwell, C. M., Schneppenheim, M., Perings, S.M., Zimmermann, T., Plehn, G. & Strauer, B.E., 2003. Alterations of left ventricular function in women with insulin-dependent diabetes mellitus during pregnancy. *Diabetologia*, **46**, 267–275, Springer Verlag. doi:10.1007/s00125-002-1029-9
- Schannwell, Christiana M, Zimmermann, T., Schneppenheim, M., Plehn, G., Marx, R. & Strauer, B.E., 2002. Left Ventricular Hypertrophy and Diastolic Dysfunction in Healthy Pregnant Women. *Cardiology*, **97**, 73–78.

- Scheufler, K.-M., Dreves, J., Velthoven, V. van, Reusch, P., Klisch, J., Augustin, H.G., Zentner, J., *et al.*, 2003. Implications of Vascular Endothelial Growth Factor, sFlt-1, and sTie-2 in Plasma, Serum and Cerebrospinal Fluid During Cerebral Ischemia in Man. *Journal of Cerebral Blood Flow & Metabolism*, **23**, 99–110. doi:10.1097/01.WCB.0000037547.46809.83
- Schlafke, S. & Enders, A.C., 1975. Cellular Basis of Interaction Between Trophoblast and Uterus at Implantation. *Biol Reprod*, **12**, 41–65. Retrieved from <https://academic.oup.com/biolreprod/article-abstract/12/1/41/2841385>
- Schmidt, W. & Cammarato, A., 2020. The Actin ‘A-Triad’s’ Role in Contractile Regulation in Health and Disease. *J Physiol*, **598**, 2908, NIH Public Access. doi:10.1113/JP276741
- Schoknecht, K., David, Y. & Heinemann, U., 2015, February 1. The blood-brain barrier- Gatekeeper to neuronal homeostasis: Clinical implications in the setting of stroke. *Semin Cell Dev Biol*, Academic Press. doi:10.1016/j.semcdb.2014.10.004
- Scholten, R.R., Sep, S., Peeters, L., Hopman, M.T.E., Lotgering, F.K. & Spaanderman, M.E.A., 2011. Prepregnancy low-plasma volume and predisposition to preeclampsia and fetal growth restriction. *Obstetrics and Gynecology*, **117**, 1085–1093. doi:10.1097/AOG.0B013E318213CD31
- Schrier, R. V. & Dürr, J.A., 1987. Pregnancy: An Overfill or Underfill State. *American Journal of Kidney Diseases*, **9**, 284–289, W.B. Saunders. doi:10.1016/S0272-6386(87)80123-3
- Schuurhof, A., Bont, L., Siezen, C.L.E., Hodemaekers, H., Houwelingen, H.C. Van, Kimman, T.G., Hoebee, B., *et al.*, 2010. Interleukin-9 polymorphism in infants with respiratory syncytial virus infection: an opposite effect in boys and girls. *Pediatr Pulmonol*, **45**, 608–613, *Pediatr Pulmonol*. doi:10.1002/PPUL.21229
- Schwartz, R.J. & Schneider, M.D., 2006, May 5. CAMTA in Cardiac Hypertrophy. *Cell*, Elsevier B.V. doi:10.1016/j.cell.2006.04.015
- Sebastião, M.J., Almeida, H. V., Serra, M., Hamdani, N., Saraiva, F., Lourenço, A.P., Barros, A.S., *et al.*, 2022. Unveiling Human Proteome Signatures of Heart Failure with Preserved Ejection Fraction. *Biomedicines*, **10**, MDPI. doi:10.3390/biomedicines10112943

- Sebire, N.J., 2017. Implications of placental pathology for disease mechanisms; methods, issues and future approaches. *Placenta*, **52**, 122–126, W.B. Saunders Ltd. doi:10.1016/j.placenta.2016.05.006
- Sedaghat, S., Sloten, T.T. Van, Laurent, S., London, G.M., Pannier, B., Kavousi, M., Mattace-Raso, F., *et al.*, 2018. Common carotid artery diameter and risk of cardiovascular events and mortality: Pooled analyses of four cohort studies. *Hypertension*, **72**, 85–92, Lippincott Williams and Wilkins. doi:10.1161/HYPERTENSIONAHA.118.11253
- Seely, E.W., Celi, A.C., Chausmer, J., Graves, C., Kilpatrick, S., Nicklas, J.M., Rosser, M.L., *et al.*, 2021. Cardiovascular Health After Preeclampsia: Patient and Provider Perspective. *J Womens Health*, **30**, 313, Mary Ann Liebert, Inc. doi:10.1089/JWH.2020.8384
- Sen, N., Paul, B.D., Gadalla, M.M., Mustafa, A.K., Sen, T., Xu, R., Kim, S., *et al.*, 2012. Hydrogen Sulfide-Linked Sulfhydration of NF- κ B Mediates Its Antiapoptotic Actions. *Mol Cell*, **45**, 13–24, Cell Press. doi:10.1016/J.MOLCEL.2011.10.021
- Sen, S.K., 2023, June 2. Messenger RNA (mRNA). *Messenger RNA - National Human Genome Research Institute*. Retrieved June 5, 2023, from <https://www.genome.gov/genetics-glossary/messenger-rna>
- Sen, U., Munjal, C., Qipshidze, N., Abe, O., Gargoum, R. & Tyagi, S.C., 2010. Hydrogen sulfide regulates homocysteine-mediated glomerulosclerosis. *Am J Nephrol*, **31**, 442–455, S. Karger AG. doi:10.1159/000296717
- Senali Abayratna Wansa, K.D., Harris, J.M. & Muscat, G.E.O., 2002. The activation function-1 domain of Nur77/NR4A1 mediates trans-activation, cell specificity, and coactivator recruitment. *J Biol Chem*, **277**, 33001–33011, J Biol Chem. doi:10.1074/JBC.M203572200
- Seo, B.J., Choi, J., La, H., Habib, O., Choi, Y., Hong, K. & Do, J.T., 2020. Role of mitochondrial fission-related genes in mitochondrial morphology and energy metabolism in mouse embryonic stem cells. *Redox Biol*, **36**, 101599, Elsevier B.V. doi:10.1016/j.redox.2020.101599

- Sep, S., Schreurs, M., Bekkers, S., Kruse, A.J., Smits, L.J. & Peeters, L., 2011. Early-pregnancy changes in cardiac diastolic function in women with recurrent pre-eclampsia and in previously pre-eclamptic women without recurrent disease. *BJOG*, **118**, 1112–1119. doi:10.1111/j.1471-0528.2011.02951.x
- Sethi, D. & Kumar, N., 2020. Peripartum cardiomyopathy with preeclampsia in a parturient: A case report with literature review. *Turk J Emerg Med*, **20**, 205, Wolters Kluwer -- Medknow Publications. doi:10.4103/2452-2473.297467
- Shaaban, C.E., Rosano, C., Cohen, A.D., Huppert, T., Butters, M.A., Hengenius, J., Parks, W.T., *et al.*, 2021. Cognition and Cerebrovascular Reactivity in Midlife Women With History of Preeclampsia and Placental Evidence of Maternal Vascular Malperfusion. *Front Aging Neurosci*, **13**, Frontiers Media SA. doi:10.3389/fnagi.2021.637574
- Shabbir, A., Cox, A., Rodriguez-Menocal, L., Salgado, M. & Badiavas, E. Van, 2015. Mesenchymal Stem Cell Exosomes Induce Proliferation and Migration of Normal and Chronic Wound Fibroblasts, and Enhance Angiogenesis in Vitro. *Stem Cells Dev*, **24**, 1635–1647, Mary Ann Liebert Inc. doi:10.1089/scd.2014.0316
- Shah, N.C., Pringle, S. & Struthers, A., 2006. Aldosterone blockade over and above ACE-inhibitors in patients with coronary artery disease but without heart failure. *J Renin Angiotensin Aldosterone Syst*, **7**, 20–30, J Renin Angiotensin Aldosterone Syst. doi:10.3317/JRAAS.2006.002
- Shahd A. Karrar & Peter L. Hong., 2023, February 23. Preeclampsia - StatPearls - NCBI Bookshelf. *Preeclampsia -Statpearls NCBI*. Retrieved May 28, 2023, from <https://www.ncbi.nlm.nih.gov/books/NBK570611/#>
- Shahul, S., Rhee, J., Hacker, M.R., Gulati, G., Mitchell, J.D., Hess, P., Mahmood, F., *et al.*, 2012. Subclinical left ventricular dysfunction in preeclamptic women with preserved left ventricular ejection fraction: A 2D speckle-tracking imaging study. *Circ Cardiovasc Imaging*, **5**, 734–739. doi:10.1161/CIRCIMAGING.112.973818
- Shai, S.Y., Harpf, A.E., Babbitt, C.J., Jordan, M.C., Fishbein, M.C., Chen, J., Omura, M., *et al.*, 2002. Cardiac myocyte-specific excision of the beta1 integrin gene results in

myocardial fibrosis and cardiac failure. *Circ Res*, **90**, 458–464, *Circ Res*. doi:10.1161/HH0402.105790

Sharma, N., Jayashree, K. & Nadhamuni, K., 2018. Maternal history and uterine artery wave form in the prediction of early-onset and late-onset preeclampsia: A cohort study. *Int J Reprod BioMed*, **16**, 109–114.

Sharma, N., Srinivasan, S., Srinivasan, K.J. & Nadhamuni, K., 2018. Role of Aspirin in High Pulsatility Index of Uterine Artery: A Consort Study. *J Obstet Gynaecol India*, **68**, 388, Springer. doi:10.1007/S13224-017-1058-4

Shimizu, Y., Polavarapu, R., Eskla, K.L., Nicholson, C.K., Koczor, C.A., Wang, R., Lewis, W., *et al.*, 2018. Hydrogen sulfide regulates cardiac mitochondrial biogenesis via the activation of AMPK. *J Mol Cell Cardiol*, **116**, 29–40, Academic Press. doi:10.1016/j.yjmcc.2018.01.011

Shin-Young Kim, Hyun-Mee Ryu, Jae Hyug Yang, Moon-Young Kim, Hyun-Kyong Ahn, Ha-Jung Lim, Joong-Sik Shin, *et al.*, 2004. Maternal Levels of Soluble Adhesion Molecules in Preeclampsia. *J Korean Med Sci*, **19**, 688–692.

Shivananjiah, C., Nayak, A. & Swarup, A., 2016. Echo Changes in Hypertensive Disorder of Pregnancy. *J Cardiovasc Echogr*, **26**, 104, Wolters Kluwer -- Medknow Publications. doi:10.4103/2211-4122.187961

Sholook, M.M., Gilbert, J.S., Sedeek, M.H., Huang, M., Hester, R.L. & Granger, J.P., 2007. Systemic hemodynamic and regional blood flow changes in response to chronic reductions in uterine perfusion pressure in pregnant rats. *AM J Physiol Heart Circ Physiol*, **293**, 2080–2084. doi:10.1152/ajpheart.00667.2007.-Pre

Shu, C., Liu, Z., Cui, L., Wei, C., Wang, S., Tang, J.J., Cui, M., *et al.*, 2014. Protein Profiling of Preeclampsia Placental Tissues. *PLoS One*, **9**, 112903, PLOS. doi:10.1371/JOURNAL.PONE.0112890

Siasos, G., Tsigkou, V., Kosmopoulos, M., Theodosiadis, D., Simantiris, S., Maria Tagkou, N., Tsimpiktsioglou, A., *et al.*, 2018. Mitochondria and cardiovascular diseases-from pathophysiology to treatment. *Ann Transl Med*, **6**, 1–22. doi:10.21037/atm.2018.06.21

- Sibai, B.M., Caritis, S. & Hauth, J., 2003. What we have learned about preeclampsia. *Semin Perinatol*, **27**, 239–246, W.B. Saunders. doi:10.1016/S0146-0005(03)00022-3
- Siedner, S., Krüger, M., Schroeter, M., Metzler, D., Roell, W., Fleischmann, B.K., Hescheler, J., *et al.*, 2003. Developmental changes in contractility and sarcomeric proteins from the early embryonic to the adult stage in the mouse heart. *J Physiol*, **548**, 505, Wiley-Blackwell. doi:10.1113/JPHYSIOL.2002.036509
- Siepmann, T., Boardman, H., Bilderbeck, A., Griffanti, L., Kenworthy, Y., Zwager, C., McKean, D., *et al.*, 2017. Long-term cerebral white and gray matter changes after preeclampsia. *American Academy of Neurology*, **88**, 1256–1264.
- Silva, S.D., Zampieri, T.T., Ruggeri, A., Ceroni, A., Aragão, D.S., Fernandes, F.B., Casarini, D.E., *et al.*, 2015. Downregulation of the vascular renin-angiotensin system by aerobic training-Focus on the balance between vasoconstrictor and vasodilator axes. *Circulation Journal*, **79**, 1372–1380, Japanese Circulation Society. doi:10.1253/circj.CJ-14-1179
- Simmons, L.A., Gillin, A.G. & Jeremy, R.W., 2002. Structural and functional changes in left ventricle during normotensive and preeclamptic pregnancy. *Am J Physiol Heart Circ Physiol*, **283**, American Physiological Society. doi:10.1152/ajpheart.00966.2001
- Singh, S.B. & Lin, H.C., 2015. Hydrogen Sulfide in Physiology and Diseases of the Digestive Tract. *Microorganisms*, **3**, 889, Multidisciplinary Digital Publishing Institute (MDPI). doi:10.3390/MICROORGANISMS3040866
- Sławek-Szmyt, S., Kawka-Paciorkowska, K., Ciepłucha, A., Lesiak, M. & Ropacka-Lesiak, M., 2022, October 1. Preeclampsia and Fetal Growth Restriction as Risk Factors of Future Maternal Cardiovascular Disease—A Review. *J Clin Med*, MDPI. doi:10.3390/jcm11206048
- Sliwa, K., Mebazaa, A., Hilfiker-Kleiner, D., Petrie, M.C., Maggioni, A.P., Laroche, C., Regitz-Zagrosek, V., *et al.*, 2017. Clinical characteristics of patients from the worldwide registry on peripartum cardiomyopathy (PPCM): EURObservational Research Programme in conjunction with the Heart Failure Association of the European Society of Cardiology Study Group on PPCM. *Eur J Heart Fail*, **19**, 1131–1141, Eur J Heart Fail. doi:10.1002/EJHF.780

- Small, H.Y., Morgan, H., Beattie, E., Griffin, S., Indahl, M., Delles, C. & Graham, D., 2016. Abnormal uterine artery remodelling in the stroke prone spontaneously hypertensive rat. *Placenta*, **37**, 34–44, W.B. Saunders Ltd. doi:10.1016/j.placenta.2015.10.022
- Smarason, A.K., Sargent, I.L., Starkey, P.M. & Redman, C.W.G., 1993. The effect of placental syncytiotrophoblast microvillous membranes from normal and pre-eclamptic women on the growth of endothelial cells in vitro. *BJOG*, **100**, 943–949, John Wiley & Sons, Ltd. doi:10.1111/j.1471-0528.1993.tb15114.x
- Smirnova, E., Griparic, L., Shurland, D.L. & Blik, A.M. Van der, 2001. Dynamin-related protein Drp1 is required for mitochondrial division in mammalian cells. *Mol Biol Cell*, **12**, 2245–2256, Mol Biol Cell. doi:10.1091/MBC.12.8.2245
- Smith, G.N., 2014. Development of preeclampsia provides a window of opportunity for early cardiovascular risk screening and intervention. <http://dx.doi.org/10.1586/eog.09.16>, **4**, 355–357, Taylor & Francis. doi:10.1586/EOG.09.16
- Smith, S.A., 2002. Peroxisome proliferator-activated receptors and the regulation of mammalian lipid metabolism. *Biochem Soc Trans*, **30**, 1086–1090, Biochem Soc Trans. doi:10.1042/BST0301086
- Sobenin, I.A., Sazonova, M.A., Postnov, A.Y., Bobryshev, Y. V & Orekhov, A.N., 2012. Mitochondrial Mutations are Associated with Atherosclerotic Lesions in the Human Aorta. *Clin Dev Immunol*, **2012**, 1–5, Hindawi Publishing Corporation. doi:10.1155/2012/832464
- Soma Pillay, P., Adeyemo, A.O., Louw, M.C., Makin, J. & Pattinson, R.C., 2018. Cardiac diastolic function after recovery from pre-eclampsia. *Cardiovasc J Afr*, **29**, 31, Clinics Cardive Publishing (Pty) Ltd. doi:10.5830/CVJA-2017-031
- Soma-Pillay, P., Nelson-Piercy, C., Tolppanen, H. & Mebazaa, A., 2016. Physiological changes in pregnancy. *Cardiovasc J Afr*, **27**, 89–94, Clinics Cardive Publishing (PTY)Ltd. doi:10.5830/CVJA-2016-021
- Sones, J.L. & Davisson, R.L., 2016. Preeclampsia, of mice and women. *Physiol Genomics*, **48**, 565–572. doi:10.1152/physiolgenomics.00125.2015

- Sophia Antipolis, 2023, January 26. Pre-eclampsia linked with four-fold higher risk of heart attack in decade after delivery. *European Society of Cardiology*. Retrieved May 23, 2023, from <https://www.escardio.org/The-ESC/Press-Office/Press-releases/pre-eclampsia-linked-with-four-fold-higher-risk-of-heart-attack-in-decade-after>
- Spaanderman, M., Ekhart, T., Eyck, J. Van, Leeuw, P. De & Peeters, L., 2001. Preeclampsia and maladaptation to pregnancy: A role for atrial natriuretic peptide? *Kidney Int*, Vol. 60.
- Spaans, F., Vos, P. De, Bakker, W.W., Goor, H. Van & Faas, M.M., 2014. Danger signals from ATP and adenosine in pregnancy and preeclampsia. *Hypertension*, **63**, 1154–1160, Lippincott Williams and Wilkins. doi:10.1161/HYPERTENSIONAHA.114.03240
- Spradley, F.T., Tan, A.Y., Joo, W.S., Daniels, G., Kussie, P., Ananth Karumanchi, S. & Granger, J.P., 2016. Placental Growth Factor Administration Abolishes Placental Ischemia-Induced Hypertension. *Hypertension*, **67**, 740–747. doi:10.1161/HYPERTENSIONAHA.115.06783
- Squire, J., 2019. Special Issue: The Actin-Myosin Interaction in Muscle: Background and Overview. *Int J Mol Sci*, **20**, 5715–5730, Multidisciplinary Digital Publishing Institute (MDPI). doi:10.3390/IJMS20225715
- Stachenfeld, N.S. & Taylor, H.S., 1991. Progesterone increases plasma volume independent of estradiol. *J Appl Physiol*, **98**. doi:10.1152/jappphysiol.00031.2005.-Adequate
- Staff, A.C., Benton, S.J., Dadelszen, P. Von, Roberts, J.M., Taylor, R.N., Powers, R.W., Charnock-Jones, D.S., *et al.*, 2013. Redefining Preeclampsia Using Placenta-Derived Biomarkers. *Hypertension*, **61**, 932–942, Lippincott Williams & Wilkins Hagerstown, MD . doi:10.1161/HYPERTENSIONAHA.111.00250
- Stallmach, T., Hebisch, G., Orban, P. & Lü, X., 1999. Aberrant positioning of trophoblast and lymphocytes in the feto-maternal interface with pre-eclampsia. *Vichows Arch*, **434**, 207–211.
- Stark, R. & Roden, M., 2007. Mitochondrial function and endocrine diseases. *Eur J Clin Invest*, **37**, 236–248, John Wiley & Sons, Ltd. doi:10.1111/J.1365-2362.2007.01773.X

- Stojanovska, V., Dijkstra, D.J., Vogtmann, R., Gellhaus, A., Scherjon, S.A. & Plösch, T., 2019. A double-hit pre-eclampsia model results in sex-specific growth restriction patterns. *Dis Model Mech*, **12**, dmm035980. doi:10.1242/dmm.035980
- Strzalka, W. & Ziemienowicz, A., 2011. Proliferating cell nuclear antigen (PCNA): a key factor in DNA replication and cell cycle regulation. *Ann Bot*, **107**, 1140, Oxford University Press. doi:10.1093/AOB/MCQ243
- Stuart, J.J., Tanz, L.J., Rimm, E.B., Spiegelman, D., Missmer, S.A., Rexrode, K.M., Mukamal, K.J., *et al.*, 2020. Abstract MP63: Established Cardiovascular Disease Risk Factors Mediate The Relationship Between Hypertensive Disorders In First Pregnancy And Maternal Cardiovascular Disease. *Circulation*, **141**, 1–3, Lippincott Williams & Wilkins Hagerstown, MD . doi:10.1161/CIRC.141.SUPPL_1.MP63
- Styrpejko, D.J. & Cuajungco, M.P., 2021. Transmembrane 163 (TMEM163) Protein: A New Member of the Zinc Efflux Transporter Family. *Biomedicines*, **9**, 1–13, Multidisciplinary Digital Publishing Institute (MDPI). doi:10.3390/BIOMEDICINES9020220
- Sugimoto, H., Hamanog, Y., Charytan, D., Cosgrove, D., Kieran, M., Sudhakar, A. & Kalluri, R., 2003. Neutralization of circulating vascular endothelial growth factor (VEGF) by anti-VEGF antibodies and soluble VEGF receptor 1 (sFlt-1) induces proteinuria. *Journal of Biological Chemistry*, **278**, 12605–12608, American Society for Biochemistry and Molecular Biology. doi:10.1074/jbc.C300012200
- Sugimoto, H., Hamanog, Y., Charytan, D., Cosgrove, D., Kieran, M., Sudhakar, A. & Kalluri, R., 2003. Neutralization of circulating vascular endothelial growth factor (VEGF) by anti-VEGF antibodies and soluble VEGF receptor 1 (sFlt-1) induces proteinuria. *Journal of Biological Chemistry*, **278**, 12605–12608, American Society for Biochemistry and Molecular Biology. doi:10.1074/jbc.C300012200
- Sun, J., Guo, X., Yu, P., Liang, J., Mo, Z., Zhang, M., Yang, L., *et al.*, 2022. Vasorin deficiency leads to cardiac hypertrophy by targeting MYL7 in young mice. *J Cell Mol Med*, **26**, 88–98, J Cell Mol Med. doi:10.1111/JCMM.17034

- Sun, Q., Liu, S., Liu, K. & Jiao, K., 2018. Role of semaphorin signaling during cardiovascular development. *J Am Heart Assoc*, **7**, American Heart Association Inc. doi:10.1161/JAHA.118.008853
- Sun, X., Wang, T., Wang, Y., Ai, K., Pan, G., Li, Y., Zhou, C., *et al.*, 2020. Downregulation of lncRNA-11496 in the Brain Contributes to Microglia Apoptosis via Regulation of Mef2c in Chronic *T. gondii* Infection Mice. *Front Mol Neurosci*, **13**, 532178, Frontiers Media S.A. doi:10.3389/FNMOL.2020.00077/BIBTEX
- Sundquist, K., Sundquist, J., Wang, X., Palmer, K. & Memon, A.A., 2022. Baseline mitochondrial DNA copy number and heart failure incidence and its role in overall and heart failure mortality in middle-aged women. *Front Cardiovasc Med*, **9**, 1–15, Frontiers Media S.A. doi:10.3389/FCVM.2022.1012403/BIBTEX
- Suri, M., Kelehan, P., O'Neill, D., Vadeyar, S., Grant, J., Ahmed, S.F., Tolmie, J., *et al.*, 2007. WT1 mutations in Meacham syndrome suggest a coelomic mesothelial origin of the cardiac and diaphragmatic malformations. *Am J Med Genet A*, **143A**, 2312–2320, Am J Med Genet A. doi:10.1002/AJMG.A.31924
- Suzuki, H., Ohkuchi, A., Matsubara, S., Takei, Y., Murakami, M., Shibuya, M., Suzuki, M., *et al.*, 2009. Effect of Recombinant Placental Growth Factor 2 on Hypertension Induced by Full-Length Mouse Soluble fms-Like Tyrosine Kinase 1 Adenoviral Vector in Pregnant Mice. *Hypertension*, **54**, 1129–1135. doi:10.1161/HYPERTENSIONAHA.109.134668
- Sweet, M.E., Cocciolo, A., Slavov, D., Jones, K.L., Sweet, J.R., Graw, S.L., Reece, T.B., *et al.*, 2018. Transcriptome analysis of human heart failure reveals dysregulated cell adhesion in dilated cardiomyopathy and activated immune pathways in ischemic heart failure. *BMC Genomics*, **19**, 1–14, BioMed Central Ltd. doi:10.1186/S12864-018-5213-9/FIGURES/7
- Szalai, G., Romero, R., Chaiworapongsa, T., Xu, Y., Wang, B., Ahn, H., Xu, Z., *et al.*, 2015. Full-Length Human Placental sFlt-1-e15a Isoform Induces Distinct Maternal Phenotypes of Preeclampsia in Mice. *PLoS One*, **10**, 1–42. doi:10.1371/journal.pone.0119547

- Szalai, G., Romero, R., Chaiworapongsa, T., Xu, Y., Wang, B., Ahn, H., Xu, Z., *et al.*, 2015. Full-Length Human Placental sFlt-1-e15a Isoform Induces Distinct Maternal Phenotypes of Preeclampsia in Mice. *PLoS One*, **10**, 1–42. doi:10.1371/journal.pone.0119547
- Szalai, G., Xu, Y., Romero, R., Chaiworapongsa, T., Xu, Z., Jen Chiang, P., Ahn, H., *et al.*, 2014. In vivo experiments reveal the good, the bad and the ugly faces of sFlt-1 in Pregnancy. *PLoS One*, **9**. doi:10.1371/journal.pone.0110867
- Szarka, A., Rigó, J., Lázár, L., Beko, G. & Molvarec, A., 2010. Circulating cytokines, chemokines and adhesion molecules in normal pregnancy and preeclampsia determined by multiplex suspension array. *BMC Immunol*, **11**, 59, BioMed Central. doi:10.1186/1471-2172-11-59
- Szczerba, E., Zajkowska, A., Bochowicz, A., Pankiewicz, K., Szewczyk, G., Opolski, G., Maciejewski, T., *et al.*, 2020. Downregulated expression of microRNAs associated with cardiac hypertrophy and fibrosis in physiological pregnancy and the association with echocardiographically-evaluated myocardial function. *Biomed Rep*, **13**, 1–10, Spandidos Publications. doi:10.3892/BR.2020.1348
- Tabuchi, C. & Sul, H.S., 2021. Signaling Pathways Regulating Thermogenesis. *Front Endocrinol (Lausanne)*, **12**, 1–14, Frontiers Media S.A. doi:10.3389/FENDO.2021.595020/BIBTEX
- Taefehshokr, S., Key, Y.A., Khakpour, M., Dadebighlu, P. & Oveisi, A., 2017. Early growth response 2 and Egr3 are unique regulators in immune system. *Cent Eur J Immunol*, **42**, 209, Termedia Publishing. doi:10.5114/CEJI.2017.69363
- Tagliafierro, L. & Chiba-Falek, O., 2016. Up-regulation of SNCA Gene Expression: Implications to Synucleinopathies. *Neurogenetics*, **17**, 157, NIH Public Access. doi:10.1007/S10048-016-0478-0
- Takano, T. & Li, S.S.L., 1989. Human testicular lactate dehydrogenase-C gene is interrupted by six introns at positions homologous to those of LDH-A (muscle) and LDH-B (heart) genes. *Biochem Biophys Res Commun*, **159**, 579–583, Biochem Biophys Res Commun. doi:10.1016/0006-291X(89)90033-8

- Tan, H., Wang, H., Ma, J., Deng, H., He, Q., Chen, Q. & Zhang, Q., 2022. Identification of human LDHC4 as a potential target for anticancer drug discovery. *Acta Pharm Sin B*, **12**, 2348–2357, Elsevier. doi:10.1016/J.APSB.2021.12.002
- Tan, Y., Zhang, Z., Zheng, C., Wintergerst, K.A., Keller, B.B. & Cai, L., 2020. Mechanisms of diabetic cardiomyopathy and potential therapeutic strategies: preclinical and clinical evidence. *Nat Rev Cardiol*, **17**, 585–607, Nature Publishing Group. doi:10.1038/s41569-020-0339-2
- Tanaka, R., Kobayashi, K. & Masuda, T., 2011. Tetrapyrrole Metabolism in *Arabidopsis thaliana*. *The Arabidopsis Book / American Society of Plant Biologists*, **9**, 1–17, American Society of Plant Biologists. doi:10.1199/TAB.0145
- Tannetta, D.S., Dragovic, R.A., Gardiner, C., Redman, C.W. & Sargent, I.L., 2013. Characterisation of Syncytiotrophoblast Vesicles in Normal Pregnancy and Pre-Eclampsia: Expression of Flt-1 and Endoglin. *PLoS One*, **8**, 1–29, Public Library of Science. doi:10.1371/journal.pone.0056754
- Tao, B.B., Liu, S.Y., Zhang, C.C., Fu, W., Cai, W.J., Wang, Y., Shen, Q., *et al.*, 2013. VEGFR2 functions as an H₂S-targeting receptor protein kinase with its novel Cys1045-Cys1024 disulfide bond serving as a specific molecular switch for hydrogen sulfide actions in vascular endothelial cells. *Antioxid Redox Signal*, **19**, 448–464. doi:10.1089/ars.2012.4565
- Taranikanti, M., 2018. Physiological Changes in Cardiovascular System during Normal Pregnancy: A Review. *Indian J Cardiovasc Dis Women WINCARS*, **03**, 062–067, Scientific Scholar. doi:10.1055/s-0038-1676666
- Taranikanti, M., 2018. Physiological Changes in Cardiovascular System during Normal Pregnancy: A Review. *Indian J Cardiovasc Dis Women WINCARS*, **03**, 062–067, Scientific Scholar. doi:10.1055/s-0038-1676666
- Tay, J., Foo, L., Masini, G., Bennett, P.R., Mceniery, C.M., Wilkinson, I.B., Dm Frcep, M.A., *et al.*, 2018. Early and late preeclampsia are characterized by high cardiac output, but in the presence of fetal growth restriction, cardiac output is low: insights from a prospective study. doi:10.1016/j.ajog.2018.02.007

- Tay, J., Foo, L., Masini, G., Bennett, P.R., McEniery, C.M., Wilkinson, I.B. & Lees, C.C., 2018. Early and late preeclampsia are characterized by high cardiac output, but in the presence of fetal growth restriction, cardiac output is low: insights from a prospective study. *Am J Obstet Gynecol*, **218**, 517.e1-517.e12, Mosby Inc. doi:10.1016/j.ajog.2018.02.007
- Tayal, U., Prasad, S. & Cook, S.A., 2017. Genetics and genomics of dilated cardiomyopathy and systolic heart failure. *Genome Med*, **9**, 1–14, BioMed Central Ltd. doi:10.1186/S13073-017-0410-8/TABLES/2
- Tei, C., Dujardw, K.S., I-lodge, D. O, Kyle, R.A., Tajhk, A.J. & Seward, J.B., 1996. Doppler index combining systolic and diastolic myocardial performance: Clinical value in cardiac amyloidosis. *Journal of American College of Cardiology*, **28**, 658–664.
- Tekay, A. & Jouppila, P., 1993. A longitudinal Doppler ultrasonographic assessment of the alterations in peripheral vascular resistance of uterine arteries and ultrasonographic findings of the involuting uterus during the puerperium. *Am J Obstet Gynecol*, **168**, 190–198, Am J Obstet Gynecol. doi:10.1016/S0002-9378(12)90913-8
- Telezhkin, V., Goecks, T., Bonev, A.D., Osol, G. & Gokina, N.I., 2008. Decreased function of voltage-gated potassium channels contributes to augmented myogenic tone of uterine arteries in late pregnancy. *Am J Physiol Heart Circ Physiol*, **294**, 272–284, American Physiological Society. doi:10.1152/AJPHEART.00216.2007/ASSET/IMAGES/LARGE/ZH40010880020009.JPG
- Telikicherla, D., Maharudraiah, J., Pawar, H., Maimuthu, A., Kashyap, M.K., Ramachandra, Y.L., Roa, J.C., *et al.*, 2012. Overexpression of Kinesin Associated Protein 3 (KIFAP3) in Breast Cancer. *J Proteomics Bioinform*, **6**, 122–126. Retrieved from <https://www.longdom.org/open-access/overexpression-of-kinesin-associated-protein-3-kifap3-in-breast-cancer-jpb.1000223.pdf>
- Teruel, J.L., Lasunción, M.A., Navarro, J.F., Carrero, P. & Ortuño, J., 1995. Pregnancy in a patient with homozygous familial hypercholesterolemia undergoing low-density lipoprotein apheresis by dextran sulfate adsorption. *Metabolism*, **44**, 929–933, Elsevier. doi:10.1016/0026-0495(95)90247-3

- Thadhani, R., Hagmann, H., Schaarschmidt, W., Roth, B., Cingoz, T., Karumanchi, S.A., Wenger, J., *et al.*, 2016. Removal of Soluble Fms-Like Tyrosine Kinase-1 by Dextran Sulfate Apheresis in Preeclampsia. *Journal of the American Society of Nephrology*, **27**, 903–913. doi:10.1681/ASN.2015020157
- Thadhani, R., Kisner, T., Hagmann, H., Bossung, V., Noack, S., Schaarschmidt, W., Jank, A., *et al.*, 2011. Pilot study of extracorporeal removal of soluble Fms-like tyrosine kinase 1 in preeclampsia. *Circulation*, **124**, 940–950. doi:10.1161/CIRCULATIONAHA.111.034793
- Thayaparan, A.S., Said, J.M., Lowe, S.A., Mclean, A. & Yang, Y., 2019. Pre-eclampsia and long-term cardiac dysfunction: A review of asymptomatic cardiac changes existing well beyond the post-partum period. *Australian Society for Ultrasound in Medicine*, **22**, 234–244. doi:10.1002/ajum.12173
- Thilaganathan, B. & Kalafat, E., 2019. Cardiovascular System in Preeclampsia and Beyond. *Hypertension*, **73**, 522–531, Lippincott Williams & Wilkins Hagerstown, MD . doi:10.1161/HYPERTENSIONAHA.118.11191
- Thilaganathan, B. & Kalafat, E., 2019. Cardiovascular system in preeclampsia and beyond. *Hypertension*, **73**, 522–531, Lippincott Williams and Wilkins. doi:10.1161/HYPERTENSIONAHA.118.11191
- Thornburg, K.L., Lindajacobson, S., Giraud, G.D. & Morton, M.J., 2000. Hemodynamic Changes in Pregnancy. *Semin Perinatol*, Vol. 24.
- Thornton, J.G. & Macdonald, A.M., 1999. Twin mothers, pregnancy hypertension and pre-eclampsia. *Br J Obstet Gynaecol*, **106**, 570–575, Br J Obstet Gynaecol. doi:10.1111/J.1471-0528.1999.TB08326.X
- Tian, Y. & Yang, X., 2022, March 3. A Review of Roles of Uterine Artery Doppler in Pregnancy Complications. *Front Med (Lausanne)*, Frontiers Media S.A. doi:10.3389/fmed.2022.813343
- Timpka, S., Markovitz, A., Schyman, T., Mogren, I., Fraser, A., Franks, P.W. & Rich-Edwards, J.W., 2018. Midlife development of type 2 diabetes and hypertension in women by history

of hypertensive disorders of pregnancy. *Cardiovasc Diabetol*, **17**, 135, *Cardiovasc Diabetol*. doi:10.1186/S12933-018-0764-2

Timpka, S., Stuart, J.J., Tanz, L.J., Rimm, E.B., Franks, P.W. & Rich-Edwards, J.W., 2017. Lifestyle in progression from hypertensive disorders of pregnancy to chronic hypertension in Nurses' Health Study II: observational cohort study. *BMJ*, **358**, 1–12, *BMJ*. doi:10.1136/BMJ.J3024

Tjoa, M.L., Cindrova-Davies, T., Spasic-Boskovic, O., Bianchi, D.W. & Burton, G.J., 2006. Trophoblastic oxidative stress and the release of cell-free feto-placental DNA. *American Journal of Pathology*, **169**, 400–404, American Society for Investigative Pathology Inc. doi:10.2353/ajpath.2006.060161

Toescu, V., Nuttall, S.L., Martin, U., Kendall, M.J. & Dunne, F., 2002. Oxidative stress and normal pregnancy. *Clin Endocrinol (Oxf)*, **57**, 609–613, John Wiley & Sons, Ltd. doi:10.1046/j.1365-2265.2002.01638.x

Toliver-Kinsky, T., Cui, W., Törö, G., Lee, S.J., Shatalin, K., Nudler, E. & Szabo, C., 2019. H₂S, a Bacterial Defense Mechanism against the Host Immune Response. *Infect Immun*, **87**, 272–290, American Society for Microbiology (ASM). doi:10.1128/IAI.00272-18

Tomasovic, A., Brand, T., Schanbacher, C., Kramer, S., Hümmert, M.W., Godoy, P., Schmidt-Heck, W., *et al.*, 2020. Interference with ERK-dimerization at the nucleocytoplasmic interface targets pathological ERK1/2 signaling without cardiotoxic side-effects. *Nature Communications* 2020 11:1, **11**, 1–16, Nature Publishing Group. doi:10.1038/s41467-020-15505-4

Tomimatsu, T., Mimura, K., Endo, M., Kumasawa, K. & Kimura, T., 2017, April 1. Pathophysiology of preeclampsia: An angiogenic imbalance and long-lasting systemic vascular dysfunction. *Hypertension Research*, Nature Publishing Group. doi:10.1038/hr.2016.152

Torres-Vergara, P., Rivera, R. & Escudero, C., 2022. How Soluble Fms-Like Tyrosine Kinase 1 Could Contribute to Blood-Brain Barrier Dysfunction in Preeclampsia? *Front Physiol*, **12**, 805082, Frontiers Media S.A. doi:10.3389/FPHYS.2021.805082/BIBTEX

- Tortorella, M.D., Burn, T.C., Pratta, M.A., Abbaszade, I., Hollis, J.M., Liu, R., Rosenfeld, S.A., *et al.*, 1999. Purification and cloning of aggrecanase-1: a member of the ADAMTS family of proteins. *Science*, **284**, 1664–1666, Science. doi:10.1126/SCIENCE.284.5420.1664
- Tranquilli, A.L., Dekker, G., Magee, L., Roberts, J., Sibai, B.M., Steyn, W., Zeeman, G.G., *et al.*, 2014. The classification, diagnosis and management of the hypertensive disorders of pregnancy: A revised statement from the ISSHP. *Pregnancy Hypertens*, **4**, 97–104, Elsevier B.V. doi:10.1016/j.preghy.2014.02.001
- Tranquilli, A.L., Dekker, G., Magee, L., Roberts, J., Sibai, B.M., Steyn, W., Zeeman, G.G., *et al.*, 2014. The classification, diagnosis and management of the hypertensive disorders of pregnancy: A revised statement from the ISSHP. *Pregnancy Hypertens*, Elsevier B.V. doi:10.1016/j.preghy.2014.02.001
- Trofimova-Griffin, M.E. & Juchau, M.R., 2002. Developmental expression of cytochrome CYP26B1 (P450RAI-2) in human cephalic tissues. *Developmental Brain Research*, **136**, 175–178, Brain Res Dev Brain Res. doi:10.1016/S0165-3806(02)00305-X
- Trogstad, L., Magnus, P. & Stoltenberg, C., 2011. Pre-eclampsia: Risk factors and causal models. *Best Pract Res Clin Obstet Gynaecol*, **25**, 329–342, Elsevier Ltd. doi:10.1016/j.bpobgyn.2011.01.007
- Tsiaras, S. & Poppas, A., 2009. Mitral valve disease in pregnancy: outcomes and management. *Obstet Med*, **2**, 6–10, SAGE Publications. doi:10.1258/om.2008.080002
- Turan, O.M., Paco, C. De, Kametas, N., Khaw, A. & Nicolaides, K.H., 2008. Effect of parity on maternal cardiac function during the first trimester of pregnancy. *Ultrasound in Obstetrics and Gynecology*, **32**, 849–854. doi:10.1002/uog.5354
- Turanov, A.A., Lo, A., Hassler, M.R., Makris, A., Ashar-Patel, A., Alterman, J.F., Coles, A.H., *et al.*, 2018. RNAi modulation of placental sFLT1 for the treatment of preeclampsia. *Nat Biotechnol*, **36**, 1164–1173. doi:10.1038/nbt.4297
- Turbeville, H.R. & Sasser, J.M., 2020. Preeclampsia beyond pregnancy: Long-term consequences for mother and child. *Am J Physiol Renal Physiol*, **318**, F1315–F1326, American Physiological Society. doi:10.1152/AJPRENAL.00071.2020

- Turco, M.Y., Gardner, L., Kay, G., Hamilton, R.S., Prater, M., Hollinshead, M.S., Mcwhinnie, A., *et al.*, 2018. Trophoblast organoids as a model for maternal-fetal interactions during human placentation. *Nature*, **564**, 263–282. doi:10.1038/s41586-018-0753-3
- Turco, M.Y. & Moffett, A., 2019. Development of the human placenta. *Development (Cambridge)*, **146**, 1–14. doi:10.1242/dev.163428
- Turi, J.L., Wang, X., McKie, A.T., Nozik-Grayck, E., Mamo, L.B., Crissman, K., Piantadosi, C.A., *et al.*, 2006. Duodenal cytochrome b: a novel ferrireductase in airway epithelial cells. *Am J Physiol Lung Cell Mol Physiol*, **291**, 272–280, *Am J Physiol Lung Cell Mol Physiol*. doi:10.1152/AJPLUNG.00342.2005
- Turi, V.R., Luca, C.T., Gaita, D., Iurciuc, S., Petre, I., Iurciuc, M., Horvath, T., *et al.*, 2022, September 1. Diagnosing Arterial Stiffness in Pregnancy and Its Implications in the Cardio-Renal-Metabolic Chain. *Diagnostics*, MDPI. doi:10.3390/diagnostics12092221
- Tyldum, E. V., Backe, B., Støylen, A. & Slørdahl, S.A., 2012. Maternal left ventricular and endothelial functions in preeclampsia. *Acta Obstet Gynecol Scand*, **91**, 566–573. doi:10.1111/j.1600-0412.2011.01282.x
- Tyldum, E. V., Backe, B., Støylen, A., Slørdahl, S.A. & Tyldum, E.V., 2011. Maternal left ventricular and endothelial functions in preeclampsia. *AOGS*, **91**, 566–573. doi:10.1111/j.1600-0412.2011.01282.x
- Umazume, T., Yamada, T., Yamada, S., Ishikawa, S., Furuta, I., Iwano, H., Murai, D., *et al.*, 2018. Morphofunctional cardiac changes in pregnant women: Associations with biomarkers. *Open Heart*, **5**, BMJ Publishing Group. doi:10.1136/openhrt-2018-000850
- Untereiner, A.A., Fu, M., Módis, K., Wang, R., Ju, Y.J. & Wu, L., 2016. Stimulatory effect of CSE-generated H₂S on hepatic mitochondrial biogenesis and the underlying mechanisms. *Nitric Oxide*, **58**, 67–76, *Nitric Oxide*. doi:10.1016/J.NIOX.2016.06.005
- Untereiner, A.A., Wang, R., Ju, Y. & Wu, L., 2016. Decreased Gluconeogenesis in the Absence of Cystathionine Gamma-Lyase and the Underlying Mechanisms. *Antioxid Redox Signal*, **24**, 129–140, *Antioxid Redox Signal*. doi:10.1089/ARS.2015.6369

- Uzun, N., 2019. Eastern Anatolian Journal of Science Cite this article as: N. Uzun, The Analysis of Glutathione Level and Superoxide Dismutase Activity in Normal and Preeclampsia Pregnant. *Eastern Anatolian Journal of Science*, **5**, 23–29.
- Vaiman, D. & Miralles, F., 2016. An Integrative Analysis of Preeclampsia Based on the Construction of an Extended Composite Network Featuring Protein-Protein Physical Interactions and Transcriptional Relationships. *PLoS One*, **11**, 1–16, PLOS. doi:10.1371/JOURNAL.PONE.0165849
- Vaka, V.R., McMaster, K.M., Jr, M.W.C., Ibrahim, T., Hazlewood, R., Usry, N., Cornelius, D., *et al.*, 2019. The role of mitochondrial dysfunction and ROS in mediating hypertension in the RUPP rat model of preeclampsia. *Hypertension*, **72**, 703–711. doi:10.1161/HYPERTENSIONAHA.118.11290.The
- Valdés, G., 2017, August 28. Preeclampsia and cardiovascular disease: Interconnected paths that enable detection of the subclinical stages of obstetric and cardiovascular diseases. *Integr Blood Press Control*, Dove Medical Press Ltd. doi:10.2147/IBPC.S138383
- Valensise, H., Novelli, G.P., Vasapollo, B., Borzi, M., Arduini, D., Galante, A. & Romanini, C., 2000. Maternal cardiac systolic and diastolic function: Relationship with uteroplacental resistances. A Doppler and echocardiographic longitudinal study. *Ultrasound in Obstetrics and Gynecology*, **15**, 487–497. doi:10.1046/j.1469-0705.2000.00135.x
- Valensise, H, Vasapollo, B., Novelli, G.P., Larciprete, G., Romanini, M.E., Arduini, D., Galante, A., *et al.*, 2001. Maternal diastolic function in asymptomatic pregnant women with bilateral notching of the uterine artery waveform at 24 weeks' gestation: a pilot study. *Ultrasound Obstetrics Gynecol*, **18**, 450–455. doi:10.1046/j.0960-7692.2001.00576.x
- Valensise, Herbert, Vasapollo, B., Gagliardi, G. & Novelli, G.P., 2008. Early and Late preeclampsia: Two different maternal hemodynamic states in the latent phase of the disease. *Hypertension*, **52**, 873–880. doi:10.1161/HYPERTENSIONAHA.108.117358
- Valiño, N., Giunta, G., Gallo, D.M., Akolekar, R. & Nicolaides, K.H., 2017. Uterine artery pulsatility index at 30-34 weeks' gestation in the prediction of adverse perinatal outcome. *Fetal Medicine*, 1–19. doi:10.1002/uog.14898

- Vannberg, F.O., Chapman, S.J., Khor, C.C., Tosh, K., Floyd, S., Jackson-Sillah, D., Crampin, A., *et al.*, 2008. CD209 genetic polymorphism and tuberculosis disease. *PLoS One*, **3**, 1388–1294, PLoS One. doi:10.1371/JOURNAL.PONE.0001388
- Vanwijk, M.J., Kublickiene, K., Boer, K. & VanBavel, E., 2000. Vascular function in preeclampsia. *Cardiovasc Res*, **47**, 38–48, Oxford Academic. doi:10.1016/S0008-6363(00)00087-0/2/47-1-38-FIG2.GIF
- Vasconcelos, M.M., Ganan, C.S., Silveira, C.F. da S.M.P. da, Malagutte, K.N.D.S., Poiati, J.R., Nunes, H.R. de C., Martin, L.C., *et al.*, 2023. Evolution of Myocardial Hypertrophy Associated With Pregnancy in Hypertensive Women Six Months Postpartum. *Curr Probl Cardiol*, **48**, 101783, Mosby. doi:10.1016/J.CPCARDIOL.2023.101772
- Vasileiou, P.V.S., Evangelou, K., Vlasis, K., Fildisis, G., Panayiotidis, M.I., Chronopoulos, E., Passias, P.-G., *et al.*, 2019. Mitochondrial Homeostasis and Cellular Senescence. *Cells*, **8**, 1–25. doi:10.3390/cells8070686
- Venkatesha, S., Toporsian, M., Lam, C., Hanai, J.I., Mammoto, T., Kim, Y.M., Bdolah, Y., *et al.*, 2006. Soluble endoglin contributes to the pathogenesis of preeclampsia. *Nat Med*, **12**, 642–649, Nat Med. doi:10.1038/NM1429
- Vento-tormo, R., Efremova, M., Botting, Rachel A., Turco, M.Y., Vento-tormo, M., Meyer, K.B., Park, J., *et al.*, 2018. Single-cell reconstruction of the early maternal-fetal interface in humans. *Nature*, **563**. doi:10.1038/s41586-018-0698-6
- Verlohren, S., Brennecke, S.P., Galindo, A., Karumanchi, S.A., Mirkovic, L.B., Schlembach, D., Stepan, H., *et al.*, 2022, March 1. Clinical interpretation and implementation of the sFlt-1/PIGF ratio in the prediction, diagnosis and management of preeclampsia. *Pregnancy Hypertens*, Elsevier B.V. doi:10.1016/j.preghy.2021.12.003
- Vinayagam, D., Thilaganathan, B., Stirrup, O., Mantovani, E. & Khalil, A., 2018. Maternal hemodynamics in normal pregnancy: reference ranges and role of maternal characteristics. *Ultrasound in Obstetrics & Gynecology*, **51**, 665–671, John Wiley and Sons Ltd. doi:10.1002/uog.17504

- Vishnyakova, P.A., Volodina, M.A., Tarasova, N. V., Marey, M. V., Tsvirkun, D. V., Vavina, O. V., Khodzhaeva, Z.S., *et al.*, 2016. Mitochondrial role in adaptive response to stress conditions in preeclampsia. *Sci Rep*, **6**, 1–9, Nature Publishing Group. doi:10.1038/srep32410
- Vitoratos, N., Hassiakos, D. & Iavazzo, C., 2012. Molecular Mechanisms of Preeclampsia. *J Pregnancy*, Hindawi Publishing Corporation. doi:10.1155/2012/298343
- Vogeser, M., Felbinger, T.W., Kilger, E., Röhl, W., Fraunberger, P. & Jacob, K., 1999. Corticosteroid-binding globulin and free cortisol in the early postoperative period after cardiac surgery. *Clin Biochem*, **32**, 213–216, Clin Biochem. doi:10.1016/S0009-9120(99)00009-0
- Vogtmann, R., Heupel, J., Herse, F., Matin, M., Hagmann, H., Bendix, I., Kräker, K., *et al.*, 2021. Circulating Maternal sFLT1 (Soluble fms-Like Tyrosine Kinase-1) Is Sufficient to Impair Spiral Arterial Remodeling in a Preeclampsia Mouse Model. *Hypertension*, **78**, 1067–1079, Lippincott Williams and Wilkins. doi:10.1161/HYPERTENSIONAHA.121.17567
- Vogtmann, R., Kühnel, E., Dicke, N., Verkaik-Schakel, R.N., Plösch, T., Schorle, H., Stojanovska, V., *et al.*, 2019. Human sFLT1 leads to severe changes in placental differentiation and vascularization in a transgenic hsFLT1/rtTA FGR mouse model. *Front Endocrinol (Lausanne)*, **10**, Frontiers Media S.A. doi:10.3389/fendo.2019.00165
- Vricella, L.K., 2017. Emerging understanding and measurement of plasma volume expansion in pregnancy. *Am J Clin Nutr*, **106**, 1620S, American Society for Nutrition. doi:10.3945/AJCN.117.155903
- Wagner, N., Wagner, K.D., Afanetti, M., Nevo, F., Antignac, C., Michiels, J.F., Schedl, A., *et al.*, 2008. A novel Wilms' tumor 1 gene mutation in a child with severe renal dysfunction and persistent renal blastema. *Pediatr Nephrol*, **23**, 1445–1453, Pediatr Nephrol. doi:10.1007/S00467-008-0845-7
- Waker, C.A., Kaufman, M.R. & Brown, T.L., 2021, July 2. Current State of Preeclampsia Mouse Models: Approaches, Relevance, and Standardization. *Front Physiol*, Frontiers Media S.A. doi:10.3389/fphys.2021.681632

- Waker, C.A., Kaufman, M.R. & Brown, T.L., 2021, July 2. Current State of Preeclampsia Mouse Models: Approaches, Relevance, and Standardization. *Front Physiol*, Frontiers Media S.A. doi:10.3389/fphys.2021.681632
- Walentowicz-Sadlecka, M., Domaracki, P., Sadlecki, P., Siodmiak, J., Grabiec, M., Walentowicz, P., Moliz, M.T.A. & Odrowaz-Sypniewska, G., 2019. Assessment of the sFlt-1 and sFlt-1/25(OH)D Ratio as a Diagnostic Tool in Gestational Hypertension (GH), Preeclampsia (PE), and Gestational Diabetes Mellitus (GDM). *Dis Markers*, **2019**, 5870239, Hindawi. doi:10.1155/2019/5870239
- Walentowicz-Sadlecka, M., Domaracki, P., Sadlecki, P., Siodmiak, J., Grabiec, M., Walentowicz, P., Moliz, M.T.A., Odrowaz-Sypniewska, G., *et al.*, 2019. Assessment of the sFlt-1 and sFlt-1/25(OH)D Ratio as a Diagnostic Tool in Gestational Hypertension (GH), Preeclampsia (PE), and Gestational Diabetes Mellitus (GDM). *Dis Markers*, **2019**, 1–12, Hindawi Limited. doi:10.1155/2019/5870239
- Walker, J.J., 2000. Preeclampsia. *The Lancet*, **356**, 1260–1265. doi:10.1016/S0140-6736(00)02800-2
- Walshe, T.E., Dole, V.S., Maharaj, A.S.R., Patten, I.S., Wagner, D.D. & D'Amore, P.A., 2009. Inhibition of VEGF or TGF- β signaling activates endothelium and increases leukocyte rolling. *Arterioscler Thromb Vasc Biol*, **29**, 1185–1192, Arterioscler Thromb Vasc Biol. doi:10.1161/ATVBAHA.109.186742
- Walshe, T.E., Saint-Geniez, M., Maharaj, A.S.R., Sekiyama, E., Maldonado, A.E. & D'Amore, P.A., 2009. TGF- β is required for vascular barrier function, endothelial survival and homeostasis of the adult microvasculature. *PLoS One*, **4**, PLoS One. doi:10.1371/JOURNAL.PONE.0005149
- Wang, Banqin, Xu, T., Li, Y., Wang, W., Lyu, C., Luo, D., Yang, Q., *et al.*, 2020. Trophoblast H2S Maintains Early Pregnancy via Regulating Maternal-Fetal Interface Immune Hemostasis. *J Clin Endocrinol Metab*, **105**, 4275–4389, J Clin Endocrinol Metab. doi:10.1210/CLINEM/DGAA357
- Wang, Bu, Chen, S., Zhao, J.Q., Xiang, B.L., Gu, X., Zou, F. & Zhang, Z.H., 2019. ADAMTS-1 inhibits angiogenesis via the PI3K/Akt-eNOS-VEGF pathway in lung cancer cells.

Transl Cancer Res, **8**, 2725–2735, AME Publishing Company.
doi:10.21037/tcr.2019.10.34

Wang, K., Ahmad, S., Cai, M., Rennie, J., Fujisawa, T., Crispi, F., Baily, J., *et al.*, 2013. Dysregulation of hydrogen sulfide producing enzyme cystathionine γ -lyase contributes to maternal hypertension and placental abnormalities in preeclampsia. *Circulation*, **127**, 2514–2522. doi:10.1161/CIRCULATIONAHA.113.001631

Wang, L., Rice, M., Swist, S., Kubin, T., Wu, F., Wang, S., Kraut, S., *et al.*, 2021. BMP9 and BMP10 Act Directly on Vascular Smooth Muscle Cells for Generation and Maintenance of the Contractile State. *Circulation*, **143**, 1394–1410, Lippincott Williams and Wilkins. doi:10.1161/CIRCULATIONAHA.120.047375

Wang, M.J., Cai, W.J., Li, N., Ding, Y.J., Chen, Y. & Zhu, Y.C., 2010. The hydrogen sulfide donor NaHS promotes angiogenesis in a rat model of hind limb ischemia. *Antioxid Redox Signal*, **12**, 1065–1077. doi:10.1089/ars.2009.2945

Wang, R., 2002. Two's company, three's a crowd: can H₂S be the third endogenous gaseous transmitter? . *The FASEB Journal*, **16**, 1792–1798, Wiley. doi:10.1096/fj.02-0211hyp

Wang, Y., Luk, A.O.Y., Ma, R.C.W., So, W.Y., Tam, C.H.T., Ng, M.C.Y., Yang, X., *et al.*, 2010. Independent predictive roles of eotaxin Ala23Thr, paraoxonase 2 Ser311Cys and beta-adrenergic receptor Trp64Arg polymorphisms on cardiac disease in Type 2 Diabetes--an 8-year prospective cohort analysis of 1297 patients. *Diabet Med*, **27**, 376–383, Diabet Med. doi:10.1111/J.1464-5491.2010.02980.X

Wang, Y. & Walsh, S.W., 1998. Placental mitochondria as a source of oxidative stress in preeclampsia. *Placenta*, **19**, 581–586, W.B. Saunders Ltd. doi:10.1016/S0143-4004(98)90018-2

Wang, Yuping & Walsh, S.W., 1996. Antioxidant Activities and mRNA Expression of Superoxide Dismutase, Catalase, and Glutathione Peroxidase in Normal and Preeclamptic Placentas. *Journal of the Society for Gynecologic* , **3**, 179–184, SAGE PublicationsSage CA: Thousand Oaks, CA. doi:10.1177/107155769600300404

- Wanschers, B., Vorstenbosch, R. Van De, Wijers, M., Wieringa, B., King, S.M. & Fransen, J., 2008. Rab6 family proteins interact with the dynein light chain protein DYNLRB1. *Cell Motil Cytoskeleton*, **65**, 183–196, Cell Motil Cytoskeleton. doi:10.1002/CM.20254
- Warrington, J.P., Drummond, H.A., Granger, J.P. & Ryan, M.J., 2015. Placental ischemia-induced increases in brain water content and cerebrovascular permeability: Role of TNF- α . *Am J Physiol Regul Integr Comp Physiol*, **309**, R1425–R1431, American Physiological Society. doi:10.1152/ajpregu.00372.2015
- Washington C. Hill, Leticia Hernandez, Angela Thuompson, Deborah Burch, Isaac Delke, Robert Yelverton, William Sappenfield, *et al.*, 2020. Cardiovascular diseases during pregnancy and postpartum in Florida, 2008-2017. *American Journal of Obstetrics&Gynecology*, **Poster session 3**, S411–S412.
- Weissgerber, T.L., Milic, N.M., Milin-Lazovic, J.S. & Garovic, V.D., 2016. Impaired Flow-Mediated Dilation Before, During, and after Preeclampsia: A Systematic Review and Meta-Analysis. *Hypertension*, **67**, 415–423, Lippincott Williams and Wilkins. doi:10.1161/HYPERTENSIONAHA.115.06554/-/DC1
- Weissgerber, T.L. & Mudd, L.M., 2015, March 1. Preeclampsia and Diabetes. *Curr Diab Rep*, Current Medicine Group LLC 1. doi:10.1007/s11892-015-0579-4
- Wen, Y.D., Wang, H., Kho, S.H., Rinkiko, S., Sheng, X., Shen, H.M. & Zhu, Y.Z., 2013. Hydrogen sulfide protects HUVECs against hydrogen peroxide induced mitochondrial dysfunction and oxidative stress. *PLoS One*, **8**, 1–13, PLoS One. doi:10.1371/JOURNAL.PONE.0053147
- Wen, Y.D., Wang, H. & Zhu, Y.Z., 2018. The Drug Developments of Hydrogen Sulfide on Cardiovascular Disease. *Oxid Med Cell Longev*, **2018**, 1–14, Oxid Med Cell Longev. doi:10.1155/2018/4010395
- Wen-Sen Lee, Justin A. Harder, Masao Yoshizu Mi, Mu-EnLee & Edgar Haber, 1997. Progesterone inhibits arterial smooth muscle cell proliferation. *Nat Med*, **3**, 1005–1008.
- Wewers, T.M., Schulz, A., Nolte, I., Pavenstädt, H., Brand, M. & Marco, G.S. Di, 2021. Circulating soluble fms-like tyrosine kinase in renal diseases other than preeclampsia.

Journal of the American Society of Nephrology, **32**, 1853–1863, American Society of Nephrology. doi:10.1681/ASN.2020111579/-/DCSUPPLEMENTAL

White, J.A., Ramshaw, H., Taimi, M., Stangle, W., Zhang, A., Everingham, S., Creighton, S., *et al.*, 2000. Identification of the human cytochrome P450, P450RAI-2, which is predominantly expressed in the adult cerebellum and is responsible for all-trans-retinoic acid metabolism. *Proc Natl Acad Sci U S A*, **97**, 6403–6408, Proc Natl Acad Sci U S A. doi:10.1073/PNAS.120161397

Wickens, D., Lunec, J., Ball, G. & Dormandy, T.L., 1981. Free-radical oxidation (peroxidation) products in plasma in normal and abnormal pregnancy. *Ann Clin Biochem*, **18**, 158–162.

Wickens, D., Wilkins, M.H., Lunec, J., Ball, G. & Dormandy, T.L., 1981. Free radical oxidation (peroxidation) products in plasma in normal and abnormal pregnancy. *Ann Clin Biochem*, **18**, 158–162, *Ann Clin Biochem*. doi:10.1177/000456328101800306

William C Mabie, Thomas G DiSessa, Lisa G Crocker, Baha M Sibai & Kristopher L Arheart, 1994. A longitudinal study of cardiac output in normal human pregnancy. *American Journal of Obstetric Gynecology*, **170**, 849–856.

Williams, D., Stout, M.J., Rosenbloom, J.I., Olsen, M.A., Joynt Maddox, K.E., Deych, E., Davila-Roman, V.G., *et al.*, 2021. Preeclampsia Predicts Risk of Hospitalization for Heart Failure With Preserved Ejection Fraction. *J Am Coll Cardiol*, **78**, 2281–2290, Elsevier. doi:10.1016/J.JACC.2021.09.1360

Williams, M.A., Sanchez, S.E., Ananth, C. V., Hevner, K., Qiu, C. & Enquobahrie, D.A., 2013. Maternal blood mitochondrial DNA copy number and placental abruption risk: Results from a preliminary study. *Int J Mol Epidemiol Genet*, **4**, 120–127, e-Century Publishing Corporation.

Williams, P.J. & Broughton Pipkin, F., 2011. The genetics of pre-eclampsia and other hypertensive disorders of pregnancy. *Best Pract Res Clin Obstet Gynaecol*, **25**, 405, Elsevier. doi:10.1016/J.BPOBGYN.2011.02.007

Williams, P.J., Bulmer, J.N., Searle, R.F., Innes, B.A. & Robson, S.C., 2009. Altered decidual leucocyte populations in the placental bed in pre-eclampsia and foetal growth restriction:

a comparison with late normal pregnancy. *Reproduction Research*, **138**, 177–184. Retrieved from <https://doi.org/10.1530/REP-09-0007>

Wisdom, S.J., Wilson, R., McKillop, J.H. & Walker, J.J., 1991. Antioxidant systems in normal pregnancy and in pregnancy-induced hypertension. *Am J Obstet Gynecol*, **165**, 1701–1704, Mosby. doi:10.1016/0002-9378(91)90018-M

Wójtowicz, A., Zembala-Szczerba, M., Babczyk, D., Kołodziejczyk-Pietruszka, M., Lewaczyńska, O. & Huras, H., 2019. Early- and Late-Onset Preeclampsia: A Comprehensive Cohort Study of Laboratory and Clinical Findings according to the New ISHHP Criteria. *Int J Hypertens*, **2019**, Hindawi Limited. doi:10.1155/2019/4108271

Wölter, M., Okai, C.A., Smith, D.S., Ruß, M., Rath, W., Pecks, U., Borchers, C.H., *et al.*, 2018. Maternal Apolipoprotein B100 Serum Levels are Diminished in Pregnancies with Intrauterine Growth Restriction and Differentiate from Controls. *Proteomics Clin Appl*, **12**, 1800017–1800025, Proteomics Clin Appl. doi:10.1002/PRCA.201800017

Wong, A.Y.H., Kulandavelu, S., Whiteley, K.J., Qu, D., Lowell Langille, B., Lee Adamson, S., Langille, B.L., *et al.*, 2002. Maternal cardiovascular changes during pregnancy and postpartum in mice. *Am J Physiol Heart Circ Physiol*, **282**, 918–925. doi:10.1152/ajpheart.00641

Wong, L.J.C., Chen, T., Wang, J., Tang, S., Schmitt, E.S., Landsverk, M., Li, F., *et al.*, 2020. Interpretation of mitochondrial tRNA variants. *Genet Med*, **22**, 917–926, Genet Med. doi:10.1038/S41436-019-0746-0

Woods, A.K., Hoffmann, D.S., Weydert, C.J., Butler, S.D., Zhou, Y., Sharma, R. V & Davisson, R.L., 2011. Adenoviral Delivery of VEGF 121 Early in Pregnancy Prevents Spontaneous Development of Preeclampsia in BPH/5 Mice. *Hypertension*, **57**, 94–102. doi:10.1161/HYPERTENSIONAHA.110.160242

Wright, D.J., Gray, L.J., Finkelstein, D.I., Crouch, P.J., Pow, D., Pang, T.Y., Li, S., *et al.*, 2016. N-acetylcysteine modulates glutamatergic dysfunction and depressive behavior in Huntington's disease. *Hum Mol Genet*, **25**, 2923–2933, Hum Mol Genet. doi:10.1093/HMG/DDW144

- Wu, F., Zhou, J., Zheng, H. & Liu, G., 2018. Decreased heart rate recovery in women with a history of pre-eclampsia. *Pregnancy Hypertens*, **13**, 25–29, Elsevier B.V. doi:10.1016/j.preghy.2018.05.002
- Wu, P., Haththotuwa, R., Kwok, C.S., Babu, A., Kotronias, R.A., Rushton, C., Zaman, A., *et al.*, 2017. Preeclampsia and future cardiovascular health. *Circ Cardiovasc Qual Outcomes*, **10**, 1–15, Lippincott Williams and Wilkins. doi:10.1161/CIRCOUTCOMES.116.003497/-/DC1
- Wu, S., Wang, Y., Zhang, M., Shrestha, S.S., Wang, M. & He, J.Q., 2018. Genetic Polymorphisms of IL1B, IL6, and TNF α in a Chinese Han Population with Pulmonary Tuberculosis. *Biomed Res Int*, **2018**, 1–6, Biomed Res Int. doi:10.1155/2018/3010898
- Xie, Y.H., Zhang, N., Li, L.F., Zhang, Q.Z., Xie, L.J., Jiang, H., Li, P., *et al.*, 2014. Hydrogen sulfide reduces regional myocardial ischemia injury through protection of mitochondrial function. *Mol Med Rep*, **10**, 1907–1914, Mol Med Rep. doi:10.3892/MMR.2014.2391
- Xu, J. & Shi, G.P., 2014. Vascular wall extracellular matrix proteins and vascular diseases. *Biochim Biophys Acta*, **1842**, 2119, NIH Public Access. doi:10.1016/J.BBADIS.2014.07.008
- Xu, M., Hua, Y., Qi, Y., Meng, G. & Yang, S., 2019. Exogenous hydrogen sulphide supplement accelerates skin wound healing via oxidative stress inhibition and vascular endothelial growth factor enhancement. *Exp Dermatol*, **28**, 776–785, Exp Dermatol. doi:10.1111/EXD.13930
- Yaling Zhai, Youxia Liu, Yuanyuan Qi, Xiaoqing Long, Jingge Gao, Xingchen Yao, Yazhuo Chen, *et al.*, 2020. The soluble VEGF receptor sFlt-1 contributes to endothelial dysfunction in IgA nephropathy. *PLoS One*, **15**, PLoS One. doi:10.1371/JOURNAL.PONE.0234492
- Yan, H., Du, J. & Tang, C., 2004. The possible role of hydrogen sulfide on the pathogenesis of spontaneous hypertension in rats. *Biochem Biophys Res Commun*, **313**, 22–27, Academic Press Inc. doi:10.1016/j.bbrc.2003.11.081

- Yancy, C.W., Jessup, M., Bozkurt, B., Butler, J., Casey, D.E., Drazner, M.H., Fonarow, G.C., *et al.*, 2013. 2013 ACCF/AHA guideline for the management of heart failure: Executive summary: A report of the American college of cardiology foundation/American Heart Association task force on practice guidelines. *Circulation*, **128**, 1810–1852, Lippincott Williams & Wilkins Hagerstown, MD . doi:10.1161/CIR.0B013E31829E8807/-/DC2
- Yang, D.B., Xu, Y.C., Wang, D.H. & Speakman, J.R., 2013. Effects of reproduction on immuno-suppression and oxidative damage, and hence support or otherwise for their roles as mechanisms underpinning life history trade-offs, are tissue and assay dependent. *Journal of Experimental Biology*, **216**, 4242–4250, J Exp Biol. doi:10.1242/jeb.092049
- Yang, G., Wu, L., Jiang, B., Yang, W., Qi, J., Cao, K., Meng, Q., *et al.*, 2008. H2S as a Physiologic Vasorelaxant: Hypertension in Mice with Deletion of Cystathionine γ -Lyase. *Science (1979)*, **322**, 587–590. doi:10.1126/science.1162667
- Yang, G., Wu, L., Jiang, B., Yang, W., Qi, J., Cao, K., Meng, Q., *et al.*, 2008. H2S as a Physiologic Vasorelaxant: Hypertension in Mice with Deletion of Cystathionine γ -Lyase. *Science (1979)*, **322**, 587–590. doi:10.1126/science.1162667
- Yang, X., Guo, L., Sun, X., Chen, X. & Tong, X., 2011. Protective effects of hydrogen-rich saline in preeclampsia rat model. *Placenta*, **32**, 681–686, W.B. Saunders. doi:10.1016/J.PLACENTA.2011.06.020
- Yang, Yijun, Kurian, J., Schena, G., Johnson, J., Kubo, H., Travers, J.G., Kang, C., *et al.*, 2021. Cardiac Remodeling during Pregnancy with Metabolic Syndrome: Prologue of Pathological Remodeling. *Circulation*, **143**, 699–712, Lippincott Williams and Wilkins. doi:10.1161/CIRCULATIONAHA.120.051264
- Yang, Ying & Wu, N., 2022. Gestational Diabetes Mellitus and Preeclampsia: Correlation and Influencing Factors. *Front Cardiovasc Med*, **9**, 1–14, Frontiers Media S.A. doi:10.3389/FCVM.2022.831297/BIBTEX
- Ye, J., Suizu, F., Yamakawa, K., Mukai, Y., Kato, M., Yoneyama, H., Yahagi, N., *et al.*, 2023. Silencing of tumoral carbohydrate sulfotransferase 15 reactivates lymph node pancreatic

- cancer T cells in mice. *Eur J Immunol*, **0**, 1–13, John Wiley & Sons, Ltd. doi:10.1002/EJI.202250160
- Yeon Lee, J., Li, S., Na, Q., Dong, J., Jia, B., Jones-Beatty, K., McLane, M.W., *et al.*, 2019. Melatonin for prevention of placental malperfusion and fetal compromise associated with intrauterine inflammation-induced oxidative stress. *Am J Obstet Gynecol*, **220**, S370–S371. doi:10.1016/j.ajog.2018.11.576
- Yin, Z., Li, Y., He, W., Li, D., Li, H., Yang, Y., Shen, B., *et al.*, 2018. Progesterone inhibits contraction and increases TREK-1 potassium channel expression in late pregnant rat uterus. *Oncotarget*, Vol. 9. Retrieved from www.impactjournals.com/oncotarget
- Yong, H.E.J., Murthi, P., Brennecke, S.P. & Moses, E.K., 2018. Genetic Approaches in Preeclampsia. *Methods Mol Biol*, **1710**, 53–72, Methods Mol Biol. doi:10.1007/978-1-4939-7498-6_5
- You, X., Chen, Z., Zhao, H., Xu, C., Liu, W., Sun, Q., He, P., *et al.*, 2017. Endogenous hydrogen sulfide contributes to uterine quiescence during pregnancy. *Reproduction*, **153**, 535–543, Reproduction. doi:10.1530/REP-16-0549
- You, X.J., Xu, C., Lu, J.Q., Zhu, X.Y., Gao, L., Cui, X.R., Li, Y., *et al.*, 2011. Expression of cystathionine β -synthase and cystathionine γ -lyase in human pregnant myometrium and their roles in the control of uterine contractility. *PLoS One*, **6**. doi:10.1371/journal.pone.0023788
- Youssef, L. & Crispi, F., 2020. Maternal and fetal cardiovascular adaptations in preeclampsia and/or fetal growth restriction. *American Journal of Obstetrics&Gynecology*, 286–287. doi:10.1016/j.ajog
- Yu, E., Calvert, P.A., Mercer, J.R., Harrison, J., Baker, L., Figg, N.L., Kumar, S., *et al.*, 2013. Mitochondrial DNA damage can promote atherosclerosis independently of reactive oxygen species through effects on smooth muscle cells and monocytes and correlates with higher-risk plaques in humans. *Circulation*, **128**, 702–712, Circulation. doi:10.1161/CIRCULATIONAHA.113.002271

- Yu, Q., Leatherbury, L., Tian, X. & Lo, C.W., 2008. Cardiovascular Assessment of Fetal Mice by In Utero Echocardiography. *Ultrasound Med Biol*, **34**, 741–752. doi:10.1016/j.ultrasmedbio.2007.11.001
- Yuan, L., Duan, Y. & Cao, T., 2006. Echocardiographic study of cardiac morphological and functional changes before and after parturition in pregnancy-induced hypertension. *Echocardiography*, **23**, 177–182. doi:10.1111/j.1540-8175.2006.00203.x
- Yung, H.W., Atkinson, D., Champion-Smith, T., Olovsson, M., Charnock-Jones, D.S. & Burton, G.J., 2014. Differential activation of placental unfolded protein response pathways implies heterogeneity in causation of early- and late-onset pre-eclampsia. *Journal of Pathology*, **234**, 262–276, John Wiley and Sons Ltd. doi:10.1002/path.4394
- Zagon, I.S., Verderame, M.F., Allen, S.S. & McLaughlin, P.J., 2000. Cloning, sequencing, chromosomal location, and function of cDNAs encoding an opioid growth factor receptor (OGFr) in humans. *Brain Res*, **856**, 75–83, Brain Res. doi:10.1016/S0006-8993(99)02330-6
- Zagon, I.S., Wu, Y. & McLaughlin, P.J., 1999. Opioid growth factor and organ development in rat and human embryos. *Brain Res*, **839**, 313–322, Brain Res. doi:10.1016/S0006-8993(99)01753-9
- Zaman, N., Abdali, N., Asif, M., Tiwari, P. & Mahmudullah Razi Mohd, 2018. Maternal Cardiovascular Hemodynamics in Preeclampsia: Echocardiographic Assessment and Evaluation of Subclinical Left Ventricular Dysfunction. *Journal of South Asian Federation Obstetric Gynaecology*, **10**, 400–404. Retrieved from <https://www.jsafog.com/doi/pdf/10.5005/jp-journals-10006-1632>
- Zanardo, R.C.O., Brancaleone, V., Distrutti, E., Fiorucci, S., Cirino, G., Wallace, J.L., Zanardo, R.C.O., *et al.*, 2006. Hydrogen sulfide is an endogenous modulator of leukocyte-mediated inflammation. *The FASEB Journal*, **20**, 2118–2120, Wiley. doi:10.1096/fj.06-6270fje
- Zanardo, R.C.O., Brancaleone, V., Distrutti, E., Fiorucci, S., Cirino, G., Wallace, J.L., Zanardo, R.C.O., *et al.*, 2006. Hydrogen sulfide is an endogenous modulator of leukocyte-mediated inflammation. *The FASEB Journal*, **20**, 2118–2120, Wiley. doi:10.1096/fj.06-6270fje

- Zenther, D., Plessis, M. Du, Brennecke, S., Wong, J., Grigg, L. & Harrap, S.B., 2009. Deterioration in cardiac systolic and diastolic function late in normal human pregnancy. *Clin Sci*, **116**, 599–606. doi:10.1042/CS20080142
- Zentner, D., Plessis, M. Du, Brennecke, S., Wong, J., Grigg, L. & Harrap, S., 2012. Cardiac function at term in human pregnancy. *Pregnancy Hypertens*, **2**, 132–138. doi:10.1016/j.preghy.2011.12.002
- Zhai, Y., Behera, J., Tyagi, S.C. & Tyagi, N., 2019. Hydrogen sulfide attenuates homocysteine-induced osteoblast dysfunction by inhibiting mitochondrial toxicity. *J Cell Physiol*, **234**, 18602–18614, *J Cell Physiol*. doi:10.1002/JCP.28498
- Zhang, C., Austin, M.A., Edwards, K.L., Farin, F.M., Li, N., Hsu, L., Srinouanprachanh, S.L., *et al.*, 2006. Functional variants of the lipoprotein lipase gene and the risk of preeclampsia among non-Hispanic Caucasian women. *Clin Genet*, **69**, 33–39, *Clin Genet*. doi:10.1111/J.1399-0004.2005.00541.X
- Zhang, J., Yu, J., Chen, Y., Liu, L., Xu, M., Sun, L., Luo, H., *et al.*, 2018. Exogenous Hydrogen Sulfide Supplement Attenuates Isoproterenol-Induced Myocardial Hypertrophy in a Sirtuin 3-Dependent Manner. *Oxid Med Cell Longev*, **2018**, *Oxid Med Cell Longev*. doi:10.1155/2018/9396089
- Zhang, Y., Zheng, D., Fang, Q. & Zhong, M., 2020. Aberrant hydroxymethylation of ANGPTL4 is associated with selective intrauterine growth restriction in monochorionic twin pregnancies. *Epigenetics*, **15**, 887–899, Bellwether Publishing, Ltd. doi:10.1080/15592294.2020.1737355/SUPPL_FILE/KEPI_A_1737355_SM4883.ZIP
- Zhao, W. & Wang, R., 2002. H₂S-induced vasorelaxation and underlying cellular and molecular mechanisms. *Am J Physiol Heart Circ Physiol*, **283**, H474–H480, *Am J Physiol Heart Circ Physiol*. doi:10.1152/AJPHEART.00013.2002
- Zhao, W., Zhang, J., Lu, Y. & Wang, R., 2001. The vasorelaxant effect of H₂S as a novel endogenous gaseous KATP channel opener. *The European Molecular Biology Organization Journal*, **20**, 6008–6016.

- Zhao, Z.Z., Wang, Z., Li, G.H., Wang, R., Tan, J.M., Cao, X., Suo, R., *et al.*, 2011. Hydrogen sulfide inhibits macrophage-derived foam cell formation. *Exp Biol Med (Maywood)*, **236**, 169–176, Exp Biol Med (Maywood). doi:10.1258/EBM.2010.010308
- Zhou, F., Chen, D., Chen, G., Liao, P., Li, R., Nong, Q., Meng, Y., *et al.*, 2021. Gene set index based on different modules may help differentiate the mechanisms of alzheimer's disease and vascular dementia. *Clin Interv Aging*, **16**, 451–463, Dove Medical Press Ltd. doi:10.2147/CIA.S297483
- Zhou, L., Sun, H., Cheng, R., Fan, X., Lai, X.S. & Deng, C., 2019. ELABELA, as a potential diagnostic biomarker of preeclampsia, regulates abnormally shallow placentation via APJ. *Am J Physiol Endocrinol Metab*, **316**, E773–E781, American Physiological Society. doi:10.1152/AJPENDO.00383.2018
- Zhou, Y., Damsky, C.H., King Chiu, I., Roberts, J.M. & Fisher, S.J., 1992. Preeclampsia Is Associated with Abnormal Expression of Adhesion Molecules by Invasive Cytotrophoblasts. *Journal of Clinical Investigation*, **91**, 950–960.
- Zhu, J., Zheng, X., Lu, D., Zheng, Y. & Liu, J., 2022. Clinical Relevance and Tumor Growth Suppression of Mitochondrial ROS Regulators along NADH:Ubiquinone Oxidoreductase Subunit B3 in Thyroid Cancer. *Oxid Med Cell Longev*, **2022**, Hindawi Limited. doi:10.1155/2022/8038857
- Zieman, S.J., Melenovsky, V. & Kass, D.A., 2005. Mechanisms, Pathophysiology, and Therapy of Arterial Stiffness. *Arterioscler Thromb Vasc Biol*, **25**, 932–943, Lippincott Williams & Wilkins. doi:10.1161/01.ATV.0000160548.78317.29
- Zintzaras, E., Kitsios, G., Harrison, G.A., Laivuori, H., Kivinen, K., Kere, J., Messinis, I., *et al.*, 2006. Heterogeneity-based genome search meta-analysis for preeclampsia. *Hum Genet*, **120**, 360–370, Hum Genet. doi:10.1007/S00439-006-0214-1
- Zoey N. Pascual & Michelle D. Langaker, 2022. Physiology, Pregnancy. *StatPearls*, 1–8. Retrieved from <https://www.ncbi.nlm.nih.gov/books/NBK559304/>
- Zong, Y., Huang, Y., Chen, S., Zhu, M., Chen, Q., Feng, S., Sun, Y., *et al.*, 2015. Downregulation of Endogenous Hydrogen Sulfide Pathway Is Involved in Mitochondrion-

Related Endothelial Cell Apoptosis Induced by High Salt. *Oxid Med Cell Longev*, **2015**, 1–12, *Oxid Med Cell Longev*. doi:10.1155/2015/754670

Zygmunt, M., Herr, F., Münstedt, K., Lang, U. & Liang, O.D., 2003. Angiogenesis and vasculogenesis in pregnancy. *European Journal of Obstetrics and Gynecology and Reproductive Biology*, Vol. 110, Elsevier Ireland Ltd. doi:10.1016/S0301-2115(03)00168-4

10. Appendices

10.1 Appendix A – Consumables and Instruments

| Laboratory Instruments/Software | Supplier |
|------------------------------------------------|----------------------------------------------------------------------------|
| Automated ELISA wash plate | ASYS Atlantis Biochrom Ltd, Cambridge, UK |
| Automated plate shaker | Stuart® SSM3, # SSL5, Staffordshire, UK |
| Bio-render software | OHSU, Canada |
| BP (Blood Pressure) Amp (Bridge Amplification) | ADInstruments Ltd, Oxford, UK |
| G:BOX Syngene system | Syngene Ltd, Cambridge, UK |
| Graph Prism v.9 software | GraphPad, California, USA |
| Homogenizer Crushing | Jencons-PLS T8.01, IKA®, Deutschland, Germany |
| LabChart® | ADInstruments Ltd, Oxford, UK |
| Multimode Microplate Reader Spark® | TECAN Group Ltd., Männedorf, Switzerland |
| Nanodrop 1000 spectrophotomer | Thermo Fisher Scientific, Warrington, UK |
| NovoMagic® Software | Novogene Ltd, Cambridge, UK |
| PCR LightCycler 480 II platform | Roche Diagnostic Ltd, Burgess Hill, UK |
| Tabletop Centrifuge | Centrifuges # 5418; # 5702; # 5424; # 5424- R, Eppendorf, Hamburg, Germany |
| TECAN plate reader | Spark-TECAN Trading AG, Switzerland. |
| ThermaSonic® Gel Warmer | Parker Laboratories, Inc, Fairfield, New Jersey, USA |
| Vevo® Lab Software | FUJIFILM Visualsonics, Amsterdam, The Netherlands |

| | |
|---------------------------------------|---------------------------------------------------|
| VisualSonics Vevo® 3100 Ultrasound | FUJIFILM Visualsonics, Amsterdam, The Netherlands |
|---------------------------------------|---------------------------------------------------|

Table S10.1: Laboratory Instruments and Software

| Reagents/Kits | Supplier |
|--------------------------------------------|-------------------------------------------|
| AdCMV | Vector Biolabs, Pennsylvania, USA |
| AdsFlt-1 | Vector Biolabs, Pennsylvania, USA |
| Agarose | Sigma-Aldrich, Dorset, UK |
| Bovine serum albumin (BSA) (#66-1252) | Fisher Scientific, Loughborough, UK |
| CSE Antibody | Proteintech Ltd, Manchester, UK |
| Cystathionine | Sigma-Aldrich, Dorset, UK |
| DirectPCR® lysis reagent | Bioquote Ltd, York, UK |
| ELISA Duoset | R&D Systems, Bio-Techne, Inc., Oxford, UK |
| Ethanol (absolute) | Sigma-Aldrich, Dorset, UK |
| Ethylenediaminetetraacetic (EDTA) (#E9884) | Sigma-Aldrich, Dorset, UK |
| Evoscript | Roche Diagnostic Ltd, Burgess Hill, UK |
| GoTaq® | Promega Ltd, Hampshire, UK |
| IsoFlo® Isoflurane | Abbott Laboratories Ltd, Maidenhead, UK |
| LightCycler® 480 SYBR Green | Roche Diagnostic Ltd, Burgess Hill, UK |
| Microsurgical Suture | InterFocus Ltd, Cambridge, UK |
| miRNeasy kit | Qiagen, Manchester, UK |
| Nair Cream | Superdrug, UK |
| Nuclease Free Water | Qiagen, Manchester, UK |
| Ocryl® Eye Gel | NewPet, Braga, Portugal |
| OCT Embedding Matrix | CellPath Ltd, Mochdre, UK |
| Paraformaldehyde (PFA) | Sigma-Aldrich, Dorset, UK |

| | |
|----------------------------------------------------------------------|------------------------------------------------|
| Primers | ID Techologies Ltd, Weston-super-Mare, UK |
| Protease inhibitor | Sigma-Aldrich, Dorset, UK |
| Proteinase K | Bioline, Nottingham, UK |
| QIAshredder | Qiagen, Manchester, UK |
| QIAzol Lysis reagent | Qiagen, Manchester, UK |
| Reagent diluent | R&D Systems, Bio-Techne, Inc., Oxford, UK |
| RIPA Lysis buffer (#89900) | ThermoFisher Scientific, Gloucester, UK |
| S&T Microsurgical Sutures 5mm Needle | InterFocus Ltd, Cambridge, UK |
| Saline | Scientific Laboratory Supplies, Nottingham, UK |
| Strip PCR tubes | ThermoFisher Scientific, Gloucester, UK |
| Substrate kit | R&D Systems, Bio-Techne, Inc., Oxford, UK |
| Trimaway Disposable Scalpel 148mm, Ideal Tek (#301-32-354) | Distelec, AG, Switzerland. |
| Tris-Borate-EDTA Buffer (TBE) (#B9-0020) | Geneflow Ltd, Staffordshire, UK |
| Ultra Fine 0.3 ml 31 G x 5/16 in. (8 mm) Insulin Syringe with Needle | Becton Dickinson Ltd, Winnersh, UK |
| Ultrasound Gel (#EE1295B) | Scientific Laboratory Supplies, Nottingham, UK |

Table S10.2 Laboratory Consumables and Kits

10.2 Appendix B – Supplementary Material

| Primer | Sequence (5'-3') |
|--------|----------------------------|
| N1 | TGCGAGGCCAGAGGCCAGTTGTGTAG |
| F1 | TGTTTCATGGTAGGTTTGGCC |
| R1 | TCAGAACTCGCAGGGTAGAA |

Table S10.3: Primer sequences for assessing the effectiveness of transgenic generation (Yang et al., 2008).

| Gene | Forward (Sequence 5' - 3') | Reverse Primer (Sequence 5' - 3') |
|------|----------------------------|-----------------------------------|
| 16S | CCGCAAGGGAAAGATGAAAGAC | TCGTTTGGTTTCGGGGTTTC |
| B2M1 | GTGAGGTAACGGCTCACCAA | GTGTCTCAGTCCCAGTGTGG |
| Cftr | CCATCAGCAAGCTGAAAGCAGG | GTAGGGTTGTAATGCCGAGACG |

Table S10.4 Mitochondrial DNA Primers

10.3 Appendix C – Supplementary Methods

C.1 Novogene mRNA Sequencing protocol

Please refer to QC report for methods of sample quality control.

Library Construction, Quality Control and Sequencing

Messenger RNA was purified from total RNA using poly-T oligo-attached magnetic beads. After fragmentation, the first strand cDNA was synthesized using random hexamer primers, followed by the second strand cDNA synthesis using either dUTP for directional library or dTTP for non-directional library.

For the non-directional library, it was ready after end repair, A-tailing, adapter ligation, size selection, amplification, and purification (**Figure S1.1 A**). For the **directional** library, it was ready after end repair, A-tailing, adapter ligation, size selection, **USER enzyme digestion**, amplification, and purification(**Figure S1.1 B**).

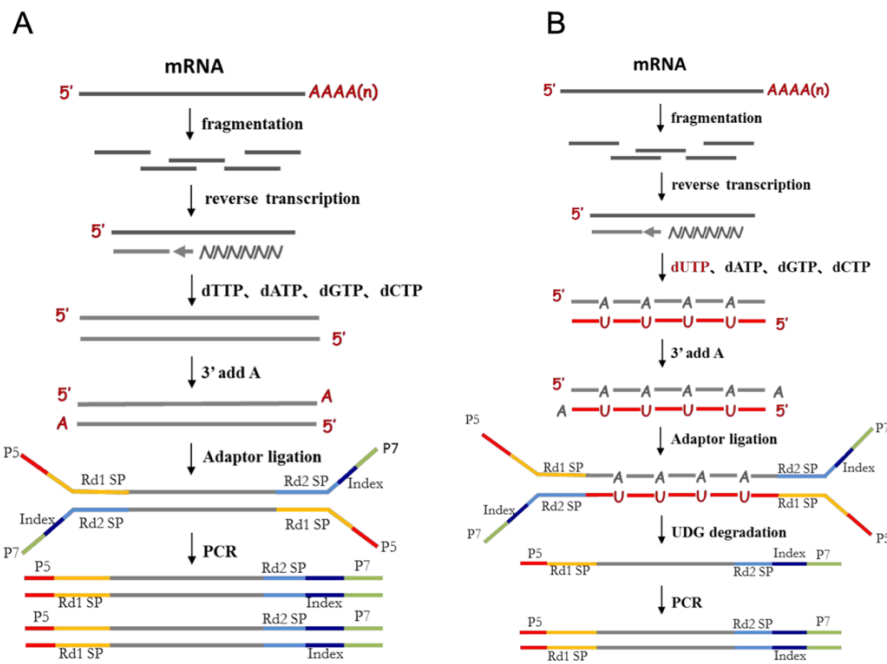


Figure S10.1 Workflow of directional library construction.

The library was checked with Qubit and real-time PCR for quantification and bioanalyzer for size distribution detection. Quantified libraries will be pooled and sequenced on Illumina platforms, according to effective library concentration and data amount.

Clustering and sequencing

The clustering of the index-coded samples was performed according to the manufacturer's instructions. After cluster generation, the library preparations were sequenced on an Illumina platform and paired-end reads were generated.

Data Analysis

Quality control

Raw data (raw reads) of fastq format were firstly processed through in-house perl scripts. In this step, clean data (clean reads) were obtained by removing reads containing adaptor, reads containing ploy-N and low quality reads from raw data. At the same time, Q20, Q30 and GC content the clean data were calculated. All the downstream analyses were based on the clean data with high quality.

Reads mapping to the reference genome

Reference genome and gene model annotation files were downloaded from genome website directly. Index of the reference genome was built using Hisat2 v2.0.5 and paired-end clean

reads were aligned to the reference genome using Hisat2 v2.0.5. We selected Hisat2 as the mapping tool for that Hisat2 can generate a database of splice junctions based on the gene model annotation

file and thus a better mapping result than other non-splice mapping tools. **Quantification of gene expression level**

featureCounts v1.5.0-p3 was used to count the reads numbers mapped to each gene. And then FPKM of each gene was calculated based on the length of the gene and reads count mapped to this gene. FPKM, expected number of Fragments Per Kilobase of transcript sequence per Millions base pairs sequenced, considers the effect of sequencing depth and gene length for the reads count at the same time, and is currently the most commonly used method for estimating gene expression levels.

Differential expression analysis

(For DESeq2 with biological replicates) Differential expression analysis of two conditions/groups (two biological replicates per condition) was performed using the DESeq2 R package (1.20.0). DESeq2 provide statistical routines for determining differential expression in digital gene expression data using a model based on the negative binomial distribution. The resulting P-values were adjusted using the Benjamini and Hochberg's approach for controlling the false discovery rate . Genes with an adjusted P-value ≤ 0.05 found by DESeq2 were assigned as differentially expressed.

(For edgeR without biological replicates) Prior to differential gene expression analysis, for each sequenced library, the read counts were adjusted by edgeR program package through one scaling normalized factor. Differential expression analysis of two conditions was performed using the edgeR R package (3.22.5). The P values were adjusted using the Benjamini & Hochberg method. Corrected P-value of 0.05 and absolute foldchange of 2 were set as the threshold for significantly differential expression.

Enrichment analysis of differentially expressed genes

Gene Ontology (GO) enrichment analysis of differentially expressed genes was implemented by the clusterProfiler R package, in which gene length bias was corrected. GO terms with corrected Pvalue less than 0.05 were considered significantly enriched by differential expressed genes. KEGG is a database resource for understanding high-level functions and utilities of the biological system, such as the cell, the organism and the ecosystem, from molecular-level information, especially large-scale molecular datasets generated by genome sequencing and other high-through put experimental technologies (<http://www.genome.jp/kegg/>). We used clusterProfiler R package to test the statistical enrichment of differential expression genes in KEGG pathways. The Reactome database brings together the various reactions and biological pathways of human model species. Reactome pathways with corrected Pvalue less than 0.05 were considered significantly enriched by differential expressed genes. The DO (Disease Ontology) database describes the function of human genes and diseases. DO pathways with corrected Pvalue less than 0.05 were considered significantly enriched by differential expressed genes. The DisGeNET database integrates human disease-related genes. DisGeNET pathways with corrected Pvalue less than 0.05 were considered significantly enriched by differential expressed genes. We used clusterProfiler software to test the statistical enrichment of differentially expressed genes in the Reactome pathway, the DO pathway, and the DisGeNET pathway.

Gene Set Enrichment Analysis

Gene Set Enrichment Analysis (GSEA) is a computational approach to determine if a pre-defined Gene Set can show a significant consistent difference between two biological states. The genes were ranked according to the degree of differential expression in the two samples, and then the predefined Gene Set were tested to see if they were enriched at the top or bottom of the list. Gene set enrichment analysis can include subtle expression changes. We use the local version of the GSEA analysis tool

<http://www.broadinstitute.org/gsea/index.jsp>, GO, KEGG, Reactome, DO and DisGeNET data sets were used for GSEA independently.

SNP analysis

GATK (v4.1.1.0) software was used to perform SNP calling. Raw vcf files were filtered with GATK standard filter method and other parameters (cluster:3; WindowSize:35; QD < 2.0 ; FS > 30.0; DP < 10.

AS analysis

Alternative Splicing is an important mechanism for regulate the expression of genes and the 3 variable of protein. rMATS(4.1.0) software was used to analysis the AS event.

PPI analysis of differentially expressed genes

PPI analysis of differentially expressed genes was based on the STRING database, which known and predicted Protein-Protein Interactions.

Fusion Analysis

Fusion gene refers to the chimeric gene formed by the fusion of all or part of the sequences of two genes, which is generally caused by chromosome translocation, deletion and other reasons. We used Starfusion software (1.9.0) to detect genes that are fused. Star-fusion is a software package uses fusion output results of STAR alignment to detect fusion transcripts, including SATR alignment, SATRfusion. predict, SATR-fusion.filter was used to correct the predicted results of Star-fusion to ensure the accuracy of the results.

Appendix D – Supplementary Figures

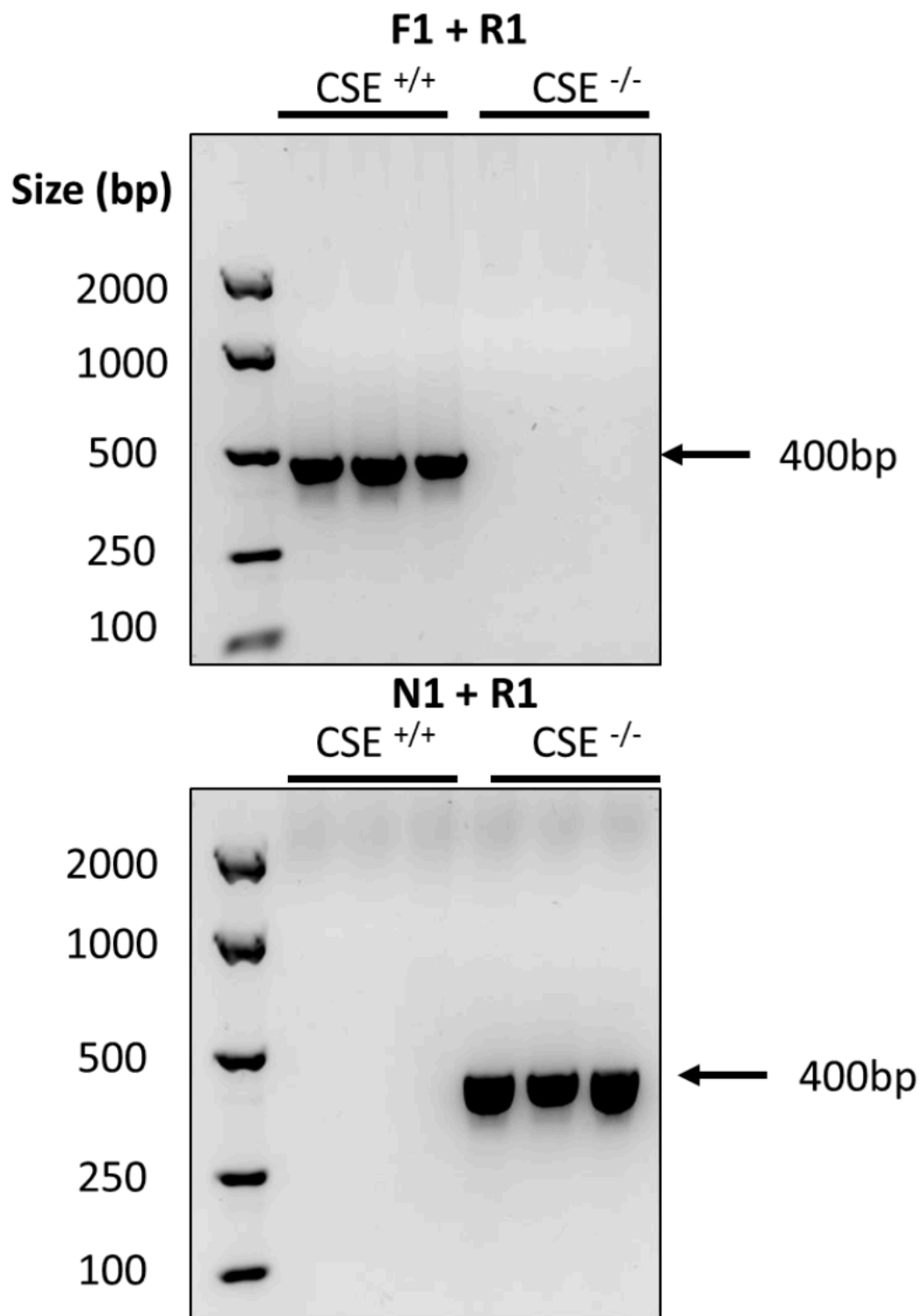


Figure S10.2 **Genotyping of cystathionine gamma lyase (CSE) knockout and wildtype mice.** Reaction 1 contained F1 and R1 primers to successfully identify Wildtype (CSE^{+/+}) mice, while reaction 2 contained N1 and R1 primers to identify the knockout (CSE^{-/-}) genotype. PCR products were run on a 1% agarose gel at 110V

for one hour in TBE buffer. Bands were identified at 400 base pairs (bp).

Echocardiographic classification of diastolic dysfunction

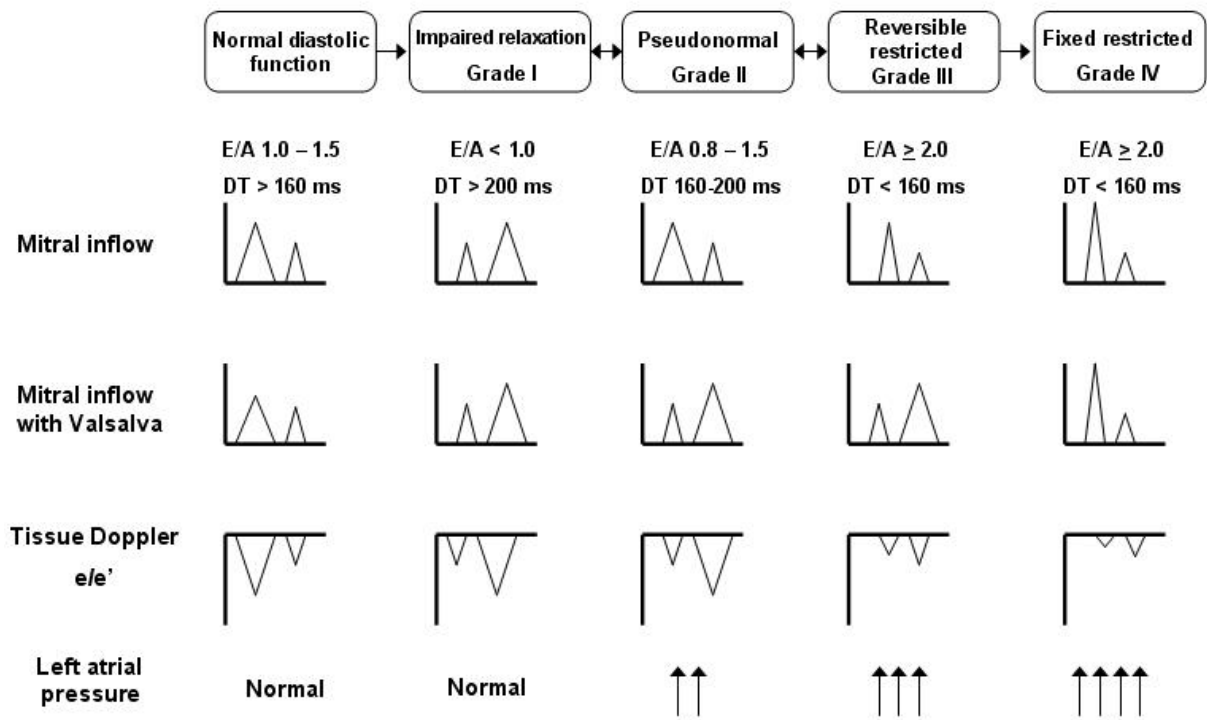


Figure S10.3 Echocardiographic MV E/A classification according to (Danzmann *et al.* 2008)

10.4 Appendix E – Publications

Published Study 1



International Journal of
Molecular Sciences



Review

Angiogenic Properties of Placenta-Derived Extracellular Vesicles in Normal Pregnancy and in Preeclampsia

Natalia Gebara ¹, Yolanda Correia ² , Keqing Wang ² and Benedetta Bussolati ^{1,*} 

¹ Department of Molecular Biotechnology and Health Sciences, University of Torino, 10124 Torino, Italy; Natalia.gebara@unito.it
² Aston Medical Research Institute, Aston Medical School, Aston University, Birmingham B4 7ET, UK; correia.yolanda94@gmail.com (Y.C.); k.wang@aston.ac.uk (K.W.)
* Correspondence: benedetta.bussolati@unito.it; Tel.: +39-011-6706453; Fax: +39-011-6331184

Abstract: Angiogenesis is one of the main processes that coordinate the biological events leading to a successful pregnancy, and its imbalance characterizes several pregnancy-related diseases, including preeclampsia. Intracellular interactions via extracellular vesicles (EVs) contribute to pregnancy's physiology and pathophysiology, and to the fetal–maternal interaction. The present review outlines the implications of EV-mediated crosstalk in the angiogenic process in healthy pregnancy and its dysregulation in preeclampsia. In particular, the effect of EVs derived from gestational tissues in pro and anti-angiogenic processes in the physiological and pathological setting is described. Moreover, the application of EVs from placental stem cells in the clinical setting is reported.

Keywords: extracellular vesicles; preeclampsia; angiogenesis

 check for updates

Citation: Gebara, N.; Correia, Y.; Wang, K.; Bussolati, B. Angiogenic Properties of Placenta-Derived Extracellular Vesicles in Normal Pregnancy and in Preeclampsia. *Int. J. Mol. Sci.* **2021**, *22*, 5402. <https://doi.org/10.3390/ijms22105402>

Academic Editors: Heriberto Rodriguez-Martinez, Jordi Roca and Emilio A. Martinez

Received: 13 April 2021
Accepted: 17 May 2021
Published: 20 May 2021

Publisher's Note: MDPI stays neutral with regard to jurisdictional claims in published maps and institutional affiliations.



Copyright: © 2021 by the authors. Licensee MDPI, Basel, Switzerland. This article is an open access article distributed under the terms and conditions of the Creative Commons Attribution (CC BY) license (<https://creativecommons.org/licenses/by/4.0/>).

Int. J. Mol. Sci. **2021**, *22*, 5402. <https://doi.org/10.3390/ijms22105402> <https://www.mdpi.com/journal/ijms>



Review

Yolanda Correia*, Julia Scheel*, Shailendra Gupta and Keqing Wang

Placental mitochondrial function as a driver of angiogenesis and placental dysfunction

<https://doi.org/10.1515/hsz-2021-0121>

Received January 22, 2021; accepted June 9, 2021;

published online July 5, 2021

Keywords: computational modelling; endothelial dysfunction; mitochondrial dysfunction; preeclampsia; systems biology; vascular deregulation.

Abstract: The placenta is a highly vascularized and complex foetal organ that performs various tasks, crucial to a healthy pregnancy. Its dysfunction leads to complications such as stillbirth, preeclampsia, and intrauterine growth restriction. The specific cause of placental dysfunction remains unknown. Recently, the role of mitochondrial function and mitochondrial adaptations in the context of angiogenesis and placental dysfunction is getting more attention. The required energy for placental remodelling, nutrient transport, hormone synthesis, and the reactive oxygen species leads to oxidative stress, stemming from mitochondria. Mitochondria adapt to environmental changes and have been shown to adjust their oxygen and nutrient use to best support placental angiogenesis and foetal development. Angiogenesis is the process by which blood vessels form and is essential for the delivery of nutrients to the body. This process is regulated by different factors, pro-angiogenic factors and anti-angiogenic factors, such as sFlt-1. Increased circulating sFlt-1 levels have been linked to different preeclamptic phenotypes. One of many effects of increased sFlt-1 levels, is the dysregulation of mitochondrial function. This review covers mitochondrial adaptations during placentation, the importance of the anti-angiogenic factor sFlt-1 in placental dysfunction and its role in the dysregulation of mitochondrial function.

Yolanda Correia and Julia Scheel contributed equally to this article.

*Corresponding authors: **Yolanda Correia** Aston Medical School, College of Health & Life Sciences, Aston University, Aston Triangle, Birmingham B4 7ET, UK, E-mail: y.correia@aston.ac.uk; and **Julia Scheel**, Department of Systems Biology and Bioinformatics, University of Rostock, D-18051 Rostock, Germany, E-mail: julia.scheel@uni-rostock.de.
<https://orcid.org/0000-0002-0034-7755>

Shailendra Gupta, Department of Systems Biology and Bioinformatics, University of Rostock, D-18051 Rostock, Germany
Keqing Wang, Aston Medical School, College of Health & Life Sciences, Aston University, Aston Triangle, Birmingham B4 7ET, UK

Introduction: preeclampsia

Preeclampsia (PE) is a multisystemic disorder (Lambert et al. 2014) that affects 1–8% of pregnancies (Duley 2009). Annually, 76,000 maternal deaths and 500,000 perinatal deaths worldwide can be attributed to PE (Khan et al. 2006) and it is accompanied by severe long-term burdens. PE is defined as *de novo* onset of hypertension ($\geq 160/110$ mmHg) (Brown et al. 2018) and proteinuria (spot urine protein/creatinine > 30 mg/mmol or > 300 mg/day) (Tranquilli et al. 2014; Trostad et al. 2011), after 20 weeks of gestation. The exact pathophysiology and phenotype subtypes of PE are poorly understood.

Although the placenta is understood to be the main actor in PE, which should thus be “cured” after delivery of the placenta, recent studies showed that preeclamptic women have an increased chance of developing various long-term cardiovascular diseases. PE strongly correlates with subsequent development of hypertension, ischaemic heart disease, stroke and venous thromboembolism (Bellamy et al. 2007). Correspondingly, several predisposing factors, such as multifetal pregnancies, chronic high blood pressure, personal or family history of PE, pre-existing diabetes, thrombophilia and obesity, are associated with increased risks of developing PE (English et al. 2015).

PE is a multifactorial disorder and the exact aetiology is still unknown. The disruption of endothelial homeostasis, abnormal placentation, excessive inflammation, and imbalance of angiogenic factors are key features of PE (Apicella et al. 2019; Possomato-Vieira and Khalil 2016; Sánchez-Aranguren et al. 2014).

To date, there are no effective treatments to prevent PE, partly due to the lack of clear knowledge behind the pathophysiology of PE. The current therapeutic strategies for PE mainly focus on alleviating the symptoms in order to delay the necessity for delivery. However, this strategy

